

NCHRP 24-17

**LOAD AND RESISTANCE FACTOR DESIGN
(LRFD) FOR DEEP FOUNDATIONS**

**APPENDIX B
LOAD AND RESISTANCE FACTOR DESIGN (LRFD)
FOR DYNAMIC ANALYSES OF DRIVEN PILES**

Prepared for
National Cooperative Highway Research Program
Transportation Research Board
National Research Council

Samuel G. Paikowsky and Kirk L. Stenerson
Geotechnical Engineering Research Laboratory
Department of Civil and Environmental Engineering
University of Massachusetts
Lowell, Massachusetts

July 2002

ACKNOWLEDGEMENT OF SPONSORSHIP

This work was sponsored by the American Association of State Highway and Transportation Officials, in cooperation with the Federal Highway Administration, and was conducted in the National Cooperative Highway Research Program, which is administered by the Transportation Research Board of the National Research Council.

DISCLAIMER

This is an uncorrected draft as submitted by the research agency. The opinions and conclusions expressed or implied in the report are those of the research agency. They are not necessarily those of the Transportation Research Board, the National Research Council, the Federal Highway Administration, the American Association of State Highway and Transportation Officials, or the individual states participating in the National Cooperative Highway Research Program.

ABSTRACT

NCHRP Project 24-17 "LRFD Deep Foundation Design" is supported by the USA National Cooperative Highway Research Program (NCHRP) under the Transportation Research Board (TRB) of the National Academy of Science (NAS). The project is aimed at rewriting AASHTO Deep Foundation Specifications for the year 2001. The AASHTO specifications are traditionally observed on all federally aided projects and generally viewed as a national code of US Highway practice, hence influencing the construction of all the deep foundations of highway bridges throughout the USA.

The new specifications are based on Load and Resistance Factor Design (LRFD) principles with resistance factors obtained from probabilistic analysis of data. This research report presents a review of methodologies, resistance factors calculation and the application of it to the dynamic analyses of driven piles. A large database (PD/LT2000) is the backbone of the dynamic methods' performance evaluation. This database originated with the work presented by Paikowsky et al. (1994), Paikowsky and LaBelle (1994), and additional information acquired since.

A review of design methodologies is presented and the application of LRFD to Geotechnical Engineering is discussed. The process of data compilation is introduced and methods to establish pile capacity based on static load test results are evaluated for the determination of a reference static capacity. A summary and careful evaluation of PD/LT 2000 database is presented, and the parameters that control the accuracy of the dynamic predictions are analyzed. The data analysis indicates the importance of certain mechanisms associated with the pile penetration and the dynamic simulations. The most important parameters are shown to be those associated with the soil inertia, namely driving resistance and pile geometry and those associated with change of pile capacity with time, namely, time of driving, [e.g. End of Driving (EOD) and Beginning of Restrike (BOR)].

The First Order Reliability Method (FORM) is introduced and applied for LRFD of Deep Foundations. Target reliability and the associated probability of failure levels are discussed. Analyses of PD/LT2000 provide statistical details for the performance of the various dynamic methods when compared to static load testing to failure. The controlling parameters and the statistical analyses along with the recommended target reliability are then utilized for the development of the resistance factors. The final resistance factors recommended for the new specifications are extracted in a three level process; (i) detailed statistical evaluation of a wide range of cases based on the identified controlling parameters, (ii) evaluation of the resistance factors for the inclusive cases (out of the 1st stage) for three target reliability levels, and, (iii) developing the final resistance factors for the most inclusive and critical cases under the recommended target reliabilities. Two concepts are introduced for the recommended resistance factors: (a) two levels of target reliability based on the criticality of the foundation, classifying the piles as redundant and non-redundant elements and, (b) efficiency evaluation of the method of analysis in conjunction with the magnitude of the resistance factors.

The obtained parameters are evaluated against FOSM (First Order Second moment method), and the actual probability of failure. Case histories allow an evaluation of the recommended parameters in an absolute way and against WSD factors of safety. The final recommendations are comprehensive and clear providing factors for a variety of dynamic methods and means to evaluate their efficiency.

ACKNOWLEDGMENTS

The American Association of State Highway and Transportation Officials (AASHTO) sponsored the presented research, under National Cooperative Highway Research Program (NCHRP) project 24-17, in cooperation with the Federal Highway Administration (FHWA). The project is supported through the Transportation Research Board (TRB) of the National Academy of Science (NAS). The panel of the research project and Mr. David Beal of the NCHRP are acknowledged for their stimulating demands. Messrs. Jerry DiMaggio, Al DiMillio and Carl Ealy of the FHWA are acknowledged for their interest, concern and support.

Dr. Gregory B. Baecher and Dr. Bilal M. Ayyub from the University of Maryland for their contributions to Chapters 2 and 9, in particular for the calculation of the presented resistance factors using FORM. Special thanks to Dr. Baecher for serving on Mr. Stenersen's M.S. thesis committee.

Dr. Frank Rausche of Goble, Rausche, Likins (GRL) and Associates for providing the data pertaining to the evaluation of GRLWEAP and for serving on Mr. Stenersen's M.S. thesis committee including the effort in traveling to the thesis defense.

Dr. John Ting from the University of Massachusetts at Lowell for serving on Mr. Stenersen's thesis committee.

Mr. Kevin O'Malley for his contributions to Chapter 7 as part of his graduate project, particularly the grueling task of compiling the data for the PD2000 database.

Dr. Michael McVay of the University of Florida for providing the data pertaining to the evaluation of the Case method in Florida.

Geosciences Testing and Research, Inc. (GTR) of North Chelmsford, Massachusetts for providing data for the research, mostly the data for the PD2000 database in Boston Blue Clay.

TABLE OF CONTENTS

LIST OF TABLES

LIST OF FIGURES

1 INTRODUCTION

- 1.1 OVERVIEW
- 1.2 BACKGROUND
- 1.3 MANUSCRIPT LAYOUT

2 BACKGROUND

- 2.1 STATE OF STRESS METHODOLOGY
 - 2.1.1 Overview
 - 2.1.2 The Working Stress (WSD) Method
 - 2.1.3 The Limit States
- 2.2 LOAD AND RESISTANCE FACTOR DESIGN (LRFD) METHOD
 - 2.2.1 Reliability Based Design – History and Background
 - 2.2.2 Development of the LRFD Method for General Geotechnical Engineering
 - 2.2.3 The Principle of the LRFD Method for Deep Foundations
 - 2.2.4 Determination of Resistance Factors by Calibration
 - a) LRFD Calibration via WSD
 - b) LRFD Calibration using Reliability Theory
 - c) Reliability-Based LRFD Using Failure Point
 - 2.2.5 The Use of Limit States in LRFD
- 2.3 THE AVAILABLE AND CHOSEN DYNAMIC METHODS
 - 2.3.1 General
 - 2.3.2 Dynamic Equations
 - a) The Basic Principle
 - b) Engineering News Record Equation
 - c) Gates Equation
 - d) FHWA modified Gates Equation
 - 2.3.3 The Wave Equation
 - a) Formulation and Principles
 - b) Pre-Driving Analysis
 - c) Post-Driving Analysis – CAPWAP/TEPWAP

- 2.3.4 The Case Method
 - a) General
 - b) The Case Method Equation
 - c) Case Damping Coefficient
 - d) Case Method Variations
- 2.3.5 The Energy Approach
- 2.4 REVIEW OF THE RECOMMENDED LRFD FACTORS FOR PILE DESIGN
 - 2.4.1 Resistance Factors Recommended by AASHTO
 - 2.4.2 Resistance Factors for Dynamic Load Testing using the Case Method
 - 2.4.3 International LRFD Codes
 - a) Australian Standard, Piling-Design and Installation
 - b) 1992 AUSTROADS Bridge Design Code
 - c) Eurocode 7, Geotechnical Design
 - d) Danish Code of Practice for Foundation Engineers
 - e) Ontario Bridge Code
 - f) Canadian Bridge Code
 - g) Japanese Specifications for Highway Bridges
 - 2.4.4 Evaluation of Recommended Resistance Factors
 - 2.4.5 Evaluation of Calculated Resistance Factors
- 2.5 DIFFICULTIES OF THE EXISTING LRFD CODES
 - 2.5.1 Overview
 - 2.5.2 Construction Difficulties
 - a) General
 - b) Observations
 - 2.5.3 Deficiency in Current Geotechnical Reliability Practice for LRFD
 - 2.5.4 Calibrations Based on State-of-Practice Reliability Methodology

3 COMPILATION OF DATABASES

- 3.1 GENERAL 90
- 3.2 PD/LT2000 DATABASE
 - 3.2.1 Overview
 - 3.2.2 Static Load Test Analysis
 - 3.2.3 Dynamic Measurements Analysis
 - a) Overview
 - b) Group 1 – Complete CAPWAP Analysis
 - c) Group 2 – Incomplete CAPWAP Analysis
 - d) Group 3 – TEPWAP Analysis
- 3.3 U-MASS LOWELL / UKRAINE DATABASE
- 3.4 GRLWEAP DATABASE

- 3.5 CASE METHOD DATABASE
- 3.6 PD2000
- 3.7 PD/LTT2000

4 REFERENCE STATIC CAPACITY

- 4.1 OVERVIEW
- 4.2 OBJECTIVES
- 4.3 PILE FAILURE / CAPACITY DETERMINATION
 - 4.3.1 Background
 - 4.3.2 Method of Approach
 - 4.3.3 Davisson's Criterion
 - 4.3.4 The Shape-of-Curve Method
 - 4.3.5 The Limited Total Settlement Methods
 - 4.3.6 DeBeer's log-log Method
 - 4.3.7 The Representative Static Capacity
- 4.4 PERFORMANCE EVALUATION OF THE DIFFERENT FAILURE CRITERION METHODS
 - 4.4.1 Method of Approach
 - 4.4.2 Davisson's Criterion
 - 4.4.3 The Shape-of-Curve Method
 - 4.4.4 Limiting Total Settlement to 25.4 mm
 - 4.4.5 Limiting Total Settlement to One Tenth of the Pile Diameter
 - 4.4.6 DeBeer's log-log Method
 - 4.4.7 Intermediate Conclusions
 - 4.4.8 Evaluation of a Modification for Davisson's Criterion
 - a) The Proposed Modification
 - b) The Performance of the Proposed Modification
- 4.5 STATIC LOAD TEST PROCEDURE
 - 4.5.1 Overview
 - 4.5.2 Load Test Procedures
 - a) ASTM Procedures
 - i) Standard Loading Procedure
 - ii) Cyclic Loading
 - iii) Quick Load Test Method for Individual Piles
 - iv) Constant Rate of Penetration
 - b) Massachusetts Highway Department Procedures
 - i) Short Duration Test
 - ii) Maintained Load Test
 - iii) Quick Load Test
 - c) Massachusetts Building Code Procedure
 - d) Texas Quick Test Procedure
 - e) Static-Cyclic Load Test Procedure
 - f) Summary

- 4.5.3 Performance Evaluation of the Load Test Procedures
 - a) Comparison of the Short Duration, Slow Maintained and Static Cyclic Tests
 - b) Comparison between the Static-Cyclic Load Testing and Slow Maintained Tests Using Davisson's Capacity
 - c) Intermediate Conclusions

4.6 CONCLUSIONS FOR REFERENCE STATIC CAPACITY

5 CONTROLLING PARAMETERS OF THE DYNAMIC METHODS

- 5.1 OVERVIEW
- 5.2 METHOD OF APPROACH
 - 5.2.1 General
 - 5.2.2 Nomenclature
 - 5.2.3 Interpretation of Statistical Results
- 5.3 THE CONTROLLING PARAMETERS
 - 5.3.1 Soil Type
 - a) General
 - b) Sand and Silt
 - c) Clay and Till
 - d) Rock
 - e) Intermediate Conclusions
 - 5.3.2 Time of Driving
 - 5.3.3 Soil Inertia Effects
 - a) Overview
 - b) Effect of Driving Resistance
 - c) Effect of Pile Type
- 5.4 INTERMEDIATE CONCLUSIONS

6 PERFORMANCE OF THE DYNAMIC METHODS DURING THE CONSTRUCTION STAGE

- 6.1 OVERVIEW
- 6.2 DYNAMIC ANALYSES WITHOUT DYNAMIC MEASUREMENTS
 - 6.2.1 WEAP Analysis
 - 6.2.2 The Dynamic Equations
 - a) General
 - b) ENR Equation
 - c) Gates Equation
 - d) FHWA modified Gates Equation
 - e) The Recommended Dynamic Equation and its Performance
 - f) Summary of the Dynamic Equations Performance
- 6.3 DYNAMIC ANALYSES WITH DYNAMIC MEASUREMENTS

- 6.3.1 Overview
- 6.3.2 Performance of the Signal Matching Technique (CAPWAP or TEPWAP)
 - a) All Pile-Cases
 - b) Performance According to Time of Driving
 - c) Performance According to Driving Resistance
 - d) Performance According to Pile Type
- 6.3.3 Field Evaluation (Energy Approach)
 - a) All Pile-Cases
 - b) Performance According to Time of Driving
 - c) Performance According to Driving Resistance
 - d) Performance According to Pile Type
- 6.3.4 Field Evaluation (Case Method)
 - a) General
 - b) Evaluation of the Case-Damping Coefficient
 - c) Evaluation of the Case Method Based on Local Calibration
 - d) Summary

6.4 SUMMARY AND INTERMEDIATE CONCLUSIONS

7 ENERGY APPROACH EOD VERSUS CAPWAP/TEPWAP BOR

- 7.1 GENERAL
- 7.2 COMPARISON BASED ON THE PD/LT2000 DATABASE
- 7.3 COMPARISON BASED ON THE PD2000 DATABASE
 - 7.3.1 Overview
 - 7.3.2 All Pile-Cases
 - 7.3.3 Driving Resistance
 - 7.3.4 Soil Types
 - a) Overview
 - b) Clay and Till
 - c) Sand and Silt
 - d) Rock
 - e) Boston Blue Clay
 - 7.3.5 Summary
- 7.4 SUMMARY AND INTERMEDIATE CONCLUSIONS

8 PILE CAPACITY GAIN WITH TIME

- 8.1 GENERAL
- 8.2 ANALYSIS OF PILE CAPACITY GAIN WITH TIME
- 8.3 INTERMEDIATE CONCLUSIONS

9 CALCULATION OF RESISTANCE FACTORS

- 9.1 METHODOLOGY

- 9.2 LEVEL OF TARGET RELIABILITY
 - 9.2.1 Overview
 - 9.2.2 General Discussion
 - a) Target Reliability Levels
 - b) Calibrated Reliability Levels
 - 9.2.3 Geotechnical Perspective
- 9.3 DEAD TO LIVE LOAD RATIO
- 9.4 THE RESISTANCE FACTORS
 - 9.4.1 Initial Evaluation
 - 9.4.2 Intermediate Conclusions
 - 9.4.3 Resistance Factors for a Range of Reliability Levels
 - 9.4.4 Recommended Resistance Factors
- 9.5 EVALUATION OF THE DYNAMIC METHODS EFFICIENCY
- 9.6 EVALUATION OF THE TARGET RELIABILITY USED
 - 9.6.1 Resistance Factors Based on the Existing AASHTO Specifications
 - 9.6.2 Evaluation of the WSD Factors of Safety (AASHTO, 1997) in Light of the Obtained Results
 - 9.6.3 Evaluation of the Chosen Target Reliability
 - a) Overview
 - b) Approximate Factors of Safety
 - c) The Actual Probability of Failure
- 9.7 THE CHOSEN TARGET RELIABILITY AND RESISTANCE FACTORS

10 EXAMPLE CASE HISTORIES

- 10.1 GENERAL
- 10.2 EVALUATION OF THE PROPOSED RESISTANCE FACTORS
- 10.3 INTERMEDIATE CONCLUSIONS

11 SUMMARY, CONCLUSIONS AND RECOMMENDATIONS

- 11.1 SUMMARY
- 11.2 CONCLUSIONS
- 11.3 RECOMMENDATIONS

REFERENCES

APPENDIX A - RELEVANT INFORMATION FROM DATABASES

APPENDIX B - BACKGROUND CALCULATIONS FOR CASE HISTORIES PRESENTED IN CHAPTER 2

**APPENDIX C - CALCULATED RESISTANCE FACTORS BY
CALIBRATING TO THE STATIC LOAD TEST
RESULTS**

**APPENDIX D - CASE HISTORY CALCULATIONS COMPARING
THE WSD METHOD, THE LRFD METHOD AND
THE PRESENT AASHTO CODE**

LIST OF TABLES**PAGE**

- | | | |
|------|---|--|
| 2.1 | Factor of Safety on Ultimate Axial Geotechnical Capacity Based on Level of Construction Control (AASHTO, 1997) | |
| 2.2 | Allowable Stresses in Piles (AASHTO, 1997) | |
| 2.3 | Resistance Factors for Geotechnical Strength Limit State for Axially Loaded Piles (AASHTO, 1998) | |
| 2.4 | Resistance Factors Calibrated by Fitting with WSD for $\gamma_D=1.25$ and $\gamma_L=1.75$ (After McVay et al., 1998) | |
| 2.5 | Resistance Factor for Driven Piles for Estimating the Axial Geotechnical Pile Capacity Using Reliability-Based Calibration (modified after Barker et al., 1991) | |
| 2.6a | Relationship Between Probability of Failure and Reliability Index for Lognormal Distribution (After Withiam et al., 1997) | |
| 2.6b | Comparison Between Rosenbleuth and Estava's Approximation and Series Expansion (Labeled "exact") | |
| 2.7 | Strength and Service Limit States for Design of Driven Pile Foundations (After Withiam et al., 1997) | |
| 2.8 | Reliability Index of Case Method Prediction (After McVay et al., 1998) | |
| 2.9 | Resistance Factor for Case Method Prediction (After McVay et al., 1998) | |
| 2.10 | Range of Values for Resistance Factors for Piles (Standard Association of Australia, 1995) | |
| 2.11 | Guide for Assessment of Resistance Factors for Piles (Standard Association of Australia, 1995) | |
| 2.12 | Material Resistance Factors for Piles (AUSTROADS, 1992) | |
| 2.13 | Typical Load and Resistance Factors for Axially Loaded Piles in Compression on Land for ULS (modified after Meyerhof, 1994) | |

- 2.14 Partial Factors from Eurocode 7 and the Equivalent Resistance Factors (After Eurocode 7, 1997)
- 2.15 Piles and Anchors (From the Danish Code)
- 2.16 Resistance Factors for Deep Foundations (From Ontario Bridge Code)
- 2.17 Resistance Factors (From the Canadian Bridge Code)
- 2.18 Summary of Ultimate and Factored Loads, Test Pile # 2, Newbury Site
- 2.19 Calculated Resistance Factors Assuming that the Resistance Factor for a Static Load Test is 1.0
- 2.20 Comparison of Recommended and Calculated Resistance Factors
- 3.1 Summary of the Data in the PD/LT2000 database
- 4.1 Summary of the Interpretation Methods applied to the Static Load Test Curves in PD/LT2000
- 4.2 Summary of Static Load Test Procedures (after Paikowsky et al., 1999)
- 4.3 Summary of the Statistical Data Comparing the Slow Maintained Load Test Results using Davisson's Criterion and the Static Cyclic Load Test Results from the UMass Lowell / Ukraine Database
- 5.1 Summary of the K_{SW} Values for the Different Soil Types used for the Soil Inertia Analysis
- 5.2 Summary of the K_{SP} Values for the Different Soil Types used for the Soil Inertia Analysis
- 5.3 Summary of the Statistics showing the Importance of the Time of Driving as a Controlling Parameter
- 5.4 Summary of the Statistics showing the Importance of the Driving Resistance as a Controlling Parameter
- 5.5 Summary of the Statistics showing the Importance of the Area Ratio as a Controlling Parameter

- 6.1 Summary of the Statistical Data Evaluating the Performance of the Dynamic Equations
- 6.2 Summary of the Statistical Analyses completed for the Dynamic Equations
- 6.3 Summary of the EOD Pile-Cases for which the K_{sx} Values Were Outside Two Standard Deviations
- 6.4 Summary of the Soil Inertia Properties for PD/LT2000, Energy Approach and CAPWAP/TEPWAP vs. Static Load Test Results for the Controlling Parameters
- 6.5 Summary of the Statistical Analyses Performed in Chapter 6
- 7.1 Summary of statistical data for the Correlation between the CAPWAP/TEPWAP predictions at the BOR to the Energy Approach predictions at the EOD using the PD/LT2000 and PD2000 databases
- 8.1 Soil properties, pile type, and relevant information for dynamic capacity gain – Data Set PD/LTT2000, predominately clay embedment (Paikowsky et al., 1995)
- 8.2 Soil properties, pile type, and relevant information for dynamic capacity gain – Data Set PD/LTT2000, partially in clay embedment
- 8.3 Summary of static and dynamic based capacity gain data sets (Paikowsky et al., 1995)
- 9.1 Approximate Relationship Between Probability of Failure and Reliability Index for Lognormal Distribution, based on Rosenbleuth and Estava (1972), see Withiam et al. (1998)
- 9.2 Comparison Between Rosenbleuth and Estava's Approximation and Series Expansion (Labeled "exact")
- 9.3 Target Reliability Levels
- 9.4 Target Reliability Levels used by Ellingwood and Galambos (1982)
- 9.5 Target Reliability Values Recommended by A.S. Veritas (Lotsberg, 1991)
- 9.6 Reliability Indices for Driven Piles (Barker et al., 1991)

- 9.7 Summary of the Performance of the Dynamic Methods
- 9.8 Recommended Resistance Factors for the Critical Dynamic Cases
- 9.9 Resistance Factors for the Critical Dynamic Cases Based on FOSM using Barker et al., (1991) versus those developed through FORM (see Table 9.8)
- 9.10 Calculated Factors of Safety Based on the Resistance Factors in Table 9.8 and the Procedure Outlined by Barker et al. (1991)
- 9.11 The Probability of Failures Associated with the Critical Dynamic Methods and Their Important Categories from the PD/LT2000 Database
- 10.1 Predictions of the Dynamic Methods for Three Case History Piles
- 10.2 Summary of Design Capacity Comparisons for Three Case History Piles
- A.1 Relevant Information Pertaining to Database PD/LT2000
- A.2 Relevant Information Pertaining to Umass – Ukraine Database
- A.3 Relevant Information Pertaining to the GRLWEAP Data
- A.4 Relevant Information Pertaining to the Case Data
- A.5 Relevant Information Pertaining to Database PD2000
- A.6 Relevant Information Pertaining to Database PD/LTT2000
- D.1 Summary of Design Capacity Comparisons for Three Case History Piles

LIST OF FIGURES

PAGE

- 2.1 Design Basis for Spread Footings in Sand (After Peck et al., 1974)
- 2.2 An Illustration of Probability Density Functions for Load Effect and Resistance (Goble, 1999)
- 2.3 An Illustration of a Probability Density Function for R-Q (Goble, 1999)
- 2.4 An Illustration of a Probability Density Function for $\ln(R/Q)$ (Goble, 1999)
- 2.5 Resistance vs. Displacement at the Top of the Pile
- 2.6 Smith's model simulating the hammer-pile-soil system for use with the one-dimensional wave equation (Smith, 1960)
- 2.7 Soil-pile model (left) and the corresponding elasto-plastic soil resistance-displacement relationship (after Smith, 1960)
- 2.8 Notations used for Model of Pile and Soil in TEPWAP Analysis (Paikowsky, 1982)
- 2.9 Flow Chart Describing the analysis process using TEPWAP (Paikowsky, 1982)
- 2.10 Force and Velocity Traces Showing Two Impact Peaks Indicative of Driving in Soils Capable of Large Deformations
- 2.11 Deep Foundation Design Process
- 3.1 Force and Velocity ($V*EA/C$) traces of pile-case 1, a steel HP12x74 that needed a force correction
- 3.2 Digitized force and velocity multiplied by the impedance (EA/C) traces for pile-case 190 used for input into INTEGRATE
- 3.3 INTEGRATE output of pile-case 190 showing the back-calculated J_c value and the Energy Approach prediction

- 3.4 Example of the pile identification information of pile-case 189 used as input for the TEPWAP analysis
- 3.5 Example of the soil and pile properties used along the pile elements of pile-case 189 as input for the TEPWAP analysis
- 3.6 Measured force and velocity multiplied by the impedance (EA/C) traces of pile-case 189 used by the TEPWAP analysis
- 3.7 Comparison between measured force near the top of pile-case 189 and the calculated force from the TEPWAP analysis
- 3.8 Summary of the final results from TEPWAP analysis performed on pile-case 189
- 4.1 Load-settlement curve of pile-case 344 with the elastic compression line inclined at 20 degrees
- 4.2 Load-settlement curve of pile-case 344 with a scale that does not consider the elastic compression of the pile
- 4.3 Load-settlement curve of pile-case 344 with the elastic compression line inclined at approximately 20 degrees
- 4.4 Load-settlement data plotted on a logarithmic graph for pile-case 344 to determine the failure load according to DeBeer's method
- 4.5 Histogram and frequency distributions of K_{SD} for 186 PD/LT2000 pile-cases in all types of soils
- 4.6 K_{SD} values vs. Pile Diameter for all PD/LT2000 pile-cases, all types of soils
- 4.7 Histogram and frequency distributions of K_{SC} for 193 PD/LT2000 pile-cases in all types of soils
- 4.8 K_{SC} values vs. Pile Diameter for all PD/LT2000 pile-cases, all types of soils
- 4.9 Histogram and frequency distributions of K_{ST} for 161 PD/LT2000 pile-cases in all types of soils
- 4.10 K_{ST} values vs. Pile Diameter for all PD/LT2000 pile-cases, all types of soils

- 4.11 Histogram and frequency distributions of K_{SL} for 90 PD/LT2000 pile-cases in all types of soils
- 4.12 K_{SL} values vs. Pile Diameter for all PD/LT2000 pile-cases, all types of soils
- 4.13 Histogram and frequency distributions of K_{SB} for 187 PD/LT2000 pile-cases in all types of soils
- 4.14 K_{SB} values vs. Pile Diameter for all PD/LT2000 pile-cases, all types of soils
- 4.15 Distribution Function Curves for the Five methods used for analysis of Static Load Test Curves based on 196 piles from PD/LT2000
- 4.16 Histogram and frequency distributions of K_{SD} and K_{SLD} for 30 and 20 PD/LT2000 pile-cases, respectively, in all types of soils
- 4.17 K_{SLD} values vs. Pile Diameter for all large diameter PD/LT2000 pile-cases, all types of soils
- 4.18 Static Pile Load Testing Procedures According to ASTM (after Paikowsky et al., 1999)
- 4.19 Static Pile Load Testing Procedures According to MHD (after Paikowsky et al., 1999)
- 4.20 Comparison of the Short Duration, Slow Maintained and Static Cyclic Load Tests for Test Pile # 2 at the Newbury Site (after Paikowsky et al., 1999)
- 4.21 Comparison of the Short Duration, Slow Maintained and Static Cyclic Load Tests for Test Pile # 3 at the Newbury Site (after Paikowsky et al., 1999)
- 4.22 Comparison of the Short Duration and Slow Maintained Static Load Tests, Reduced for Creep, for Test Pile # 2 at the Newbury Site
- 4.23 Comparison of the Short Duration and Slow Maintained Static Load Tests, Reduced for Creep, for Test Pile # 3 at the Newbury Site
- 4.24 Davisson Capacity vs. Static Cyclic Load Test Capacity for 75 pile-cases from the UMass Lowell / Ukraine Database (after Paikowsky et al., 1999)

- 5.1 Static Load Test Results vs. CAPWAP or TEPWAP predictions for 382 PD/LT2000 pile-cases in all types of soils (AAA)
- 5.2 Static Load Test Results vs. Energy Approach predictions for 378 PD/LT2000 pile-cases in all types of soils (AAA)
- 5.3 Static Load Test Results vs. CAPWAP or TEPWAP predictions for 265 PD/LT2000 pile-cases in sand & silt (AAS)
- 5.4 Static Load Test Results vs. Energy Approach predictions for 260 PD/LT2000 pile-cases in sand & silt (AAS)
- 5.5 Static Load Test Results vs. CAPWAP or TEPWAP predictions for 100 PD/LT2000 pile-cases in clay & till (AAC)
- 5.6 Static Load Test Results vs. Energy Approach predictions for 101 PD/LT2000 pile-cases in clay & till (AAC)
- 5.7 Static Load Test Results vs. CAPWAP or TEPWAP predictions for 15 PD/LT2000 pile-cases in rock (AAR)
- 5.8 Static Load Test Results vs. Energy Approach predictions for 15 PD/LT2000 pile-cases in rock (AAR)
- 5.9 Static Load Test Results vs. CAPWAP or TEPWAP predictions for 377 PD/LT2000 pile-cases in all types of soils (AAA)
- 5.10 Static Load Test Results vs. CAPWAP or TEPWAP predictions for 125 PD/LT2000 pile-cases at EOD in all types of soils (AEA)
- 5.11 Static Load Test Results vs. CAPWAP or TEPWAP predictions for 162 PD/LT2000 pile-cases at BOR(last) in all types of soils (ABA)
- 5.12 Static Load Test Results vs. Energy Approach predictions for 371 PD/LT2000 pile-cases in all types of soils (AAA)
- 5.13 Static Load Test Results vs. Energy Approach predictions for 128 PD/LT2000 pile-cases at EOD in all types of soils (AEA)
- 5.14 Static Load Test Results vs. Energy Approach predictions for 153 PD/LT2000 pile-cases at BOR(last) in all types of soils (ABA)
- 5.15 Static Load Test Results vs. CAPWAP or TEPWAP predictions for 108 PD/LT2000 pile-cases with Blow Count < 16 BP10cm in all types of soils (AAA)

- 5.16 Static Load Test Results vs. CAPWAP or TEPWAP predictions for 274 PD/LT2000 pile-cases with Blow Count ≥ 16 BP10cm in all types of soils (AAA)
- 5.17 Static Load Test Results vs. Energy Approach predictions for 109 PD/LT2000 pile-cases with Blow Count < 16 BP10cm in all types of soils (AAA)
- 5.18 Static Load Test Results vs. Energy Approach predictions for 269 PD/LT2000 pile-cases with Blow Count ≥ 16 BP10cm in all types of soils (AAA)
- 5.19 K_{SW} versus Blow count for all pile-cases in PD/LT2000
- 5.20 K_{SP} versus Blow count for all pile-cases in PD/LT2000
- 5.21 Static Load Test Results vs. CAPWAP or TEPWAP predictions for 250 PD/LT2000 pile-cases with Area Ratio < 350 in all types of soils (AAA)
- 5.22 Static Load Test Results vs. CAPWAP or TEPWAP predictions for 132 PD/LT2000 pile-cases with Area Ratio ≥ 350 in all types of soils (AAA)
- 5.23 Static Load Test Results vs. Energy Approach predictions for 250 PD/LT2000 pile-cases with Area Ratio < 350 in all types of soils (AAA)
- 5.24 Static Load Test Results vs. Energy Approach predictions for 128 PD/LT2000 pile-cases with Area Ratio ≥ 350 in all types of soils (AAA)
- 5.25 K_{SW} versus Area Ratio for all pile-cases in PD/LT2000
- 5.26 K_{SP} versus Area Ratio for all pile-cases in PD/LT2000
- 5.27 K_{SW} versus Area Ratio for 71 PD/LT2000 pile-cases at EOD with Blow Count ≥ 16 BP10cm in all types of soils
- 6.1 Flow Chart Depicting the Various Investigated Dynamic Analyses of Driven Piles
- 6.2 Static Load Test Results vs. GRLWEAP Predictions for 99 pile-cases at EOD provided by GRL Inc., in all types of soils (AEA)

- 6.3 Static Load Test Results vs. GRLWEAP Predictions for 99 pile-cases at BOR provided by GRL Inc., all types of soils (ABA)
- 6.4 Static Load Test Results vs. ENR Equation Capacity for 384 PD/LT2000 pile-cases in all types of soils
- 6.5 Static Load Test Results vs. ENR Equation Capacity with Factor of Safety of 6 for 384 PD/LT2000 pile-cases in all types of soils
- 6.6 Static Load Test Results vs. Gates Dynamic Equation Capacity for 384 PD/LT2000 pile-cases in all types of soils
- 6.7 Static Load Test Results vs. Pile Capacity according to the FHWA Version of the Gates Equation for 384 PD/LT2000 pile-cases in all types of soils
- 6.8 Static Load Test Results vs. Pile Capacity according to the FHWA Version of the Gates Equation for 135 PD/LT2000 EOD pile-cases in all types of soils (AEA)
- 6.9 Static Load Test Results vs. Pile Capacity according to the FHWA Version of the Gates Equation for 159 PD/LT2000 BOR(last) pile-cases in all types of soils (ABA)
- 6.10 Static Load Test Results vs. Pile Capacity according to the FHWA Version of the Gates Equation for 62 PD/LT2000 pile-cases at the EOD with Blow Count < 16 BP10cm in all types of soils (AEA)
- 6.11 Static Load Test Results vs. Pile Capacity according to the FHWA Version of the Gates Equation for 32 PD/LT2000 pile-cases at the BOR(last) with Blow Count < 16 BP10cm in all types of soils (ABA)
- 6.12 Static Load Test Results vs. Pile Capacity according to the FHWA Version of the Gates Equation for 73 PD/LT2000 pile-cases at the EOD with Blow Count ≥ 16 BP10cm in all types of soils (AEA)
- 6.13 Static Load Test Results vs. Pile Capacity according to the FHWA Version of the Gates Equation for 127 PD/LT2000 pile-cases at the BOR(last) with Blow Count ≥ 16 BP10cm in all types of soils (ABA)

- 6.14 Static Load Test Results vs. CAPWAP or TEPWAP predictions for all 377 PD/LT2000 pile-cases at all times and in all types of soils (AAA)
- 6.15 Static Load Test Results vs. CAPWAP or TEPWAP predictions for 125 PD/LT2000 pile-cases at EOD in all types of soils (AEA)
- 6.16 Static Load Test Results vs. CAPWAP or TEPWAP predictions for 162 PD/LT2000 pile-cases at BOR (last) in all types of soils (ABA)
- 6.17 Static Load Test Results vs. CAPWAP or TEPWAP predictions for 54 PD/LT2000 pile-cases at the EOD with Blow Count < 16 BP10cm in all types of soils (AEA)
- 6.18 Static Load Test Results vs. CAPWAP or TEPWAP predictions for 71 PD/LT2000 pile-cases at the EOD with Blow Count ≥ 16 BP10cm in all types of soils (AEA)
- 6.19 Static Load Test Results vs. CAPWAP or TEPWAP predictions for 32 PD/LT2000 pile-cases at the BOR (last) with Blow Count < 16 BP10cm in all types of soils (ABA)
- 6.20 Static Load Test Results vs. CAPWAP or TEPWAP predictions for 130 PD/LT2000 pile-cases at the BOR (last) with Blow Count ≥ 16 BP10cm in all types of soils (ABA)
- 6.21 Static Load Test Results vs. CAPWAP or TEPWAP predictions for 37 PD/LT2000 pile-cases at the EOD with Blow Count < 16 BP10cm and Area Ratio < 350 in all types of soils (AEA)
- 6.22 Static Load Test Results vs. CAPWAP or TEPWAP predictions for 22 PD/LT2000 pile-cases at the EOD with Blow Count < 16 BP10cm and Area Ratio ≥ 350 in all types of soils (AEA)
- 6.23 Static Load Test Results vs. CAPWAP or TEPWAP predictions for 37 PD/LT2000 pile-cases at the EOD with Blow Count ≥ 16 BP10cm and Area Ratio < 350 in all types of soils (AEA)
- 6.24 Static Load Test Results vs. CAPWAP or TEPWAP predictions for 34 PD/LT2000 pile-cases at the EOD with Blow Count ≥ 16 BP10cm and Area Ratio ≥ 350 in all types of soils (AEA)
- 6.25 Static Load Test Results vs. CAPWAP or TEPWAP predictions for 22 PD/LT2000 pile-cases at the BOR (last) with Blow Count < 16 BP10cm and Area Ratio < 350 in all types of soils (ABA)

- 6.26 Static Load Test Results vs. CAPWAP or TEPWAP predictions for 10 PD/LT2000 pile-cases at the BOR (last) with Blow Count < 16 BP10cm and Area Ratio ≥ 350 in all types of soils (ABA)
- 6.27 Static Load Test Results vs. CAPWAP or TEPWAP predictions for 83 PD/LT2000 pile-cases at the BOR (last) with Blow Count ≥ 16 BP10cm and Area Ratio < 350 in all types of soils (ABA)
- 6.28 Static Load Test Results vs. CAPWAP or TEPWAP predictions for 47 PD/LT2000 pile-cases at the BOR (last) with Blow Count ≥ 16 BP10cm and Area Ratio ≥ 350 in all types of soils (ABA)
- 6.29 Static Load Test Results vs. Energy Approach predictions for 371 PD/LT2000 pile-cases at all times and in all types of soils (AAA)
- 6.30 Static Load Test Results vs. Energy Approach predictions for 128 PD/LT2000 pile-cases at EOD in all types of soils (AEA)
- 6.31 Static Load Test Results vs. Energy Approach predictions for 153 PD/LT2000 pile-cases at BOR(last) in all types of soils (ABA)
- 6.32 Static Load Test Results vs. Energy Approach predictions for 56 PD/LT2000 pile-cases at the EOD with Blow Count < 16 BP10cm in all types of soils (AEA)
- 6.33 Static Load Test Results vs. Energy Approach predictions for 72 PD/LT2000 pile-cases at the EOD with Blow Count ≥ 16 BP10cm in all types of soils (AEA)
- 6.34 Static Load Test Results vs. Energy Approach predictions for 29 PD/LT2000 pile-cases at the BOR (last) with Blow Count < 16 BP10cm in all types of soils (ABA)
- 6.35 Static Load Test Results vs. Energy Approach predictions for 124 PD/LT2000 pile-cases at the BOR (last) with Blow Count ≥ 16 BP10cm in all types of soils (ABA)
- 6.36 Static Load Test Results vs. Energy Approach predictions for 39 PD/LT2000 pile-cases at the EOD with Blow Count < 16 BP10cm and Area Ratio < 350 in all types of soils (AEA)
- 6.37 Static Load Test Results vs. Energy Approach predictions for 23 PD/LT2000 pile-cases at the EOD with Blow Count < 16 BP10cm and Area Ratio ≥ 350 in all types of soils (AEA)

- 6.38 Static Load Test Results vs. Energy Approach predictions for 39 PD/LT2000 pile-cases at the EOD with Blow Count ≥ 16 BP10cm and Area Ratio < 350 in all types of soils (AEA)
- 6.39 Static Load Test Results vs. Energy Approach predictions for 34 PD/LT2000 pile-cases at the EOD with Blow Count ≥ 16 BP10cm and Area Ratio ≥ 350 in all types of soils (AEA)
- 6.40 Static Load Test Results vs. Energy Approach predictions for 19 PD/LT2000 pile-cases at the BOR (last) with Blow Count < 16 BP10cm and Area Ratio < 350 in all types of soils (ABA)
- 6.41 Static Load Test Results vs. Energy Approach predictions for 10 PD/LT2000 pile-cases at the BOR (last) with Blow Count < 16 BP10cm and Area Ratio ≥ 350 in all types of soils (ABA)
- 6.42 Static Load Test Results vs. Energy Approach predictions for 82 PD/LT2000 pile-cases at the BOR (last) with Blow Count ≥ 16 BP10cm and Area Ratio < 350 in all types of soils (ABA)
- 6.43 Static Load Test Results vs. Energy Approach predictions for 42 PD/LT2000 pile-cases at the BOR (last) with Blow Count ≥ 16 BP10cm and Area Ratio ≥ 350 in all types of soils (ABA)
- 6.44 Tip Soil Conditions versus calculated Case Damping Coefficient, J_c , based on Static Load Test Results for 290 PD/LT pile-cases (Paikowsky et al., 1994)
- 6.45 Static Load Test Results vs. the Case Method (RMX) predictions for 77 pile-cases with varied J_c in all types of soils, (data obtained from the University of Florida)
- 6.46 Static Load Test Results vs. the Case Method (RMX) predictions for 40 EOD pile-cases with varied J_c in all types of soils, (data obtained from the University of Florida)
- 6.47 Static Load Test Results vs. the Case Method (RMX) predictions for 40 BOR pile-cases with varied J_c in all types of soils, (data obtained from the University of Florida)
- 7.1 CAPWAP (last Restrike) Predictions vs. Energy Approach (EOD) Predictions for 83 PD/LT2000 pile-cases in all types of soils (AAA)

- 7.2 CAPWAP (last Restrike) Predictions vs. Energy Approach (EOD)
Predictions for 47 PD/LT2000 pile-cases with Blow Count < 16
BP10cm in all types of soils (AAA)
- 7.3 CAPWAP (last Restrike) Predictions vs. Energy Approach (EOD)
Predictions for 36 PD/LT2000 pile-cases with Blow Count \geq 16
BP10cm in all types of soils (AAA)
- 7.4 CAPWAP (last Restrike) Predictions vs. Energy Approach (EOD)
Predictions for 228 PD2000 pile-cases in all soil types
- 7.5 CAPWAP (last Restrike) Predictions vs. Energy Approach (EOD)
Predictions for 43 PD2000 pile-cases with Blow Count < 16
BP10cm in all soil types
- 7.6 CAPWAP (last Restrike) Predictions vs. Energy Approach (EOD)
Predictions for 185 PD2000 pile-cases with Blow Count \geq 16
BP10cm in all soil types
- 7.7 CAPWAP (last Restrike) Predictions vs. Energy Approach (EOD)
Predictions for 90 PD2000 pile-cases in clay & till
- 7.8 CAPWAP (last Restrike) Predictions vs. Energy Approach (EOD)
Predictions for 15 PD2000 pile-cases with Blow Count < 16
BP10cm in clay & till
- 7.9 CAPWAP (last Restrike) Predictions vs. Energy Approach (EOD)
Predictions for 75 PD2000 pile-cases with Blow Count \geq 16
BP10cm in clay & till
- 7.10 CAPWAP (last Restrike) Predictions vs. Energy Approach (EOD)
Predictions for 42 PD2000 pile-cases in sand & silt
- 7.11 CAPWAP (last Restrike) Predictions vs. Energy Approach (EOD)
Predictions for 16 PD2000 pile-cases with Blow Count < 16
BP10cm in sand & silt
- 7.12 CAPWAP (last Restrike) Predictions vs. Energy Approach (EOD)
Predictions for 26 PD2000 pile-cases with Blow Count \geq 16
BP10cm in sand & silt
- 7.13 CAPWAP (last Restrike) Predictions vs. Energy Approach (EOD)
Predictions for 94 PD2000 pile-cases in rock

- 7.14 CAPWAP (last Restrike) Predictions vs. Energy Approach (EOD)
Predictions for 12 PD2000 pile-cases with Blow Count < 16
BP10cm in rock
- 7.15 CAPWAP (last Restrike) Predictions vs. Energy Approach (EOD)
Predictions for 82 PD2000 pile-cases with Blow Count ≥ 16
BP10cm in rock
- 7.16 CAPWAP (last Restrike) Predictions vs. Energy Approach (EOD)
Predictions for 72 PD2000 pile-cases with Boston Blue Clay
- 7.17 CAPWAP (last Restrike) Predictions vs. Energy Approach (EOD)
Predictions for 8 PD2000 pile-cases with Blow Count < 16
BP10cm with Boston Blue Clay
- 7.18 CAPWAP (last Restrike) Predictions vs. Energy Approach (EOD)
Predictions for 64 PD2000 pile-cases with Blow Count ≥ 16
BP10cm with Boston Blue Clay
- 8.1 Kws values vs. log – Time for PD/LTT2000 pile-cases with multiple
Restrikes with the majority of the skin friction coming from the clay
layers (Paikowsky et al., 1995)
- 8.2 Kws values vs. log - Time for PD/LTT2000 pile-cases with multiple
Restrikes partially in clay
- 9.1 Resistance Factor Analysis Flow Chart (after Ayyub & Assakkaf, 1999,
Ayyub et al., 2000)
- 9.2 Calculated Resistance Factors for the CAPWAP and Energy Approach
General Cases showing the Influence of the Dead to Live Load Ratio
- 9.3 Flow Chart Presenting the Sub-Grouping of the Dynamic Analyses
According to the Controlling Parameters and the Resulting Statistical
Parameters for a Normal Distribution Function
- 9.4 Histogram and frequency distributions of K_{sw} for 377 PD/LT2000
CAPWAP pile-cases in all types of soils (AAA)
- 9.5 Histogram and frequency distributions of K_{sw} for 125 PD/LT2000
CAPWAP pile-cases at the EOD in all types of soils (AEA)

- 9.6 Histogram and frequency distributions of K_{SW} for 37 PD/LT2000 CAPWAP pile-cases at the EOD with Blow Counts < 16 BP10cm and Area Ratio < 350 in all types of soils (AEA)
- 9.7 Histogram and frequency distributions of K_{SW} for 162 PD/LT2000 CAPWAP pile-cases at the BOR(last) in all types of soils (ABA)
- 9.8 Histogram and frequency distributions of K_{SP} for 371 PD/LT2000 Energy Approach pile-cases in all types of soils (AAA)
- 9.9 Histogram and frequency distributions of K_{SP} for 128 PD/LT2000 Energy Approach pile-cases at the EOD in all types of soils (AEA)
- 9.10 Histogram and frequency distributions of K_{SP} for 39 PD/LT2000 Energy Approach pile-cases at the EOD with Blow Counts < 16 BP10cm and Area Ratio < 350 in all types of soils (AEA)
- 9.11 Histogram and frequency distributions of K_{SP} for 153 PD/LT2000 Energy Approach pile-cases at the BOR(last) in all types of soils (ABA)
- 9.12 Histogram and frequency distributions of K_{SENR} (without FS = 6) for 384 PD/LT2000 pile-cases in all types of soils (AAA)
- 9.13 Histogram and frequency distributions of K_{SENR} (with FS = 6) for 384 PD/LT2000 pile-cases in all types of soils (AAA)
- 9.14 Histogram and frequency distributions of K_{SG} for 384 PD/LT2000 pile-cases in all types of soils (AAA)
- 9.15 Histogram and frequency distributions of K_{SFG} for 384 PD/LT2000 pile-cases in all types of soils (AAA)
- 9.16 Histogram and frequency distributions of K_{SFG} for 135 PD/LT2000 pile-cases at the EOD in all types of soils (AAA)
- 9.17 Histogram and frequency distributions of K_{SFG} for 62 PD/LT2000 pile-cases at the EOD with Blow Counts < 16 BP10cm in all types of soils (AAA)
- 9.18 Histogram and frequency distributions of K_{SWP} for 99 PD/LT2000 GRLWEAP pile-cases at the EOD in all types of soils (AAA)
- 9.19 Histogram and frequency distributions of K_{SWP} for 99 PD/LT2000 GRLWEAP pile-cases at the BOR in all types of soils (AAA)

- B.1 Blow Count vs. Depth for Newbury Site
- B.2 Vertical Effective Stress vs. Depth for Newbury Site
- B.3 Tip Resistance vs. Depth, CPT's, Newbury Site
- B.4 Side Resistance vs. Depth, CPT's, Newbury Site
- B.5 Load vs. Deflection Curve, Compression Test, Newbury Site
- B.6 Load vs. Deflection Curve, Tension Test, Newbury Site
- D.1 Soil Profile and SPT values with Depth for the Newbury Site
- D.2 CPT data, f_s profile with Depth for the Newbury Site
- D.3 CPT data, q_c profile with Depth for the Newbury Site
- D.4 Soil Profile and SPT values with Depth for the Choctawhatchee River Project
- D.5 CPT data, f_s profile with Depth for the Choctawhatchee River Project
- D.6 CPT data, q_c profile with Depth for the Choctawhatchee River Project

CHAPTER 1

INTRODUCTION

1.1 OVERVIEW

An ongoing project supported by the USA National Cooperative Highway Research Program (NCHRP) under the Transportation Research Board (TRB) of the National Academy of Science (NAS), is aimed at rewriting AASHTO Deep Foundation Specifications for the year 2001. The AASHTO specifications are traditionally observed on all federally aided projects and generally viewed as a national code of US Highway practice, hence influencing the construction of all the deep foundations of highway bridges throughout the USA.

The new code is based on Load and Resistance Factor Design (LRFD) principles with resistance factors obtained from probabilistic analysis of data. A large database (PD/LT2000) is the backbone of the dynamic methods' performance evaluation. This database originated with the work presented by Paikowsky et al. (1994), Paikowsky and LaBelle (1994), and additional information acquired since.

A summary and careful evaluation of the large database is presented, detailing the performance of various dynamic methods when compared to static load testing to failure. The parameters that control the accuracy of the dynamic predictions are

analyzed, suggesting the importance of certain mechanisms associated with the pile penetration and the dynamic simulations.

The controlling parameters and the statistical analyses are then utilized for the development of resistance factors to be recommended for the new specifications.

1.2 BACKGROUND

National Cooperative Highway Research Program, project, NCHRP 24-17, "LRFD Deep Foundations Design" was initiated to: (i) Provide recommended revisions to the driven pile and drilled shaft portions of section 10 of AASHTO Specifications and (ii) Provide a detailed procedure for calibrating deep foundation resistance factors. The current AASHTO specifications as well as other existing codes based on Load and Resistance Factor Design (LRFD) principles were developed using insufficient data, hence they utilized mostly back-calculated factors. The main challenges of the project are therefore: (a) Compilation of large, high quality databases and (b) Framework for a procedure and data management to enable: (i) LRFD parameter evaluation and (ii) Future updates. These challenges include two requirements: (i) Organization of the factors following the design - construction - quality control sequence (i.e. independence in resistance factors according to the chronological stage and the evaluation procedure) and (ii) Overcome the generic difficulties of applying the LRFD methodology to geotechnical applications, i.e. incorporation of indirect variability, (e.g. site or parameters interpretation), judgment (e.g. previous experience), and other similar factors.

The project team, headed by Samuel G. Paikowsky, is divided into three major groups dealing with static analyses (University of Florida), probabilistic approaches and structural analyses (University of Maryland), and dynamic analyses (University of Massachusetts at Lowell). The present paper provides a background for design methodologies and the LRFD. Database PD/LT2000 is presented and analyzed. The state of practice and the selected dynamic methods are described, followed by an initial evaluation of the signal matching technique and examination of the controlling parameters. The performance of the dynamic methods is then provided, categorized according to the controlling parameters. The obtained results are used for the development of resistance factors to be recommended for the new specifications.

1.3 MANUSCRIPT LAYOUT

The following is a brief description of the contents of each chapter:

CHAPTER 2 presents a summary of the Working Stress Design (WSD) method and the Load and Resistance Factor Design (LRFD) method as they apply to Geotechnical Engineering. Also presented is a review of the recommended LRFD factors based on many international codes.

CHAPTER 3 describes the processes that were used in compiling the data presented in each of the databases for use in the present research. The actual data is presented in Appendix A but will be discussed in detail in this chapter.

CHAPTER 4 discusses the methodology used to determine which method of determining pile capacity based on the static load test curve should be used as the

reference static capacity when comparing the dynamic pile capacity predictions to the static load test results.

CHAPTER 5 presents the analysis used to determine the controlling parameters that effect the pile capacity based on the dynamic methods. The controlling parameters that are analyzed are the effects of soil type, time of driving (EOD – End Of Driving and BOR – Beginning Of Restrike), and the soil inertia effects (driving resistance and pile type).

CHAPTER 6 discusses the performance of the dynamic methods during the construction phase. The performance of the dynamic methods is analyzed for two cases, with dynamic measurements and without dynamic measurements. The analysis that is presented for the case without dynamic measurements includes the WEAP analysis and the dynamic equations. The CAPWAP method, the Energy Approach method, and the Case Method are all presented in the case with dynamic measurements.

CHAPTER 7 presents a comparison between the Energy Approach pile capacity predictions at the EOD and the CAPWAP pile capacity predictions at the BOR based on the controlling parameters presented in Chapter 5.

CHAPTER 8 briefly discusses the effects of pile capacity gain with time due to pore water pressure dissipation.

CHAPTER 9 presents the methodology that was used to calculate the proposed resistance factors for the dynamic methods, which are also presented in this chapter.

CHAPTER 10 discusses the difficulty of comparing the pile capacities determined using the LRFD method with the proposed resistance factors and previous codes. A comparison is made although it is limited due to the discussed difficulties.

CHAPTER 11 presents the conclusions of the present research.

CHAPTER 2

BACKGROUND

2.1 STATE OF STRESS METHODOLOGY

2.1.1 Overview

Working Stress Design (WSD) method, also called the Allowable Stress Design (ASD) method, has been the traditional design basis in Civil Engineering since it was first introduced in the early 1800's. In the 1950's the continued demand for a more economical design of piles brought about the use of Limit States or Limit States Design (LSD). The two types of limit states are the Ultimate Limit State (ULS) and the Serviceability Limit State. Both limit states must be satisfied when using the Limit States Design method. A more detailed description of the two limit states is presented in the following sections. The material in the overview section is based primarily on Becker (1996) and Allen (1994).

The latest method of pile design to be introduced is the Load and Resistance Factor Design (LRFD) method. This method relies heavily on the use of limit states and reliability theory, which is also known as Reliability Based Design (RBD). The reliability theory introduced the determination of factors of safety based on the combined probability of load and resistance looking into the probability of pile failure or the probability of failure of the soil in bearing capacity. The most recent methods of pile design, i.e. LRFD, RBD and LSD can be utilized in a simple manner for a specific site or can be involved as need

be for more complex subsurface conditions. “Regardless of the design philosophy and approach used, the basic design criteria is that the capacity or resistance of the system must be greater than the demand or loads on the system for an acceptable or required level of safety” (Becker, 1996).

2.1.2 The Working Stress Design (WSD) Method

The Working Stress Design (WSD) method is aimed to ensure that when the structure is subjected to the “working” or service applied load; the induced stresses are less than the allowable stresses. The WSD method combines all of the uncertainties in the loads and the soil and accounts for them by using one factor of safety, FS. The design loads, Q, consist of the actual forces estimated to be applied directly to the structure, (Becker, 1996 and Withiam et al. 1998). This can be seen in the fundamental equation that governs WSD:

$$Q \leq Q_{all} = \frac{R_n}{FS} = \frac{Q_{ult}}{FS} \quad (2.1)$$

Where: Q = Design load (kN)
 Q_{all} = Allowable design load (kN)
 $R_n = Q_{ult}$ = Ultimate geotechnical pile force resistance of a pile; and
 FS = Factor of safety

Equation 2.1 can also be written as:

$$\frac{R_n}{FS} \geq \sum Q_i \quad (2.2)$$

Where: R_n = Nominal resistance
 $\sum Q_i$ = Load effect
 FS = Factor of safety

The factor of safety is commonly defined as the ratio of the resistance of the structure (R_n) to the load effects (Q) acting on the structure. The determination of the factor of safety is the most difficult part of the design process. Rearranging Equation 2.2 to solve for the factor of safety (FS), the factor of safety can be expressed as a variable or a constant. The factor of safety mostly depends on the level of control that was used in the design and construction phases. For example, if data from a subsurface exploration program is used, a static analysis is completed, and the results from a wave equation analysis are used to determine the ultimate geotechnical resistance of a pile, then the factor of safety must be greater than 2.75, (see Table 2.1). On the other hand, if more reliable methods for determining the ultimate geotechnical resistance of a pile are used, then a reduced factor of safety can be incorporated. "Traditionally, the factor of safety is applied to the resistance as in Equation 2.2. This method gives sensible results when material strength (resistance) represents the greatest uncertainty in design", (Simpson et al., 1981).

Table 2.1, after AASHTO (1997), provides different factors of safety that are used in the analysis of the ultimate geotechnical resistance of a piles. Table 2.1 relates to both design and construction phases and demonstrates that the WSD method allows the factor of safety to vary depending on the level of control. When a more reliable and consistent level of Construction Control is used, a smaller factor of safety can be implemented, leading to a more economical construction.

Equation 2.1 can also be rewritten for structural design based on allowable stress as:

$$\Sigma Q \leq \sigma_{all} A = P_{all} \quad (2.3)$$

Where: σ_{all} = Allowable axial stress in pile (kPa)
 P_{all} = Allowable axial structural capacity (kN); and
 A = Cross sectional area of pile (m²)

Equation 2.3 can be rewritten so as to solve for the allowable axial load, P_{all} :

$$P_{all} = \Sigma \sigma_{all} A \quad (2.4)$$

The applied load is limited by the maximum allowable load. The maximum allowable axial load that can be applied to the pile is obtained from Equation 2.4 by multiplying the allowable stress (see Table 2.2) by the cross sectional area of the pile.

In addition to axial geotechnical and structural capacity evaluation, the design of driven piles by WSD requires evaluations of pile displacements and comparisons with deformation criteria using the following:

$$\delta_i \leq \delta_n \quad (2.5)$$

Where: δ_i = Estimated displacement (mm); and
 δ_n = Tolerable displacement established by designer (mm).

The tolerable displacement is typically associated with the structure type and function, for example the allowable displacement of bridges depends on the structural concept (e.g., simply supported versus integral), and the type of supports that are being utilized for the superstructure.

2.1.3 The Limit States

Limit states are defined as the conditions under which a structure or its component members can no longer perform their intended functions. Whenever a structure or a part of it fails to satisfy one of its designated operational criteria, it is

said to have reached a limit state. The two limit states that are checked in the design of piles are the Ultimate Limit State (ULS) or Strength Limit State and the Serviceability Limit State (SLS).

Ultimate limit states pertain to structural safety and define dangerous conditions. The ULS involves the collapsing of the structure and in relation to piles the event under which the ultimate bearing capacity of the soil is exceeded. Serviceability limit states (SLS) represent the conditions that affect the function or service requirements (performance) of the structure under expected service/ working loads. These conditions can include excessive deformations and settlement or deterioration of the structure pile(s). "The serviceability limit states are checked by using a partial factor of unity on all specified or characteristic service loads and load effects", (Meyerhof, 1994).

In WSD, the term "allowable soil bearing pressure" may be controlled by either bearing capacity (ULS) or by settlement (SLS) considerations. WSD implicitly accounts for these two key limit states, but generally does not do so explicitly, (Becker, 1996). In other words, the WSD method does not require that the calculations be made to check both of the limit states, instead, there are charts that are used to show whether the designer needs to check the ultimate limit state or the serviceability limit state. Figure 2.1 is an example of the type of charts used for determining whether the design of spread footings is controlled by bearing capacity or settlement. The LRFD method for piles checks both the ultimate and serviceability

limit states explicitly. The calculations are done to insure that the design criteria have been met for both; the ultimate and serviceability limit states.

When limit states were first introduced, the design method encountered opposition because designers and engineers thought it to be too complicated for practice. The limit state design calculations and analyses can however range from estimates and back-of-the envelope calculations to three-dimensional finite element analysis. "Simple calculations that capture the essence of the behavior and promote thinking are preferred for preliminary design and checking, rather than complex computer programs", (Allen, 1994). Regardless of the complexity of the analysis and calculations, all limit states designs are carried out to satisfy the following criteria:

Ultimate limit state (ULS):

$$\text{Factored resistance} \geq \text{Factored load effects} \quad (2.6)$$

Serviceability limit state (SLS):

$$\text{Deformation} \leq \text{Tolerable deformation to remain serviceable} \quad (2.7)$$

(Becker, 1996)

According to Duncan et al. (1989) the SLS have a higher probability of occurrence than the ULS. The allowable settlement of a structure generally controls the design of shallow foundations rather than the ultimate bearing capacity of the soil. "In geotechnical design, a serviceability condition or settlement criterion frequently constitutes the primary limit state. Accordingly, the design would be based on specific SLS; the ULS would be checked subsequently", (Becker, 1996). By and large, the design of deep foundations is controlled by the ultimate limit state. However, O'Neill

(1999) suggests that this is not always the case, deep foundations need to be checked for settlement, therefore, it is required that their serviceability limit state be evaluated as well. Examples for such cases are group settlement of driven piles in certain soil/pile stiffness conditions and large diameter drilled shafts (say 4m), especially when carrying a large portion of the load at the toe of the deep foundation.

2.2 LOAD AND RESISTANCE FACTOR DESIGN (LRFD) METHOD

2.2.1 Reliability Based Design - History and Background

The design of a pile depends upon predicted loads and the pile's capacity to resist them. Both loads and capacity have various types and levels of uncertainty that needs to be considered in design. Historically, engineering design methods and processes have compensated for these uncertainties by experience and subjective judgment. However, with reliability technology, these uncertainties can be considered more quantitatively. Specifically, the use of probability-based design criteria, or safety check expressions, has the promise of producing better-engineered designs with consistent levels of reliability. The load and resistance factor design (LRFD) format is a commonly used reliability-based format in many areas. It consists of the requirement that a factored (reduced) strength of a pile is larger than a linear combination of factored (magnified) load effects. In this format, load effects are increased, and strength is reduced, by multiplying the corresponding characteristic (nominal) values with factors, which are called strength (resistance) and load factors, respectively. The characteristic value of some quantity is the value that is used in current design practice, and it is usually equal to a certain percentile of the probability

distribution of that quantity. The load and strength factors are different for each type of load and strength. The higher the uncertainty associated with a load, the higher the corresponding load factor. These factors are determined probabilistically so that they correspond to a prescribed safety level. It is also common to consider two classes of performance functions that correspond to ultimate strength (or simply strength) and serviceability requirements. The difference between working stress and LRFD formats is that the latter use different safety factors for each type of load and strength thereby allowing to take into account uncertainties in load and strength, and to scale their characteristic values accordingly in the design equation. Working stress formats cannot do that as it uses only one safety factor. Relative to a conventional factor of safety code, a probability-based design code has the promise of producing a better engineered structure. Experience has shown that adoption of a probability-based design code has resulted in significant savings in materials and/or an efficient use of materials. Reliability improvements are still under evaluation even though, the new codes are specifically designed so that the reliability is equal to or better than the older codes they replace. Experiences are not well documented at this time, but designers have commented that, relative to the conventional working stress code, the new AISC-LRFD (American Institute of Steel Construction) requirements are saving anywhere from 5% to 30% steel weight, with about 10% being typical. This may or may not be the case for other industries. Specific benefits in pile design include the following:

1. A more efficiently balanced design results in weight/cost savings and/or an improvement of reliability.
2. Uncertainties in the design are treated more rationally and rigorously.

3. An improved perspective of the overall design and construction process (substructure and superstructure) and the development of probability-based design procedures can stimulate advances in pile analysis and design.
4. The codes become a living document that can be easily revised to include new information reflecting statistical data on design factors.
5. The partial safety factor format used herein also provides a framework for extrapolating existing design practice to new foundation concepts and materials where experience is limited.

The concept of using the probability of failure as a criterion for structural design can be credited to the Russians N. F. Khotsialov and N. S. Streletskii who presented the idea in the late 1920s. The first exposition of the idea in the United States was made by A. M. Freudenthal in 1947. Considerable interest by many industries and engineering disciplines has evolved in developing reliability-based design codes. Reliability-based design codes using an LRFD format were developed using first-order second-moment reliability methods (Ayyub and McCuen 1997) such as by the American Institute of Steel Construction (AISC 1994, and Galambos and Ravindra 1978) and by the American Concrete Institute (ACI). An effort was made by the National Standards Institute (ANSI) to develop probability-based load criteria for buildings (Ellingwood et al. 1982a and 1982b) that was published as ASCE 7-93 (ASCE 1993). The American Petroleum Institute (API) extrapolated LRFD technology for its use in fixed offshore platforms (API 1989, and Moses (1985 and 1986)). Other efforts which provide excellent and comprehensive summaries of implementation of modern probabilistic design theory into design codes include those of Siu, et al. (1975) for the National Building Code of Canada (1977), Ellingwood et

al. (1980) for the National Bureau of Standards, and the CIRIA 63 (1977) report. Ayyub et al. (1998) provide details on LRFD rules for naval surface ship structures developed for the US Navy.

The AASHTO LRFD Bridge Design and Construction Specifications (1994) as a result of NCHRP Project 12-33 by Nowak, (1993) provide design guidance for girders. To enable uniform treatment of all bridge subsystems, this study is required to provide design and construction specifications for piles that are consistent with the AASHTO LRFD Bridge Design and Construction Specifications.

2.2.2 Development of the LRFD Method for General Geotechnical Engineering

The following section is based on a comprehensive review presented by Goble, (1999). Figure 2.2 shows the probability density functions for the load effect, Q , and the resistance, R . (The term load effect refers to the load calculated to act on the particular element in question). The area where the two curves overlap illustrates the region where the load effect is greater than the resistance indicating a scenario where there is a high probability of failure. The shaded area under the probability density function for the resistance represents the probability that the resistance will have a value between a and b .

In probability-based design, a prescribed value that is based on previous case histories similar to the one that is being evaluated is chosen for the probability of failure. The probability of the failure for the specific case in question should be greater than the prescribed value.

In Figure 2.2, the probability density function for the load effect is narrower than for the resistance because the loads are usually much more deterministic than the resistances. In terms of probability and statistics, the load effect has much less variability than the resistance. This is measured by the standard deviation, which is not shown in Figure 2.2. \bar{Q} and \bar{R} as shown in the Figure 2.2 are the mean of the load effect and the mean of the resistance, respectively. The strength or resistance that is determined by the method, which is being used to evaluate the case history, is the nominal strength, R_n , shown in Figure 2.2. This strength is not necessarily the mean strength or resistance. When the probability density functions are available for both the load effect and the resistance the probability of failure can be determined directly.

There are two different approaches that are used to determine the probability of failure and they are illustrated in Figure 2.3 and Figure 2.4. Figure 2.3 shows the combined probability density function of $R-Q$. The probability of failure is the shaded region that is shown to the left of the y-axis. The principle of the method is that $\bar{R} - \bar{Q}$ needs to be larger than $R-Q = 0$. Usually the mean value is used to define the reference value and the distance of the mean above zero is taken as a multiple of the standard deviation of the distribution. The multiple of the standard deviation, shown in Figure 2.3 as β , is called the reliability index. Figure 2.4 shows the second approach for determining the probability of failure and this is done by using the natural log of R/Q ($\ln R/Q$). The limiting condition is when $\ln R/Q = 0$ or when $R/Q = 1$. The reliability index is defined the same for both approaches. The reliability

index is defined in greater detail in a later section entitled *LRFD Calibration using Reliability Theory*.

2.2.3 The Principle of the LRFD Method for Deep Foundations

The Load and Resistance Factor Design (LRFD) method takes into consideration the variability in the loads placed on the structure by applying a load factor (γ). A resistance factor (ϕ) is applied to the resistance to take into account its variability. According to O'Neill (1995), the intent of this design method is to separate uncertainties in loading from uncertainties in resistance and to assure a prescribed margin of safety. The load and resistance factors are present in the fundamental LRFD equations used for checking the resistance and deformation of the supporting soil and rock materials as well as the structural components. Following the 1999 AASHTO LRFD Highway Bridge Design Specifications:

For the strength limit states:

$$R_r = \phi R_n \geq \eta \sum \gamma_i Q_i \quad (2.8)$$

and for the serviceability limit states:

$$\eta \sum \gamma_i \delta_i \leq \phi \delta_n \quad (2.9)$$

Where: $\eta = \eta_D \eta_R \eta_I > 0.95 \quad (2.10)$

- η = Factors to account for effects of ductility (η_D), redundancy (η_R), and operational importance (η_I) (dimensionless)
- γ_i = Load factor (dimensionless);
- Q_i = Force effect, stress or stress resultant (F or F/A);
- ϕ = Resistance factor (dimensionless);
- R_n = Ultimate or nominal resistance (F or F/A);
- R_r = Factored resistance (F or F/A);
- δ_i = Estimated displacement (L); and

δ_n = Tolerable displacement (L).

The method for determining the ultimate geotechnical resistance (R_n) of a single pile is basically the same for both, the LRFD and WSD methods. The difference between the methods is the resistance factors used in the LRFD method. The ultimate axial geotechnical resistance of piles subjected to axial loading, R_n is:

$$R_n = Q_{ult} = Q_p + Q_s \quad (2.11)$$

And the factored axial geotechnical resistance, Q_R is:

$$Q_R = R_r = Q_{ult} = \phi_{qp}Q_p + \phi_{ps}Q_s \quad (2.12)$$

For which:

$$Q_p = q_p A_p \quad (2.13)$$

$$Q_s = q_s A_s \quad (2.14)$$

Where: ϕ_{qp}, ϕ_{qs} = Resistance factors based on Barker et al. (1991), see Table 2.3
 Q_p, Q_s = Ultimate pile tip and side resistance
 q_p, q_s = Unit tip and side resistance
 A_p, A_s = Area of pile tip and side surface

(AASHTO, 1998)

The reduction multiplier factor λ_v as shown in Table 2.3 is to account for the level of field capacity verification. As an example, a piles capacity is calculated using the SPT-method for a site where the pile has end bearing and friction in sand, for which the corresponding resistance factor is $0.45\lambda_v$. If the ENR equation is used to verify the calculated capacity without stress wave measurements during driving the

corresponding reduction multiplier factor is 0.80, which results in a resistance factor of 0.36.

Various procedures can be used to determine the ultimate axial capacity of driven piles. Whenever using a design method, the resistance factor that is associated with (calibrated to) that particular design procedure, must be used. For example; when using the AASHTO LRFD Specification, only those methods referred to in Table 2.3, for which the calibrated ϕ -factors have been developed, can be used (Withiam et al., 1998). The methods commonly used in practice today are briefly described below:

- Static Methods of Analysis
 - α – method - A semi-empirical, total stress static method of analysis for estimating the ultimate unit side resistance, q_s , and the ultimate unit tip resistance, q_p , as a function of the undrained shear strength, S_u , of cohesive soil (Drewry et al., 1977)
 - β – method - a semi-empirical, effective stress method of analysis for estimating q_s and q_p in soil as a function of the effective overburden pressure (Burland, 1973)
 - λ – method - A semi-empirical, effective stress method of analysis for estimating q_s in soil as a function of the passive effective lateral earth pressure (Vijayvergiva and Focht, 1972)
 - End-Bearing Pile on Rock - Semi-empirical method (Canadian Geotechnical Society, 1992) for estimating q_p as a function of the uniaxial compressive strength of the rock, c , and the spacing of discontinuities
- In-Situ Methods of Analysis
 - SPT-method - Semi-empirical developed by Meyerhof (1976) which correlates q_s with the SPT blow count for cohesionless soils
 - CPT-method - Semi-empirical method developed by Nottingham and Schmertmann (1975) which correlates q_s and q_p with CPT results for cohesionless soils

- Methods Based on Field Testing of Pile
 - Dynamic Measurements - Methods based on data obtained during pile driving for estimating total load capacity based on monitored performance of driven piles and wave equation analyses. Several methods fall under this category, among the field methods: (a) the Case method (see Goble et al., 1970 and Goble et al., 1975) and (b) the Energy Approach (Paikowsky et al. 1994) and the office method: CAPWAP (Goble et al., 1970).
 - Static Load Test - A method for determining the total load capacity based on quasi-static loading (ASTM, 1996) representative of pile, load and subsurface conditions expected for the prototype piles (AASHTO, 1997).

The above procedures are used to determine the ultimate axial geotechnical capacity of driven piles in soil using semi-empirical methods and in-situ testing, and for piles bearing on or in rock using semi-empirical methods.

The load factors that are generally used in practice range from 1.25 for structural loads (dead loads) to 1.75 for moving or live loads. AASHTO has conducted an extensive testing program to determine the load factors that should be used for the different types of loads and these general values can be found in the AASHTO manual. When using Equation 2.8 for driven pile foundation design at the Strength Limit States, the following values of η can normally be used:

- $\eta_D = \eta_R = 1.00$; and
- $\eta_I = 1.05$ for structures deemed operationally important, 1.00 for typical structures and 0.95 for relatively less important structures, (AASHTO, 1997)

The determination of the resistance factor (ϕ) is the challenging element when using LRFD. The following sections describe in detail the calibration processes that are used in conjunction with the LRFD method.

2.2.4 Determination of Resistance Factors by Calibration

The resistance factor can be obtained via calibration utilizing the Working Stress Design (WSD) method (in order to achieve approximately the same factor of safety that WSD would provide) or using the Reliability Theory. The Reliability Theory emphasizes the use of probability analysis via statistical parameters. The following sections describe the calibration process using the WSD method and the reliability theory, respectively.

a) *LRFD Calibration via WSD*

Calibration through fitting to the WSD method is used when insufficient statistical data does not allow the performance of a calibration process by optimization, (Withiam et al., 1998). The method of calibrating by fitting with WSD is a simple process in which the fundamental LRFD equation (Eq. 2.8) is divided by the fundamental ASD equation (Eq. 2.2) to determine an equation for the resistance factor (ϕ). If an average value of 1.0 is used for the load modifier η , then the equation obtained is:

$$\phi \geq \frac{\sum \gamma_i Q_i}{FS \sum Q_i} \quad (2.15)$$

If only the dead loads and live loads are considered the equation becomes:

$$\phi = \frac{\gamma_D Q_D + \gamma_L Q_L}{FS(Q_D + Q_L)} \quad (2.16)$$

Dividing both the numerator and denominator by Q_L the equation becomes:

$$\phi = \frac{\frac{\gamma_D Q_D}{Q_L} + \gamma_L}{FS(\frac{Q_D}{Q_L} + 1)} \quad (2.17)$$

Where: ϕ = Resistance factor
 γ_D, γ_L = Load factors for dead and live loads, respectively
 Q_D, Q_L = Force effect for dead and live loads, respectively
 FS = WSD method factor of safety

(After O'Neill, 1995)

Equation 2.17 can be used to determine the resistance factors that need to be used in the LRFD equations in order to obtain a factor of safety equal to that of the WSD method. “While the load and resistance factor design method represented by equation 8 as calibrated using Equation 2.17 provides the designer a clearer means of visualizing uncertainty than the lumped factor of safety method, use of the current load and resistance factors are not likely to result in improved design. Such can only occur if the resistance factors are evaluated directly, rather than through calibration with existing factors of safety”, (O'Neill, 1995). Table 2.4 presents values of the resistance factors using Equation 2.17 for factors of safety varying between 1.5 to 4 and average dead and live load factors of 1.25 and 1.75 respectively. The table presents the resistance factors that would be used to obtain a factor of safety of 1.5 to 4.0 (in 0.5 intervals) related to ratios of dead to live load of 1 to 9. The obtained relations provide an important scale of values, but when using the resistance factors calibrated via the WSD in the LRFD equation (2.8) it is no different from using the WSD method.

b) LRFD Calibration using Reliability Theory

Based on Withiam et al. (1998) the resistance factor chosen for a particular limit state must take into account: (i) the variability of the soil and rock properties, (ii) the reliability of the equations used for predicting resistance, (iii) the quality of the construction workmanship, (iv) the extent of soil exploration (little versus extensive), and (v) the consequence of failure. In order to take into account the inherent uncertainties of the resistance and load in a consistent manner, first-order, second-moment principles can be used to establish Equation 2.18 from Equation 2.8 with $\eta = 1$:

$$\phi = \frac{\lambda_R (\sum \gamma_i Q_i) \sqrt{\frac{1 + COV_Q^2}{1 + COV_R^2}}}{Q \exp\{\beta_T \sqrt{\ln[(1 + COV_R^2)(1 + COV_Q^2)]}\}} \quad (2.18)$$

Where: λ_R = Overall bias for resistance
 COV_Q = Coefficient of variation of the load
 COV_R = Coefficient of variation of the resistance
 β_T = Target reliability index

When just the dead and live loads are considered Equation 2.18 can be written as:

$$\phi = \frac{\lambda_R (\frac{\gamma_D Q_D}{Q_L} + \gamma_L) \sqrt{\frac{(1 + COV_{QD}^2 + COV_{QL}^2)}{(1 + COV_R^2)}}}{(\frac{\lambda_{QD} Q_D}{Q_L} + \lambda_{QL}) \exp\{\beta_T \sqrt{\ln[(1 + COV_R^2)(1 + COV_{QD}^2 + COV_{QL}^2)]}\}} \quad (2.19)$$

Where: $\lambda_{QD}, \lambda_{QL}$ = Overall bias for the dead and live loads
 COV_{QD}, COV_{QL} = Coefficient of variation of the dead and live loads

(After Barker et. al., 1991)

Table 2.5 summarizes the calculated resistance factors for five different methods of Axial Pile Capacity. The five methods are the α -method, the β -method, the λ -method, the CPT method and the SPT method. Both the α -method and the λ -method show a Type I and a Type II method of axial pile capacity estimation. Type I refers to soils with undrained shear strength, S_u , less than 50 kPa and Type II refers to soils with S_u greater than 50 kPa. The calculations allow the examination of the way the pile's length affects the value of the resistance factor. The presented results indicate that the resistance factor does not vary much for the different pile lengths. The selected values of resistance factors for the five methods shown here are the recommended resistance factors in the LRFD AASHTO Specification for the different methods. The selected values of ϕ are all relatively close to the average value of ϕ that was determined, the exception being the ϕ factor selected for the β -method. According to Withiam et al. (1998) the ϕ factor for the β -method chosen in the LRFD AASHTO Specification is much lower than the average value based on the limited number of reported cases where the method had been used in conjunction with performance testing, and the engineering judgment of the code developers.

The following paragraphs describe in detail the different statistical parameters that are being used in the calculation of the resistance factor when calibrating utilizing the reliability theory. The coefficient of variation, bias factors, and the reliability index and its correlation with the probability of failure are described.

The coefficient of variation, COV, is a dimensionless measure of the variability of the data. The COV is defined as the standard deviation (σ) divided by the mean value (\bar{x}):

$$\text{coefficient of variation, } COV = \frac{\sigma}{\bar{x}} \quad (2.20)$$

Where, for a given set of data, $x_i = (x_1, x_2, \dots, x_N)$ the mean (\bar{x}) is defined by:

$$\bar{x} = \sum \frac{x_i}{N} \quad (2.21)$$

for which N is equal to the total number of data values and the standard deviation (σ) is determined by:

$$\sigma = \sqrt{\frac{\sum (x_i - \bar{x})^2}{(N - 1)}} \quad (2.22)$$

The COV expresses the magnitude of the variability as a percentage or fraction of the mean value. There can be many different types of coefficients of variation including those related to the dead load, live load and the piles resistance.

The bias factor, (λ), is defined as the ratio of the measured resistance to the predicted or nominal resistance. In equation form it is:

$$\text{Bias factor, } \lambda = \frac{R_m}{R_n} \quad (2.23)$$

Where: R_m = Measured resistance; and
 R_n = Predicted (nominal) resistance.

Bias factors are used for live loads, dead loads and the resistance, as can be seen in Equation 2.19.

The term β , the reliability index, is also determined using different statistical parameters and is defined as the number of standard deviations, ζ_g , between the mean value, \bar{g} , and the origin (i.e., $\beta = \bar{g}/\zeta_g$). Using this definition the reliability index, β , can be expressed as:

$$\beta = \frac{\ln \left[\left(\frac{R}{Q} \right) \sqrt{\frac{(1 + COV_Q^2)}{(1 + COV_R^2)}} \right]}{\sqrt{\ln \left[\frac{(1 + COV_R^2)}{(1 + COV_Q^2)} \right]}} \quad (2.24)$$

For further detail on the derivation of this equation the reader is referred to the National Highway Institute Reference Manual and Participant Workbook, NHI Course No. 13068 by Withiam et al. (1998).

There is a correlation between the reliability index and the probability of failure for the pile or structure, presented in the following two equations:

$$p_f = 460e^{(-4.3\beta)} \quad 2 < \beta < 6 \quad (2.25)$$

$$\beta = \frac{\ln\left(\frac{460}{p_f}\right)}{4.3} \quad 10^{-1} < p_f < 10^{-9} \quad (2.26)$$

(Rosenblueth and Esteva, 1972)

Table 2.6a presents the normal PDF approximation generated using the two equations above. Table 2.6a can be used to: (i) determine the target reliability index for a prescribed maximum probability of failure in a design, and (ii) determine the probability of failure for a certain target reliability index. Rosenbleuth and Estava

base this relationship used by Withiam, Barker et al. (1991) and others, on an approximation. Unfortunately, although they say that the approximation pertains to log normal distributions (because they use the mean of the logs and the standard deviation of the logs to calculate), the approximation is not so good below β of about 2.5. Table 2.6b prepared by Greg Baecher provides the comparison between the "exact" numbers to the approximation and suggests significant errors, especially in our zone of interest ($\beta = 2$ to 3). The "exact" numbers will be used in the presented research.

c) *Reliability-Based LRFD Using Failure Point*

The First-Order Reliability Method (FORM) is conveniently used to assess the reliability of a pile according to a specified limit state. FORM also provides a means for calculating the partial safety factors ϕ and γ_i for a specified target reliability level β_0 . The simplicity of the FORM approach stems from the fact that this method, beside the requirement that the distribution types must be known, requires only first and second moments of the distribution, namely, the mean values and standard deviations of the respective random variables.

In design practice, there are usually two types of limit states: ultimate limit states and serviceability limit state. Each can be represented by a performance function of the form,

$$g(\mathbf{X}) = g(X_1, X_2, \dots, X_n) \quad (2.27)$$

in which \mathbf{X} is a vector of basic random variables (X_1, X_2, \dots, X_n) for strengths and loads. The performance function $g(\mathbf{X})$ is sometimes called the limit state function. It

relates the random variables for the limit-state of interest. The limit state is defined when $g(\mathbf{X}) = 0$, and therefore, failure occurs when $g(\mathbf{X}) < 0$. The reliability index β is defined as the shortest distance from the origin to the failure surface at the most probable failure point (MPFP).

As indicated earlier, the basic approach to develop a reliability-based strength standard is to determine the relative reliability of designs based on current practice. Therefore, reliability assessments of existing designs are needed to estimate representative values of the reliability index β . FORM is well suited to perform such a reliability assessment.

The following are computational steps for determining β using FORM:

1. Assume a design point x_i^* and obtain its corresponding point, $x_i'^*$ in a reduced coordinate system using the normalizing transformation:

$$x_i'^* = \frac{x_i^* - \mu_{X_i}}{\sigma_{X_i}} \quad (2.28)$$

Where: μ_{X_i} = mean value of the basic random variable X_i , and
 σ_{X_i} = standard deviation of the basic random variable.

The mean values of the basic random variables can be used as initial guesses for the design points, to be later solved for iteratively. The notation x^* and x'^* is used respectively for the design point in the regular coordinates and in the reduced (normalized) coordinates.

2. Evaluate the equivalent normal distributions for the non-normal basic random variables at the design point using the following equations:

$$\mu_X^N = x^* - \Phi^{-1}(F_X(x^*))\sigma_X^N \quad (2.29)$$

and

$$\sigma_X^N = \frac{\left(\Phi^{-1}(F_X(x^*))\right)}{f_X(x^*)} \quad (2.30)$$

where μ_X^N = mean of the equivalent normal distribution, σ_X^N = standard deviation of the equivalent normal distribution, $F_X(x^*)$ = original cumulative distribution function (CDF) of X_i evaluated at the design point, $f_X(x^*)$ = original probability density function (PDF) of X_i evaluated at the design point, $\Phi(\cdot)$ = CDF of the standard normal distribution, and $\phi(\cdot)$ = PDF of the standard normal distribution.

3. Set $x_i^* = -\alpha_i^* \beta$, in which the α_i^* are direction cosines. Compute the directional cosines (α_i^* , $i = 1, 2, \dots, n$) using the equations:

$$\alpha_i^* = \frac{\left(\frac{\partial g}{\partial x_i}\right)_*}{\sqrt{\sum_{i=1}^n \left(\frac{\partial g}{\partial x_i}\right)_*^2}} \quad \text{for } i = 1, 2, \dots, n \quad (2.31)$$

Where:

$$\left(\frac{\partial g}{\partial x_i}\right)_* = \left(\frac{\partial g}{\partial x_i}\right) \sigma_{X_i}^N \quad (2.32)$$

4. With α_i^* , $\mu_{X_i}^N$, and $\sigma_{X_i}^N$ now known, the following equation can be solved for β :

$$g[(\mu_{x_1}^N - \alpha_{x_1}^* \sigma_{x_1}^N \beta), \dots, (\mu_{x_n}^N - \alpha_{x_n}^* \sigma_{x_n}^N \beta)] = 0 \quad (2.33)$$

5. Using the β obtained from step 4, a new design point is obtained from:

$$x_i^* = \mu_{x_i}^N - \alpha_i^* \sigma_{x_i}^N \beta \quad (2.34)$$

6. Repeat steps 1 to 5 until a convergence of β is achieved. This reliability index is the shortest distance to the failure surface from the origin in the reduced coordinates.

The first-order reliability method (FORM) can be used to estimate partial safety factors such as those found in the design format. At the failure point $(R^*, L_1^*, \dots, L_n^*)$, the limit state is given by

$$g = R^* - L_1^* - \dots - L_n^* = 0 \quad (2.35)$$

or, in a general form

$$g(X) = g(x_1^*, x_2^*, \dots, x_n^*) = 0 \quad (2.36)$$

For given target reliability index β_0 , probability distributions and statistics (means and standard deviations) of the load effects, and the coefficient of variation of strength, the mean value of the resistance, and the partial safety factors can be determined by the iterative solution as previously presented. The mean value of the resistance and the design point can be used to compute the mean required partial design safety factors as,

$$\phi = \frac{R^*}{\mu_R} \quad (2.37)$$

$$\gamma_i = \frac{L_i^*}{\mu_{L_i}} \quad (2.38)$$

In developing design code provisions for piles, it is sometimes necessary to follow the current design practice to insure consistent levels of reliability over various pile types. Calibrations of existing design codes are needed to make the new design formats as simple as possible and to put them in a form that is familiar to users or designers. Moreover, the partial safety factors for the new codes provide consistent levels of safety or reliability. For a given reliability index β and probability characteristics for the resistance and load effects, the partial safety factors determined by the FORM approach might be different for different failure modes for the same or differing component. For this reason, calibration of the calculated partial safety factors (PSF's) is important in order to maintain the same values for all loads at different failure modes.

Normally, the calibration is performed on the strength factor ϕ for a given set of load factors. The following algorithm can be used to accomplish this objective:

1. For a given value of the reliability index β , probability distributions and statistics of the load variables, and the coefficient of variation for the strength, compute the mean of the strength R using the first-order reliability method as outlined previously.

2. With the mean value for R computed in step 1, the partial safety factor ϕ can be revised as follows:

$$\phi = \frac{\sum_{i=1}^n \gamma_i \mu_{L_i}}{\mu_R} \quad (2.39)$$

Where μ_{L_i} and μ_R are the mean values of the loads and strength variables, respectively and $\gamma_i, i = 1, 2, \dots, n$, are the given set of load factors.

2.2.5 The Use of Limit States in LRFD

The design of driven pile foundations using LRFD requires evaluation of pile suitability at various strength limit states and the service I limit state (Withiam et al., 1997). The service I limit state is defined as the load combination relating to the normal operational use of the bridge with a 56-mph (90 km/hr) wind. For driven piles supporting bridges, two different strength limit states can be used depending on the type of loading that is applied to the pile(s). If the loading is designed for vehicles without wind then the strength I limit state is used and if the loading is a permit vehicle loading then the strength II limit state is used. Table 2.7 shows the design considerations that must be taken into account for piles that are designed at the different limit states. There are many different types of ultimate and serviceability limit states that are used in pile design with the LRFD method.

2.3 THE AVAILABLE AND CHOSEN DYNAMIC METHODS

2.3.1 General

The materials presented in this section are based on the review of the dynamic methods by Paikowsky et al., 1994 and Paikowsky, 1995. Dynamic analyses of piles are methods that predict pile capacity based on behavior during driving. The evaluation of static capacity from pile driving is based on the concept that the driving operation induces failure in the pile-soil system – in other words, a very fast load test is carried out under each blow. There are basically two methods of estimating the ultimate capacity of driven piles on the basis of dynamic driving resistance: pile-driving formulas (i.e., dynamic equations) and wave-equation analysis.

2.3.2 Dynamic Equations

a) *The Basic Principle*

The theoretical equations have been formulated around analyses that evaluate the total resistance of the pile, based on the work done by the pile during penetration. Observations of the hammer's ram stroke and the pile set are used in determining this work done by the hammer and the pile. These theoretical equation formulations assume elasto-plastic force-displacement relations (see figure 2.5). The total work is computed as:

$$W = R_u \left(S + \frac{Q}{2} \right) \quad (2.40)$$

Where: R_u = Yield resistance
 S = Pile set, denoting the permanent displacement (plastic deformation) of the pile under each hammer blow

Q = Quake, denoting the elastic deformation of the pile-soil system.

b) Engineering News Record Equation

The Engineering New Record (ENR) Equation was developed for timber piles using a drop hammer with a factor of safety of approximately 6. Since the equation was first introduced it has been modified for different types of hammers and piles. The ENR equation is based on Wellington (1892). The following overview is also presented in Bowles, 1996 as follows (length units of s and h must be the same):

(2.41)

Where:

P_u	=	Ultimate pile capacity (F)
e_h	=	Hammer efficiency
W_r	=	Weight of ram (for double-acting hammers include weight of casing) (F)
h	=	Height of fall of ram (L)
s	=	Amount of point penetration per blow (L)
C	=	A single factor which contains all the elastic compression, $C=25$ mm or 1 inch for drop hammers and $C=2.54$ mm or 0.1 inch for all other hammers

When using the ENR equation with SI units the weight of the ram should be in kN and the set and height of fall of the ram need to be expressed in millimeters. When expressing the ultimate pile capacity in English units the weight of the ram can be in tons, kips or pounds, but the set and height of fall of the ram need to be expressed in inches.

c) Gates Equation

The Gates equation is empirical in nature (using sound relations of energy and resistance) based on 130 static load tests to failure. Details are not provided but it is

reasonable to assume that the data set represents different pile and soil conditions.

Recommended F.S. = 3, (Gates, 1957). The equation is presented as follows:

$$B = \frac{1}{7} \times \sqrt{E} \times (1 - \log s) \quad (2.42)$$

Where:

B	=	Safe load-carrying capacity of pile, in tons
E	=	Gross energy of pile-driving hammer, in ft-lb, times 75 percent for drop hammers, and 85 percent for all other hammers unless otherwise stated by manufacturer
s	=	Set per blow, in inches

d) FHWA modified Gates Equation

The FHWA version of the Gates equation was derived through corrections suggested by Olsen and Flaate, 1967 (using a small database) and then further simplified by Dick Cheney of the FHWA (DiMaggio, 2000). The FHWA modified Gates equation is presented as follows:

$$R_u = 1.75 \times \sqrt{E} \times \log 10N - 100 \quad (2.43)$$

Where:

R_u	=	Ultimate capacity (tons)
E	=	Gross energy of pile hammer, ft-lb 0.75E for drop hammers 0.85E for all other hammers
N	=	Number of blows per inch

2.3.3 The Wave Equation

a) Formulation and Principles

Issacs (1931) concluded that many pile-driving formulas were incorrectly based on Newtonian mechanics for the pile/hammer impact and he became the first person to suggest the use of an analysis based on the one-dimensional wave equation instead. This proposed solution assumed that the toe of the pile was fixed and that no

side resistance existed (Lowery et al., 1969). Fox (1932) proposed an exact solution to Issacs formulation; however, without the aid of computers, many simplified assumptions were necessary because of the complexity of his solution (Smith, 1960).

Stress-wave propagation in a pile during driving can be described by the following one-dimensional wave equation (after Paikowsky and Whitman, 1990) modified to include frictional resistance along the pile:

$$E_p \frac{\partial^2 u}{\partial x^2} - \frac{S_p}{A_p} f_s = \rho_p \frac{\partial^2 u}{\partial t^2} \quad (2.44)$$

Where: E_p, ρ_p = Modulus of elasticity and unit density of the pile material
 $u(x,t)$ = Longitudinal displacement of infinitesimal segment
 f_s = Frictional stress along the pile
 A_p, S_p = Pile area and circumference, respectively

The displacement (u) causes strains in each pile element that can be used to calculate pile stresses as well as the resistance developed in the soil. This displacement can be determined with respect to time and location. The friction stresses (f_s) are generated by the movement of the pile. When the pile is subjected to free-wave motion ($f_s = 0$), the stress propagation equation becomes the familiar one-dimensional wave equation:

$$c^2 \frac{\partial^2 u}{\partial x^2} = \frac{\partial^2 u}{\partial t^2} \quad (2.45)$$

Where: $c = \sqrt{\frac{E_p}{\rho_p}} \quad (2.46)$

c = Wavespeed of the pile material
 E_p = Modulus of elasticity of the pile
 ρ_p = Density of the pile material

Among the assumptions implicit in the development of the one-dimensional wave equation are prismatic shape and homogeneity. Also, it is assumed that under loading, plane parallel cross sections remain plane and parallel and that a uniform distribution of stress exists across each plane. The assumption of uniaxial stress does not include uniaxial strain and, therefore, lateral expansions and contractions (Poisson's effect) arise from the axial stresses associated with lateral inertia (Graff, 1975). The additional friction term (after Paikowsky and Whitman, 1990) was included under the assumption that the soil is stationary (having no inertia effects), and the action of the friction forces does not violate any of the previous assumptions.

The so-called "wave equation methods" are based on a numerical solution of the one-dimensional wave equation. The numerical solution utilizes mathematical models for the pile and pile-soil system. When the one-dimensional wave equation numerical solution is used for pre-driving analysis, the driving system is also modeled.

In 1960, Smith developed a numerical model to simulate the dynamic behavior of the hammer-pile-soil system during driving. This model is represented by a series of discrete masses and springs used for solving the one-dimensional wave equation (see Figure 2.6). The soil resistance is modeled via a spring, slider, and dashpot, which represent the static and dynamic soil resistances (see Figure 2.7). The elastoplastic soil model is employed for the static soil resistance in Smith's solution. The distance traveled by the pile toe during the elastic deformation of the soil is represented by the soil quake (Smith, 1960). As the elastic limit of the soil is reached (represented by the slider in sequence with the spring), plastic deformation takes

place. The plastic deformation, or irreversible compression of the soil, is denoted by the permanent set of the soil (see Figure 2.7).

According to this model, point A represents the ground resistance buildup to the ultimate resistance, R_u . Plastic failure occurs as the ground resistance has reached its maximum and the adjacent pile segment displaces, plastically, to point B. Unloading the soil at point B produces an elastic rebound, equal to the quake, to point C. The permanent set is, therefore, equal to the distance OC, which, in turn, is equal to distance AB (Smith, 1960). The static soil resistance-displacement relationship, as presented by Smith (1960), is modeled by a spring (K_s) and a slider, where W represents the mass of the pile element.

The dynamic component of the soil's resistance is assumed to viscous (soiltype related) and is, therefore, velocity-dependent. This dynamic resistance is modeled by a dashpot (J) parallel to the spring (see Figure 2.7). The resisting soil force (R_{max}) developed under each hammer blow is a combination of the static and dynamic soil resistances:

$$R_{max} = R_s + R_d \quad (2.47)$$

Where:

R_{max}	=	Total resistance
R_s	=	Static resistance
R_d	=	Dynamic resistance

The wave equation formulation is used in two general ways: pre-driving analysis and post-driving analysis.

b) Pre-Driving Analysis

The so-called "wave equation analysis" utilizes the one-dimensional wave equation to predict dynamic pile behavior before construction and models the pile-soil system and the driving system (i.e., the hammer, cushion, and capblock), as suggested by Smith (1960). This computerized solution is used for the evaluation of the penetration resistance (i.e., blow count) and the driving stresses in the modeled pile under given conditions. The static capacity is then determined by relating the computed static capacity-penetration resistance relationship for a certain energy rating to observed dynamic resistances during driving. Such analyses enable engineers to determine a suitable pile-site-equipment combination.

c) Post-Driving Analysis - CAPWAP/TEPWAP

Post-driving analyses utilize the measured force signal (calculated from strain readings) and the measured velocity signal (integrated from acceleration readings) obtained near the pile top during driving. These analyses model the pile-soil system as shown in Figure 2.8 with the element denoted as number 3 representing the point of measurement. The velocity signal is used as a boundary condition at that point while varying the parameters describing the soil resistance in order to match the calculated and measured force signals. These parameters include the side and tip quake, side and tip damping, the pile shaft resistance, and the pile tip resistance. Additional parameters may be used to describe soil resistance and rebound ratio for unloading different from that of loading. The process is described in the form of a flow chart in Figure 2.9. The subscripts *msd.* and *cal.* denote measured and calculated values,

respectively. Iterations are performed by changing the soil-model variables for each pile element in contact with the soil until the best match between the force signals is obtained. The results of these analyses are assumed to represent the actual distribution of the ultimate static capacity of the pile.

This procedure was first suggested by Goble, Likins, and Rausche (1970), utilizing the computer program CAPWAP. Similar analyses were developed by others (see Paikowsky, 1982 and Paikowsky and Whitman, 1989) utilizing the program code TEPWAP.

2.3.4 The Case Method

a) General

The Case method (see Goble et al., 1970 and Rausche et al., 1975), is a simple field procedure used by the PDA to estimate pile capacities. Analysis by the Case method is based on the assumptions of a uniform elastic pile, ideal plastic soil behavior, and a simplified wave propagation formulation. Employed are force and velocity measurements taken at the pile top and a correlation between the soil at the pile tip to a damping parameter.

b) The Case Method Equation

The Case method calculates the total soil resistance (*RTL*) active during pile-driving, using the following equation:

$$RTL = \frac{\left[F(T1) + F\left(T1 + \frac{2L}{C}\right) \right]}{2} + \left[v(T1) - v\left(T1 + \frac{2L}{C}\right) \right] \times \frac{MC}{2L} \quad (2.48)$$

Where:	$F(T1)$	=	Measured force at the time $T1$
	$F(T1+2L/C)$	=	Measured force at the time $T1$ plus $2L/C$
	$v(T1)$	=	Measured velocity at the time $T1$
	$v(T1 + 2L/C)$	=	Measured velocity at the time $T1$ plus $2L/C$
	L, M	=	Length and mass of the pile, respectively
	C	=	Speed of wave propagation in the pile

Different variations of the Case method have been developed taking $T1$ as the time of impact or modified to include a time delay constant allowing higher RTL values to be obtained. The time $T1$ is defined, in equation form, as:

$$T1 = TP + \delta \quad (2.49)$$

Where:	TP	=	Time of the impact peak
	δ	=	Time delay

The time delay is required in soils capable of large deformations before achieving full resistance (see Figure 2.10). A time delay is also used in situations where the hammer impact is uneven (PDA Manual, 1999).

The total resistance calculated is a combination of the static resistance (S) which is displacement-dependent, and the dynamic resistance (D) which is velocitydependent. Therefore, the total resistance (Goble et al., 1975) is:

$$RTL = S + D \quad (2.50)$$

Several factors that influence the pile-soil system must be considered when the total predicted resistance is evaluated. These factors include the damping coefficient, time-dependent soil strength changes, and refusal driving when the soil's resistance is not fully mobilized under a single hammer blow.

c) Case Damping Coefficient

The dynamic resistance (D) is considered to be viscous in nature, hence, a function of the velocity at the pile toe (V_{toe}) and a damping constant (J) where:

$$D = J \times V_{toe} \quad (2.51)$$

By applying the wave propagation theory, the pile toe velocity can be calculated as a function of the velocity at the pile top (Goble et al., 1975):

$$V_{toe} = 2V_{top} - \frac{L}{MC} RTL \quad (2.52)$$

Where:

L	=	Pile length
M	=	Pile mass
C	=	Wave speed of the pile material
R	=	Total resistance
V_{top}	=	Velocity at pile top

V_{top} is taken as the pile top velocity at the time TL .

According to Goble et al. (1975), remolding effects cause the majority of the damping resistance to be concentrated near the pile tip. Consequently, the damping constant is determined according to the soil type at the pile tip. In most cases, the damping constant (J) is proportional to the pile properties (EA/C) and, therefore, is represented by a dimensionless coefficient (J_c) using the following equation:

$$J = J_c \frac{EA}{C} \quad (2.53)$$

The recommended values for J_c are based on soil type. These recommended values can be found in the PDA Manual.

d) Case Method Variations

Variations of the Case method have evolved for adopting the analysis to different driving situations and soil types. The variations are similar in that they all begin with the initial total resistance prediction (*RTL*) of equation 2.48. Five distinct methods are used to employ the predicted *RTL*: Damping Factor Method (RSP), the Maximum Resistance Method (RMX), the Minimum Resistance Method (RMN), the Unloading Method (RSU), and the Automatic Method (RAU), PDA Manual (1999).

The Damping Factor Method (RSP) uses the standard Case method equation for normal driving conditions. The method utilizes damping constants empirically derived from static load tests.

The Maximum Resistance Method (RMX) is useful for short rise time impacts or large soil quakes where the full toe resistance is not activated by the time the stress wave first reaches the pile toe. RMX is often helpful for displacement piles with large end bearing. RX# can be used for $J = 0.6$ (i.e., RX6 is RMX with $J_c = 0.6$). With a fixed $2L/C$, time T_1 is varied from T_p to $T_p + 30$ msec to search for the maximum resistance RMX. This method is advantageous for large displacement piles with substantial end bearing (PDA Manual, 1999).

The minimum capacity (RMN) is determined using the tip reflection time. This method can be used with confidence if the blow count is less than 131 blows per meter (PDA Manual, 1999).

For long piles with high frictional resistance, the measured velocity can become negative before a reflection from the tip is observed at T_2 . Under such

conditions, the upper portion of the pile experiences decreasing displacement or rebounding. This results in an unloading of the upper soil layers resistance and the computed capacities are under-predicted. The Unloading Method (RSU) compensates for this by calculating the total friction in the upper unloading layers from the force velocity difference.

The Automatic Method computes the capacity (RAU) for the first time where the computed pile toe velocity (V_{toe}) is zero. This method, originally proposed by Goble et al. (1967), does not select a damping coefficient because damping must be zero when V_{toe} is zero; therefore, the resistance at this time is completely static. This method provides an exact solution for the end bearing for piles with no skin friction and is recommended for use on piles with very little frictional resistance.

2.3.5 The Energy Approach

This review of the Energy Approach method was taken from Paikowsky and Stenersen (2000). The Energy Approach uses basic energy relations in conjunction with dynamic measurements to determine pile capacity; the concept was presented by Paikowsky (1982) and was examined on a limited scale by Paikowsky and Chernauskas (1992). Extensive studies of the Energy Approach method were carried out by Paikowsky et al. (1994), and Paikowsky and LaBelle (1994). The underlying concept of this approach is the energy balance between the total energy delivered to the pile and the work done by the pile/soil system. The basic Energy Approach equation is:

$$R_u = \frac{E_{max}}{Set + \frac{(D_{max} - Set)}{2}} \quad (2.54)$$

Where:

- R_u = Maximum pile resistance
- E_{max} = Measured maximum energy delivered to the pile
- D_{max} = Measured maximum pile top displacement
- Set = permanent displacement of the pile at the end of the analyzed blow, or 1/measured blow count

For further details regarding the Energy Approach method see Paikowsky et al. (1994) and Paikowsky (1995).

2.4 REVIEW OF RECOMMENDED LRFD FACTORS FOR PILE DESIGN

2.4.1 Resistance Factors Recommended by AASHTO

Table 2.3 presents the recommended resistance factors (ϕ) AASHTO (1998), related to the methods employed for determining the ultimate axial pile capacity, described earlier. The resistance factors shown in Table 2.3 are for the ultimate bearing resistance of single piles and are additionally multiplied by a factor λ_v as specified in the table. This factor is accounting for the method that was used to control the pile's installation and to verify the pile's capacity during or after driving.

2.4.2 Resistance Factors for Dynamic Load Testing using the Case Method

The majority of the piles installed by the Florida Department of Transportation (FDOT) require dynamic load testing using Pile Driving Analyzer (PDA) monitoring. The FDOT Standard Specifications for Road and Bridge Construction Section A455 recommends that a factor of safety of 2.5 be used for all dynamic pile capacity evaluations based on the PDA. The piles are generally monitored throughout the entire driving but the static capacity is usually evaluated for the end of driving (EOD)

and beginning of restrike (BOR) cases only. McVay et al. (1998) stated that the pile bearing capacity for the EOD case is generally underestimated when compared with the static load test results due to the freezing (set-up) effect with time. This will result in a low probability of failure for the Case method EOD case. The Case method BOR analysis usually gives a prediction that is closer to the static load test results because at the time of the restrike sufficient time has passed to allow for set-up (freezing effects) to occur. Therefore, the Case method BOR analysis will generally result in a higher probability of failure.

The dead and live load factors that are recommended in the AASHTO LRFD Bridge Design Specification (1994) are 1.25 and 1.75, respectively. Barker et al., (1991) recommended the following values be used for the bias factors for dead and live loads 1.05 and 1.15, respectively and for the coefficients of variation for dead and live loads 0.1 and 0.18, respectively. Resistance factors based on the Case method using the maximum resistance method predictions were predominantly for piles driven in Florida and were analyzed and reported by McVay et al. (1998). The pile-cases that were provided by McVay are related to different damping factors. The influence of this damping factor on the predicted static capacity depends on the reflected wave from the pile's tip, and hence on the driving resistance. It needs to be noted that because of the different damping factors that were used the presented data is not entirely reliable. Table 2.8 shows the back-calculated reliability index for a WSD factor of safety of 2.5 and the statistical parameters defined above. The reliability indices for the Case method EOD and BOR cases ranged from 3.04 to 3.14 and from

2.40 to 2.50, respectively, for dead to live load ratios from 1 to 9. The reliability analysis showed that the medians of the reliability index for the Case method EOD and BOR cases are 3.09 and 2.45, respectively. These values relate to a probability of failure of approximately 7.8×10^{-4} and 1.2×10^{-2} , respectively.

Table 2.9 shows the resistance factors that were calculated for both the Case method EOD and BOR cases for target reliability indices of 2.0, 2.5, 3.0 and dead to live load ratios from 1 to 9. Using the target reliability index of 2.5 as an example, the resistance factors ranged from 0.70 to 0.63 for the Case method EOD analysis and from 0.55 to 0.50 for the Case method BOR analysis. From Table 2.4 it can be seen that for a factor of safety of 2.5 and calibrating directly with the WSD the resistance factors ranged from 0.60 to 0.52 for dead to live load ratios from 1 to 9. As a general rule, the dead to live load ratios are in the order of 2 to 4 for the majority of highway bridges. Based on the results of the calibration by reliability analysis and ASD fitting in conjunction with the engineering judgements, a resistance factor of 0.65 is selected for using the Case method EOD condition of dynamic load test to estimate the axial compression capacity of driven pile, and 0.55 for the Case method BOR condition (McVay et al., 1998).

Table 2.8 shows the bias factor for the BOR case as 1.052, which indicates that for the average BOR condition an accurate prediction of the pile capacity is provided. The bias factor for the EOD condition was calculated as 1.552, which indicates that the Case method EOD analysis underestimates the pile capacity. A higher resistance factor was calculated for the EOD condition as compared with the BOR condition,

0.65 and 0.55, respectively. A higher risk is posed when using the Case method BOR condition than when using the Case method EOD condition because of the high uncertainty of the pile freeze effect. As a result, the recommendation by McVay et al., 1998 is that for the general procedure of piling control, the Case method EOD condition be used with a resistance factor of 0.65. The Case method BOR condition can be used with a resistance factor of 0.55 in special cases where the pile freeze effect is well documented.

2.4.3 International LRFD Codes

a) Australian Standard, Piling-Design and Installation

A review of the "Australian Standard, Piling-Design and Installation" (1995) is provided by Goble (1999). Table 2.10 presents the resistance factors recommended in the Australian Standard and Table 2.11 is used to determine the final value of the resistance factor to be used from the recommended range of resistance factors given in Table 2.10. In traditional structural design specifications, a nominal value is given and the value used is based primarily on engineering judgement and cannot exceed the nominal value. The Australian Standard is therefore a unique code providing a guide for assessing which resistance factor to use for piles. It is noted that no recommendations are given in regard to the dynamic measurements for the use of EOD or BOR and the method by which the resistance factors were generated is not provided in the code.

b) 1992 AUSTROADS Bridge Design Code

Table 2.12 presents the resistance factors specified by AUSTROADS (1992) for different methods used to determine the axial pile capacity. The range of resistance factors in Table 2.12 is quite large and the resistance factor that is provided for the static load test is larger than those provided by other modern codes. No explanation as to how the resistance factors were obtained is given in the specification. Goble (1999) states that the resistance factors were probably calibrated via the WSD method.

c) Eurocode 7, Geotechnical Design

Given in this section is the method that is used to determine the ultimate axial geotechnical resistance using Eurocode 7 (1993) and its partial factors (γ). Eurocode 7 uses the LRFD method of design with one major difference, the factors used for the resistance are greater than unity and the resistances are divided by the Eurocode partial factors. Eurocode 7 also uses different symbols to describe the different terms in the resistance equations. The design bearing resistance, R_{cd} , of a pile shall be found from:

$$R_{cd} = R_{bd} + R_{sd} \quad (2.55)$$

Where:

$$R_{bd} = \frac{R_{bk}}{\gamma_b} \quad (2.56)$$

$$R_{sd} = \frac{R_{sk}}{\gamma_s} \quad (2.57)$$

In which:

$$R_{bk} = q_{bk} A_b, \text{ and} \quad (2.58)$$

$$R_{sk} = \sum q_{sik} A_{si} \quad (2.59)$$

Where the following symbols are used:

R_{bk} and R_{sk}	the characteristic values of the base and shaft resistances
A_b	the nominal plan area of the base of the pile
A_{si}	the nominal surface area of the pile in soil layer I
q_{bk}	the characteristic value of the resistance per unit area of the base
q_{sik}	the characteristic value of the resistance per unit area of the shaft in layer i (Eurocode, 1993)

Table 2.13 provides the equivalent load and resistance factors for Eurocode 7 in comparison with the factors provided by the Canadian Geotechnical Society and AASHTO.

Table 2.14 presents the partial factors for Eurocode 7 that are to be used in Equation 2.55. The partial factors that are to be used are constant and independent of soil types or soil tests that are performed on the piles to check their ultimate capacity.

The comparison between the recommended resistance factors of Eurocode 7, the Canadian Geotechnical Society and AASHTO, (presented in Table 2.13) suggest that the load factors recommended by AASHTO, are more conservative than those of the Canadian Geotechnical Society and Eurocode 7. "It is observed that the AASHTO resistance (ϕ) factors tend to be higher than those for the other codes because they have been calibrated to generally higher load factors (O'Neill, 1995)". Fellenius (1994) reports that foundation engineers espousing LRFD have generally accepted the load factors for the superstructure and have focused on establishing resistance factors. Neither Eurocode 7 nor the Canadian Geotechnical Society provide resistance factors for bored piles. Eurocode 7 does not differentiate between resistances that are

determined using load tests or SPT tests and do not use a different resistance factor for compression and tension load tests.

d) Danish Code of Practice for Foundation Engineers

The Danish Code (see Goble, 1999) is similar to Eurocode 7, where partial factors are used instead of resistance factors. For easy comparison with the AASHTO parameters Table 2.15 presents the inverse of the partial coefficients from the Danish Code. In the code the use of static analysis based on soil properties as well as the use of static load tests to determine the axial pile capacity are discussed. Also discussed in the Danish Code is the Danish Formula for dynamic analysis.

The resistance factors (inverse of the partial coefficients) shown in Table 2.15 were calibrated to provide the same level of safety existing in the current practice and do not rely on actual data and its analysis.

e) Ontario Bridge Code

Table 2.16 presents resistance factors for deep foundations recommended by the Ontario Highway Bridge Code. No differentiation exists between the various static analysis methods and the provided resistance factors seem to be very small compared to those recommended by other codes. No information is given as to the way in which the resistance factors were obtained.

f) Canadian Bridge Code

The Canadian Bridge Code is brief in its design requirements for deep foundations. The three categories that are dealt with for the soil limit state in the Canadian Bridge Code are routine static load testing, dynamic testing and the

geotechnical formula (static analysis). For routine static load tests a resistance factor of 0.5 is to be used while for high-level static load tests a resistance factor of 0.6 is recommended. The two types are defined but only qualitatively. For dynamic load testing a resistance factor of 0.4 is recommended for routine testing and when the analysis is based on parameters obtained from dynamic field measurements a resistance factor of 0.5 is recommended.

In the Canadian Bridge Code the static analysis is defined as the geotechnical formula, the particular formula that is used is not given but whatever formula a designer chooses to use must be approved. When soil properties are used to determine the axial pile capacity such as the cohesion or the friction angle the resistance factors used are 0.5 and 0.8, respectively. The resistance factors presented in Table 2.17, based on pile type, are then multiplied by the pile capacity that was obtained using the soil properties modified by the resistance factors for the particular soil property. The code states that the calculated capacity shall not be greater than EAp/C or the structural nominal resistance, where E is the modulus of elasticity of the pile and C is the velocity of the stress wave propagation. The other two terms, ρ and A , are not defined in the code but represent the density of the pile's material and its average cross-sectional area, respectively. The basis for determining the resistance factors was not provided in the code.

g) Japanese Specifications for Highway Bridges

The Japanese Design Standards are in the process of being revised to a more generically performance based design, such as LRFD, in conformity to other

international design standards. The presented limited review is based on a report entitled "Foundation Design Standards in the World - Toward Performance-Based Design" written by Kusakabe, 1998. The current specifications for highway bridges are based on two design concepts, the allowable stress design method and the ductility method. Three limit states are considered for the allowable stress design: (i) normal conditions, (ii) at the time of a medium scaled earthquake and (iii) during the time of a storm. At the time of a large scaled earthquake the ductility design method is used. The acceptance criterion for a static load test is based on the "Standard for vertical loading of test piles (JGS, 1811)" Japanese Geotechnical Society.

2.4.4 Evaluation of Recommended Resistance Factors

A detailed test pile case history was used to evaluate the AASHTO recommended resistance factors. The relevant calculations and a summary of results are presented in Table 2.18. The test pile is part of a research test program conducted in Newbury, Massachusetts by the Geotechnical Engineering Research Laboratory at the University of Massachusetts - Lowell. Detailed reports about the site and the piles are provided by Paikowsky and Chen, (1998) and Paikowsky and Hajduk, (1999), respectively. The ultimate capacity, Q_{ult} , and the factored axial capacity, Q_R , of the pile were evaluated using the CPT, SPT, static load test results, the traditional methods based on soil properties, and a computer program, Driven 1.0, which is a windows based update to the program S-Pile.

The information presented in Table 2.18 suggests that the factored axial capacity, Q_R , for all methods is relatively equal with the exception of the results from

Driven 1.0. Driven 1.0 uses the Nordlund method to determine the static pile capacity and resulted in conservative values. A resistance factor of 0.55 was used for Driven 1.0 based on a recommendation by Withiam et al. (1998).

The designated pile capacities in Table 2.18 under the category "traditional methods" refer to calculations using soil properties to evaluate the skin friction and end bearing resistance of a pile. The designated ultimate loads under this category are an average of the ultimate loads based on a combination of many different methods. The subsurface profile for test pile # 2 consists of both sand and clay layers. For the clay layers the designated skin resistance is the average of the one obtained using the α and the λ -methods. An average of the skin resistance found using four different methods was used as the designated skin resistance for each sand layer (refer to Appendix B for details). The methods that were used are the General Values after Mansur and Hunter (1970), the API (1989) charts, the McClelland method (McClelland et al., 1969), and Meyerhof's method using the SPT values (Meyerhof, 1956). The average skin resistance found for each of the layers was summed and this value was used as the total side friction for the pile. To determine the tip resistance the methods used were the General Values after Coyle and Castello (Coyle and Castello, 1981), the API (1989) charts, Meyerhof's method using the SPT values (Meyerhof, 1956), the Vesic-Simplified method (Vesic, 1965), the Vesic-Advanced method (Vesic, 1977), the Berezantzev method (Berezantzev et al., 1961), and the simplified SPT method (Meyerhof, 1976). The values determined by each of these methods were summed and an average was taken and this average value was used as

the tip resistance for the traditional methods. AASHTO (1997) recommends resistance factors for some of these different methods individually, but not for the case when they are combined and averaged, such as was done here. Due to the large variability of the subsurface and for illustration purposes a resistance factor of 0.35 was used. This resistance factor is translated to a factor of safety of approximately three in the Working Stress Design method.

The proposed resistance factors from AASHTO (1997) provide parity between the factored axial pile capacities when the ultimate capacity is calculated using the SPT method, CPT method, and the load test data. The problem arises when the ultimate pile capacity is calculated using the computer programs (Nordlund method), because the proposed resistance factor does not give a factored axial pile capacity that is comparable with that calculated using the other methods. Many more case histories will have to be reviewed before any conclusions can be made whether the resistance factors provided by AASHTO and the FHWA are acceptable for practice today.

2.4.5 Evaluation of Calculated Resistance Factors

Contained in this section are the resistance factors that were calculated by calibrating to the ultimate load that was determined from the static load test results, assuming that the resistance factor for a static load test is 1.00. The calculations were done using the following equations.

$$Q_R = Q_R \quad (2.60)$$

If the resistance factor for end bearing and skin friction are equal then:

$$Q_R = Q_{ult}\phi \quad (2.61)$$

$$Q_{ultA}\phi_A = Q_{ultB}\phi_B \quad (2.62)$$

Where:

- Q_{ultA} = Ultimate Load calculated from static load test results
- Q_{ultB} = Ultimate Load for the method that is being analyzed
- ϕ_A = Resistance Factor for the static load test = 1.0 (assumed)
- ϕ_B = Resistance Factor to be calculated for the method that is being analyzed

Rearranging Equation 2.62 to solve for ϕ_B , Equation 2.63 is obtained:

$$\phi_B = \frac{Q_{ultA}}{Q_{ultB}} \quad (2.63)$$

Equation 2.60 is a fundamental equation that can be written for the LRFD method of driven pile design. The equation basically states that in the theoretical aspect of LRFD the factored axial capacity calculated using the different methods should be equal. Equation 2.62 is obtained by making the assumption that the resistance factors for both the end bearing and skin friction resistances are equal for the different methods being analyzed. Looking at Table 2.3 it can be seen that this is not an entirely incorrect assumption according to the resistance factors as recommended by AASHTO. Equation 2.63 is obtained by rearranging Equation 2.62 to solve for the resistance factor for the method that is being analyzed.

Table 2.19 shows the resistance factors that were calculated for the SPT method, the CPT method, the Nordlund method (Driven 1.0), and the traditional methods using Equation 2.63. Four different test piles were analyzed to calculate an average resistance factor for each of the four different methods shown in the table. These test piles case histories come from two different project sites, the Newbury Site Project in Newbury, Massachusetts and the West Bay Project in Bay County, Florida. These are two projects in

which the soils data and load test data were well documented, enabling for detailed calculations as presented in Appendix B. The calculations that were done to obtain the resistance factors shown in Table 2.19 are presented in Appendix C.

Table 2.19 shows that for the CPT method there is no consistency between the resistance factors calculated for the different test piles. The resistance factors that were calculated for the SPT method are approximately the same for the two test piles of each site. The problem is that there is a substantial difference between the resistance factors for the test piles of the Newbury Project and the resistance factors for the test piles of the West Bay Project. For both the Nordlund method and the traditional methods the resistance factors that were calculated for the different test piles are approximately the same.

Again referring to Table 2.19 it can be seen that the calculated resistance factor for the CPT method, for test pile # 9 at the West Bay Project is incorrect because it is greater than one (1.38). This is saying that the engineer has so much confidence in the CPT method that instead of reducing the calculated ultimate load it is increased. The resistance factors that are used for the Load and Resistance Factor Design method are all less than one, which states that an ultimate load can never be increased to obtain a factored load. A major problem arises when a resistance factor is greater than one because it essentially shows that a factor of safety that is less than one can be used in the Working Stress Design method.

A direct comparison between the recommended resistance factors and the average calculated resistance factors as well as the average calculated resistance factors multiplied by the AASHTO recommended resistance factor for a static load test of 0.80 are presented

in Table 2.20. This table shows that the average calculated resistance factors were higher (except for the Nordlund method) when compared with the recommended resistance factors. This is reasonable, as by and large the recommended resistance factors need to provide safe design capacities. The fact that the calculated resistance factor for the Nordlund method is lower than the recommended suggests that using the AASHTO specification would result in less than anticipated safe design.

Based on the presented case history calculations and keeping in mind that the resistance factor for the traditional methods is just an assumed resistance factor that provides a factor of safety of approximately three, the statement can be made that there needs to be some research done which looks into the basis for the AASHTO recommended resistance factors. The AASHTO recommended resistance factors need to be founded on large high quality databases.

2.5 DIFFICULTIES OF THE EXISTING LRFD CODES

2.5.1 Overview

All existing codes suffer from two major difficulties. One is the application of LRFD to geotechnical problems due to uncertainties in resistance principally manifested in site characterization, soil behavior, and construction quality. The other problem is lack of data. None of the reviewed codes and associated resistance factors were developed based on databases enabling the calculation of resistance factors from case histories.

The current AASHTO specifications encounter additional difficulty due to the irrational multiplication of the resistance factor by the modifier λ_v . This procedure

requires the interaction of two independent evaluations (e.g. static analysis and dynamic methods) and results in unnecessary and confusing conservatism. A clear separation of the resistance factors on the basis of design and construction is required.

2.5.2 Construction Difficulties

a) General

In geotechnical practice, uncertainties in resistance principally manifest in site characterization, soil behavior, and construction quality. The uncertainties have to do with interpreting site conditions, understanding soil behavior, and accounting for construction effects. Uncertainties in external loads are small compared with uncertainties in soil and water loads and the strength-deformation behaviors of soils. The approach for selecting load and resistance factors developed in structural practice, though a useful starting point for geotechnical applications, is not sufficient. Work is needed to incorporate in the LRFD formulation factors that are unique to geotechnical design.

Philosophically, the selection of load and resistance factors need not be made probabilistically, although in current structural practice a reliability-theory-based calibration is commonly used. This approach focuses more on load uncertainties than resistance uncertainties, and does not include many subjective factors unique to geotechnical practice. An expanded approach is needed if the full benefits of LRFD are to be achieved for foundation design.

The initial LRFD specification for driven piles uses uncertainties associated with pile capacity equations in calibrating resistance factors. In practice, engineers

use more than just the equations in designing piles. Load test results provide additional information, and quality assurance procedures are implemented on the construction process. These other factors intend to reduce uncertainty, and thus by not including them the LRFD design is more conservative than needed. The 1997 specification attempts to address this issue by introducing a parameter λ to be multiplied by the resistance factor, ϕ . These λ factors are typically less than 1.0. Unfortunately, this adds a further level of conservatism, rather than giving credit to the additional information provided by load tests and construction controls.

The current specifications in the dynamic evaluation of pile capacity area are completely disassociated from (a) common design and construction procedures and (b) the understanding and utilization of the instruments and methods of analyses employed for dynamic evaluations. The specified numbers can neither be used to write specifications (i.e. contract documents) nor can they be used by a practicing engineer as a design guideline. Such critical statements call for (a) a detailed review of these specifications and (b) suggested revisions. This chapter has provided the review and suggested revisions are given in this manuscript.

b) Observations

The following observations are made regarding the review of the current specifications:

- (a) The provided information seems not to be founded on actual data (database) assuming unavailability at the time of the original code development.

- b) The specifications provided for the dynamic evaluation of driven piles are by and large unrelated to the actual design / QA process used in practice (see for example Figure 2.11). The methods referred to are by no means absolute (or just do not exist). For example: the performance of a wave equation analysis in the design stage requires the modeling of the pile, soil and the driving system. The obtained results can be varied markedly based on the input parameters and hence cannot be referred to as 'a' specific method without a guideline. Moreover, the reference to the pile driving analyzer (PDA) is not clear. This is an instrument that acquires data. These data can be analyzed in different ways. One method employed by the PDA most commonly used in the USA (manufactured by Pile Dynamics Inc. of Cleveland, Ohio) in analyzing the data is the Case Method (Goble et al., 1970, Rausche et al., 1975, and PDA, 1999). This method has many (at least five!) variations and is often highly dependent (related to the driving conditions) on a 'Case damping' parameter that is assumed to be associated with soil conditions, (Paikowsky, 1982, Paikowsky et al. 1994, Paikowsky and LaBelle, 1994, Paikowsky 1995, Paikowsky and Chernauskas, 1996).
- (c) The specifications seem to be concerned mostly with the structural integrity aspect of the driven piles. While being one important aspect of the construction process, the specifications provide only a qualitative unclear guideline for monitoring pile driving, (e.g. severe driving, good driving).
- (d) The methodology lumps together multiple sources of uncertainties. The oversimplification in the geotechnical approach results in a crude procedure of

questionable calibration ability. This is true for all parameter sources; superstructure loading, soil conditions, design procedure and field-testing.

- (e) A limited use of databases in conjunction with the aforementioned crude procedure results in recommended parameters that by and large mimic or parallel the WSD. As such, the LRFD approach loses its effectiveness and becomes a burden to the practicing engineer.

2.5.3 Deficiency in Current Geotechnical Reliability Practice for LRFD

While the use of LRFD for the design of structures enjoyed a deep involvement of professionals in the probability area (Ellingwood et al. 1980; Ravindra and Galambos 1978), geotechnical applications of reliability in the US lag behind their counterparts in structural engineering (Meyerhof 1994). Earlier work performed in Europe as the preparation for Eurocode 7 (Baecher 1982; Standardization 1993) has been slow to make its way into American practice, and the "design point" approach to calibrating partial factors based on advanced second-moment methodology (the basis for most load factors in current LRFD codes) has yet to replace the mathematically inconsistent first-order second-moment approach in geotechnical applications. The current project presents unique opportunities to bring geotechnical implementations of LRFD into align with more advanced structural implementations.

The current literature on LRFD for deep foundations is inconsistent on the definition of reliability index as used in calibrating resistance factors, either against ASD or statistical data. FHWA publications (Barker et al. 1991; Withiam et al. 1997) define reliability index, β , on the logarithms of load and resistance; in other places in

the literature β is defined on arithmetic values (O'Neill 1995). These two definitions give different answers. A reliability index calculated on arithmetic values of logNormally distributed parameters is not consistently related to probability of failure, p_f , and the same is true of converse is true with β calculated on the logarithms of Normally distributed parameters. In fact, geotechnical design methods for pile resistance confound multiplicative and additive sources of uncertainty. This is especially obvious in static formulas that add tip and shaft resistance, while multiplying uncertainties having to do with soil conditions and construction effects. While current procedures incorporate extensive knowledge of geomechanics, they do not incorporate the state-of-practice in reliability analysis of data.

2.5.4 Calibrations Based on State-of-Practice Reliability Methodology

It is important that the calibrations of resistance factors for piles and shafts make use of modern methodology consistent with procedures used to calibrate load factors. If it is not based on the current approach, the calibrated resistance factors, which result run the risk of being inconsistent with corresponding load factors for bridge superstructures. Also of being internally inconsistent with respect to the statistical assumptions of distributional form, uncertainty structure, and correlation among variables on which they are based (Nowak 1999).

In the proposed work, calibrations will be performed in two, redundant ways and compared to obtain appropriate resistance factors:

- (1) Using the first-order second-moment, one-dimensional formulation discussed in current FHWA publications (Withiam et al. 1997).

- (2) Using "design-point" methodology of current reliability theory, incorporating both resistances and loads (see for example Ayyub and McCuen 1997, and Melchers 1987). By comparing and contrasting results obtained, the objective will be to take advantage of the more modern and mathematically consistent approach of advanced second-moment reliability, while at the same time attempting to ensure continuity with past practice. This redundant approach also contributes to quality assurance in the analysis.

The first-order second-moment approach reflected in current geotechnical documents combines the many sources of uncertainty that contribute to error in resistance predictions into a single variable, and then calculates a coefficient of variation for that single dimension. This approach is straightforward, and produces accurate results when the probabilistic models are sufficiently well known and simple that approximations are not required. This is, however, not the case in most predictions of pile and shaft resistance. In these cases the calculation is usually an approximation, the first order approach implicitly takes that approximation at the joint means of the uncertain qualities. This introduces well-known inaccuracies in which, for example, mechanically equivalent definitions of failure may yield different reliability indices based on the same parameter uncertainties.

Current practice in reliability theory is to represent each limiting state as a surface in the space of uncertain parameters, and to center approximations at the point (R^*, Q^*) along the limiting state surface which has the highest probability with respect to the uncertain parameters. This point is called the "design point," and is solved for

iteratively (Ayyub and McCuen 1997, Madsen et al. 1985; Melchers 1987; Thoft-Christensen and Baker 1982). Using this approach, the reliability index β can be defined geometrically as the vector distance between the design point in the joint means (m_R, m_Q) of the uncertain parameters [Hasofer, 1974 #19]. The partial factors on loads and resistances can be found the ratio of the coordinate of the design point on each parameter axis divided by the respective mean of the parameter (i.e., $\phi = R^*/m_R$; $\gamma = Q^*/m_Q$, and so forth for resistance and load components).

The design-point methodology provides greater internal consistency among the load resistance factors calculated, better consistency with load factors (which is a not uncommon concern at the state level), and an efficient way for dealing with correlations among parameters. Uncertainties in geotechnical parameters typically exhibit substantial correlations with one another, and significant errors can be made if these are ignored, as they usually have been in past practice using the first-order second-moment approach. An important additional benefit of design-point methodology is that it allows partial factors to be calculated on the individual components of geotechnical uncertainty, providing greater insight on how the uncertainties combine (Cf., (Taylor 1948) on the appropriateness of separate factors of safety for cohesion and friction angle). One example of this is the relative contributions of uncertainty in tip resistance and skin friction in static formula calculations.

Most LRFD calibration work for resistance factor ϕ addresses total pile resistance, ignoring the possibly differing uncertainties attending the components of

resistance (e.g., end bearing vs. side friction). The reasons are understandable. Only a small fraction of pile load tests have sufficient instrumentation to discriminate among resistance components, and more advanced data analysis procedures than those based on equation 2.63 are required to evaluate the data.

A sufficient number of test results exist in the database to analyze partial resistance factors for static design formulas. An analysis of these data will be made using advanced second-moment reliability to separate out partial factors on end bearing and side friction. The separately calibrated partial factors will be compared to total resistance factors calibrated using the first-order second-moment equation.

Table 2.1. Factor of Safety on Ultimate Axial Geotechnical Capacity
Based on Level of Construction Control (AASHTO, 1997).

Basis for Design and Type of Construction Control	Increasing Design/Construction Control				
Subsurface Exploration	X	X	X	X	X
Static Calculation	X	X	X	X	X
Dynamic Formula	X				
Wave Equation		X	X	X	X
CAPWAP Analysis			X		X
Static Load Test				X	X
Factor of Safety (FS)	3.50	2.75	2.25	2.00 ⁽¹⁾	1.90

⁽¹⁾ For any combination of construction control that includes a static load test, FS = 2.0.

Table 2.2. Allowable Stresses in Piles (AASHTO, 1997).

Pile Type	Maximum Allowable Stress, σ_{all} , (kPa)
Steel	
• Driving Damage Likely	0.25 F_y
• Driving Damage Unlikely	0.33 F_y
Concrete-Filled Steel Pipe	0.25 F_y + 0.40 f'_c ⁽¹⁾
Prestressed Concrete	0.33 f'_c - 0.27 f_{pe} ⁽²⁾
Round Timber	
• Douglas-Fir - Coast	8.3
• Douglas-Fir - Interior	7.6
• Lodgepole Pine	5.5
• Red Oak	7.6
• Southern Pine	8.3
• Western Hemlock	6.9

⁽¹⁾ Applied over cross-sectional area of steel pipe and cross-sectional area of concrete;

⁽²⁾ Applied over gross cross-sectional area of concrete; F_y = Yield strength of steel (kPa); f'_c = Concrete compressive strength (kPa); and f_{pe} = Concrete compressive strength due to prestressing (kPa).

Table 2.3. Resistance Factors for Geotechnical Strength Limit State for Axially Loaded Piles (AASHTO, 1998).

Method/Soil/Condition		Resistance Factor, ϕ
Ultimate Bearing Resistance of Single Piles	Skin Friction: Clay	
	α -method	$0.70\lambda_v$
	β -method	$0.50\lambda_v$
	λ -method	$0.55\lambda_v$
	End Bearing: Clay and Rock	
	Clay	$0.70\lambda_v$
	Rock	$0.50\lambda_v$
	Skin Friction and End Bearing: Sand	
	SPT-method	$0.45\lambda_v$
	CPT-method	$0.55\lambda_v$
	Wave equation analysis with assumed driving resistance	$0.65\lambda_v$
	Load Test	$0.80\lambda_v$
Block Failure	Clay	0.65
Uplift Resistance of Single Piles	α -method	0.60
	β -method	0.40
	λ -method	0.45
	SPT-method	0.35
	CPT-method	0.45
	Load Test	0.80
Group Uplift Resistance	Sand	0.55
	Clay	0.55
Method of controlling installation of piles and verifying their capacity during or after driving to be specified in the contract documents		Value of λ_v
Pile Driving Formulas, e.g., ENR, equation without stress wave measurements during driving		0.80
Bearing graph from wave equation analysis without stress wave measurements during driving		0.85
Stress wave measurements on 2% to 5% of piles, capacity verified by simplified methods, e.g., the pile driving analyzer		0.90
Stress wave measurements on 2% to 5% of piles, capacity verified by simplified methods, e.g., the pile driving analyzer, and static load test to verify capacity		1.00
Stress wave measurements on 2% to 5% of piles, capacity verified by simplified methods, e.g., the pile driving analyzer, and CAPWAP analyses to verify capacity		1.00
Stress wave measurements on 10% to 70% of piles, capacity verified by simplified methods, e.g., the pile driving analyzer		1.00

Table 2.4. Resistance Fsfactors Calibrated by Fitting with WSD for $\gamma_D = 1.25$ and $\gamma_L = 1.75$ (After McVay et al., 1998).

Q_D/Q_L	Resistance Factor, ϕ					
	FS=1.5	FS=2.0	FS=2.5	FS=3.0	FS=3.5	FS=4.0
1	1.00	0.75	0.60	0.50	0.43	0.38
2	0.94	0.71	0.57	0.47	0.40	0.35
3	0.92	0.69	0.55	0.46	0.39	0.34
4	0.90	0.68	0.54	0.45	0.39	0.34
5	0.89	0.67	0.53	0.44	0.38	0.33
6	0.88	0.66	0.53	0.44	0.38	0.33
7	0.88	0.66	0.53	0.44	0.38	0.33
8	0.87	0.65	0.52	0.44	0.37	0.33
9	0.87	0.65	0.52	0.43	0.37	0.33
Median	0.94	0.70	0.56	0.47	0.39	0.34
Recommended	0.90	0.65	0.55	0.45	0.35	0.30

Table 2.5. Resistance Factor for Driven Piles for Estimating the Axial Geotechnical Pile Capacity Using Reliability-Based Calibration (modified after Barker, et al., 1991).

Pile Length (m)	β_T	ϕ Values by Method of Axial Pile Capacity Estimation						
		α		β	λ		CPT	SPT
		Type I	Type II		Type I	Type II		
10	2.0	0.78	0.92	0.79	0.53	0.65	0.59	0.48
30	2.0	0.84	0.96	0.79	0.55	0.71	0.62	0.51
10	2.5	0.65	0.69	0.68	0.41	0.56	0.48	0.36
30	2.5	0.71	0.73	0.68	0.44	0.62	0.51	0.38
Average ϕ		0.78		0.74	0.56		0.55	0.43
Selected ϕ		0.70		0.50	0.55		0.55	0.45

Type I refers to soils with $S_u < 50$ kPa; Type II refers to soils with $S_u > 50$ kPa

Table 2.6a. Relationship Between Probability of Failure and Reliability Index for Lognormal Distribution (After Withiam et al., 1997).

Reliability Index, β	Probability of Failure, p_f	Probability of Failure, p_f	Reliability Index, β
2.5	0.99×10^{-2}	1×10^{-1}	1.96
3.0	1.15×10^{-3}	1×10^{-2}	2.50
3.5	1.34×10^{-4}	1×10^{-3}	3.03
4.0	1.56×10^{-5}	1×10^{-4}	3.57
4.5	1.82×10^{-6}	1×10^{-5}	4.10
5.0	2.12×10^{-7}	1×10^{-6}	4.64
5.5	2.46×10^{-8}	1×10^{-7}	5.17

Table 2.6b. Comparison Between Rosenbleuth and Estava's Approximation and Series Expansion (Labeled "exact").

β	Rosenbleuth and Estavas' p_f	"exact" p_f	Percent Error
2.0	8.4689E-2	2.2750E-2	272.3%
2.5	9.8649E-3	6.2097E-3	58.9%
3.0	1.1491E-3	1.3500E-3	-14.9%
3.5	1.3385E-4	2.3267E-4	-42.5%
4.0	1.5592E-5	3.1686E-5	-50.8%
4.5	1.8162E-6	3.4008E-6	-46.6%
5.0	2.1156E-7	2.8711E-7	-26.3%
5.5	2.4643E-8	1.9036E-8	29.5%
6.0	2.8705E-9	9.9012E-10	189.9%

Table 2.7. Strength and Service Limit States for Design of Driven Pile Foundations
(After Withiam et al., 1997).

Performance Limit	Strength Limit State(s)	Service I Limit State
Bearing Resistance of Single Pile/Group	X	
Pile/Group Punching	X	
Settlement of Pile Group		X
Tensile Resistance of Uplift-Loaded Piles	X	
Lateral Displacement of Pile/Group		X
Structural Capacity of Axially/Laterally-Loaded Piles	X	

Table 2.8. Reliability Index of Case Method Prediction (After McVay et al., 1998).

Q_D/Q_L	β		COV_R		λ_R		COV_{QD}	λ_D	COV_{QL}	λ_L	ASD FS
	EOD	BOR	EOD	BOR	EOD	BOR					
1	3.04	2.40	0.325	0.318	1.355	1.052	0.1	1.05	0.18	1.15	2.5
2	3.08	2.44	0.325	0.318	1.355	1.052	0.1	1.05	0.18	1.15	2.5
3	3.10	2.46	0.325	0.318	1.355	1.052	0.1	1.05	0.18	1.15	2.5
4	3.11	2.47	0.325	0.318	1.355	1.052	0.1	1.05	0.18	1.15	2.5
5	3.12	2.48	0.325	0.318	1.355	1.052	0.1	1.05	0.18	1.15	2.5
6	3.13	2.49	0.325	0.318	1.355	1.052	0.1	1.05	0.18	1.15	2.5
7	3.13	2.49	0.325	0.318	1.355	1.052	0.1	1.05	0.18	1.15	2.5
8	3.13	2.49	0.325	0.318	1.355	1.052	0.1	1.05	0.18	1.15	2.5
9	3.14	2.50	0.325	0.318	1.355	1.052	0.1	1.05	0.18	1.15	2.5

Table 2.9. Resistance Factor for Case Method Prediction (After McVay et al., 1998).

Q_D/Q_L	Resistance Factor, ϕ					
	EOD			BOR		
	$\beta=2.0$	$\beta=2.5$	$\beta=3.0$	$\beta=2.0$	$\beta=2.5$	$\beta=3.0$
1	0.85	0.70	0.58	0.66	0.55	0.46
2	0.81	0.67	0.56	0.64	0.53	0.44
3	0.79	0.66	0.54	0.62	0.52	0.43
4	0.78	0.65	0.54	0.61	0.51	0.42
5	0.77	0.64	0.53	0.61	0.51	0.42
6	0.77	0.64	0.53	0.60	0.50	0.42
7	0.77	0.63	0.53	0.60	0.50	0.41
8	0.76	0.63	0.52	0.60	0.50	0.41
9	0.76	0.63	0.52	0.60	0.50	0.41

Table 2.10. Range of Values for Resistance Factors for Piles
(Standard Association of Australia, 1995).

Method of Assessment of Ultimate Geotechnical Strength	Range of Values of ϕ_g
Static load testing to failure	0.70-0.90
Static proof (not to failure) load testing ¹	0.70-0.90
Dynamic load testing to failure supported by signal matching ²	0.65-0.85
Dynamic load testing to failure not supported by signal matching	0.50-0.70
Dynamic proof (not to failure) load testing supported by signal matching ^{1,2}	0.65-0.85
Dynamic proof (not to failure) load testing not supported by signal matching ¹	0.50-0.70
Static analysis using CPT data	0.45-0.65
Static analysis using SPT data in cohesionless soils	0.40-0.55
Static analysis using laboratory data for cohesive soils	0.45-0.55
Dynamic analysis using wave equation method	0.45-0.55
Dynamic analysis using driving formulae for piles in rock	0.50-0.65
Dynamic analysis using driving formulae for piles in sand	0.45-0.55
Dynamic analysis using driving formulae for piles in clay	Note 2
Measurement during installation of proprietary displacement piles, using well established in-house formulae	0.50-0.65

Notes:

¹ ϕ_g should be applied to the maximum load applied.

²Signal matching of the recorded data obtained from dynamic load testing should be undertaken on representative test piles using a full wave signal matching process.

³Caution should be exercised in the sole use of dynamic formulae (e.g., Hiley) for the determination of the ultimate geotechnical strength of piles in clays. In particular, the dynamic measurements will not measure the 'set up' which occurs after completion of driving. It is preferable that assessment be first made by other methods, with correlation then made with dynamic methods on a site-specific basis if these latter are to be used for site driving control.

For cases not covered in Table 10, values of ϕ_g should be chosen using the stated values as a guide.

Table 2.11. Guide for Assessment of Resistance Factors for Piles
(Standard Association of Australia, 1995).

Circumstances in Which Lower End of Range May be Appropriate	Circumstances in Which Upper End of Range May be Appropriate
Limited site investigation	Comprehensive site investigation
Simple method of calculation	More sophisticated design method
Average geotechnical properties used	Geotechnical properties chosen conservatively
Use of published correlations for design parameters	Use of site-specific correlations for design parameters
Limited construction control	Careful construction control
Less than 3 percent of piles dynamically tested	15 percent or more piles dynamically tested
Less than 1 percent of piles statically tested	3 percent or more of piles statically tested

Table 2.12. Material Resistance Factors for Piles
(AUSTROADS, 1992).

Routine proof load tested	0.8
Load tested to failure	0.9
Piles analyzed by dynamic formulae or wave equation methods based on assumed driving system energy and soil parameters	0.4 - 0.5*
Piles subjected to closed-form dynamic solutions, e.g., Case method	0.5
Piles subjected to closed-form dynamic solutions correlated against static load test or dynamic load tests using measured field parameters in a wave equation analysis (e.g., CAPWAP)	0.6
Piles subjected to dynamic load tests using measured field parameters in a wave equation (e.g., CAPWAP)	0.8

* Note: A value of 0.4 should be used for cohesive soils and structures where permanent loads dominate. In noncohesive soils and for structures where transient loads dominate, values up to 0.5 may be used.

Table 2.13. Typical Load and Resistance Factors for Axially Loaded Piles in Compression on Land for ULS (modified after Meyerhof, 1994).

Code Factor	Eurocode 7 (1993)	Canadian Geotechnical Society (1992)	AASHTO (1994)
Dead Load	1.1	1.25	1.3
Live Load	1.5	1.5	2.17
Resistance (driven pile with load tests)	0.4 - 0.6	0.5 - 0.6	0.80
Resistance (driven piles from SPT tests)	---	0.33 - 0.5	0.45
Resistance (bored piles with load tests)	---	---	0.80
Resistance (bored piles from static analysis)	---	---	0.45 - 0.65

Table 2.14. Partial Factors from Eurocode 7 and the Equivalent Resistance Factors (After Eurocode 7, 1997).

Component factors	γ_b	γ_s
Driven piles	1.30	1.30
Bored piles	1.60	1.30
CFA (Continuos flight auger) piles	1.45	1.30

Table 2.15. Piles and Anchors¹ (From the Danish Code).

Partial Coefficient	Safety Class	
	Normal	High
γ_{b1} without test loading	0.50	0.45
γ_{b2} with test loading	0.63	0.57
γ_{b3} for piles and anchor actually subjected to test loading	0.71	0.65

¹ The γ -values are inverted here to more easily compare with United States practice.

Table 2.16. Resistance Factors for Deep Foundations
(From Ontario Bridge Code).

Axial Load	Factor
Static analysis, compression	0.4
Static analysis, tension	0.3
Static test, compression	0.6
Static test, tension	0.4
Dynamic analysis, compression	0.4
Dynamic analysis, compression field measurements and analysis	0.5

Table 2.17. Resistance Factors (From the Canadian Bridge Code).

Type of Unit	Resistance Factor
Precast reinforced concrete	0.4
Cast-in-place concrete	0.4
Expanded-base concrete	0.4
Prestressed concrete	0.4
Steel H-section	0.5
Unfilled steel pipe pile	0.5
Concrete-filled steel pipe pile	0.4
Wood	0.4

Table 2.18. Summary of Ultimate and Factored Loads, Test Pile # 2, Newbury Site.

Method	Q _p (tons)	Q _s (tons)	Q _{ult} (tons)	φ-factor	Q _R (tons)
SPT	61	71	132	0.45	59
CPT	50	50	100	0.55	55
Traditional Methods	77	86	163	0.35	57
Driven 1.0 (Nordlund)	48	119	167	0.55	92
Static Load Test	28	46	74	0.80	59
Average	53	74	127	-----	64
Standard Deviation	18	30	40	-----	16

Table 2.19. Calculated Resistance Factors Assuming that the Resistance Factor for a Static Load Test is 1.0.

	Newbury Site Project		West Bay Project		Average ϕ -factor for Method
Test Pile Method	#2	#3	#9	#15	
SPT	0.56	0.51	0.79	0.75	0.65
CPT	0.74	0.62	1.38	0.88	0.91
Driven 1.0 (Nordlund)	0.44	0.33	0.42	0.40	0.40
Traditional Methods	0.45	0.41	0.53	0.51	0.48

Table 2.20. Comparison of Recommended and Calculated Resistance Factors.

	Calculated ϕ -factors	Recommended ϕ -factors	0.80 * Calculated ϕ -factors
SPT	0.65	0.45	0.52
CPT	0.91	0.55	0.73
Driven 1.0 (Nordlund)	0.40	0.55	0.32
Traditional Methods	0.48	0.35	0.38

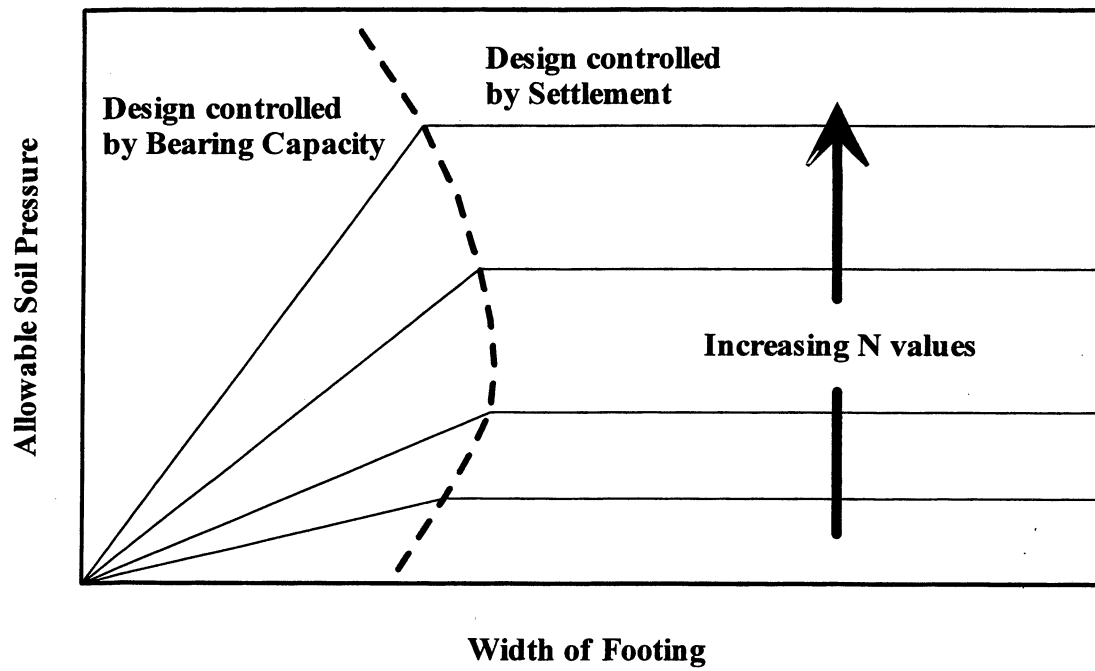


Figure 2.1. Design Basis for Spread Footings in Sand (after Peck et al., 1974).

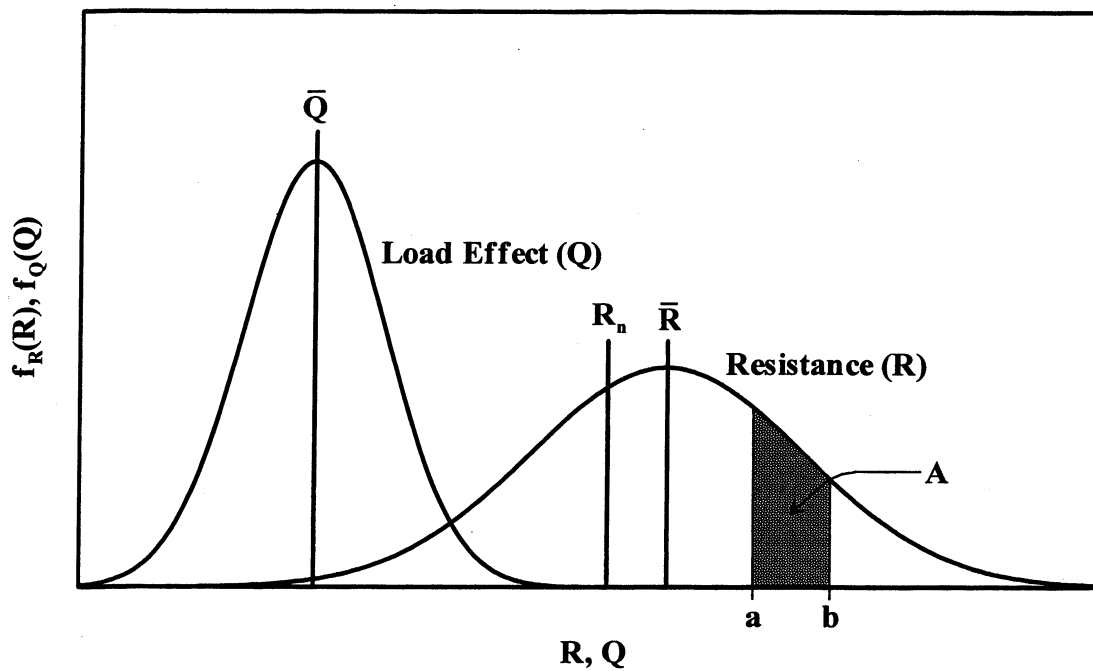


Figure 2.2. An Illustration of Probability Density Functions for Load Effect and Resistance (Goble, 1999).

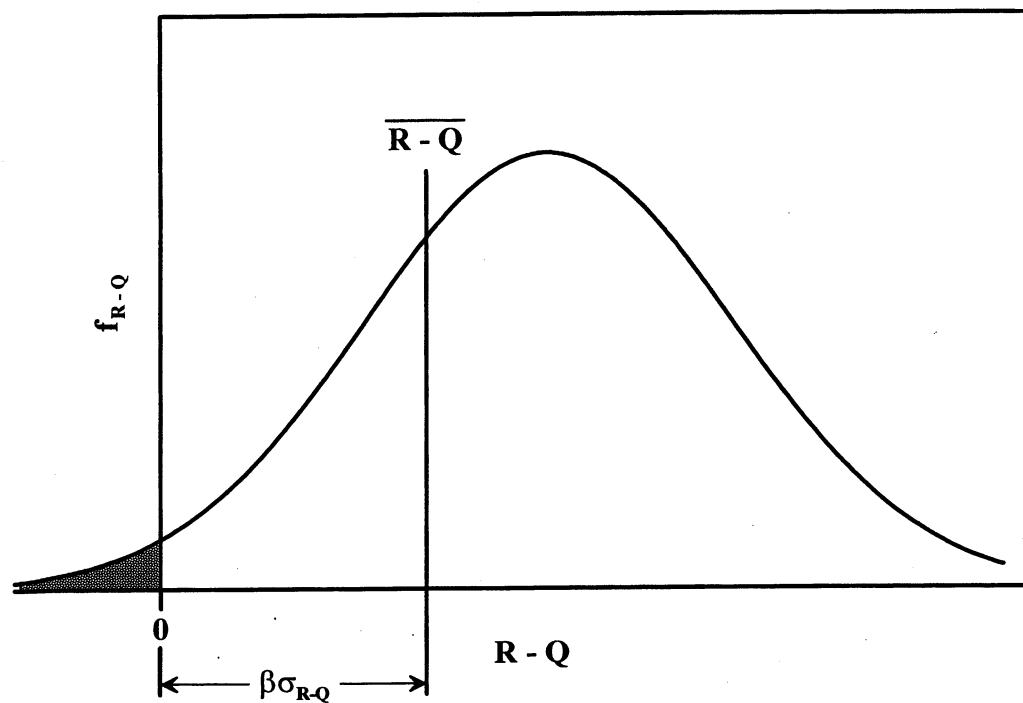


Figure 2.3. An Illustration of a Probability Density Function for $R - Q$ (Goble, 1999).

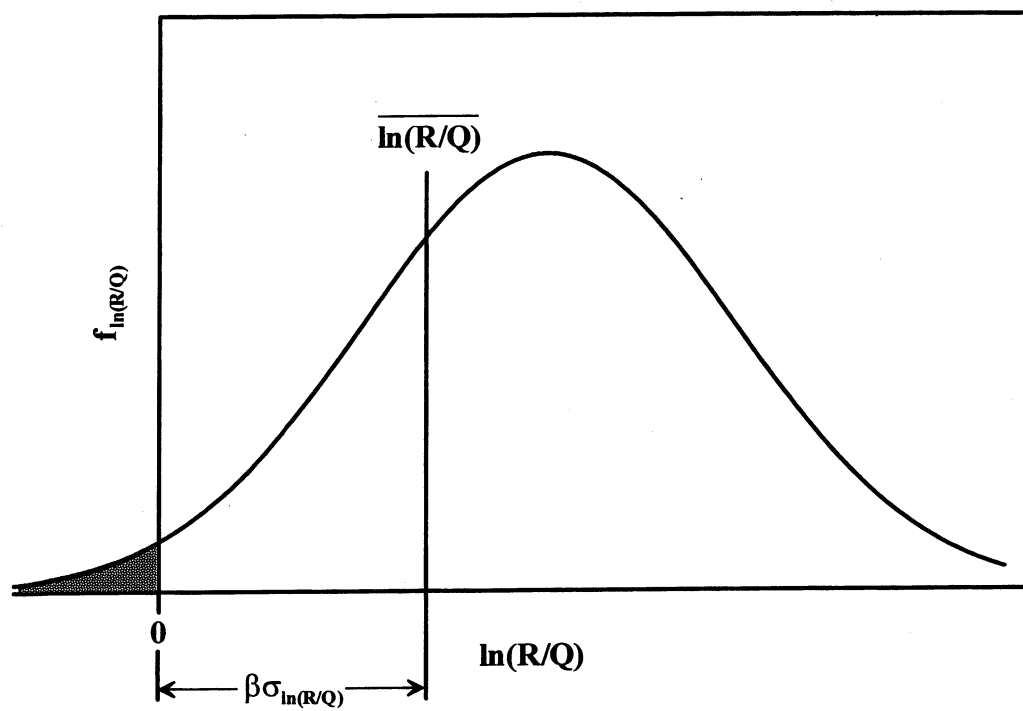


Figure 2.4. An Illustration of a Probability Density Function for $\ln(R/Q)$ (Goble, 1999).

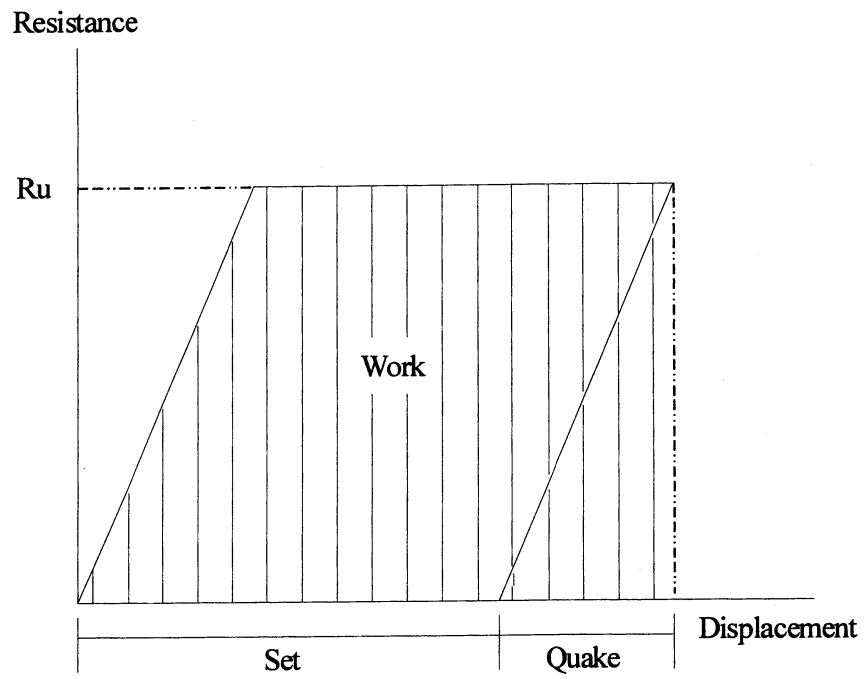


Figure 2.5. Resistance vs. Displacement at the Top of the Pile.

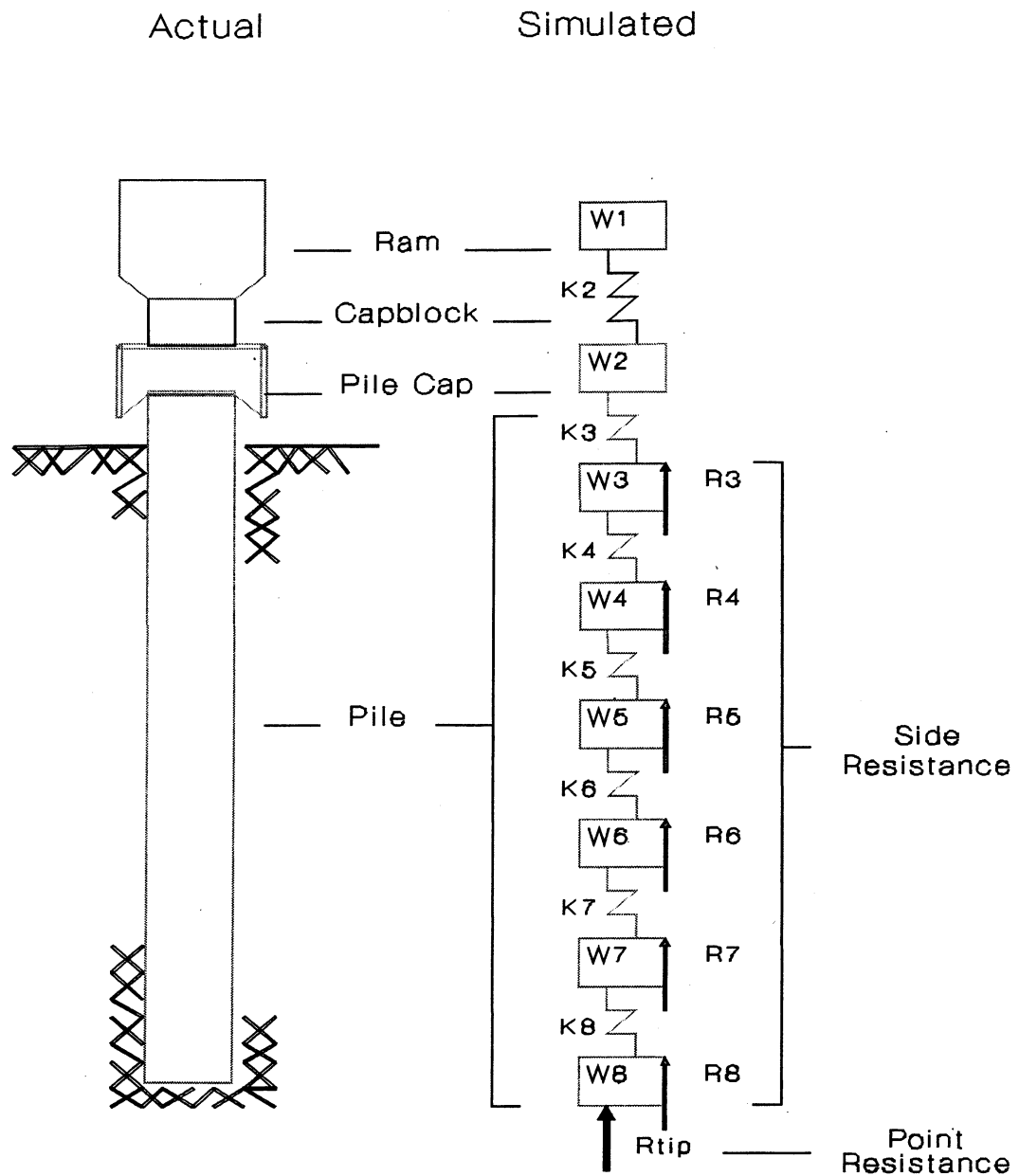


Figure 2.6. Smith's model simulating the hammer-pile-soil system for use with the one-dimensional wave equation (Smith, 1960).

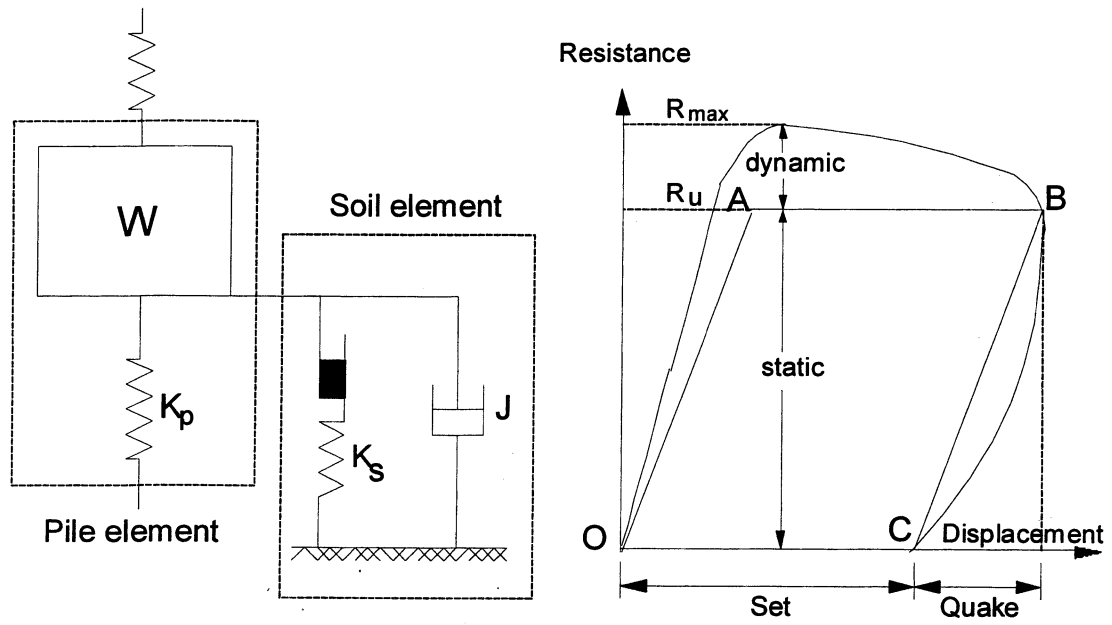


Figure 2.7. Soil-pile model (left) and the corresponding elasto-plastic soil resistance-displacement relationship (after Smith, 1960).

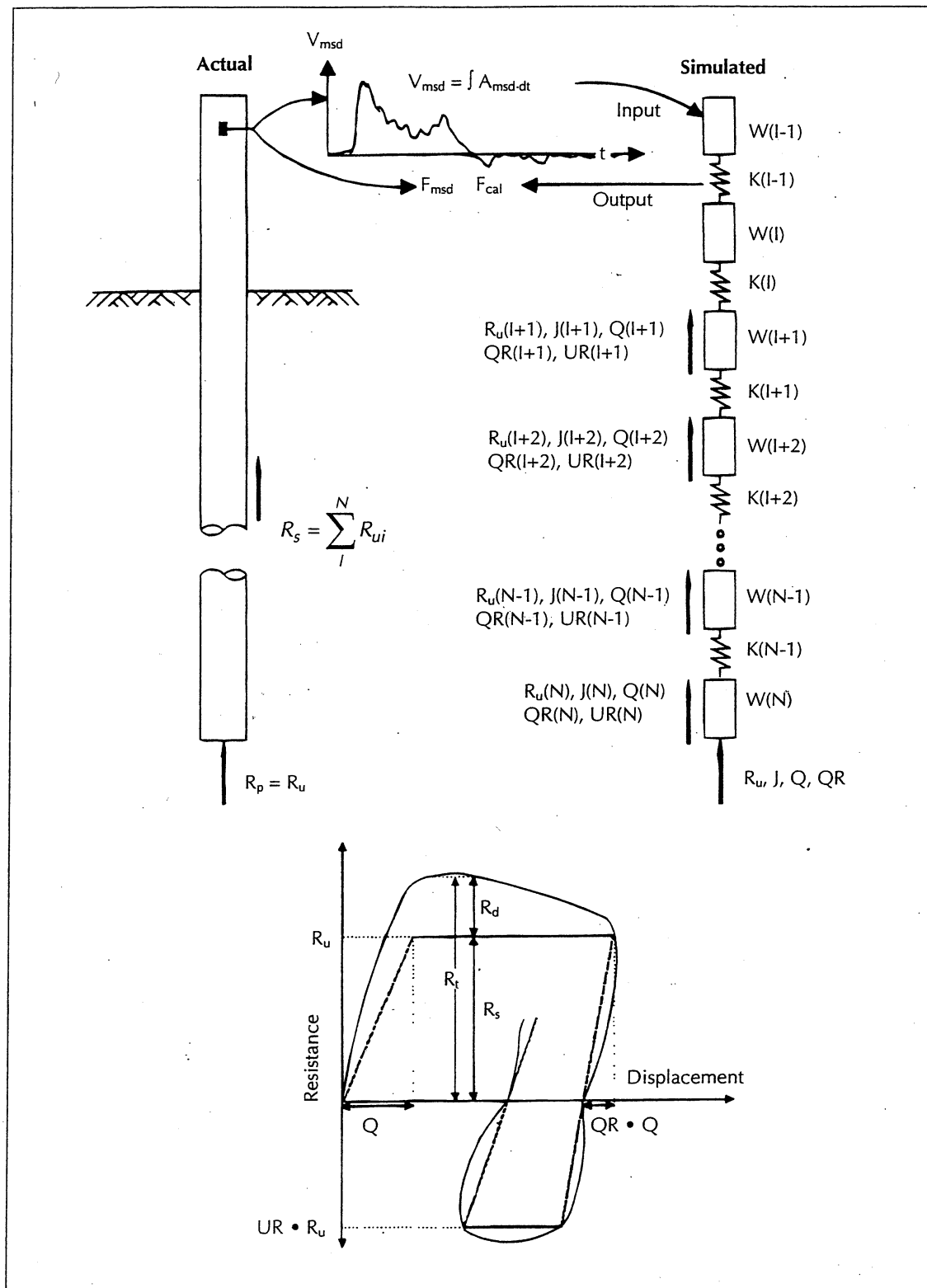


Figure 2.8. Notations used for Model of Pile and Soil in TEPWAP Analysis (Paikowsky, 1982)

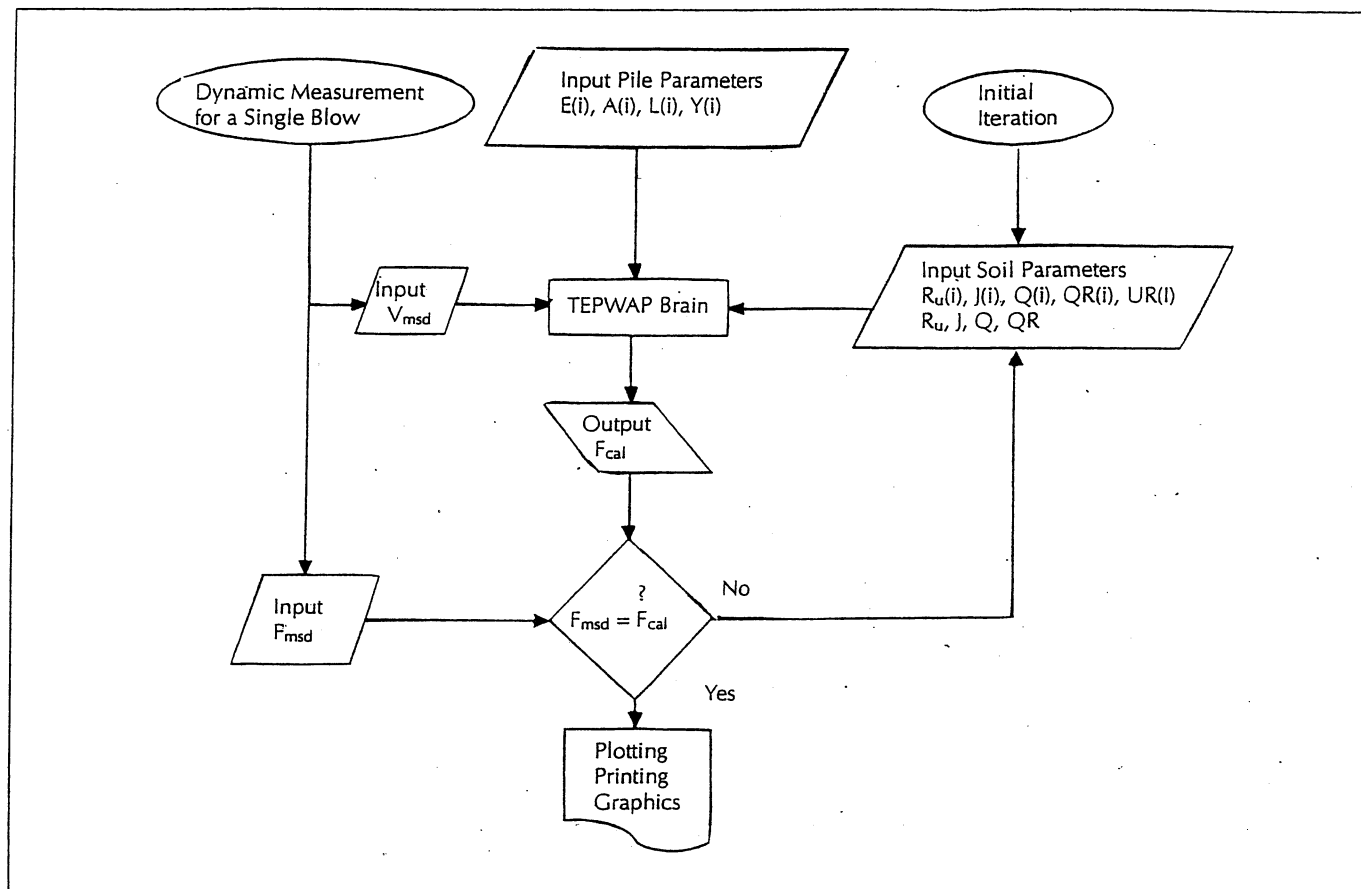


Figure 2.9. Flow Chart Describing the analysis process using TEPWAP (Paikowsky, 1982).

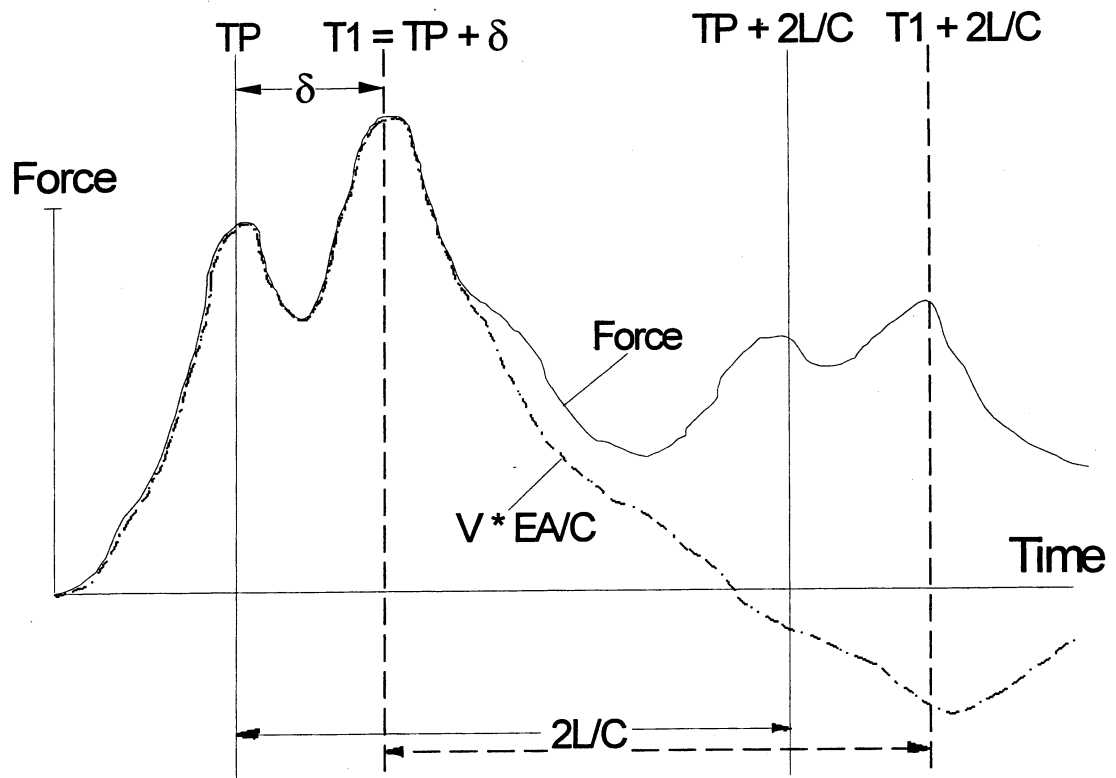


Figure 2.10. Force and Velocity Traces Showing Two Impact Peaks Indicative of Driving in Soils Capable of Large Deformations.

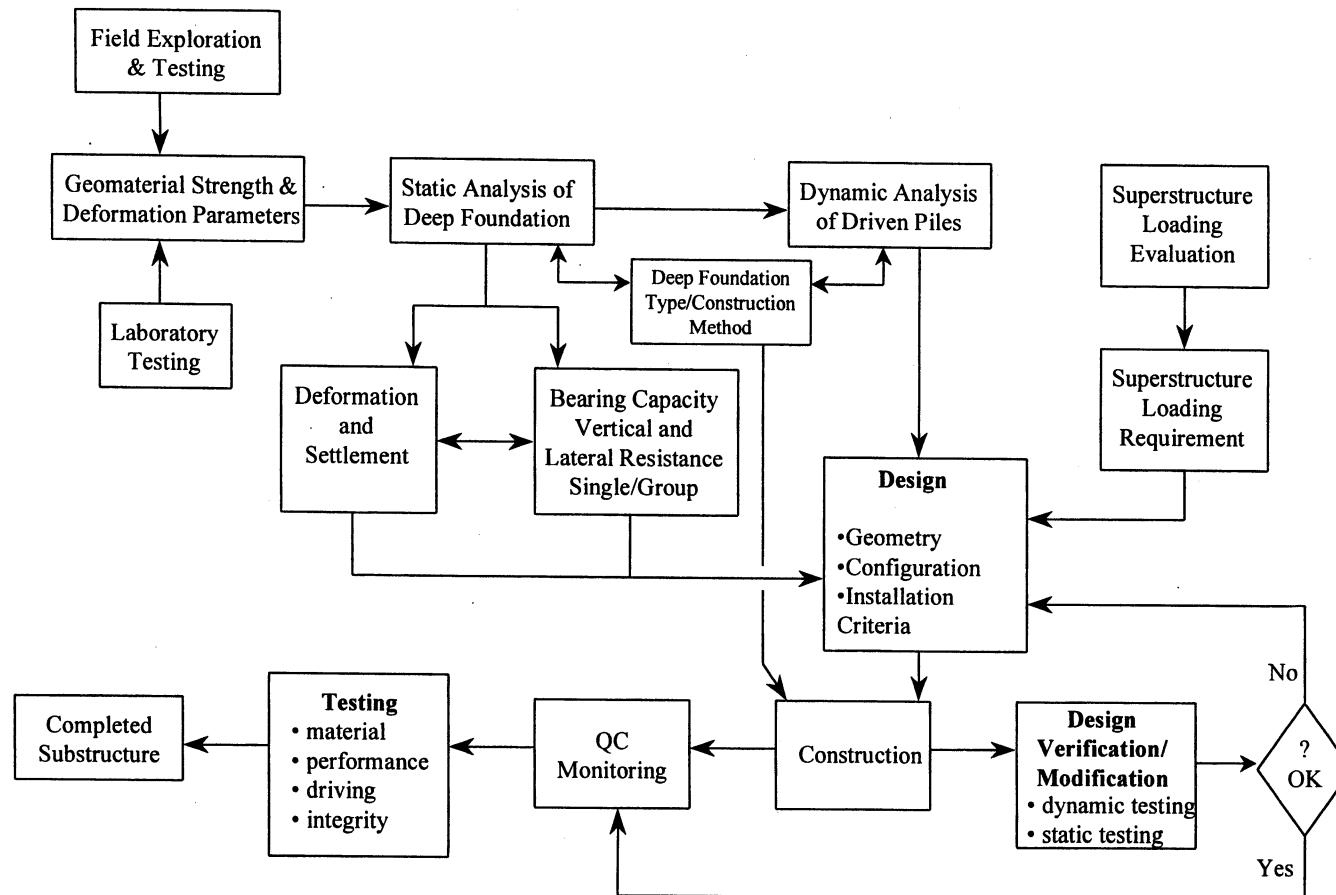


Figure 2.11. Deep Foundation Design Process.

CHAPTER 3

COMPILATION OF THE DATA BASES

3.1 GENERAL

This chapter presents the databases that were compiled to allow for the statistical analyses required in this research. Each section briefly describes the method that was used to obtain the data and the purpose for which the data were used. The five databases that were used in the presented research are the PD/LT2000 database, the U-MASS LOWELL/UKRAINE database, the GRLWEAP database, the PD2000 database, and the PD/LTT2000 database. The PD/LT2000 database is used for the majority of the dynamic analyses while the other databases are used to examine specific issues such as the influence of the type of static load test procedure on the pile's capacity, the performance of the WEAP method, the comparison of the Energy Approach End Of Driving (EOD) predictions in relation to the CAPWAP/TEPWAP Beginning Of Restrike (BOR) predictions, and the optimum time to perform a restrike to obtain the most accurate prediction of the pile's capacity.

3.2 PD/LT2000 DATABASE

3.2.1 Overview

The data found in the PD/LT2000 database is widely used throughout this thesis for analyzing the dynamic methods. In this section a detailed description of the

processes used to obtain this data will be described. Table 3.1 presents a brief summary of the types of data that make up the PD/LT2000 database. The data was sub-grouped according to pile type, geographical location, soil type along the side of the pile and at the tip of the pile, soil inertia properties based on the blow counts and area ratios, time of driving, i.e., End Of Driving (EOD and Beginning Of Restrike (BOR), and the pile capacity as determined by the static load test results. The table shows that the data was obtained from many different areas of the United States as well as from many countries around the world. The data was taken from approximately 77 different project sites around the world. A full table presenting all of the data found in PD/LT2000 is in Appendix A.

3.2.2 Static Load Test Analysis

Each pile-case that was incorporated into PD/LT2000 was required to have a static load test to failure. The methodology used to analyze the load-settlement curves for each pile will be described in detail in sections 4.3.1 and 4.3.2 and therefore will not be discussed in this section.

3.2.3 Dynamic Measurement Analysis

(a) Overview

This section is based on previous research completed by Paikowsky et al. (1994). The text, tables and figures were taken directly from the previous report therefore the units that are used in this section are English units with SI units in parentheses were applicable.

The analyses performed on piles in data set PD/LT employed office analysis (i.e., CAPWAP or TEPWAP) as well as several computer programs developed to process and manage force and velocity signals, including DIGITIZE, PDAP, INTEGRATE, and FILECHNG.

The dynamic analyses were performed in different ways depending on the completeness of each pile-case. In all cases, the pile geometry (i.e., type, material, length of penetration, the soil at the pile' tip and side, and the blow count) was known before any type of analysis was initiated. The individual cases were divided into three distinct groups:

- (a) Group 1 - pile-cases with complete CAPWAP summaries, including E_{\max} , D_{\max} , $F1$, and $V1$.
- (b) Group 2 - pile-cases with incomplete CAPWAP summaries, such as those missing E_{\max} , D_{\max} , $F1$, and/or $V1$.
- (c) Group 3 - pile-cases that were analyzed using TEPWAP.

(b) *GROUP 1 – Complete CAPWAP Analyses*

Pile group 1 contains the complete cases available in data set PD/LT. The most common adjustment necessary for the pile cases in this group was a ratio correction between the force at impact ($F1$) and the velocity at impact ($V1$). Theoretically, the force and velocity multiplied by the pile impedance are identical under a passing disturbance, as long as no other external forces act. The ratio between these values is:

$$\frac{V1 \left(\frac{EA}{C} \right)}{F1} \quad (3.1)$$

Where: E = modulus of elasticity of the pile material
A = cross-sectional area of the pile
C = wave speed of the pile

and should be equal to unity. An acceptable ratio was considered to be 1.0 ± 0.1 . Beyond this ratio, a linear multiplier was applied to either or both parameters (force, velocity, or both) and to their byproducts, e.g., displacement and energy. The ratio between force and velocity may also be influenced by the pre-compression of a diesel hammer and hammer misalignment.

Pre-compression in a diesel hammer occurs as the air-fuel mixture is compressed by the ram just prior to combustion. This results in a force that is applied to the pile top. However, as the force is applied relatively slowly and before the actual impact between the ram and the pile top, there is not a corresponding velocity wave. This scenario results in a discrepancy between the impact force (F1) and the impact velocity ($V1(EA/C)$), as shown in Figure 3.1. The force and velocity traces of pile-case 1, driven with a Delmag 30 diesel hammer, are shown in Figure 3.1. The observed relations indicate the need for a force reduction (Δ_{total}), which is equal to the difference between Δ_k and Δ_s . Prior to a correction, the ratio ($V1(EA/C)/F1$) for pile-case 1 was 0.874. The factor (Δ_{total}) represents the number of units by which the force must be reduced in order to produce an acceptable ratio according to Equation 3.2. The magnitude of Δ_{total} and the reduction of F1 are performed as follows:

$$\Delta_{total} = \Delta_{pk} - \Delta_{ps} = 2 \text{ units} \Rightarrow \frac{2 \text{ units}}{38.5 \text{ units}} \times 250 \text{ kips} = 13 \text{ kips} (58 \text{ kN}) \quad (3.2)$$

$$F1 = F1_{uncorrected} - \Delta_{total} = 335.4 \text{ kips} - 13 \text{ kips} = F1_{corrected} = 322.4 \text{ kips} (1434 \text{ kN}) \quad (3.3)$$

The corrected F1 yields a new V1(EA/C)/F1 ratio, and adjusted E_{\max} , and a corresponding uncorrected Energy Approach prediction (R_u) as follows:

$$\frac{V1\left(\frac{EA}{C}\right)}{F1_{corrected}} = 0.909 \quad (3.4)$$

$$E_{mas} = 18 \text{ kip} - \text{ft} \times \frac{322.4 \text{ kips}}{335.4 \text{ kips}} = 17.3 \text{ kip} - \text{ft} \Rightarrow R_u = 362 \text{ kips (1610 kN)} \quad (3.5)$$

The procedure for correcting F1 is also performed in a similar manner for adjusting V1 and the corresponding D_{\max} , where $D_{\max} = \int V(t) dt$. This is sometimes necessary when either there is a significant hammer-pile misalignment that creates disturbance in the force and velocity measurements or there is a discrepancy in the measurement itself. The correction procedure for decreasing V1(EA/C) also uses the factor Δ_{total} as determined by the discrepancy in the F1 and V1(EA/C) measurements where Δ_{total} is converted to units of force. Similarly, V1(EA/C) is decreased by:

$$V1\left(\frac{EA}{C}\right)_{Corrected} = V1\left(\frac{EA}{C}\right)_{uncorrected} - \Delta_{total} \quad (3.6)$$

producing a corrected ratio:

$$\frac{\left(V1\frac{EA}{C}\right)_{corrected}}{F1} \quad (3.7)$$

and an adjusted D_{\max} :

$$D_{\max(corrected)} = \int V1_{corrected} dt \quad (3.8)$$

The corresponding uncorrected Energy Approach prediction is calculated using the adjusted D_{\max} as follows:

$$R_u = \frac{E_{\max}}{Set + \frac{D_{\max(\text{corrected})} - Set}{2}} \quad (3.9)$$

It should be noted that it is sometimes necessary to correct both the force and the velocity measurements given the proper circumstances. In general, very few pile-cases required correction, the majority of which needed very small adjustments. These corrections usually had an insignificant effect on the obtained J_c and R_u values.

After the static load test analysis and the dynamic analysis were completed, the Case damping coefficient (J_c) was back-calculated using equation 6 as outlined by Goble *et al.* (1980).

(c) GROUP 2 - Incomplete CAPWAP Analyses

The pile cases categorized in group 2 include piles from data set PD/LT that were analyzed via CAPWAP. Difficulties associated with retrieving and accumulating complete pile data cause pile-cases to require more analysis in order to produce missing information essential for the study. Typical information missing from pile cases included E_{\max} (the maximum energy delivered to the pile top) and D_{\max} (the maximum displacement of the pile top). A typical pile-case in group 2 includes a static load test plot, subsurface site information, blow count records, and CAPWAP predictions at EOD, BOR, and/or EOR, excluding the CAPWAP summary tables. The CAPWAP summary tables include pile characteristics, Case method predictions and crucial dynamic measurements (V_{\max} , V_{fin} , $V1*Z$, $F1$, F_{\max} , D_{\max} , D_{fin} , E_{\max} , and E_{fin}). In order to determine these missing dynamic parameters, a program was developed at UMASS-Lowell called INTEGRATE (written by L. Chernauskas). This program was

specifically developed to calculate the uncorrected Energy Approach and the Case method similar to a more extensive and versatile program called PDAP (Pile Driving Analysis Program), which was developed by Paikowsky (1984). The program PDAP uses recorded field data from the PDA, enables it's manipulation and correction, and produces an Energy Approach prediction and a range of Case method predictions based on all the different variations for different J_c values.

INTEGRATE processes digitized force and velocity ($V*EA/C$) traces (see Figure 3.2 for example) and, using the pile parameters as given by the user, produces the dynamic measurements listed above. INTEGRATE also calculates the uncorrected Energy Approach prediction and back-calculates the Case damping coefficient (J_c) using the following relationship after (Goble et al., 1980):

$$J_c = \frac{RTL - FINAL R_s}{V1 \frac{EA}{C} + F1 - RTL} \quad (3.10)$$

The static load test results are denoted FINAL R_s , and must be supplied by the user. An example of the results of an INTEGRATE analysis of the force and velocity traces shown in Figure 3.2 for pile-case 192 (33P1BOR) is shown in Figure 3.3. After reviewing the force and velocity (EA/C) traces for a given pile case and the $(V1*EA/C)/F1$ ratio, calculated by INTEGRATE, any necessary corrections and corresponding adjustments to E_{max} and D_{max} can be made, as outlined in section 3.2.2(a); and the uncorrected Energy Approach calculations can be performed.

(d) GROUP 3 - TEPWAP Analyses

Several pile cases in data set PD/LT were lacking the CAPWAP office analysis and, therefore, required wave match analysis to be performed. These pile cases were categorized in group 3 and all of them were analyzed using a computer program called TEPWAP. TEPWAP (Paikowsky, 1982; Paikowsky and Whitman, 1990; and Chernauskas, 1993) utilizes a procedure somewhat similar to the CAPWAP analysis described by Goble *et al.* (1970). This program allows the input of the measured velocity at the pile top as a function of time, solving for a set of parameters describing the soil resistance (dynamic and static) along the pile. Adjustments of the matches are made until the calculated force at the top matches that measured. A good agreement between CAPWAP and TEPWAP analyses was presented by Paikowsky (1982) and further confirmed by Chernauskas (1993).

The pile cases in group 3 were initially analyzed in the same manner as those in group 2, whereby their force and velocity traces were digitized with respect to time using the program DIGITIZE and processed using INTEGRATE. After these steps were successfully completed, three data files were created for each case: an input file, an identification file, and a pile/soil file. An input file for TEPWAP is created using the program DIGPWAP that processes digitized force and velocity traces and prepares them in the same manner as the PDA. Figures 3.4 and 3.5 show the identification file and the pile/soil file for pile-case 191, respectively. These files, along with the digitized force and velocity traces (see Figure 3.6 for example), are necessary for TEPWAP analyses. Iterations are performed, where the user is required

to adjust the soil properties (i.e., side and tip damping and quake, and side and tip resistance) until an acceptable force wave match is made. Figure 3.7 presents the comparison between the calculated forces at the top (obtained from the above procedure) to the measured force at the top of pile-case 191.

This particular pile case appears to be exhibiting pile plugging near the tip as indicated by the sudden observed force "jump" near $2L/C$ and again near $4L/C$. Pile plugging is most commonly associated with open-pipe piles or H-piles. It usually refers to the phenomenon that occurs when soil enters the open-pipe pile during driving until the inner-soil cylinder develops sufficient resistance to prevent further soil intrusion (see Paikowsky et al., 1989; Paikowsky and Whitman, 1990). The development of friction along the web of an H-pile can also develop enough resistance to prevent soil intrusion, causing the H-pile to become "plugged." When an H-pile becomes plugged, it then assumes the penetration characteristics of a large displacement pile (i.e., with a closed rectangular tip). Pile plugging is shown to have the following marked effects: significant contribution to the capacity of piles driven in sand; delay in capacity gain with time for piles driven in clay; and changes in the behavior of piles during installation, causing it to differ from that described by the models commonly used to predict and analyze pile driving (Paikowsky and Whitman, 1990). Further investigation into pile-case 191 shows that the H-pile is embedded over 114 ft (35 m) into silty sand. These conditions are ideal for pile plugging to occur and, therefore, plugging can be attributed to the force match disagreement at $2L/C$ and again at $4L/C$ by TEPWAP as shown in Figure 3.2.

The final summary of results from TEPWAP analyses is produced for each case (see Figure 3.8 for example). These summaries allow the user to investigate the compressive and tensile stresses developed in the pile during driving (e.g., concrete piles) as well as the side and tip resistance and the measured and calculated energy delivered to the pile. All of the pile-cases that were analyzed using TEPWAP are footnoted in the data set tables found in Appendix A. The Case damping coefficients for these cases were calculated as part of the INTEGRATE output as previously stated.

It should be noted that the additional pile-cases that were added to the PD/LT and PD/LT2 databases (Paikowsky et al., 1994 and Paikowsky and LaBelle, 1994) all fell into Group 1 as described above. For each pile-case of the added data there was a complete CAPWAP analysis as well as a static load test to failure.

3.3 U-MASS LOWELL/UKRAINE DATABASE

The U-Mass Lowell/Ukraine database consists of static load test data compiled by Dr. Operstein from the Research Design Institute at Dniepropetvorsk, Ukraine. Dr. Operstein, currently with the Technion, Israel Institute of Technology, revisited the research Design Institute in 1997 and obtained data and graphical results for about 176 full-scale pile cases carried out to failure. The piles were tested under the conventional static load-test method (Standard test) and the static cyclic test. The reader is referred to the research report entitled "Express Method of Pile testing by Static Cyclic Loading" by Paikowsky et al., (1999) for more detailed analysis of this database. The data from the U-Mass Lowell/Ukraine database was used to evaluate

the effect of the type of static load test that is completed on the static pile capacity that is determined from the static load test results. A total of 81 piles that had both a standard static load test completed as well as static cyclic load test were used in this analysis. The analysis of the effect of the type of static load test that is completed on the static load test results is presented in section 4.5.3. The database is presented in its entirety in Appendix A as well as in the above referenced report.

3.4 GRLWEAP DATABASE

The GRLWEAP database was compiled for the sole purpose of analyzing the performance of the WEAP method for determining pile capacity at the EOD using default values. Therefore, each of the pile-cases obtained contain a static load test to failure as well as a WEAP analysis at the end of pile driving. The data were obtained from GRL Inc. and consists of 99 pile-cases that have a static load tests to failure that were analyzed using Davisson's criterion, as well standard and corrected WEAP analyses at the EOD and BOR. The evaluation of the performance of the WEAP method is presented in section 6.2.1. Table A.3 in Appendix A presents the data in the GRLWEAP database.

3.5 CASE METHOD DATABASE

Similar to the GRLWEAP database the Case method database was compiled to evaluate the performance of the Case method at the EOD. The data found in this database was obtained from Mike McVay of the University of Florida. All of the piles found within the database were driven in Florida. A total of 40 piles with a Case method evaluation at the EOD and a static load test to failure are contained within the

Case database. Also found in the Case database are 37 piles with a Case method analysis at the BOR as well as a static load test to failure. The evaluation of the Case method is presented in section 6.3.4 and a table showing all of the data in the Case database is presented in Appendix A.

3.6 PD2000 DATABASE

The PD2000 database was compiled by Kevin O'Malley and was compiled in such a manner that the Energy Approach results at the EOD could be compared to the CAPWAP/TEPWAP results at the BOR. The database includes pile-cases for which dynamic analysis was completed both at the EOD (Energy Approach) and the BOR (CAPWAP/TEPWAP). There was no record showing that a static load test to failure was completed on any of these piles. Chapter 7 presents the comparison between the Energy Approach predictions at the EOD and the CAPWAP/TEPWAP predictions at the BOR. A presentation of the data found in the PD2000 database is shown in Appendix A.

3.7 PD/LTT2000 DATABASE

The PD/LTT2000 database consists of driven piles that had a static load test to failure as well as dynamic measurements taken at the EOD and on two or more restrikes. The data contained in this database was taken directly out of the PD/LT2000 database; it also contains two test piles that were analyzed by Edward Hajduk of the Geotechnical Engineering Research Laboratory at the University of Massachusetts Lowell (Paikowsky and Hajduk, 1999 and Paikowsky and Hajduk, 2000). The database presents the phenomenon of pile capacity gain over time for piles driven into

cohesive soils. The database was also used to evaluate the optimum time to perform restrikes on driven piles to obtain the most accurate prediction of pile capacity. The analyses that were completed using this database are presented in chapter 8. All of the data found in the PD/LTT2000 database is presented in Appendix A.

Table 3.1. Summary of the Data in the PD/LT2000 database.

Pile Types		Geographical Location		Soil Types			Soil Inertia			Type of Data		Pile Capacities	
Pile Type	No.	Location	No.	Soil Type	Side	Tip	Criteria	Blow Count	A _R	Time	No.	Range (kN)	No.
<i>H-Pile</i>	37	<i>NE USA</i>	44	<i>Clay & Till</i>	67	61	≥ 16 blows per 10cm	272	-----	<i>EOD & BOR</i>	92	0-445	2
<i>OEP</i>	10	<i>SE USA</i>	69									445-890	6
<i>CEP</i>	61	<i>North USA</i>	24							<i>EOD & BOR's</i>	30	890-1334	17
<i>Voided Conc.</i>	35	<i>South USA</i>	10									1334-1779	44
<i>Sq. Conc.</i>	254	9	<i>NW USA</i>	<i>Rock</i>	0	11	< 16 blows per 10cm	112	-----	<i>EOD</i>	135	1779-2224	27
	305	5	<i>SW USA</i>									2224-2669	25
	356	8	<i>Australia</i>							<i>BOR</i>	239	2669-3114	15
	406	1	<i>Brunswick</i>									3114-3559	10
	457	8	<i>Holland</i>	<i>Sand & Silt</i>	140	137	≥ 350	-----	134	<i>EOR</i>	11	3559-4003	13
	508	8	<i>Hong Kong</i>									4003-4448	13
	610	16	<i>Israel</i>				< 350	-----	255	<i>DD</i>	2	4448-4893	11
	762	5	<i>Ontario</i>									4893-5338	6
<i>Octagonal Concrete</i>	3	<i>Sweden</i>	1	<i>NA</i>	3	1	<i>Unknown</i>	5	-----	<i>DR</i>	1	5338-5783	5
		<i>NA</i>	6									5783-6228	4
<i>Timber</i>	2									<i>ALT</i>	1	6228-6672	6
<i>Monotube</i>	2											>6672	6
Total	210	-----	210	-----	210	210	-----	389	389	-----	389	-----	210

- Notes:**
- | | | |
|--------------------------------|------------------------------------|---------------------------------------|
| 1. OEP - Open Ended Pipe Pile | 7. DR - During Restrike | 13. North USA - FHWA Regions 5, 7 & 8 |
| 2. CEP - Close Ended Pipe Pile | 8. ALT - Alternate measurement | 14. South USA - FHWA Region 6 |
| 3. EOD - End of Driving | 9. A _R - Area Ratio | 15. NE USA - FHWA Regions 1, 2 & 3 |
| 4. BOR - Beginning of Restrike | 10. No. - Number of Piles/Cases | 16. SE USA - FHWA Region 4 |
| 5. EOR - End of Restrike | 11. NA - Non-Applicable/Unknown | 17. NW USA - FHWA Region 10 |
| 6. DD - During Driving | 12. USA - United States of America | 18. SW USA - FHWA Region 9 |

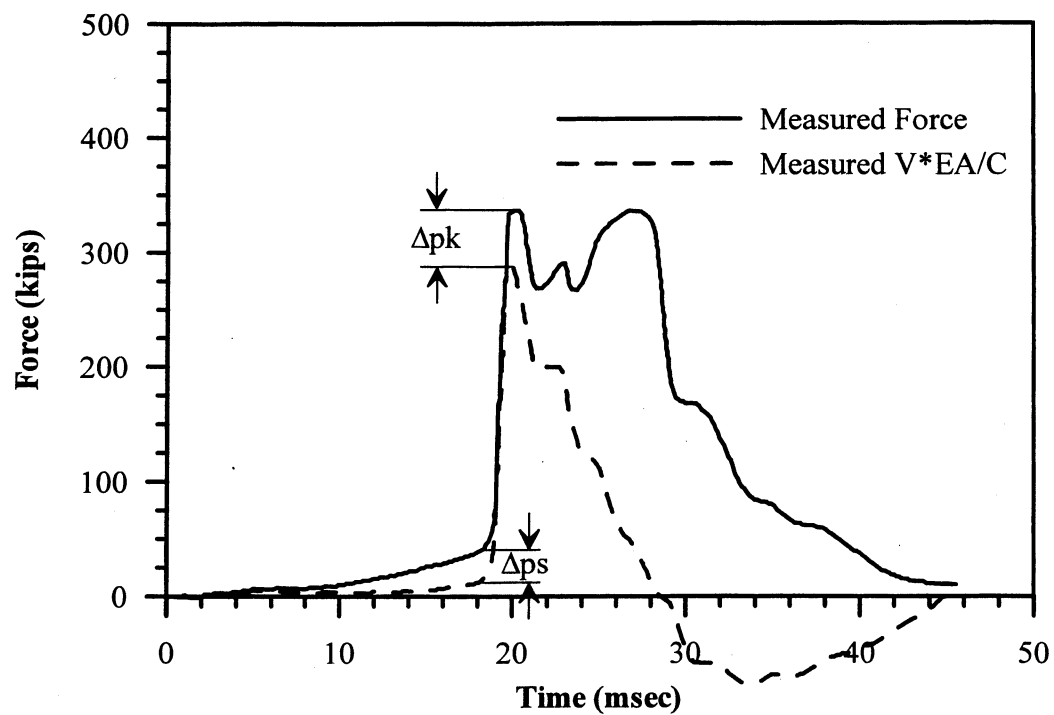


Figure 3.1. Force and velocity ($V \cdot EA/C$) traces of pile-case 1, a steel HP12x74 that needed a force correction (not to scale).

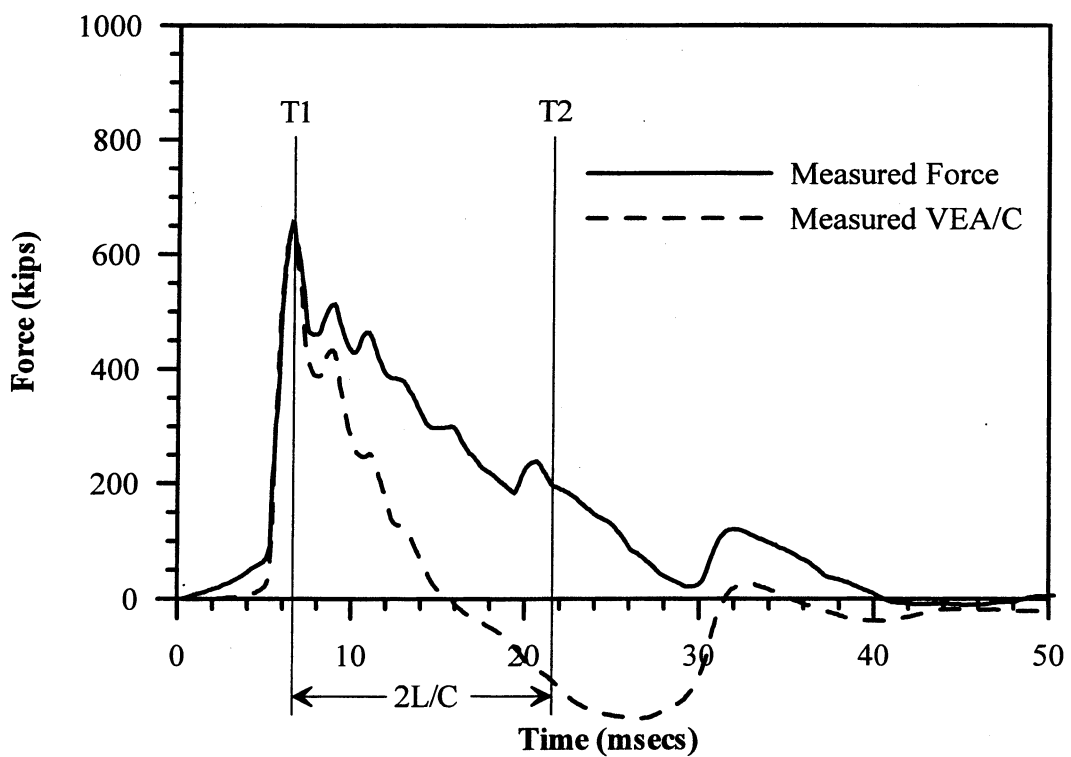


Figure 3.2. Digitized force and velocity multiplied by the impedance (EA/C) traces for pile-case 190 used for input into INTEGRATE.

**UMASS-LOWELL GEOTECHNICAL ENGINEERING
DYNAMIC PILE TESTING**

SUMMARY OF INPUT PARAMETERS

File	33P1BOR
Pile Location	Site 33
Date of Analysis	2-10-92
Pile Designation	33P1-BOR
Pile Type	HP12x74
Hammer Type	B-400
Nominal Energy of Hammer (ft-kips)	46
Penetration Depth (ft)	114.4
2L/C (msecs)	14.39
Time Interval (msecs)	0.1
Pile Impedance – EA/C (kip/sec/ft)	38.9
Final Blow Count (blows/inch)	16
T2 (offset from T1) (msecs)	14.39

SUMMARY OF OUTPUT PARAMETERS

D _{max}	0.787
D _{final}	0.164
Hammer Efficiency (%)	69.14
E _{max} (kip-ft)	31.80
E _{final} (kip-ft)	25.55
V _{max} (ft/sec)	15.78
V _{final} (ft/sec)	0.420
F _{max} (kips)	637.38
F _{final} (kips)	42.02
J	-0.017
F1 (kips)	637.38
F2 (kips)	192.10
V1 (ft/sec)	15.78
V2 (ft/sec)	-3.59
(V1*EA/C)/F1	0.963

PILE CAPACITY (kips)

Davisson's Criteria	800
Shape of Curve	800
D = 0.1B	598
D = 1 inch	522
DeBeers log method	800
Final R _s	800
CASE RTL	792
CAPWAP	715
Energy Approach R _u (uncorrected)	898

Figure 3.3. INTEGRATE output of pile-case 190 showing the back-calculated Jc value and the Energy Approach prediction.

UNIVERSITY OF MASSACHUSETTS - LOWELL
GEOTECHNICAL ENGINEERING
TEPWAP ANALYSIS

=====

IDENTIFICATION DATA

=====

Job Number TP1EOD
 Job Name 33_P
 Date of Driving 10-28-77
 Pile Designation H
 Type of Pile HP 12x74
 Pile Length (ft) 121
 Type of Hammer B-400
 Nominal Energy of Hammer (ft-kips) 46
 Depth of Penetration (ft) 114.4
 Element Length (ft) 5.26
 Damping Model Smith
 Number of Blows per last three inches 13, 13, 12
 Date of Analysis 9-16-92
 PDA Blow # 2
 Iteration # 1
 Time Interval 0.200
 Option Number 2

=====

Figure 3.4. Example of the pile identification information of pile-case 189 used as input for the TEPWAP analysis.

UNIVERSITY OF MASSACHUSETTS - LOWELL
GEOTECHNICAL ENGINEERING
TEPWAP ANALYSIS

=====

SOIL AND PILE PROPERTIES ALONG PILE ELEMENTS

=====

element no.	dist. from gauges (ft)	area (in ²)	weight (lbs)	stiffn (k/in)	resist (kips)	sum of resist (kips)	damp (s/ft)	quake (in)	quake rebnd ratio (%)	upwrd resist ratio (%)
3	5.3	21.8	390.1	10364	0.0	439.0	0.000	0.000	0.0	0.0
4	10.5	21.8	390.1	10364	5.0	434.0	0.020	0.300	100.0	-50.0
5	15.8	21.8	390.1	10364	5.0	429.0	0.020	0.300	100.0	-50.0
6	21.0	21.8	390.1	10364	5.0	424.0	0.020	0.300	100.0	-50.0
7	26.3	21.8	390.1	10364	5.0	419.0	0.020	0.300	100.0	-50.0
8	31.6	21.8	390.1	10364	5.0	414.0	0.020	0.300	100.0	-50.0
9	38.8	21.8	390.1	10364	0.0	414.0	0.010	0.300	100.0	-50.0
10	42.1	21.8	390.1	10364	0.0	414.0	0.010	0.300	100.0	-50.0
11	47.3	21.8	390.1	10364	0.0	414.0	0.010	0.300	100.0	-50.0
12	52.6	21.8	390.1	10364	0.0	414.0	0.010	0.300	100.0	-50.0
13	57.9	21.8	390.1	10364	0.0	414.0	0.010	0.300	100.0	-50.0
14	63.1	21.8	390.1	10364	5.0	409.0	0.010	0.300	100.0	-50.0
15	68.4	21.8	390.1	10364	5.0	404.0	0.010	0.300	100.0	-50.0
16	73.6	21.8	390.1	10364	8.0	396.0	0.010	0.300	100.0	-50.0
17	78.9	21.8	390.1	10364	8.0	388.0	0.010	0.300	100.0	-50.0
18	84.2	21.8	390.1	10364	8.0	380.0	0.010	0.300	100.0	-50.0
19	89.4	21.8	390.1	10364	8.0	372.0	0.010	0.300	100.0	-50.0
20	94.7	21.8	390.1	10364	8.0	364.0	0.010	0.300	100.0	-50.0
21	99.9	21.8	390.1	10364	8.0	356.0	0.010	0.300	100.0	-50.0
22	105.2	21.8	390.1	10364	8.0	348.0	0.010	0.300	100.0	-50.0
23	110.5	21.8	390.1	10364	8.0	340.0	0.010	0.300	100.0	-50.0
24	115.7	21.8	390.1	10364	80.0	260.0	0.090	0.150	100.0	-50.0
25	121.0	21.8	390.1	10364	100.0	160.0	0.080	0.150	100.0	-50.0
tip					160.0	0.0	0.080	0.150	100.0	

Figure 3.5. Example of the soil and pile properties used along the pile elements of pile-case 189 as input for the TEPWAP analysis.

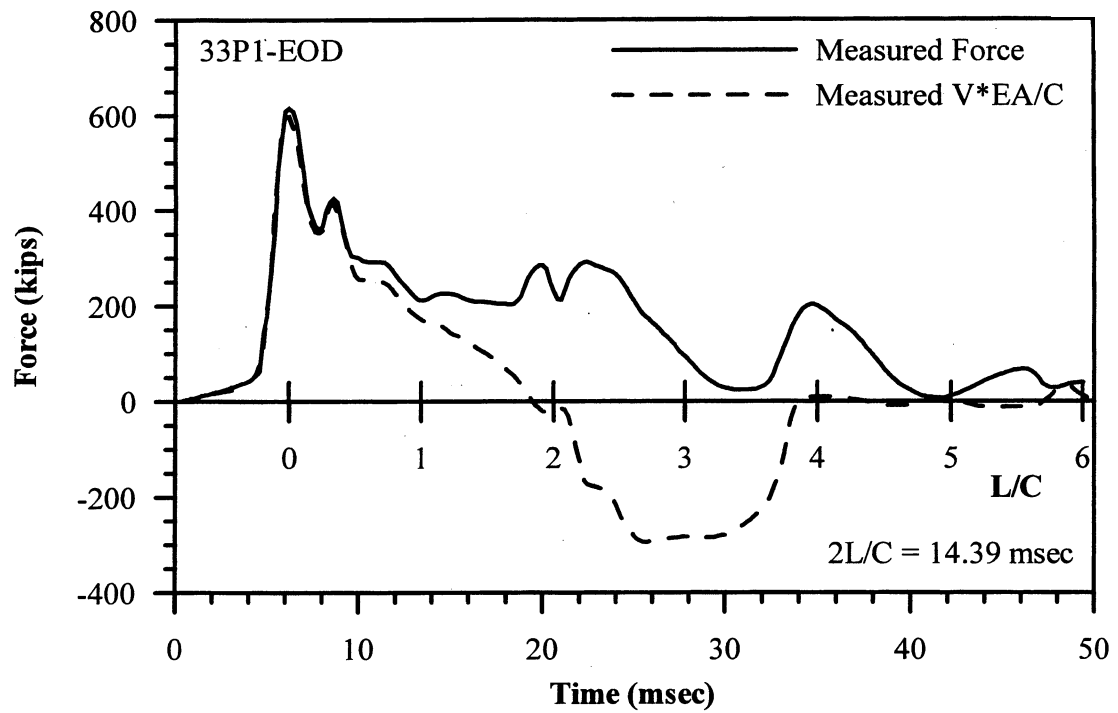


Figure 3.6. Measured force and velocity multiplied by the impedance (EA/C) traces of pile-case 189 used by the TEPWAP analysis.

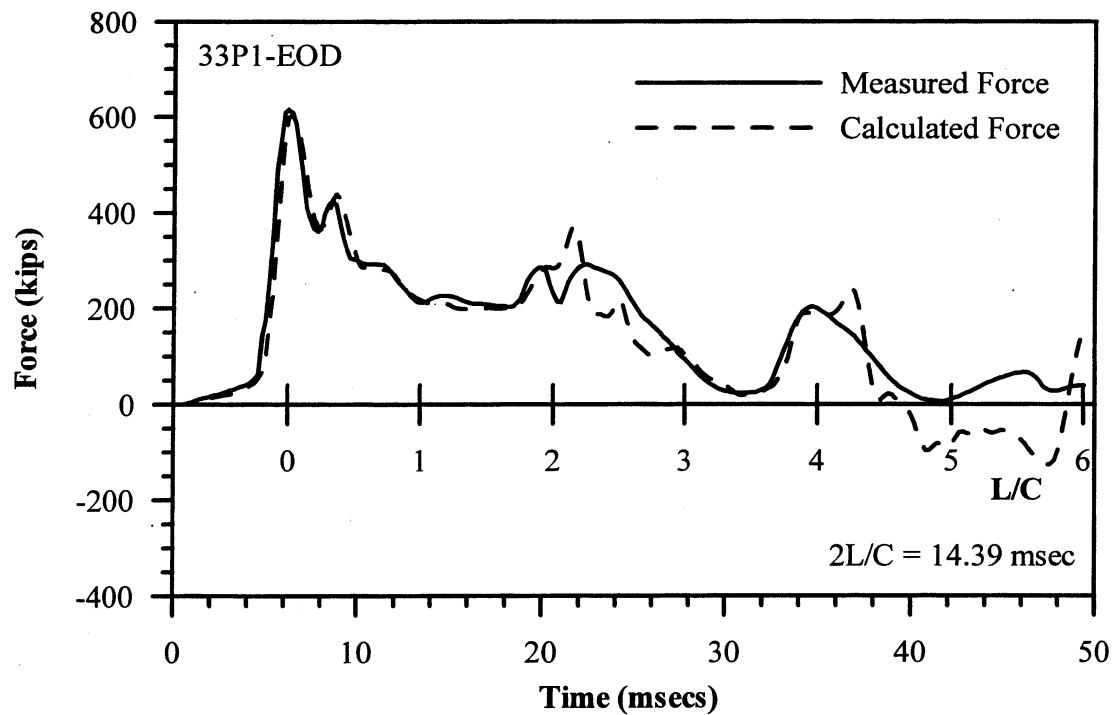


Figure 3.7. Comparison between measured force near the top of pile-case 189 and the calculated force from the TEPWAP analysis.

UNIVERSITY OF MASSACHUSETTS - LOWELL
GEOTECHNICAL ENGINEERING
TEPWAP ANALYSIS

SUMMARY OF FINAL RESULTS

End Resistance	-	160.0 kips
Side Friction	-	279.0 kips
Total Capacity	-	439.0 kips

Percent in Friction	-	63.6%
---------------------	---	-------

Top Quake	-	0.79 inches
Set at Tip	-	0.32 inches

The Set Corresponds to 3 Blows Per Inch.

Maximum Calculated Energy	-	32.362 kip*ft
Maximum Measured Energy	-	32.674 kip*ft

Energy Difference (Calc – Measured)	-	-0.312 kip*ft
-------------------------------------	---	---------------

Maximum Compression force is in element #3 on iteration 32	-	636.49 kips
---	---	-------------

Maximum Tension force is in element #19 on iteration 181	-	-139.18 kips
---	---	--------------

The Maximum Stress is	-	29.20 kips/in ²
The Minimum Stress is	-	-6.38 kips/in ²

Figure 3.8. Summary of the final results from TEPWAP analysis performed on pile-case 189.

CHAPTER 4

REFERENCE STATIC CAPACITY

4.1 OVERVIEW

Different methods of analysis are used for the interpretation of load-settlement curves obtained from static load tests of piles. Many of the methods are subjective, resulting in a different static capacity from method to method and from engineer to engineer for the same static load test curve.

4.2 OBJECTIVES

The aim of the work presented in this chapter is to determine statistically if there is one method for analyzing pile capacity based on the static load-settlement curve that provides consistent and "correct" results. The main purposes in assigning one method for use in analyzing pile capacity are; (a) that there will be consistency in the pile capacity determination in general and (b) in the present LRFD parameter determination, predictive methods are compared to the "correct" capacity and one uniform approach is required.

4.3 PILE FAILURE / CAPACITY DETERMINATION

4.3.1 Background

A universal criterion capable of establishing the ultimate capacity of a pile is essential in improving the accuracy of static load test interpretations. Various ultimate

load criteria have been proposed and used by researchers and design organizations (see for example Vesic, 1977 and Fellenius, 1989). Significant disagreements remain among these methods as they are based on different principles and produce different values under varying pile types and sizes, load test procedures, and surrounding soils.

Vesic (1972) pointed out that interpreting a pile's ultimate load based solely on a visual examination of its load-settlement curve (i.e. shape of the curve) may be misleading and can result in different pile capacities depending on the scale used to plot the curve. Figure 4.1 and 4.2 demonstrate this point by presenting the same load-settlement relations using two different scales. Figure 4.1 shows a load-settlement curve indicating a pile capacity of approximately 4430 kN whereas the curve in Figure 4.2 suggests that the pile's displacement at 4430 kN may still be based on the elastic compression of the pile and that the pile capacity is approximately 4800 kN. One solution to this problem is to implement a common scale, based on the pile's elastic deformation. When plotting load-settlement curves, the elastic deformation of a fixed end column, (i.e., frictionless pile) is expressed as:

$$\delta = \frac{PL}{EA} \quad (4.1)$$

Where:

- δ = the calculated elastic deformation of the pile
- P = the applied load
- L = pile length
- E = elastic modulus of the pile material
- A = cross sectional area of the pile.

The elastic compression line obtained by Equation 4.1 is based on the assumption that the entire load applied to the pile top is transferred to the pile toe. To implement a

scale proportional to all load settlement curves, the elastic compression line should be inclined at an angle of approximately 20 degrees to the load axis (see Figure 4.3).

4.3.2 Method of Approach

In order to facilitate the aforementioned uniform scale, all of the load-settlement curves in the dataset PD/LT were digitized using the program DIGITIZE, developed at UMASS-Lowell by Chernauskas and Paikowsky. These curves were then replotted, using the graphics software GRAPHER, to produce curves that were proportional to each pile's elastic compression line inclined at 20 degrees.

After replotting, each load-settlement curve was analyzed using five different failure load interpretation procedures: Davisson's Criterion, the Shape of Curve method, Limited Total Settlement methods ($\Delta = 25.4$ mm (1 inch) and $\Delta = 0.1B$), and DeBeer's method.

4.3.3 Davisson's Criterion

The Davisson Criterion, (Davisson, 1972), or offset limit, defines the failure load of a pile as the load corresponding to the settlement which exceeds the elastic compression of the pile, by an offset, X , equal to 3.81 mm plus a factor equal to the diameter of the pile divided by 120. The offset is simply:

$$X = 3.81 + \frac{B}{120} \quad (4.2)$$

Where: B = the diameter of the pile in mm.

The Davisson's Criterion line is parallel to the elastic compression line and predicts the failure load at its intersection with the load-settlement curve. Figure 4.3 illustrates

the use of Davisson's failure criterion for load-settlement relations of pile-case 344, yielding a capacity of 4235 kN.

4.3.4 The Shape of Curve Method

The Shape of Curve method is a failure load approximation, which usually yields a range of values over which the pile is considered at or near failure. The boundaries of this range can be determined by examining the minimum curvature in the load-settlement curve through lines drawn tangent to the load-settlement curve (similar to the method proposed by Butler and Hoy (1977)). The failure range is relatively easy to define for load-settlement curves that exhibit general failure or plunging failure (rapid settlement with slightly increased loads) (see Figure 4.3 for example). Piles that experience local failure, or non-plunging failure, are difficult to analyze using the shape of curve method because of the uniform changes in slope of lines drawn tangent to the curve. Figure 4.3 illustrates the use of the 'shape of curve' procedure yielding an estimated capacity as a range between 4060 kN and 4800 kN.

4.3.5 The Limited Total Settlement Methods

The Limited Total Settlement methods, $\Delta = 25.4 \text{ mm}$ and $\Delta = 0.1B$ (Terzaghi, 1942), define the failure load as the load corresponding to settlements of 25.4 mm and 0.1B, respectively, where B is the diameter of the pile. These methods are not applicable in many cases. For example, the elastic compression for a very long steel pile often exceeds 25.4 mm and/or 0.1B without inducing any plastic deformation in the soil. Figure 4.3 shows as an example a load-settlement curve for pile-case 344, a 16" square concrete pile, that experiences a plunging failure before a displacement of

25.4 mm. Also, it is obvious that a settlement of 0.1B, or 40.64 mm in this case, does not represent the failure load of this pile and therefore is not applicable.

4.3.6 DeBeer's log-log Method

DeBeer (1970) defines the failure load as the load corresponding to the intersection of two distinct slopes created by the load-settlement data plotted using logarithmic scales. Figure 4.4 illustrates the use of DeBeer's criteria for the load-settlement curve of pile-case 344 leading to an estimated capacity as a range between 3960 kN and 4800 kN. The two slopes are especially visible for piles that experience plunging failures, yet when using DeBeer's method piles that undergo local failures, the result may be a range of values, such as illustrated here. As mentioned earlier, each load-settlement curve was digitized from the standard linear plots that they were presented on and the data was stored. This data was later plotted in logarithmic scales to utilize DeBeer's method.

4.3.7 The Representative Static Capacity

The capacity results for each method were reviewed independently based on the load-settlement curves for each pile. After considering the pile type, soil type, size of each pile and the load test procedure, unrealistic results were eliminated, and the acceptable values were averaged, yielding a final static capacity, R_s . For example, for pile-case 344 presented in Figures 4.3 and 4.4 the considered criteria were: Davisson's = 4235 kN, shape of curve = 4060 - 4800 kN, 25.4 mm settlement = 4800 kN, 0.1B settlement = NA, and DeBeer's = 3960 - 4804 kN. Excluding the 0.1B settlement

method, which is not applicable, the average of all the criteria led to a final static resistance assessment of $R_s = 4462$ kN.

4.4 PERFORMANCE EVALUATION OF THE DIFFERENT FAILURE CRITERION METHODS

4.4.1 Method of Approach

Each of the methods described above was evaluated by comparing the capacity determined by that particular method to the representative pile capacity. The analysis was completed using 196 piles from the database PD/LT2000. The analysis used a K_{SX} value, which is the ratio of the representative capacity to the capacity determined by the method being analyzed. The subscript S in the K value corresponds to the representative static capacity. The X value is substituted for different letters depending on the method that was being analyzed. The subscripts were used as follows; D is used for the Davisson's criterion, B is used for the DeBeer method, L is used for the method of limiting the total settlement to $\Delta = 0.1B$, T is used for the method of limiting total settlement to 25.4 mm, and C is used for the Shape of Curve method. As an example, if the ratio is labeled K_{SD} it is the representative pile capacity divided by the Davisson's criterion capacity. A mean and standard deviation of the K_{SX} value were calculated for each of the five methods of pile capacity analysis. To evaluate each method a graph was generated presenting the normal and lognormal distributions as well as the actual data distribution in the form of a bar chart. The bar charts were generated by graphing the total number of K_{SX} values within a 0.02 interval versus that range of K_{SX} values. The graphs for all methods of analysis were plotted at the same scale so that comparisons could be made between them.

Conclusions could then be drawn, by comparing the figures, as to which method should be used in the analysis of static load test curves if the analysis is limited to one method. The following sections present the results of these analyses.

4.4.2 Davisson's Criterion

Figure 4.5 shows the normal and lognormal distributions of the K_{SD} value, which represents the ratio of the representative pile capacity to the capacity determined by Davisson's criterion. A total of 186 piles were used in the evaluation of the Davisson's criterion. For 10 piles, Davisson's criterion could not be applied. In nine (9) of these piles, the maximum settlement was less than the failure criterion and for the tenth pile; the pile capacity according to Davisson's criterion was below the the range of load in which the failure took place. The mean K_{SD} is 1.018 with a standard deviation of 0.1010 while the mean using the lognormal distribution is 1.013 with a standard deviation of 0.0892. The coefficient of variation, which is the ratio of the standard deviation to the mean, is 9.9%; statistically indicating that Davisson's criterion is a good method for use in analyzing static load test curves as it matches well the designated representative capacity. The bar chart, which shows the actual data for the K_{SD} values compares relatively well with the normal and lognormal distributions, the major exception being the large number of K_{SD} values, (40 and 36), concentrating in the ranges from 0.970 to 0.990 and 0.990 to 1.010, respectively, (total of 41% between 0.970 and 1.010). Figure 4.6 shows that there is no clear correlation between the K_{SD} value and the pile diameter. From the presented results the

Davisson's criterion method is an adequate method to use in the analysis of static load tests.

4.4.3 The Shape of Curve Method

The normal and lognormal distributions of the K_{SC} value, which is the ratio of the representative pile capacity to the capacity determined by the Shape of Curve method, are presented in Figure 4.7. A total of 193 piles were used in the evaluation of the Shape of Curve method. There were three cases for which the Shape of Curve method could not be applied; as the load settlement relationship was a gradual consistent curve without a clear point of failure. The mean K_{SC} for the 193 piles is 1.019 with a standard deviation of 0.0661 while the mean for the lognormal distribution is 1.017 with a standard deviation of 0.0596. The bar chart shows a good comparison between the actual data and the normal and lognormal distributions. The ranges from 0.990 to 1.010 and 1.010 to 1.030 show a large number of K_{SC} values, 57 and 38, respectively, (total of 49.2% between 0.990 and 1.030), which are close to the calculated mean values. This shows that for the majority of the cases the performance of the method is actually better than what is shown by the means and standard deviations. The relationships presented in Figure 4.8 suggest that there is no correlation between the K_{SC} value and the pile diameter. The obtained results indicate that the Shape of Curve method is an excellent method to use in the analysis of static load tests, with the only drawback being that the method is subjective.

4.4.4 Limiting Total Settlement to 25.4 mm

The K_{ST} value is the ratio of the representative pile capacity to the capacity determined by the load that relates to the settlement of the pile equal to 25.4 mm. There were 161 piles that met the failure criterion of $\Delta = 25.4$ mm. There were 35 piles for which the limiting total settlement to 25.4 mm could not be applied, as the maximum settlement of the piles was smaller than the failure criterion. The normal and lognormal distributions of the K_{ST} values are shown in Figure 4.9 with a mean and standard deviation of 0.971 and 0.0981, respectively, for the normal distribution and 0.967 and 0.0959, respectively, for the lognormal distribution. There is a superior match between the bar chart, which shows the actual data, and the calculated normal and lognormal distributions. There are 4 ranges that have the highest and approximately the same number of K_{ST} values, 18 and 19, and the ranges are from 0.910 to 0.990 in 0.02 intervals, (total of 46.6% between 0.910 and 0.990). Figure 4.10 shows that there may be a correlation between the K_{ST} value and the pile diameter but there is not enough data to allow for conclusive observations. These results suggest that limiting the total settlement to 25.4 mm provides a good method to use in the analysis of static load tests, the drawback being that there are a significant number of piles that have failed before the failure criterion is reached, hence, the criterion maybe associated with the pile geometry and type of failure.

4.4.5 Limiting Total Settlement to One Tenth of the Pile Diameter

Figure 4.11 shows the normal and lognormal distributions of the K_{SL} value, which is the ratio of the representative pile capacity to the capacity determined by

taking the pile capacity as the load at a settlement equal to one tenth of the diameter of the pile. There were only 90 piles for which this method could have been applied. For 106 piles this failure criterion could not have been applied because the maximum settlement of the piles did not reach ten percent of the pile's diameter. The mean K_{SL} value for the normal distribution is 0.938 with a standard deviation of 0.1144 while the mean for the lognormal distribution is 0.932 with a standard deviation of 0.1215. The match between the bar chart, which shows the actual data, and the normal and lognormal distributions is not very good because the actual data is erratic. The highest number of K_{SL} values, 17, is in the range from 0.970 to 0.990, (total of 18.9% between 0.970 and 0.990), which is slightly higher than the mean of 0.938. Figure 4.12 in general shows that as the pile diameter increases this criterion shows more and more higher results than the designated static capacity (lower K_{SL}). These results show that the limiting total settlement to one tenth of the pile diameter is not a good method to use in the analysis of static load tests because over half of the piles have failed before the failure criterion is reached and the statistical data is not very supportive of the method.

4.4.6 DeBeer's log-log Method

The normal and lognormal distributions of the K_{SB} value, which is the ratio of the representative pile capacity to the capacity determined by the DeBeer's method, are shown in Figure 4.13. A total of 187 piles were used in the evaluation of DeBeer's method of analysis for static load test curves. There were 9 piles for which the method could not have been applied because the load settlement relationship on a log-log scale

did not result in an identifiable change in orientation. The mean K_{SB} value for the 187 piles is 1.033 with a standard deviation of 0.0877 while the mean for the lognormal distribution is 1.030 with a standard deviation of 0.0816. These statistics show that this is a good method of analysis as the coefficient of variation is approximately 8.5%. The bar chart shows a good comparison between the actual data and the normal and lognormal distributions, the exception being the two peaks with a high number of K_{SB} values, 39 and 29, in the ranges from 0.990 to 1.010 and 1.010 to 1.030, respectively, (total of 36.4% between 0.990 and 1.030). Figure 4.14 shows that there is no correlation between the K_{SB} value and the pile diameter. The obtained results suggest that the DeBeer method is an excellent procedure to be used in the analysis of static load tests. The drawback of the DeBeer method is that it is by and large a subjective method that provides a narrow band of possible capacity outcome under the conditions of a clear general failure.

4.4.7 Intermediate Conclusions

The analyses and their graphical representation as provided in the previous section allows for an educated evaluation of the load test interpretation methods and the possible selection of a single method of analysis rather than a representative pile capacity. Table 1 provides a complete summary of the mean and standard deviation of the K_{SX} value for each of the methods as well as some other significant information for comparison purposes. Figure 4.15 shows a comparison of the normal distribution curves for the five methods used to determine the pile capacities.

The Shape of Curve and DeBeer methods show a good correlation between the normal and lognormal distributions to the actual data. The mean K_{SX} value for each of the methods is close to one with a small standard deviation. For the majority of the pile-cases using the Shape of Curve method, 179 of 193 pile-cases, the K_{SC} values fall within the range of 0.90 to 1.10. For most of the pile-cases using the DeBeer method (153 of 187 pile-cases) the K_{SB} values fall within the range of 0.90 to 1.10. According to these statistics alone the conclusion can be drawn that the Shape of Curve and DeBeer's methods are preferable methods for evaluating static load tests. The problem with these two methods (in particular the Shape of Curve) is that they are both subjective, the results can vary greatly from engineer to engineer, and therefore they cannot be recommended for evaluating static load test capacity under conditions that require objectivity and repetitiveness.

The method of determining the pile capacity using a total settlement ($\Delta = 25.4$ mm) seems to perform well judging by the mean and standard deviations as well as the number of K_{ST} values that fall in the range of 0.90 to 1.10, 120 of 161 pile-cases. The method is objective, but 35 piles out of the examined 196 piles did not meet the failure criterion. The method of determining pile capacity by limiting the total settlement to 25.4 mm is therefore not recommended because of the above stated disadvantage.

The method of determining the pile capacity using the failure criterion of $\Delta = 0.1B$ seemed to perform well judging by the mean and standard deviation. The number of piles that have K_{ST} values that fall within the range of 0.90 to 1.10 is also very small (59 of 90 pile-cases) compared to the other interpretation methods. These

disadvantages as well as the fact that the method could be applied to only 90 of the 196 piles that were evaluated lead to the conclusion that this method of analysis should not be used by itself (stand alone).

The intermediate conclusion of this analysis is that the one method to use in evaluating the pile capacity based on the static load test results is the Davisson's criterion. This method has a mean K_{SD} value that is close to one and the standard deviation is relatively small. In addition; for 160 of 186 pile-cases the K_{SD} value falls within the range of 0.90 to 1.10, which is satisfactory by itself. The method's major additional advantage is its objectivity so the results from the analysis should not vary much from one engineer to another. Based on the minimum and maximum K_{SD} values it is clear however that the method must be examined and judgment needs to be applied.

4.4.8 Evaluation of a Modification for Davisson's Criterion

a) The Proposed Modification

Davisson's Criterion as concluded above is the method that should be used to analyze static load test curves if only one method of analysis needs to be used. Static load tests on large diameter piles require larger settlements to develop the toe resistance, therefore, Kyfor et al., (1992), proposed that for large diameter piles (diameter greater than 610 mm), the offset to be used for Davisson's criterion should be:

$$X = \frac{B}{30} \quad (4.3)$$

Where B is the pile diameter in the units consistent with the calculated elastic deformation. The following section presents an evaluation of the proposed criterion.

b) The Performance of the Proposed Modification

Thirty-one (31) piles of database PD/LT2000 belong to the large diameter pile category, for which the load-settlement curves were reanalyzed based on the modified criterion and new pile capacities were determined. Figure 4.16 presents the normal and lognormal distributions of the K_{SD} and K_{SLD} values for the large diameter piles in PD/LT2000. K_{SLD} represents the ratio of the representative pile capacity to the capacity determined by the Davisson's criterion method using the offset given in Equation 4.3 for the large diameter piles. Of the 31 piles that fall into the large diameter pile category only 20 meet the Davisson's failure criterion using the modified offset. Using the original offset there was only one pile that did not meet the Davisson's failure criterion. Using the modified offset caused ten additional cases (out of the 31) to be excluded from the Davisson's failure criterion. These were excluded because the settlement of the pile did not reach the failure criterion. This information alone raises doubts about the applicability of the modified offset for large diameter piles as it significantly decreases the number of piles that meet the failure criterion. As shown in Figure 4.16 for the thirty-one large diameter piles, the mean K_{SLD} is 0.920, while the mean K_{SD} is 0.994, which is much better. The standard deviation of the K_{SLD} values is 0.0714, which is slightly better than that of the standard deviation for the K_{SD} values, 0.0749. The lognormal distribution statistics also show that the original offset gives better results than the modified offset based on the 31

large diameter piles. The bar chart, which shows the actual data for the K_{SLD} values compares relatively well with the normal and lognormal distributions, with the exception being the two ranges from 0.970 to 0.990 and 0.990 to 1.010 with large numbers of K_{SLD} values, 36 and 31, respectively. Figure 4.17 shows that there is no correlation between the K_{SLD} value and the pile diameter. The results of this analysis has lead the authors to the conclusion that the single method of choice for analyzing static load test results is the Davisson's criterion method and the correction for large diameter piles should not be used.

4.5 STATIC LOAD TEST PROCEDURE

4.5.1 Overview

This section reviews common procedures used when performing a static load test in the United States. The ASTM, Massachusetts Highway Department, Massachusetts Building Code, and the Texas Quick Test procedures are described and briefly analyzed. Detailed comparisons are held between two methods; the slow maintained and short duration load tests as well as the static cyclic test. The influence of creep on the static load test results when using two different static load test procedures is examined and some new research data are presented. The material presented in this section is based on the Paikowsky et al., (1999).

4.5.2 Load Test Procedures

a) ASTM Procedures

The American Standard for Testing and Materials (ASTM) provides four static load test procedures, which include the standard loading procedure, cyclic loading,

quick load test, and constant rate of penetration. These procedures are described briefly below, for more details refer to ASTM (1998).

Standard Loading Procedure

The standard ASTM method calls for piles to be loaded to 200% of the anticipated design load, unless failure occurs first. The pile shall be loaded in increments of 25% of the total test load. Each load increment will be held until the rate of settlement is not greater than 0.25 mm/hr (0.01 inches per hour) but no longer than two hours per increment. In the event the pile has not failed, hold the total load on the test pile between 12 and 24 hours until the butt settlement is not greater than 0.25 mm/hr (0.01 inches per hour). After the settlement rates have been satisfied, remove the load in decrements of 25% of the total test load with one hour between decrements.

Cyclic Loading

The pile is loaded in a series of four cycles. The first cycle is loaded in increments of 25% of the total design load up to 50% and each load increment is held for one hour. At 50% the pile is unloaded in decrements of 25% until the entire load is removed from the pile with 20 minutes between decrements. Cycles two, three, and four are loaded to 100%, 150%, and 200%, respectively in increments of 50% of the total design load. Each load increment is held for one hour during each cycle. Once the maximum load is reached per cycle, the pile is unloaded to zero in decrements of 50% of the maximum applied load with 20 minutes between each unloading.

Quick Load Test Method for Individual Piles

The load is applied in increments of 10 to 15% of the design load with a constant time interval of 2.5 minutes between loading increments. Load increments are added until continuous jacking is required to hold the test load or until the specified capacity of the loading device is reached. After one of these criteria is reached, the load is held for five minutes and the full load is removed from the pile.

Constant Rate of Penetration

The pile is loaded at a constant rate of penetration 0.3 to 1.3 mm/min (0.01 to 0.05 in/min) for cohesive soils or 0.8 to 2.5 mm/hr (0.03 to 0.1 in/min) for granular soils. The pile is continually loaded until no further increase in load is necessary for the constant rate of penetration of the pile under the predetermined rate or the capacity of the pile is reached. If the pile continues to settle under the constant load, the load is held until the pile has moved at least 15% of the pile diameter and then the pile is unloaded completely. If maximum capacity of the pile is reached before failure, the total load is released.

b) Massachusetts Highway Department Procedures

The Massachusetts Highway Department uses a set of load test procedures similar to the ASTM methods. The procedures described by the Massachusetts Highway Department encompass the short duration test, maintained load test, and the quick load test. The procedures are described in detail by the Massachusetts Highway Department (1995) and briefly reviewed below.

Short Duration Test

Massachusetts Highway Department requires the load to be applied up to 200% of the design load in increments of 25%. Each load increment is held for half an hour. Once the maximum applied load is achieved, it is held for one hour and until the settlement rate is less than 25 mm/hr (1 inch per hour). After both of the above criteria are met, the load is removed in decrements of 25% of the design load every 15 minutes until zero load is reached. Finally, zero load is held for one hour to complete the test.

Maintained Load Test

The pile is tested under load increments equal to 50, 100, 150, 175, and 200% of the design load and maintained for a period of two hours. Once the maximum load is achieved, it is held until the settlement does not exceed 0.02 inches (0.5 millimeters) in a 12-hour time frame. After completion of the loading, the unloading is conducted in decrements not exceeding one quarter of the total test load and maintained for a period of four hours each.

Quick Load Test

The test shall be applied in increments of 50 to 100 kN (11 to 22 kips) and maintained for 2.5 minutes until continuous jacking is required to maintain the test load. The final load increment shall be held for no more than five minutes and then unloaded in four equal decrements.

c) *Massachusetts Building Code Procedure*

Massachusetts Building Code (5th Edition, 1996) requires the pile to be loaded to 200% of the design load in increments of 25% and each increment is held for half an hour. Once the maximum applied load is achieved, it is held for one hour or until the settlement rate is less than 25 mm/hr (1 inch per hour). After both of the above criteria are met, the load is removed in decrements of 25% of the design load every 15 minutes until zero load is reached. Finally, zero load shall be held for one hour to complete the test.

d) *Texas Quick Test Procedure*

The Texas quick test (Butler and Hoy, 1977) is a modification of the Constant Rate of Penetration Test (CRP). The CRP test advances a pile into the ground at a constant penetration rate while the force required to sustain the rate is continually adjusted. Engineers at the Texas State Department of Highways and Public Transportation simplified the CRP test. The new test requires that load be applied in 44 to 89 kN (5 to 10 ton) (or 10-15% of the design load) increments while recording the load and settlement data immediately after each load increment. Each load increment is held for 2.5 minutes before the next load increment is applied. Once the maximum load is achieved, it is held for 2.5 minutes before complete removal of the load from the pile.

e) *Static-Cyclic Load Test Procedure*

The static-cyclic approach is based on a methodology developed by Dr. Valery Operstein during her work as the Chief Engineer at Ukrspetsstroiproekt, a soils and

foundations research design institute in Dniepropetvorsk, Ukraine. A pile is loaded to failure by applying a load at a high constant rate of approximately 150 kN/min and then unloaded at a fast rate of approximately 325 kN/min. Typically a series of three load-unload cycles is performed within a time period of less than one hour. The method enables the unique determination of the ultimate pile capacity based on the load-settlement relations in the load-unload cycle, which is closely related to the fundamental physical mechanism of soil/pile interaction.

f) Summary

The static load test procedures discussed in the above sections are compiled in Table 4.2. The table summarizes the loading and unloading increments and hold times associated with each test. Figure 4.18 displays the ASTM procedures in a graphical format. The figure depicts the duration in minutes vs. percent of design load for each test and testing stage. Figure 4.19 shows the MHD procedures using the same format. The loading procedure (MBC) and standard tests are not displayed on any graph because they replicate the short duration test (MHD) and maintained load test (MHD), respectively. General hold times were used to complete each graph and it should be noted that the hold times for each test would vary depending on the soil conditions.

4.5.3 Performance Evaluation of the Load Test Procedures

a) Comparison of the Short Duration, Slow Maintained and Static Cyclic Tests

To evaluate the influence of creep on static load test results two pile case histories were analyzed. The two piles were part of a research project conducted by the University of Massachusetts Lowell Geotechnical Engineering Research

Laboratory at a bridge reconstruction site in Newbury, Massachusetts. The two test piles were labeled test pile # 2 and test pile # 3; both of these piles were tested under slow maintained, short duration and static cyclic load test procedures. The load test curves for both the slow maintained and short duration static load test types were reduced for creep and compared for both test piles.

Figure 4.20 and Figure 4.21 present the static load test curves, using the original data, for the short duration, slow maintained and static cyclic tests for test piles # 2 and # 3, respectively. In both figures it is seen that a significant creep takes place during the holding times for both the slow maintained and short duration load test types. The figures show that, even with the large settlements due to creep, the pile capacity determined by Davisson's criterion is approximately equivalent for both load test types. The static cyclic capacities, which is the load equivalent to the intersection of the load and unload curves on the load displacement graph, is approximately the same load that was determined using Davisson's criterion for both load test piles. Static cyclic load test results will be compared to pile capacities determined using Davisson's criterion on slow maintained static load tests in the following section. These two test piles load-displacement curves show that there is an insignificant influence on the load test results from the type of static load test that is completed.

To evaluate the effect of creep on the results of the load test analysis the load test curves for both test pile # 2 and # 3 were replotted using the original data reduced for creep. The new load-settlement curves are shown in Figures 4.22 and 4.23 for test piles # 2 and # 3, respectively.

Figure 4.22 presents the original short duration and slow maintained static load test curves for test pile # 2 as well as the curves that were reduced for creep. When reducing both static load test curves for creep it was apparent that the significant amount of settlement at a load of approximately 700 kN could no longer be attributed to creep but the pile had begun to plunge. The pile capacity based on Davisson's criterion for both types of static load test is approximately the same. The analysis of test pile # 2 suggests that there is no influence of the static load test results (designated failure) based on the type of static load test performed.

Figure 4.23 presents the slow maintained and short duration static load test curves using both the original data and the data reduced for creep for test pile # 3. The presented load-settlement relations suggest that test pile # 3 begins to fail by plunging at approximately 1200 kN. The settlement at this load is too large to be attributed to creep. Evaluating this pile's capacity based on Davisson's criterion and the two types of static load tests; results in a pile capacity of approximately 1200 kN with little or no influence of the load test type.

b) Comparison between the Static-Cyclic Load Testing and Slow Maintained Tests Using Davisson's Capacity

In order to further evaluate whether the static load test capacity is influenced by the static load test procedure, a comparison between results obtained using the static cyclic and slow maintained load tests was made. A database compiled by Dr. Valerie Operstein and the University of Massachusetts - Lowell presented by Paikowsky et al., (1999) was used. The database contains 81 piles, which were statically load tested using both methods, but there were 6 piles for which the

Davisson's criterion did not apply to the slow maintained test. Figure 4.24 shows a comparison between the pile capacity determined using Davisson's criterion for the slow maintained load test and the static cyclic capacity. The mean K_{SCYC} of 0.930 and standard deviation of 0.136 show that the results determined using each load test method are very similar and there is no significant difference. A few of the cases shown on the graph do show a fairly large discrepancy between the results from each of the load tests. This is due to limiting the analysis of the slow maintained test to a single method. As shown in Table 4.3 the statistics, the mean of 1.023 for the ratio between the representative pile capacity for the slow maintained test and the static cyclic results and its standard deviation, 0.057, show that when a representative pile capacity is used the two load test methods give almost identical results. The results of this analysis show that the load test results are not significantly influenced by the procedure of the static load test.

c) *Intermediate Conclusions*

The influence of the static load test procedure on the chosen pile capacity based on the above two analyses is insignificant. As only a small number of pile-cases exist for which multiple types of static load tests to failure were completed the above analysis of the two piles at the Newbury site is rare but it has lead the authors to the above conclusion. The extensive research on the static-cyclic load testing procedure that was recently completed (Paikowsky et al., 1999) also shows that the static load test procedure has little to no influence on the pile capacity.

4.6 CONCLUSIONS FOR REFERENCE STATIC CAPACITY

It is recommended that the traditional Davisson's criterion will be used for determining the pile capacity based on static load-settlement curves. The correction for the large diameter piles suggested by Kyfor et al., 1992 did not prove to be worthwhile. The static capacity used for the evaluation of the dynamic methods will make use of the static pile's capacity as evaluated based on Davisson's criterion regardless of the load testing procedure.

Table 4.1. Summary of the Interpretation Methods applied to the Static Load Test Curves in PD/LT2000.

Interpretation Method	Number of Valid Cases	Mean Ratio K_{SX}	Standard Deviation	Max Value of K_{SX}	Min Value of K_{SX}	Number of Cases for the Range of K_{SX} from 0.95 to 1.05	Number of Cases for the Range of K_{SX} from 0.90 to 1.10	Non-Applicable Cases and Reason why they are non-applicable
Davisson's Criteria	186	1.018	0.101	1.734	0.766	111	161	9 - max settlement less than failure criterion 1 - load below the failure range
DeBeer	187	1.033	0.088	1.429	0.750	119	153	9 - no clear failure point on log - log graph of load settlement curve
$\Delta = 0.1B$	90	0.938	0.114	1.367	0.647	39	59	106 - max settlement less than failure criterion
$\Delta = 1''$	161	0.971	0.098	1.538	0.714	73	120	35 - max settlement less than failure criterion
Shape of Curve	193	1.019	0.066	1.600	0.833	145	179	3 - load settlement curve did not have a clear failure point
Representative Pile Capacity	196	1.000	0.000	1.000	1.000	196	196	0

Notes:

K_{SX} – The ratio between the representative pile capacity to the capacity obtained by the examined method.

Table 4.2. Summary of Static Load Test Procedures (after Paikowsky et al., 1999)

Code	Test Name	Loading		Hold Time at Max. Load	Unloading		Hold time at Zero Load
		Increments	Hold Time		Increments	Hold Time	
ASTM	<i>Standard Loading Procedure</i>	25%	0.01 in/hr	12-24 hr	25%	1 hr & .01 in/hr	1 hr
	<i>Cyclic Loading</i>	50%	1 hr	0 hr	50%	0.33 hr	1 hr
		50%	0.33 hr	12-24 hr	25%	1 hr	0 hr
	<i>Quick Load Test</i>	10-15%	2.5 min	5 min	1 step	Instantaneous	0 hr
	<i>Constant Rate of Penetration</i>	.01 - .1 in/min	0 hr	-	-	-	-
MHD	<i>Short Duration</i>	25%	0.5 hr	1 hr	25%	0.25 hr	1 hr
	<i>Maintained Load Test</i>	50%	2 hr	12-24 hr	25%	4 hr	4 hr
	<i>Quick Load Test</i>	50-100kN	2.5 min	5 min	25% of max.	2.5 min	15 min
MBC	<i>Loading Procedure</i>	25%	0.5 hr	1 hr	25%	0.25 hr	1 hr
TQT	<i>Quick Load Method</i>	10-15%	2.5 min	2.5 min	1 step	Instantaneous	2.5 min
	<i>Static-Cyclic Test</i>	150 kN/min	0 hr	0 hr	325 kN/min	0 hr	0 hr

Notes:

1. ASTM – American Standard for Testing and Materials.
2. MHD – Massachusetts Highway Department.
3. MBC – Massachusetts Building Code.
4. TQT – Texas Quick Test.
5. All percentages are in percent of total design load of the pile.
6. The loading increment for the standard test is based on the assumed bearing capacity of the pile.

Table 4.3. Summary of the Statistical Data Comparing the Slow Maintained Load Tests Results using Davisson's Criterion and the Static Cyclic Load Test Results from the UMass Lowell / Ukraine Database.

	<u>Representative Load Test Results</u> Static Cyclic Capacity	<u>Davissons Capacity</u> Static Cyclic Capacity
Mean K_{SC}	1.023	0.930
Standard Deviation	0.057	0.136
Number of Cases	81	75
Maximum K_{SC}	1.216>1.215	
Minimum K_{SC}	0.893	0.577

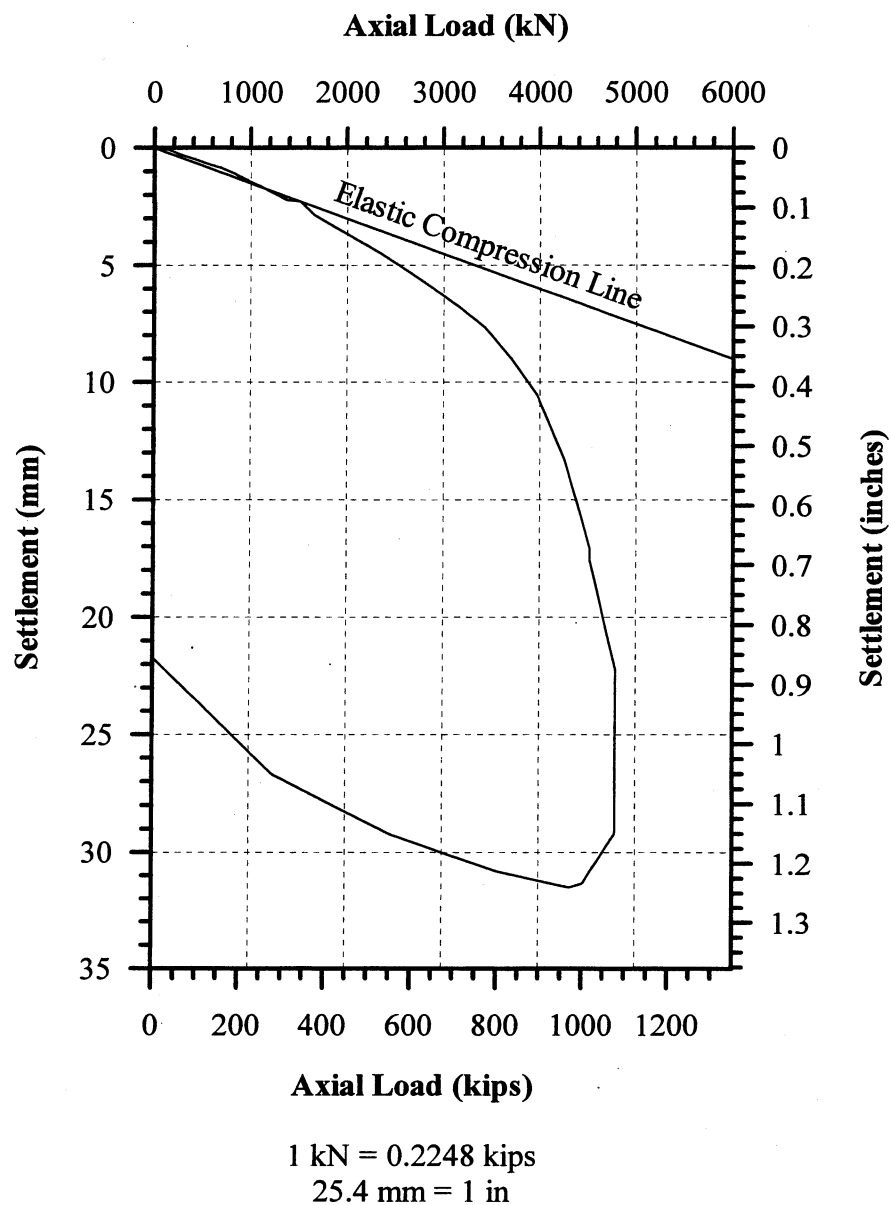


Figure 4.1. Load-settlement curve of pile-case 344 with the elastic compression line inclined at 20 degrees.

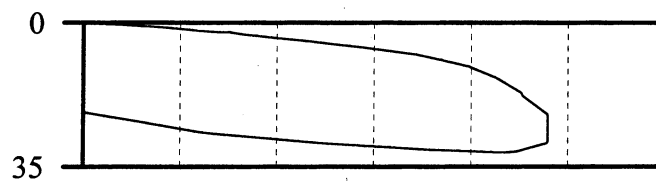


Figure 4.2. Load-settlement curve of pile-case 344 with a scale that does not consider the elastic compression of the pile.

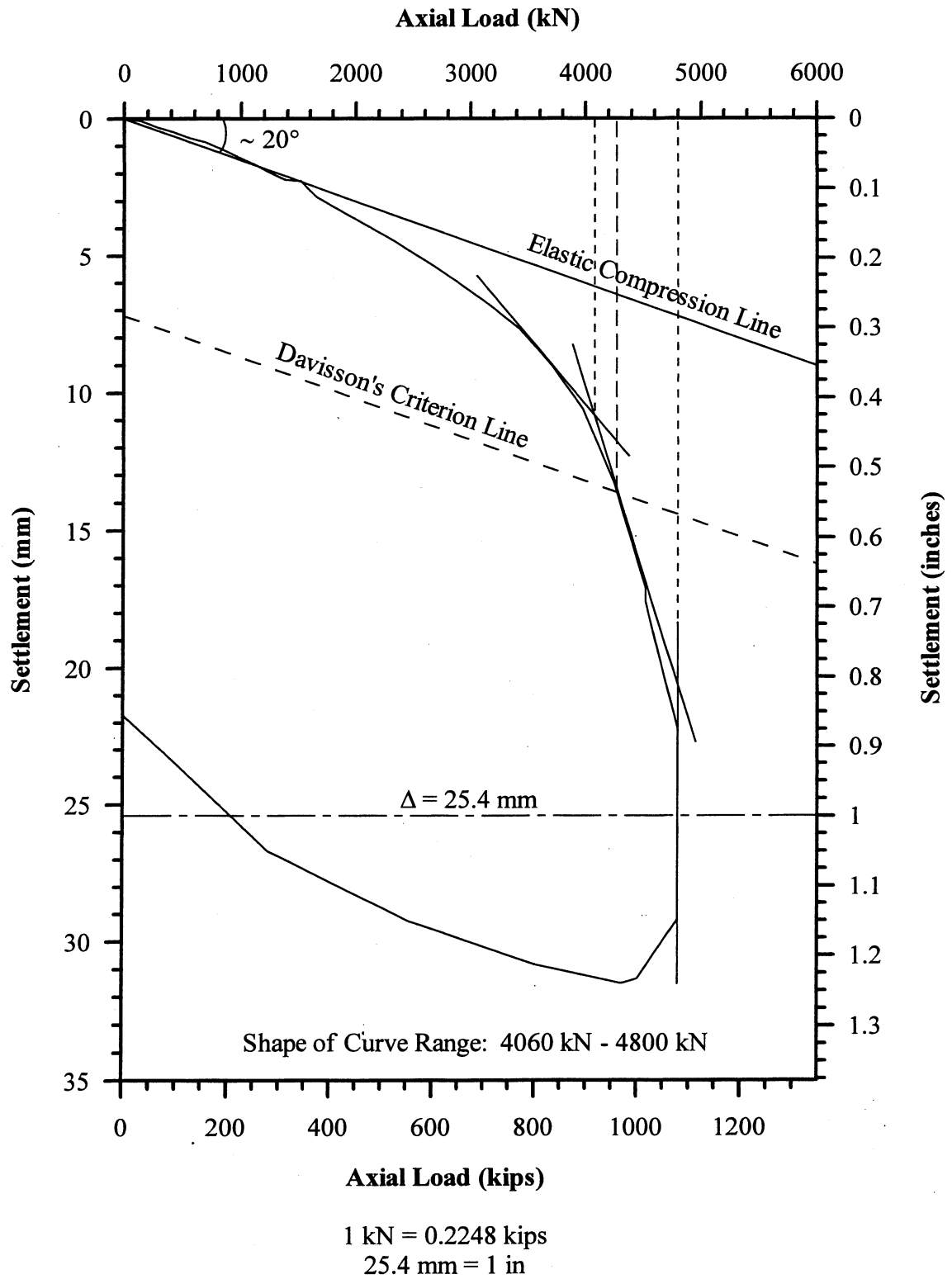


Figure 4.3. Load-settlement curve of pile-case 344 with the elastic compression line inclined at approximately 20 degrees.

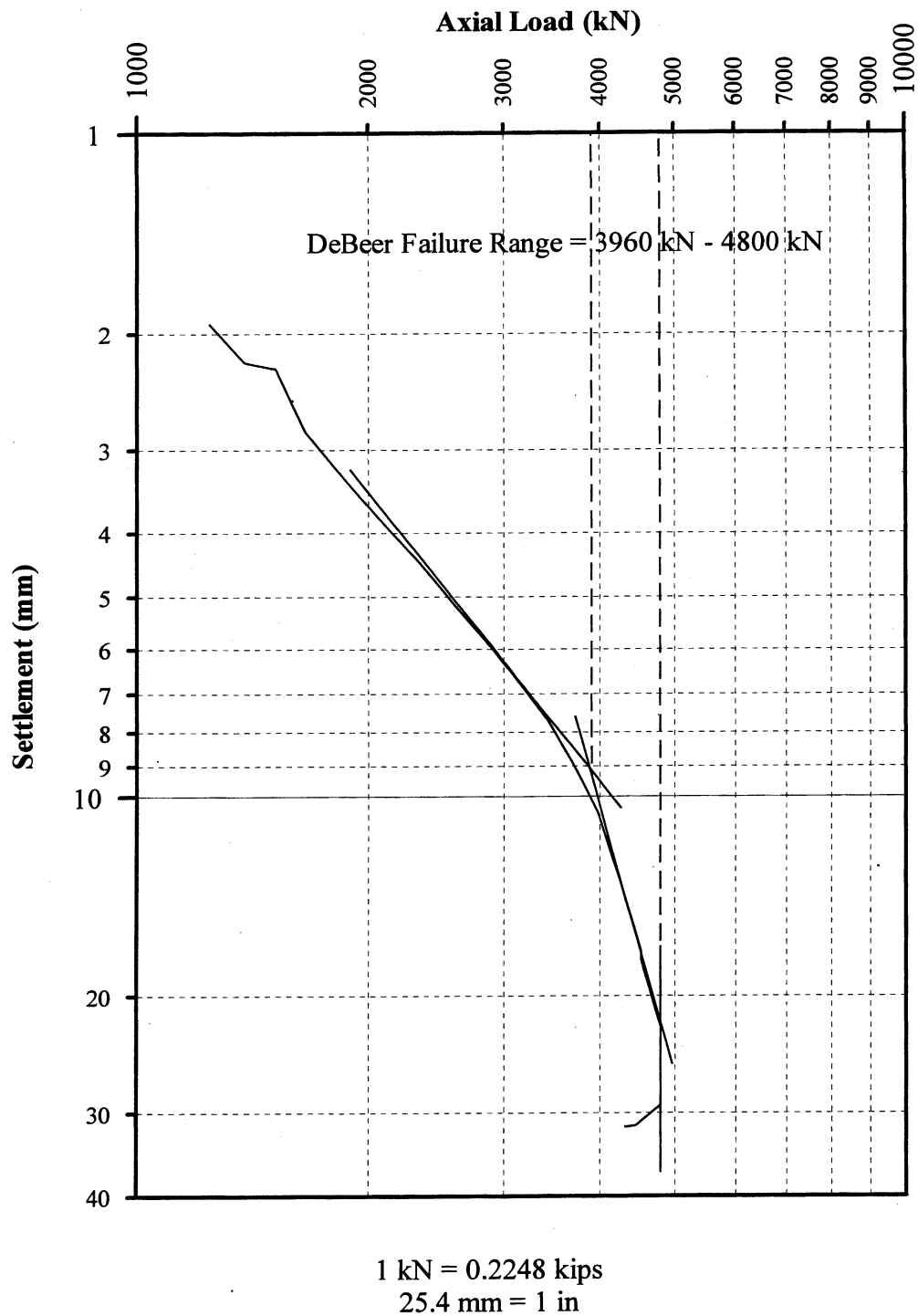


Figure 4.4. Load-settlement data plotted on a logarithmic graph for pile-case 344 to determine the failure load according to DeBeer's method.

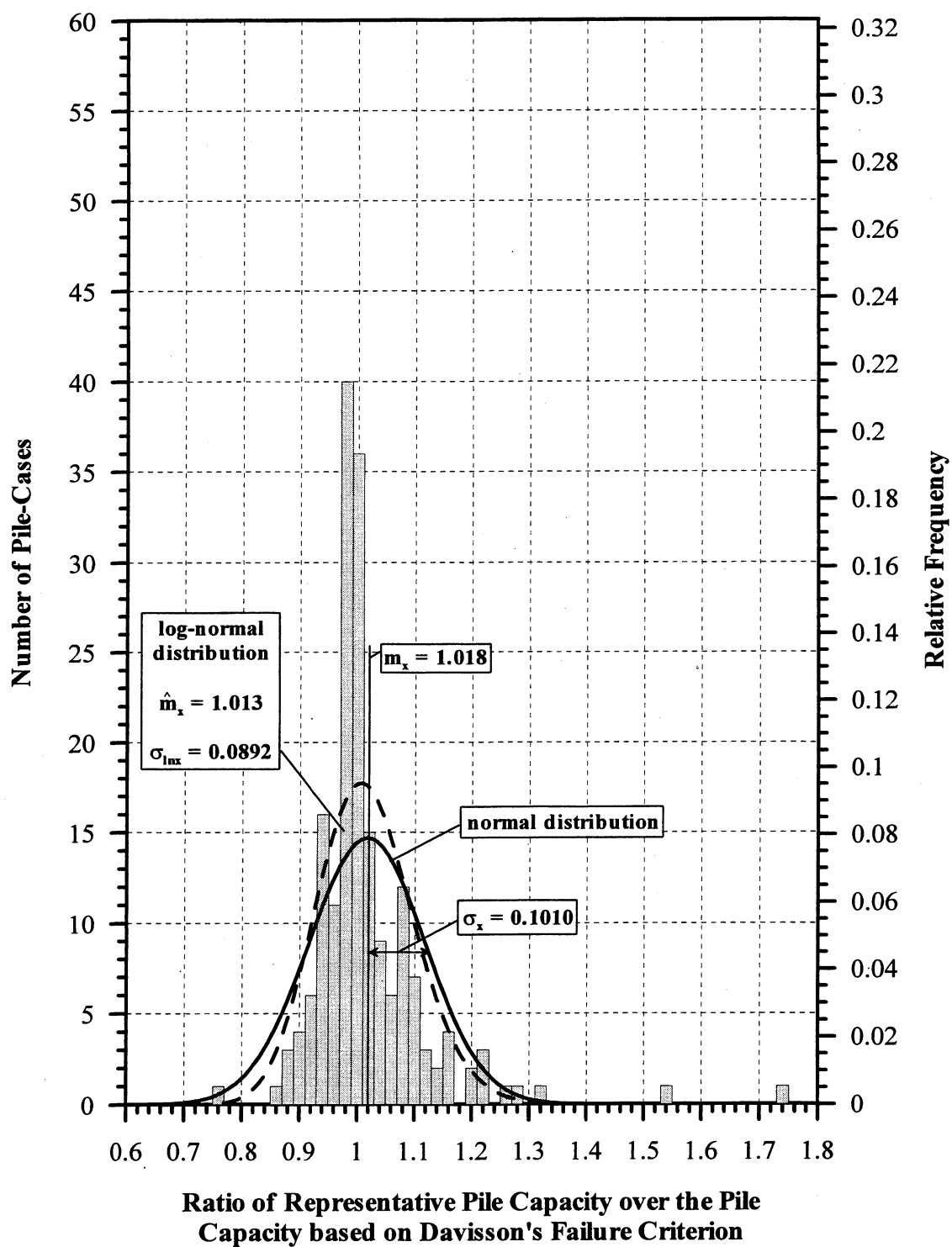


Figure 4.5. Histogram and frequency distributions of K_{SD} for 186 PD/LT2000 pile-cases in all types of soils.

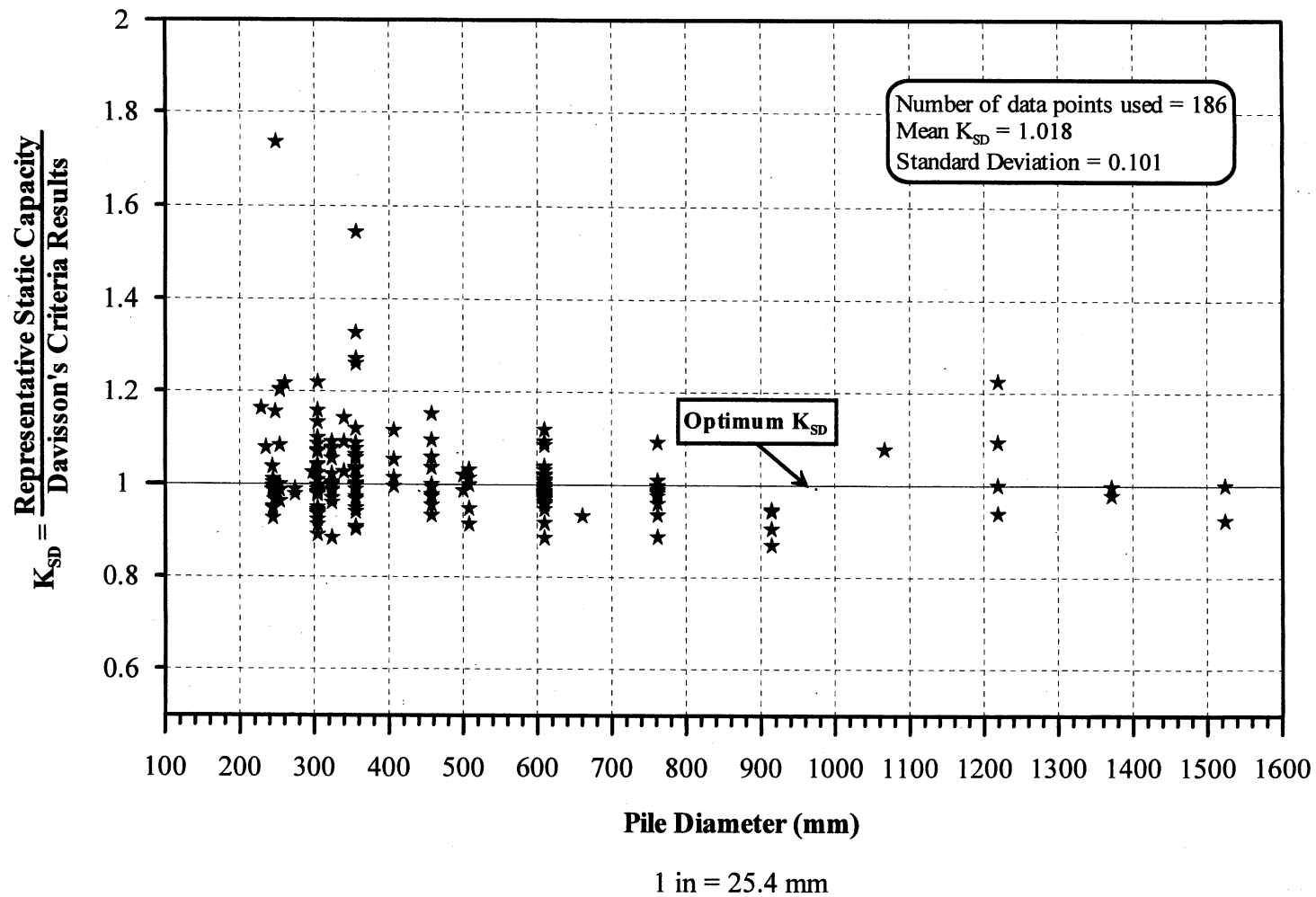


Figure 4.6. K_{SD} values vs. Pile Diameter for all PD/LT2000 pile-cases, all types of soils.

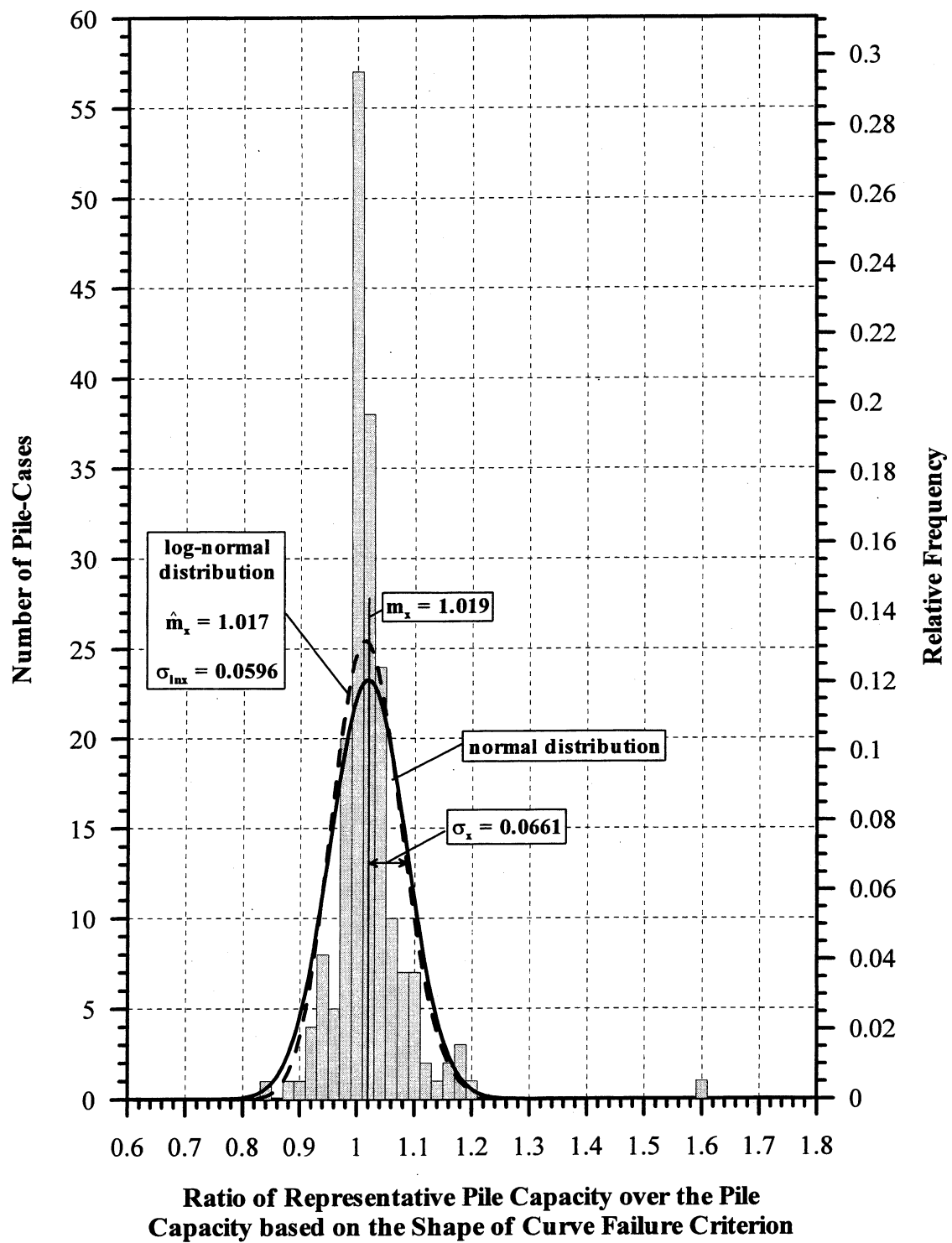


Figure 4.7. Histogram and frequency distributions of K_{sc} for 193 PD/LT2000 pile-cases in all types of soils.

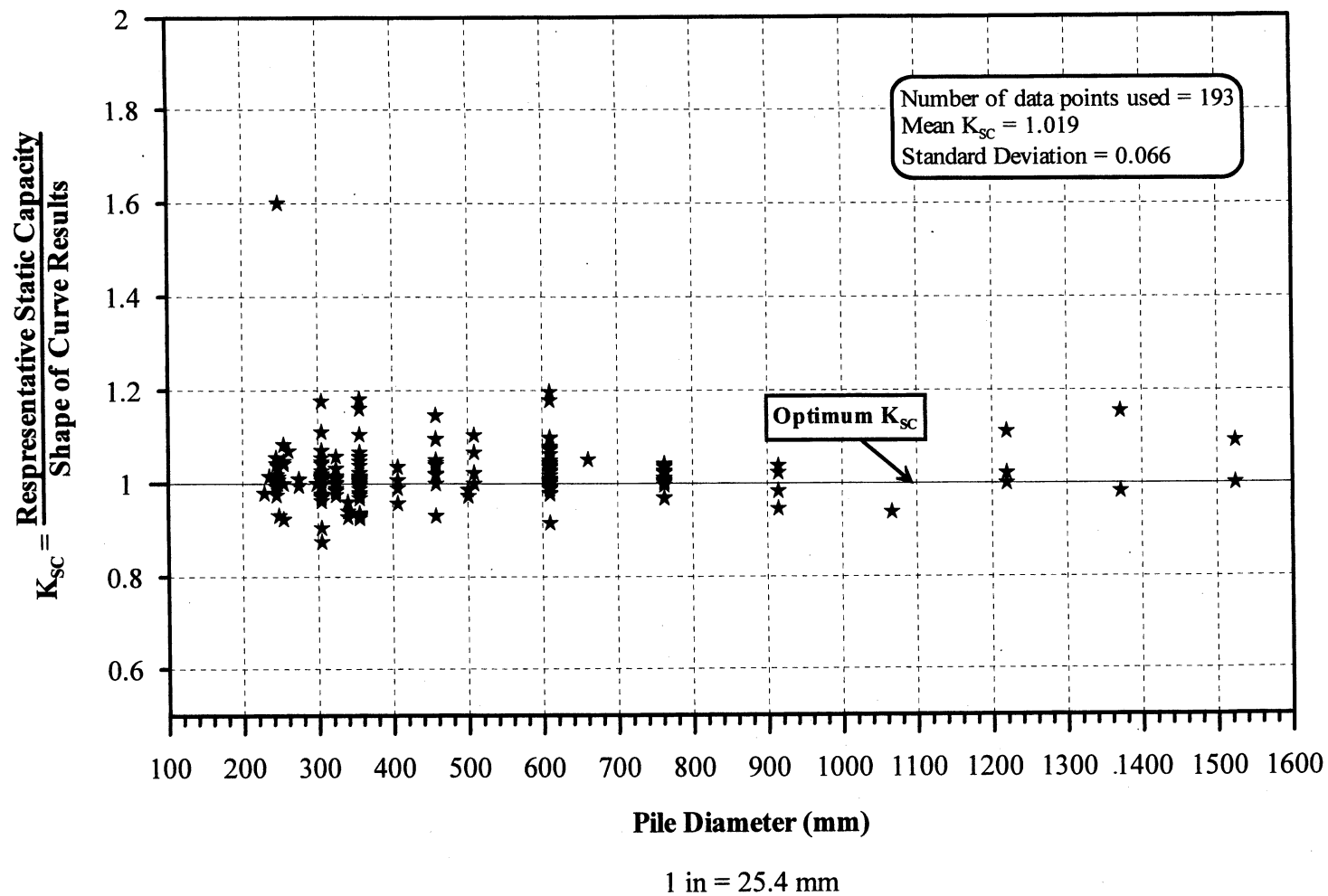


Figure 4.8. K_{sc} values vs. Pile Diameter for all PD/LT2000 pile-cases, all types of soils.

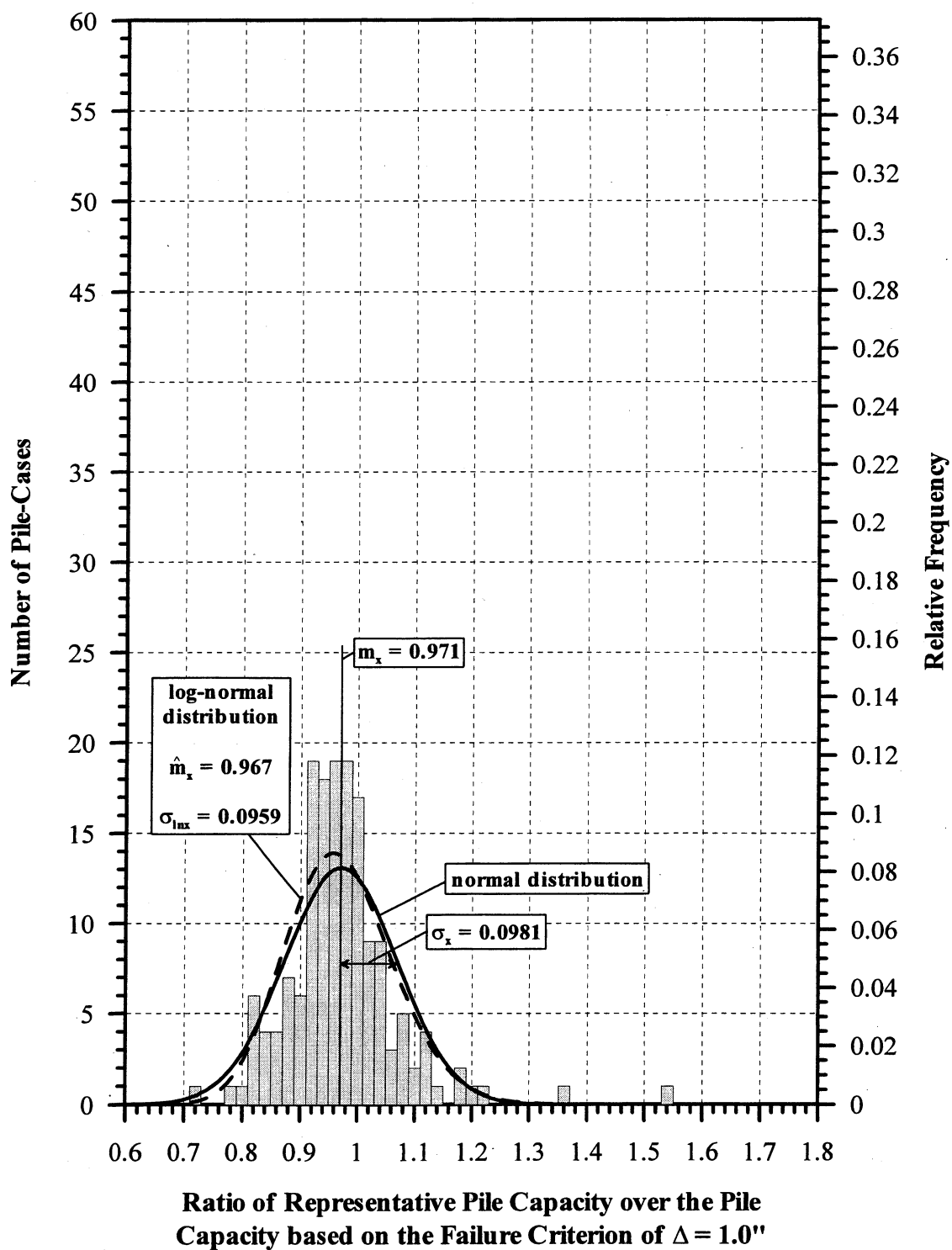


Figure 4.9. Histogram and frequency distributions of K_{ST} for 161 PD/LT2000 pile-cases in all types of soils.

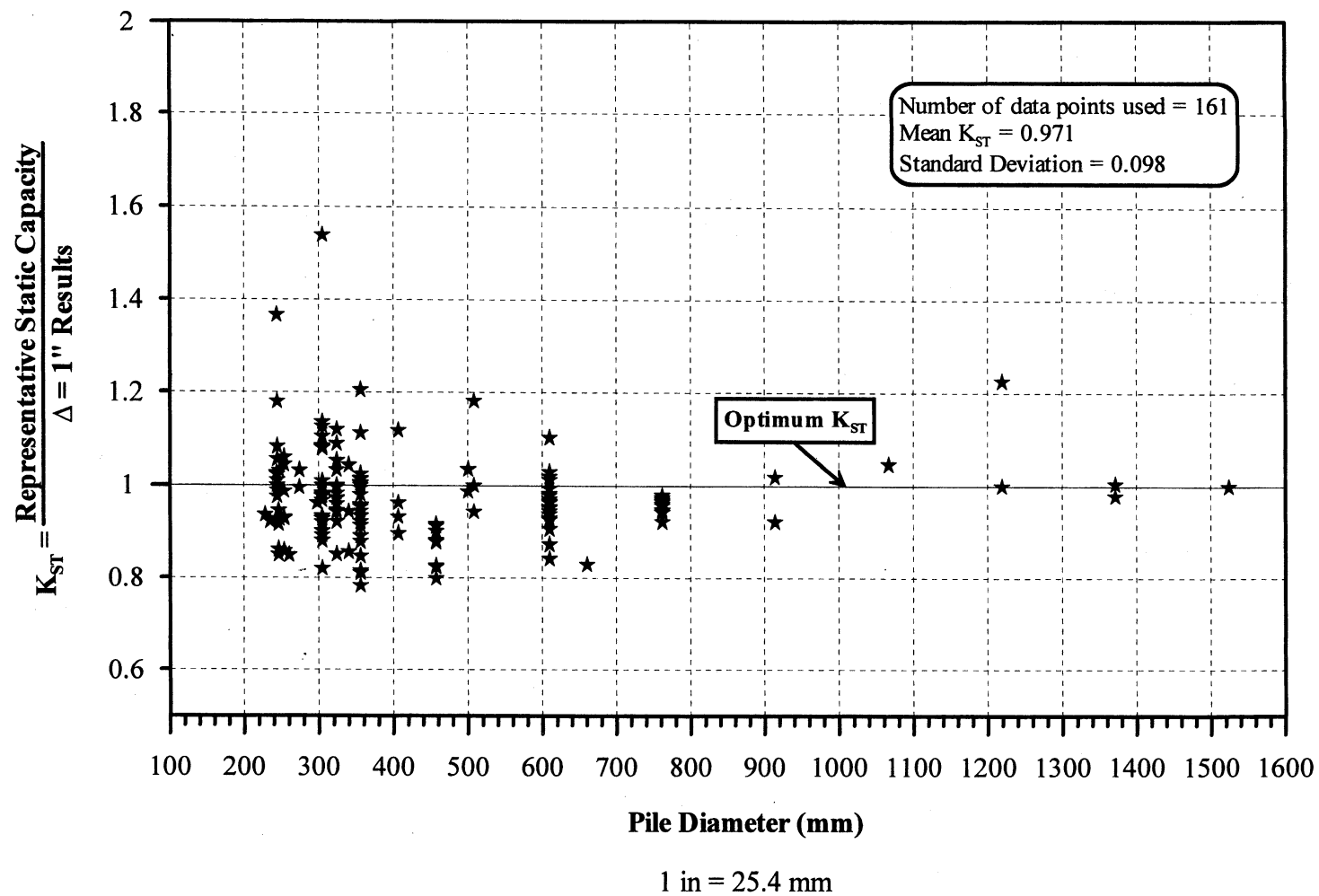


Figure 4.10. K_{ST} values vs. Pile Diameter for all PD/LT2000 pile-cases, all types of soils.

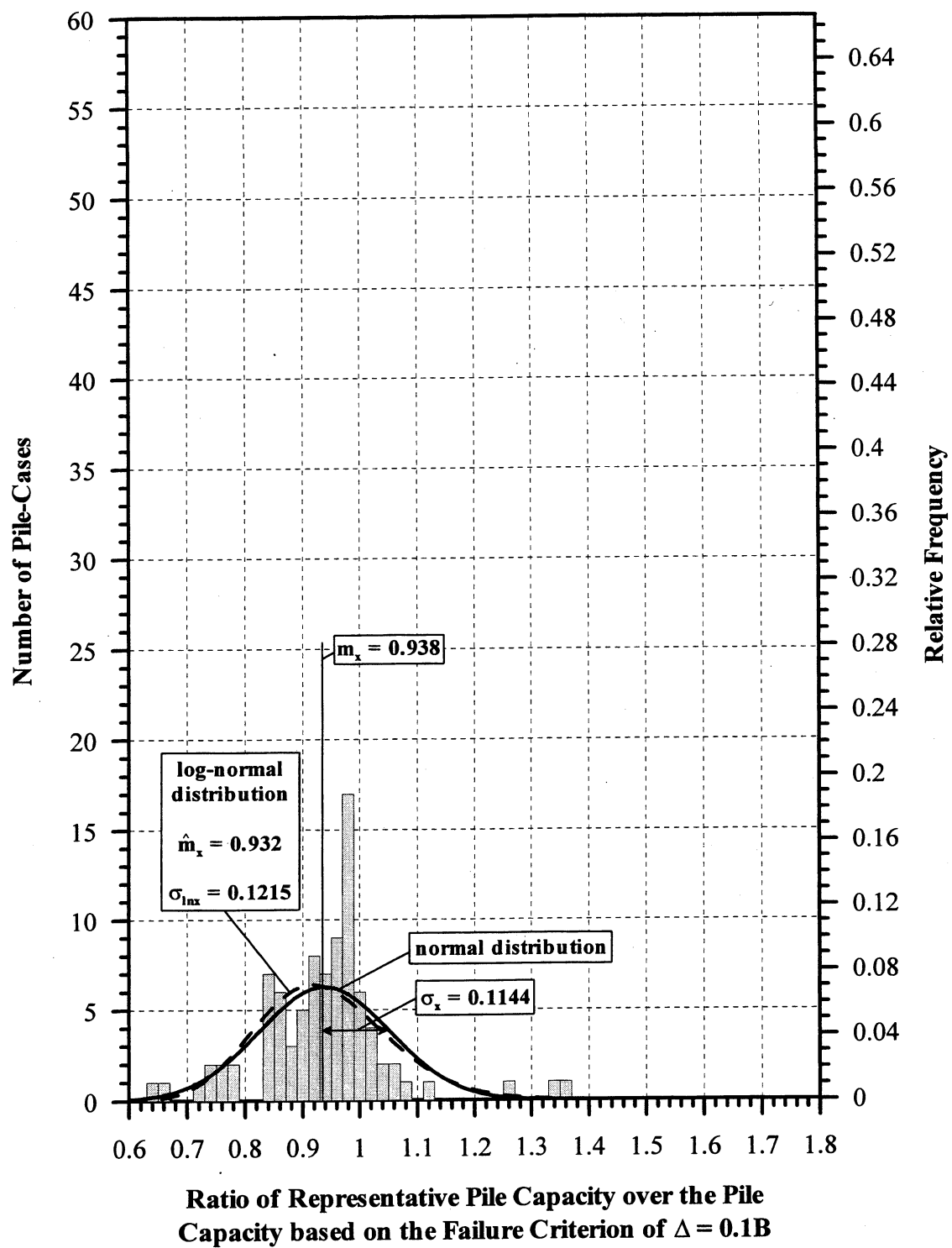


Figure 4.11. Histogram and frequency distributions of K_{SL} for 90 PD/LT2000 pile-cases in all types of soils.

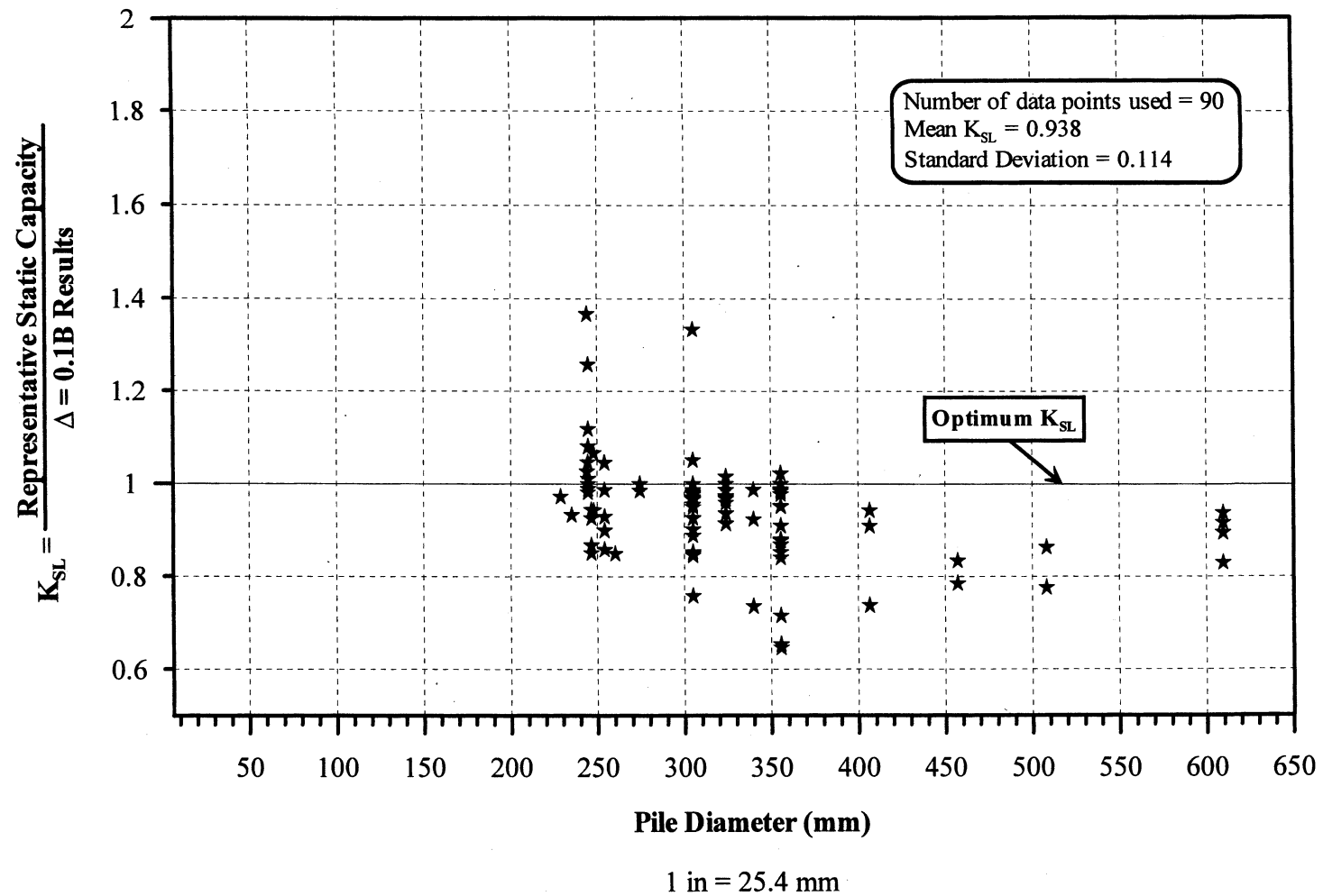


Figure 4.12. K_{SL} values vs. Pile Diameter for all PD/LT2000 pile-cases, all types of soils.

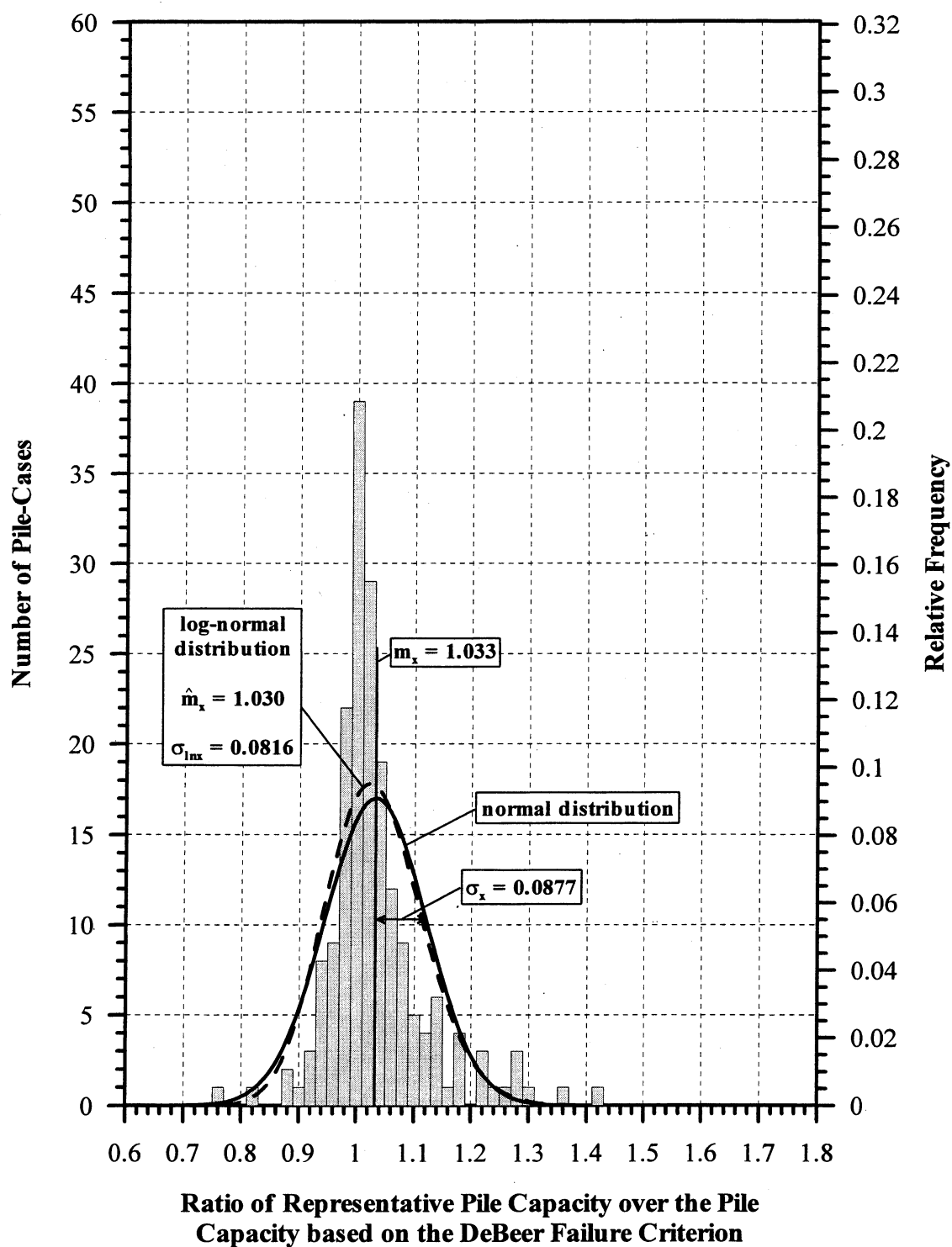
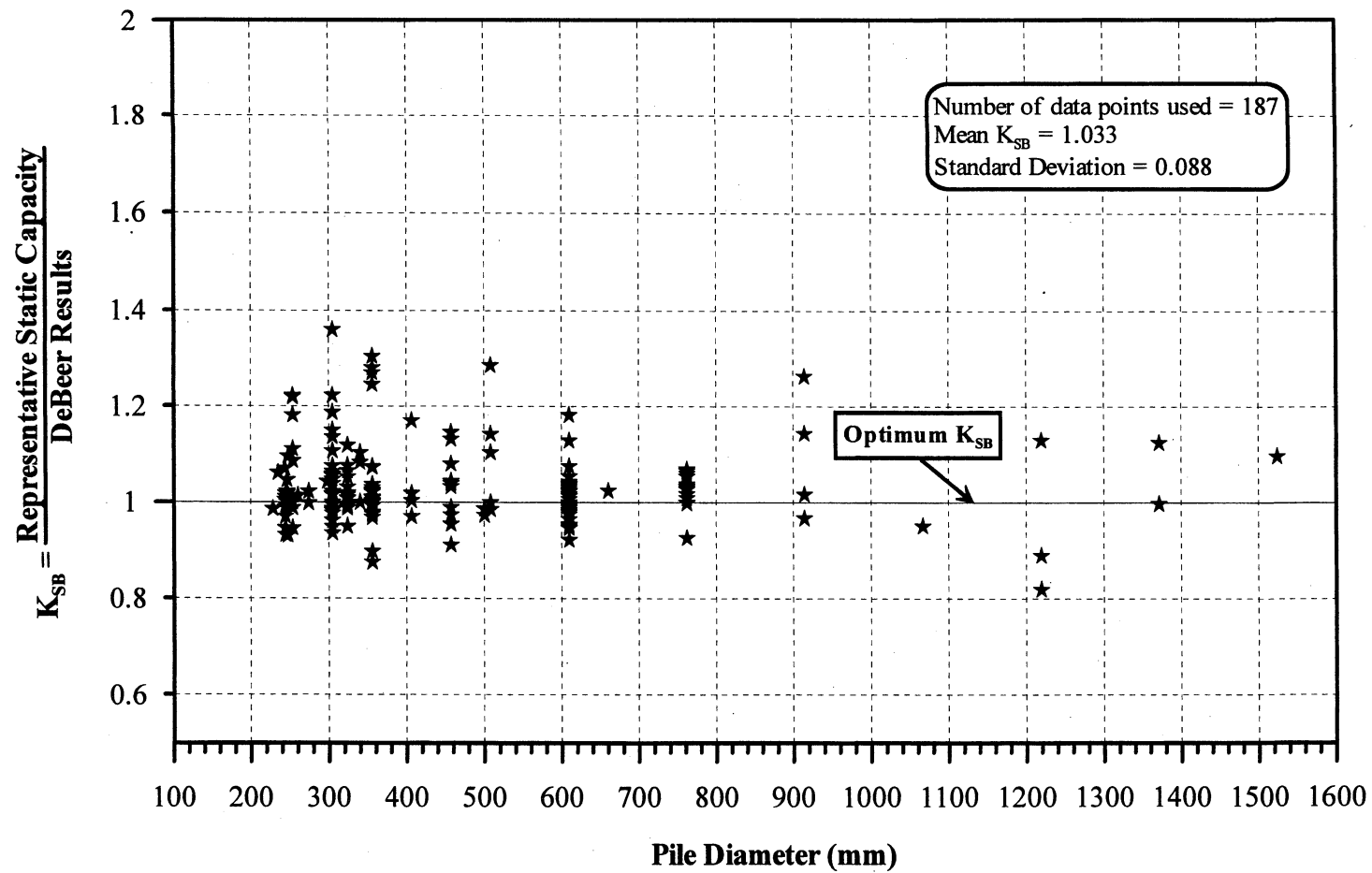


Figure 4.13. Histogram and frequency distributions of K_{SB} for 187 PD/LT2000 pile-cases in all types of soils.



1 in = 25.4 mm

Figure 4.14. K_{SB} values vs. Pile Diameter for all PD/LT2000 pile-cases, all types of soils.

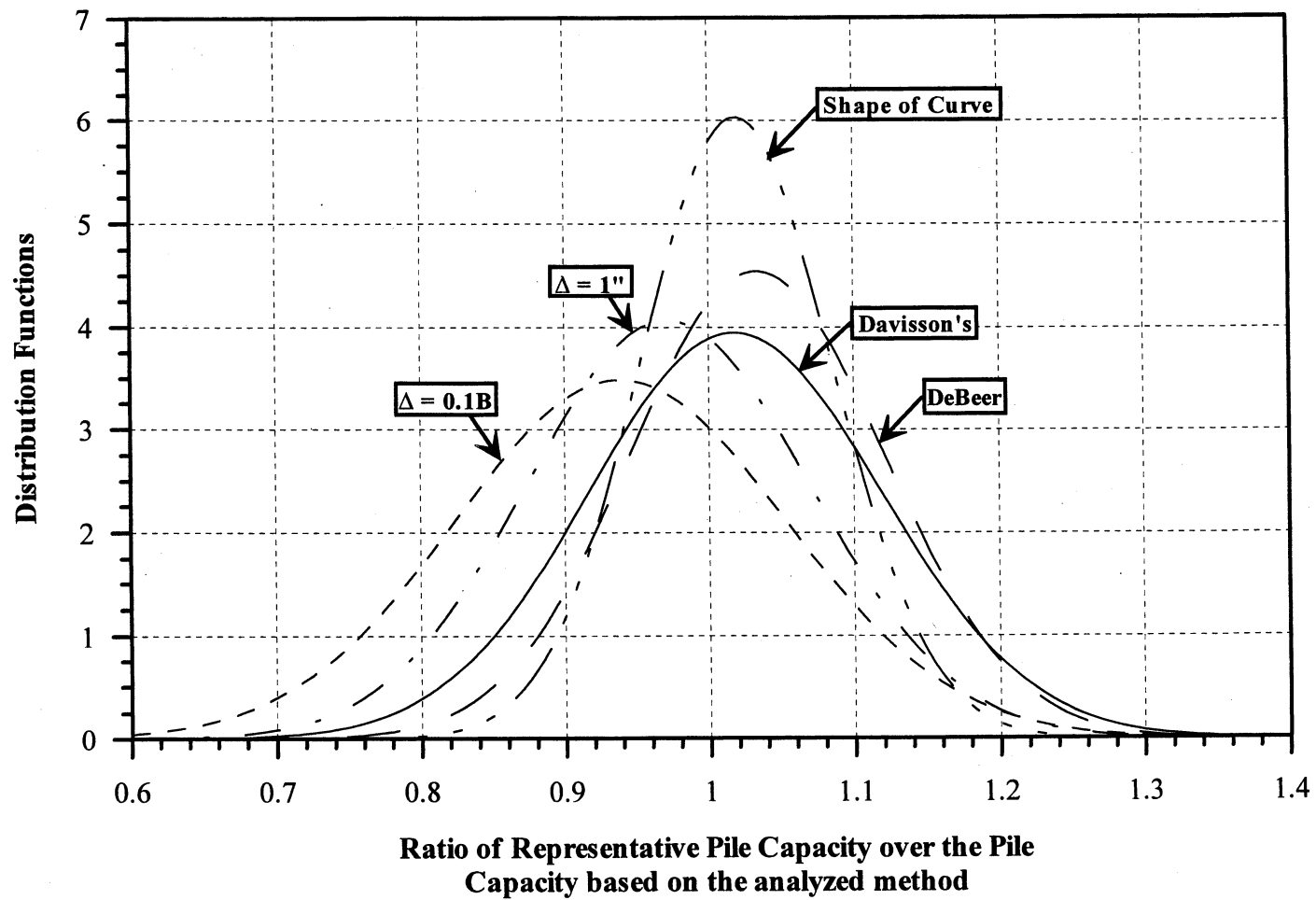
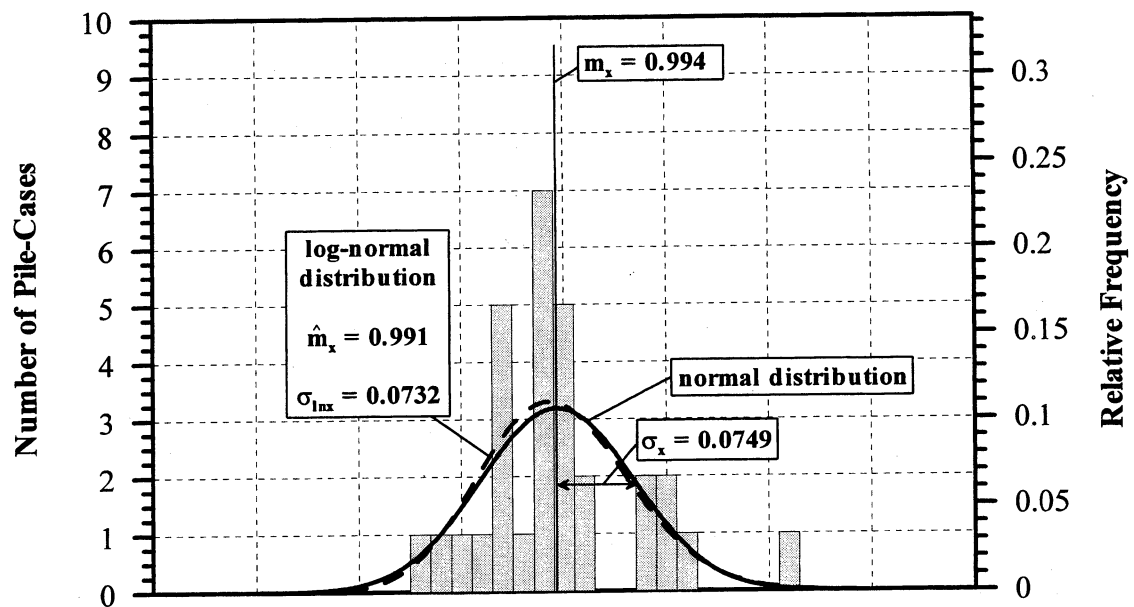
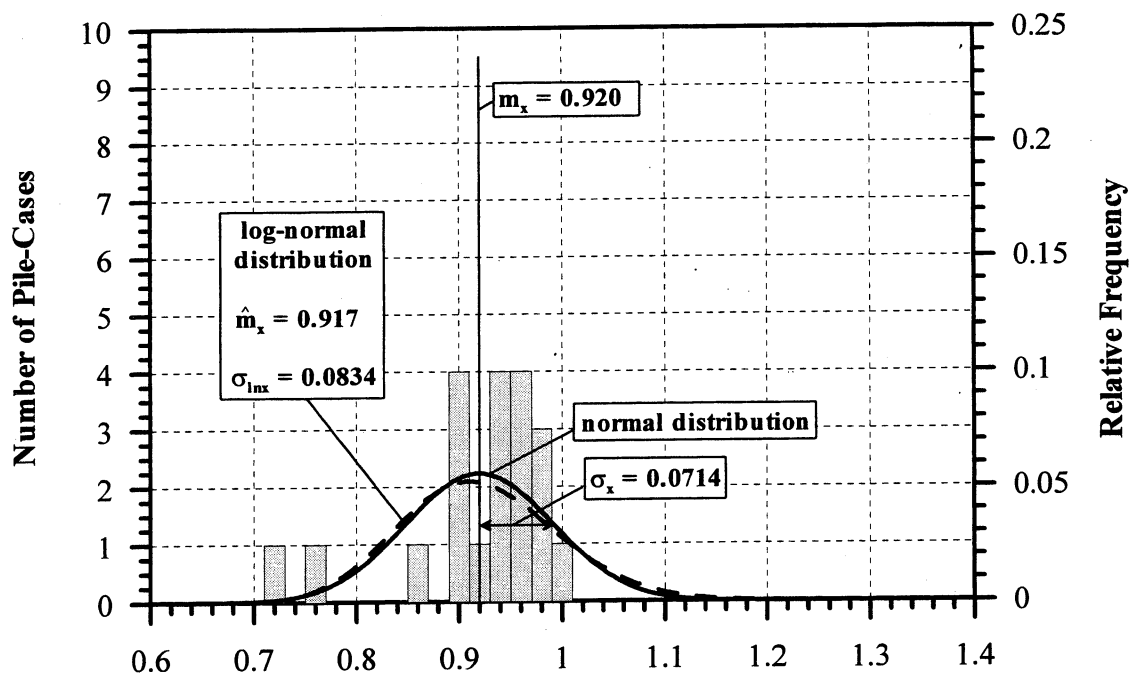


Figure 4.15. Distribution Function Curves for the Five methods used for analysis of Static Load Test Curves based on 196 piles from PD/LT2000.

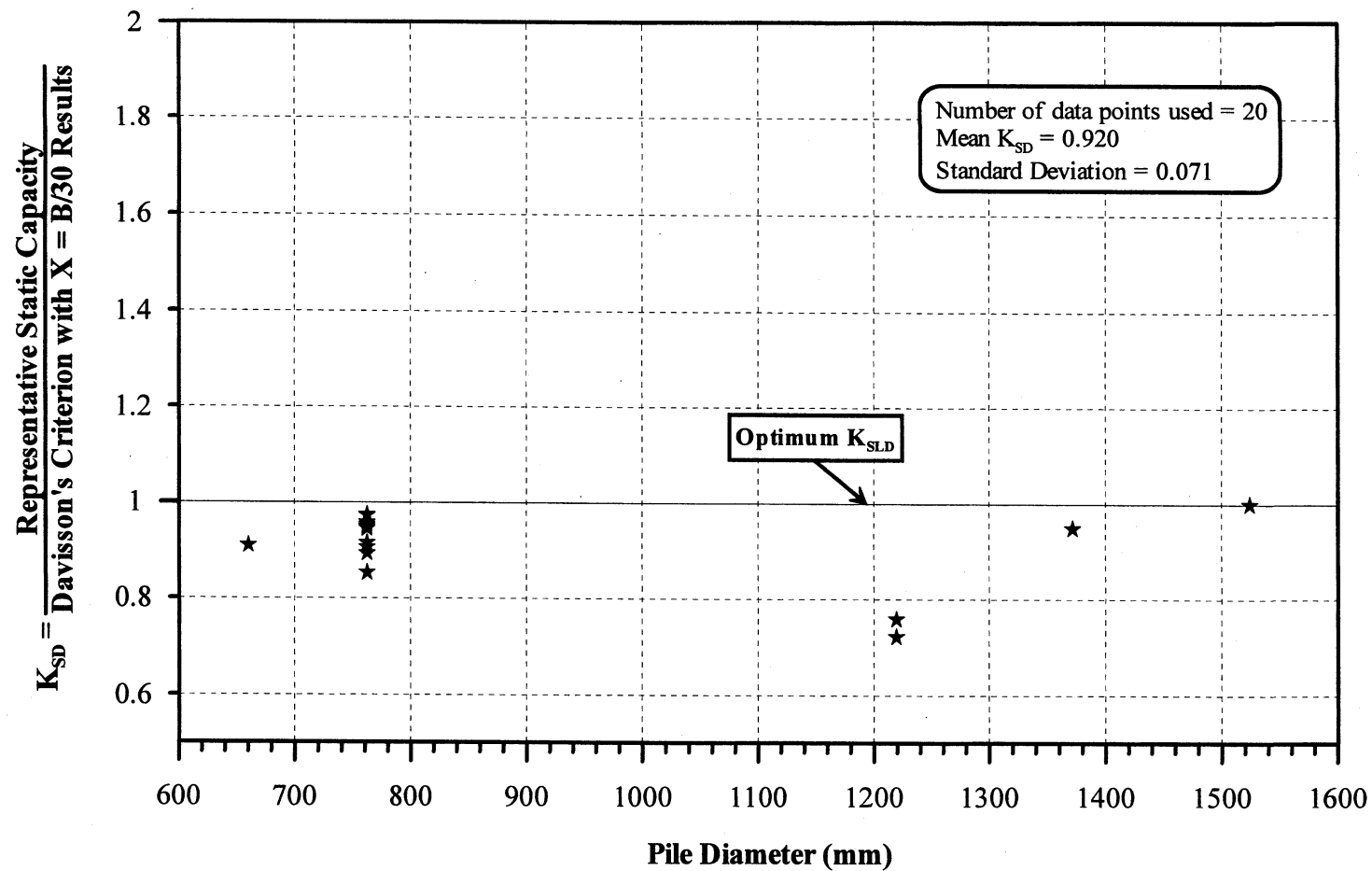


Ratio of Representative Pile Capacity over the Pile Capacity based on Davisson's Failure Criterion with offset $X = 3.81 + B/120$, K_{SD}



Ratio of Representative Pile Capacity over the Pile Capacity based on Davisson's Failure Criterion with offset $X = B/30$, K_{SLD}

Figure 4.16. Histogram and frequency distributions of K_{SD} and K_{SLD} for 30 and 20 PD/LT2000 pile-cases, respectively, in all types of soils.



1 in = 25.4 mm

Figure 4.17. K_{SLD} values vs. Pile Diameter for all large diameter PD/LT2000 pile-cases, all types of soils.

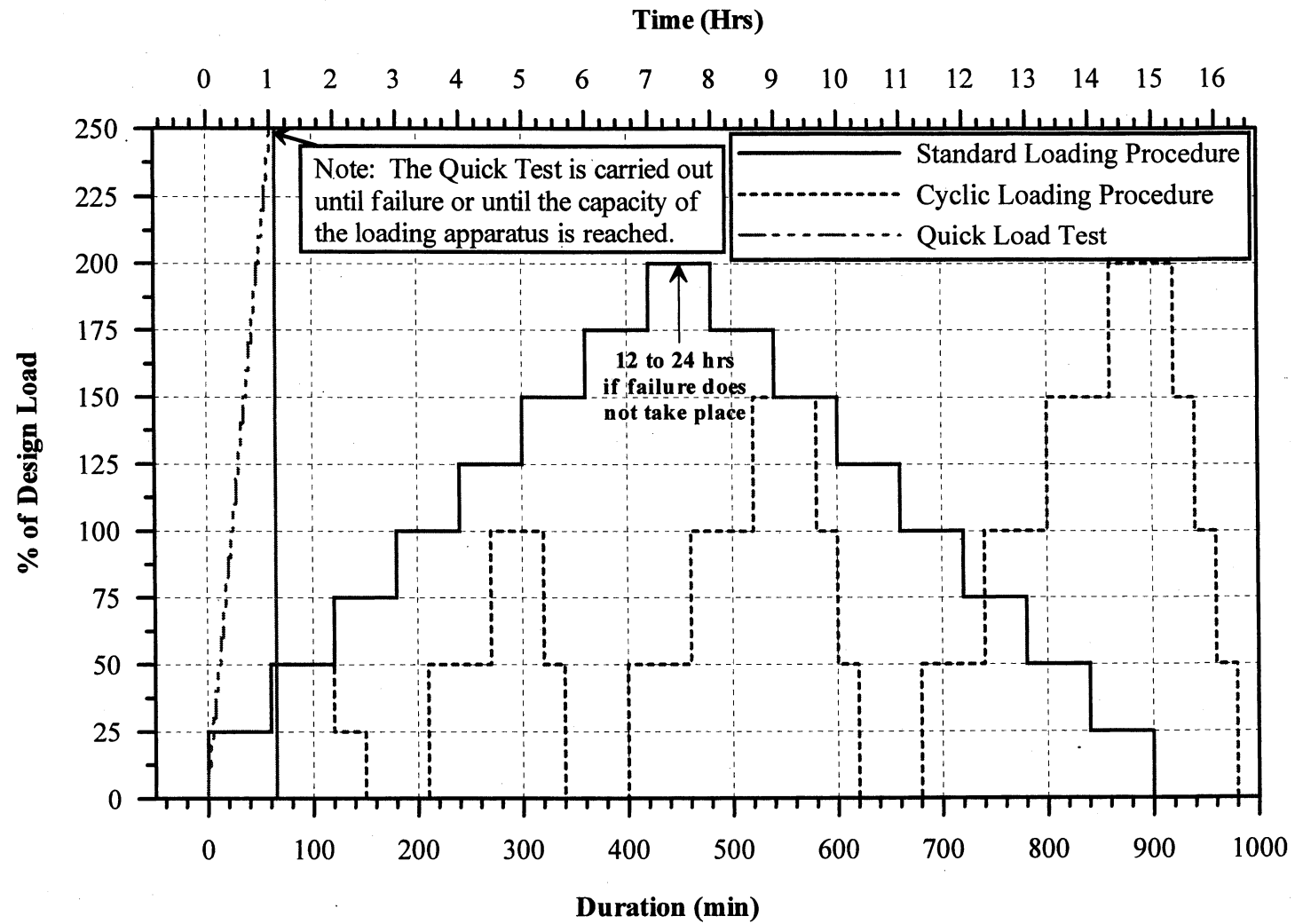


Figure 4.18. Static Pile Load Testing Procedures According to ASTM (after Paikowsky et al., 1999)

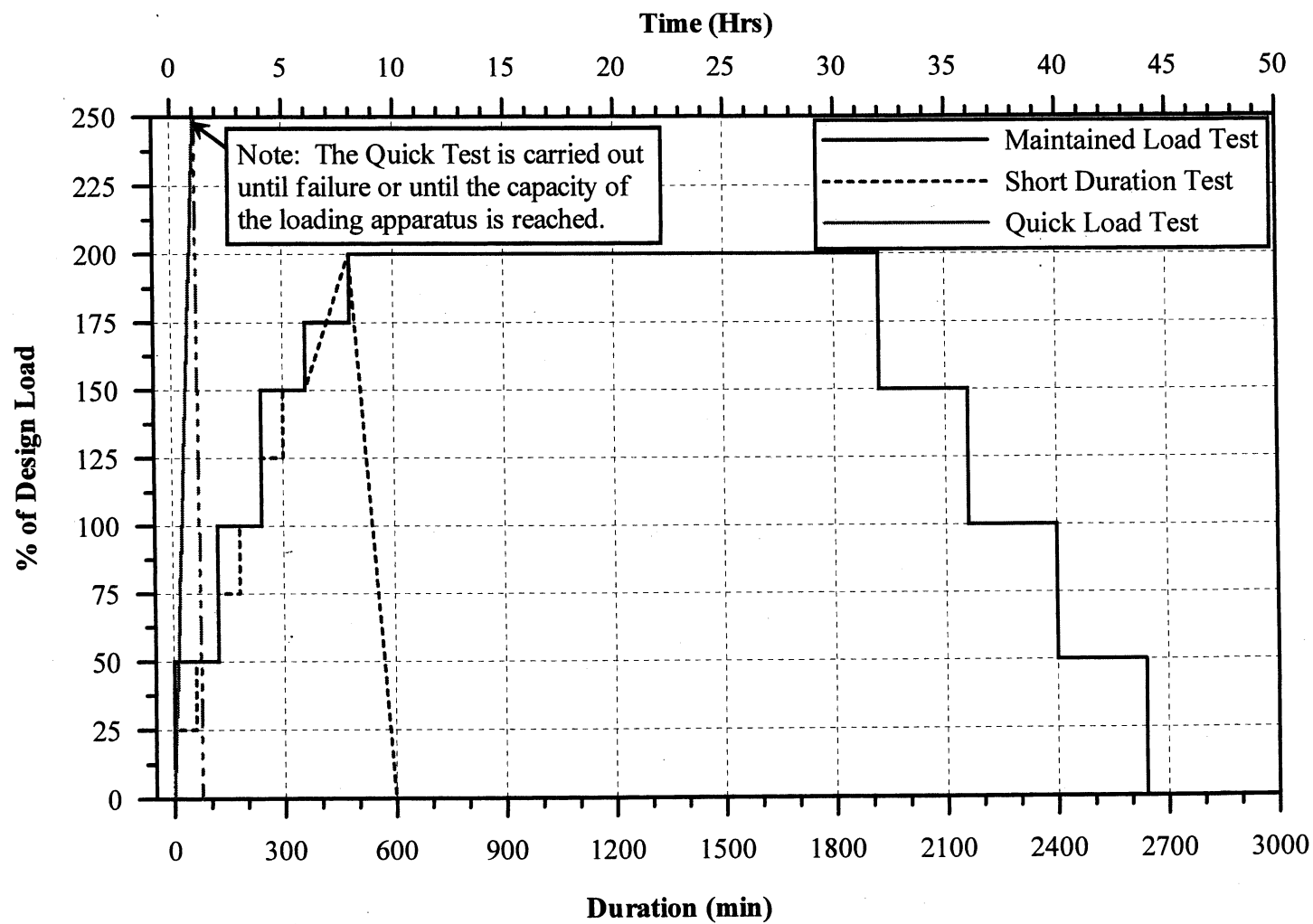


Figure 4.19. Static Pile Load Testing Procedures According to MHD (after Paikosky et al., 1999)

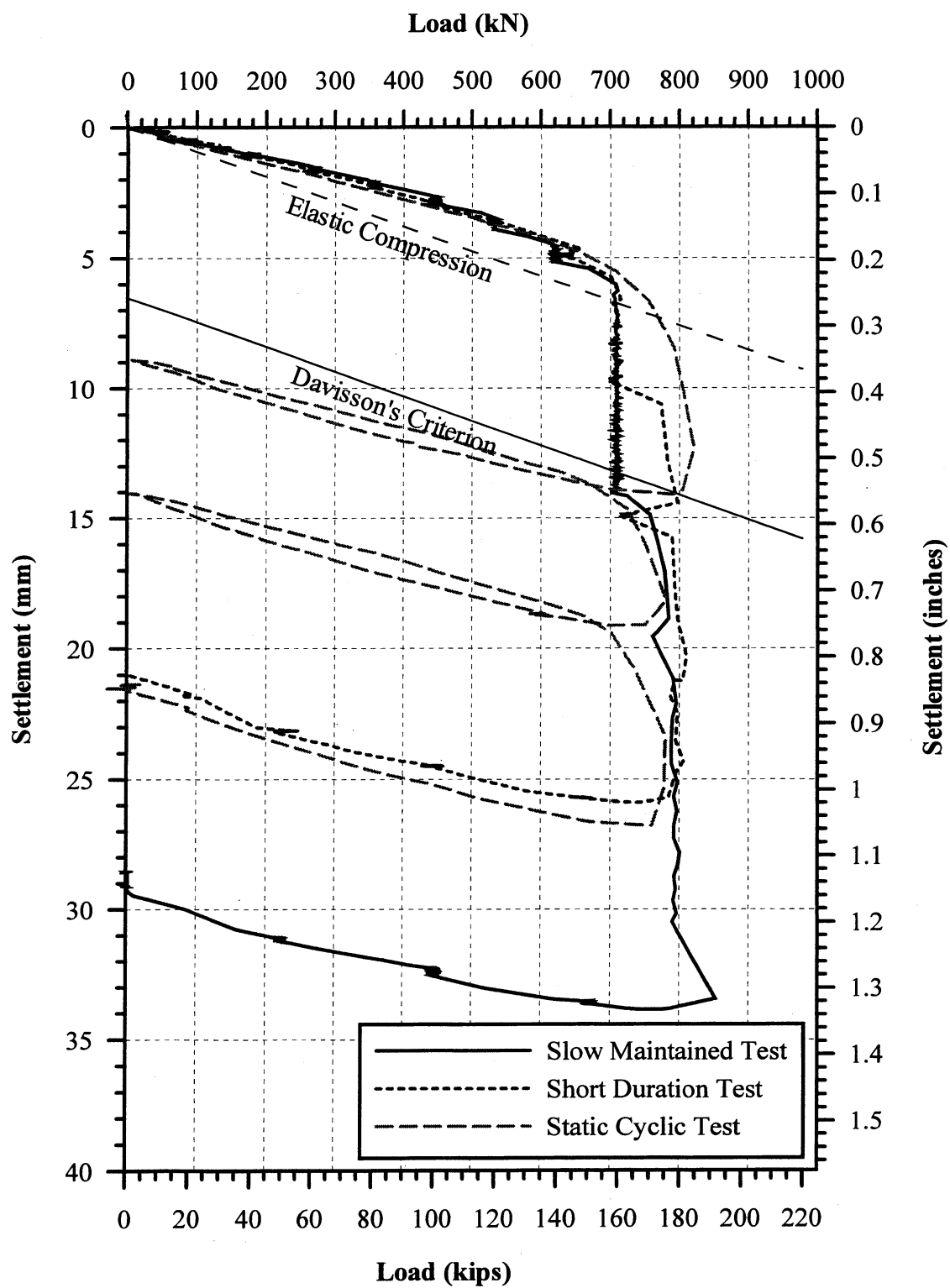


Figure 4.20. Comparison of the Short Duration, Slow Maintained and Static Cyclic Load Tests for Test Pile # 2 at the Newbury Site (after Paikowsky et al., 1999).

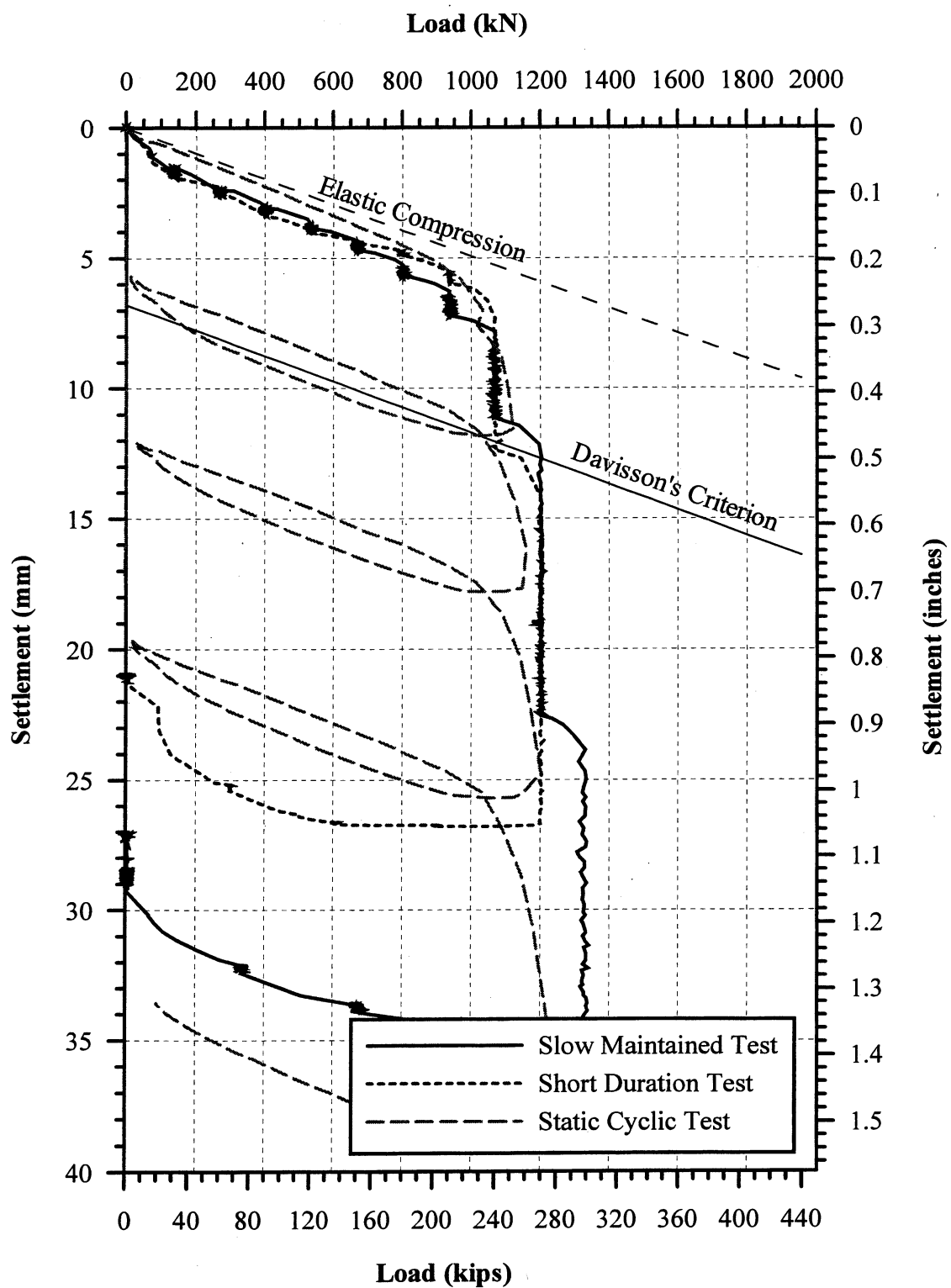


Figure 4.21. Comparison of the Short Duration, Slow Maintained and Static Cyclic Load Tests for Test Pile # 3 at the Newbury Site (after Paikowsky et al., 1999).

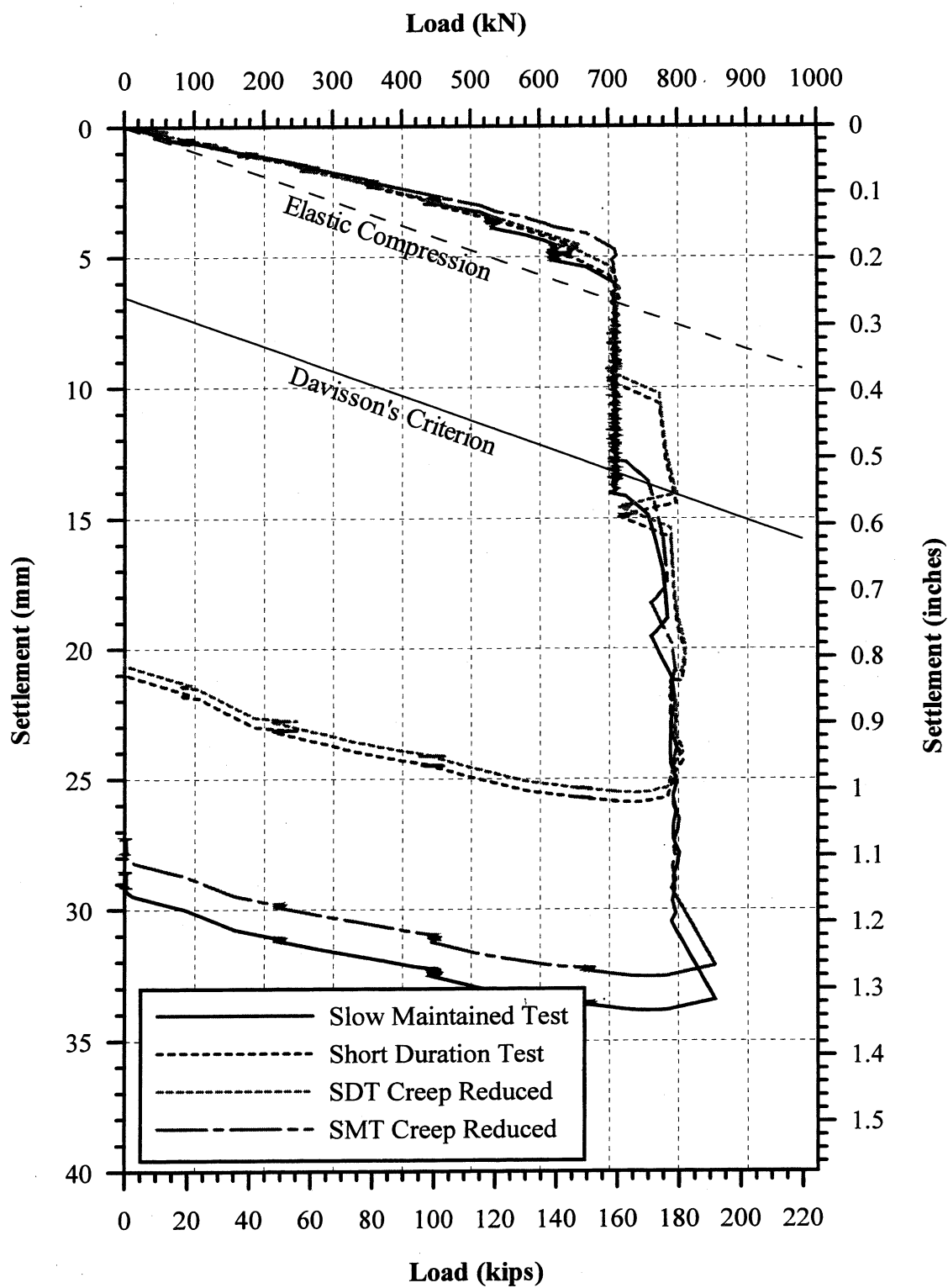


Figure 4.22. Comparison of the Short Duration and Slow Maintained Static Load Tests, Reduced for Creep, for Test Pile # 2 at the Newbury Site.

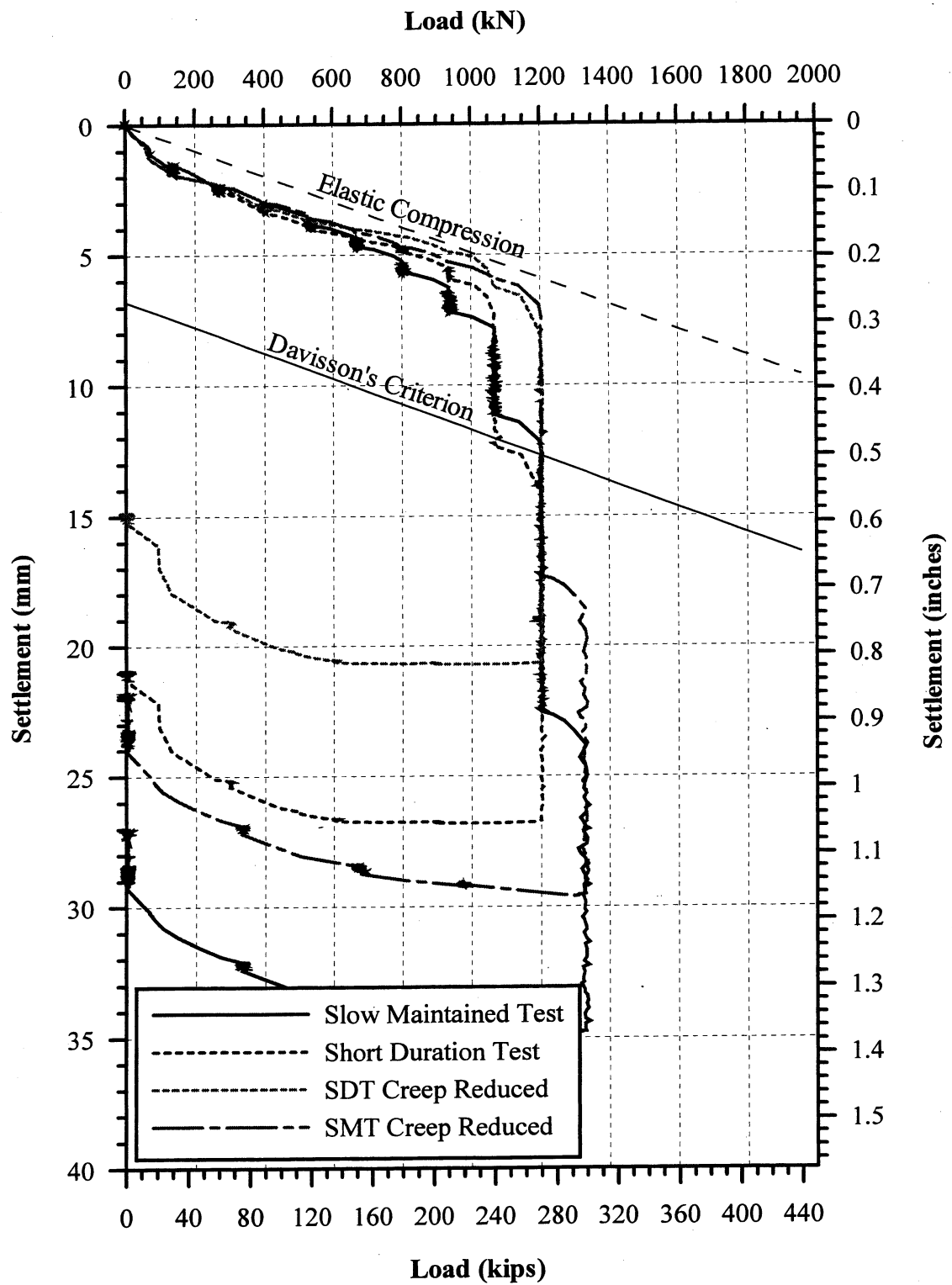


Figure 4.23. Comparison of the Short Duration and Slow Maintained Static Load Tests, Reduced for Creep, for Test Pile # 3 at the Newbury Site.

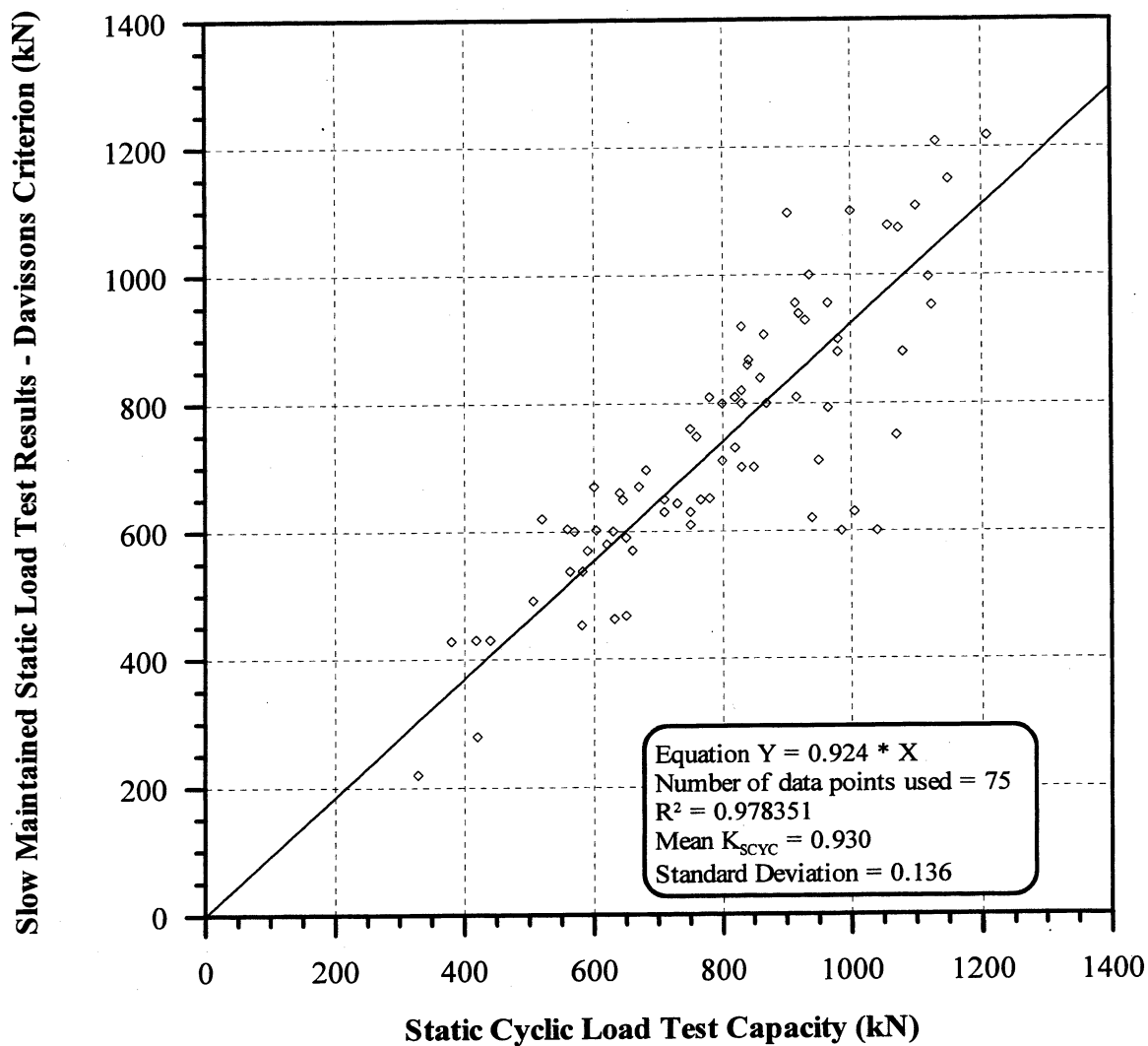


Figure 4.24. Davisson Capacity vs. Static Cyclic Load Test Capacity for 75 pile-cases from the UMass Lowell / Ukraine Database (after Paikowsky et al., 1999).

CHAPTER 5

CONTROLLING PARAMETERS OF THE DYNAMIC METHODS

5.1 OVERVIEW

The performance of the dynamic methods has been assumed to depend on the type of soil (cohesive or cohesionless) the pile is driven into, the time of driving (End of Driving - EOD or Beginning of Restrike - BOR), and the soil inertia effects (type of pile and difficulty of driving). The controlling effect of each these parameters on the dynamic predictions vary for each pile-case. In this chapter the parameters will be analyzed using the data from PD/LT2000 in an attempt to determine the significance of each parameter. The performance of the dynamic methods can then be evaluated according to the controlling parameters.

5.2 METHOD OF APPROACH

5.2.1 General

The first parameter to be analyzed is the effect of the soil type on the accuracy of the dynamic prediction. This factor has been traditionally assumed to be a major controlling parameter on the accuracy of the dynamic methods. The second controlling parameter to be evaluated is the time of driving. When a dynamic test is completed at the EOD no time has been given to allow for pile setup (freeze effects) to take place, hence, the pile resistance at the time of the measurement differs from that

exhibited at the time of a static load test. If a dynamic test is conducted, during a restrike, generally, a reasonable amount of time after driving has passed and the freeze effects are accounted for. The final parameter that is analyzed is that of the soil inertia effects. In this category are the effects contributing to the soil motion, i.e., the type of pile (small or large displacement) and the driving resistance (easy or hard driving). The analysis in this chapter will evaluate the soil inertia effect and will determine what constitutes a small vs. large displacement pile and hard vs. easy driving.

5.2.2 Nomenclature

The nomenclature that is used throughout this manuscript and extensively in this chapter is based on a method we will label the XXX method. The first letter denotes the pile type, where A = all piles, L = large displacement piles and S = small displacement piles. The second letter denotes the time at which the dynamic measurements were taken, A = all times, E = End Of Driving (EOD) and B = Beginning Of Restrike (BOR). The third letter denotes the soil type along the side of the pile, where A = all soils, S = sand and silt, C = clay and till and R = rock. As an example, pile-cases labeled LES are large displacement piles with dynamic measurements taken at the EOD where the pile was driven into a sand and silt material or AAA would be all types of piles at all times of driving in all types of soils.

5.2.3 Interpretation of Statistical Results

The relationship between the predicted static pile capacity and the actual measured static pile capacity (based on Davisson's criterion from the load-settlement test curves) is presented as a scatter-gram of the two values. The best-fit line (forced

through the origin) was plotted on each of the graphs comparing the actual and predicted static pile capacity. The best-fit line was forced through the origin of the axes as the predicted pile capacity is expected to be zero when the actual capacity is zero. The coefficient of determination values (r^2) were found to be only slightly affected (lower) due to the forced best-fit line through zero, compared to those passing through the y-intercept (Paikowsky et al., 1994).

The following review of the coefficient of determination follows that presented by Paikowsky et al., (1994). The coefficient of determination (r^2) represents the proportion of the sum of squares of deviations of the y-values about their mean, and it is a measure of the contribution of "x" in prediction "y". By definition, a scatter at higher x-values will influence this coefficient more than a scatter close to the origin of axes. The coefficient of determination varies between 0 and 1; the first indicating no correlation or contribution and the last ($r^2 = 1$) is a perfect match where all the points fall on the best-fit, least-squares line. For example, $r^2 = 0.6$ means that 60 percent of the sum of squares of deviations of the observed y-values about their mean is attributed to the linear relations between y and x (actual vs. predicted). In other words, 60 percent of the variability in y is explained by the regression equation. According to Ryan (1989), a meaningful correlation is obtained with $r^2 \geq 0.80$, which coincides with $p \leq 0.0011$; p is the probability of obtaining an F-value as or larger than the calculated value. This value of $r^2 = 0.80$ may be rigorous relative to correlations in geotechnical engineering. The results, therefore, may be reviewed in the following ranges (Veneziano, 1993):

$r^2 \geq 0.80$	good correlation
$0.60 \leq r^2 < 0.80$	moderate correlation
$r^2 < 0.60$	poor correlation

A second parameter that can be used to determine whether there is a good or poor correlation between data is the coefficient of variation (COV), which was defined in section 2.2.4b as the ratio of the standard deviation over the mean. Based on previous geotechnical experience the results will be reviewed in the following ranges:

$COV < 0.30$	very good correlation
$0.30 \leq COV < 0.45$	good correlation
$0.45 \leq COV < 0.60$	moderate correlation
$COV \geq 0.60$	poor correlation

5.3 THE CONTROLLING PARAMETERS

5.3.1 Soil Type

a) General

The soil type sub-groupings are based on a research report submitted to the Federal Highway Department by Paikowsky et al., 1994. The soil groupings, which refer to the soil type along the side of the pile, are as follows; clay and till, sand and silt, and rock. During the soil type analysis the question arose whether the soil groupings should not follow a more conventional sub-grouping of cohesive soils, non-cohesive soils and rock. This would lead to the sub-groupings of sand and gravel, clay and silt, and till and rock. The analysis was done comparing both sets of sub-groupings and it was found that no matter what the soil groupings were the effect of soil type on the dynamic predictions is minimal. The analysis was therefore continued using the original soil sub-groupings.

The figures used in evaluating the effect of the soil type on the performance of the dynamic predictions present the data sub-grouped according to small and large displacement piles. This is based on the definition of small displacement piles being H-piles and open-ended pipe piles (OEP) and large displacement piles being categorized as all piles that are not H-piles or OEP piles.

Figures 5.1 and 5.2 show the relationship between the static load test results compared to the CAPWAP/TEPWAP predictions and the Energy Approach predictions, respectively. The data shown are sub-grouped into soil types and type of pile as described above. Based on the r^2 values of 0.542 and 0.521 the figures show that there is a poor correlation between the static load test results and the CAPWAP/TEPWAP predictions or Energy Approach predictions for both types of piles in all types of soils. The poor correlation is also shown by the large amount of scatter in both figures. To further analyze the effect of the soil types each sub-grouping was plotted separately to better see if there is any relationship between the static load test results and the dynamically predicted results.

b) Sand and Silt

Figure 5.3 presents a comparison between the static load test results and the CAPWAP/TEPWAP predictions. The r^2 value of 0.679 for the best-fit line forced through zero shows that a moderate correlation exists between the actual and predicted pile capacities for piles that are embedded into sand and silt. A poor correlation is shown by the COV of 0.715. The change in the mean and standard deviation is minimal when compared to the mean and standard deviation for all soil types ($1.452 \pm$

0.985 for all cases compared to 1.517 ± 1.085 for cases in sand and silt). The best-fit line forced through zero shows an under-prediction ratio of 1.260 for pile-cases in sand and silt compared to 1.161 for all pile-cases. There are some cases where CAPWAP/TEPWAP under-predicts the pile capacity by as much as 90 percent, which is an under-prediction ratio of 10.

A correlation between the static load test results and the Energy Approach predictions are shown in Figure 5.4. As is shown in the figure there is a significant amount of scatter, which is also shown by the r^2 value of 0.879, which shows a poor correlation between the actual and predicted results based on the sub-grouping by soil type to sand and silt. The COV of 0.518 shows a moderate correlation between the actual and predicted values. The mean and standard deviation (0.968 ± 0.501) has not changed significantly from that shown for all soil types in Figure 5.2 (0.936 ± 0.485). The graph shows that the Energy Approach over-predicts the actual static capacity of the pile by an over-prediction ratio of 0.790, this is the slope of the best-fit line forced through zero. There is no significant change here, either, from the over-prediction ratio for all cases in all types of soils. The majority of the data points do fall within the ratios of 0.40 to 2.50 (load test results over the prediction). The scatter is still fairly large and has not changed significantly from that shown in Figure 5.2 for all of the Energy Approach predictions in all types of soils.

c) *Clay and Till*

The data shown in Figure 5.5 is a comparison between the static load test results and the CAPWAP/TEPWAP predictions for those piles embedded in clay and

till. The figure shows a poor correlation between the actual and predicted results based on the r^2 value of 0.141, while based on the COV of 0.535 there is a moderate correlation. The mean and standard deviation for the piles in clay and till (1.352 ± 0.723) has not notably changed from that for all the piles in all types of soils (1.452 ± 0.985). The under-prediction ratio changed slightly from that for all the piles in all types of soils (0.988 from 1.161) but the change is insignificant when evaluating the soil types as a controlling parameter. The majority of the extreme cases where CAPWAP or TEPWAP under-predicted the pile's capacity do not fall into the category of piles in clay and till.

Figure 5.6 shows the comparison between the static load test results and the Energy Approach predictions. A poor correlation exists between the load test results and the predicted results based on the r^2 value of 0.320 and a moderate correlation exists based on the COV of 0.527. The mean, 0.873, and standard deviation, 0.460, for the piles which are embedded in clay and till has not changed considerably from the mean, 0.936, and standard deviation, 0.485, for all piles embedded in all types of soils. The figure does show that there is a slight decrease in the over-prediction ratio for the piles that are in clay from the piles that are in all types of soils; the ratio decreases from 0.744 to 0.660. The upper end of the ratios, load test results over the predictions, meaning the amount that the method under-predicts, did decrease from 2.50 to 1.67.

d) Rock

The results that are presented in this section show a significant increase in the performance of each of the dynamic analysis methods, the CAPWAP/TEPWAP and the Energy Approach methods. It should be noted that there is a significant less number of pile-cases for which the piles are embedded in rock compared to the number of piles that are embedded into sand and silt and clay and till. The small number of pile-cases accounts for the increased performance as well as the fact that with the exception of one pile all 15 have a driving resistance that is greater 16 BP10cm and two thirds of the piles have area ratios greater than 350. These two parameters are determined to have a significant effect on the performance of the dynamic methods and are discussed later in this chapter.

Figure 5.7 shows the comparison between the static load test results and the CAPWAP/TEPWAP predictions, there is a good correlation between the actual and the predicted results as the mean and standard deviation have decreased from 1.452 ± 0.985 for all piles in all types of soils to 0.930 ± 0.172 for those piles embedded in rock. The r^2 value of 0.790 shows that there is a moderate to good correlation between the actual and predicted pile capacities, while the COV of 0.185 shows a very good correlation between the data. The mean over-prediction ratio is 0.879, which has changed from an under-prediction ratio of 1.161 for all pile-cases. All of the data points fall within a fairly narrow band of ratios (load test results over the predictions); the ratios range from approximately 0.60 to 1.25 showing that there is minimal scatter when comparing the actual and predicted results for piles that are embedded in rock.

Presented in Figure 5.8 is the comparison between the static load test results and the Energy Approach predictions for all pile-cases that are embedded in rock. As is shown the Energy Approach method also performs very well for piles that are embedded in rock with a mean of 0.744 and a standard deviation of 0.154; this is a decrease from a mean of 0.936 and a standard deviation of 0.485 for all pile-cases in all types of soils. The over-prediction ratio has also decreased from 0.744 for piles in all types of soils to 0.620 for piles that are driven into rock. Again as seen in the figure the data points fall with a narrow range of ratios (load test results over the predictions); the range is from an over-prediction ratio of 0.40 to 1.00.

e) Intermediate Conclusions

Tables 5.1 and 5.2 summarize the statistical data for the sub-groupings according to soil types for the wave matching methods (CAPWAP/TEPWAP predictions) and the field evaluation method (Energy Approach predictions), respectively. The tables also present a summary of the statistics for the sub-groupings by time of driving and the driving resistance. The above analyses show that the soil type does not have a significant effect on the results of the dynamic analyses excluding the small pile group that are driven into rock. Later in this chapter it will be seen that the soil inertia effects (the driving resistance of the pile and the type of pile that is driven) control the performance of the dynamic methods in rock and not necessarily just the fact that the pile is driven into rock.

5.3.2 Time of Driving

The time of driving (EOD versus BOR) has a significant effect on the results of the dynamic analyses. This section does not detail the effect of the time of driving on each one of the dynamic methods, but establishes the need for the time of driving to be considered in any further analyses that are done. As shown in Tables 5.1 and 5.2 the statistics for the CAPWAP/TEPWAP and Energy Approach predictions drastically improve from the end of driving cases to the beginning of restrike cases. To further evaluate the effect of time of driving on the performance of the dynamic methods, the wave matching predictions and the Energy Approach predictions will be compared to the static load test results for both EOD and BOR cases.

The wave matching predictions (CAPWAP/TEPWAP) are shown in Figure 5.9 compared to the static load test results for all pile-cases with the exception of the 5 extreme pile-cases (refer to section 6.3.1 for explanation). The mean and standard deviation of the ratio of the static load test results to the CAPWAP/TEPWAP predictions are 1.368 and 0.620, respectively. The wave matching predictions under predict the pile capacity by a mean ratio (load test results over the prediction) of 1.160.

Figures 5.10 and 5.11 present the CAPWAP/TEPWAP predictions compared to the static load test results for the end of driving and beginning of restrike pile-cases, respectively. A comparison between the means and standard deviations for all cases, the EOD cases and the BOR (last) pile-cases reveals that the time of driving has a major influence on the performance of the CAPWAP/TEPWAP methods. The mean for the EOD pile-cases is 1.626 with a standard deviation of 0.797 while the mean for

the BOR (last) pile-cases is 1.158 with a standard deviation of 0.393. The BOR (last) pile-cases have a significant less amount of scatter compared to all of the pile-cases and the EOD pile-cases. The under-prediction ratio decreases from 1.284 for the EOD pile-cases to 1.104 for the BOR (last) pile-cases. The above statistics and analysis of the wave matching methods reveals that any further analysis that is completed should take into consideration the time of driving.

Figure 5.12 presents a comparison of the static load test results and the Energy Approach predictions for all pile-cases, with the exception of the 7 extreme pile-cases (refer to section 6.3.1 for details), at all driving times. The mean and standard deviation all pile-cases is 0.894 and 0.367, respectively. The scatter is fairly significant ($r^2 = 0.542$) and the ratios (load test results over the predictions) range from approximately 0.40 and 2.50. The Energy Approach over-predicts the pile capacity by an average ratio of 0.743, which is the slope of the best-fit line through zero.

Presented in Figures 5.13 and 5.14 are the graphs comparing the static load test results and the Energy Approach predictions for the EOD and BOR (last) pile-cases. A comparison between the statistics for all pile-cases, the EOD pile-cases, and the BOR (last) pile-cases shows that there is a significant improvement from the EOD pile-cases to BOR (last) pile-cases. The mean for the EOD pile-cases is 1.084 with a standard deviation of 0.431, while the mean for the BOR (last) piles-cases is 0.785 with a standard deviation of 0.290. The scatter improves slightly for the BOR (last) pile-cases from the EOD pile-cases. The range of ratios (load test results over the predictions) for the BOR (last) pile-cases is 0.40 to 1.67 while for the EOD pile-cases

the range is from 0.40 to 2.50. The mean over-prediction for the EOD pile-cases is 0.926 while for the BOR (last) pile-cases it is 0.695, this shows that for the BOR (last) pile-cases the Energy Approach over-predicts by a significant amount but it consistently over-predicts so it can be corrected with a multiplying factor. The statistics for the Energy Approach also show that any further analysis that is completed needs to take into consideration the effects of the time of driving. The time of driving effects are not as obvious for the Energy Approach predictions as for the CAPWAP/TEPWAP predictions.

Table 5.3 summarizes the statistics of the data that were presented in Figures 5.9 through 5.14 for the comparison of the static load test results and the CAPWAP/TEPWAP predictions as well as the Energy Approach predictions. Based on these statistics it can be seen that the time of driving has a major influence on the performance of the dynamic methods and needs to be considered in any further analysis.

5.3.3 Soil Inertia Effects

a) Overview

Paikowsky and Chernauskas (1996) had shown that the stationary soil assumption, under which the soil/pile interaction models were developed, does not reflect the physical phenomenon that occurs during pile driving. The use of pseudo viscous damping serves as a mechanism to absorb energy, but, as it does not reflect the actual phenomenon, its correlation to physical properties (e.g. soil type) or time of driving cannot be achieved. If the motion of the displaced soil is a major factor

contributing to the energy loss during driving, a substantial portion of the dynamic resistance should be a function of two parameters: (i) mass/volume of the displaced soil that is a function of the pile geometry, namely, small vs. large displacement piles, and (ii) acceleration of the displaced soil, (especially at the tip) that can be conveniently examined as a function of the driving resistance (Paikowsky and Stenersen, 2000).

The soil inertia effects consist of the driving resistance of the pile, hard or easy driving, and the type of pile that is used, small or large displacement. This section will first show the controlling effect of the driving resistance and then present the method used to determine the dividing point between hard and easy driving.

Through analysis previously done by Paikowsky et al. 1994 it was determined that small and large displacement piles are not defined only by the type of pile (e.g. H-piles and OEP piles are small displacement) but rather they are defined by the area ratio. The area ratio is defined by Paikowsky et al., 1994, as follows:

$$A_R = \frac{A_{\text{skin}}}{A_{\text{tip}}} = \frac{\text{Surface area in contact with the soil}}{\text{Area of the pile tip}} \quad (5.1)$$

Paikowsky et al. (1994) proposed that piles that have an area ratio above 350 are small displacement piles and piles with an area ratio less than 350 are classified as large displacement piles. The controlling effect of the type of pile driven will be shown in this section, as well as a statistical analysis used to verify the area ratio boundary between small and large displacement piles.

b) Effect of Driving Resistance

The initial analysis in this section shows that there is a controlling effect due to driving resistance. The initial boundary between hard and easy driving is based on research by Paikowsky et al. (1994). A blow count boundary between hard and easy driving of 16 blows per 10 cm (4 blows/inch) is used in Figures 5.15 through 5.18 to show the controlling effect of driving resistance. Paikowsky et al. (1994) suggested to use 6 BPI (Blows Per Inch), (24 blows/10cm) as the boundary between easy driving and hard driving. A later study by Paikowsky and Chernauskas (1996) found that 4 BPI (16 blows/10cm) is a better indicator of that boundary. A 3 BPI (12 blows/10cm) boundary is used by GRL for such differentiation (Rausche, 2001).

Shown in Figures 5.15 and 5.16 are the comparisons between the static load test results and the CAPWAP/TEPWAP predictions for the pile-cases that fall into the categories of easy and hard driving, respectively. The mean and standard deviation of ratio of static load test results to the wave matching predictions for the easy driving case is 1.874 and 1.580, respectively, which shows that for low blow counts the wave matching methods do not perform very well. As seen in Figure 5.16 the mean ratio of the static load test results to the CAPWAP/TEPWAP predictions is 1.285 with a standard deviation of 0.528, representing a significant improvement in the performance of the wave matching methods. The scatter for both the easy and hard driving pile case is approximately the same with the ratios (load test results over the predictions) ranging from 0.60 to 2.50. The mean under-prediction for the easy driving pile-cases is 1.308 and the mean under-prediction for the hard driving pile-

cases is 1.130, which is consistent with the improvement in the mean and standard deviations. The analysis comparing the static load test results to the CAPWAP/TEPWAP predictions for the easy and hard driving pile-cases shows that the effect of driving resistance needs to be considered in any further analysis that is completed.

Figures 5.17 and 5.18 show the comparisons of the static load test results and the Energy Approach predictions for the easy and hard driving pile-cases, respectively. The figures show an improvement in the performance of the Energy Approach method from the easy driving pile-cases to the hard driving pile-cases. This is seen in the improvement of the mean and standard deviation, which for the easy driving pile-cases are 1.173 and 0.693, respectively, and for the hard driving pile-cases are 0.840 and 0.324, respectively. The scatter for both the easy and hard driving cases are similar ranging from a ratio (load test results over the predictions) of 0.40 to 2.50. The mean over-prediction decreases from 0.871 for the easy driving pile-cases to 0.720 for the hard driving pile-cases, this is consistent with the decreasing in the mean K_{SP} value. The results from analyzing the Energy Approach predictions based on blow count show that driving resistance is a parameter that controls the performance of the dynamic methods.

A summary of the above mentioned statistics analyzing the effect of the driving resistance on the performance of the dynamic methods is presented in Table 5.4. The table shows the sub-grouping of the PD/LT2000 database into the dynamic

methods according to the CAPWAP/TEPWAP predictions and the Energy Approach predictions, as well as by the blow count according to easy and hard driving.

The continuation of the analysis reexamines the boundary between easy and hard driving using a statistical analysis of the data found in PD/LT2000. Figures 5.19 and 5.20 present the method that was used to determine this boundary. The figures show the relationship between the K_{SW} and K_{SP} values, which are the ratios of the static load test results to the CAPWAP/TEPWAP and Energy Approach predictions respectively, and the blow count. From these graphs it can be seen that at low blow counts there is larger scatter between the blow count and the K_{SW} and K_{SP} values.

To determine the blow count boundary at which the CAPWAP/TEPWAP and the Energy Approach methods perform poorly for blow counts below that boundary and better for blow counts above that boundary, the means and standard deviations were taken for all K_{SW} and K_{SP} values within ranges of 8 BP10cm (2 BPI). The mean K_{SX} (the ratio of the static load test results to the CAPWAP/TEPWAP or Energy Approach predictions depending on which method is being analyzed) values for each range of blow counts were plotted versus the midpoint blow count of that specific range. Shown on the bottom graphs for each of the figures are these relationships as well as the mean for all pile cases and their standard deviations. The figures show that at blow counts less than 8 BP10cm the Energy Approach and signal-matching methods have a mean that is approximately one standard deviation (for all pile-cases) larger than the mean for all pile-cases. The mean for the pile-cases that are within the range of 8 to 16 BP10cm is approximately equal to the mean for all cases (1.472 vs.

1.368 for CAPWAP/TEPWAP and 0.975 vs. 0.894 for the Energy Approach) but the standard deviation is still large compared to that of the means for the pile-cases in the ranges above 16 BP10cm (0.765 vs. 0.528 for CAPWAP/TEPWAP and 0.478 vs. 0.324 for the Energy Approach). The standard deviations for the ranges of 8 BP10cm above a blow count of 16 BP10cm are all fairly consistent and are significantly smaller than the standard deviations for the two ranges below 16 BP10cm. The boundary between easy and hard driving is therefore taken as 16 BP10cm (4 BPI) and will subsequently be used in all analyses.

c) Effect of Pile Type

The second aspect of the soil inertia effects is the volume of the displaced soil, i.e., the pile type (small or large displacement piles). The preliminary analysis to determine the pile size effect on the dynamic predictions was presented by Paikowsky et al., 1994, suggesting that the boundary between small and large displacement piles is an area ratio of 350. Figures 5.21 through 5.24 use the area ratio of 350 as the boundary between small and large displacement piles demonstrating that there is a controlling effect based on the size of the driven pile.

Figures 5.21 and 5.22 show the comparisons between the static load test results and the wave matching techniques (CAPWAP/TEPWAP) for pile-cases with area ratios below and above 350, respectively. The mean and standard deviations for the two sub-groupings show that there is a significant increase in the performance of the wave matching techniques from large displacement (area ratio < 350) piles to small displacement piles (area ratio ≥ 350). The mean and standard deviation decreases

from 1.536 ± 1.137 to 1.295 ± 0.582 . There is a minimal decrease in the mean under-prediction ratio from the pile-cases with area ratios less than 350 to those with area ratios above 350; the mean decreases from 1.168 to 1.150. There are a significant number of pile-cases with area ratios less than 350 for which the wave matching techniques under-predict the pile capacity by more than sixty percent. The number of pile-cases for which the wave matching techniques under-predicts the pile capacity by more than sixty percent for pile-cases with an area ratio greater than 350 is significantly less than those for pile-cases with area ratios less than 350. Based on the predictions of the wave matching techniques there is a significant effect of the pile type on the predicted pile capacity.

The comparisons between the static load test results and the Energy Approach predictions are shown in Figures 5.23 and 5.24 for pile-cases with area ratios less than 350 and greater than 350, respectively. There is no significant difference between the mean and standard deviations for these two sub-groupings, 0.914 ± 0.473 for the pile-cases with an area ratio below 350 and 0.980 ± 0.508 for pile-cases with an area ratio above 350. There is a slight improvement in the mean over-prediction from the pile-cases with an area ratio less than 350 to the pile-cases with an area ratio greater than 350 (0.712 to 0.832). The scatter for both sub-groupings is very similar and the prediction ratios range from approximately 0.40 to 2.50. Based on the Energy Approach predictions there is little to no effect on the predicted pile capacity due to the pile type.

The statistics that were shown in the above analyses for the effect of pile type on the pile capacities based on the wave matching techniques and the Energy Approach are summarized in Table 5.5. The conclusion from the analysis is that there is an effect on the pile capacity determined using the dynamic methods due to the pile type, which is based on the area ratio, especially for the CAPWAP/TEPWAP predictions. The continued analysis to determine the area ratio boundary, which differentiates between small and large displacement piles, will show that even for the Energy Approach method the results are affected by the pile type.

The data presented in Figures 5.25 and 5.26 is similar to the approach that was used to determine the boundary between easy and hard driving (refer to Figures 5.19 and 5.20). The top portion of each of the figures (5.25 and 5.26) presents the comparison between the K_{SX} values (the ratio of the static load test results to the CAPWAP/TEPWAP or Energy Approach predictions depending on which method is being analyzed) and the area ratio for the CAPWAP/TEPWAP and Energy Approach predictions, respectively. The data is sub-grouped by soil type and it can be seen that there is no real correlation between the K_{SX} values and the area ratio. The bottom portions of the figures were created by plotting the mean K_{SX} values and the standard deviations for the pile-cases within a range of area ratios of 175 versus the mid-point area ratio for that specific range. As is shown in Figures 5.25 and 5.26 for both the wave matching techniques and the Energy Approach predictions the mean K_{SX} value for the range of area ratios from 0 to 175 is approximately equal to the mean for all pile-cases (1.382 vs. 1.452 for CAPWAP/TEPWAP and 0.864 vs. 0.936 for the

Energy Approach) and the standard deviations are within the standard deviation for all pile-cases (0.569 vs. 0.985 for CAPWAP/TEPWAP and 0.326 vs. 0.485 for the Energy Approach). The range in which the standard deviations become drastically larger than the standard deviations for all pile-cases is from 175 to 350 (1.425 vs. 0.985 for CAPWAP/TEPWAP and 0.563 vs. 0.485 for the Energy Approach). The majority of the means and standard deviations for the ranges above 350 fall within the range of the standard deviations of all pile-cases. The boundary between small and large displacement was therefore taken at an area ratio of 350. Piles having an area ratio greater than 350 are classified as small displacement and pile having an area ratio less than 350 are classified as large displacement piles.

In an effort to examine the true influence of the area ratio three things needed to be done. The first is to isolate, to the extent possible, the influence of the acceleration on the inertia from that of the mass on the inertia, i.e., look on blow counts greater than 16 BP10cm. The second is to look at the data when the soil inertia effects most likely exist during driving, i.e., EOD, whereas, it may not be mobilized at BOR. The final thing is the method of analysis to evaluate, the CAPWAP (wave matching techniques) were chosen because of the easier influence on the method as a full analysis of the phenomenon is done. The conclusion is that in order to look closely at the influence of the area ratio the pile-cases related to the wave matching techniques at the EOD for blow counts greater than 16 BP10cm needed to be evaluated.

Figure 5.27 presents the analysis that was completed to isolate the CAPWAP/TEPWAP pile-cases at the EOD for blow counts greater than 16 BP10cm. The top portion of the figure is a comparison between the K_{SW} values and their corresponding area ratios. This graph shows that there is a point in which the K_{SW} values begin to go asymptotically towards a K_{SW} value of 1.0. The bottom graph of the figure presents the actual analysis used to verify the boundary between small and large displacement piles. The mean K_{SW} values as well as the standard deviations for a range of area ratios were plotted versus the midpoint area ratio for that range. The ranges for these pile-cases varied due to the lesser number of pile-cases compared to all of the wave matching technique pile-cases. As is shown the means for the first two ranges of area ratios, (0 - 175 and 175- 350), are slightly higher than the mean for all cases in the specific sub-grouping being analyzed. It is apparent by the standard deviations for these two ranges that the dynamic methods performance will be less accurate for piles that have an area ratio less than 350. The means for the ranges above an area ratio of 350 are significantly smaller than the mean for all pile-cases in this sub-grouping but they are approximately one as is shown in the figure. The standard deviations are relatively small for the pile-cases that have an area ratio greater than 350 compared to the overall standard deviation for all pile-cases in this sub-grouping.

The conclusion from this analysis is that there is a significant effect on the performance of the dynamic methods due to the type of pile that is driven. The boundary between poor performance (large displacement piles) and good performance

(small displacement piles) of the CAPWAP/TEPWAP and Energy Approach predictions is taken at an area ratio of 350. The analysis that is done from this point forward will incorporate the effect of the pile type.

5.4 INTERMEDIATE CONCLUSIONS

The above analyses show that the controlling parameters that have a significant effect on the pile capacity predictions are, in order of importance, the time of driving, the driving resistance and the type of pile (small or large displacement) that was driven. The analyses showed that the effect of soil type is minimal when compared to the other controlling parameters. The boundary between easy and hard driving will be taken at a blow count of 16 BP10cm (4 BPI) and the boundary between small and large displacement piles will be taken at an area ratio of 350.

Table 5.1. Summary of the K_{SW} Values for the Different Soil Types used for the Soil Inertia Analysis.

	Clay & Till				Sand & Silt				Rock			
Mean	1.352				1.517				0.930			
Standard Deviation	0.723				1.085				0.172			
Number of Cases	100				265				15			
	EOD		BOR(last)		EOD		BOR(last)		EOD		BOR(last)	
Mean	1.634		1.133		2.068		1.193		0.968		0.925	
Standard Deviation	0.899		0.444		1.765		0.391		0.132		0.203	
Number of Cases	45		40		77		116		7		7	
	< 5 BPcm	≥ 5 BPcm	< 5 BPcm	≥ 5 BPcm	< 5 BPcm	≥ 5 BPcm	< 5 BPcm	≥ 5 BPcm	< 5 BPcm	≥ 5 BPcm	< 5 BPcm	≥ 5 BPcm
Mean	1.725	1.315	1.254	0.985	2.191	1.458	1.126	1.283	1.070	0.952	0.960	0.879
Standard Deviation	0.807	1.160	0.489	0.340	1.901	0.512	0.386	0.355	-----	0.136	0.209	0.230
Number of Cases	35	10	22	18	64	13	74	40	1	6	4	3

Table 5.2. Summary of the K_{SP} Values for the Different Soil Types used for the Soil Inertia Analysis.

	Clay & Till				Sand & Silt				Rock			
Mean	0.873				0.968				0.744			
Standard Deviation	0.460				0.501				0.154			
Number of Cases	101				260				15			
	EOD		BOR(last)		EOD		BOR(last)		EOD		BOR(last)	
Mean	1.037		0.717		1.310		0.821		0.778		0.729	
Standard Deviation	0.588		0.231		0.670		0.314		0.092		0.207	
Number of Cases	46		40		81		107		7		7	
	< 5 BPcm	≥ 5 BPcm	< 5 BPcm	≥ 5 BPcm	< 5 BPcm	≥ 5 BPcm	< 5 BPcm	≥ 5 BPcm	< 5 BPcm	≥ 5 BPcm	< 5 BPcm	≥ 5 BPcm
Mean	1.127	0.750	0.686	0.751	1.345	1.122	0.789	0.863	0.645	0.801	0.772	0.671
Standard Deviation	0.637	0.241	0.235	0.229	0.716	0.292	0.330	0.267	-----	0.077	0.249	0.163
Number of Cases	35	11	21	19	68	13	72	34	1	6	4	3

Table 5.3. Summary of the Statistics showing the Importance of the Time of Driving as a Controlling Parameter.

Dynamic Method	CAPWAP		Energy Approach	
Mean	1.368		0.894	
Standard Deviation	0.620		0.367	
Number of Cases	377		371	
Time of Driving	EOD	BOR (last)	EOD	BOR (last)
Mean	1.626	1.158	1.084	0.785
Standard Deviation	0.797	0.393	0.431	0.290
Number of Cases	125	162	128	153

Table 5.4. Summary of the Statistics showing the Importance of the Driving Resistance as a Controlling Parameter.

Dynamic Method	CAPWAP		Energy Approach	
Mean	1.368		0.894	
Standard Deviation	0.620		0.367	
Number of Cases	377		371	
Driving Resistance	< 16 BP10cm	≥ 16 BP10cm	< 16 BP10cm	≥ 16 BP10cm
Mean	1.874	1.285	1.173	0.840
Standard Deviation	1.580	0.528	0.693	0.324
Number of Cases	108	274	109	269

Table 5.5. Summary of the Statistics showing the Importance of the Area Ratio as a Controlling Parameter.

Dynamic Method	CAPWAP		Energy Approach	
Mean	1.368		0.894	
Standard Deviation	0.620		0.367	
Number of Cases	377		371	
Area Ratios	< 350	≥ 350	< 350	≥ 350
Mean	1.536	1.295	0.914	0.980
Standard Deviation	1.137	0.582	0.473	0.508
Number of Cases	250	132	250	128

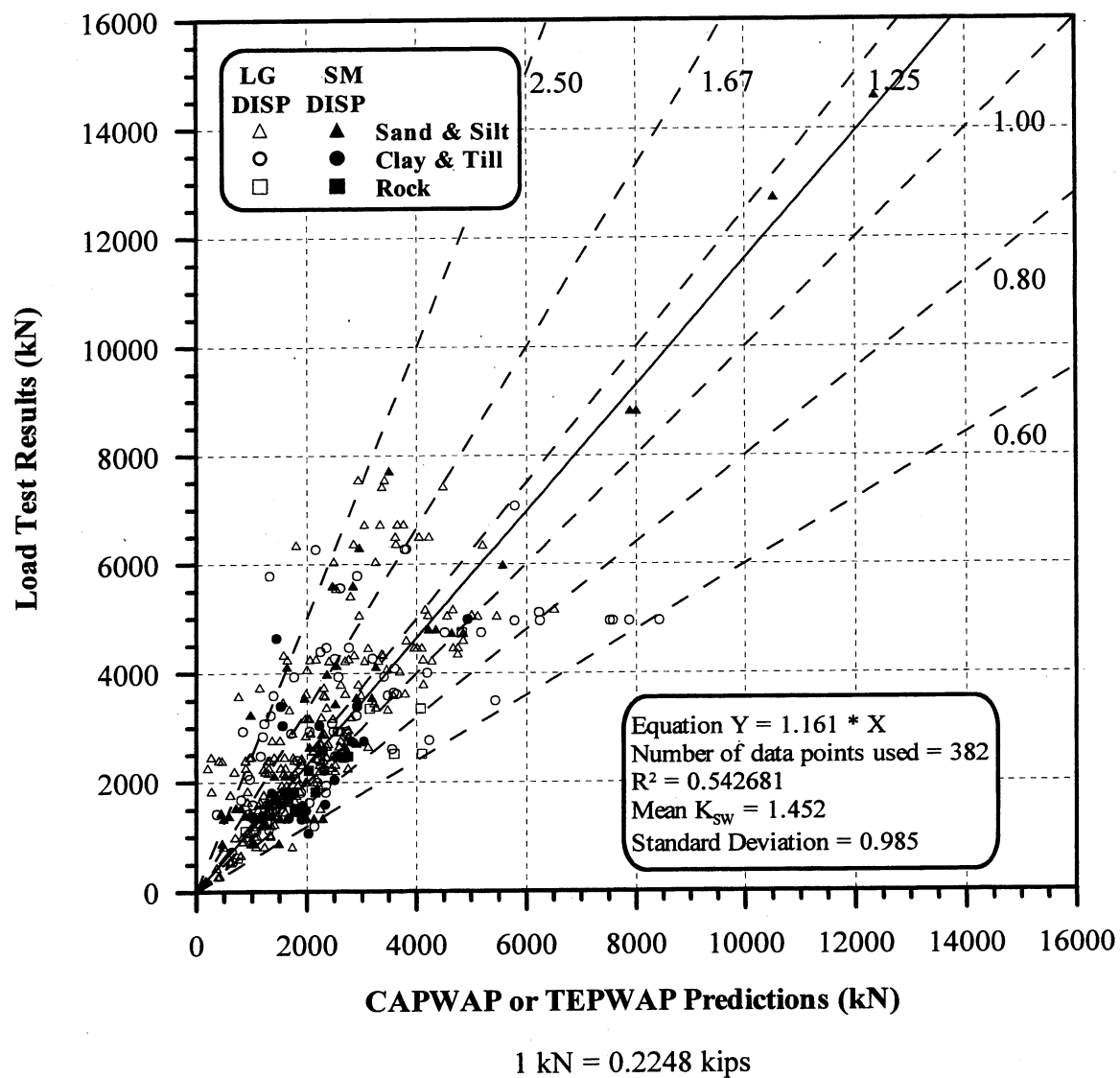


Figure 5.1. Static Load Test Results vs. CAPWAP or TEPWAP predictions for 382 PD/LT2000 pile-cases in all types of soils (AAA).

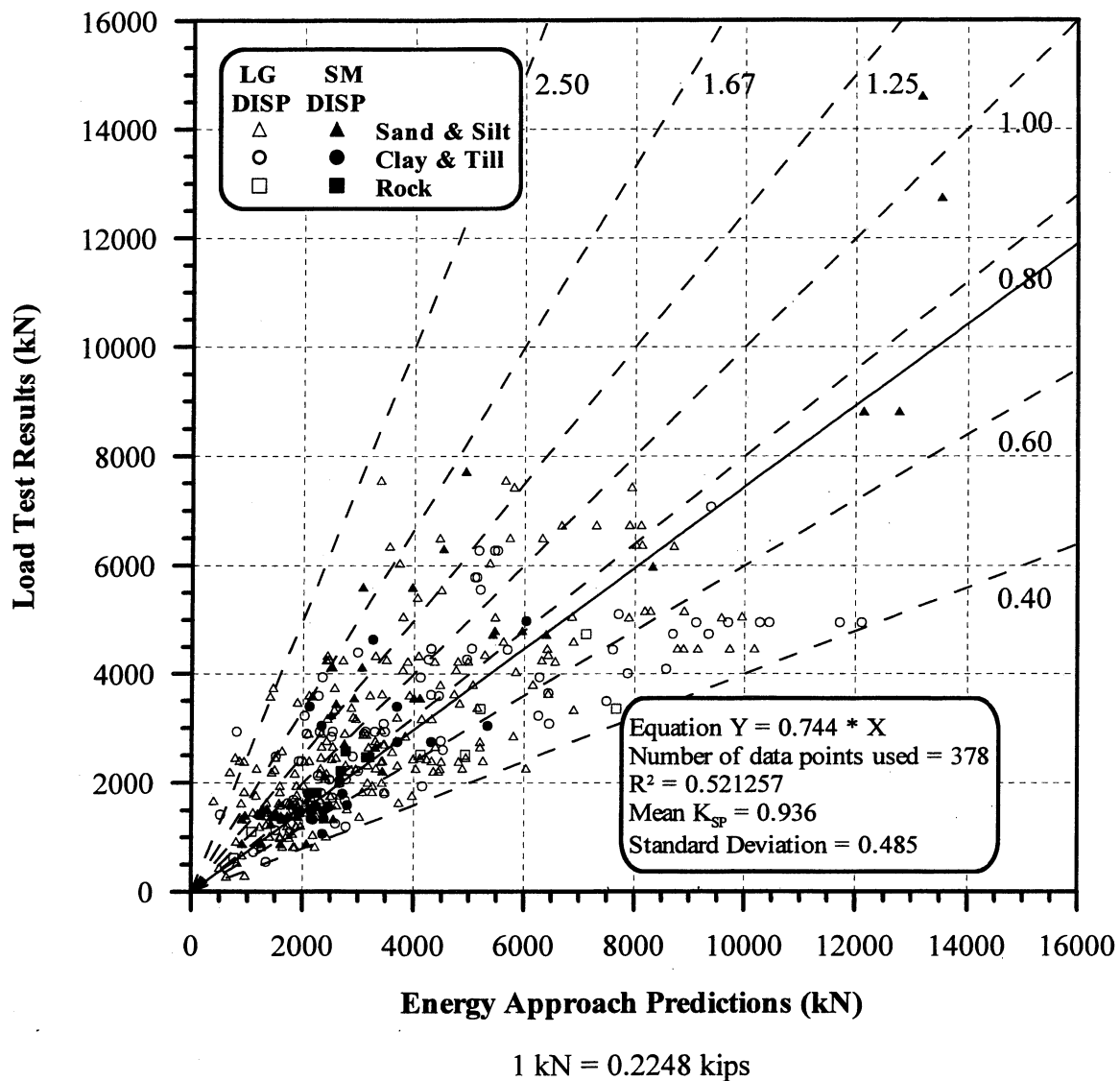


Figure 5.2. Static Load Test Results vs. Energy Approach predictions for 378 PD/LT2000 pile-cases in all types of soils (AAA).

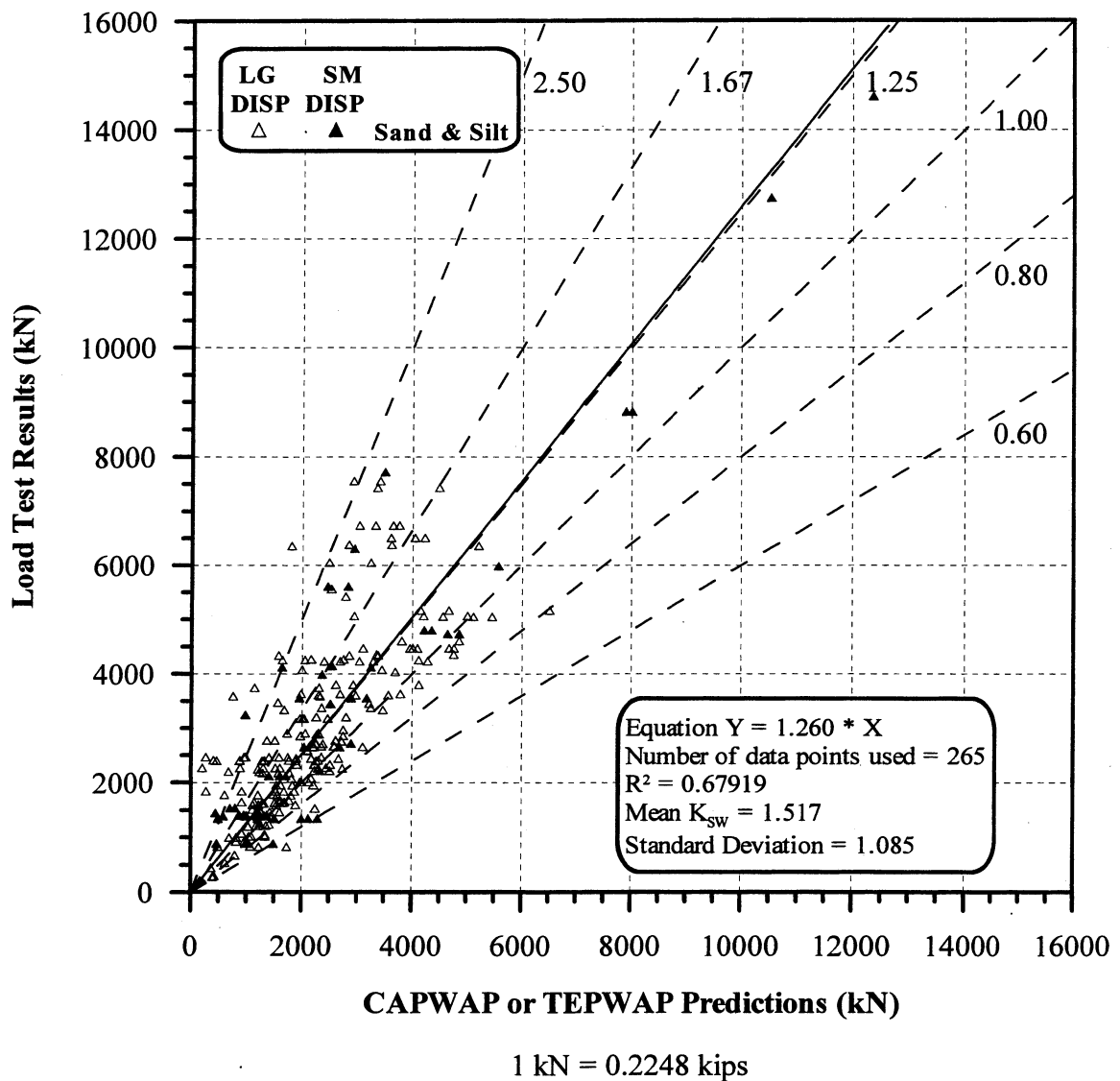


Figure 5.3. Static Load Test Results vs. CAPWAP or TEPWAP predictions for 265 PD/LT2000 pile-cases in sand & silt (AAS).

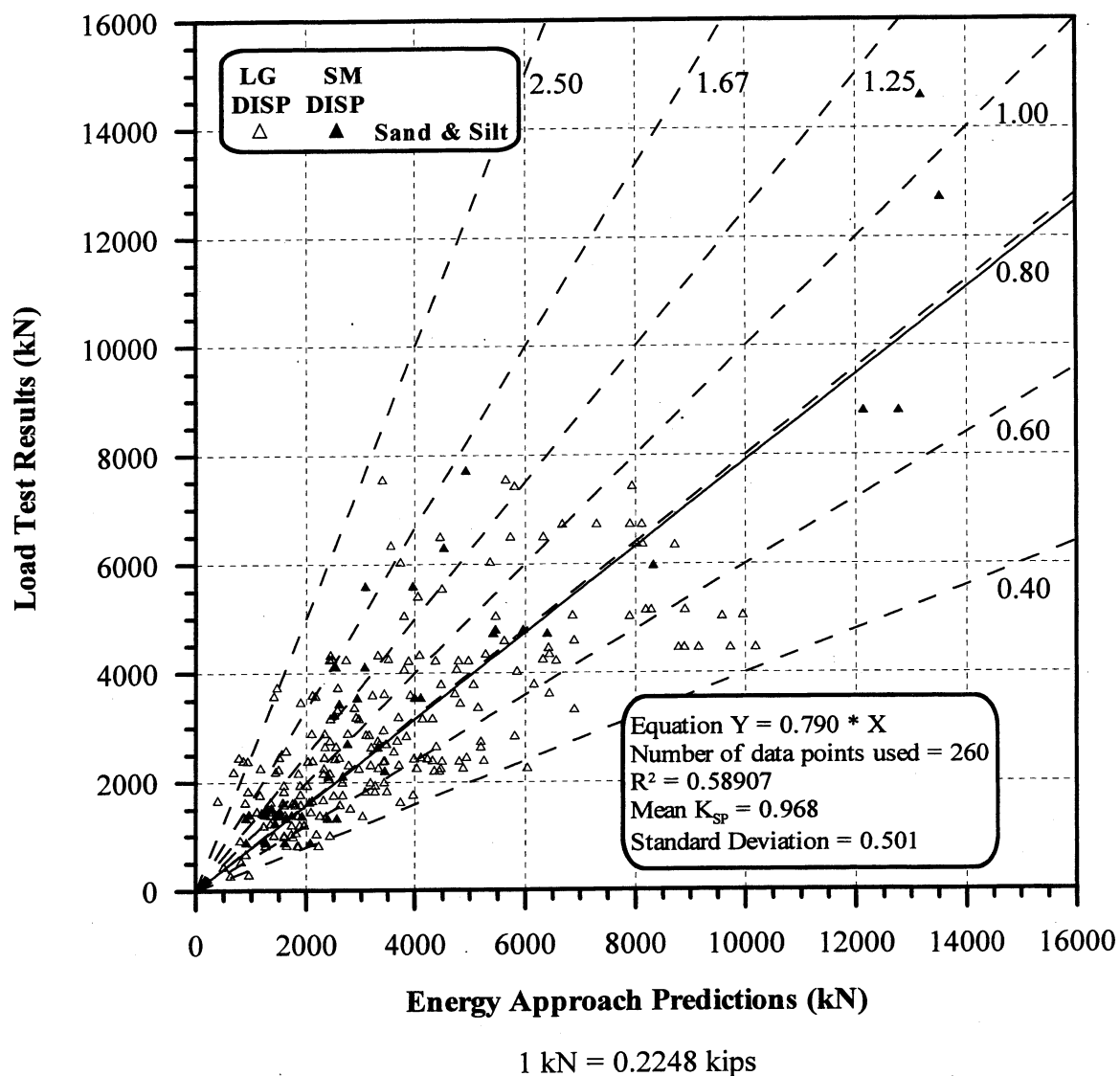


Figure 5.4. Static Load Test Results vs. Energy Approach predictions for 260 PD/LT2000 pile-cases in sand & silt (AAS).

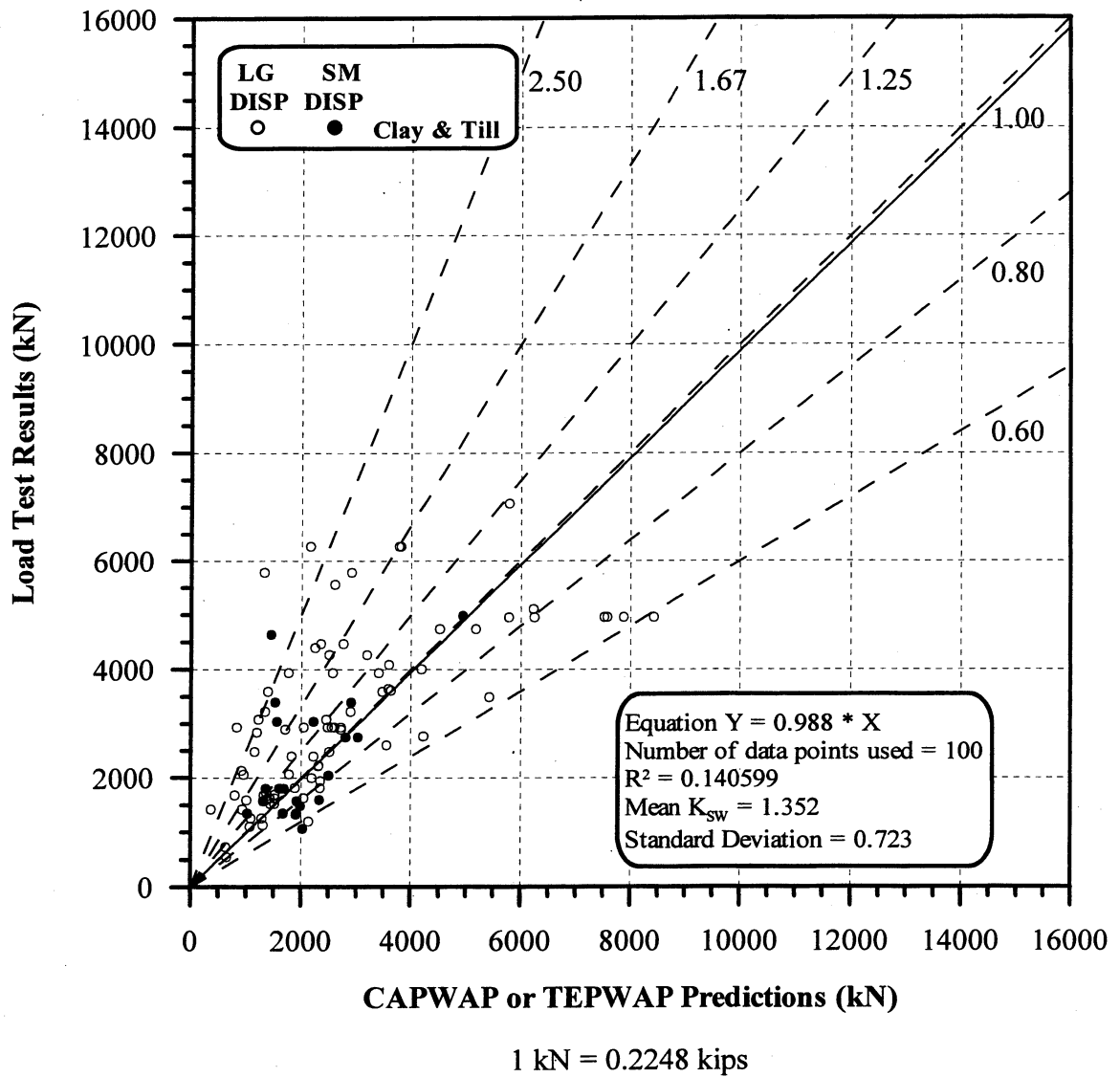


Figure 5.5. Static Load Test Results vs. CAPWAP or TEPWAP predictions for 100 PD/LT2000 pile-cases in clay & till (AAC).

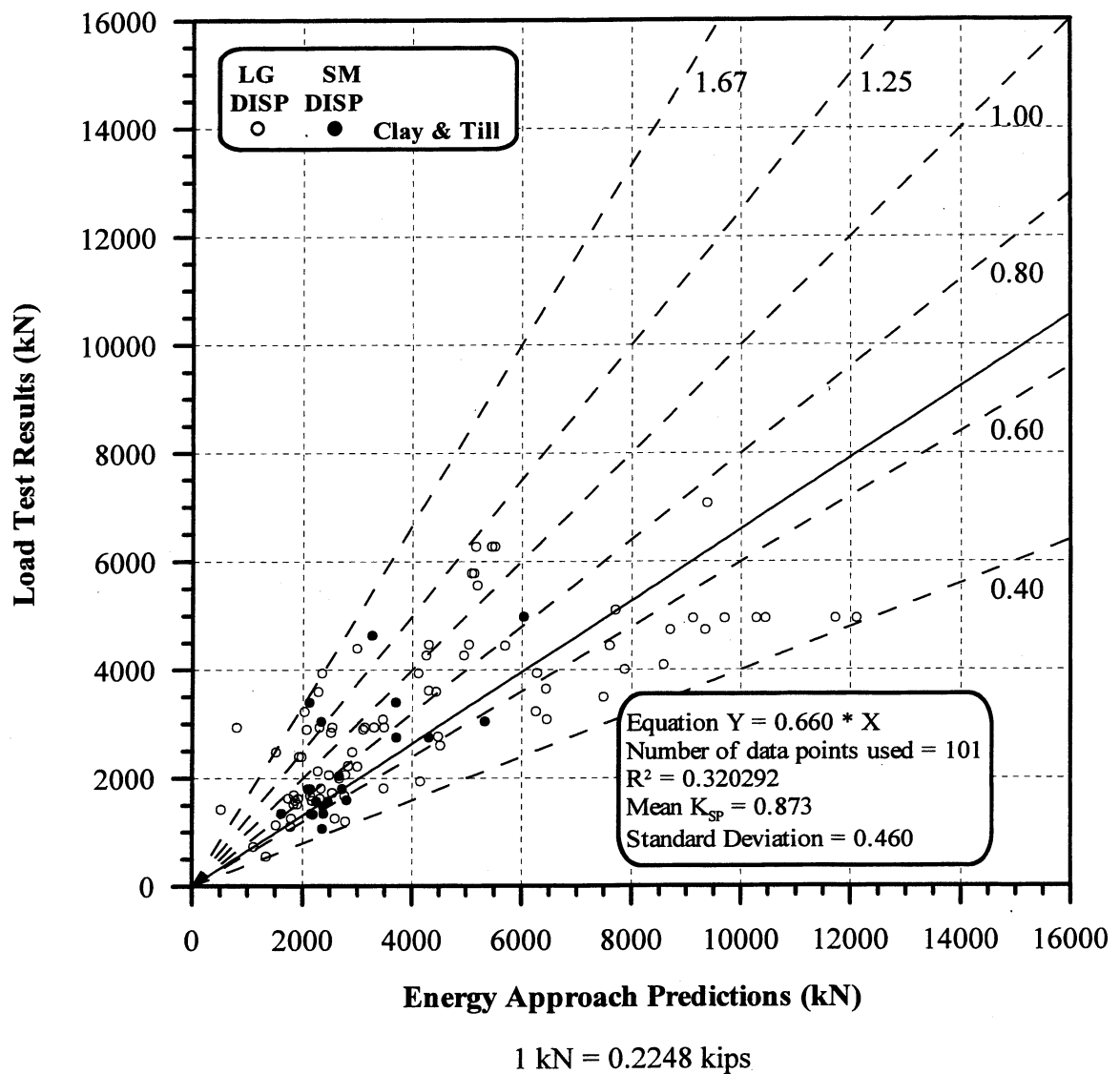


Figure 5.6. Static Load Test Results vs. Energy Approach predictions for 101 PD/LT2000 pile-cases in clay & till (AAC).

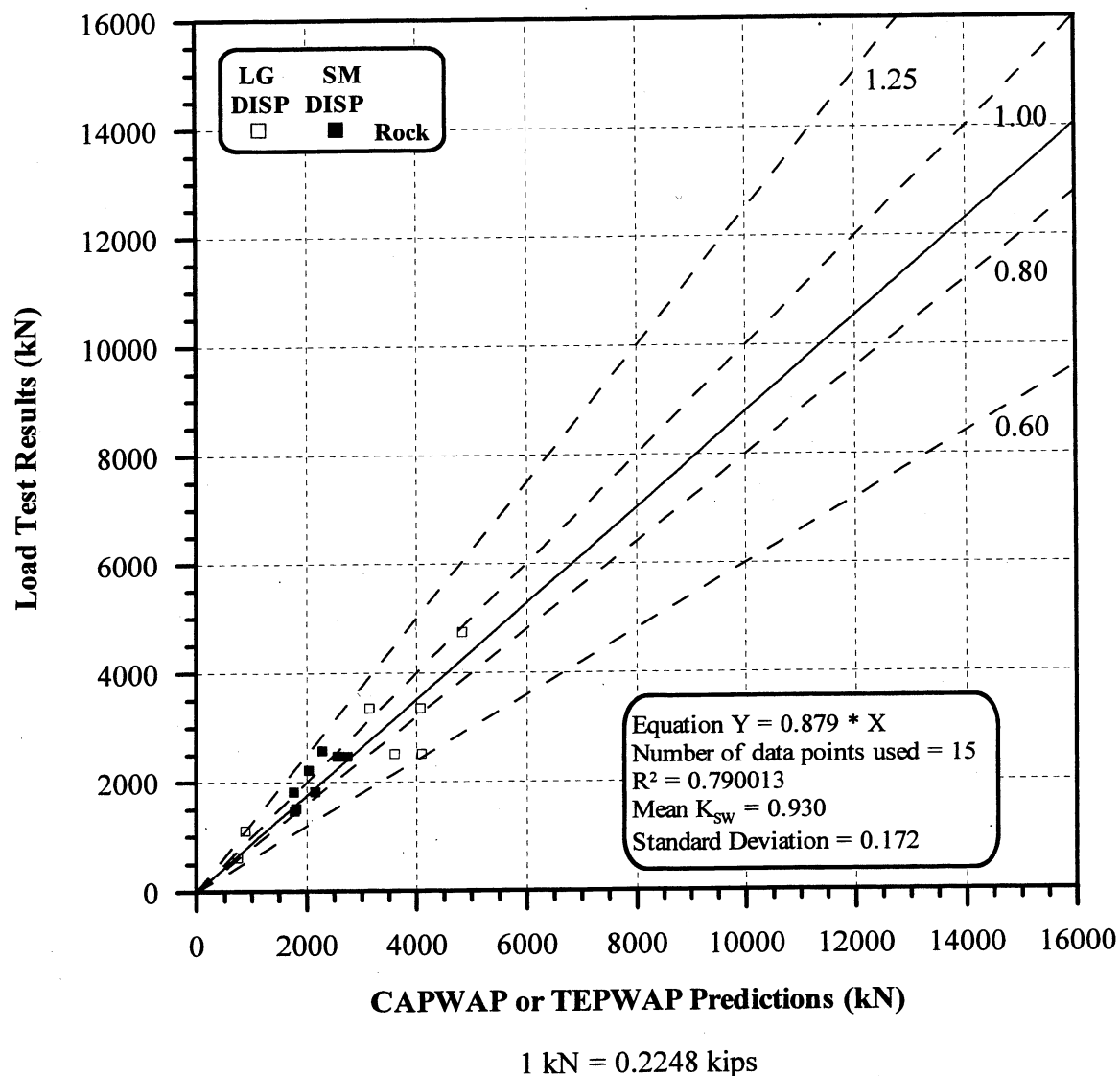


Figure 5.7. Static Load Test Results vs. CAPWAP or TEPWAP predictions for 15 PD/LT2000 pile-cases in rock (AAR).

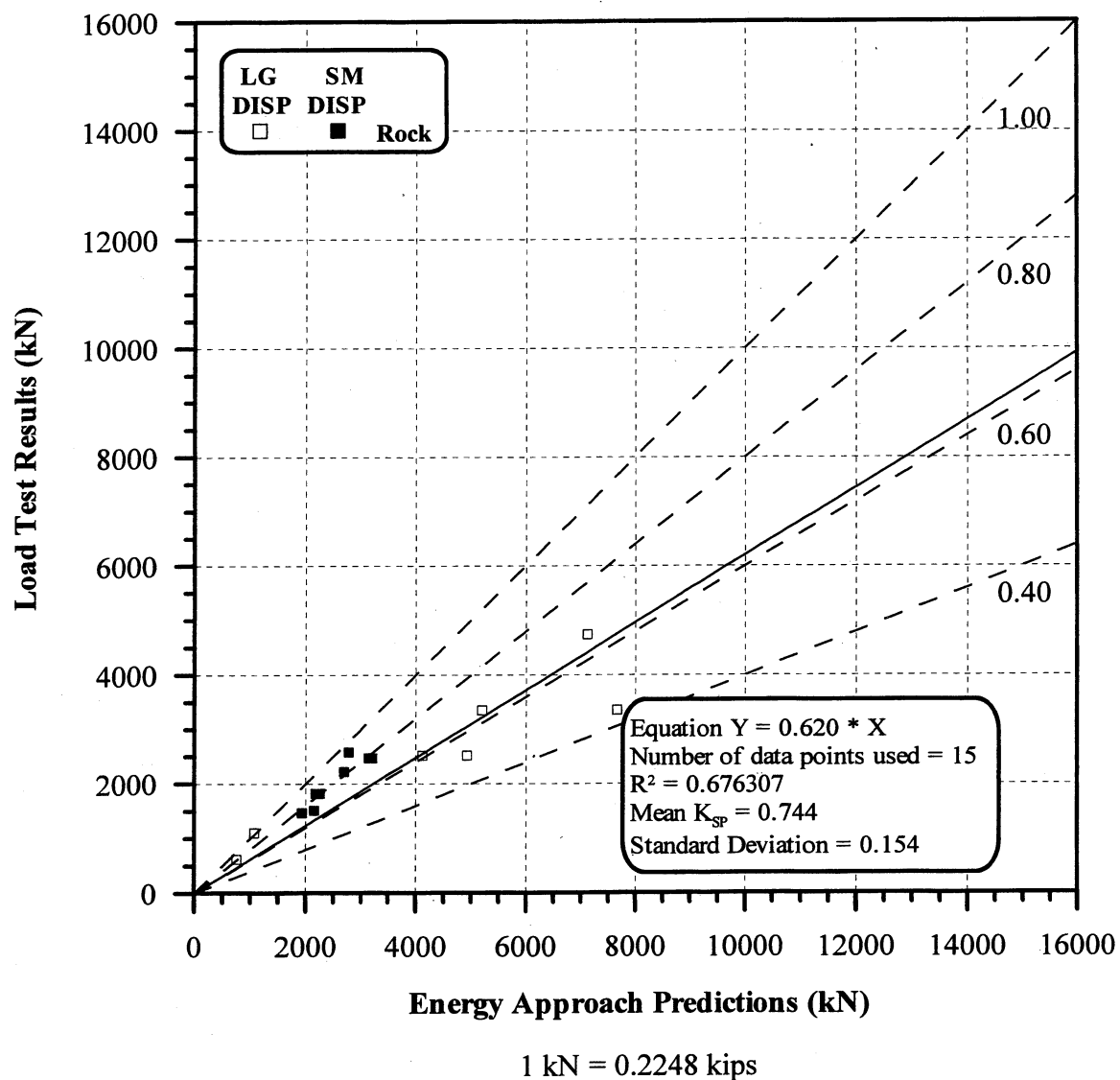


Figure 5.8. Static Load Test Results vs. Energy Approach predictions for 15 PD/LT2000 pile-cases in rock (AAR).

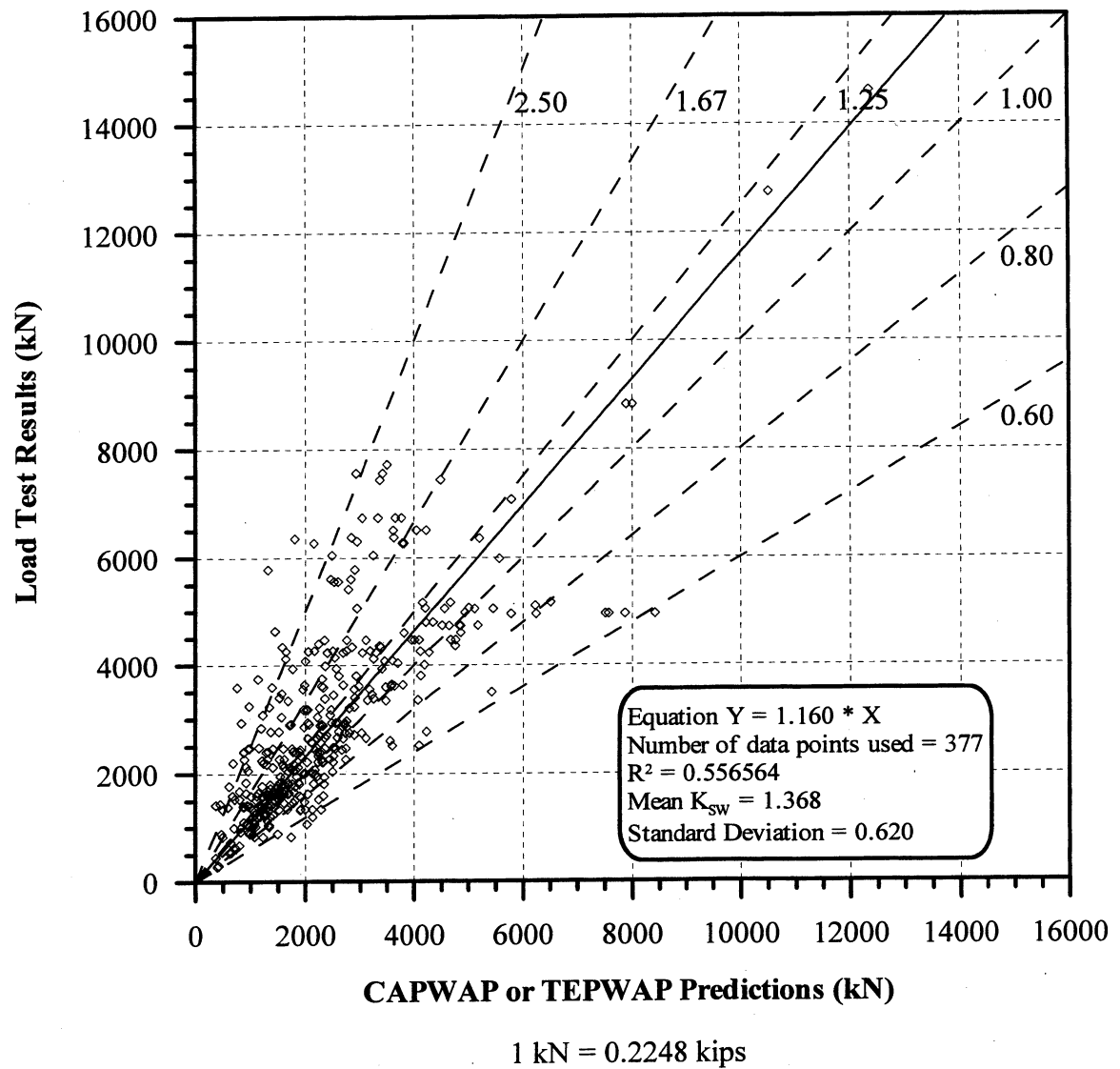


Figure 5.9. Static Load Test Results vs. CAPWAP or TEPWAP predictions for 377 PD/LT2000 pile-cases in all types of soils (AAA).

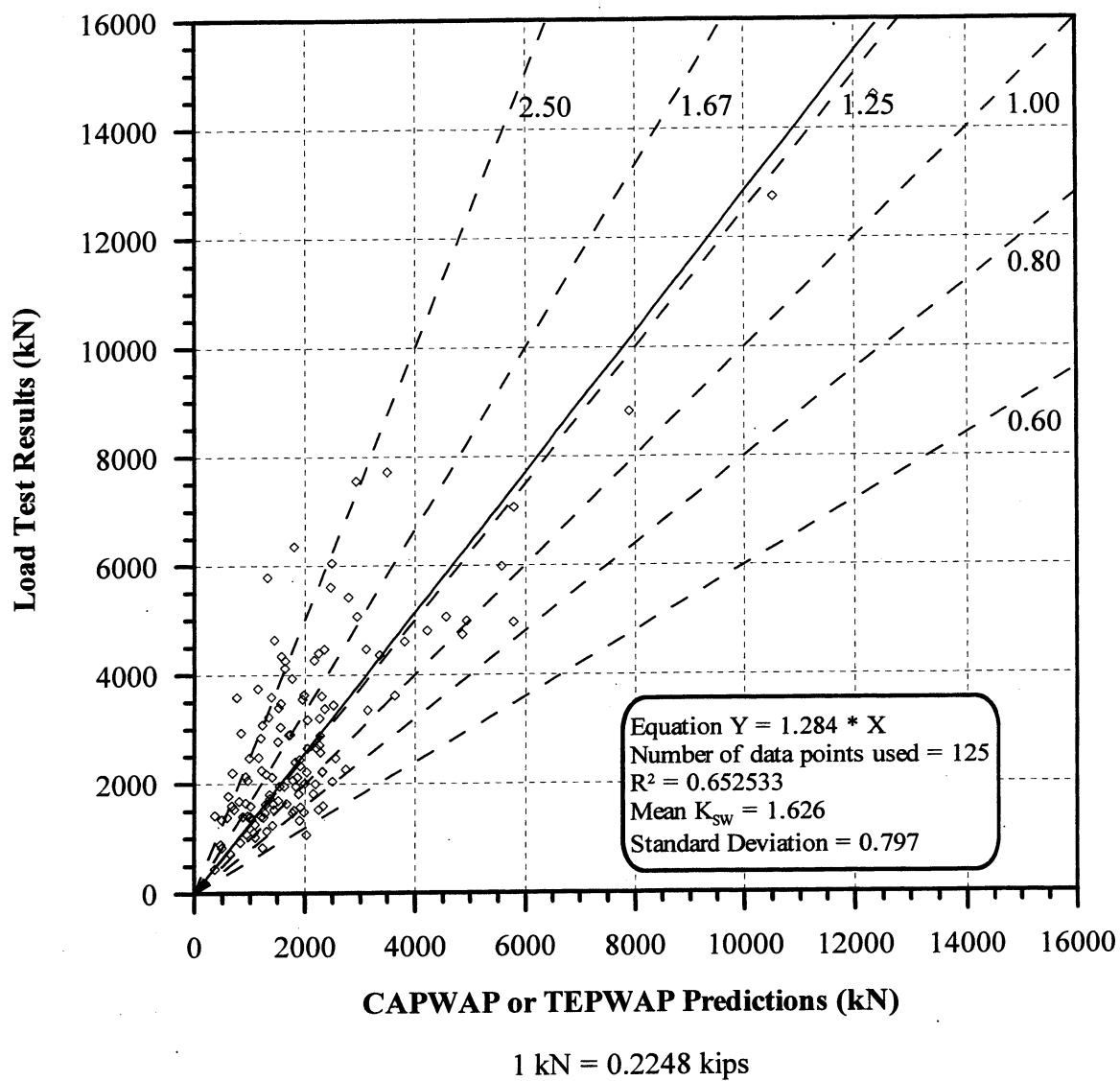


Figure 5.10. Static Load Test Results vs. CAPWAP or TEPWAP predictions for 125 PD/LT2000 pile-cases at EOD in all types of soils (AEA).

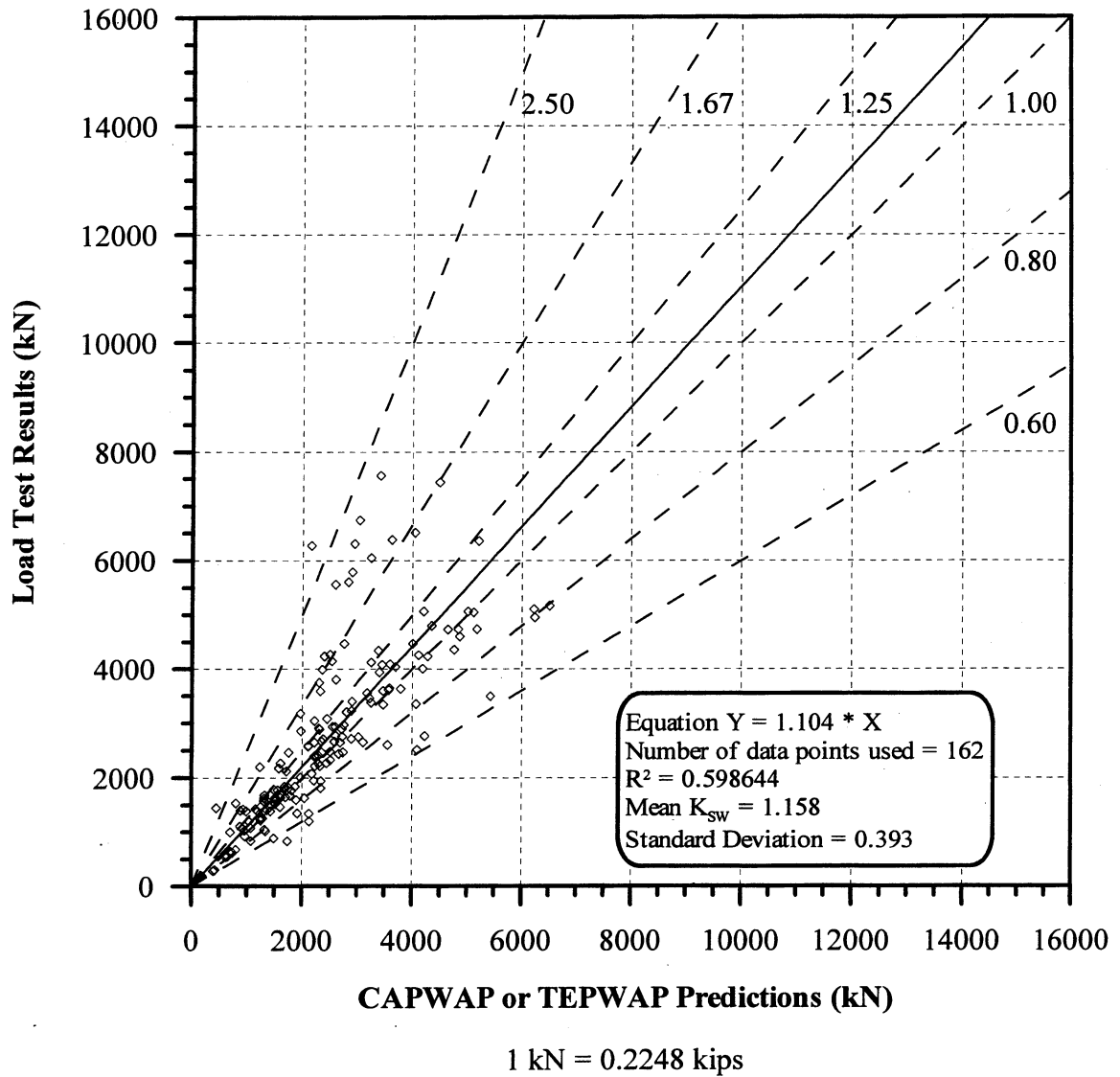


Figure 5.11. Static Load Test Results vs. CAPWAP or TEPWAP predictions for 162 PD/LT2000 pile-cases at BOR(last) in all types of soils (ABA).

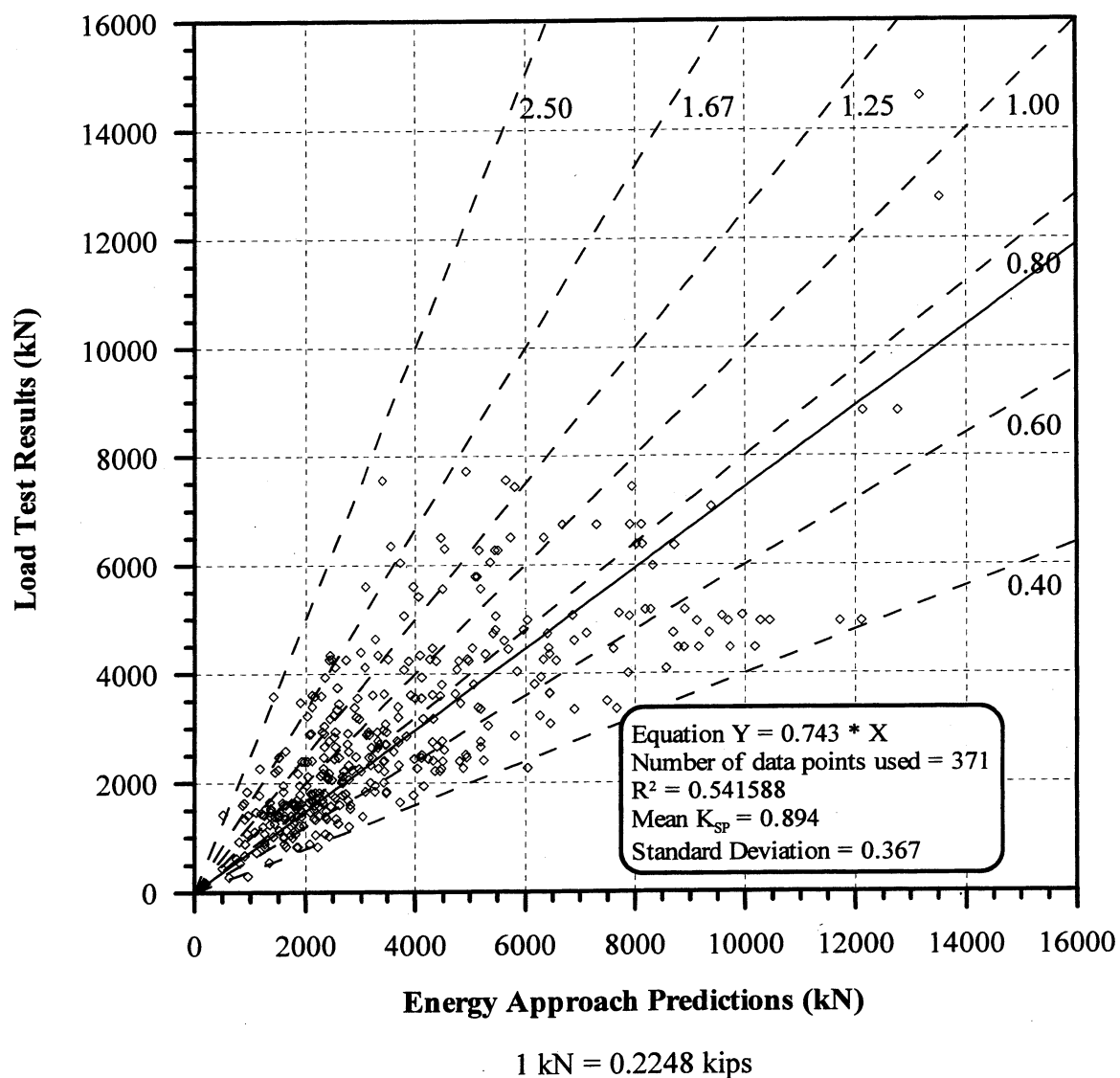


Figure 5.12. Static Load Test Results vs. Energy Approach predictions for 371 PD/LT2000 pile-cases in all types of soils (AAA).

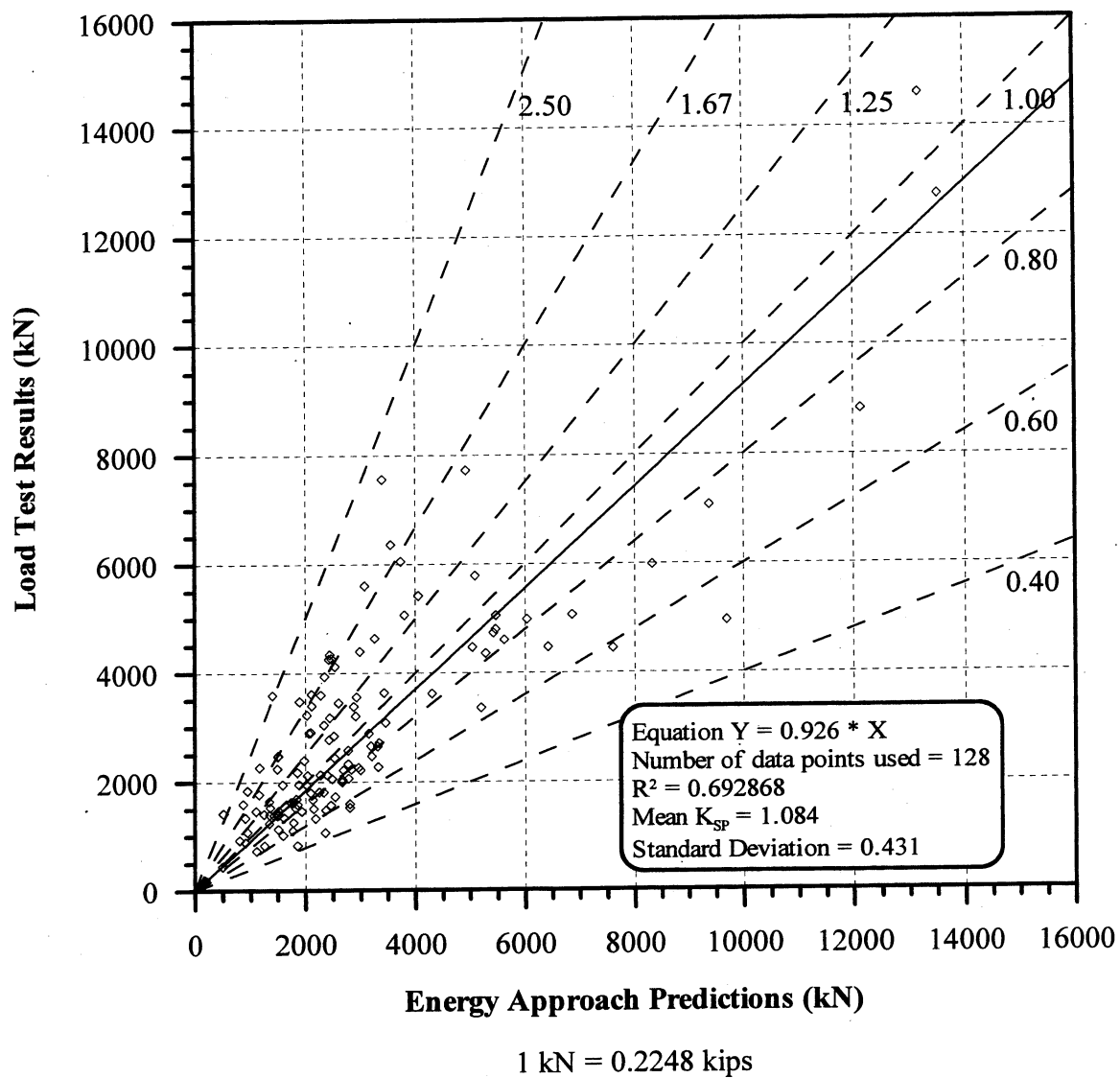


Figure 5.13. Static Load Test Results vs. Energy Approach predictions for 128 PD/LT2000 pile-cases at EOD in all types of soils (AEA).

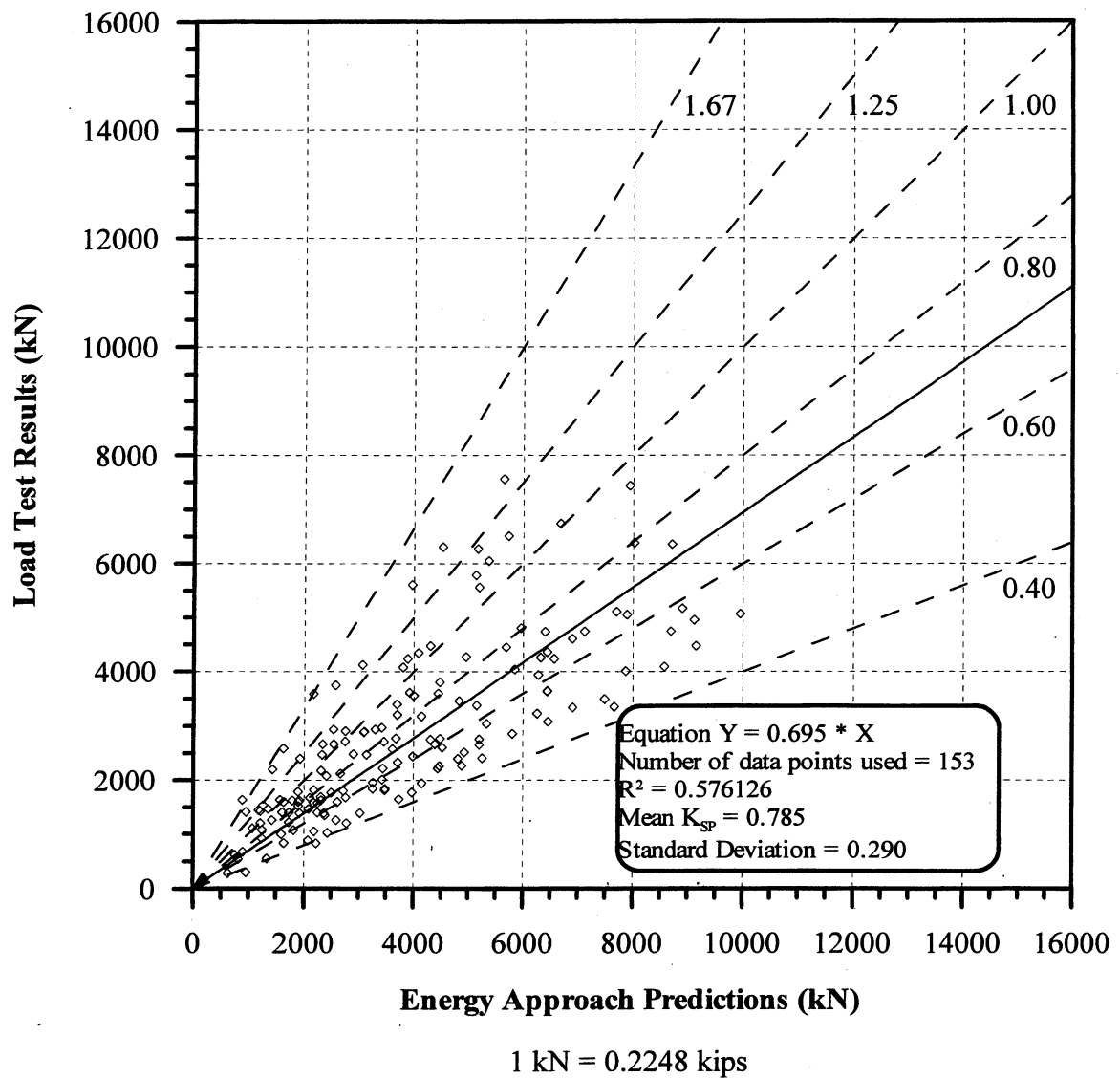
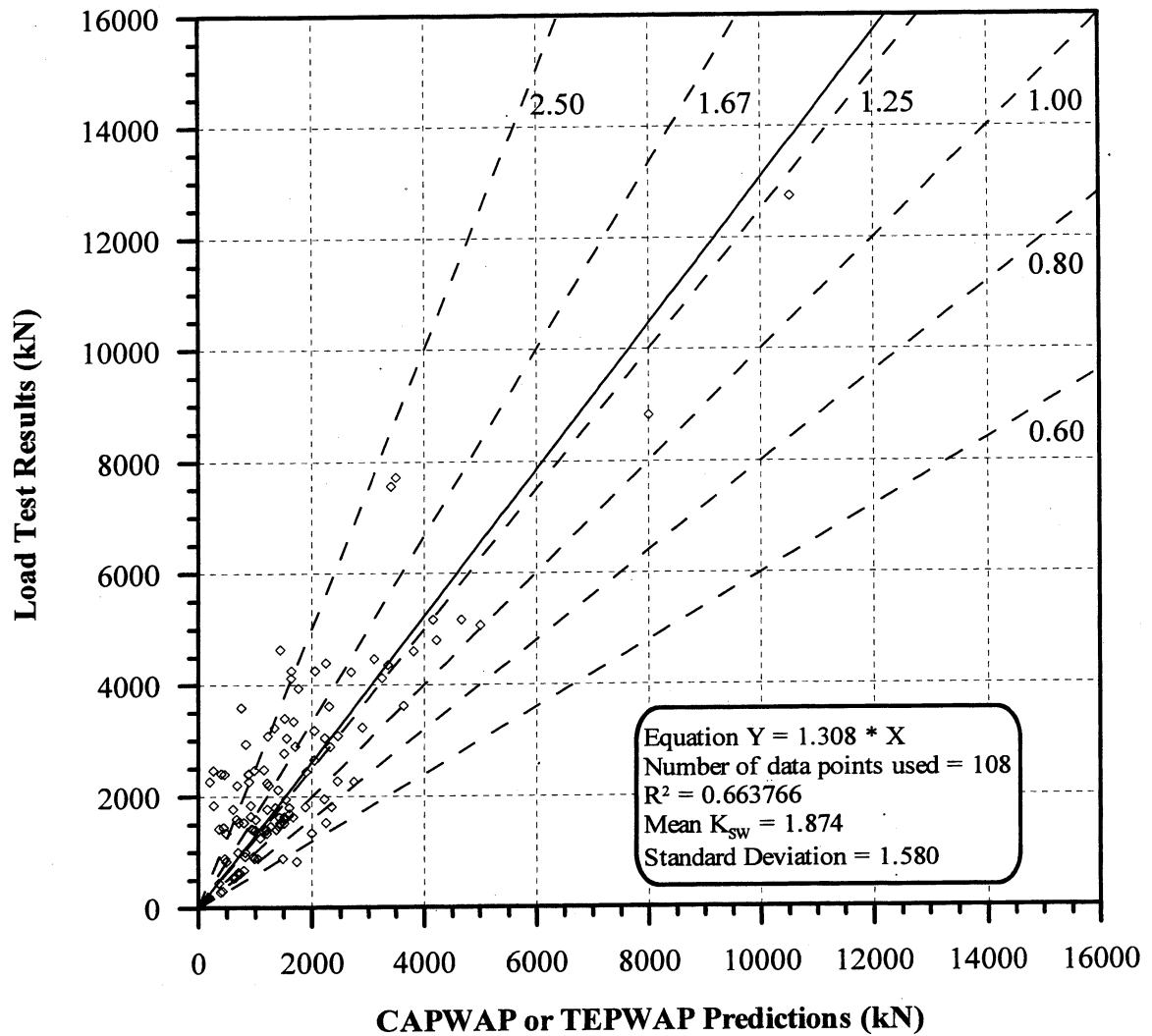


Figure 5.14. Static Load Test Results vs. Energy Approach predictions for 153 PD/LT2000 pile-cases at BOR(last) in all types of soils (ABA).



1 kN = 0.2248 kips

Figure 5.15. Static Load Test Results vs. CAPWAP or TEPWAP predictions for 108 PD/LT2000 pile-cases with Blow Count < 16 BP10cm in all types of soils (AAA).

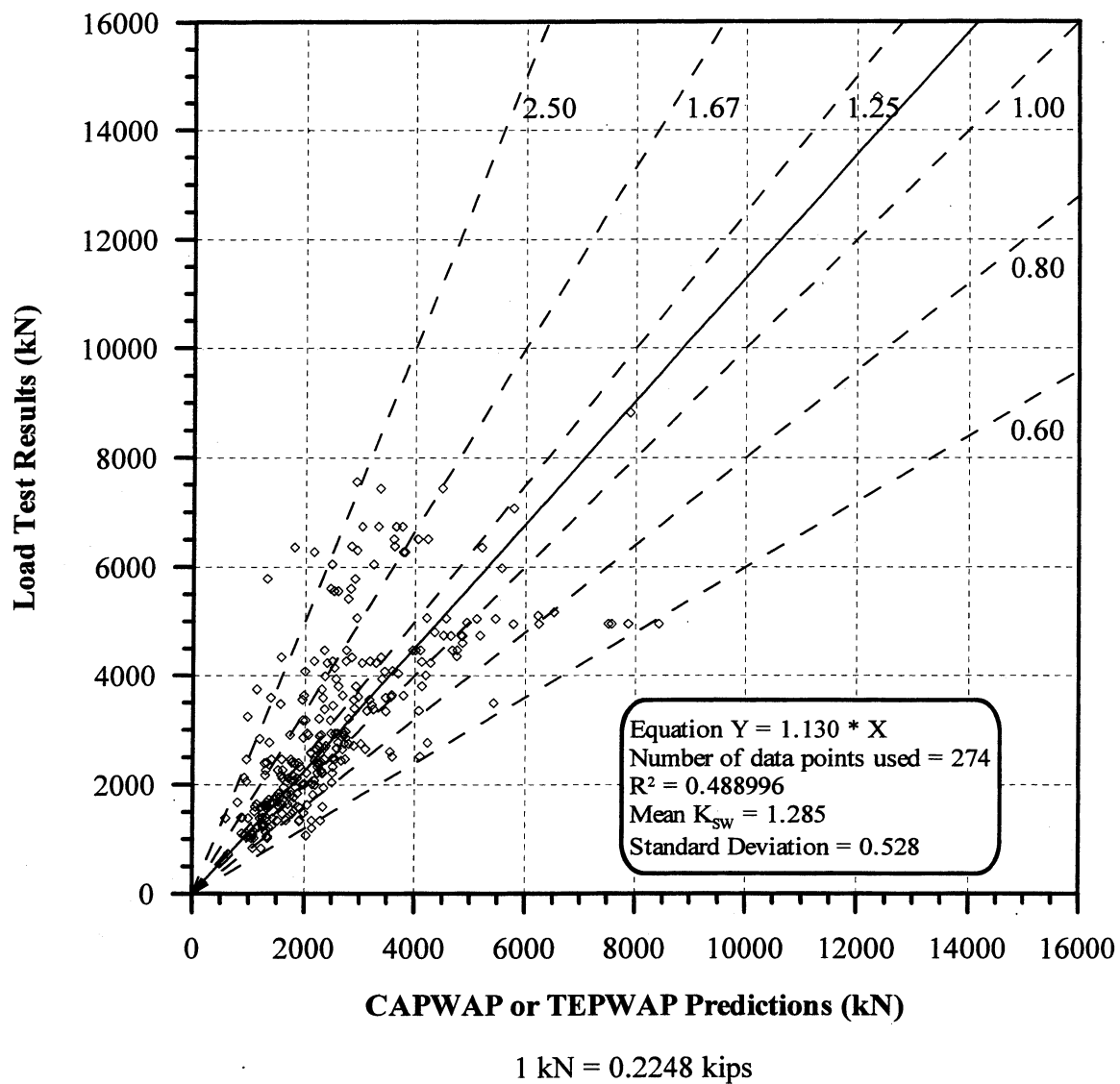


Figure 5.16. Static Load Test Results vs. CAPWAP or TEPWAP predictions for 274 PD/LT2000 pile-cases with Blow Count ≥ 16 BP10cm in all types of soils (AAA).

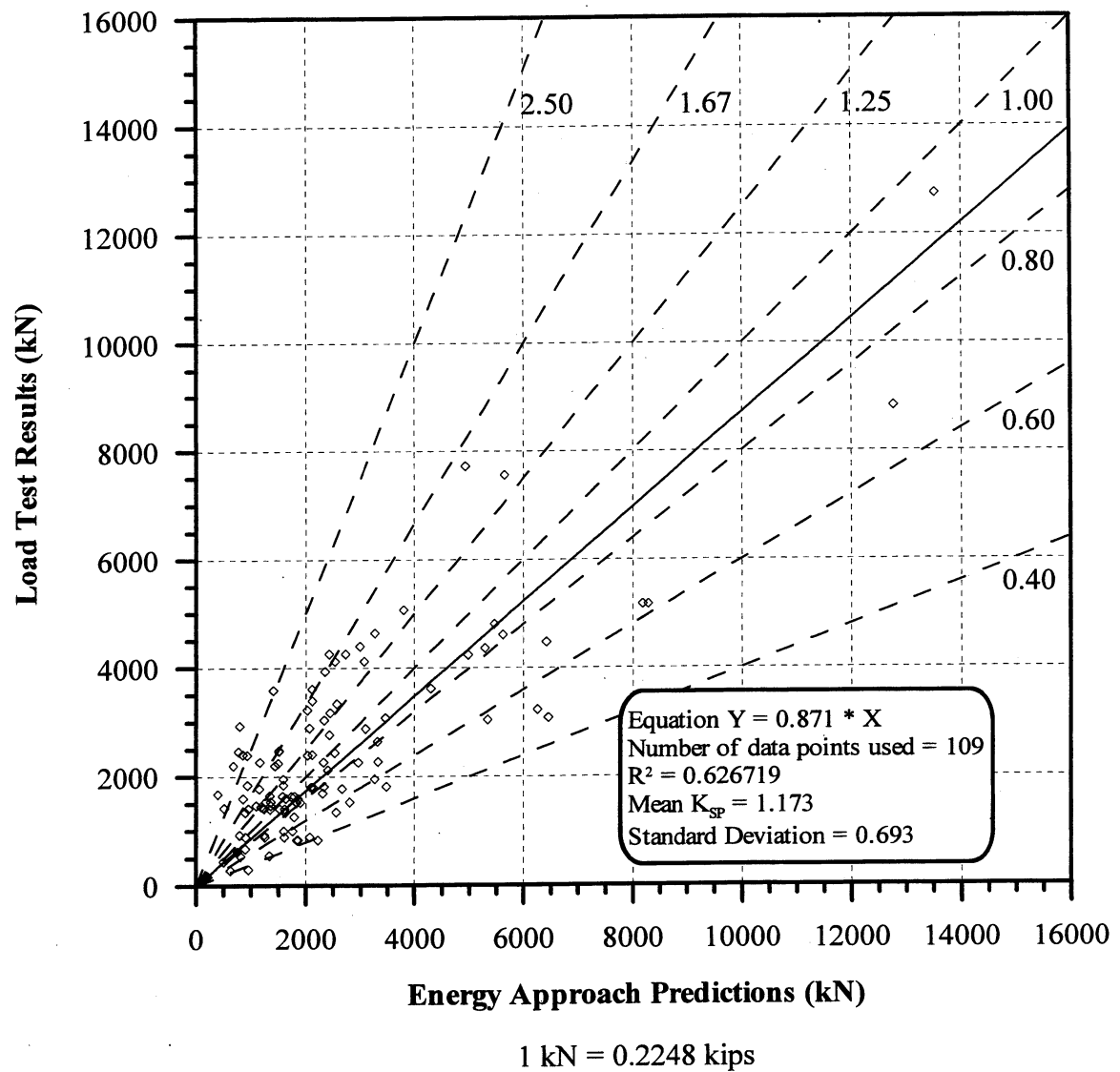


Figure 5.17. Static Load Test Results vs. Energy Approach predictions for 109 PD/LT2000 pile-cases with Blow Count < 16 BP10cm in all types of soils (AAA).

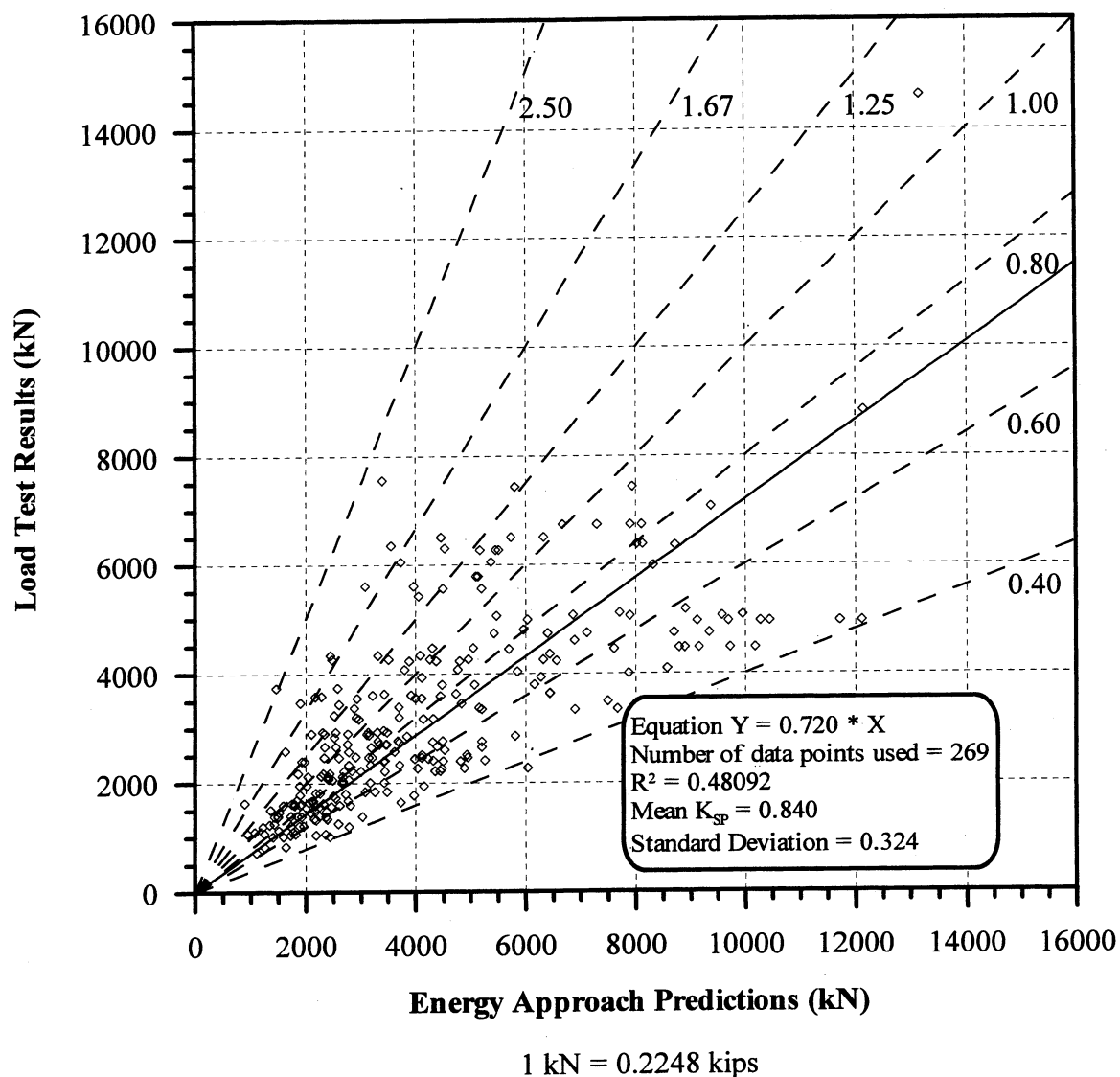


Figure 5.18. Static Load Test Results vs. Energy Approach predictions for 269 PD/LT2000 pile-cases with Blow Count ≥ 16 BP10cm in all types of soils (AAA).

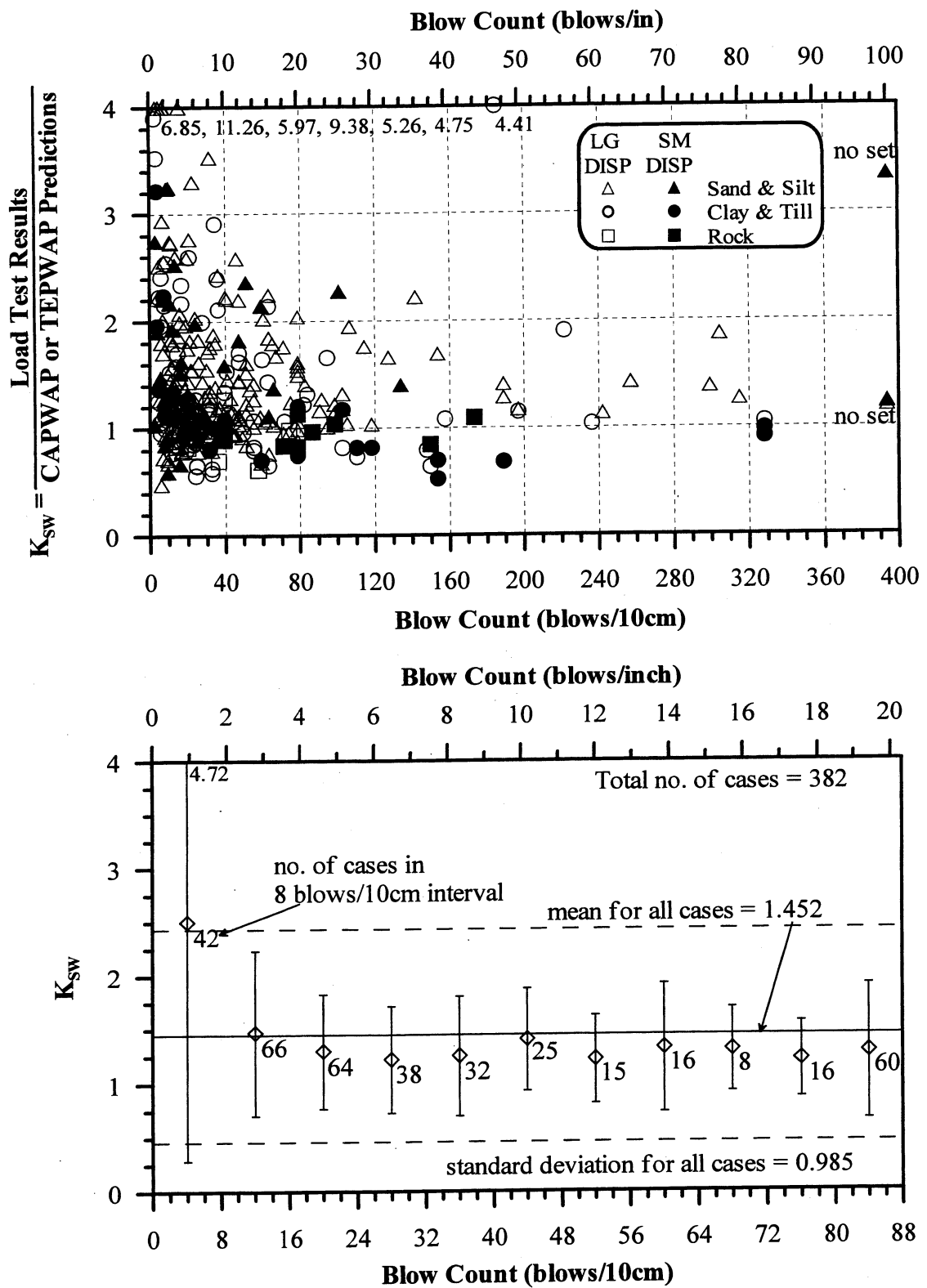


Figure 5.19. K_{sw} versus Blow count for all piles cases in PD/LT2000.

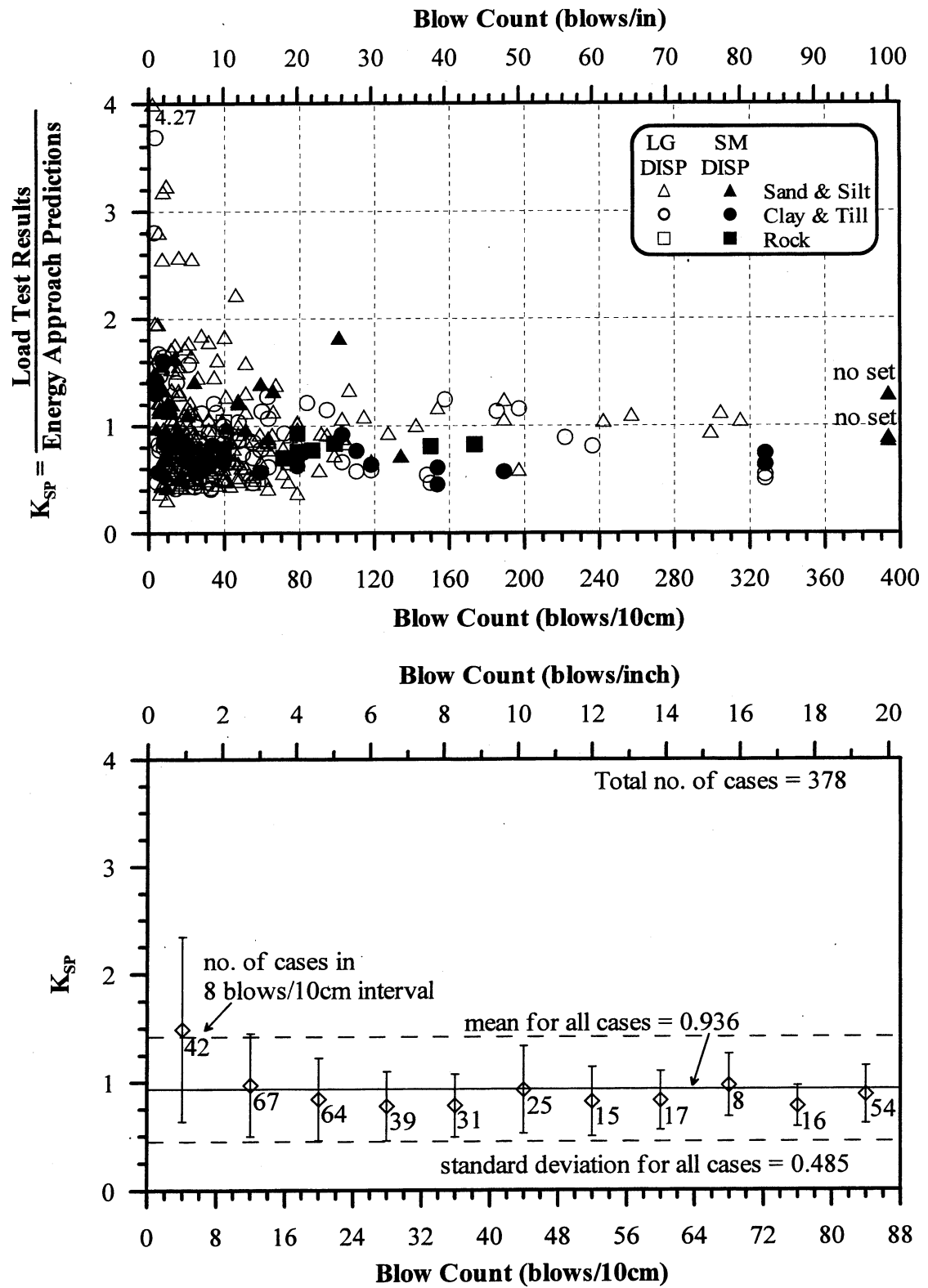


Figure 5.20. K_{SP} versus Blow count for all piles cases in PD/LT2000.

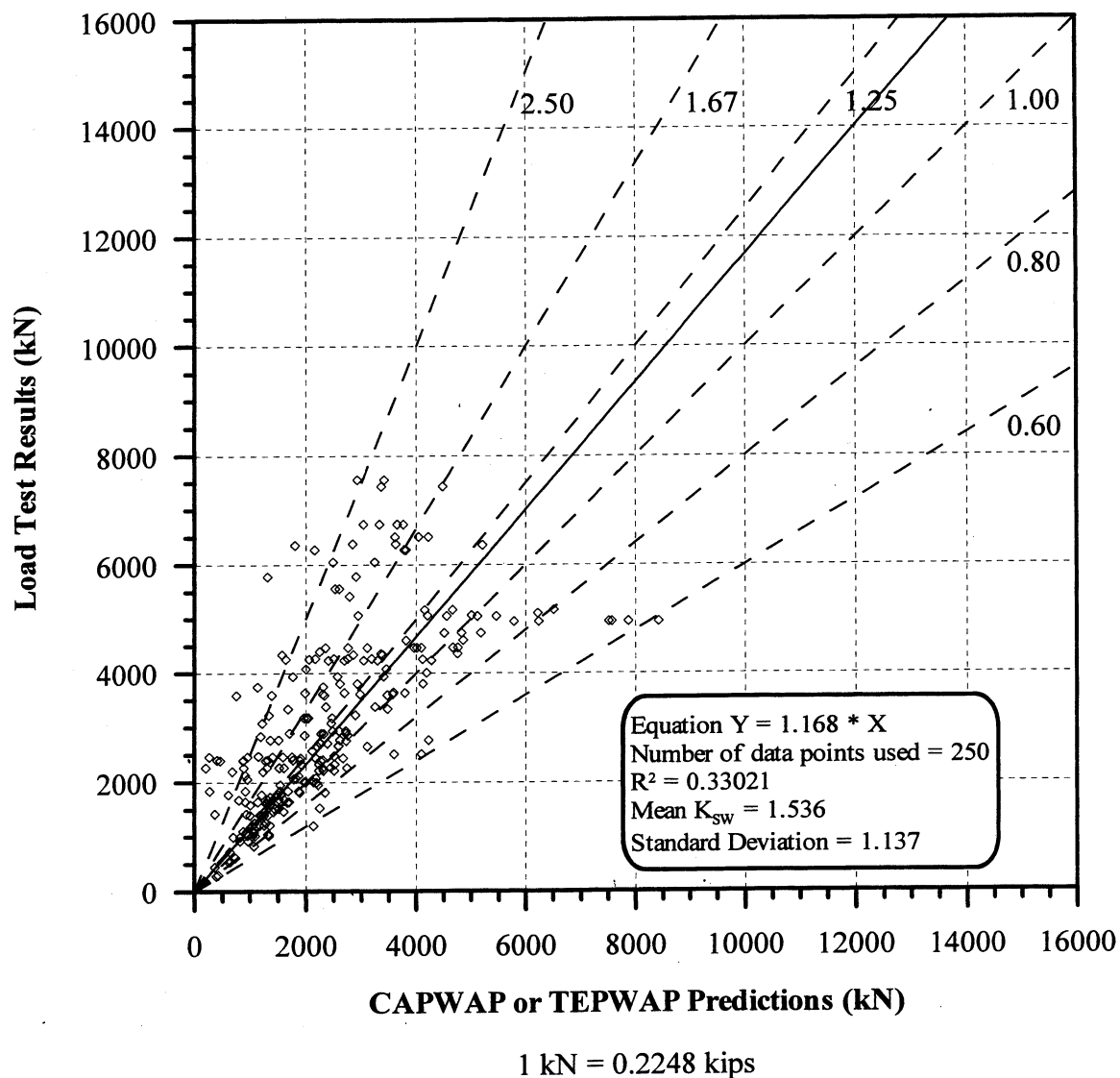
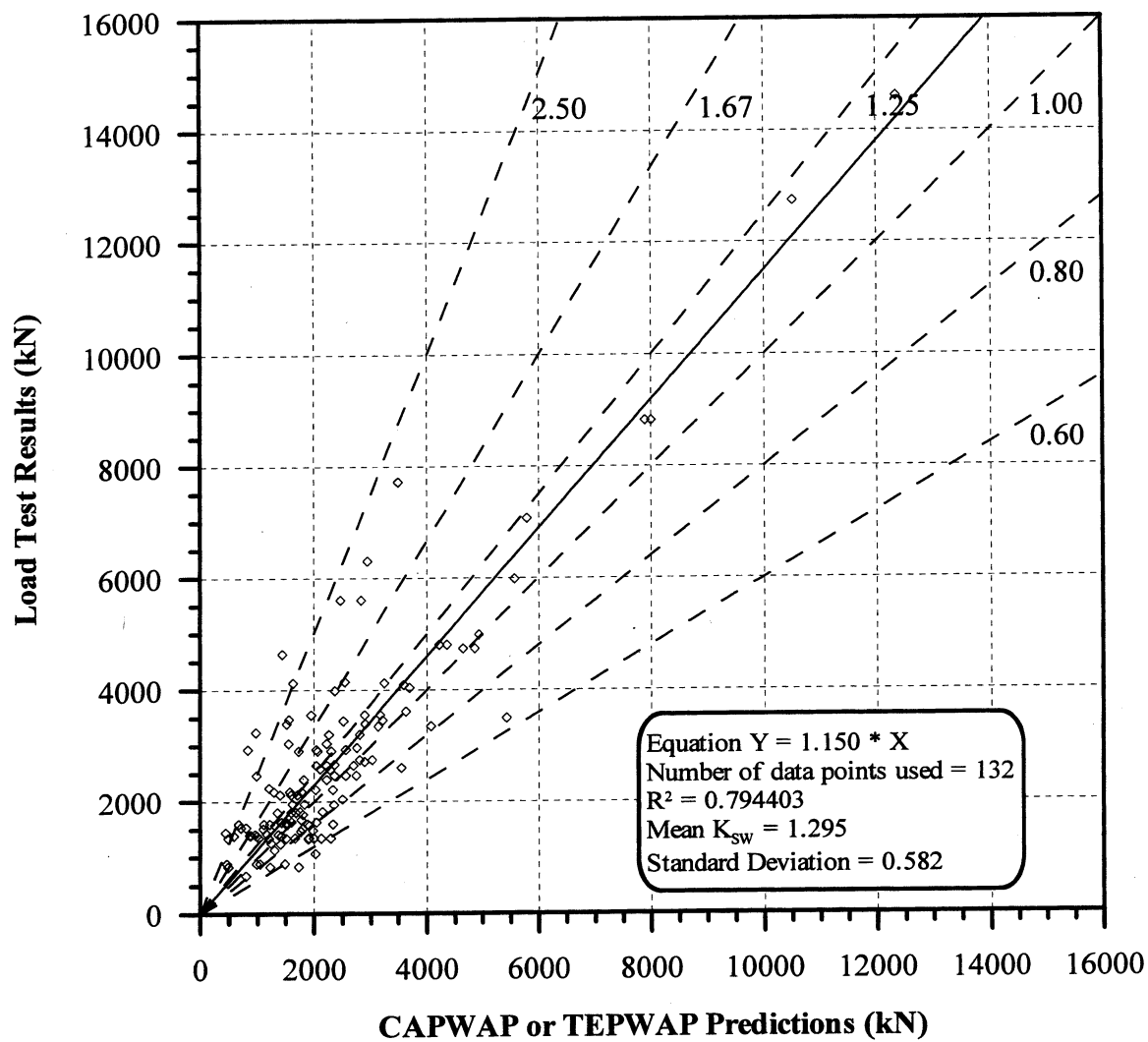


Figure 5.21. Static Load Test Results vs. CAPWAP or TEPWAP predictions for 250 PD/LT2000 pile-cases with Area Ratio < 350 in all types of soils (AAA).



1 kN = 0.2248 kips

Figure 5.22. Static Load Test Results vs. CAPWAP or TEPWAP predictions for 132 PD/LT2000 pile-cases with Area Ratio ≥ 350 in all types of soils (AAA).

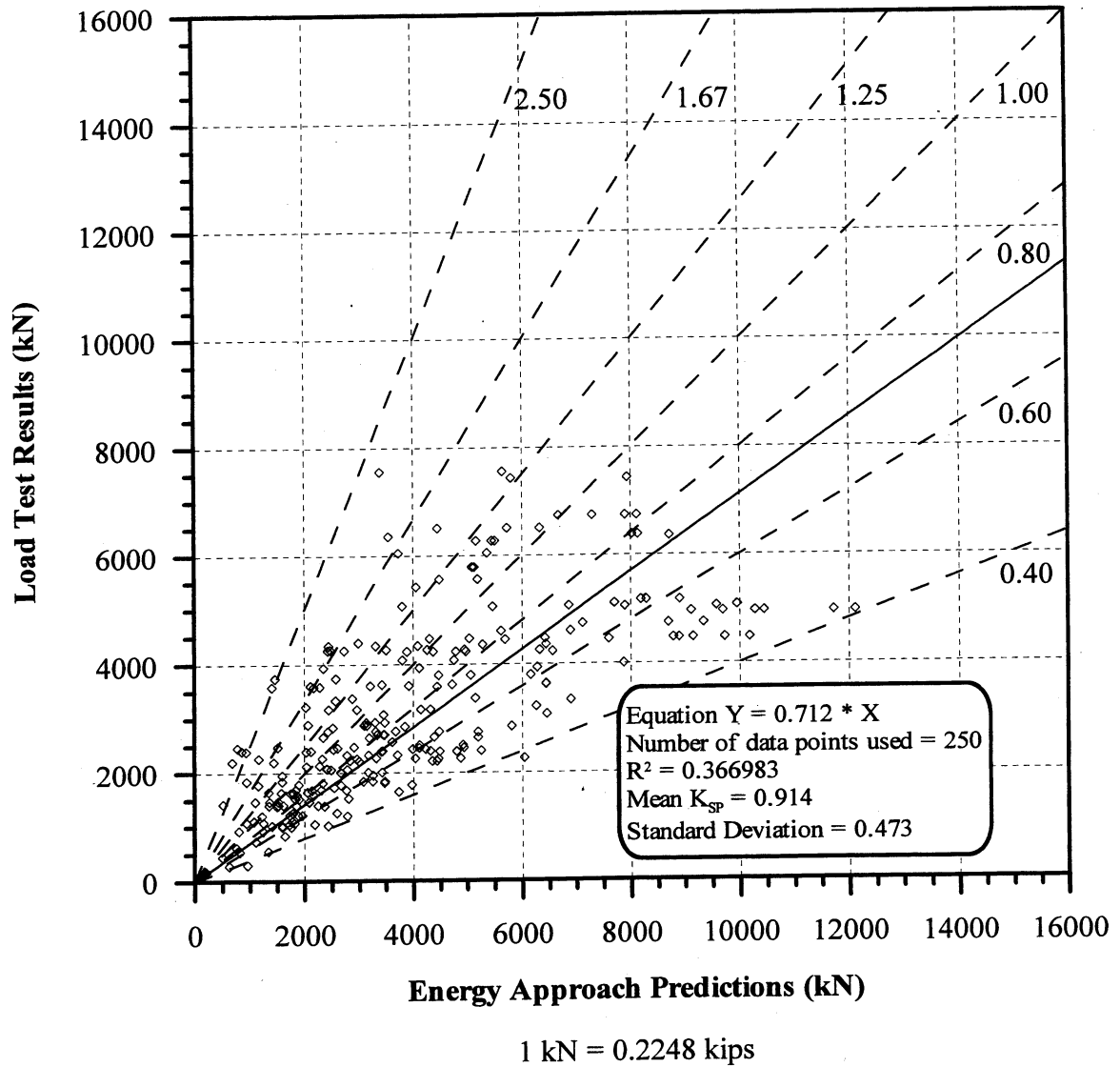


Figure 5.23. Static Load Test Results vs. Energy Approach predictions for 250 PD/LT2000 pile-cases with Area Ratio < 350 in all types of soils (AAA).

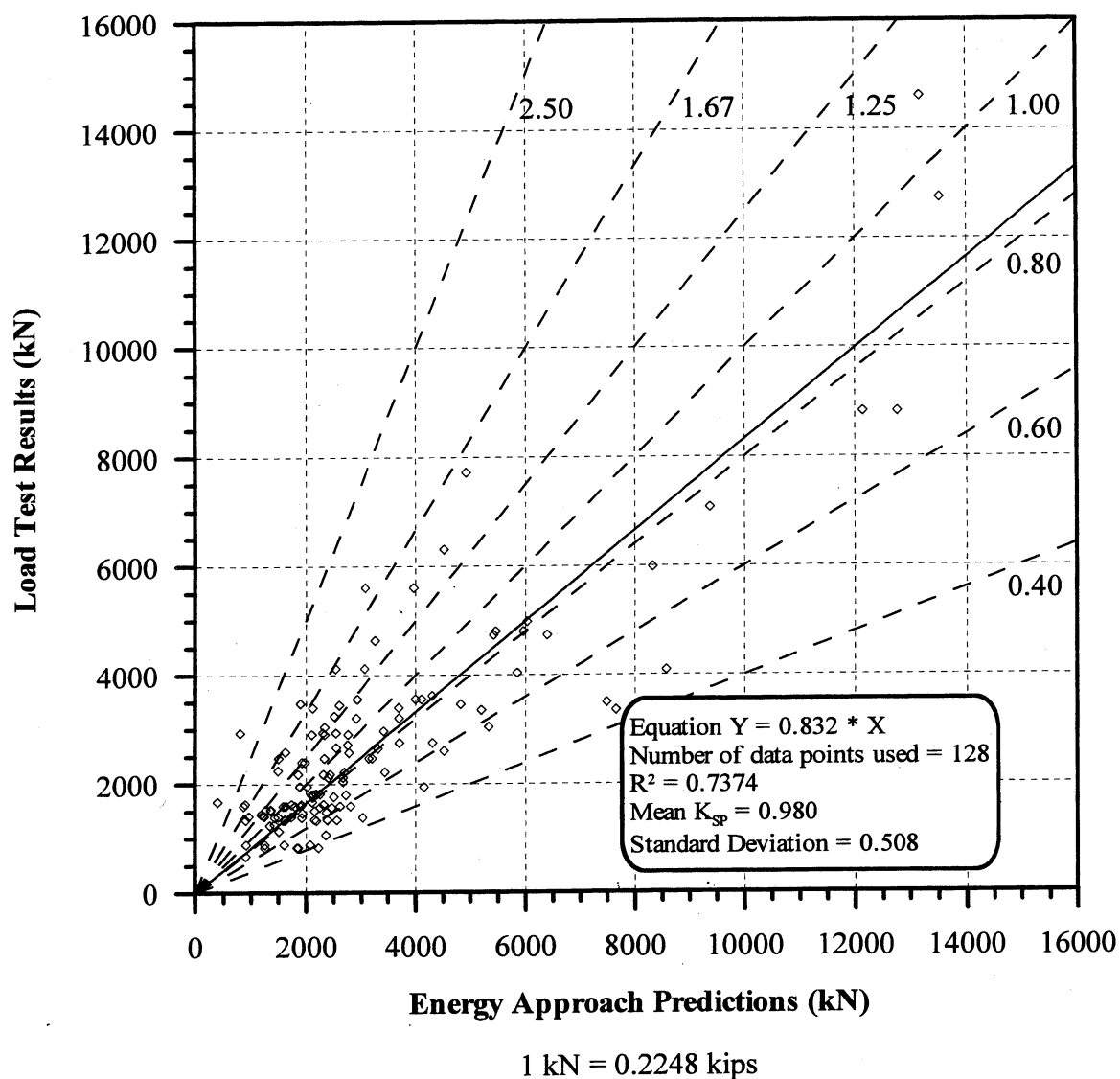


Figure 5.24. Static Load Test Results vs. Energy Approach predictions for 128 PD/LT2000 pile-cases with Area Ratio ≥ 350 in all types of soils (AAA).

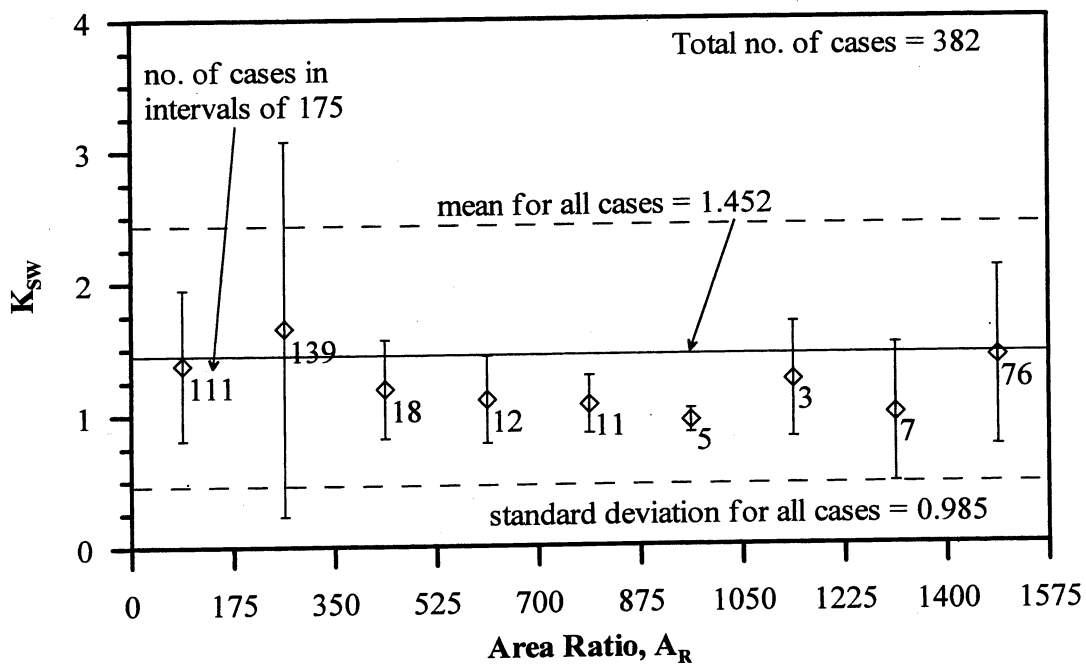
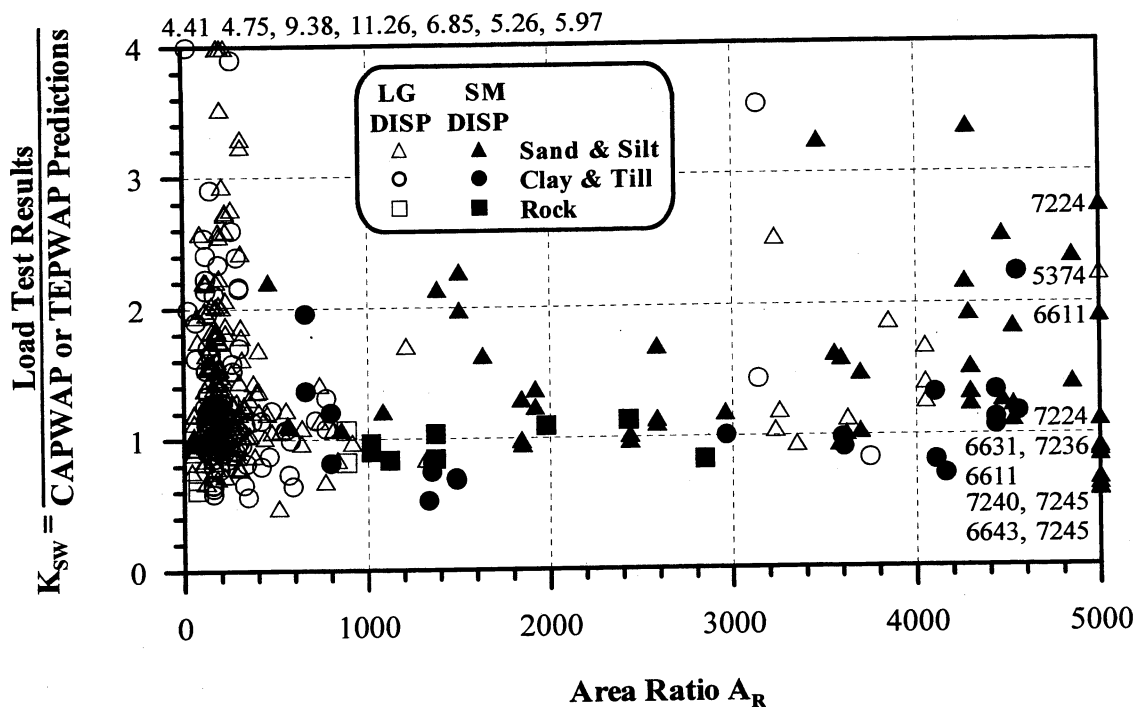


Figure 5.25. K_{SW} versus Area Ratio for all piles cases in PD/LT2000.

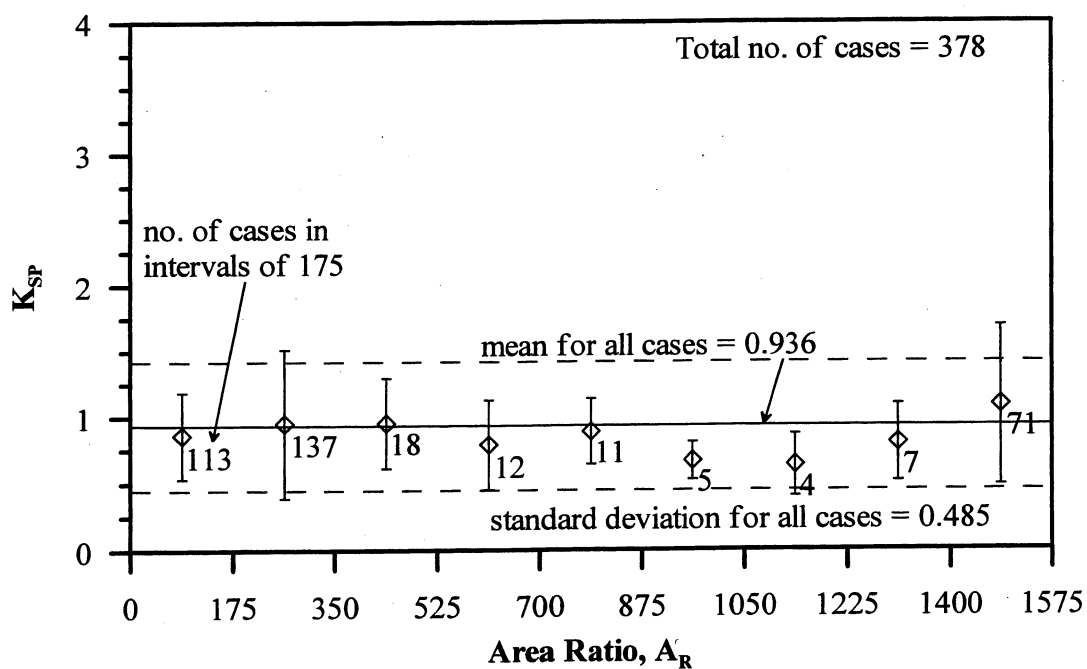
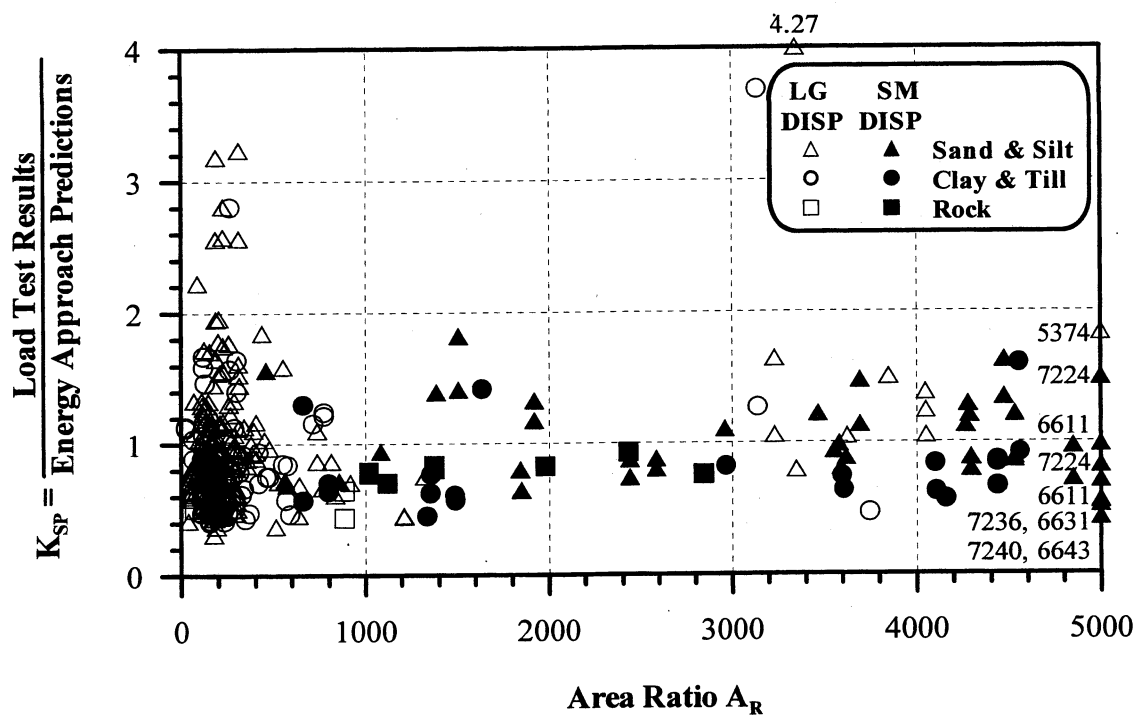


Figure 5.26. K_{SP} versus Area Ratio for all piles cases in PD/LT2000.

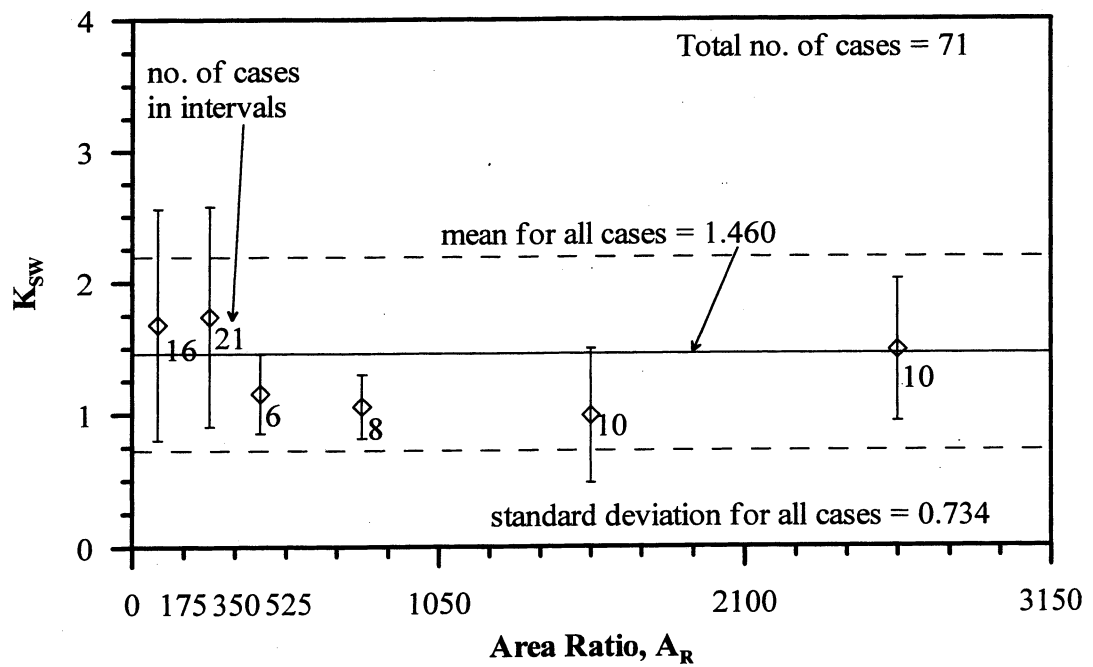
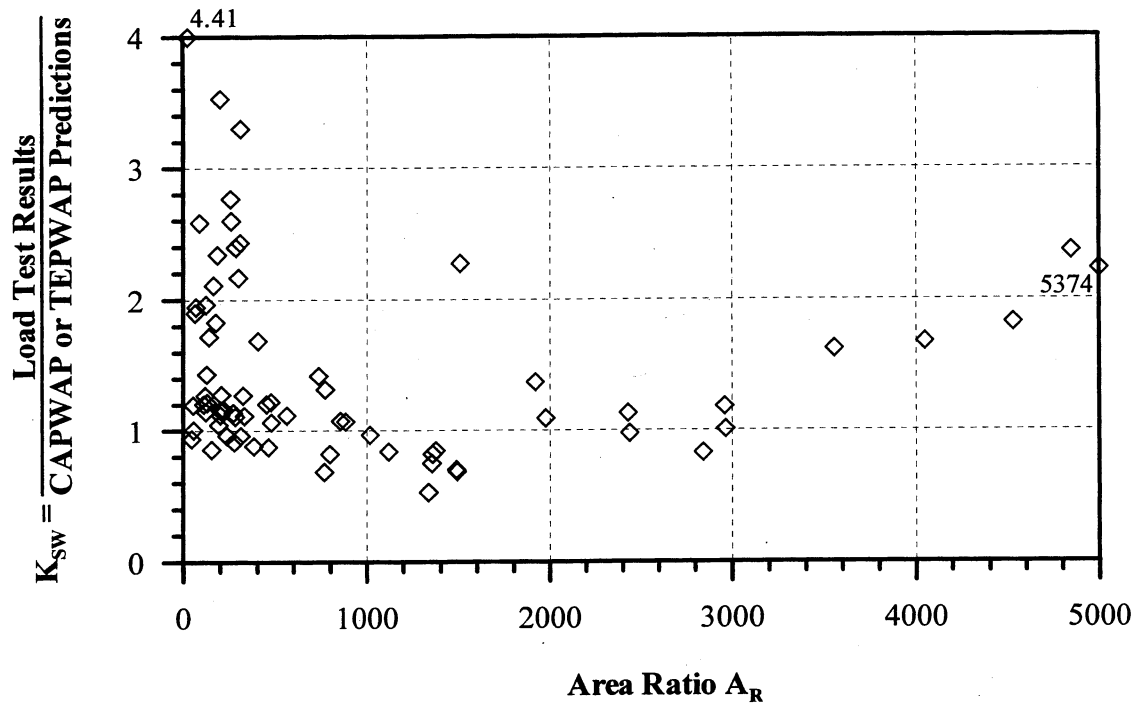


Figure 5.27. K_{sw} versus Area Ratio for 71 PD/LT2000 pile-cases at EOD with Blow Count ≥ 16 BP10cm in all types of soils.

CHAPTER 6

PERFORMANCE OF THE DYNAMIC METHODS DURING THE CONSTRUCTION STAGE

6.1 OVERVIEW

Figure 6.1 presents a flow chart outlining the breakdown of the dynamic analyses to be carried out. The dynamic methods can be broadly subdivided into two categories associated with the project stages: the design stage, employing a wave equation analysis (WEAP) to determine the driving system and the pile's drivability and the construction stage, in which capacity, driving criterion and quality control are required. The performance of the WEAP for drivability and pile design is highly important. The evaluation of the WEAP in pile design includes for example stress analysis, leading to load factors (see Figure 6.1). This evaluation was not included in this research. The wave equation analysis program is reviewed however in this chapter as a dynamic method for determining static pile capacity. This practice is questionable due to a high variability in the input parameters and the difficulties associated with the monitoring of the driving system without dynamic measurements. Generally, dynamic analyses are carried out using one of two methods, depending on whether dynamic measurements were recorded during pile driving. The first method, the dynamic equations, are commonly used when dynamic measurements are not recorded in the field. When dynamic measurements are taken during driving the wave

matching techniques or the field evaluation methods are used to determine the pile's capacity.

6.2 DYNAMIC ANALYSES WITHOUT DYNAMIC MEASUREMENTS

6.2.1 WEAP Analysis

The evaluation of WEAP (Wave Equation Analysis Program) effectiveness for capacity predictions is difficult as a large number and range of input parameters is possible, and the results are greatly affected by the actual field conditions. Examination of the method through analyses making use of default values is probably the only possible avenue. Other evaluations including WEAP analysis adjustments following dynamic measurements (e.g. matching energy) seem to be impractical in light of other available methods once dynamic measurements are performed. Such procedures lead to questionable results regarding their quality and meaning (Rausche et al., 2000 and Rausche, 2000). The wave equation analysis in this section will be evaluated using WEAP default input values and the pile's driving resistance at the End Of Driving (EOD) and Beginning Of Restrike (BOR) compared to the static load test results.

Figure 6.2 presents a comparison between the static load test results and the pile capacity prediction using the WEAP analysis at the EOD. This comparison is possible using a database obtained from GRL Inc., as described in chapter 3. The mean and standard deviation, 1.656 and 1.199, respectively, show that the WEAP analysis at the EOD performs poorly. The slope of the line forced through zero of actual results over the predicted results is 1.081. The scatter is very large as the

prediction ratios range from an under-prediction ratio of over 10 to an over-prediction ratio of about 0.6. The R^2 value of 0.359 and COV of 0.724 show the poor performance of the WEAP analysis as a method for determining pile capacity at the EOD. This conclusion should not be mistaken with the importance of the use of the wave equation analysis during the design stage and its role in the determination of the driving equipment, drivability and the stresses in the pile during driving.

A comparison between the static load test results and the standard WEAP predictions at the BOR (provided by GRL, Inc.) is shown in Figure 6.3. The mean and standard deviation are 0.939 and 0.399, respectively, which results in a COV of 0.425, indicating a good correlation between the actual and predicted capacities. Based on the R^2 value of 0.494 there is a poor correlation between the data and the best-fit line. It needs to be noted that this is not representative of how the WEAP method performs as an analysis program because knowledge of the specific site has generally been obtained from the initial driving of the pile and therefore, default input values are generally not used. Moreover, the hammer performance and driving system behavior is more difficult to assess at restrikes than at the EOD after a period of operation during driving.

6.2.2 The Dynamic Equations

a) General

The dynamic equations are commonly used to evaluate pile capacity when dynamic measurements are not recorded in the field at either the EOD or BOR, (see section 2.3.2). The two most commonly used dynamic equations in practice (USA)

are the Engineering News Record (ENR) equation (Wellington, 1892) and the Gates equation (Gates, 1957). These equations are evaluated in this research as well as the Federal Highway Administrations (FHWA) version of the Gates equation as suggested previously by Richard Cheney, (FHWA, 1988).

b) ENR Equation

The Engineering News Record (ENR) equation (Wellington, 1892) has a factor of safety of 6 incorporated directly into the equation (see section 2.3.2b). As the LRFD principles substitute for the factors of safety, the evaluation of the ENR equation was performed with and without the built in factor of safety.

Figure 6.4 presents the relationship between the static load test results and the pile capacity as calculated using the ENR equation (eliminating the factor of safety) for 384 pile-cases. The mean KSEN value, which is the ratio of the static load test results over the pile capacity prediction using the ENR equation, is 0.267 with a standard deviation of 0.243. The coefficients of variation and determination of 0.910 and 0.223, respectively, indicate the extremely poor performance of the equation. When the factor of safety of six is not incorporated into the equation the mean over-prediction ratio is 0.162 with the prediction ratios ranging from less than 0.1 to approximately 2.0. This shows that in addition to the method over-predicting by a considerable amount there is a very large amount of scatter in the prediction ratios (static load test results over the predicted results).

Figure 6.5 shows the relationship between the static load test results and the ENR equation pile capacity predictions in its typical format, with the built in factor of

safety of 6. The mean (1.600) and standard deviation (1.458) increase, logically, by a multiple of the factor of safety (6) from the case where the built in factor of safety is excluded, (Figure 6.4). The COV and R^2 values remain the same whether or not the built in factor of safety is applied to the ENR equation, i.e., 0.910 and 0.223, respectively. Due to the poor performance of the ENR equation further evaluation of the prediction on the basis of sub categorization was not carried out.

c) *Gates Equation*

A comparison between the static load test results and the pile capacity as determined by the Gates equation is presented in Figure 6.6 using 384 pile-cases from the database PD/LT2000. The mean and standard deviation of the ratio of the static load test results over the Gates equations predictions are 1.787 and 0.848, respectively. The data shows that the Gates equation performs relatively well but there is a significant bias (under-prediction) indicated by the slope of the best fit line (forced through zero), which is 1.828. There is also a large amount of scatter of the data as the prediction ratios (static load test results over the predicted results) range from approximately 0.6 to 6.0. Based on the R^2 value of 0.412 and the COV of 0.475 there is poor and moderate correlation, respectively, between the actual and predicted pile capacities.

d) *FHWA modified Gates Equation*

Figure 6.7 shows the comparison of the static load test results and the pile capacity predictions using the FHWA version of the Gates equation for 384 pile-cases from PD/LT2000. The mean K_{SFG} value, which is the ratio of the static load test

results to the pile capacity determined using the FHWA version of the Gates equation, is 0.940 with a standard deviation of 0.472. The mean over-prediction ratio, which is the ratio of the static load test results over the pile capacity, as calculated using the FHWA version of the Gates equation, is 0.922. The scatter is fairly significant ($R^2 = 0.417$) with prediction ratios (static load test results over the predictions) ranging from about 0.4 to 4.0. Correcting for the bias of the original Gates equation, the FHWA version of the Gates equation performs overall better with a small over prediction (0.922), but a slightly higher COV (0.502 vs. 0.475).

e) The Recommended Dynamic Equation and its Performance

Table 6.1 presents a summary of the statistical data for the three evaluated dynamic equations with ENR presented with and without the built in factor of safety. The table shows that the FHWA version of the Gates equation has the smallest bias of the three dynamic equations that were reviewed. While the bias is smaller in the FHWA modified equation the coefficient of variation is slightly higher than the original Gates equation. The mean is close to one and the standard deviation is reasonably small considering that the equation does not utilize any field measurements other than the blow count. The FHWA version of the Gates equation seems to be suitable to evaluate pile capacity if no dynamic measurements are taken and is further evaluated in this section according to the controlling parameters described in chapter 5. The evaluation of the controlling parameters in chapter 5 showed that the time of driving (EOD and BOR) and the driving resistance (blow count) had the largest effect on the performance of the dynamic methods. The FHWA version of the Gates

equation is further evaluated based on the combinations of these controlling parameters.

Shown in Figure 6.8 is the comparison between the static load test results and the pile capacity predictions as obtained using the FHWA version of the Gates equation for 135 EOD pile-cases from PD/LT2000. The mean K_{SFG} value is 1.073 with a standard deviation of 0.573, which is a slight decrease in the performance of the equation compared to all pile-cases. The COV is 0.534, which shows that there is a moderate correlation between the actual and predicted results. The mean under prediction ratio (static load test results over the predicted results) is 1.048, while the scatter ranges from an over prediction ratio of approximately 0.4 to an under-prediction ratio of approximately 3.2, which shows no to little change from the scatter for all pile-cases. The R^2 value of 0.412 also shows that there is a significant scatter in the data.

Figure 6.9 presents the comparison between the static load test results and the pile capacity prediction using the FHWA version of the Gates equation for 159 BOR (last) pile-cases from the PD/LT2000 database. The mean and standard deviation are 0.833 and 0.403, respectively and have decreased minimally from that for all pile-cases as shown in Figure 6.7. There is a moderate correlation between the actual and predicted pile capacities based on the COV of 0.484. The mean over-prediction ratio (static load test results over the predicted results) is 0.828, which is a slight increase from that for all pile-cases. The scatter remains approximately the same as for all pile-

cases as the prediction ratios for the BOR (last) pile-cases ranges from approximately 0.4 to 2.5 and the R^2 value is 0.487.

A comparison between the static load test results and the pile capacity predictions using the FHWA version of the Gates equation for 62 PD/LT2000 pile-cases at the EOD with blow counts less than 16 BP10cm is shown in Figure 6.10. The mean K_{SFG} for these pile-cases is 1.306 with a standard deviation of 0.643, which is a significant increase from the mean and standard deviation for all pile-cases (refer to Figure 6.7). The coefficient of variation 0.492, which is approximately equal to that for all cases (0.502), shows that there is a moderate correlation between the actual and predicted results. The mean under-prediction ratio (static load test results over the predicted results) is 1.282, which is significant increase from the mean over-prediction ratio of 0.922 for all pile-cases. The amount of scatter did not change from that for all pile-cases as the prediction ratios still range from approximately 0.6 to 2.5 and the R^2 value is still 0.418.

Figure 6.11 presents the comparison between the static load test results and the pile capacity prediction for 32 BOR (last) pile-cases with blow counts less than 16 BP10cm using the FHWA version of the Gates equation. The mean K_{SFG} value of 0.929 is basically the same as that for all pile-cases, 0.940, while the standard deviation has increased significantly from 0.472 for all pile-cases to 0.688 for this specific case. The COV (0.741) shows that there is a poor correlation between the actual and predicted pile capacities. The mean over-prediction ratio also basically remains unchanged, as it is 0.929. The scatter is still significant as the prediction

ratios (static load test results over the predicted results) range from approximately 0.4 to 2.0. There are a few pile-cases that do not fall within the range of scatter described above, which causes the low R^2 value of 0.215, which also shows the poor correlation between the data.

The mean and standard deviation for the comparison between the static load test results and the pile capacity determined using the FHWA version of the Gates equation for 73 PD/LT2000 pile-cases at the EOD with blow count greater than 16 BP10cm as shown in Figure 6.12 is 0.876 and 0.419, respectively. This is an insignificant change from the mean and standard deviation for all pile-cases with a pile capacity prediction using the FHWA version of the Gates equation as shown in Figure 6.7. The mean over-prediction ratio has increased slightly from 0.922 for all pile-cases to 0.967 for the pile-cases at the EOD with blow counts greater than 16 BP10cm. The R^2 value of 0.468 shows that there is significant scatter in the data. The prediction ratios range from 0.4 to 2.5, which also shows that there is significant scatter in the data.

Figure 6.13 presents the comparison between the static load test results and the pile capacity prediction using the FHWA version of the Gates equation for 73 pile-cases at the BOR (last) with blow counts greater than 16 BP10cm. The mean K_{SFG} value for these pile-cases is 0.809, which is a slight decrease from the mean for all pile-cases of 0.940. The standard deviation of 0.290 has decreased significantly from that for all pile-cases (0.472). There is a good correlation between the actual and predicted results based on the COV of 0.358. The mean over-prediction ratio has also

decreased from 0.922 for all pile-cases to 0.820 for these specific pile-cases. The scatter has also decreased slightly as the upper range of the prediction ratio decreased from approximately 2.5 for all pile-cases to 1.7 for the pile-cases analyzed in Figure 6.13. This decrease in scatter is also shown by the increase in the R^2 value from 0.417 to 0.499.

The analysis presented in this section shows that the performance of the FHWA version of the Gates equation for all sub-groupings is approximately the same as for all pile-cases, the exceptions being for the EOD cases and the EOD cases with blow counts less than 16 blows per 10 cm.

f) Summary of the Dynamic Equations Performance

Table 6.2 presents a summary of the statistics representing the performance of the ENR equation (with and without the built in factor of safety), the Gates equation and the modified Gates equation. This table includes the data shown in Table 6.1 as well as the sub-categorization of the FHWA version of the Gates equation. A relatively small over-prediction exists in the FHWA version of the Gates equation for the BOR condition compared to the EOD. The data in the table shows that the FHWA version of the Gates equation performs more accurately for the BOR cases with high blow counts ($COV = 0.358$) compared to those with low blow counts ($COV = 0.741$).

6.3 DYNAMIC ANALYSES WITH DYNAMIC MEASUREMENTS

6.3.1 Overview

Three dynamic analysis methods are evaluated in this section, the wave matching techniques (CAPWAP or TEPWAP) and the field evaluation methods (the

Energy Approach and the Case method). Each of the methods is evaluated using the sub-groupings (described in chapter 5) according to the major controlling parameters.

The first step to the analysis was to evaluate the effect of the extreme pile-cases. For these cases, the ratio of the static load test results to the predicted pile capacity (using either the wave matching techniques or the Energy Approach) was either extremely small or large, relative to the overall performance of the examined method. The pile-cases for which the K_{SX} value was outside two standard deviations for all pile-cases were isolated to determine if there were any problems with the data. No problems were found with the BOR data but some difficulties that were identified with the EOD pile-cases are shown in Table 6.3. The identified EOD pile-cases are shown in Table 6.3. These data were removed from the general population and a brief explanation is provided in Table 6.3 as to why the data were removed. The extreme data that were removed from the general population of the PD/LT2000 database were kept for the area ratio sub-groupings where its extreme performance is relevant.

6.3.2 Performance of the Signal Matching Technique (CAPWAP or TEPWAP)

a) All Pile-Cases

The pile capacity predictions of the signal matching analyses are shown in Figure 6.14 compared to the static load test results for all pile-cases (377). The mean and standard deviation of the ratio of the static load test results to the CAPWAP/TEPWAP predictions are 1.368 and 0.620, respectively. The COV (0.453) shows that there is a moderate correlation between the compared data. The wave matching analyses under predict the pile capacity by a mean prediction ratio (load test

results over the prediction) of 1.368, with is the slope of the best-fit line forced through the origin being 1.160. There is a significant amount of scatter in the CAPWAP/TEPWAP predictions as the COV is 0.453 with the prediction ratios ranging from approximately 0.6 to over 4.5 and the R^2 value is 0.557.

b) Performance According to Time of Driving

The wave matching technique predictions were sub-grouped according to the time of driving (i.e., End Of Driving, EOD, or Beginning Of Restrike, BOR). Each of these categories was then compared to the static load test results. The BOR (last) refers to the piles that had multiple restrikes; for which only the last restrike was used in the evaluation of the wave matching technique predictions. Figures 6.15 and 6.16 present the comparison between the static load test results and the wave matching technique predictions for EOD and BOR, respectively.

Shown in Figure 6.15 is the comparison between the static load test results and the CAPWAP/TEPWAP predictions at the EOD for 125 PD/LT2000 pile-cases. The statistics show that the signal matching techniques do not perform well at the EOD as the mean K_{SW} value is 1.626 with a standard deviation of 0.797, this is a significant decrease in performance from the statistics for all pile-cases as shown in Figure 6.14. The scatter is significant with the predictions ratios (static load test results over the predicted results) ranging from 0.6 to above 2.5 with a mean under-prediction ratio of 1.626 and a best line through the origin slope of 1.284. The coefficient of variation and determination are 0.490 and 0.653, respectively, which also indicate the

significant scatter and moderate to poor correlation between the actual and predicted results.

Figure 6.16 presents the comparison between the static load test results and the predicted pile capacity at the beginning of restrike (BOR) by the CAPWAP/TEPWAP wave matching techniques for 162 PD/LT2000 pile-cases. The method in this category performed very well with the mean K_{sw} value being 1.158 and a relatively small standard deviation of 0.393. The scatter ranges from approximately an over-prediction ratio 0.60 to an under prediction ratio 2.50 but the majority of the predictions (about 81%) fall within the range of predictions ratios between 0.8 and 1.67. The R^2 value of 0.599 and the COV value of 0.339 indicate a moderate to good correlation between the actual and the predicted results. The mean under-prediction ratio is 1.158 and a best-fit line through the origin has a slope of 1.104, both suggest good agreement between the measured and predicted values.

The categorization according to the time of driving for the wave matching technique predictions compared to the static load test results show a significant improvement in the CAPWAP/TEPWAP methods from the end of driving cases to the beginning of restrike cases. As is shown in Figures 6.15 and 6.16 the wave matching techniques perform exceptionally well at the beginning of restrike but they perform very poorly at the end of driving.

c) *Performance According to Driving Resistance*

The pile capacity prediction of the CAPWAP/TEPWAP methods are analyzed by comparing the performance of the pile-cases that had a driving resistance greater

than 16 BP10cm against those with a driving resistance lower than 16 BP10cm, both at the end of driving and beginning of restrike. The four combinations of the above-described comparisons are presented in Figures 6.17 through 6.20.

Figure 6.17 shows the comparison between the static load test results and the wave matching technique predictions for 54 PD/LT2000 pile-cases at the end of driving with blow counts less than 16 BP10cm. The mean K_{SW} value and its standard deviation are 1.843 and 0.831, respectively, which have not changed significantly from the mean (1.626) and standard deviation (0.797) for all pile-cases at the end of driving. There is a moderate correlation between the actual and predicted pile capacities as is shown by the COV (0.451) and the R^2 value (0.677). The mean under-prediction ratio is 1.843 with the ratios ranging from approximately 0.8 to 3.2, the slope of the best-fit line forced through the origin, is 1.388.

A comparison between the static load test results and the wave matching technique predictions for 71 PD/LT2000 pile-cases at the end of driving with blow counts greater than or equal to 16 BP10cm is presented in Figure 6.18. The mean K_{SW} for these pile-cases is 1.460, which is lower than that for the pile-cases with blow counts less than 16 BP10cm (1.843). The standard deviation is 0.734, which is approximately equal to that for pile-cases with blow counts less than 16 BP10cm (0.831). There is a moderate correlation between the actual and predicted data as shown by the COV (0.502) and the R^2 value (0.647). The mean under-prediction ratio is 1.460 with the ratios ranging from approximately an over-prediction of 0.6 to an under-prediction of 3.2; the slope of the best-fit line forced through the origin is 1.236.

Figure 6.19 presents the comparison between the static load test results and the pile capacity prediction based on the signal matching techniques for 32 PD/LT2000 pile-cases at the beginning of restrike with blow counts less than 16 BP10cm. The slope of the best-fit line through the origin is 1.189. The mean K_{SW} value and its standard deviation for these pile-cases are 1.176 and 0.530, respectively, with the data ranging from K_{SW} values of approximately 0.6 to 2.5. The COV (0.451) shows a moderate to good correlation between the actual and predicted results, while the R^2 value (0.717) shows a good correlation and a small amount of scatter.

Figure 6.20 presents the comparison of the static load test results and the wave matching predictions for 130 PD/LT2000 pile-cases at the beginning of restrike with blow counts greater than or equal to 16 BP10cm. The mean K_{SW} value is 1.153 with a standard deviation of 0.354, with the ratio ranging from an over-prediction ratio of approximately 0.6 to an under-prediction ratio of 2.5. The slope of the best-fit line forced through the origin, is 1.096. The COV (0.307) shows that there is a good to very good correlation between the actual and predicted results and a significant improvement over the data in Figure 6.19 (COV = 0.451). The R^2 value (0.526) shows that there is a meaningful amount of scatter and a moderate to poor correlation between the data.

The figures presented in this section show that for the beginning of restrike pile-cases there is a significant effect on the performance of wave matching techniques based on the driving resistance. This effect is not as apparent for the end of driving

pile-cases and becomes clearer only when the pile type (through area ratio) is considered.

d) *Performance According to Pile Type*

The performance of the wave matching techniques based on the soil displacement / pile type, utilizes the area ratio as described in section 5.3.3a. Four combinations of cases based on driving resistance and area ratio (see Figure 6.1) are explored and presented in Figures 6.21 through 6.28.

Figure 6.21 presents the static load test results compared to the wave matching predictions for 37 PD/LT2000 pile-cases at the end of driving with blow counts less than 16 BP10cm and area ratio less than 350 (this sub-grouping includes the 5 extreme CAPWAP pile-cases, detailed in Table 6.3). The mean K_{SW} value and the standard deviation are 2.589 and 2.385, respectively; show a very poor performance of the CAPWAP/TEPWAP predictions for large displacement piles under easy driving resistance at the end of driving. The coefficients of variation and determination are 0.921 and -0.082, respectively, indicating the extremely poor performance of the method and the large scatter of the data under the analyzed conditions.

The static load test results compared to the wave matching technique predictions are presented in Figure 6.22 for 22 PD/LT2000 pile-cases at the end of driving with blow counts less than 16 BP10cm and area ratios greater than or equal to 350. The mean K_{SW} value for these pile-cases is 1.929 with a standard deviation of 0.698 resulting in a COV of 0.362. The R^2 value (0.776) shows a moderate to good correlation between the actual and predicted pile capacities with the ratio ranging from

1.0 to an under-prediction ratio of approximately 2.5 with all pile-cases under-predicting the pile's capacity.

A comparison between the static load test results and the wave matching technique predictions for 37 PD/LT2000 pile-cases at the end of driving with blow counts greater than or equal to 16 BP10cm and area ratios less than 350 is presented in Figure 6.23. The mean K_{SW} value is 1.717 with a standard deviation of 0.841, resulting in a COV of 0.490, which shows a moderate correlation between the actual and predicted results. The ratio of the static load test results over the predicted capacity ranges from an over-prediction ratio of 0.8 to an under-prediction ratio of about 3.4. The R^2 value (0.185) further indicates a poor correlation between the actual and predicted pile capacities.

Figure 6.24 presents a comparison between the static load test results and the wave matching technique predictions for 34 PD/LT2000 pile-cases at the end of driving with blow counts greater than or equal to 16 BP10cm and area ratios greater than or equal to 350. The mean K_{SW} value is 1.181, with a standard deviation of 0.468, resulting in a COV of 0.396; presenting a much better predictive performance than for the large displacement pile-cases shown in Figure 6.23. The R^2 value (0.904) shows that there is little scatter and a good correlation to the best-fit line with a slope of 1.139 passing through the origin.

The static load test results are compared to the wave matching techniques in Figure 6.25 for 22 PD/LT2000 pile-cases at the beginning of restrike with blow counts less than 16 BP10cm and area ratios less than 350. The statistics show that for this

specific sub-category, the CAPWAP/TEPWAP method performs reasonably well with a mean K_{SW} value of 1.116 and a standard deviation of 0.362, which results in a COV of 0.324. The prediction ratios range approximately between 0.8 and 1.7, which also shows the good performance of the wave matching techniques for this specific sub-category. The R^2 value (0.730) shows some scatter and a moderate correlation to the best-fit line with a slope of 1.207 passing through the origin.

Figure 6.26 presents the comparison between the static load test results and the wave matching techniques for 10 PD/LT2000 pile-cases at the beginning of restrike with blow counts less than 16 BP10cm and area ratios greater than or equal to 350. The mean K_{SW} value is 1.308 with a standard deviation 0.796, which gives a COV of 0.609, indicating a poor performance of the CAPWAP/TEPWAP methods for this specific category compared to the large displacement pile-cases as presented in Figure 6.25. The data ranges from prediction ratios of about 0.4 to 3.0. The large range in the data and the R^2 value of 0.637 shows the moderate to poor performance of the CAPWAP/TEPWAP methods for this specific category.

Figure 6.27 presents the comparison of the static load test results and the wave matching technique predictions for 83 PD/LT2000 pile-cases at the beginning of restrike with blow counts greater than or equal to 16 BP10cm and area ratios less than 350. The mean K_{SW} value is 1.178 with a standard deviation of 0.379 and a COV of 0.321, which shows there is a good correlation between the actual and predicted pile capacities. The ratios range from an over-prediction ratio of 0.6 to an under-prediction ratio of about 2.9. The R^2 value of 0.522 also shows the significant scatter in the data

around the best-fit line through the origin with a slope of 1.109 and a poor correlation between the actual and predicted results.

The static load test results are compared to the wave matching technique predictions for 47 PD/LT2000 pile-cases at the beginning of restrike with blow counts greater than or equal to 16 BP10cm and area ratios greater than or equal to 350 in Figure 6.28. The mean K_{SW} value is 1.110 with a standard deviation of 0.303, resulting in a COV of 0.273. The scatter is fairly significant around the best-fit line passing through the origin with a slope of 1.064. The prediction ratios range from approximately 0.6 to 2.4 and the R^2 value is 0.484.

The analysis presented in this section shows that the performance of the signal matching methods (CAPWAP/TEPWAP) is affected by the pile type (small or large displacement) with the exception of the pile-cases at the beginning of restrike with blow counts greater than or equal to 16 BP10cm as presented in Figures 6.27 and 6.28.

6.3.3 Field Evaluation (Energy Approach)

a) All Pile-Cases

The Energy Approach predictions compared to the static load test results for 371 PD/LT2000 pile-cases are presented in Figure 6.29. The mean and standard deviation of the ratio of the static load test results to the Energy Approach predictions are 0.894 and 0.367, respectively, resulting in a COV of 0.411. The slope of the best-fit line forced through the origin is 0.73 and the R^2 value is 0.542. The Energy Approach method for predicting pile capacity performs reasonably well overall,

however there is a significant amount of scatter in the predictions with the prediction ratios ranging from approximately 0.4 to 2.5.

b) Performance According to Time of Driving

To evaluate the effect of the time of driving, the Energy Approach predictions were sub-grouped according to the End Of Driving (EOD) and Beginning Of Restrike (BOR) (last) pile-cases and each of these categories were compared to the static load test results. The BOR (last) refers to the piles that had multiple restrikes; where only the last restrike was used in the evaluation of the method.

Figure 6.30 presents the comparison between the static load test results and the Energy Approach predictions at the EOD for 128 PD/LT2000 pile-cases. The mean K_{SP} value (ratio of the static load test results to the Energy Approach predictions) is 1.084 with a standard deviation of 0.431, which results in a COV of 0.398. The Energy Approach method performs very well compared to other methods for evaluating pile capacity based on the EOD data. The scatter of the data is significant with prediction ratios (static load test results over the predicted results) ranging from 0.4 to 2.5 with a best-fit line through the origin having slope of 0.926 and R^2 of 0.542, indicating the significant amount of scatter in the data.

Figure 6.31 present the Energy Approach pile capacity predictions at the beginning of restrike (BOR) in comparison with the static load test results for 153 PD/LT2000 pile-cases. The mean K_{SP} value of 0.785, suggests mostly over prediction with a standard deviation of 0.290, resulting in a coefficient of variation of 0.369. The data ranges from approximately an over-prediction ratio of 0.4 to an under

prediction ratio of 1.7. The best-fit line through the origin has a slope of 0.695, which indicates a typical over prediction. The R^2 value of 0.576 for this line suggests a large amount of scatter in the data in difference from the small COV.

The data in Figures 6.30 and 6.31 suggests that the Energy Approach performs reasonably well for both cases, but it significantly over predicts the piles capacity for the beginning of restrike case. It should be noted that the Energy Approach method was developed for use at the end of driving only (Paikowsky et al., 1994).

c) *Performance According to Driving Resistance*

The performance of the Energy Approach is analyzed in this section based on the driving resistance. Hard driving is categorized as blow counts greater than or equal to 16 BP10cm and easy driving is categorized as those pile-cases with blow counts less than 16 BP10cm. The Energy Approach method is analyzed by comparing the predicted capacity to the measured capacity based on hard and easy driving pile-cases, both at the end of driving and beginning of restrike as presented in Figures 6.32 through 6.35.

Figure 6.32 shows the comparison between the static load test results and the Energy Approach predictions for 56 PD/LT2000 pile-cases at the end of driving with blow counts less than 16 BP10cm. The mean K_{SP} value and its standard deviation are 1.227 and 0.474, respectively, (COV = 0.386), which are similar to the mean (1.084) and standard deviation (0.431) for all pile-cases at the end of driving. The slope of the best-fit line forced through the origin, is 1.012 with a R^2 value of 0.739 indicating that there is a moderate correlation.

A comparison between the static load test results and the Energy Approach predictions for 72 PD/LT2000 pile-cases at the end of driving with blow counts greater than or equal to 16 BP10cm is presented in Figure 6.33. The mean K_{SP} for these pile-cases is 0.972, with a standard deviation of 0.359, resulting in a COV of 0.369, indicating a good correlation between the actual and predicted pile capacities. The best-fit line through the origin has a slope of 0.885 and a R^2 value of 0.680 with the scatter of data ranging from approximately a prediction ratio of 0.5 to 2.1.

Figure 6.34 presents the comparison between the static load test results and the pile capacity prediction based on the Energy Approach for 29 PD/LT2000 pile-cases at the beginning of restrike with blow counts less than 16 BP10cm. The mean K_{SP} value and its standard deviation are 0.830 and 0.352, respectively, resulting in a COV of 0.424, indicating a good correlation between the actual and predicted pile capacities. The R^2 value of 0.553 suggests a significant scatter in the data around the best-fit line through the origin with a slope of 0.742.

Figure 6.35 presents the comparison of the static load test results and the Energy Approach predictions for 124 PD/LT2000 pile-cases at the beginning of restrike with blow counts greater than or equal to 16 BP10cm. The mean K_{SP} value is 0.775 with a standard deviation of 0.274, which results in a COV of 0.354. The slope of the best-fit line through the origin, 0.691, and the mean indicate that for this specific sub-category the Energy Approach over predicts the pile's capacity. The ratio ranges from an over-prediction of 0.4 to an under-prediction of approximately 1.7 with a scatter shown by the low R^2 value of 0.525.

The figures presented in this section show that similarly to the signal matching analyses, the Energy Approach predicts the pile capacity for pile-cases with a hard driving resistance much more accurately than for the pile-cases with an easy driving resistance. This is shown for both the end of driving pile-cases as presented in Figures 6.32 and 6.33 as well as for the beginning or restrike pile-cases as presented in Figures 6.34 and 6.35.

d) *Performance According to Pile Type*

The performance of the Energy Approach method is evaluated in this section based on pile type, defining small and large displacement piles as those with area ratios greater and lower than 350, respectively. A comparison between the Energy Approach pile capacity predictions for small and large displacement piles to the static load test results is conducted for each of the analyses in the above section, i.e., eight comparisons all together, presented in Figures 6.36 through 6.43.

Figure 6.36 presents the static load test results compared to the Energy Approach predictions for 39 PD/LT2000 pile-cases at the end of driving with blow counts less than 16 BP10cm and area ratios less than 350 (this sub-grouping includes 4 of the extreme Energy Approach pile-cases, see Table 6.3). The mean K_{SP} value and its standard deviation are 1.431 and 0.727, respectively, which results in a COV of 0.508. The best-fit line through the origin has a slope of 1.018, with a large scatter shown by the range of prediction ratios from approximately 0.6 to 2.7 and a coefficient of determination, R^2 of 0.134.

The static load test results compared to the Energy Approach predictions are presented in Figure 6.37 for 23 PD/LT2000 pile-cases at the end of driving with blow counts less than 16 BP10cm and area ratios greater than or equal to 350 (this sub-grouping includes 2 of the extreme Energy Approach pile-cases, see Table 6.3). The mean K_{SP} value is 1.422 with a standard deviation of 0.888, which results in a COV of 0.624. The best-fit line through the origin has a slope of 1.031 with the scatter ranging from prediction ratios of approximately 0.5 to about 3.3. The R^2 value of 0.831 indicates smaller scatter mostly due to reasonably good predictions in the high capacity range.

A comparison between the static load test results and the Energy Approach predictions for 39 PD/LT2000 pile-cases at the end of driving with blow counts greater than or equal to 16 BP10cm and area ratios less than 350 is presented in Figure 6.38 (this sub-grouping includes 1 of the extreme Energy Approach pile-cases, see Table 6.3). The mean K_{SP} value for these pile-cases is 1.054 with a standard deviation of 0.459, resulting in a COV of 0.435. The best-fit line through the origin has a slope of 0.902 with the scatter ranging approximately from an over-prediction ratio of 0.5 to an under-prediction ratio of 1.8 with a coefficient of determination, R^2 of 0.247 indicating the poor correlation of the method in this subcategory.

Figure 6.39 presents the comparison between the static load test results and the Energy Approach predictions for 34 PD/LT2000 pile-cases at the end of driving with blow counts greater than or equal to 16 BP10cm and area ratios greater than or equal to 350. The mean K_{SP} value is 0.926, with a standard deviation of 0.320, which results

in a COV of 0.346. The slope of the best-fit line through zero is 0.879, with the scatter ranging from ratios of approximately 0.4 to 1.8 with a coefficient of determination, R^2 of 0.850 suggesting along with the COV value a relatively small amount of scatter in the data and a good performance of the Energy Approach for large displacement piles with a high driving resistance.

The static load test results are compared to the Energy Approach predictions in Figure 6.40 for 19 PD/LT2000 pile-cases at the beginning of restrike with blow counts less than 16 BP10cm and area ratios less than 350. The mean K_{SP} is 0.764 with a standard deviation of 0.318, resulting in a COV of 0.416. The Energy Approach method overall over predicts the pile capacity during restrike as also indicated by the slope of the best-fit line through zero, 0.736. There is a significant amount of scatter shown by the range of prediction ratios of approximately 0.4 to 1.4 with R^2 value of 0.600.

Figure 6.41 presents the comparison between the static load test results and the Energy Approach predictions for 10 PD/LT2000 pile-cases at the beginning of restrike with blow counts less than 16 BP10cm and area ratios greater than or equal to 350. The mean K_{SP} value is 0.954 with a standard deviation 0.396, which results in a COV of 0.415. The slope of the best-fit line through the origin is 0.761 with a significant scatter shown by the R^2 value of 0.334 and the range in prediction ratios of approximately 0.4 to 1.3. The amount of data is small and hence the information derived from it is limited.

Shown in Figure 6.42 is the comparison of the static load test results and the Energy Approach predictions for 82 PD/LT2000 pile-cases at the beginning of restrike with blow counts greater than or equal to 16 BP10cm and area ratios less than 350. The mean K_{SP} value is 0.736 with a standard deviation of 0.249, which results in a COV of 0.338. The Energy Approach method performs well for this sub-category, with over prediction of the pile capacity shown by the mean and by the slope of the best-fit line through zero of 0.685. The scatter ranges from an over-prediction ratio of 0.4 to an under-prediction ratio of about 1.8 and by the coefficient of determination, R^2 of 0.573.

The static load test results are compared to the Energy Approach predictions for 42 PD/LT2000 pile-cases at the beginning of restrike with blow counts greater than or equal to 16 BP10cm and area ratios greater than or equal to 350 in Figure 6.43. The mean K_{SP} value is 0.851 with a standard deviation of 0.305, which results in a COV of 0.358. Again the Energy Approach method performs well for this specific category with the exception of the consistent over-prediction. The mean slope of the best-fit line through the origin is 0.712, while the scatter ranges from a prediction ratio of about 0.4 to 1.7 with a coefficient of determination, R^2 of 0.269 indicating a large amount of scatter in the data.

The analysis presented in this section shows that the performance of the Energy Approach method is not affected by the pile type (small or large displacement) as much as the wave matching techniques. There is a slight effect on the Energy

Approach predictions based on pile type but none that are significant enough to require different resistance factors based on pile type.

6.3.4 Field Evaluation (Case Method)

a) General

A background of the Case method is presented in section 2.3.4 (Goble et al., 1970 and Rausche et al., 1975). The method is often used in field evaluations, as it is built into Pile Dynamics Inc.'s Pile Driving Analyzer (PDA), and is commonly used in the USA. The method is based on a simplified pile and soil behavior assumptions (free end and plastic soil), resulting in a closed form solution related to the impact and its reflection from the tip. With the years, the method has evolved to be implemented into at least five different variations (GRL, 1999). The Case method utilizes a damping coefficient (J_c) that is assumed to be associated with soil type. The influence of this factor on the predicted static capacity depends on the reflected wave from the pile's tip, and hence on the driving resistance. The case-damping coefficient was investigated through back calculation (to match the measured static capacity). The results, described in the next section, suggest no correlation between the soil type and the case-damping coefficient. The common recommended practice suggests the use of the method based on a specific site/area calibration (GRL, 1999).

b) Evaluation of the Case-Damping Coefficient

A comparison between the back-calculated case-damping coefficient, J_c , based on the static load test result and the soil type at the pile tip is presented in Figure 6.44. J_c was calibrated using the static capacity R_s and the "standard" Case method, as

outlined by Goble et al. (1975). Paikowsky et al., (1994) originally presented this figure that shows data for 290 PD/LT pile-cases. The data in the figure shows that there is no correlation between the J_c value and the soil type at the tip as commonly assumed. The negative J_c values, which were back calculated from matching the load test results to the dynamic measurements, have no physical meaning and only demonstrate the limitations of the J_c coefficient.

c) *Evaluation of the Case Method Based on Local Calibration*

A statistical examination of local calibration (in Florida) was performed by McVay et al. (2000). The results of this analysis suggested that for 48 cases, the ratio between the static pile capacities to the Case method predictions at the end of driving was 1.344 ± 0.443 (mean \pm 1 standard deviation). The data was obtained by the Geotechnical Engineering Research Laboratory at the University of Massachusetts Lowell from Professor Michael McVay of the UFL (see section 3.5). The data contained 40 EOD cases as well as 37 BOR cases. The RMX variation of the Case method was used to determine the static pile capacity and the J_c values that were used in each of the analyses range from 0.02 to 0.44. It should be noted that the presented data was obtained from 13 different sites throughout the state of Florida; and although considered as a local calibration, the use of the varied J_c leaves the analysis questionable.

Presented in Figure 6.45 is a comparison between the static load test results and the Case method predictions for 77 pile-cases at both the EOD and BOR. The mean K_{SCASE} value, which is the ratio of the static load test results over the case

predictions, is 1.183 with a standard deviation of 0.403, which results in a COV of 0.341. There is a large amount of scatter indicated by the R^2 value of 0.361 and the range of prediction ratios from 0.6 to 2.7 while the slope of the best fit-line through the origin is 1.049.

Figure 6.46 presents the comparison between the static load test results and the Case method predictions for 40 EOD pile-cases. The mean K_{SCASE} value is 1.334 with a standard deviation of 0.438, which results in a COV of 0.328. These statistics are similar to that observed for the data presented in Figure 6.45 for all piles-cases. The scatter of the ratio ranges from approximately 0.6 to 3.1 and the R^2 value is 0.470. The slope of the best-fit line through the origin is 1.165.

The comparison between the static load test results and the Case method predictions for 37 BOR pile-cases are shown in Figure 6.47. The statistics show a significant improvement in the performance of the case method for the BOR pile-cases as the mean is approximately one (1.019) and the standard deviation is relatively small (0.285) resulting in a COV of 0.280 which is also small compared to the COV for the EOD pile-cases. The best-fit line through the origin has a slope of 0.957 with a scatter shown by the R^2 value of 0.366 and a range of ratios from an over-prediction ratio of 0.6 to an under-prediction ratio of 1.6.

d) Summary

The data presented in Figures 6.45 through 6.47 suggest that the Case method performs reasonably well under local conditions for both the EOD and BOR cases. The method performs better for the BOR cases than for the EOD pile-cases. The Case

method application in the maximum resistance form (RMX) has proven therefore effective for local conditions. Accumulated experience on extensive number of sites in the Boston area (e.g., GTR, 1997, 1998) has demonstrated the effectiveness of the Case method, when locally calibrated. As the data from Florida represents varied J_c and no generic conditions exist for the use of the Case method, international or national calibrations are not possible at this time. The projection of local calibration (of good experience and practice) beyond the geographical location and under non-uniform J_c is at this time impossible; hence, resistance factors will not be calibrated for the Case method.

6.4 SUMMARY AND INTERMEDIATE CONCLUSIONS

The evaluation of the dynamic methods used during the construction stage (indicator and production piles), was presented in this chapter. Figure 6.1 presented a flow chart that outlines the analysis methods and the conditions under which they were examined. A statistical evaluation was completed for each of the sub-categories presented in Figure 6.1 excluding the development of load factors for the stress evaluation of WEAP analyses.

The wide spread use of the WEAP analysis for pile capacity predictions has required the statistical evaluation of this method. The statistics presented in section 6.2.1 showed the use of the WEAP method for evaluating pile capacity is very limited at the EOD and somehow better at the BOR. Resistance factors are presented in Chapter 9 for these WEAP cases due to its wide spread use and demand of the research project panel.

A summary of the statistics describing the performance of the dynamic equations was presented in Table 6.2. The obtained results show that the FHWA version of the Gates equation had the lowest bias and the evaluation of this method was therefore carried out to examine its performance under different times of driving and driving resistances.

Table 6.4 presents a summary of the statistical evaluation of the methods that use dynamic measurements, namely the signal matching methods (CAPWAP/TEPWAP) and the Energy Approach method with their subcategories based on the controlling parameters. The statistics show that the Energy Approach performs the best as a construction control during driving (for the EOD pile-cases) while the signal matching methods perform the best for overall accuracy verification when used for the last BOR pile-cases. Also shown by the statistics is that both methods perform better for pile-cases with blow counts that are greater than 16 blows per 10cm than for pile-cases with blow counts less than 16 blows per 10cm. The extreme pile-cases that were discussed in section 6.3.1 result in Table 6.4 in a poor performance for the category of low driving resistance and low area ratio (large displacement piles). The most unreliable performance is that of the signal matching related to the sub-category of EOD pile-cases with blow counts of less than 16 blows per 10cm and area ratios less than 350. The EOD cases with blow count less than 16 blows per 10cm and area ratio greater than 350 resulted in a large bias but a good coefficient of variation. The unreliable categories for the Energy Approach method are the EOD pile-cases with blow counts less than 16 blows per 10cm and area ratios both less than and greater

than 350. The moderate to poor performance of the Energy Approach is therefore very noticeable for blow counts less than 16 blows per 10cm. However, its bias in these cases is on the safe side and hence would result with resistance factors similar to other categories (to be discussed in Chapter 9). The following cases for the Energy Approach and CAPWAP/TEPWAP methods are recommended to have resistance factors calculated:

1. For the CAPWAP/TEPWAP methods, the general case, the EOD case, the BOR case and the EOD case with blow counts less than 16 blows per 10cm and area ratios less than 350.
2. For the Energy Approach method, the general case, the EOD case, the BOR case and the EOD case with blow counts less than 16 blows per 10cm and area ratios less than 350.

These are only the preliminary recommended cases to have resistance factors evaluated and may not necessarily be the final cases that have recommended resistance factors assigned for them.

A resistance factor will not be calculated for the Case method for two reasons: (a) the Case method performs really well for local calibrations, but calibration based on a national scale (beyond the local geographical conditions) could not be evaluated and (b) the presented assessment of the Case method although uses a uniform interpretation methodology (RMX) used different J_c values for each case. The reevaluation of the capacity based on a uniform application of the method (i.e., RMX,

say with $J_c = 0.6$) requires data not available in this study and may be a well-justified expansion of this research in the future.

Table 6.5 is a summary of the statistics that were calculated for each of the sub-categories presented in this chapter. For each sub-category the number of cases, the mean K value, the standard deviation, the coefficient of variation, the slope of the best-fit line through the origin, and the coefficient of determination are presented.

Table 6.1. Summary of the Statistical Data Evaluating the Performance of the Dynamic Equations.

	<u>ENR Equation</u> Load Test Results	<u>ENR Equation (w/FS)</u> Load Test Results	<u>Gates Formula</u> Load Test Results	<u>FHWA Version</u> Load Test Results
Mean K_{SX}	0.267	1.600	1.787	0.940
Standard Deviation	0.243	1.458	0.848	0.472
Coefficient of Variation	0.910	0.911	0.475	0.502
Minimum K_{SX}	0.058	0.347	0.374	0.223
Maximum K_{SX}	2.208	13.249	7.063	3.907
No. of Cases	384	384	384	384

Table 6.2. Summary of the Statistical Analyses Performed for the Dynamic Equations.

Method	ENR Equation	ENR Equation (w/FS)	Gates Equation	FHWA Version of Gates Equation			
$\mu_{K_{SX}}$	0.267	1.600	1.787	0.940			
$\sigma_{K_{SX}}$	0.243	1.458	0.848	0.472			
COV	0.910	0.911	0.475	0.502			
No.	384	384	384	384			
Time of Driving	----	----	----	EOD	BOR (last)		
$\mu_{K_{SX}}$	----	----	----	1.073	0.833		
$\sigma_{K_{SX}}$	----	----	----	0.573	0.403		
COV	----	----	----	0.534	0.484		
No.	----	----	----	135	159		
Blow Count	----	----	----	< 16 BP10cm	≥ 16 BP10cm	< 16 BP10cm	≥ 16 BP10cm
$\mu_{K_{SX}}$	----	----	----	1.306	0.876	0.929	0.809
$\sigma_{K_{SX}}$	----	----	----	0.643	0.419	0.688	0.290
COV	----	----	----	0.492	0.478	0.741	0.358
No.	----	----	----	62	73	32	127

NOTES: COV = Coefficient of Variation K_{SX} = Static Load Test Results over the Dynamic Equation Prediction.
EOD = End of Driving BOR = Beginning of Restrike μ = mean value σ = standard deviation

Table 6.3. Summary of the EOD Pile-Cases for which the K_{SX} Values Were Outside Two Standard Deviations.

Energy Approach Pile-Cases						
No.	Pile-Case Number	Location	Area Ratio	Blow Count (BP10cm)	K _{SP}	Reason for Removal
226	CH39-EOD	Jones Island, WI	3142	3.3	3.687	Blow Counts were measured in BPF and not BPI at the EOD. D _{max} is less than the measured set.
229	CH6-5B-EOD	Jones Island, WI	3349	2.0	4.273	
286	DD22-EOD	Orlando, FL	309	22.3	2.567	Blow Counts were measured in BPF and not BPI at the EOD.
288	DD23-EOD	Orlando, FL	309	8.9	3.242	
300	LB5-EOD	Kenner, LA	189	7.2	3.188	See reason below for this same site.
305	LB6-EOD	Kenner, LA	226	4.9	2.813	
310	LB7-EOD	Kenner, LA	225	15.5	2.580	
CAPWAP Pile-Cases						
No.	Pile-Case Number	Location	Area Ratio	Blow Count (BP10cm)	K _{SW}	Reason for Removal
291	LB3-EOD	Kenner, LA	203	3.3	6.854	Pile-cases are all from the same site and all have very low blow counts and very low area ratios. These 5 pile-cases fall into the category of Blow Count less than 16 BP10cm (4 BPI) and Area Ratio less than 350, and were retained for that specific combination of the analysis.
295	LB4-EOD	Kenner, LA	189	4.6	11.256	
300	LB5-EOD	Kenner, LA	189	7.2	9.375	
305	LB6-EOD	Kenner, LA	226	4.9	5.969	
310	LB7-EOD	Kenner, LA	225	15.5	5.258	

Notes: EOD = End of Driving
 K_{SP} = Ratio of Static Load Test Results to Energy Approach Predictions
 K_{SW} = Ratio of Static Load Test Results to CAPWAP Predictions

BP10cm = Blows per 10 centimeters
BPI = Blows per inch
BPF = Blows per foot

Table 6.4. Summary of the Soil Inertia Properties for PD/LT2000, Energy Approach and CAPWAP/TEPWAP vs. Static Load Test Results for the Controlling Parameters.

Method	CAPWAP/TEPWAP								Energy Approach							
$\mu_{K_{SX}}$	1.368								0.894							
$\sigma_{K_{SX}}$	0.620								0.367							
COV	0.453								0.411							
No.	377								371							
Time	EOD				BOR (last)				EOD				BOR (last)			
$\mu_{K_{SX}}$	1.626				1.158				1.084				0.785			
$\sigma_{K_{SX}}$	0.797				0.393				0.431				0.290			
COV	0.490				0.339				0.398				0.369			
No.	125				162				128				153			
Bl. Count	< 16 BP10cm		≥ 16 BP10cm		< 16 BP10cm		≥ 16 BP10cm		< 16 BP10cm		≥ 16 BP10cm		< 16 BP10cm		≥ 16 BP10cm	
$\mu_{K_{SX}}$	1.843		1.460		1.176		1.153		1.227		0.972		0.830		0.775	
$\sigma_{K_{SX}}$	0.831		0.734		0.530		0.354		0.474		0.359		0.352		0.274	
COV	0.451		0.503		0.451		0.307		0.386		0.369		0.424		0.354	
No.	54		71		32		130		56		72		29		124	
A_R	< 350	≥ 350	< 350	≥ 350	< 350	≥ 350	< 350	≥ 350	< 350	≥ 350	< 350	≥ 350	< 350	≥ 350	< 350	≥ 350
$\mu_{K_{SX}}$	2.589	1.929	1.717	1.181	1.116	1.308	1.178	1.110	1.431	1.422	1.054	0.926	0.764	0.954	0.736	0.851
$\sigma_{K_{SX}}$	2.385	0.698	0.841	0.468	0.362	0.796	0.379	0.303	0.727	0.888	0.459	0.320	0.318	0.396	0.249	0.305
COV	0.921	0.362	0.490	0.396	0.324	0.609	0.446	0.273	0.508	0.624	0.435	0.346	0.416	0.415	0.338	0.358
No.	37	22	37	34	22	10	83	47	39	23	39	34	19	10	82	42

NOTES: COV = Coefficient of Variation K_{SX} = Static Load Test Results over the CAPWAP/TEPWAP or Energy Approach Predictions.
EOD = End of Driving BOR = Beginning of Restrike μ = mean σ = standard deviation

Table 6.5. Summary of the Statistical Analyses Performed in Chapter 6.

Method	No.	Mean K _{sx}	Standard Deviation	COV	m ₀	R ²
GRLWEAP, EOD	99	1.656	1.199	0.724	1.081	0.359
GRLWEAP, BOR	99	0.939	0.399	0.425	0.803	0.495
ENR w/out FS	384	0.267	0.243	0.910	0.162	0.223
ENR w/FS	384	1.600	1.458	0.910	0.972	0.223
Gates, General	384	1.787	0.848	0.475	1.828	0.412
FHWA, General	384	0.940	0.472	0.502	0.922	0.417
FHWA, EOD	135	1.073	0.573	0.534	1.048	0.413
FHWA, BOR	159	0.833	0.403	0.484	0.828	0.487
FHWA, EOD, ED	62	1.306	0.643	0.492	1.282	0.419
FHWA, BOR, ED	32	0.929	0.688	0.741	0.929	0.215
FHWA, EOD, HD	73	0.876	0.419	0.478	0.967	0.468
FHWA, BOR, HD	127	0.809	0.290	0.358	0.820	0.499
CAPWAP, General	377	1.368	0.620	0.453	1.160	0.557
CAPWAP, EOD	125	1.626	0.797	0.490	1.284	0.653
CAPWAP, BOR	162	1.158	0.393	0.339	1.104	0.599
CAPWAP, EOD, ED	54	1.843	0.831	0.451	1.388	0.677
CAPWAP, EOD, HD	71	1.460	0.734	0.503	1.236	0.647
CAPWAP, BOR, ED	32	1.176	0.530	0.451	1.189	0.717
CAPWAP, BOR, HD	130	1.153	0.354	0.307	1.096	0.526
CAPWAP, EOD, ED, LD	37	2.589	2.385	0.921	1.467	-0.082
CAPWAP, EOD, ED, SD	22	1.929	0.698	0.362	1.360	0.776
CAPWAP, EOD, HD, LD	37	1.717	0.841	0.490	1.479	0.185
CAPWAP, EOD, HD, SD	34	1.181	0.468	0.396	1.139	0.904

Notes: K_{sx} = Ratio of Static Load Test Results to the Predicted Results
m₀ = Slope of the best-fit line forced through the origin
No. = Number of pile-cases
R² = coefficient of determination
BOR = Beginning of Restrike
ED = Easy Driving
LD = Large Displacement
EA = Energy Approach
COV = Coefficient of Variation
EOD = End of Driving
FS = Factor of Safety
HD = Hard Driving
SD = Small Displacement

Table 6.5 (con't). Summary of the Statistical Analyses Performed in Chapter 6

Method	No.	Mean K_{sx}	Standard Deviation	COV	m₀	R²
CAPWAP, BOR, ED, LD	22	1.116	0.362	0.324	1.207	0.730
CAPWAP, BOR, ED, SD	10	1.308	0.796	0.609	1.133	0.638
CAPWAP, BOR, HD, LD	83	1.178	0.379	0.322	1.109	0.522
CAPWAP, BOR, HD, SD	47	1.110	0.303	0.273	1.064	0.484
EA, General	371	0.894	0.367	0.411	0.743	0.542
EA, EOD	128	1.084	0.431	0.398	0.926	0.693
EA, BOR	153	0.785	0.290	0.369	0.695	0.576
EA, EOD, ED	56	1.227	0.474	0.386	1.012	0.739
EA, EOD, HD	72	0.972	0.359	0.369	0.885	0.680
EA, BOR, ED	29	0.830	0.352	0.424	0.742	0.554
EA, BOR, HD	124	0.775	0.274	0.354	0.691	0.525
EA, EOD, ED, LD	39	1.431	0.727	0.508	1.018	0.134
EA, EOD, ED, SD	23	1.422	0.888	0.624	1.031	0.831
EA, EOD, HD, LD	39	1.054	0.459	0.435	0.902	0.247
EA, EOD, HD, SD	34	0.926	0.320	0.346	0.879	0.850
EA, BOR, ED, LD	19	0.764	0.318	0.416	0.736	0.600
EA, BOR, ED, SD	10	0.954	0.396	0.415	0.761	0.334
EA, BOR, HD, LD	82	0.736	0.249	0.338	0.685	0.573
EA, BOR, HD, SD	42	0.851	0.305	0.358	0.712	0.269
Case, General	77	1.183	0.403	0.341	1.049	0.361
Case, EOD	40	1.334	0.438	0.328	1.165	0.470
Case, BOR	37	1.019	0.285	0.280	0.957	0.366

Notes: K_{sx} = Ratio of Static Load Test Results to the Predicted Results
m₀ = Slope of the best-fit line forced through the origin
No. = Number of pile-cases COV = Coefficient of Variation
R² = coefficient of determination EOD = End of Driving
BOR = Beginning of Restrike FS = Factor of Safety
ED = Easy Driving HD = Hard Driving
LD = Large Displacement SD = Small Displacement
EA = Energy Approach

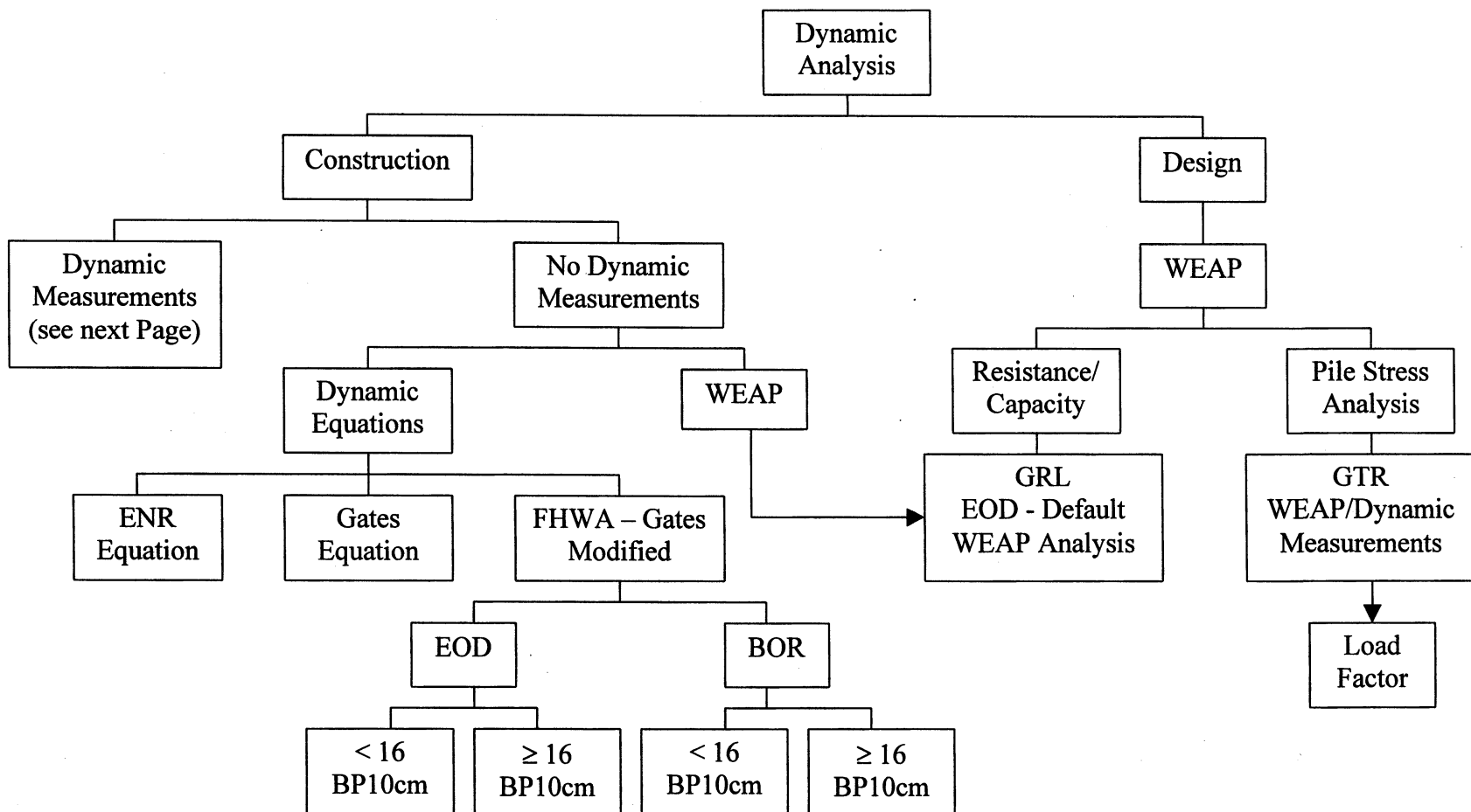


Figure 6.1. Flow Chart Depicting the Various Investigated Dynamic Analyses of Driven Piles (Pile Stress Analysis Excluded)

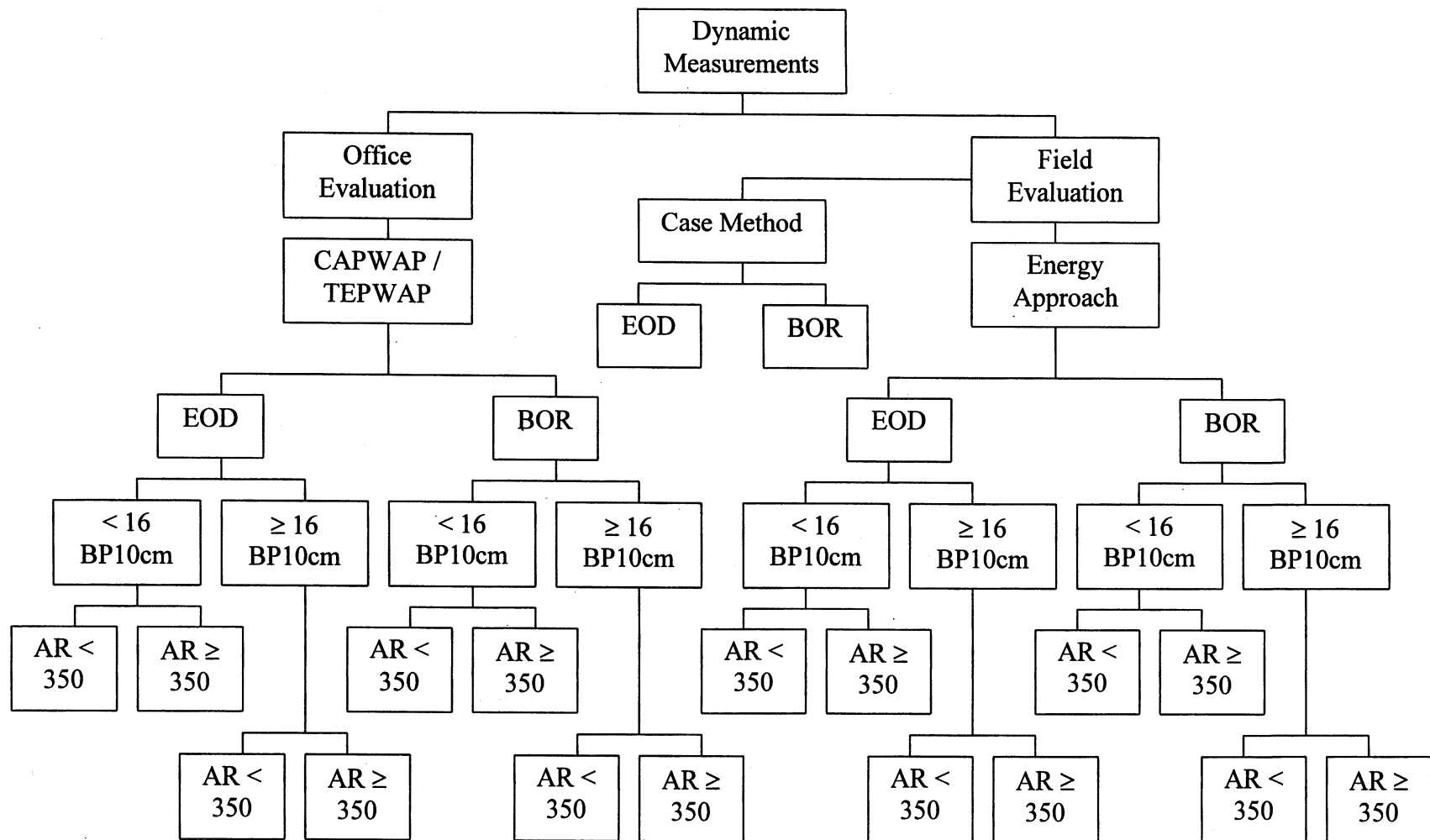


Figure 6.1 (con't). Flow Chart Depicting the Various Investigated Dynamic Analyses of Driven Piles (Pile Stress Analysis Excluded).

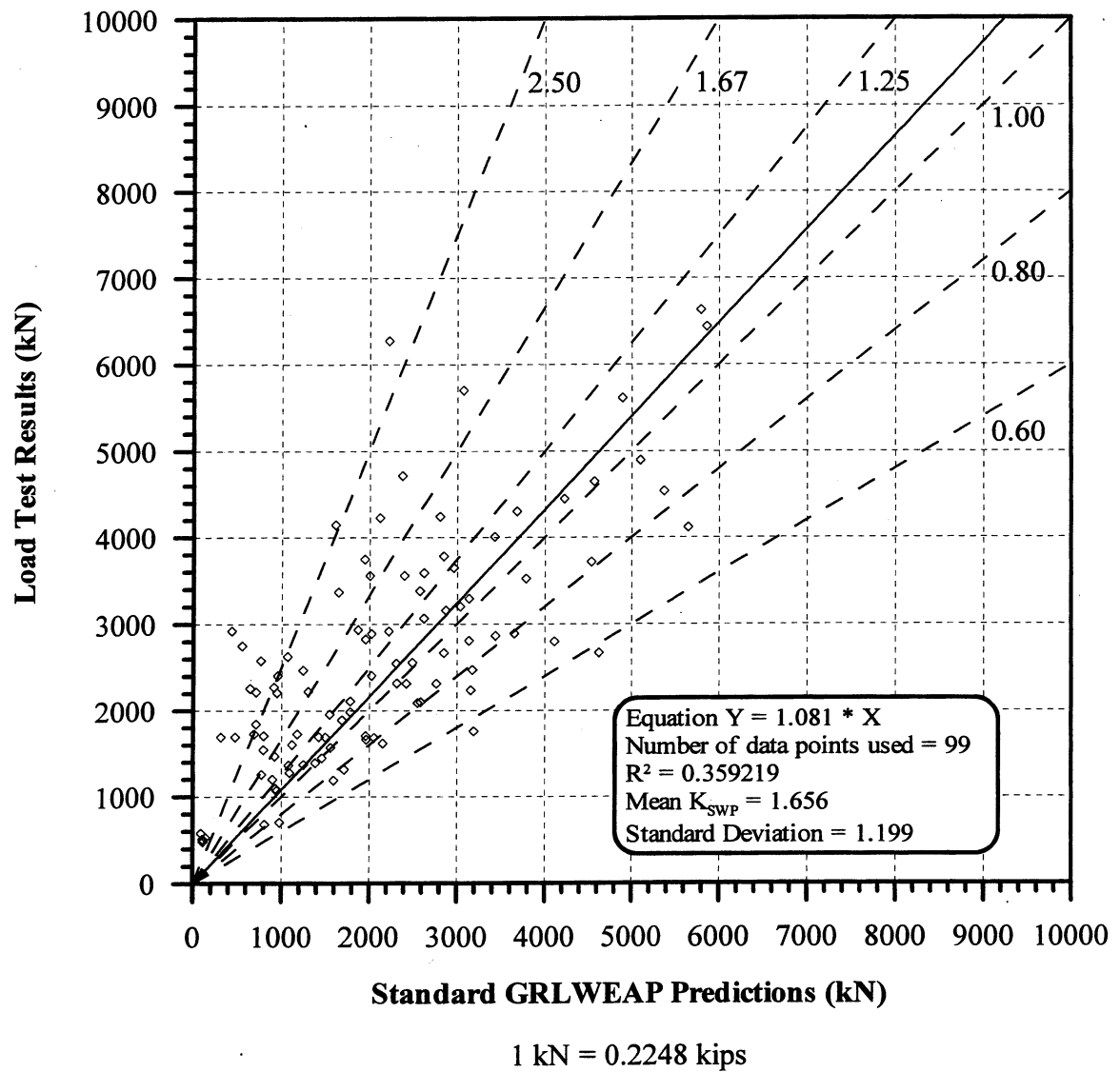


Figure 6.2. Static Load Test Results vs. GRLWEAP Predictions for 99 pile-cases at EOD provided by GRL Inc., in all types of soils (AEA).

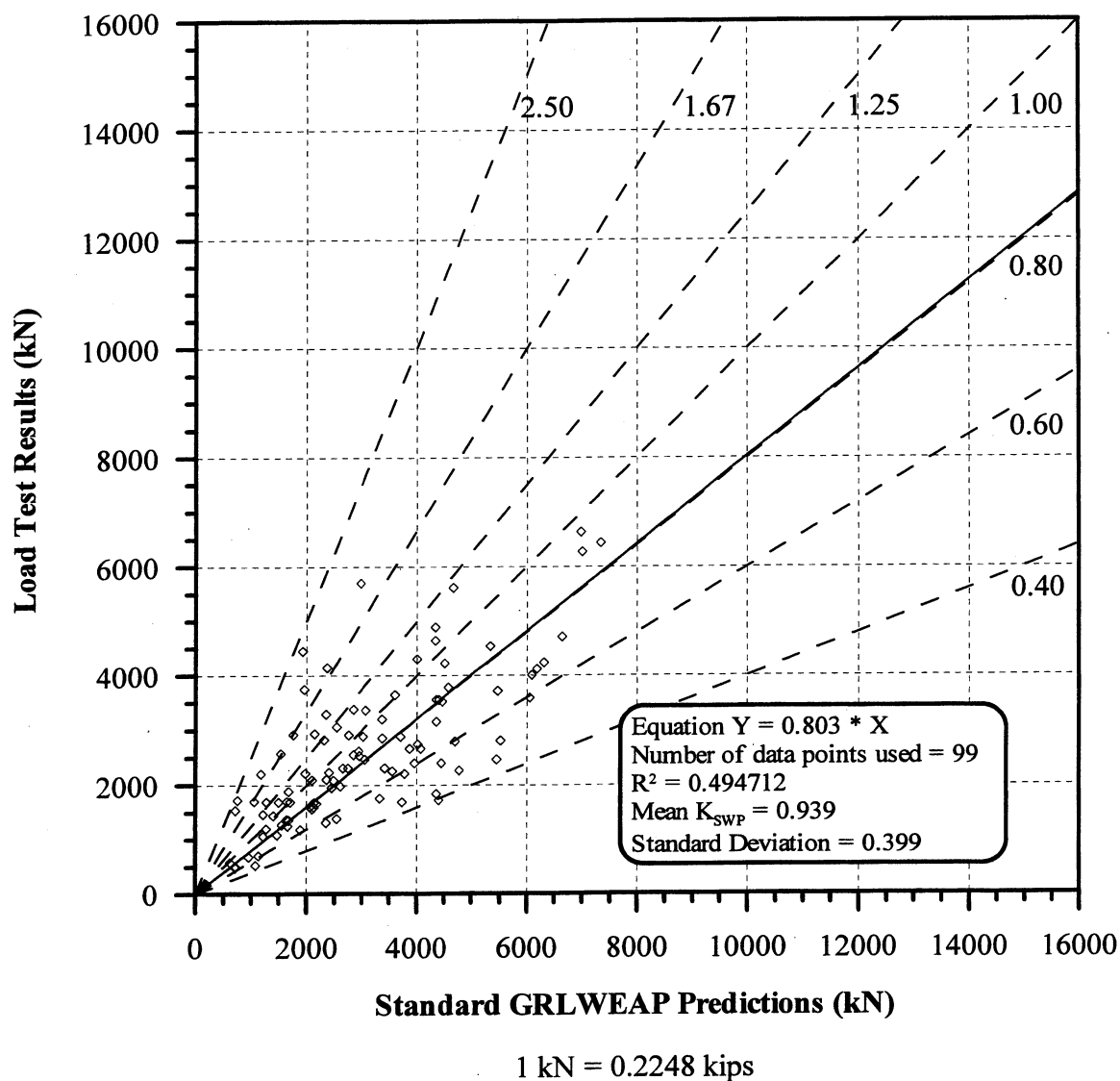


Figure 6.3. Static Load Test Results vs. GRLWEAP Predictions for 99 pile-cases at BOR provided by GRL Inc., all types of soils (ABA).

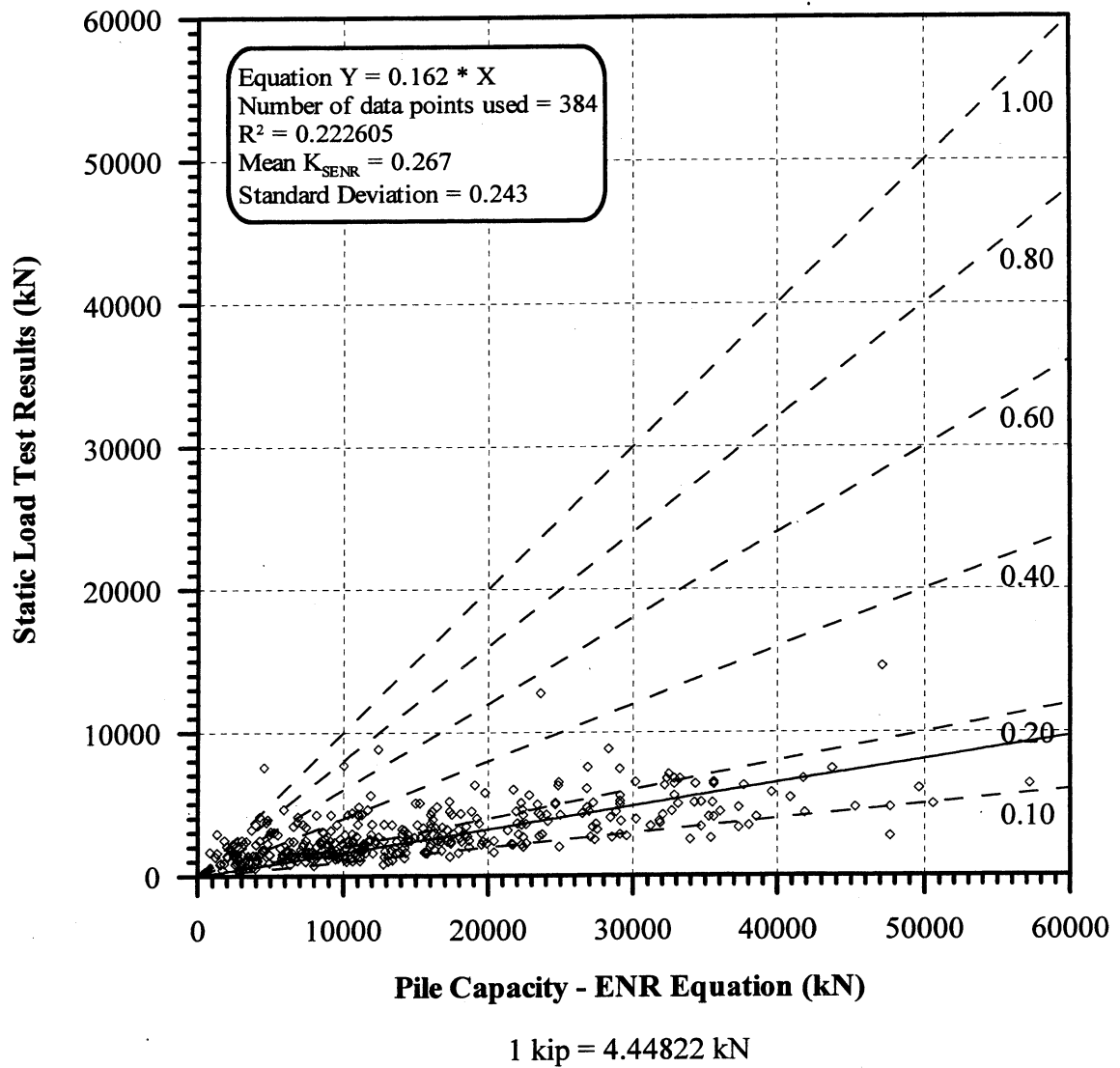


Figure 6.4. Static Load Test Results vs. ENR Equation Capacity for 384 PD/LT2000 pile-cases at all times and in all types of soils (AAA).

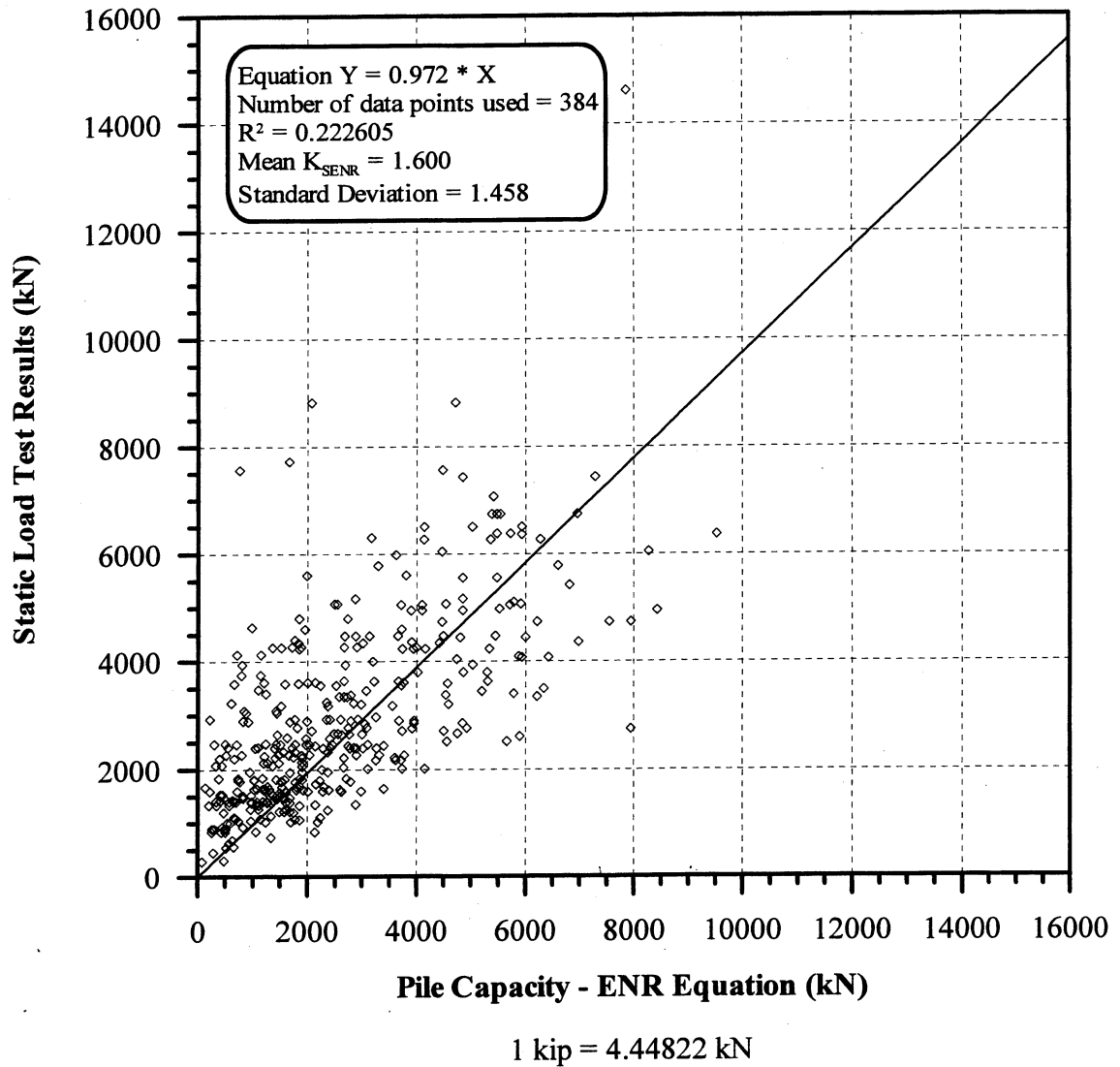


Figure 6.5. Static Load Test Results vs. ENR Equation Capacity with Factor of Safety of 6 for 384 PD/LT2000 pile-cases at all times and in all types of soils (AAA).

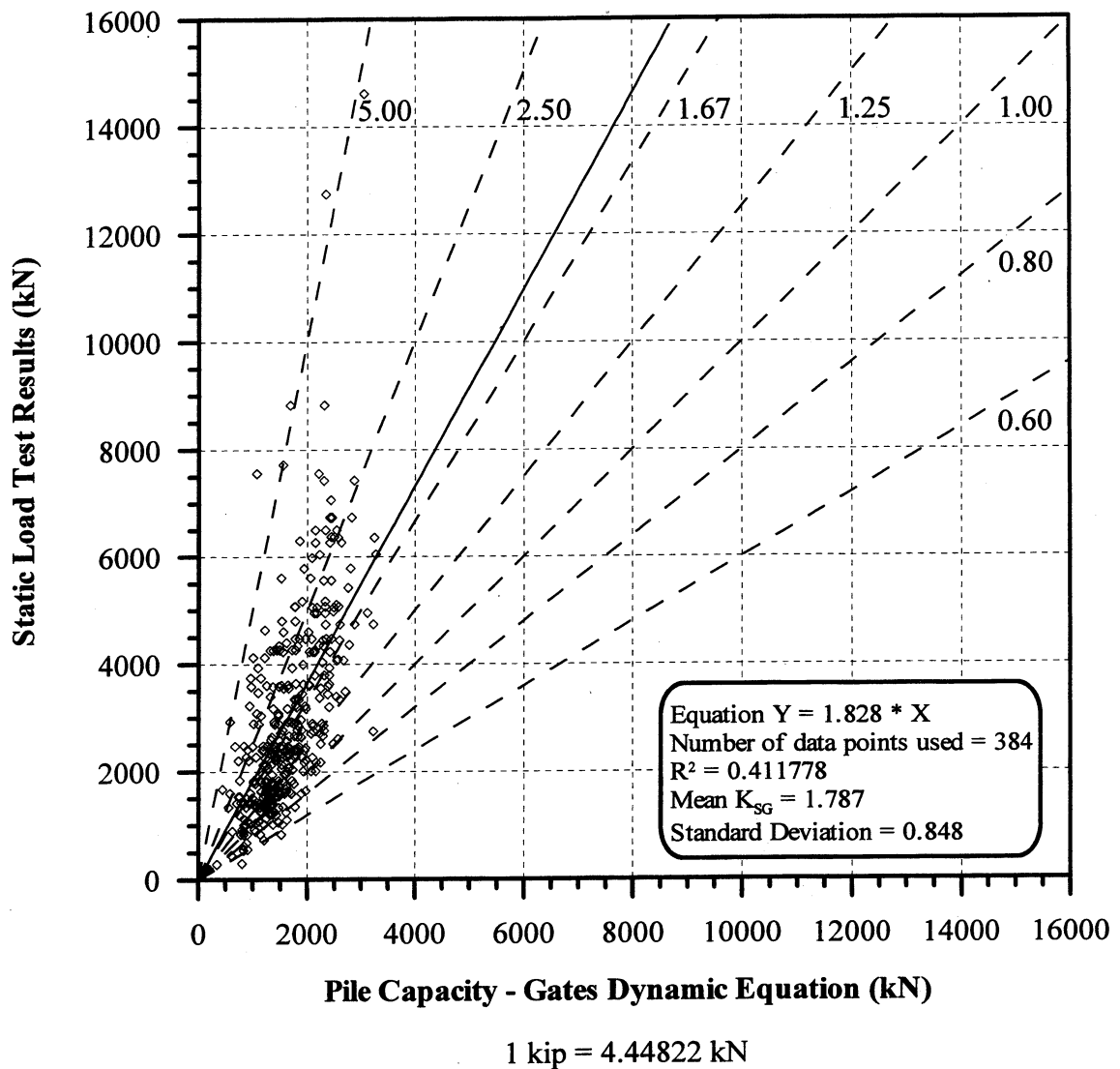
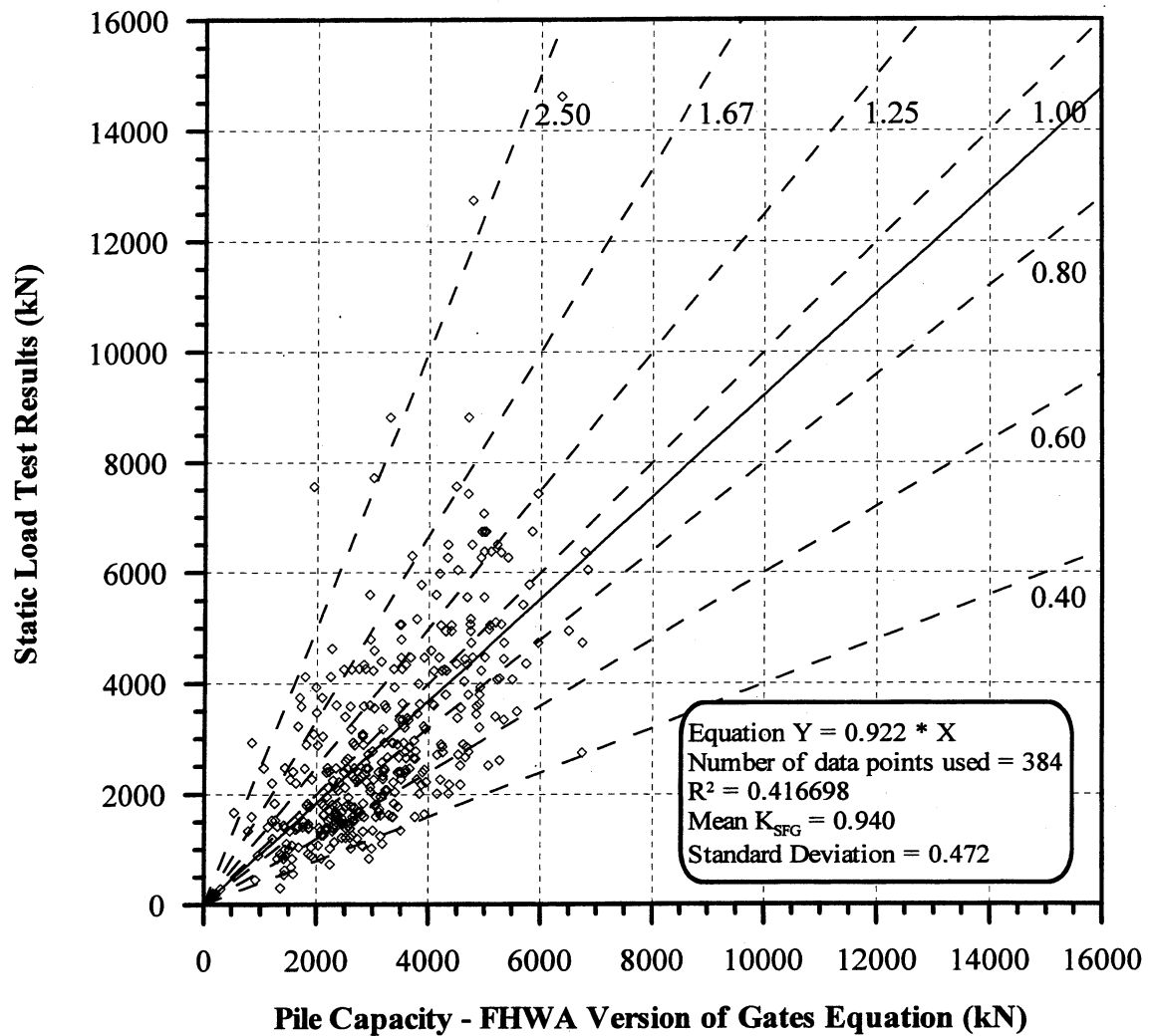


Figure 6.6. Static Load Test Results vs. Gates Dynamic Equation Capacity for 384 PD/LT2000 pile-cases at all times and in all types of soils (AAA).



1 kip = 4.44822 kN

Figure 6.7. Static Load Test Results vs. Pile Capacity according to the FHWA Version of the Gates Equation for 384 PD/LT2000 pile-cases at all times and in all types of soils (AAA).

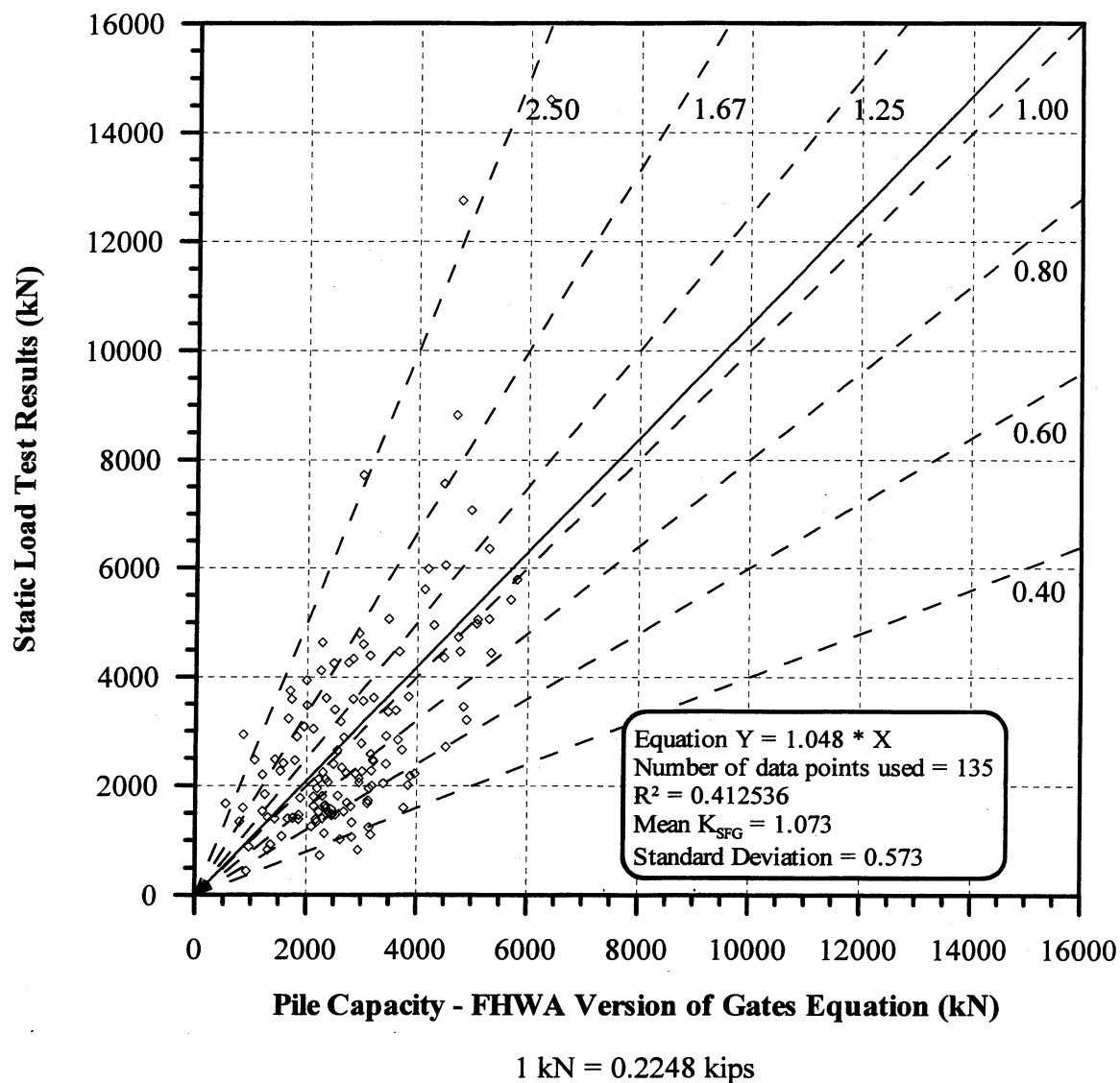


Figure 6.8. Static Load Test Results vs. Pile Capacity according to the FHWA Version of the Gates Equation for 135 PD/LT2000 EOD pile-cases in all types of soils (AEA)

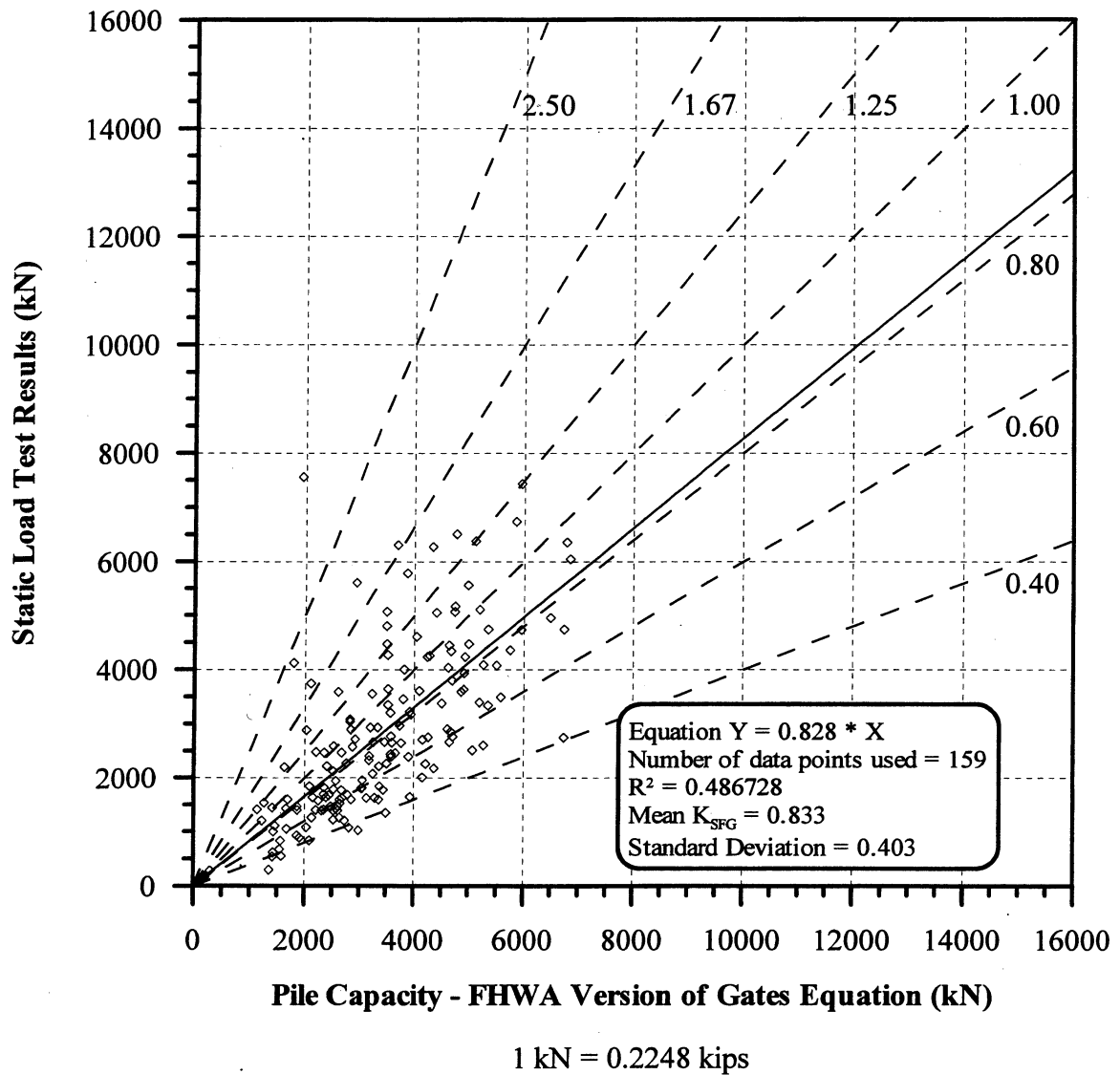


Figure 6.9. Static Load Test Results vs. Pile Capacity according to the FHWA Version of the Gates Equation for 159 PD/LT2000 BOR(last) pile-cases in all types of soils (ABA).

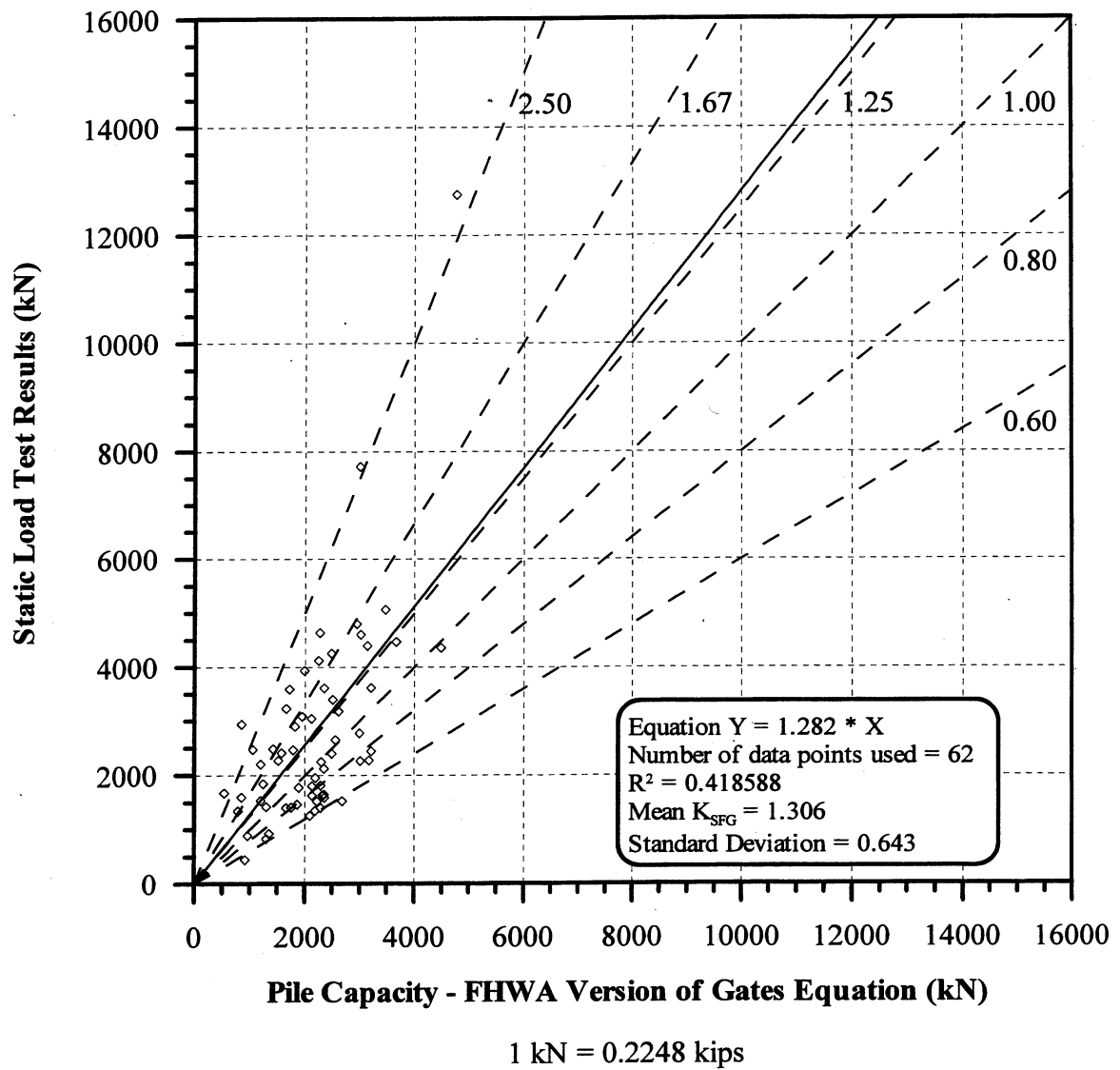


Figure 6.10. Static Load Test Results vs. Pile Capacity according to the FHWA Version of the Gates Equation for 62 PD/LT2000 pile-cases at the EOD with Blow Count < 16 BP10cm in all types of soils (AEA).

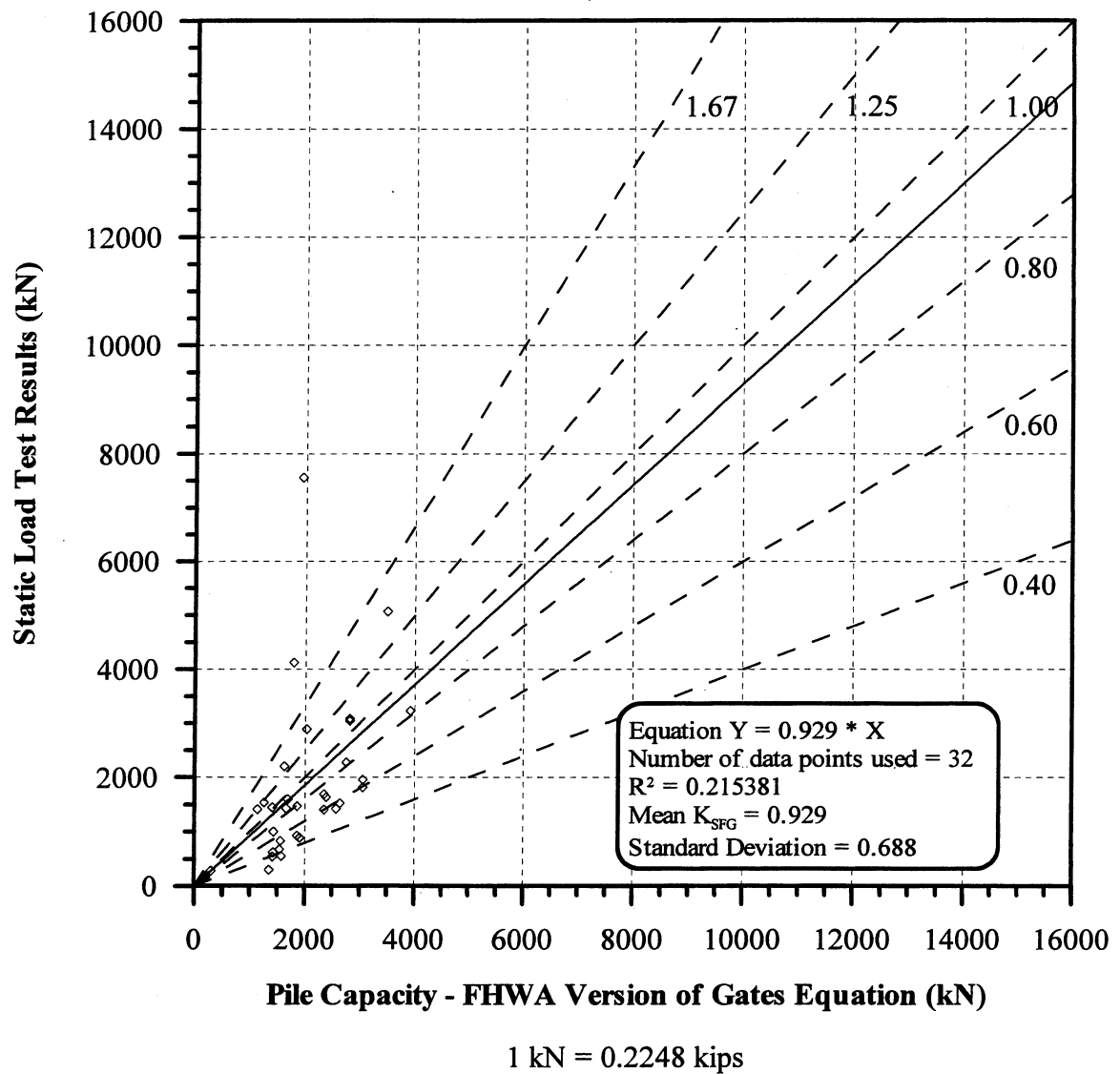


Figure 6.11. Static Load Test Results vs. Pile Capacity according to the FHWA Version of the Gates Equation for 32 PD/LT2000 pile-cases at the BOR (last) with Blow Count < 16 BP10cm in all types of soils (ABA).

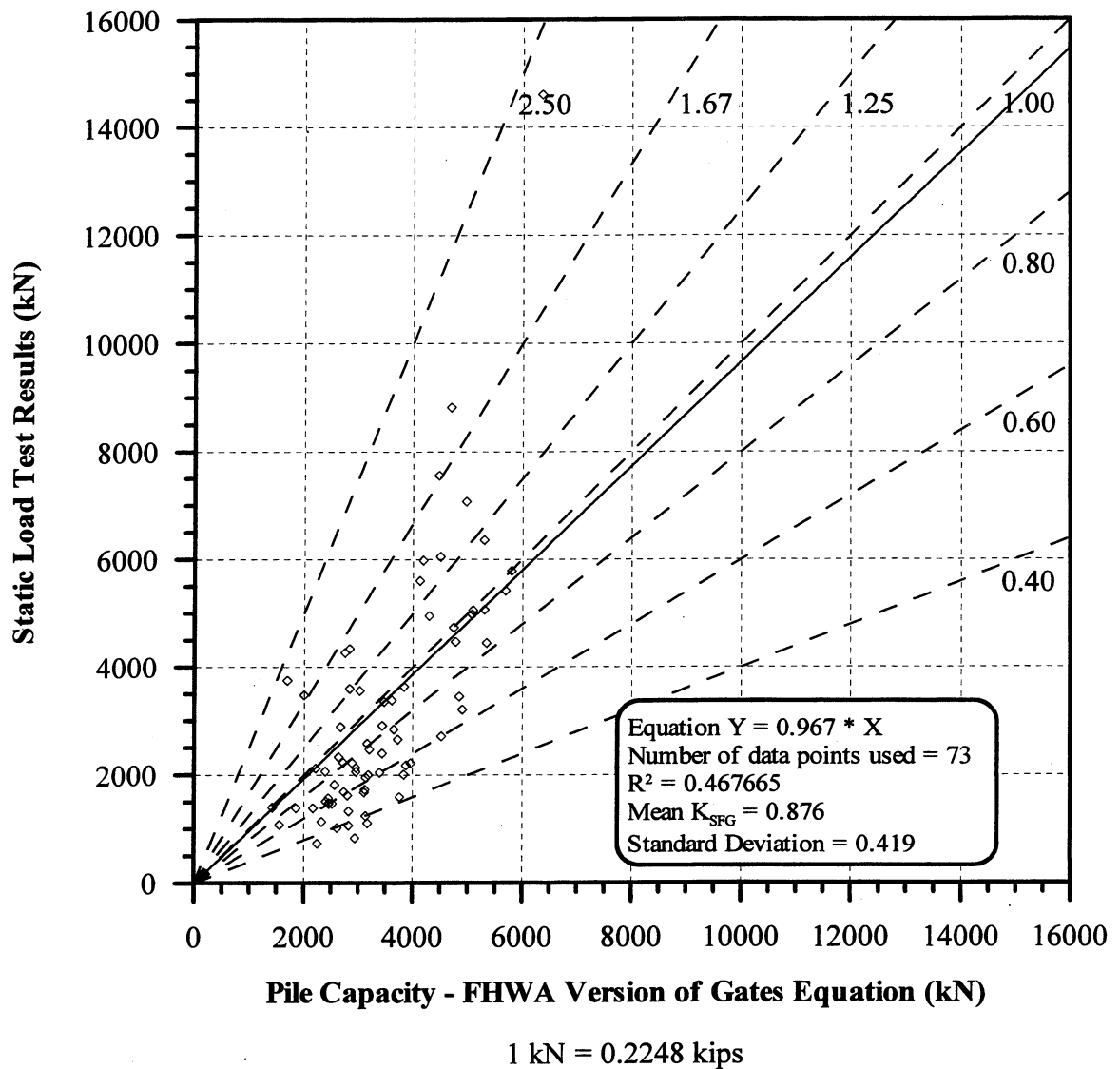


Figure 6.12. Static Load Test Results vs. Pile Capacity according to the FHWA Version of the Gates Equation for 73 PD/LT2000 pile-cases at the EOD with Blow Count ≥ 16 BP10cm in all types of soils (AEA).

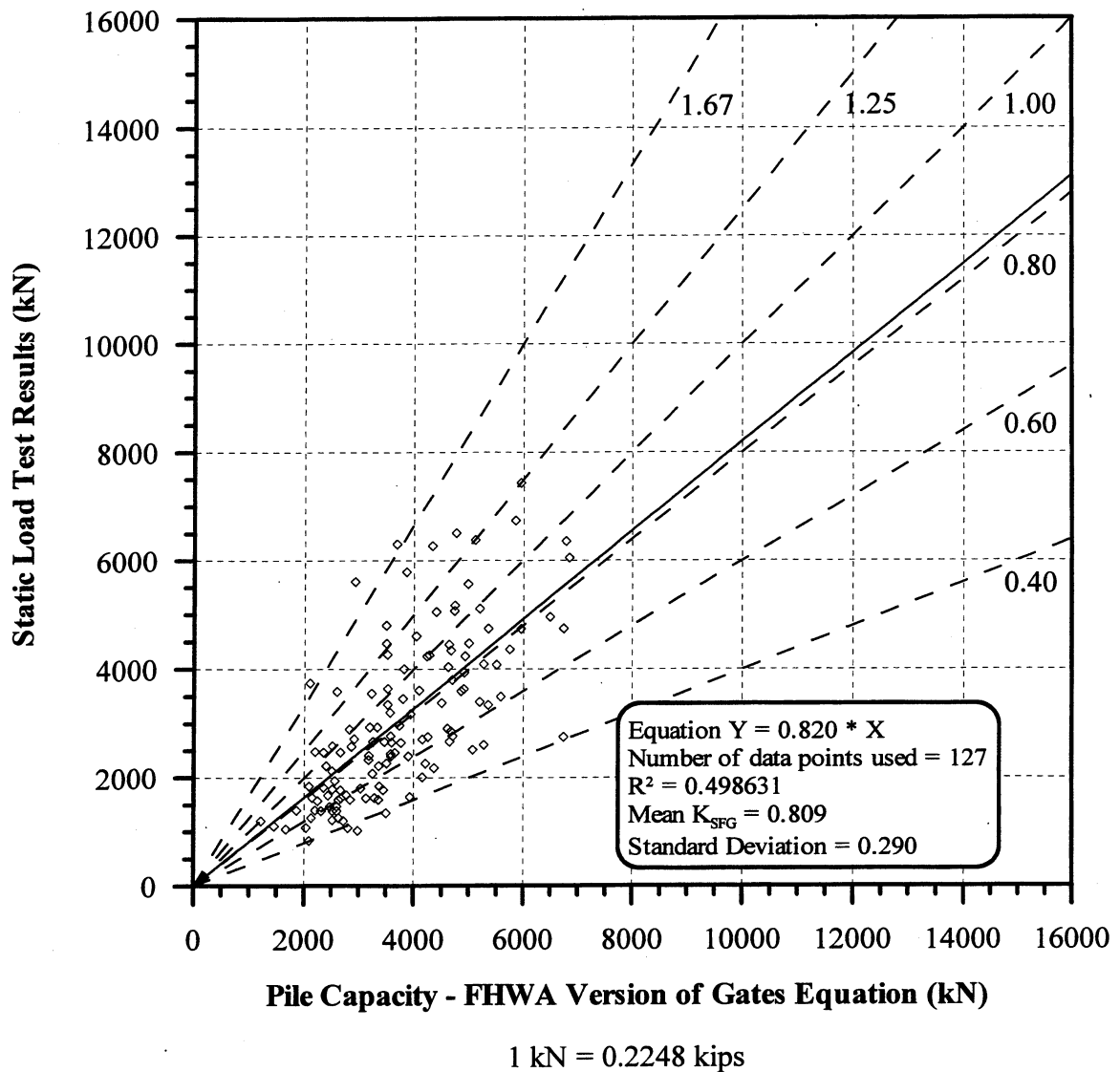
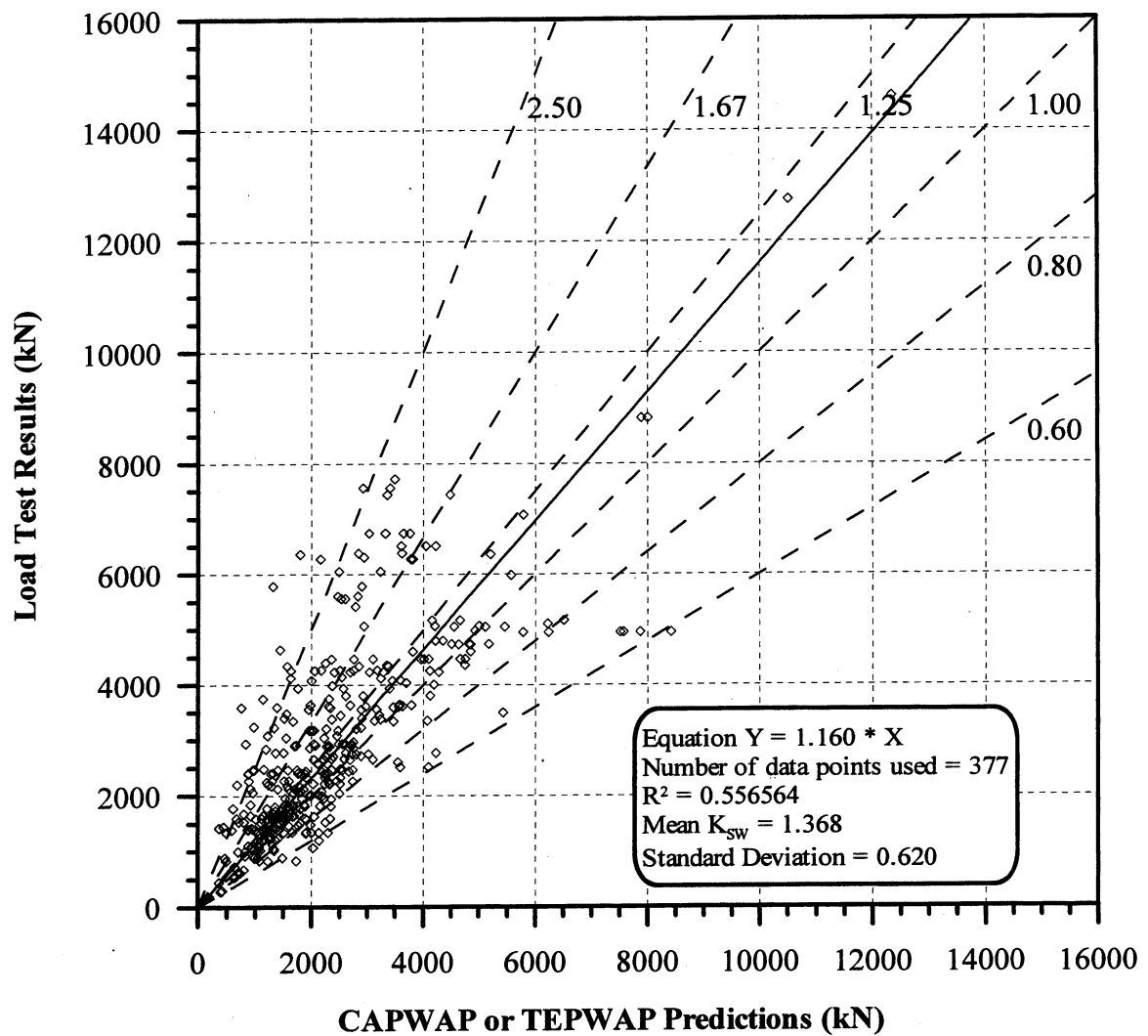


Figure 6.13. Static Load Test Results vs. Pile Capacity according to the FHWA Version of the Gates Equation for 127 PD/LT2000 pile-cases at the BOR (last) with Blow Count ≥ 16 BP10cm in all types of soils (ABA).



1 kN = 0.2248 kips

Figure 6.14. Static Load Test Results vs. CAPWAP or TEPWAP predictions for all 377 PD/LT2000 pile-cases at all times and in all types of soils (AAA).

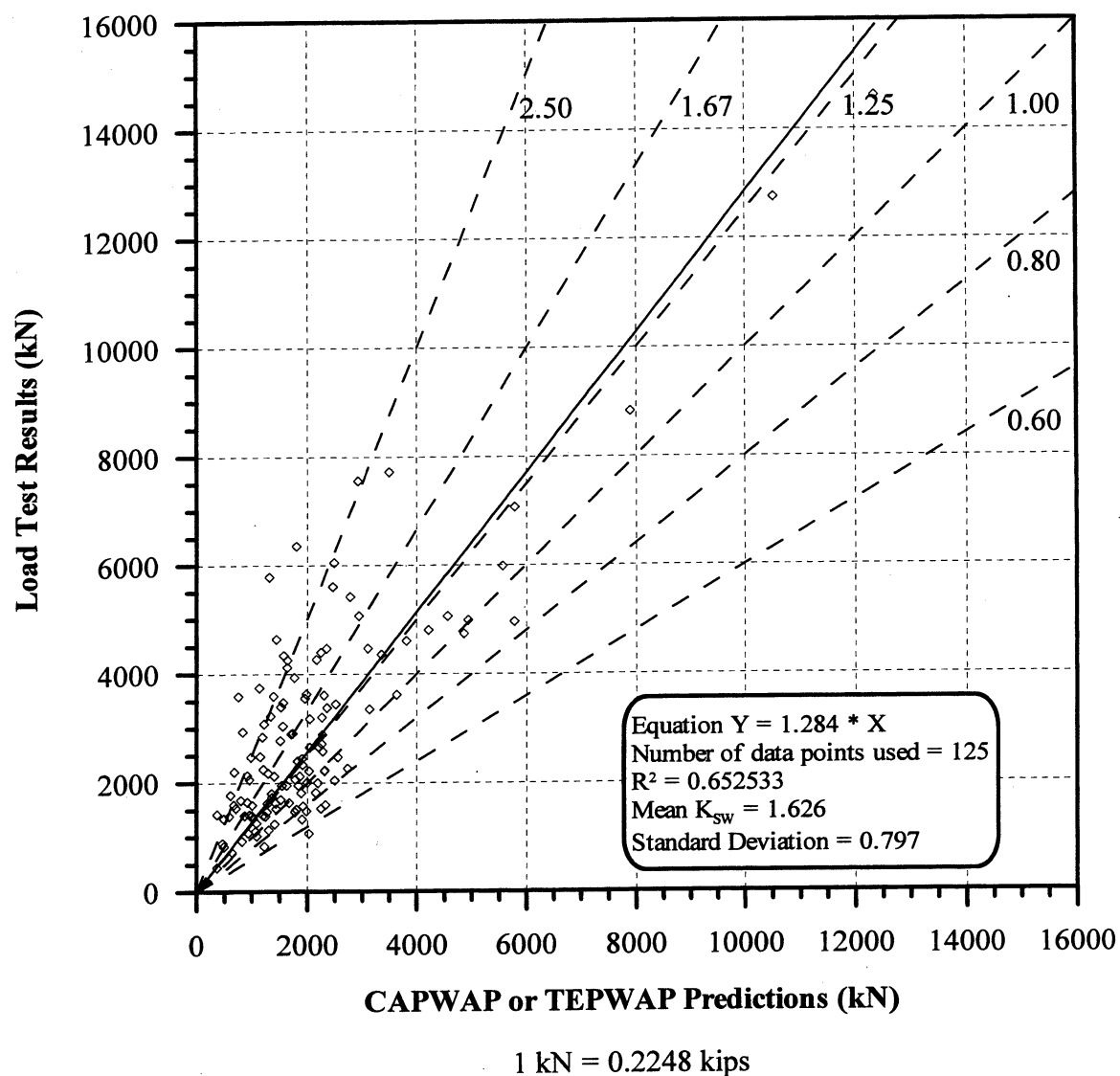


Figure 6.15. Static Load Test Results vs. CAPWAP or TEPWAP predictions for 125 PD/LT2000 pile-cases at EOD in all types of soils (AEA).

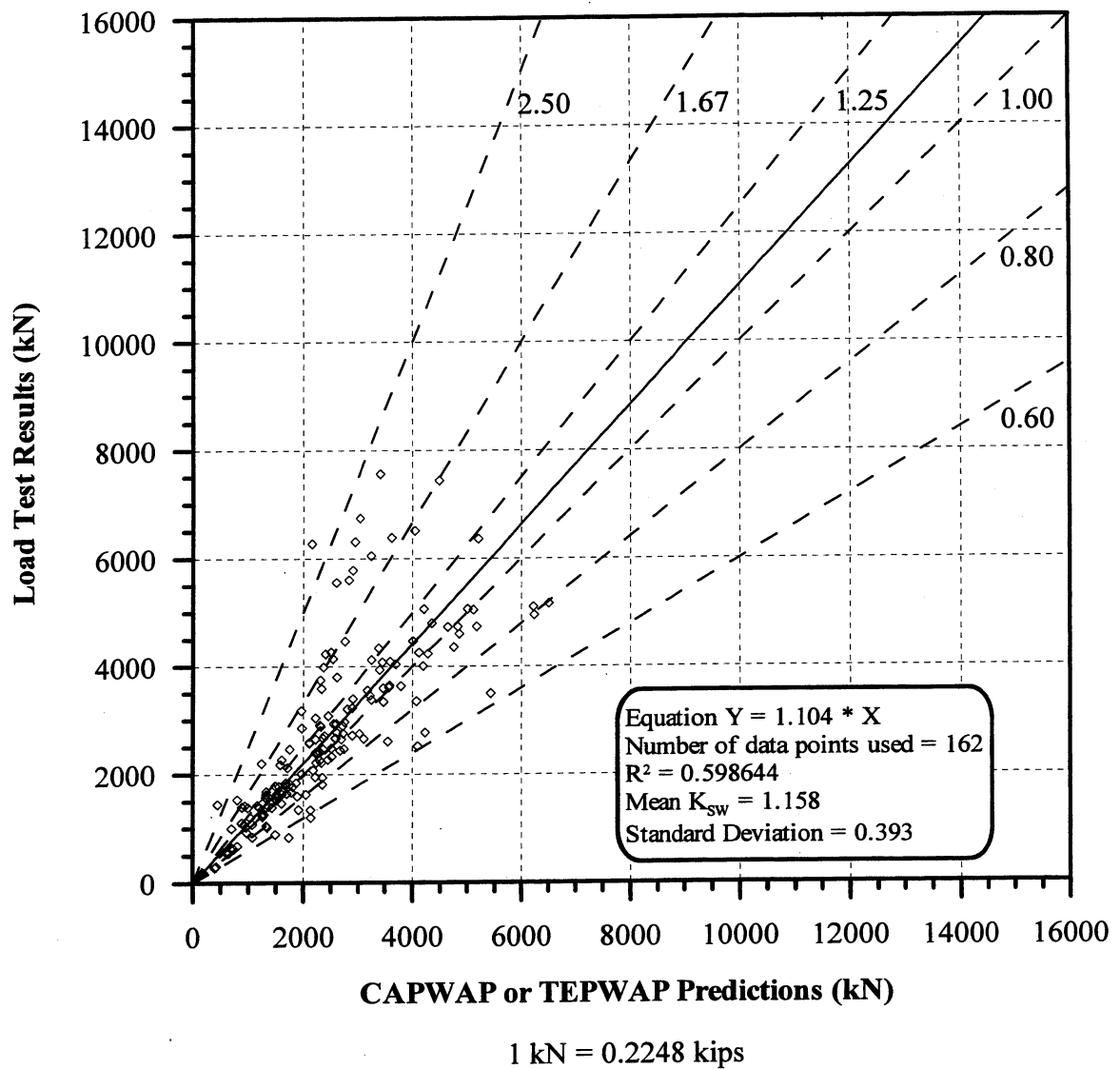


Figure 6.16. Static Load Test Results vs. CAPWAP or TEPWAP predictions for 162 PD/LT2000 pile-cases at BOR(last) in all types of soils (ABA).

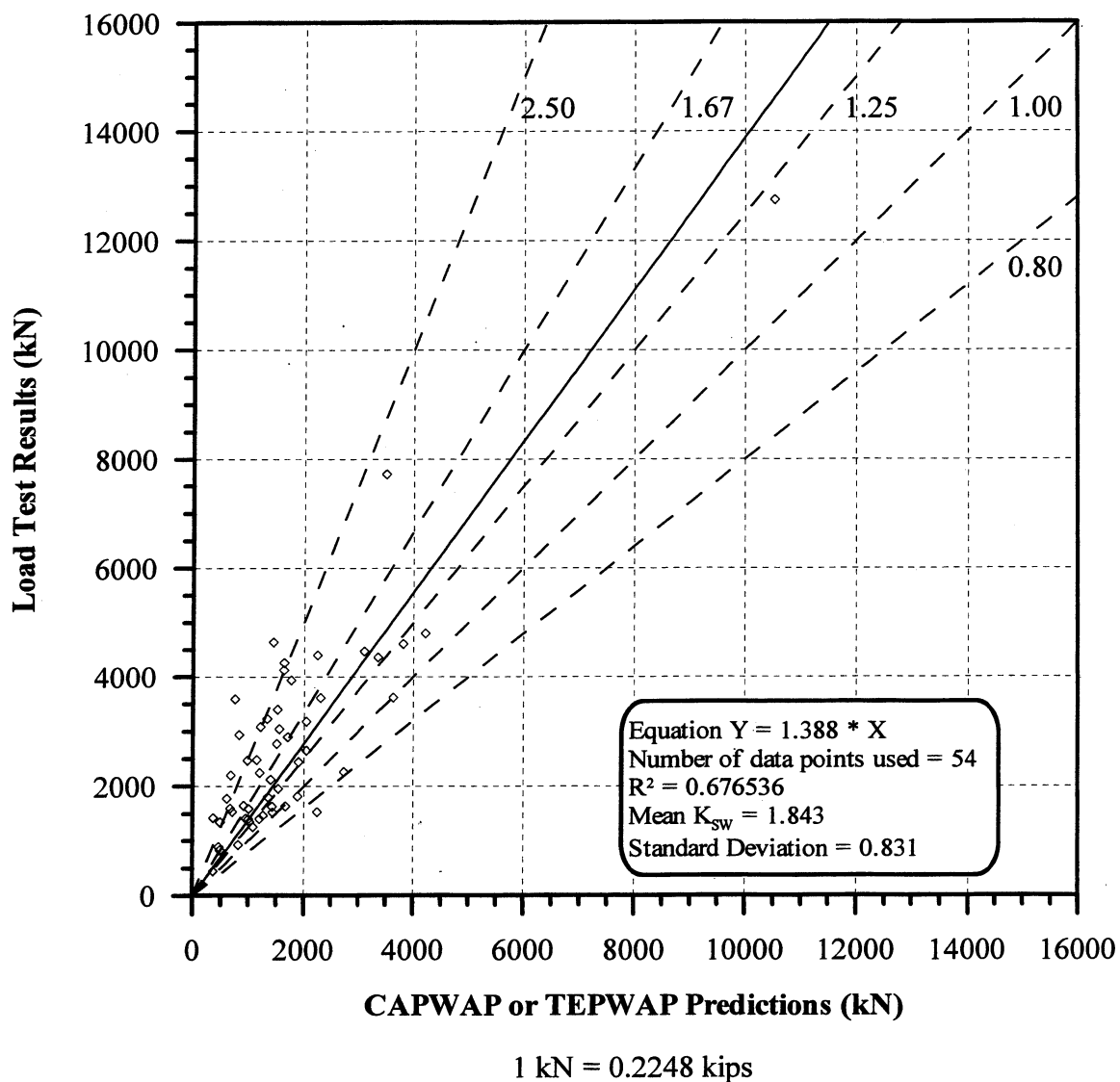
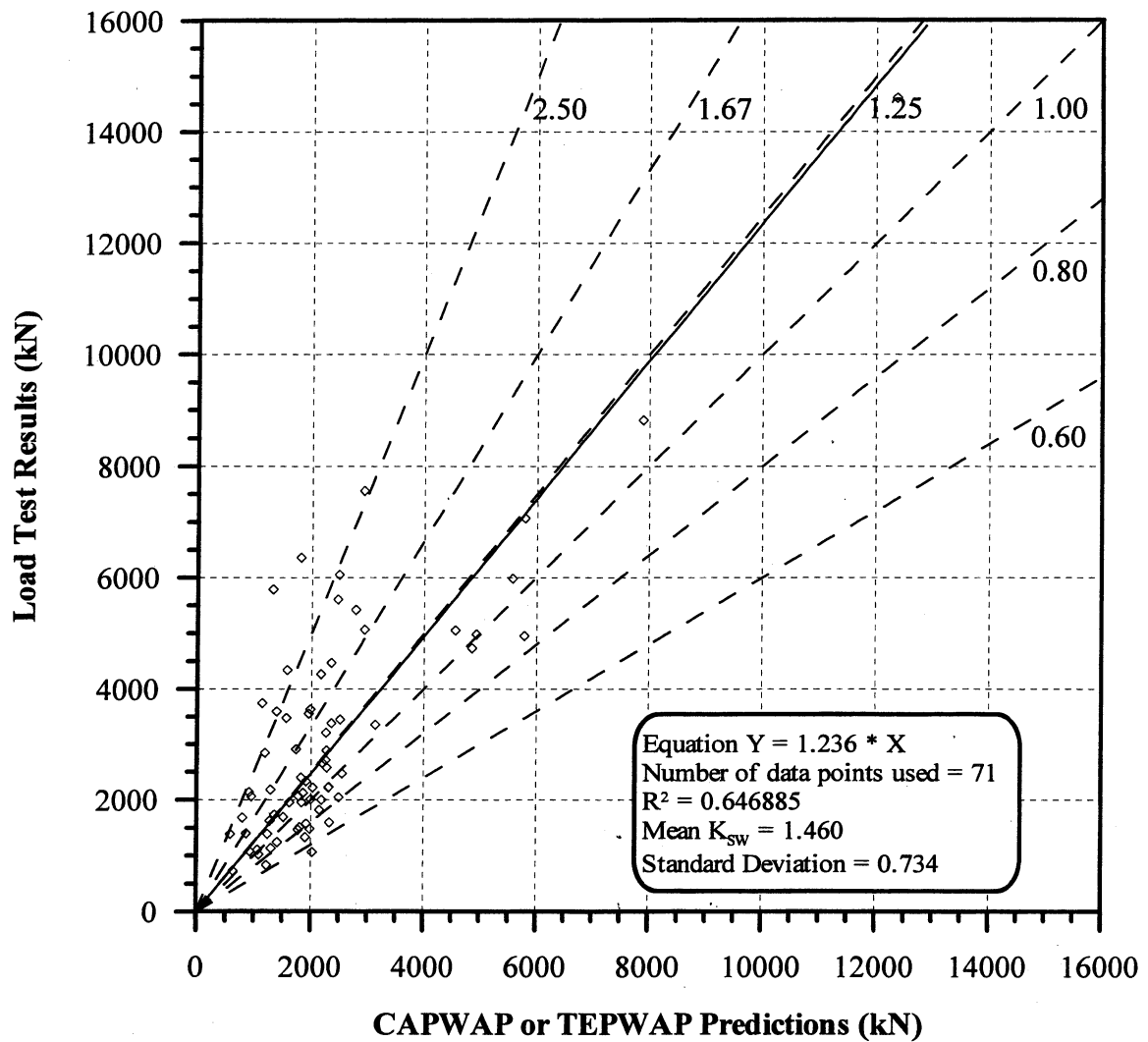


Figure 6.17. Static Load Test Results vs. CAPWAP or TEPWAP predictions for 54 PD/LT2000 pile-cases at the EOD with Blow Count < 16 BP10cm in all types of soils (AEA).



1 kN = 0.2248 kips

Figure 6.18. Static Load Test Results vs. CAPWAP or TEPWAP predictions for 71 PD/LT2000 pile-cases at the EOD with Blow Count ≥ 16 BP10cm in all types of soils (AEA).

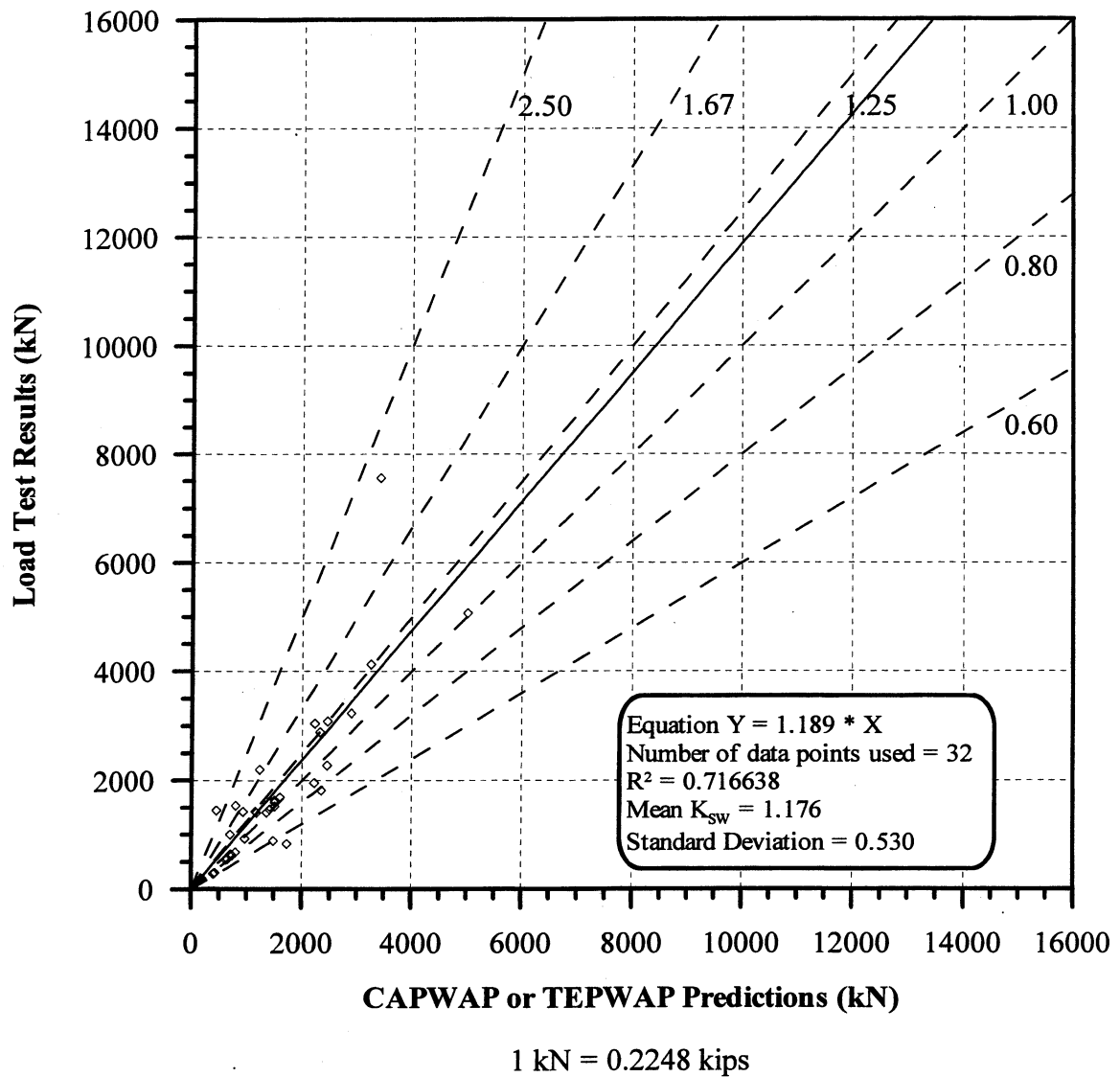


Figure 6.19. Static Load Test Results vs. CAPWAP or TEPWAP predictions for 32 PD/LT2000 pile-cases at the BOR(last) with Blow Count < 16 BP10cm in all types of soils (ABA).

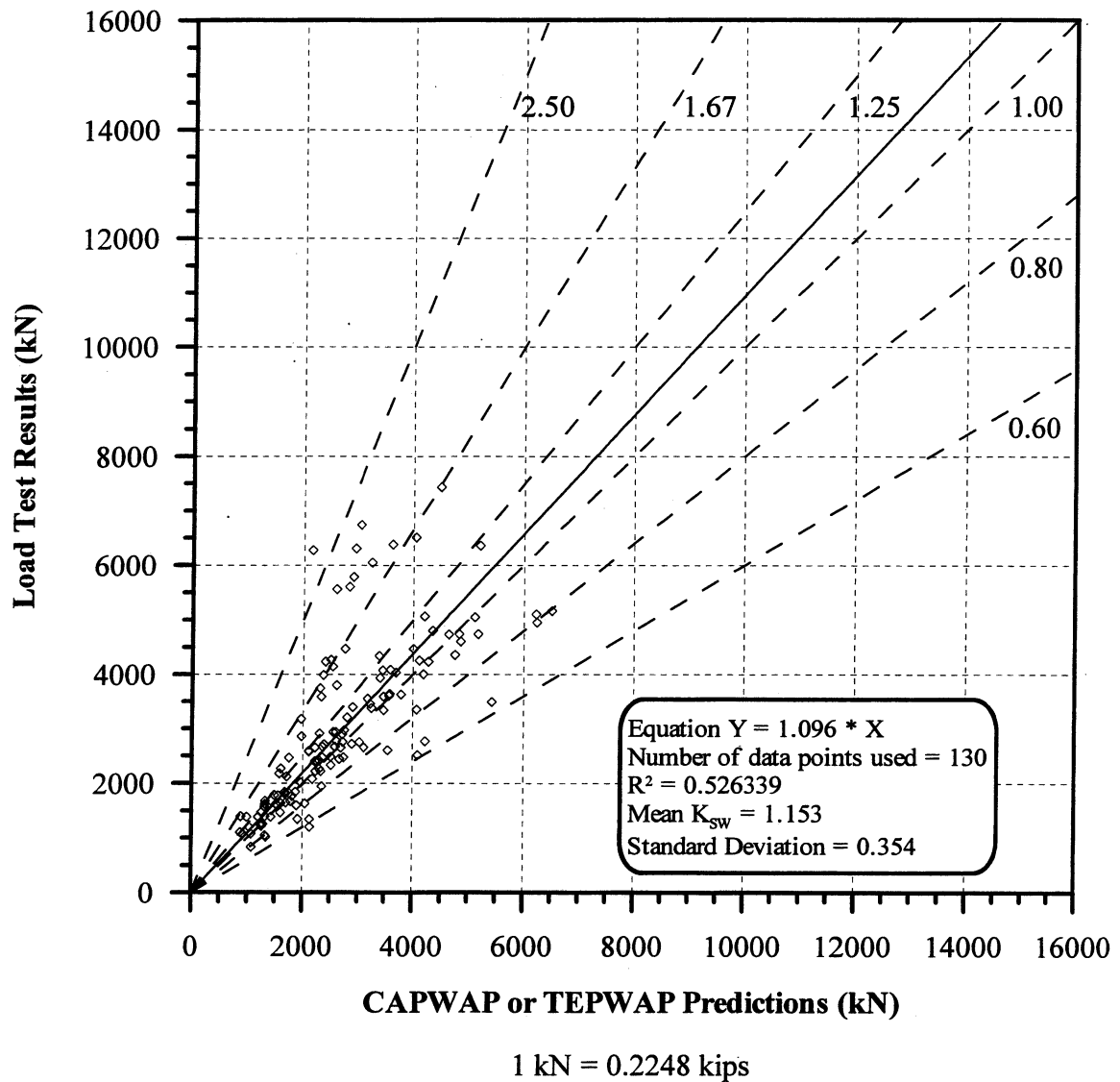


Figure 6.20. Static Load Test Results vs. CAPWAP or TEPWAP predictions for 130 PD/LT2000 pile-cases at the BOR(last) with Blow Count ≥ 16 BP10cm in all types of soils (ABA).

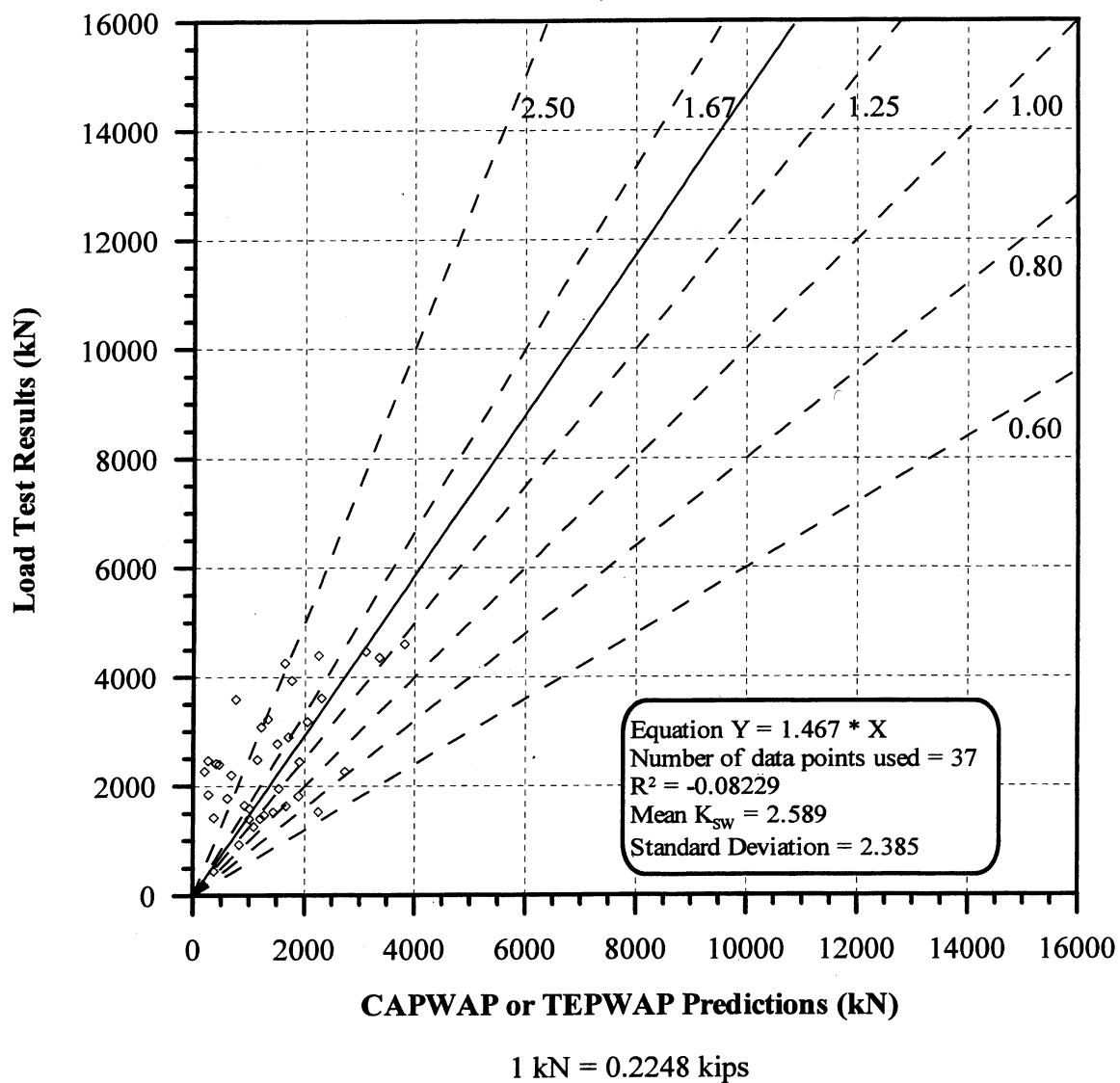


Figure 6.21. Static Load Test Results vs. CAPWAP or TEPWAP predictions for 37 PD/LT2000 pile-cases at the EOD with Blow Count < 16 BP10cm and Area Ratio < 350 in all types of soils (AEA).

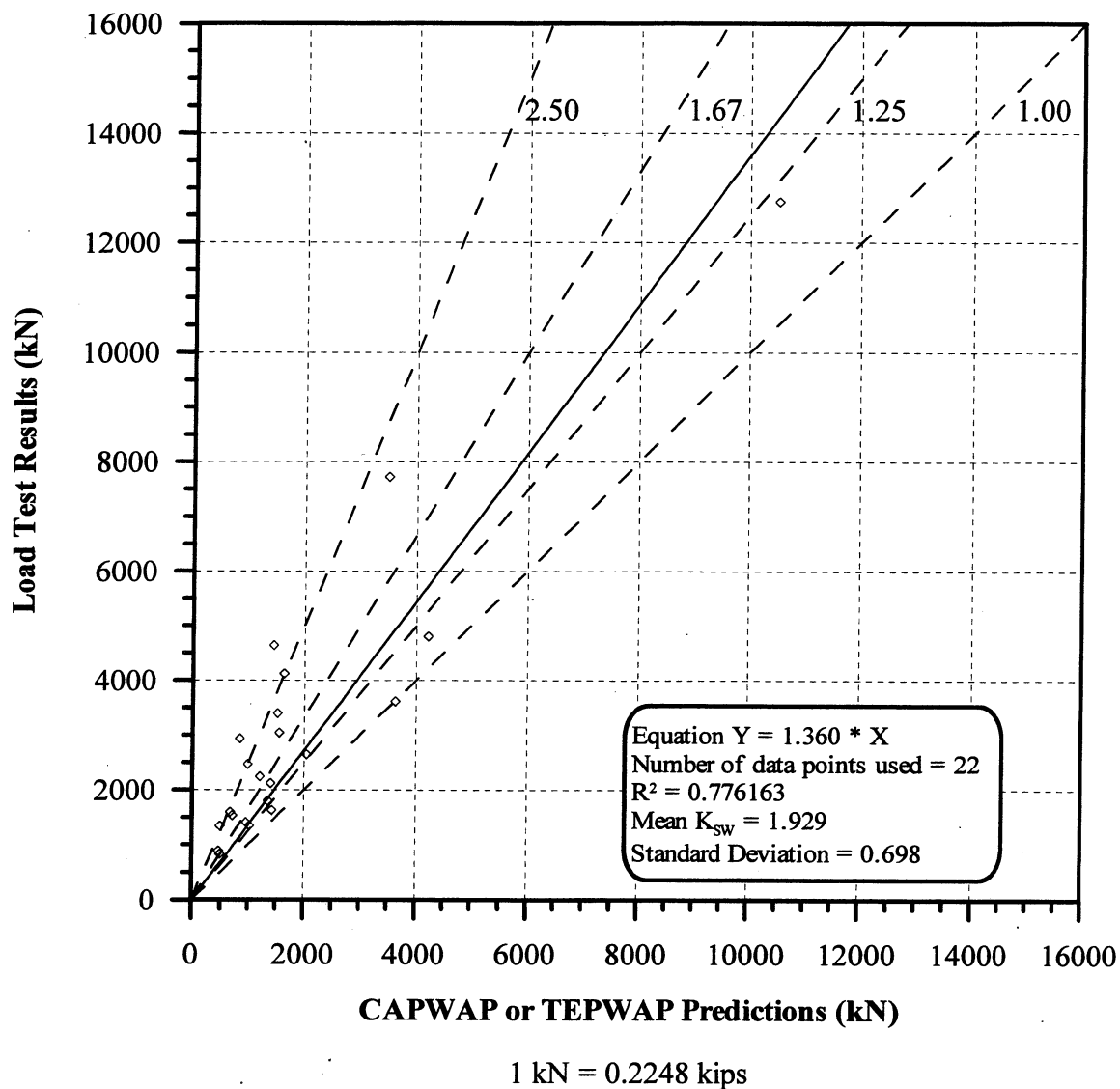


Figure 6.22. Static Load Test Results vs. CAPWAP or TEPWAP predictions for 22 PD/LT2000 pile-cases at the EOD with Blow Count < 16 BP10cm and Area Ratio ≥ 350 in all types of soils (AEA).

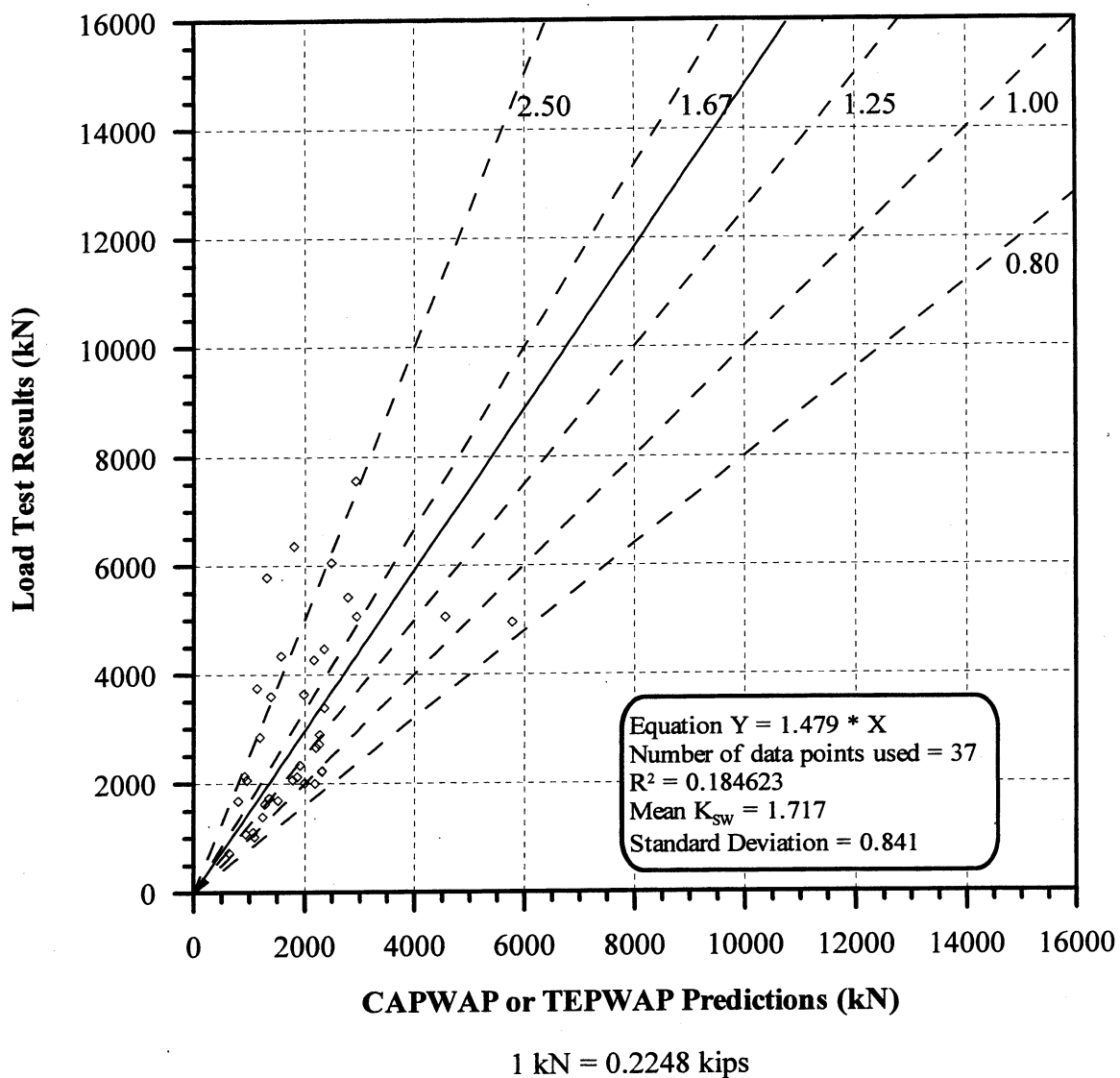


Figure 6.23. Static Load Test Results vs. CAPWAP or TEPWAP predictions for 37 PD/LT2000 pile-cases at the EOD with Blow Count ≥ 16 BP10cm and Area Ratio < 350 in all types of soils (AEA).

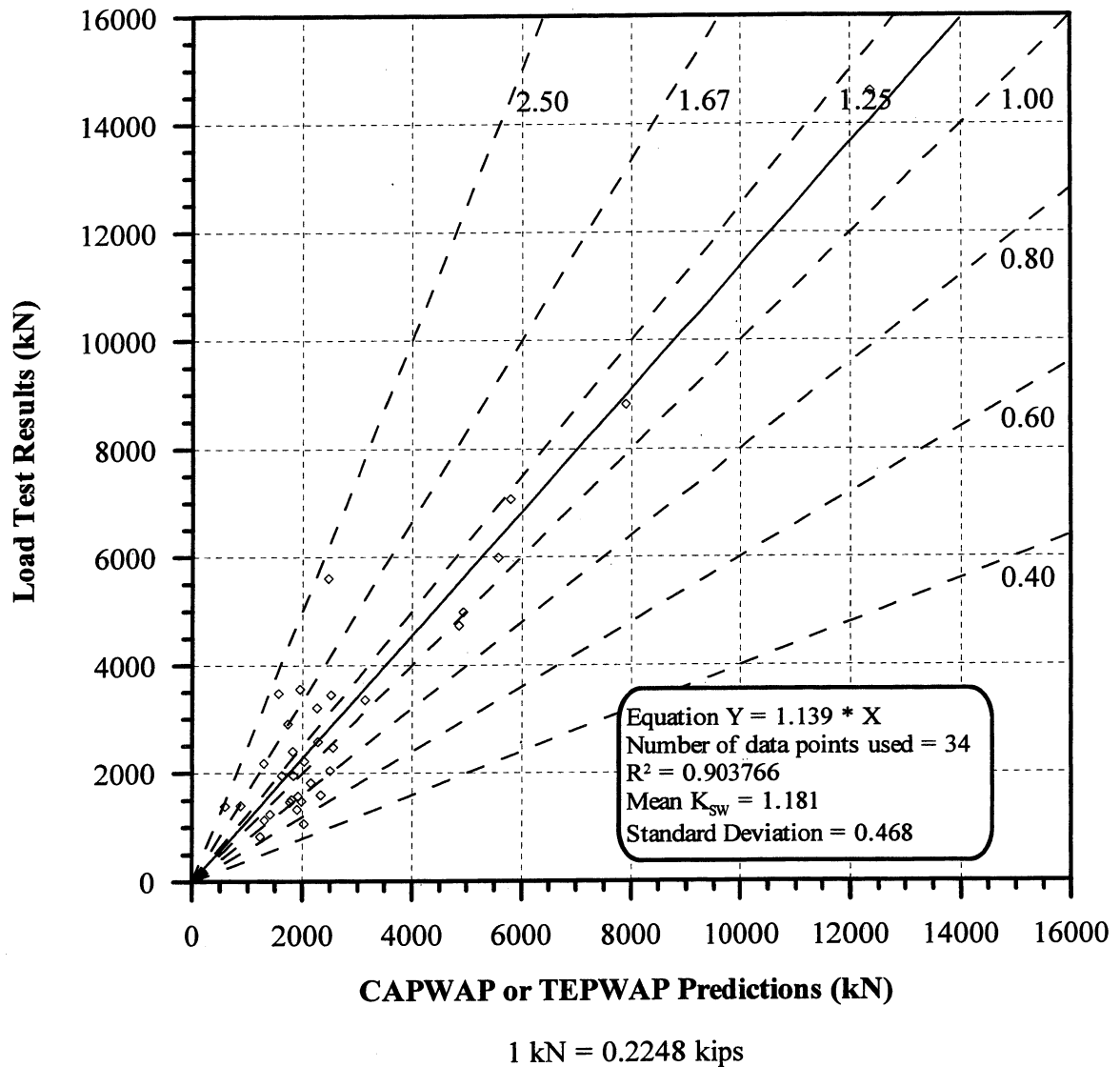


Figure 6.24. Static Load Test Results vs. CAPWAP or TEPWAP predictions for 34 PD/LT2000 pile-cases at the EOD with Blow Count ≥ 16 BP10cm and Area Ratio ≥ 350 in all types of soils (AEA).

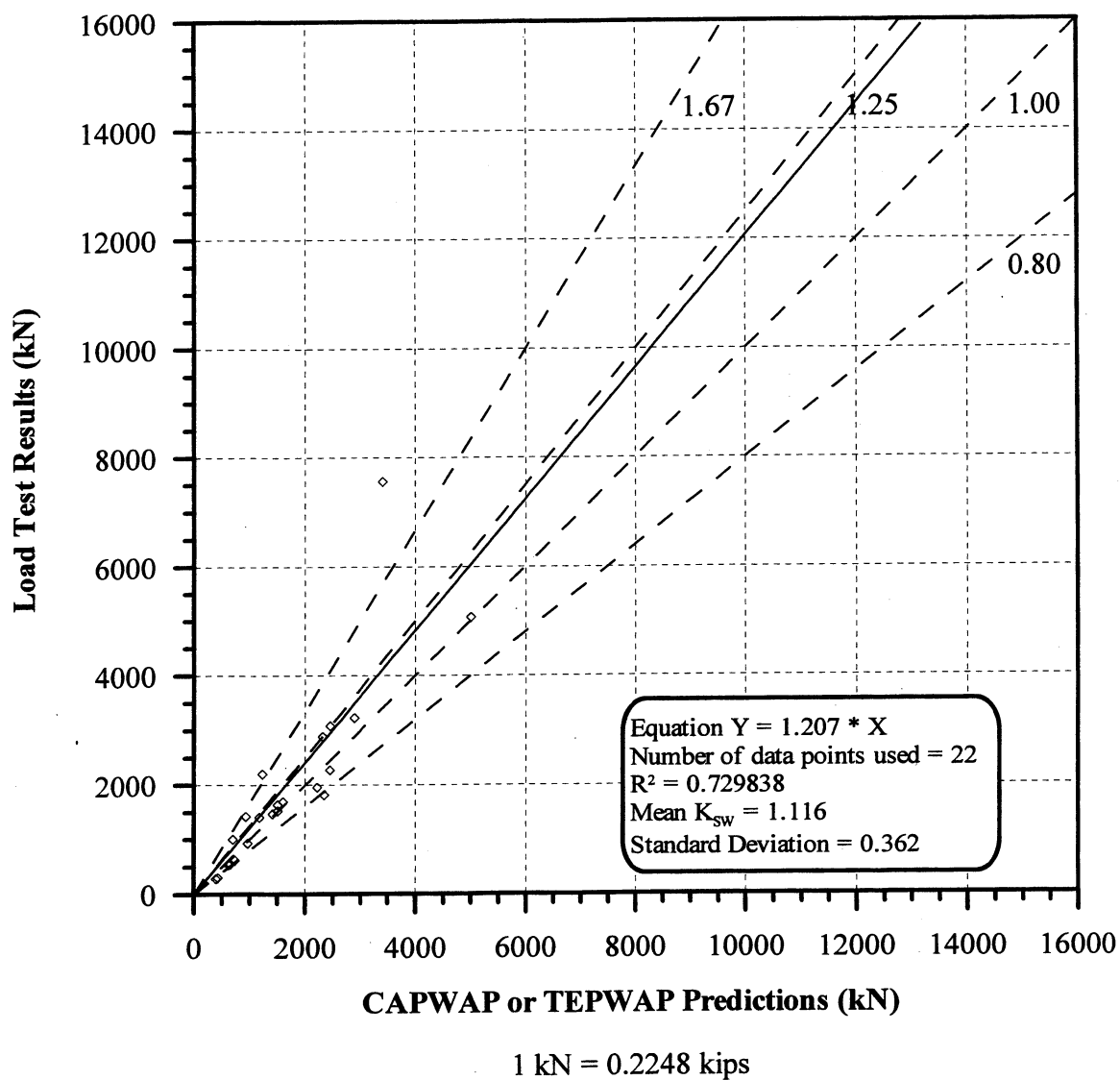


Figure 6.25. Static Load Test Results vs. CAPWAP or TEPWAP predictions for 22 PD/LT2000 pile-cases at the BOR (last) with Blow Count < 16 BP10cm and Area Ratio < 350 in all types of soils (ABA).

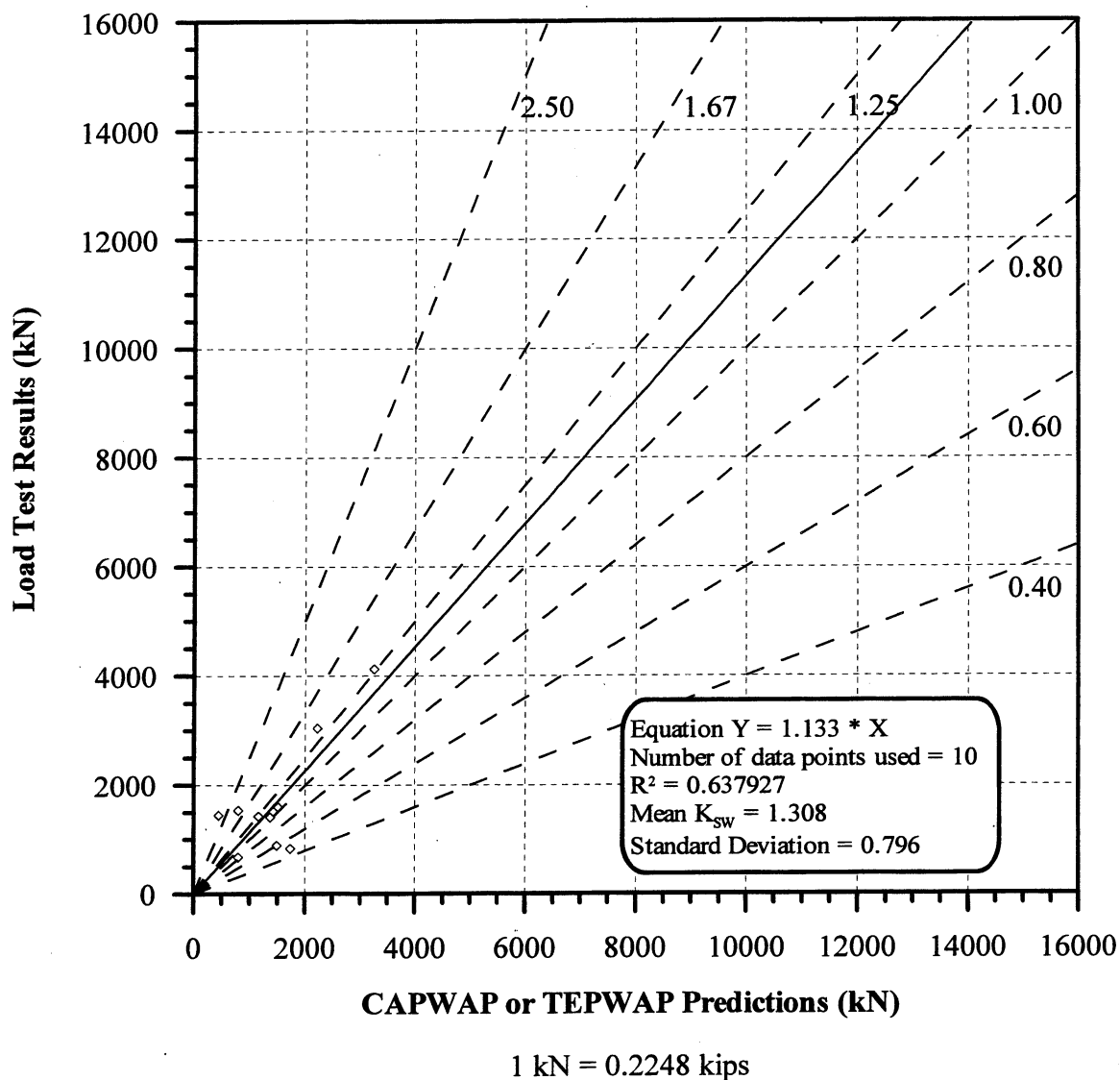


Figure 6.26. Static Load Test Results vs. CAPWAP or TEPWAP predictions for 10 PD/LT2000 pile-cases at the BOR (last) with Blow Count < 16 BP10cm and Area Ratio ≥ 350 in all types of soils (ABA).

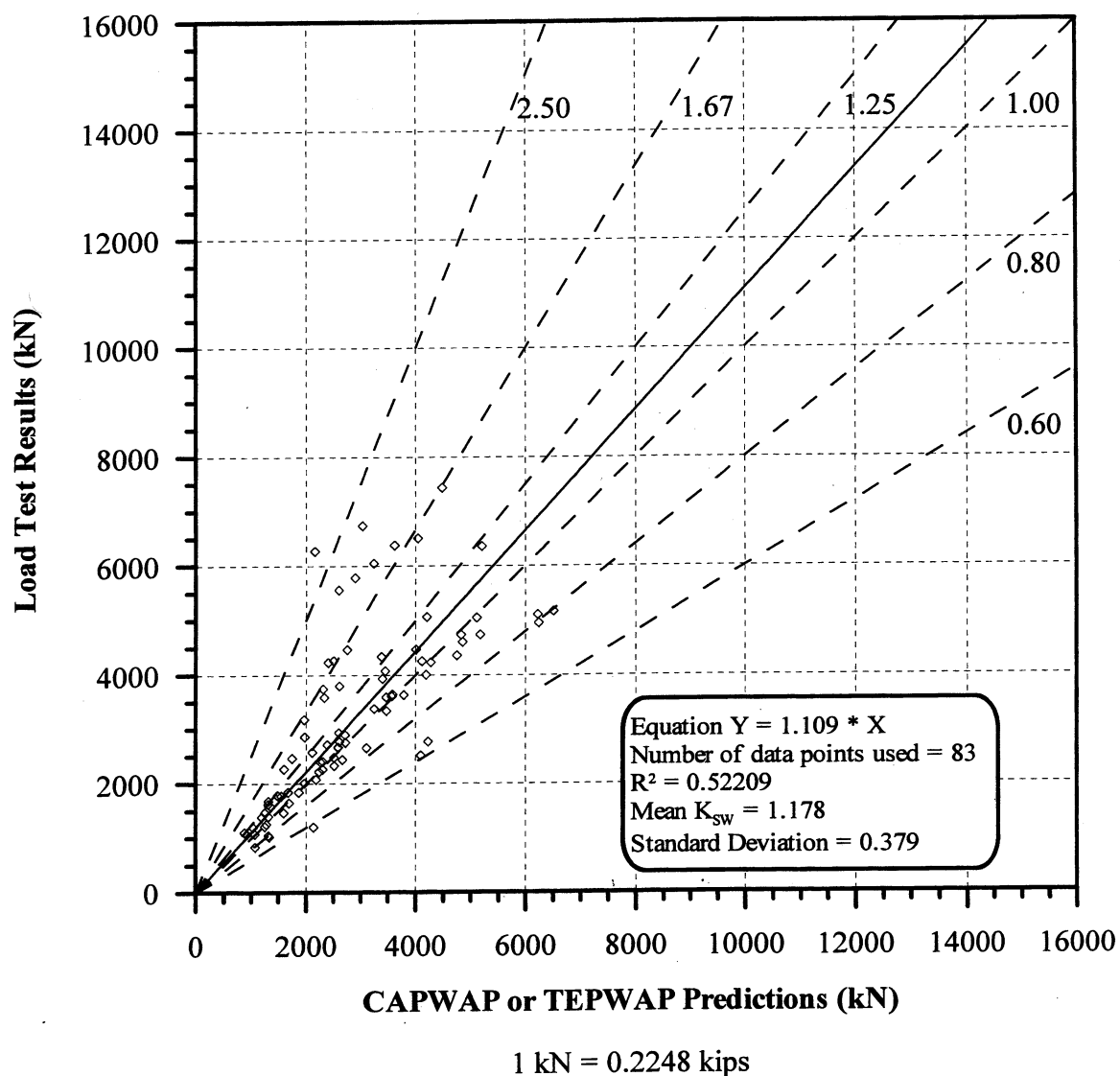


Figure 6.27. Static Load Test Results vs. CAPWAP or TEPWAP predictions for 83 PD/LT2000 pile-cases at the BOR (last) with Blow Count ≥ 16 BP10cm and Area Ratio < 350 in all types of soils (ABA).

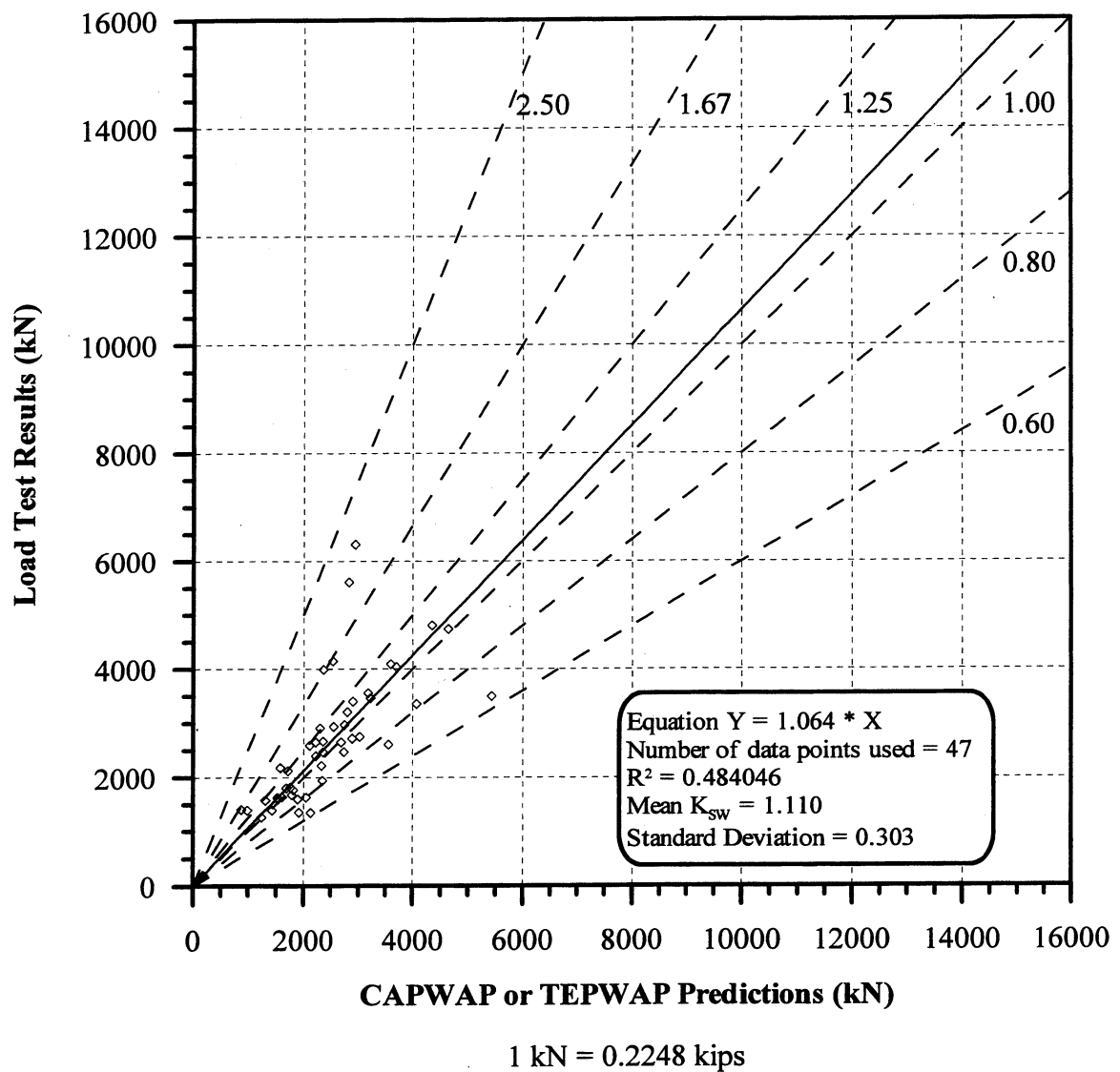


Figure 6.28. Static Load Test Results vs. CAPWAP or TEPWAP predictions for 47 PD/LT2000 pile-cases at the BOR (last) with Blow Count ≥ 16 BP10cm and Area Ratio ≥ 350 in all types of soils (ABA).

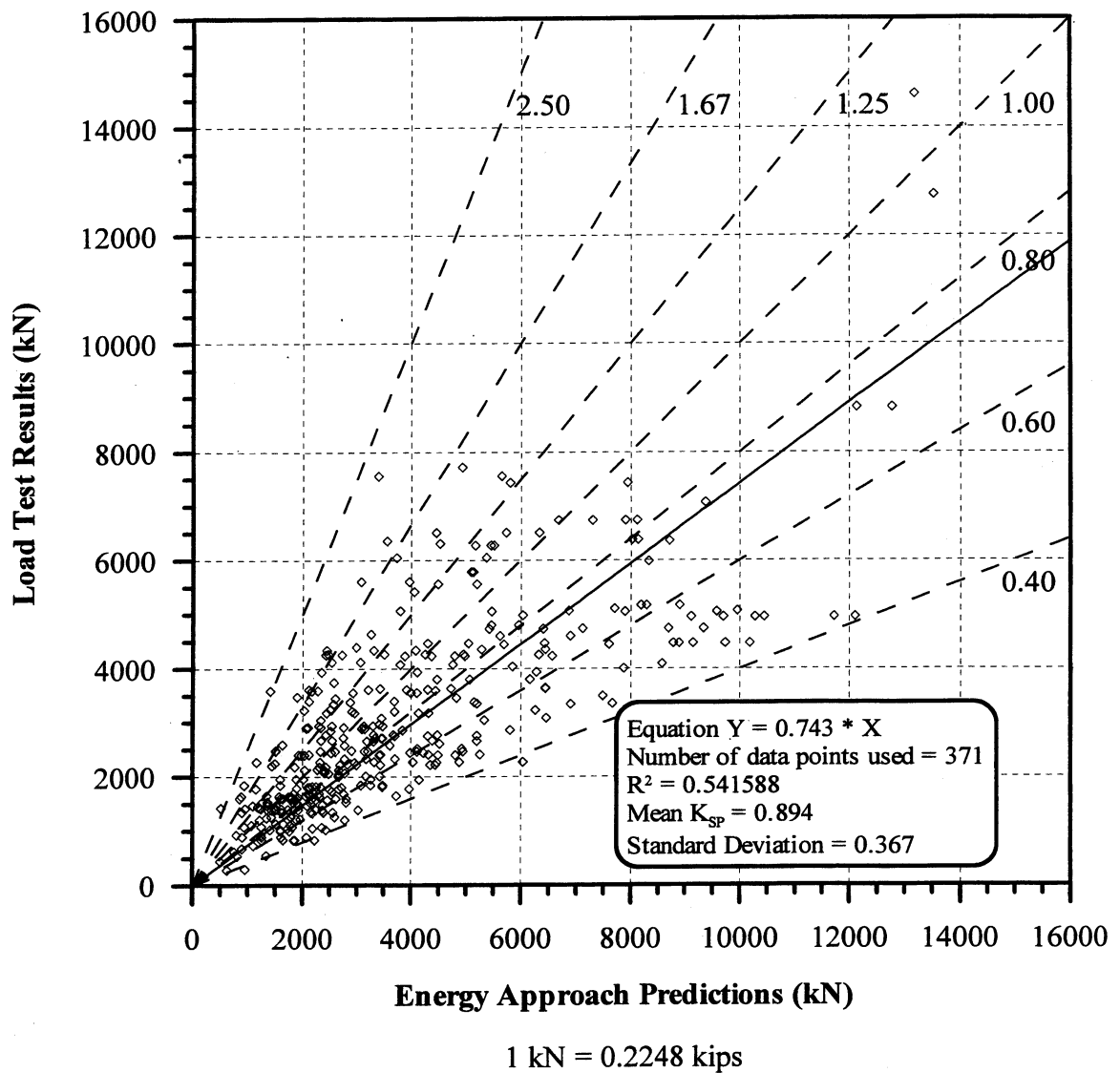


Figure 6.29. Static Load Test Results vs. Energy Approach predictions for 371 PD/LT2000 pile-cases at all times and in all types of soils (AAA).

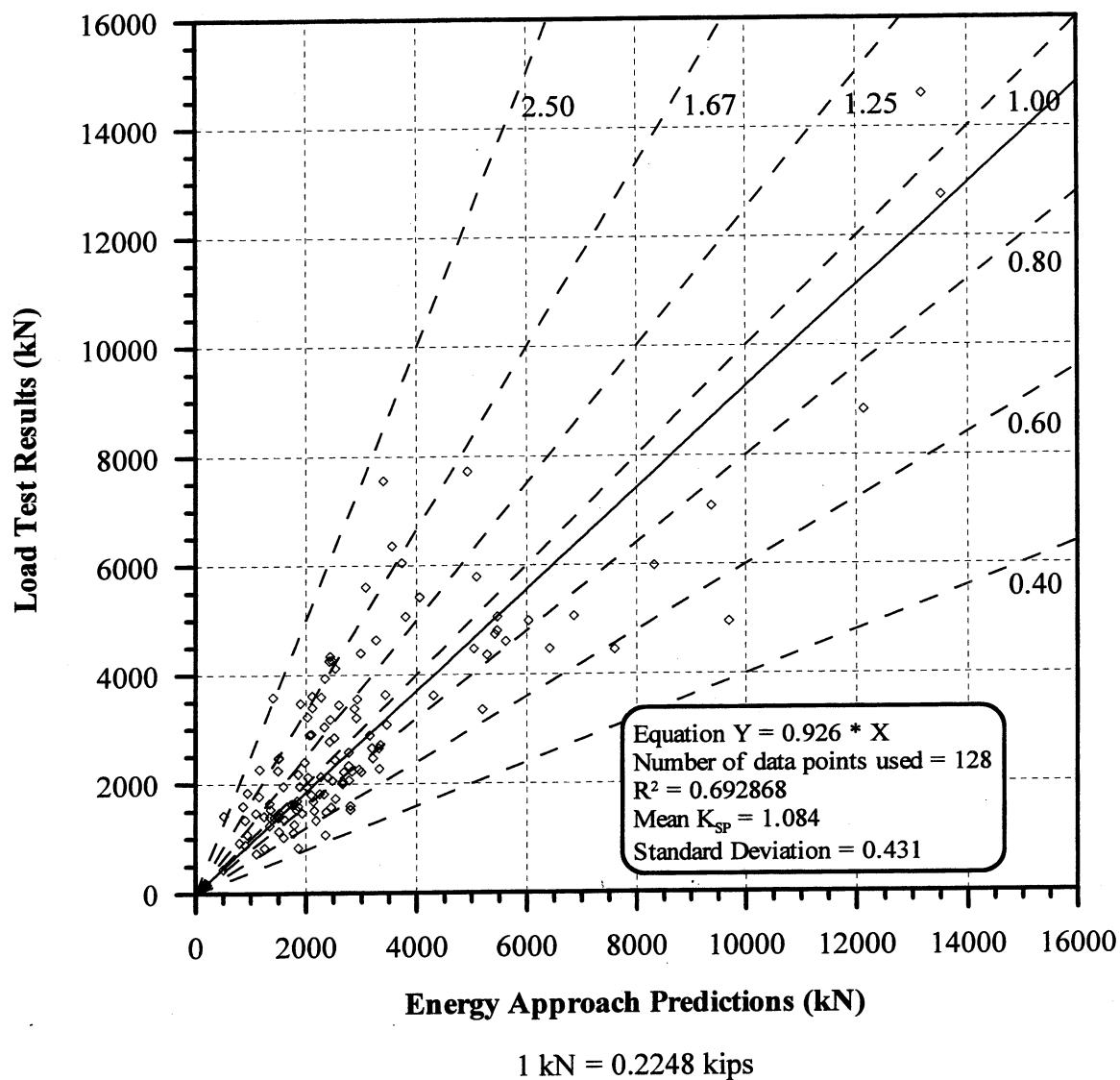


Figure 6.30. Static Load Test Results vs. Energy Approach predictions for 128 PD/LT2000 pile-cases at EOD in all types of soils (AEA).

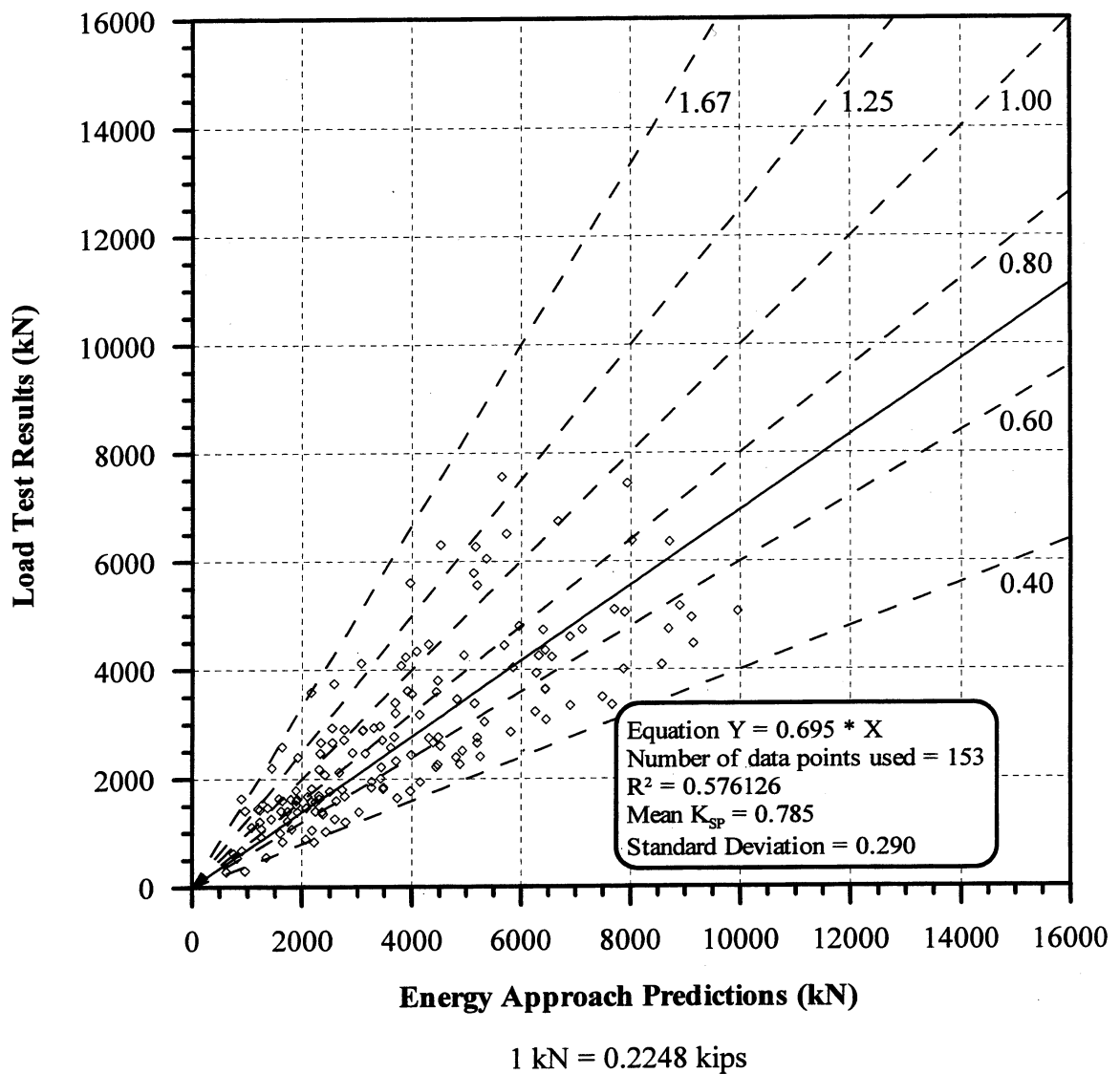


Figure 6.31. Static Load Test Results vs. Energy Approach predictions for 153 PD/LT2000 pile-cases at BOR (last) in all types of soils (ABA).

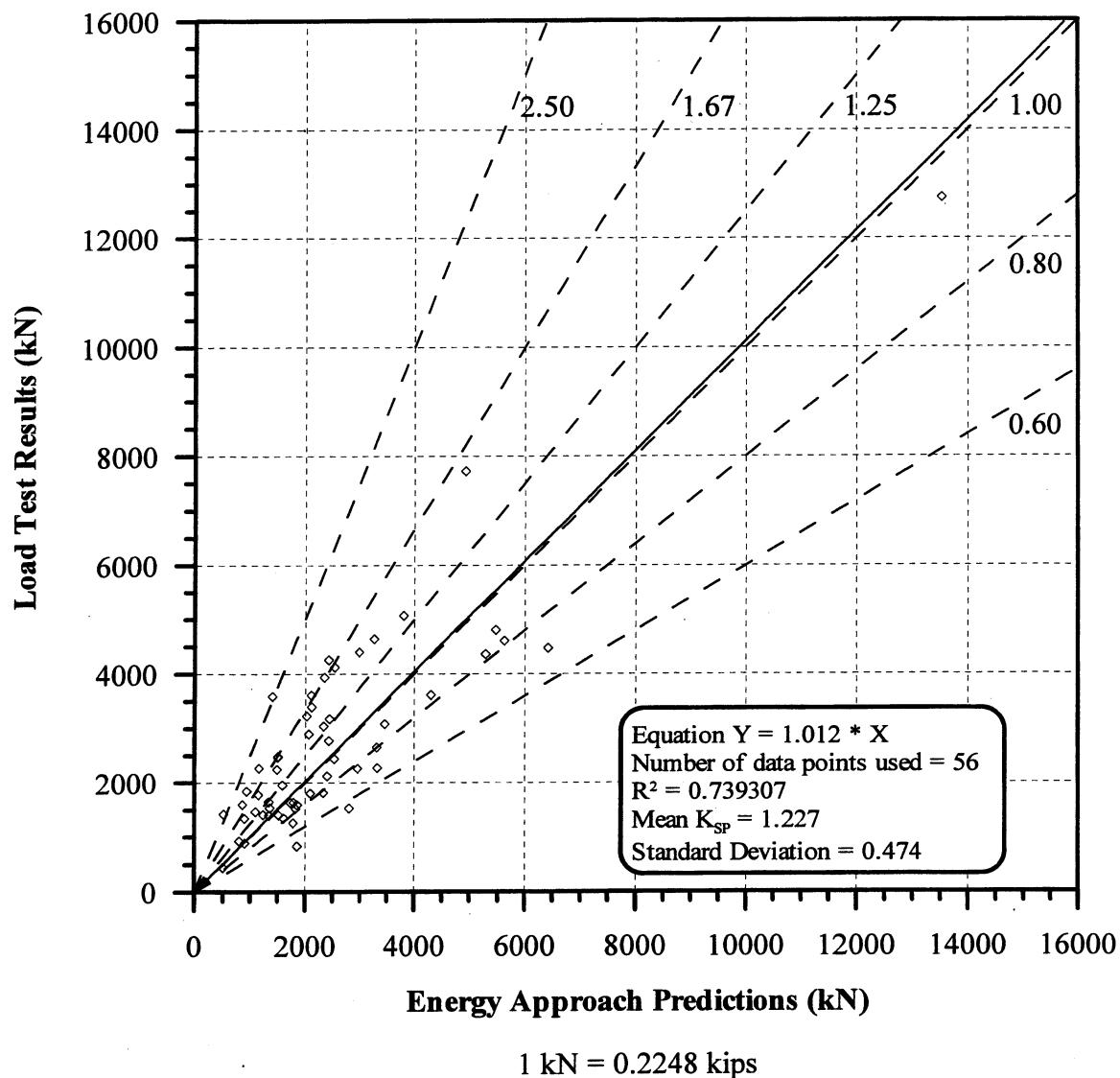


Figure 6.32. Static Load Test Results vs. Energy Approach predictions for 56 PD/LT2000 pile-cases at the EOD with Blow Count < 16 BP10cm in all types of soils (AEA).

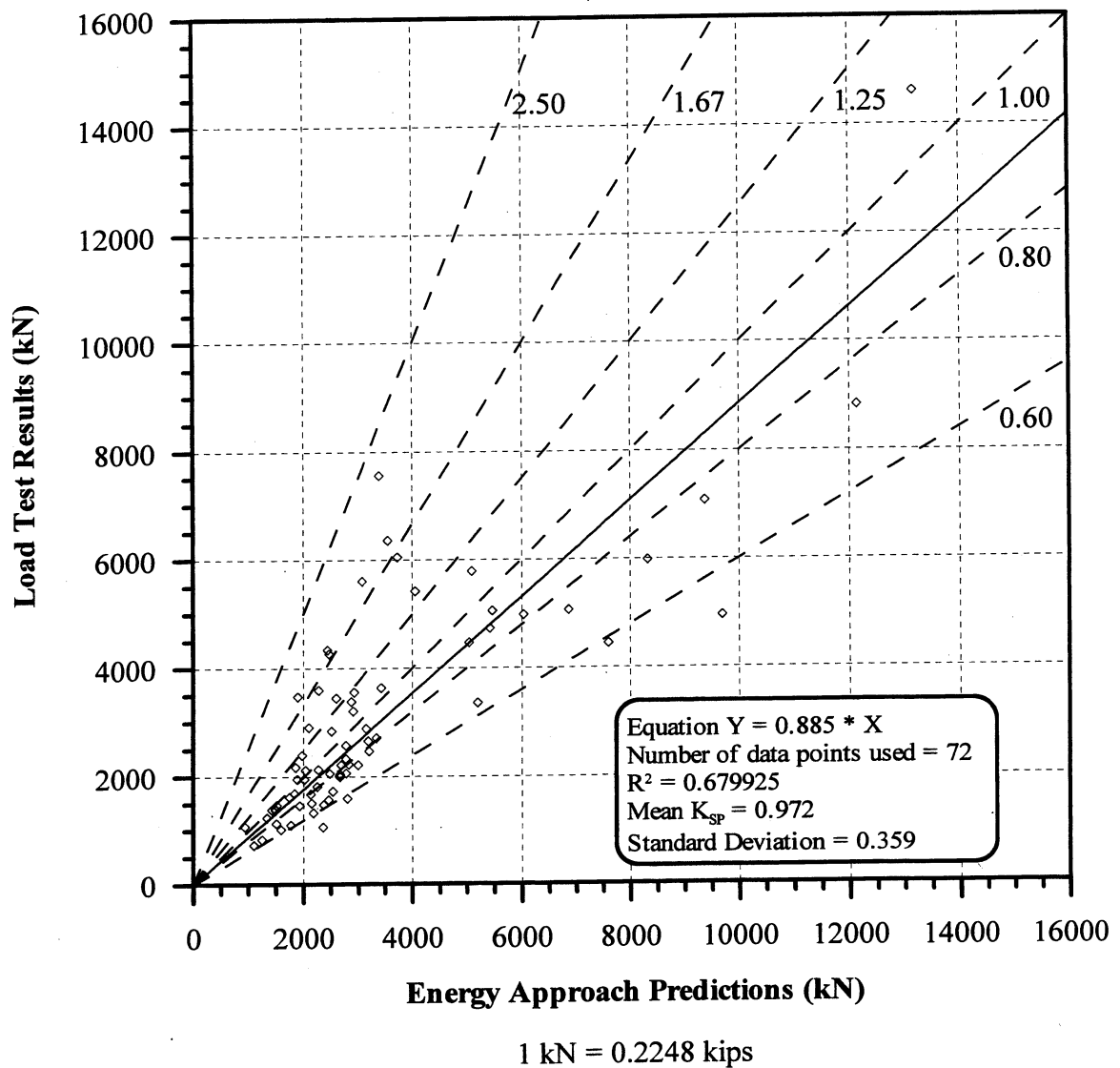


Figure 6.33. Static Load Test Results vs. Energy Approach predictions for 72 PD/LT2000 pile-cases at the EOD with Blow Count ≥ 16 BP10cm in all types of soils (AEA).

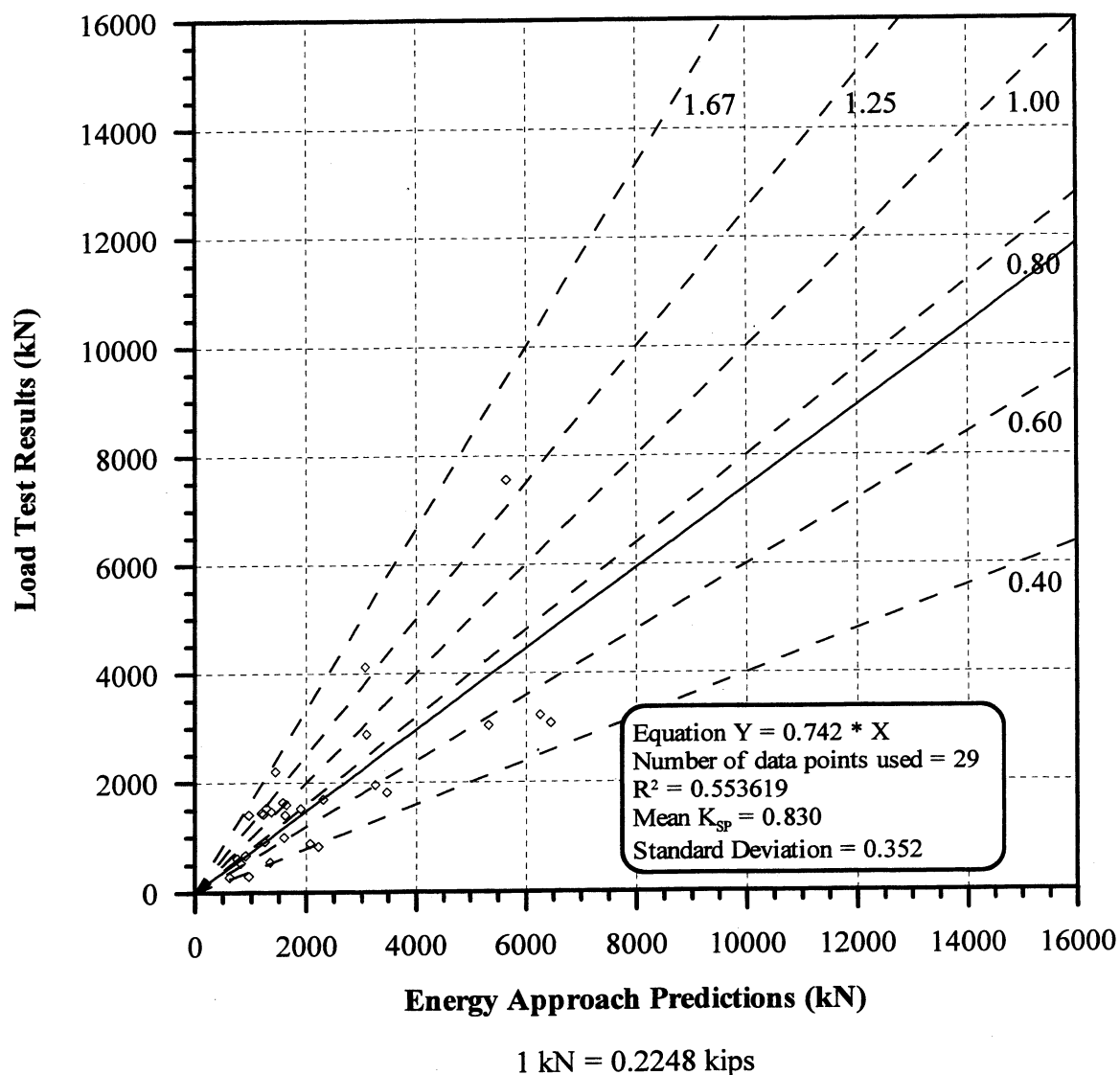


Figure 6.34. Static Load Test Results vs. Energy Approach predictions for 29 PD/LT2000 pile-cases at the BOR (last) with Blow Count < 16 BP10cm in all types of soils (ABA).

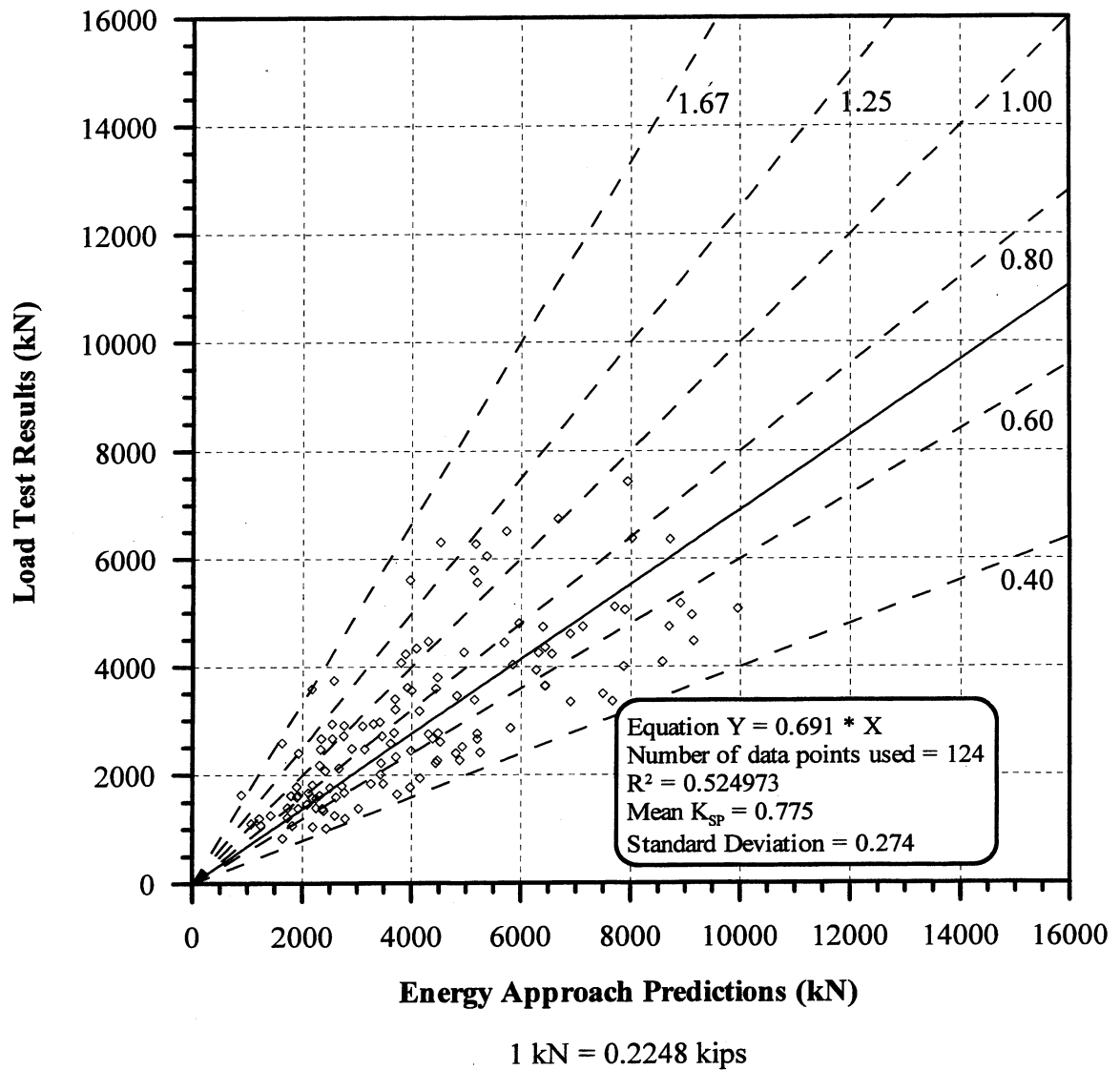


Figure 6.35. Static Load Test Results vs. Energy Approach predictions for 124 PD/LT2000 pile-cases at the BOR (last) with Blow Count ≥ 16 BP10cm in all types of soils (ABA).

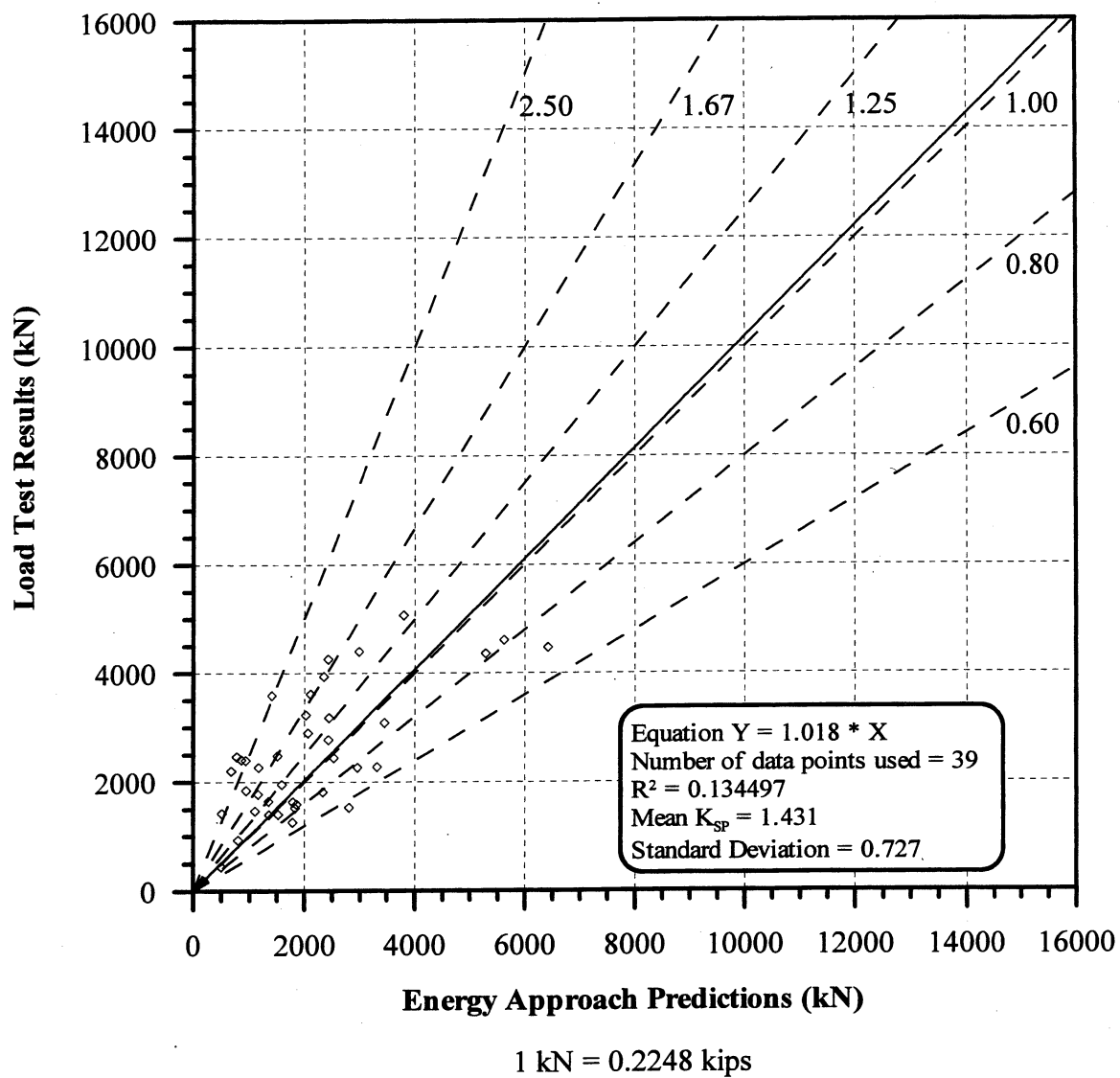


Figure 6.36. Static Load Test Results vs. Energy Approach predictions for 39 PD/LT2000 pile-cases at the EOD with Blow Count < 16 BP10cm and Area Ratio < 350 in all types of soils (AEA).

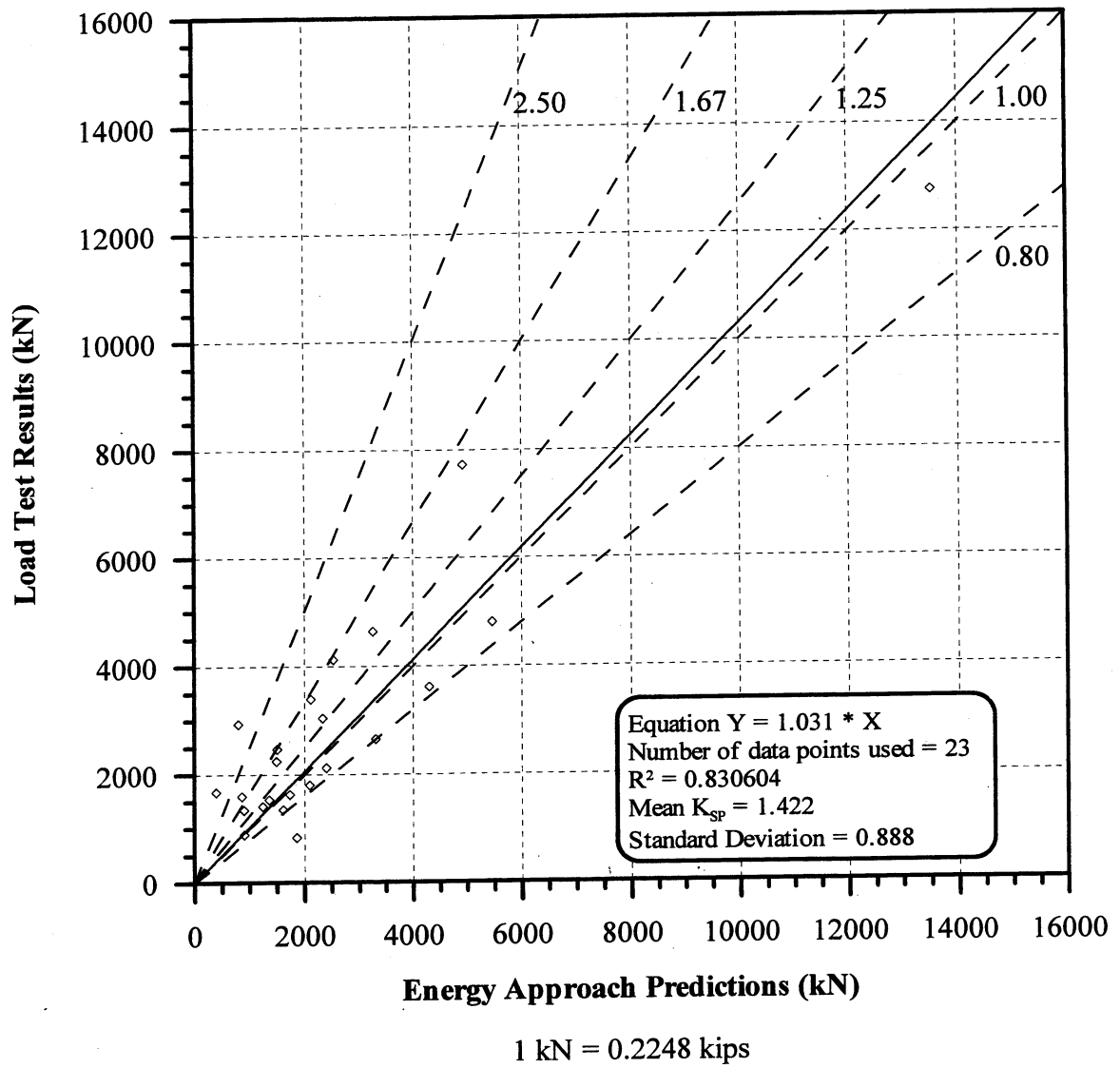


Figure 6.37. Static Load Test Results vs. Energy Approach predictions for 23 PD/LT2000 pile-cases at the EOD with Blow Count < 16 BP10cm and Area Ratio ≥ 350 in all types of soils (AEA).

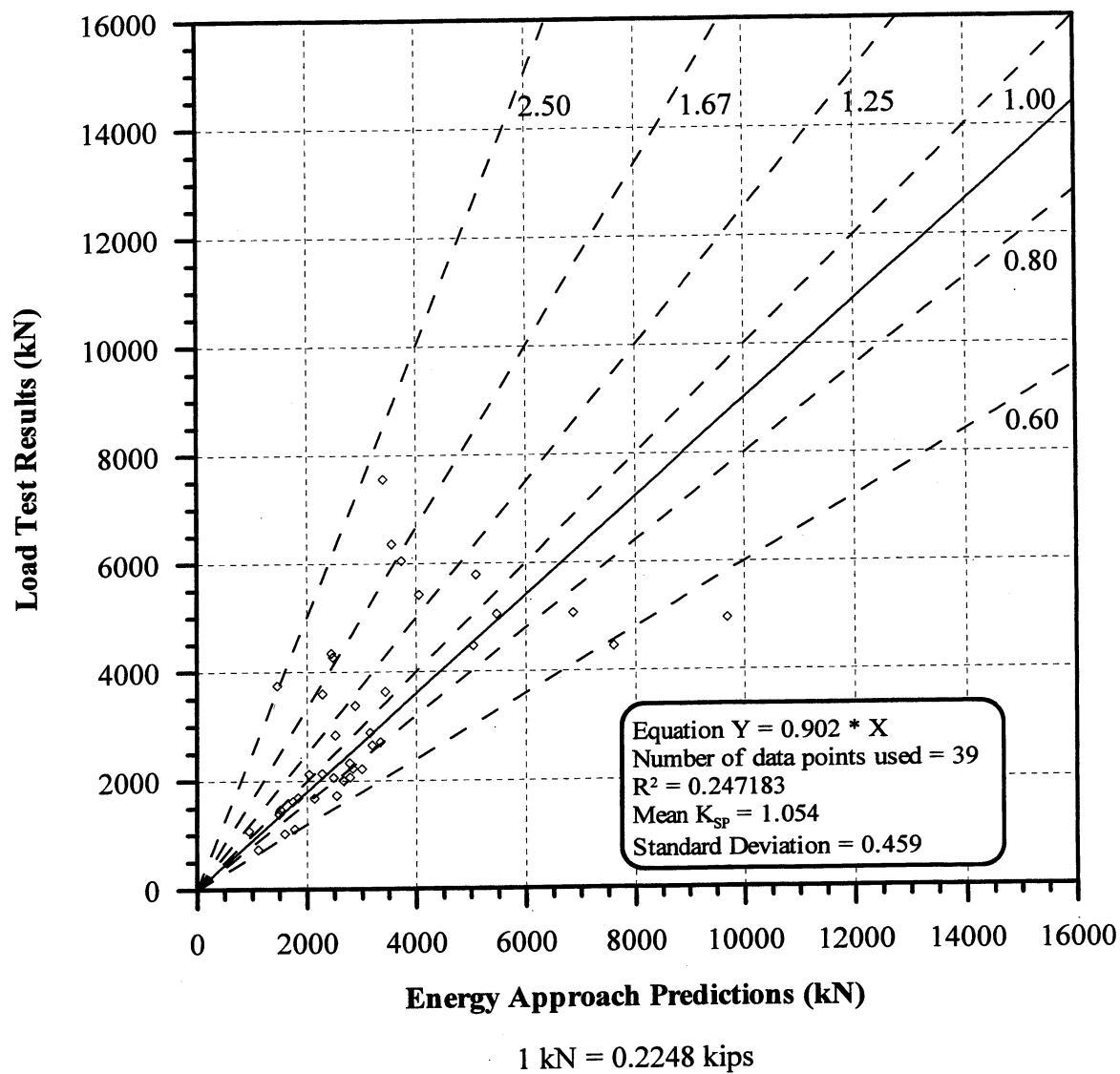


Figure 6.38. Static Load Test Results vs. Energy Approach predictions for 39 PD/LT2000 pile-cases at the EOD with Blow Count ≥ 16 BP10cm and Area Ratio < 350 in all types of soils (AEA).

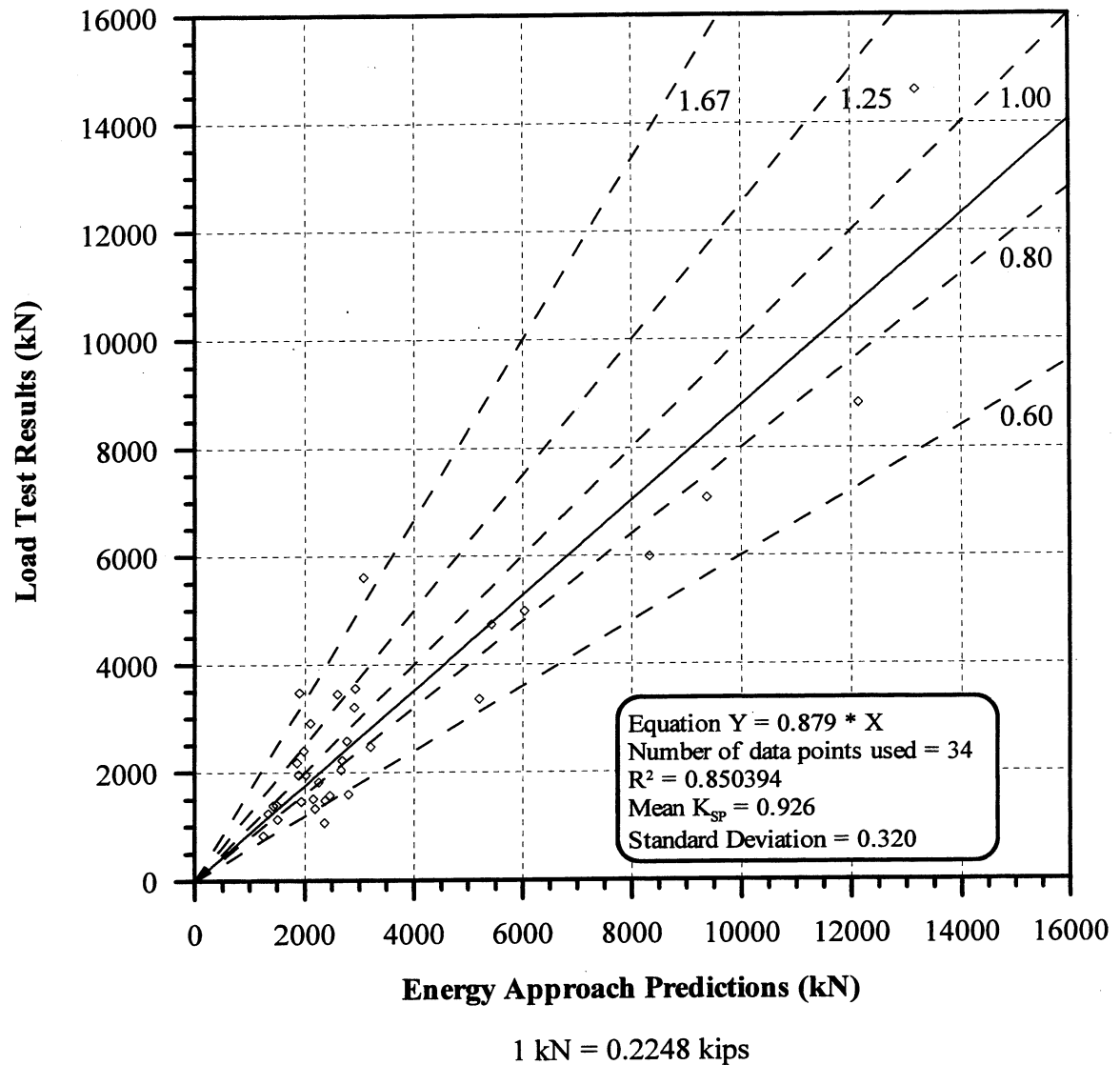


Figure 6.39. Static Load Test Results vs. Energy Approach predictions for 34 PD/LT2000 pile-cases at the EOD with Blow Count ≥ 16 BP10cm and Area Ratio ≥ 350 in all types of soils (AEA).

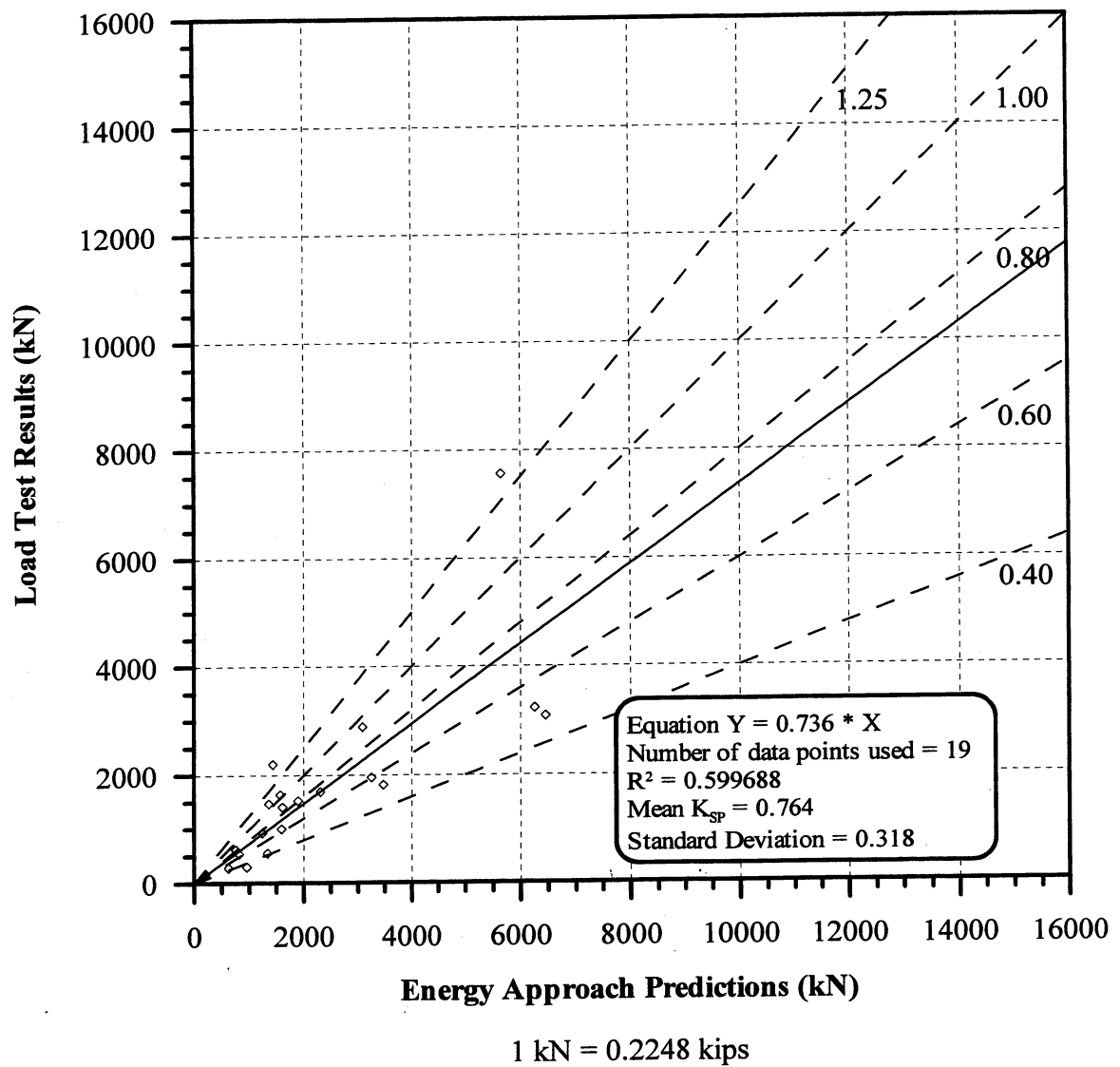


Figure 6.40. Static Load Test Results vs. Energy Approach predictions for 19 PD/LT2000 pile-cases at the BOR (last) with Blow Count < 16 BP10cm and Area Ratio < 350 in all types of soils (ABA).

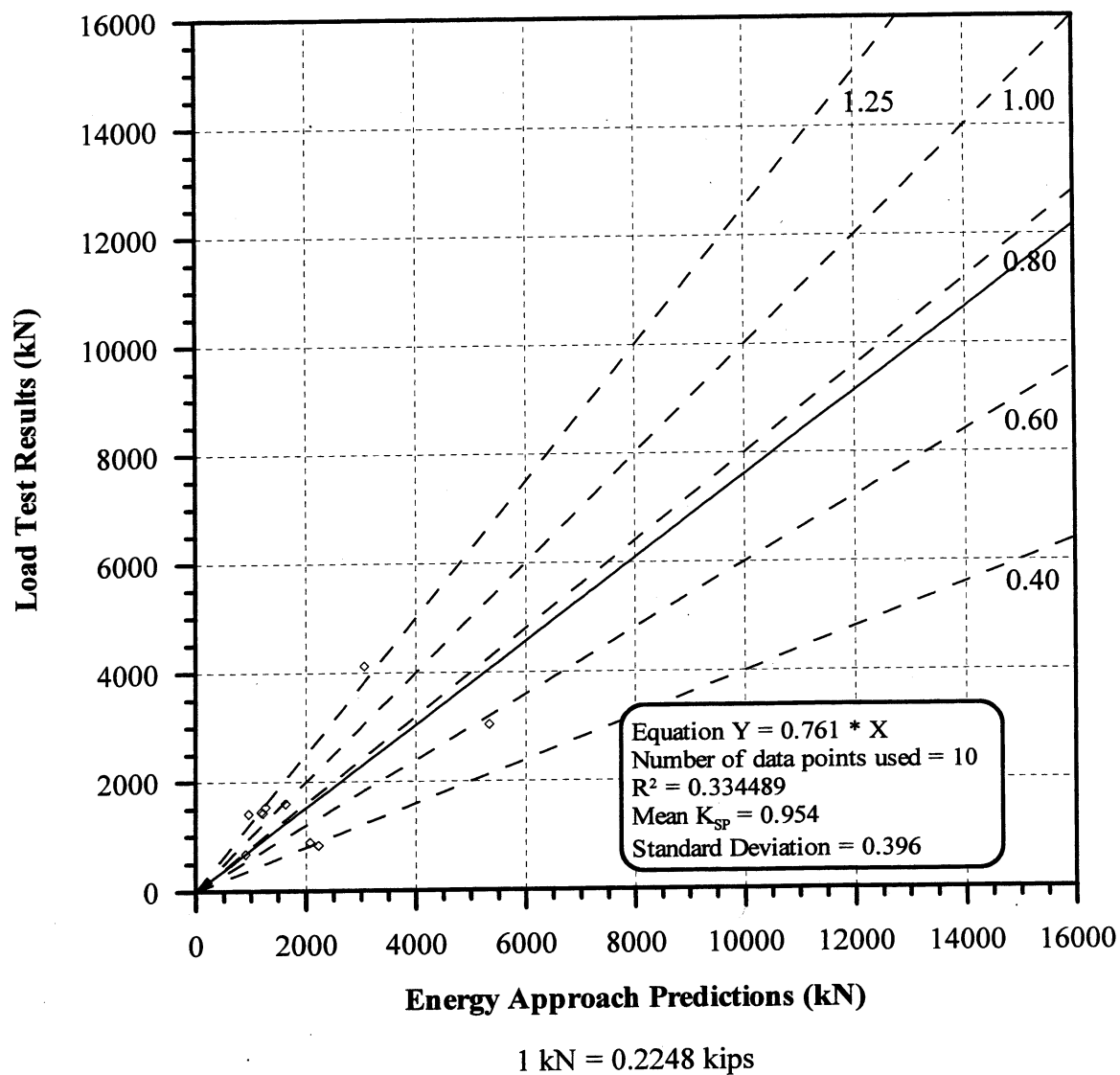


Figure 6.41. Static Load Test Results vs. Energy Approach predictions for 10 PD/LT2000 pile-cases at the BOR (last) with Blow Count < 16 BP10cm and Area Ratio ≥ 350 in all types of soils (ABA).

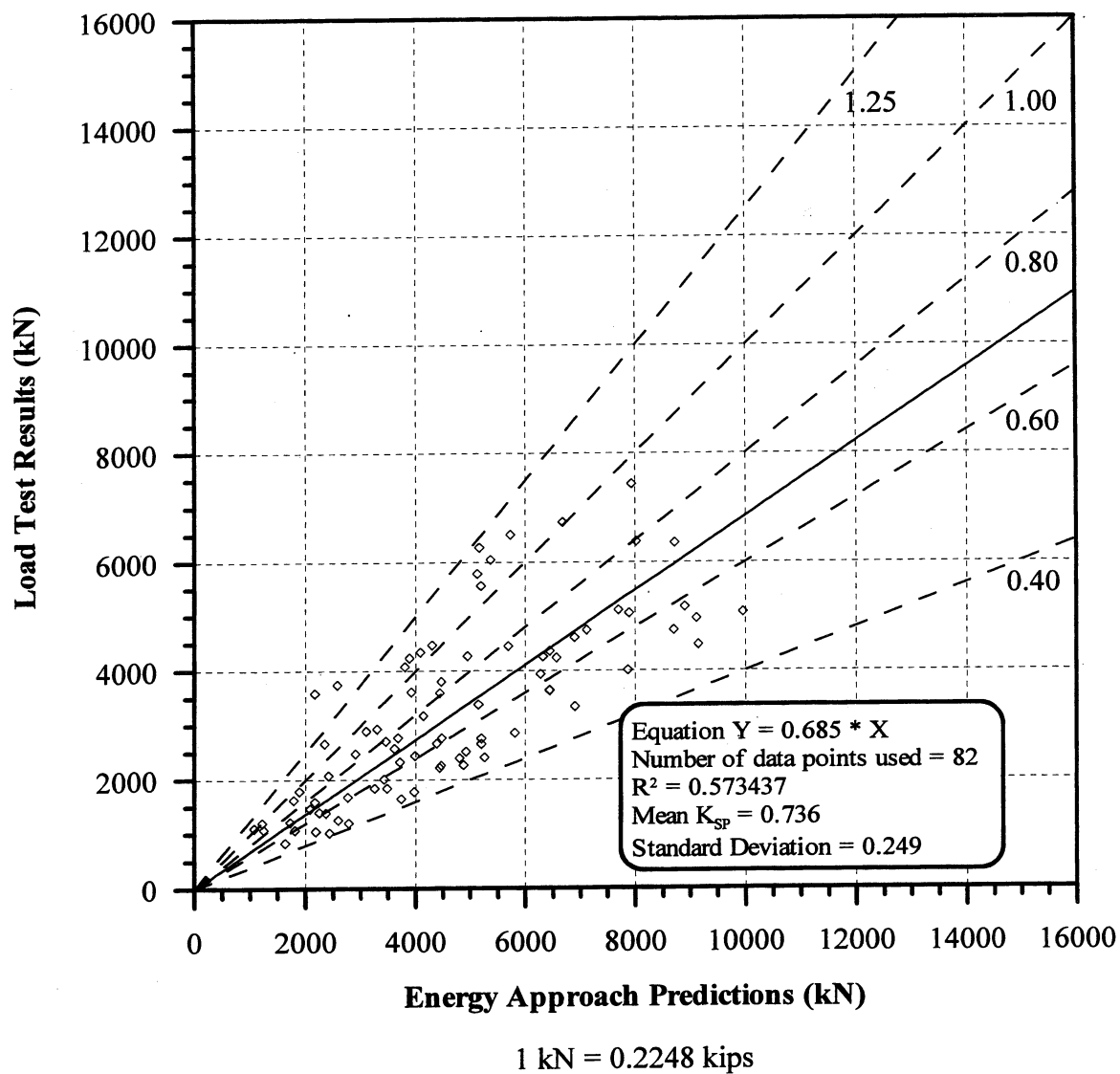


Figure 6.42. Static Load Test Results vs. Energy Approach predictions for 82 PD/LT2000 pile-cases at the BOR (last) with Blow Count ≥ 16 BP10cm and Area Ratio < 350 in all types of soils (ABA).

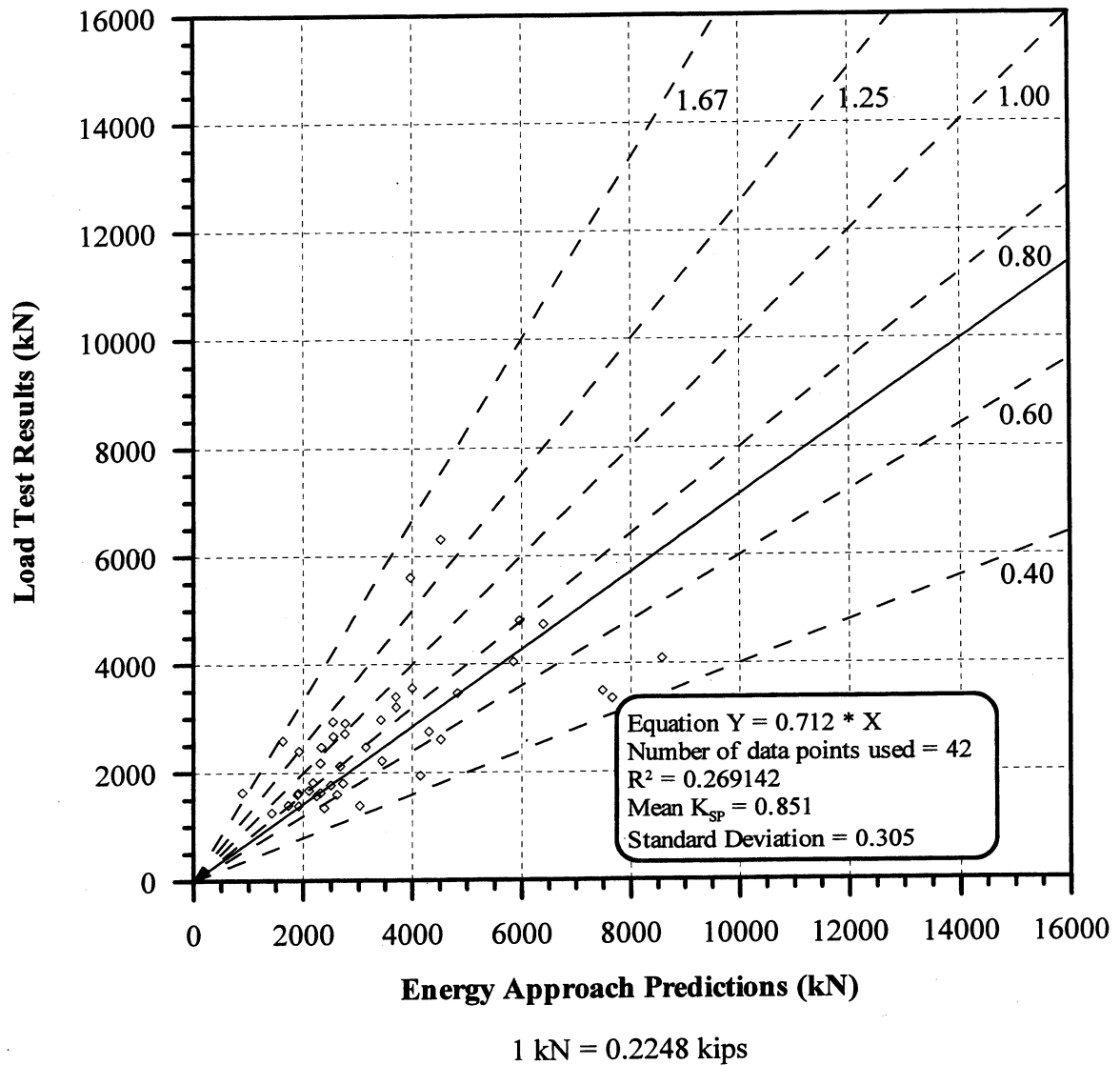


Figure 6.43. Static Load Test Results vs. Energy Approach predictions for 42 PD/LT2000 pile-cases at the BOR (last) with Blow Count ≥ 16 BP10cm and Area Ratio ≥ 350 in all types of soils (ABA).

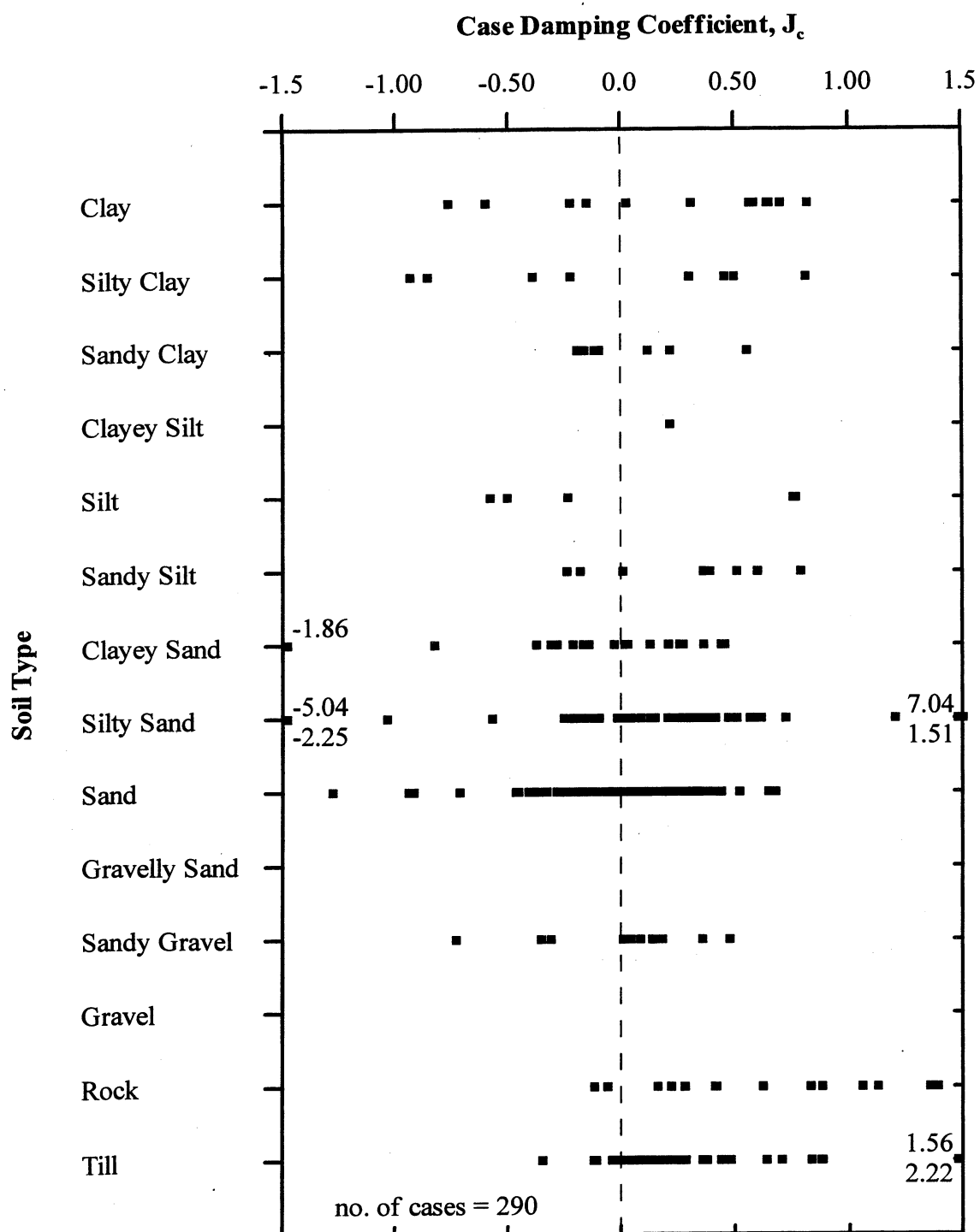
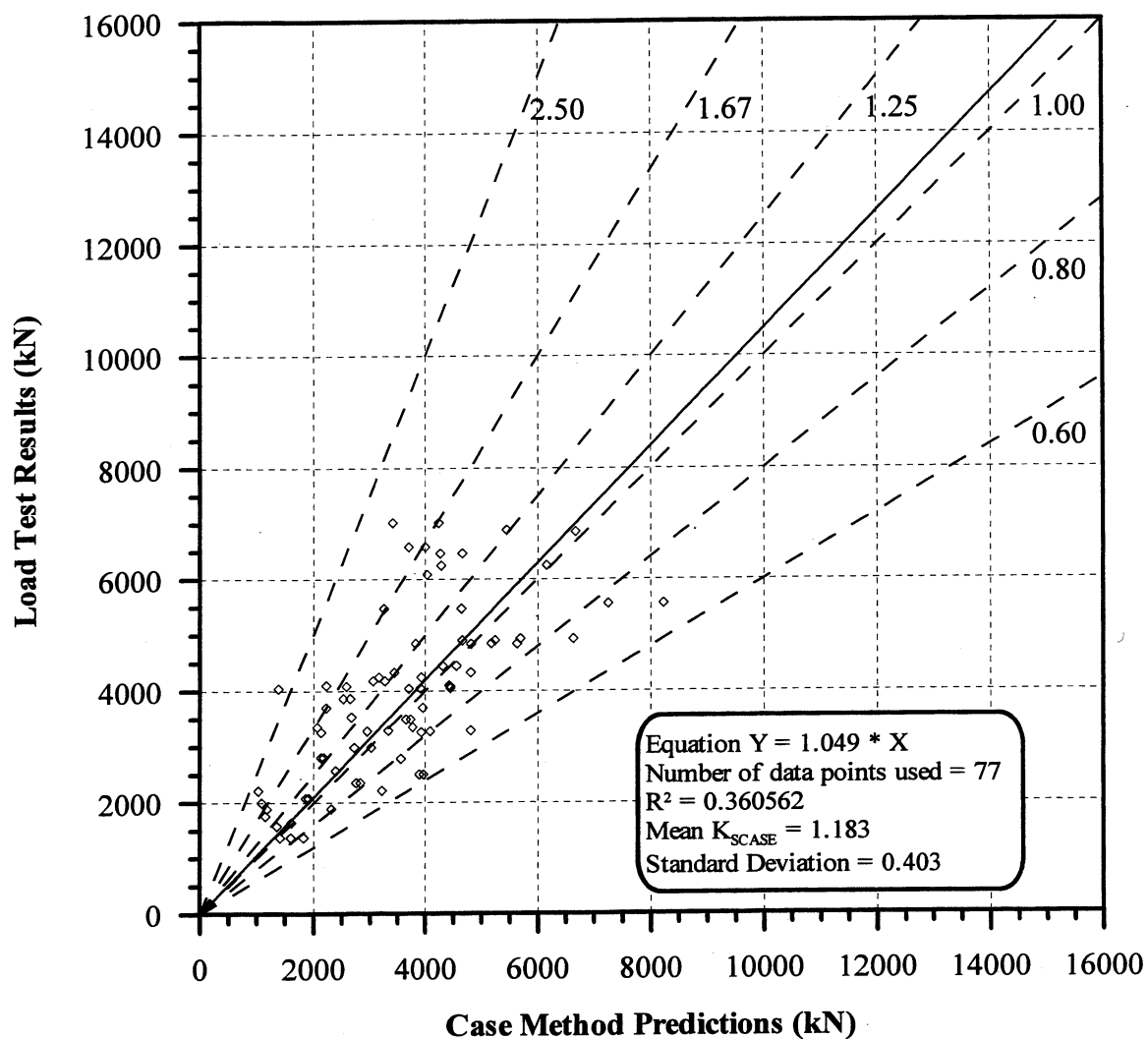


Figure 6.44. Tip Soil Conditions versus calculated Case Damping Coefficient, J_c , based on Static Load Test Results for 290 PD/LT pile-cases (Paikowsky et al., 1994).



1 kN = 0.2248 kips

Figure 6.45. Static Load Test Results vs. the Case Method (RMX) predictions for 77 pile-cases in Florida with varied J_c in all types of soils, (data obtained from the University of Florida).

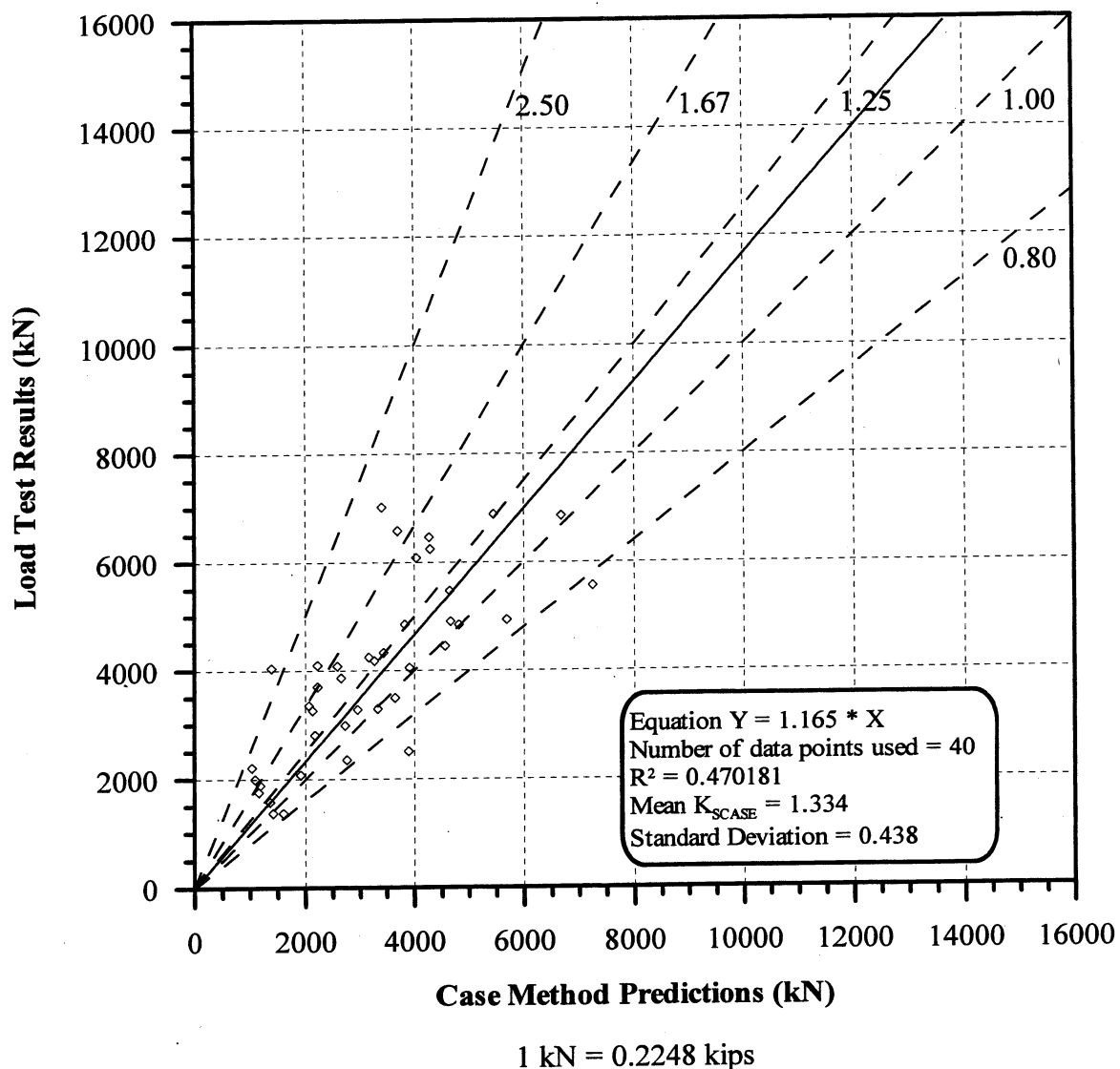


Figure 6.46. Static Load Test Results vs. the Case Method (RMX) predictions for 40 EOD pile-cases in Florida with varied J_c in all types of soils, (data obtained from the University of Florida).

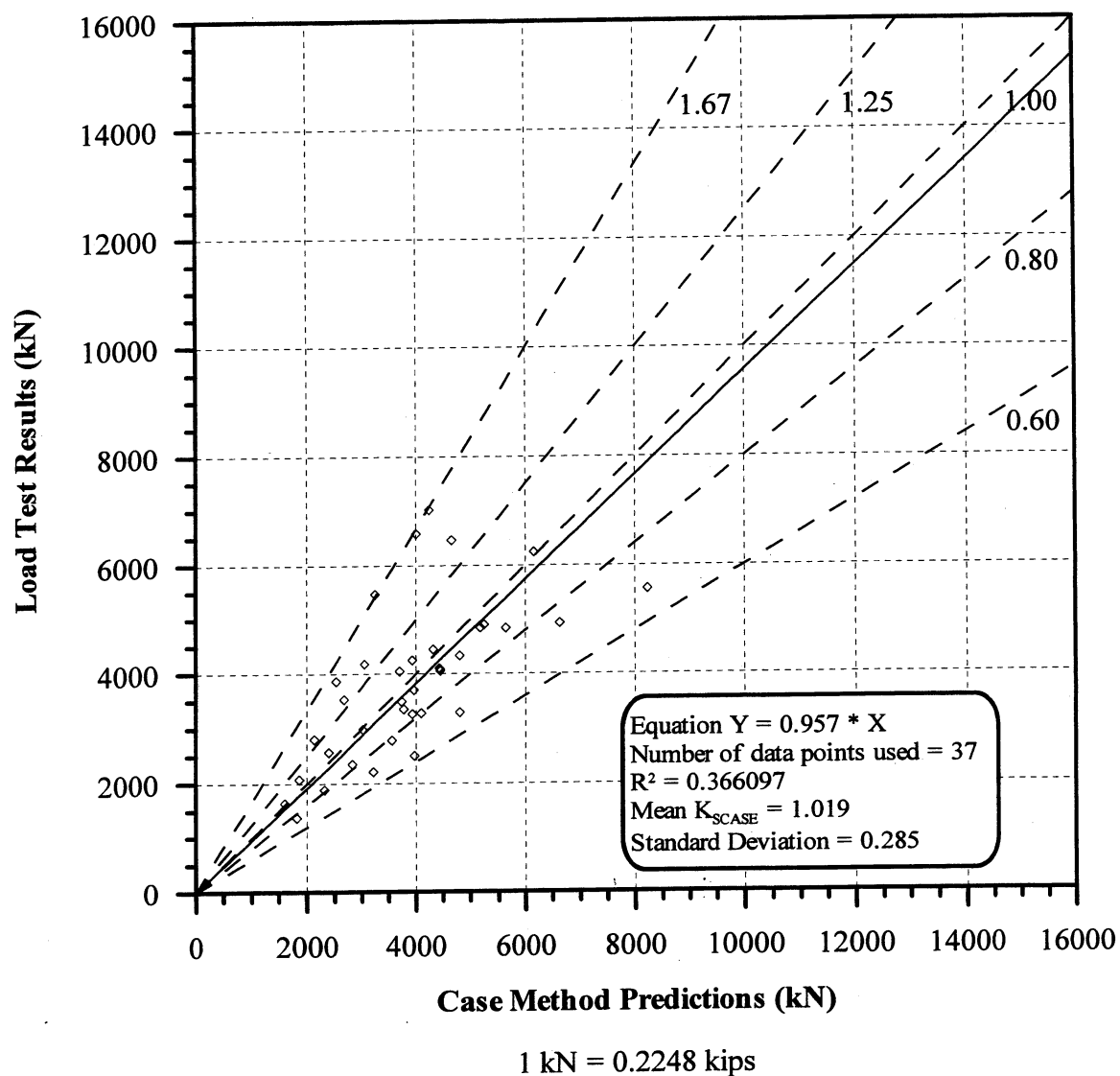


Figure 6.47. Static Load Test Results vs. the Case Method (RMX) predictions for 37 BOR pile-cases in Florida with varied J_c in all types of soils, (data obtained from the University of Florida).

CHAPTER 7

ENERGY APPROACH EOD VERSUS CAPWAP / TEPWAP BOR

7.1 GENERAL

The statistics presented in Chapter 6 confirmed the findings of previous studies; high accuracy of predictions for the signal matching analyses (e.g. CAPWAP) when performed at the BOR (Beginning of Restrike) and for the Energy Approach, when carried out during driving as indicated by the EOD (End of Driving) analyses. This chapter evaluates the practicality of using the Energy Approach method at the EOD in conjunction with or instead of performing a CAPWAP analysis at the BOR. The performance of the Energy Approach method at the EOD and the CAPWAP/TEPWAP methods at the BOR are presented compared to the static load test results. A comparison between the Energy Approach predictions at the EOD to the CAPWAP/TEPWAP predictions at the BOR is then made using 83 pile-cases from PD/LT2000 for which both analyses were available for the same piles. The evaluation comparing the two methods is continued using the database PD2000, which contains 228 pile-cases that have both an Energy Approach analysis at the EOD and a CAPWAP analysis at the BOR without static load test results, this data was compiled by Mr. Kevin O'Malley using data provided by Geosciences Testing and Research

Inc, (GTR). In all BOR analyses the CAPWAP predictions of the last restrike are utilized.

7.2 COMPARISON BASED ON THE PD/LT2000 DATABASE

A comparison between the static load test results and the Energy Approach predictions at the EOD was presented in Figure 6.30. The mean K_{SP} value, which is the ratio of the static load test results over the Energy Approach predictions, is 1.084 with a standard deviation of 0.431. These statistics show a fairly high accuracy of the Energy Approach predictions at the EOD. The CAPWAP/TEPWAP predictions at the BOR also show a high accuracy as was presented in Figure 6.16, where the mean K_{SW} value (static load test results over the CAPWAP/TEPWAP predictions) is 1.158 with a standard deviation of 0.393.

The accuracy of both the Energy Approach at the EOD and the CAPWAP/TEPWAP methods at the BOR improve when the blow counts are greater than 16 blows per 10cm (see Chapter 6). The mean K_{SP} value and its standard deviation for the Energy Approach at the EOD with blow counts less than 16 blows per 10cm are 1.227 and 0.474, respectively, while for blow counts greater than 16 blows per 10cm the mean K_{SP} value is 0.972 with a standard deviation of 0.359. For the CAPWAP/TEPWAP methods at the BOR with blows counts less than 16 blows per 10cm the mean K_{SW} value is 1.176 with a standard deviation of 0.530, while for the pile-cases with blow counts greater than 16 blows per 10cm the mean K_{SW} value and its standard deviation are 1.153 and 0.354, respectively. The presented statistics

show that both methods provide more accurate results for pile-cases in which the blow counts are greater than 16 blows per 10cm.

The relationship between the CAPWAP/TEPWAP predictions at the BOR and the Energy Approach predictions at the EOD is presented in Figure 7.1 for 83 PD/LT2000 pile-cases. The figure shows a good correlation between the results of the two methods at the different driving times as the mean K_{WP} value (ratio of the CAPWAP/TEPWAP predictions at the BOR over the Energy Approach predictions at the EOD) is 1.054 with a standard deviation of 0.370, which results in a COV of 0.351. The slope of the best-fit line forced through the origin for the presented data is 0.861 with a coefficient of determination (R^2) of 0.484, which shows a poor correlation between the two predictions. The R^2 value shows that there is significant scatter in the data. The ratios between the two predictions (CAPWAP/TEPWAP predictions over the Energy Approach predictions) ranges from approximately 0.50 to 2.5, which also shows significant scatter in the data.

Figure 7.2 presents the relationship between the CAPWAP/TEPWAP predictions at the BOR and the Energy Approach predictions at the EOD for 47 PD/LT2000 pile-cases with blow counts less than 16 blows per 10cm. The correlation is approximately the same as that for all pile-cases as the mean K_{WP} value increased slightly to 1.180, the standard deviation increased slightly to 0.400 and the COV decreased slightly to 0.339. The slope of the best-fit line forced through the origin increased to 0.958. The R^2 value (0.464) suggests that the scatter remained approximately the same as that for all pile-cases presented in Figure 7.1.

The relationship between the CAPWAP/TEPWAP predictions at the BOR and the Energy Approach predictions at the EOD for 36 PD/LT2000 pile-cases with blow counts greater than 16 blows per 10cm is presented in Figure 7.3. As is expected, the statistics have improved from that for all pile-cases, (presented in Figure 7.1), with the mean K_{WP} value being 0.890 with a standard deviation of 0.248, which results in a COV of 0.279. The slope of the best-fit line forced through the origin is 0.795, with $R^2 = 0.571$, which shows a significant amount of scatter in the data. The scatter is also shown by the prediction ratios that range from approximately 0.5 to 1.4.

The statistical information presented in this section suggests a high correlation between the Energy Approach at the EOD and CAPWAP during the BOR. The relationship suggests that from the construction point of view in many cases the use of the Energy Approach at the EOD can be much more cost effective than conducting dynamic testing and completing a complex CAPWAP or TEPWAP analysis at the BOR. This is less true for pile-cases where the blow counts at the end of driving are less than 16 blows per 10cm as the Energy Approach methods performance is more limited under such conditions with possible significant pile capacity gain with time.

7.3 COMPARISON BASED ON THE PD2000 DATABASE

7.3.1 Overview

Presented in this section are the comparisons between the CAPWAP predictions at the BOR and the Energy Approach predictions at the EOD for the pile-cases contained in database PD2000. The above comparison is made for all pile-cases as well as for the pile-cases with blow counts less and greater than 16 blows per 10cm.

The analysis is continued by comparing the two predictions based on the soil type at the tip of the pile for both cases where the blow count is less than and greater than 16 blows per 10cm.

7.3.2 All Pile-Cases

The comparison between the CAPWAP predictions at the BOR and the Energy Approach predictions at the EOD for the 228 pile-cases in PD2000 is presented in Figure 7.4. The figure shows a very good correlation between the two predictions as the mean K_{WP} value, (CAPWAP predictions over the Energy Approach predictions), is 0.962 with a standard deviation of 0.269. The data is plotted according to soil type at the tip with no clear correlation for any specific soil type. The slope of the best-fit line forced through the origin, which is an indicator of the accuracy of the correlation between the two prediction methods, is 0.901, with a coefficient of determination (R^2) of 0.738. These measures indicate a moderate correlation between the predicted capacities using the two different methods at different times of driving. The scatter is relatively insignificant as shown by the R^2 value and the prediction ratios (CAPWAP predictions over Energy Approach predictions), which range from approximately 0.5 to approximately 1.7.

7.3.3 Driving Resistance

Figure 7.5 presents the comparison between the CAPWAP predictions at the BOR and the Energy Approach predictions at the EOD for 43 PD2000 pile-cases with blow counts less than 16 blows per 10cm. The data is plotted according to soil type with no clear correlation for any specific soil type at the pile tip. The mean and

standard deviation are 1.167 and 0.434, respectively, have increased from that for all PD2000 EOD pile-cases. The COV (0.372) also increased from that for all EOD PD2000 pile-cases, but still shows that there is a good correlation between the prediction methods. The slope of the best-fit line is 0.979, with a coefficient of determination (R^2) of 0.556, which shows a significant scatter in the data as shown also by the ratios of the CAPWAP predictions to the Energy Approach predictions ranging from approximately 0.7 to 1.8.

Figure 7.6 presents a comparison between the CAPWAP predictions at the BOR and the Energy Approach predictions at the EOD for 185 PD2000 pile-cases with blow counts greater than 16 blows per 10cm. The plotted data according to soil type at the tip suggests that a larger scatter exists for the piles in clay and till but no clear correlation was established based on a specific soil type. The mean K_{WP} value is 0.915 with a standard deviation of 0.185, which is a significant improvement from the statistics for all pile-cases as was shown in Figure 7.4 or those for the EOD case in easy driving (Figure 7.5). An excellent correlation exists between the predictions using the two dynamic methods with the slope of the best-fit line forced through zero being 0.895, and a coefficient of determination (R^2) of 0.725. The scatter is small based on the R^2 and COV values and the small range of ratios of CAPWAP predictions over Energy Approach predictions (approximately 0.5 to 1.5, with only 5 pile-cases falling above the ratio of 1.25 or below 0.6).

The statistics presented in this section showed that the correlation between the two methods for pile-cases with blow counts greater than 16 blows per 10cm is

excellent while the correlation is not so good for pile-cases with blow counts less than 10 blows per 10cm. This again leads to the conclusion that if the blow counts are less than 16 blows per 10cm at the EOD then a restrike and a signal matching analysis may be advantageous. The data for each of the presented figures was plotted according to soil types at the tip and from these figures it appears that there is no clear correlation based on soil types. The next section will examine the correlation between the CAPWAP predictions at the BOR and the Energy Approach predictions at the EOD based on soil type.

7.3.4 Soil Type

a) Overview

This section presents the correlations between the CAPWAP predictions at the BOR and the Energy Approach predictions at the EOD based on the type of soil at the pile's tip. The correlation is also shown for a special group of pile-cases driven through Boston Blue Clay. Each of the correlations based on soil type are also sub-grouped according to the driving resistance distinguishing between less and greater than 16 blows per 10cm.

b) Clay and Till

The comparison between the CAPWAP predictions at the BOR and the Energy Approach predictions at the EOD for 90 PD2000 pile-cases embedded in clay and till is presented in Figure 7.7. The mean K_{WP} value is 0.999 with a standard deviation of 0.293, which results in a COV of 0.293 suggesting a very good correlation between the two dynamic method predictions for piles embedded in clay and till. The slope of

the best-fit line forced through the origin is 0.943, with a coefficient of determination of 0.820, which also shows the good correlation between the two dynamic method predictions. The scatter of data is relatively small as the data ranges from ratios of CAPWAP predictions to Energy Approach predictions of approximately 0.6 to approximately 1.8 and the R^2 value is greater than 0.8.

Figure 7.8 presents the comparison between the CAPWAP predictions at the BOR and the Energy Approach predictions at the EOD for 15 PD2000 pile-cases embedded in clay and till with blow counts less than 16 blows per 10cm. Based on the mean K_{WP} value of 1.272 and a standard deviation of 0.539, the COV is 0.424, which shows a reasonably good correlation between the two prediction methods. The slope of the best-fit line forced through the origin is 1.037, with a coefficient of determination (R^2) of 0.608, indicating a borderline moderate correlation (to poor) between the predictions based on the two dynamic methods for pile-cases embedded in clay and till with blow counts less than 16 blows per 10cm. The ratios of the CAPWAP predictions over the Energy Approach predictions range from 0.7 to above 2.4 and with the marginal R^2 value and only 15 pile-cases in this category, the correlation of the method in this case is rather limited.

Figure 7.9 presents the comparison between the CAPWAP predictions at the BOR and the Energy Approach predictions at the EOD for 75 PD2000 pile-cases with blow counts greater than 16 blows per 10cm embedded in clay and till. The mean K_{WP} value is 0.944 with a standard deviation of 0.173, which results in a COV of 0.183. These statistics show a very good correlation between the two dynamic method

predictions, as does the slope of the best-fit line forced through the origin, 0.939 and the coefficient of determination, R^2 value of 0.800. The ratios of the CAPWAP predictions over the Energy Approach predictions range from approximately 0.6 to 1.5 with only 2 pile-cases falling above the ratio of 1.25.

c) *Sand and Silt*

Figure 7.10 presents a comparison between the CAPWAP predictions at the BOR and the Energy Approach predictions at the EOD for 42 PD2000 pile-cases of piles embedded in sand and silt. The mean K_{WP} value, which is the ratio of the CAPWAP predictions over the Energy Approach prediction, is 1.028 with a standard deviation of 0.333, which results in a COV of 0.324. The slope of the best-fit line forced through the origin is 0.871; with a coefficient of determination (R^2) of 0.721. These statistics show a good correlation between the two dynamic methods at the different times of driving with the ratios (CAPWAP predictions over the Energy Approach predictions) ranging from approximately 0.6 to 1.7 and the R^2 value suggests moderate to good correlation.

Presented in Figure 7.11 is the comparison between the CAPWAP predictions at the BOR and the Energy Approach predictions at the EOD for 16 PD2000 pile-cases with blow counts of less than 16 blows per 10cm embedded in sand and silt. Based on the COV of 0.320 the performance in this category has not changed from that for all pile-cases in sand and silt, although the mean K_{WP} value, 1.254, and the standard deviation of 0.401 have increased. The standard deviation (0.401) has also increased. The slope of the best-fit line is 1.148, with a coefficient of determination

(R^2) of 0.441 shows a poor correlation between the pile capacity predictions using the two methods. The scatter is fairly significant as it ranges from ratios of CAPWAP predictions over Energy Approach predictions of approximately 0.8 to 1.7.

The comparison between the CAPWAP predictions at the BOR and the Energy Approach predictions at the EOD for 26 PD2000 pile-cases with blows counts greater than 16 blows per 10cm embedded in sand and silt is presented in Figure 7.12. The data in the figure shows a good correlation between the pile capacity predictions based on the two dynamic methods, as the mean K_{WP} value is 0.888 with a standard deviation of 0.179, which results in a COV of 0.202. The slope of the best-fit line is 0.837, with a coefficient of determination (R^2) of 0.804, which shows a small amount of scatter and a good correlation between the predictions.

d) Rock

Figure 7.13 presents a comparison between the CAPWAP predictions at the BOR and the Energy Approach predictions at the EOD for 94 PD2000 pile-cases embedded in rock. The mean K_{WP} value is 0.906 with a standard deviation of 0.187, which results in a COV of 0.206, suggesting an excellent correlation between the pile capacity predictions using the two dynamic methods. The slope of the best-fit line forced through the origin is 0.902; with a R^2 value of 0.708. The ratios of the CAPWAP predictions over the Energy Approach predictions range from approximately 0.5 to 1.3, which shows a small amount of scatter and a moderate correlation between the two methods predictions.

Figure 7.14 presents the comparison between the CAPWAP predictions at the BOR and the Energy Approach predictions at the EOD for 12 PD2000 pile-cases with blow counts less than 16 blows per 10cm embedded in rock. The statistics have not changed from that presented for all pile-cases. The mean K_{WP} value is 0.918 with a standard deviation of 0.188, which results in a COV of 0.205. The slope of the best-fit line forced through the origin is 0.887, with a R^2 value of 0.590, suggesting a significant amount of scatter in the data and a moderate to poor correlation between the predictions using these two dynamic methods at different times of driving. These conclusions are subjected however to the small sample size of 12 cases only.

The comparison between the CAPWAP predictions at the BOR and the Energy Approach predictions at the EOD for 82 PD2000 pile-cases with blow counts greater than 16 blows per 10cm embedded in rock is presented in Figure 7.15. Again the mean and standard deviation did not change from that for all pile-cases embedded in rock. The mean K_{WP} value is 0.905 with a standard deviation of 0.188, which results in a COV of 0.208 and the slope of the best-fit line forced through the origin is 0.904, with a R^2 value of 0.713. The ratios of the CAPWAP predictions to the Energy Approach predictions range from approximately 0.5 to 1.5, which along with the other parameters suggests a moderate correlation between the pile capacity predictions based on the two dynamic methods.

e) Boston Blue Clay

The comparison between the CAPWAP predictions at the BOR and the Energy Approach predictions at the EOD for 72 PD2000 pile-cases with Boston blue clay as

the major soil type along the side of the pile is presented in Figure 7.16. The mean K_{WP} value, 0.920, and its standard deviation, 0.178, result in a COV of 0.193, which shows an excellent correlation between the pile capacity predictions based on the two dynamic methods. The slope of the best-fit line forced through the origin, 0.940, with a R^2 value of 0.821, which also suggests a good correlation between the predictions. The scatter is relatively small based on the ratios of the CAPWAP predictions over the Energy Approach predictions, which range from approximately 0.5 to 1.5 with only 3 pile-cases having a ratio greater than 1.25.

Presented in Figure 7.17 is the comparison between the CAPWAP predictions at the BOR and the Energy Approach predictions at the EOD for 8 PD2000 pile-cases with blow counts less than 16 blows per 10cm and with Boston blue clay as the major soil type along the side of the pile. The mean K_{WP} value is 0.845 with a standard deviation of 0.136, which results in COV of 0.161, which shows a very good correlation between the pile capacity predictions using the two dynamic methods. The slope of the best-fit line forced through the origin is 0.841, with a R^2 value of 0.144. The small sample size of this category provides limited ability to conclude decisively regarding the meaning of the data.

Figure 7.18 presents the comparison between the CAPWAP predictions at the BOR and the Energy Approach predictions at the EOD for 64 PD2000 pile-cases with blow counts greater than 16 blow per 10cm and with Boston blue clay as the major soil type along the side of the pile. The mean K_{WP} value, 0.930, and its standard deviation, 0.181, result in a COV of 0.195 which is approximately the same as the

COV for all pile-cases with Boston blue clay as the major soil type along the side of the pile. These values again suggest an excellent correlation between the predictions of the two dynamic methods. The slope of the best-fit line is 0.947; with an R^2 value of 0.825 also remained relatively unchanged. The relatively small change between this case to the total case is expected as 64 out of the 72 cases of Figure 7.16 relate to a blow count greater than 16 BP10cm.

7.3.5 Summary

As the best performing dynamic methods for BOR and EOD, the correlation between the CAPWAP predictions (at the BOR) and the Energy Approach predictions (at the EOD) was evaluated using the database PD2000. The conclusion from the presented analyses is that if the blow counts at the end of driving are less than 16 blows per 10cm, it is wise to complete a CAPWAP analysis at the beginning of a restrike. Chapter 8 will discuss a way to evaluate the time required to perform a restrike after the end of driving to obtain the most accurate predictions of the pile capacity. If the blow count at the end of driving is greater than 16 blows per 10cm the high accuracy of the Energy Approach and the good correlation between the methods suggest that it is much more cost effective to complete a quick field evaluation of the pile capacity using the Energy Approach rather than performing a delayed and more expensive wave matching technique evaluation in the office. The correlation developed in this section also showed that the soil type has a minimal effect on the accuracy of the direct correlation between the CAPWAP predictions at the BOR and the Energy Approach predictions at the EOD. Piles that are driven into cohesive soils

such as Boston blue clay often exhibit a significant gain of capacity with time. The analysis based on the criteria that all pile-cases have Boston blue clay as the major soil type along the side of the pile showed that the pile capacity gain with time does not affect the proposed correlation with the Energy Approach at the EOD matching well with CAPWAP results at the BOR. Demonstrating again the high accuracy of the Energy Approach for the long-term pile capacity.

7.4 SUMMARY AND INTERMEDIATE CONCLUSIONS

The analysis presented in this chapter has shown that there is a very good correlation between the CAPWAP predictions at the BOR and the Energy Approach predictions at the EOD. A summary of the analyses that were performed is presented in Table 7.1. The statistical data of Table 7.1 suggests the following:

- (i) Soil type has a minimal effect on the accuracy of the correlation between the pile capacity predictions using the two dynamic methods at different times of driving.
- (ii) A better correlation exists between the two dynamic method predictions for pile-cases with blow counts greater than 16 blows per 10cm compared to those with blow counts less than 16 blows per 10cm.
- (iii) A reasonable practical suggestion is therefore to use the Energy Approach method to evaluate the pile capacity at the end of driving unless the recorded blow counts are less than 16 blows per 10cm. If the blow count is smaller than 16 blows per 10cm a CAPWAP analysis should be completed for a restrike performed some time after the driving of the pile, to be discussed in Chapter 8.

Table 7.1. Summary of statistical data for the Correlation between the CAPWAP/TEPWAP predictions at the BOR to the Energy Approach predictions at the EOD using the PD/LT2000 and PD2000 databases.

	Ratios	All Cases	Blow Count < 16 BP10cm	Blow Count \geq 16 BP10cm
PD/LT2000 Database	K_{SP} (all soil types) End of Driving	$\mu = 1.084$ $\sigma = 0.431$ no. = 128	$\mu = 1.227$ $\sigma = 0.474$ no. = 56	$\mu = 0.972$ $\sigma = 0.359$ no. = 72
	K_{SW} (all soil types) Beginning of Restrike	$\mu = 1.158$ $\sigma = 0.393$ no. = 162	$\mu = 1.176$ $\sigma = 0.530$ no. = 32	$\mu = 1.153$ $\sigma = 0.354$ no. = 130
	K_{WP} (all soil types)	$\mu = 1.054$ $\sigma = 0.370$ no. = 83	$\mu = 1.180$ $\sigma = 0.400$ no. = 47	$\mu = 0.890$ $\sigma = 0.248$ no. = 36
PD2000 Database	K_{WP} (all soil types)	$\mu = 0.962$ $\sigma = 0.269$ no. = 228	$\mu = 1.167$ $\sigma = 0.434$ no. = 43	$\mu = 0.915$ $\sigma = 0.185$ no. = 185
	K_{WP} (clay & till)	$\mu = 0.999$ $\sigma = 0.293$ no. = 90	$\mu = 1.272$ $\sigma = 0.539$ no. = 15	$\mu = 0.944$ $\sigma = 0.173$ no. = 75
	K_{WP} (sand & silt)	$\mu = 1.028$ $\sigma = 0.333$ no. = 42	$\mu = 1.254$ $\sigma = 0.401$ no. = 16	$\mu = 0.888$ $\sigma = 0.179$ no. = 26
	K_{WP} (rock)	$\mu = 0.906$ $\sigma = 0.187$ no. = 94	$\mu = 0.918$ $\sigma = 0.188$ no. = 12	$\mu = 0.905$ $\sigma = 0.188$ no. = 82
	K_{WP} (BBC side)	$\mu = 0.920$ $\sigma = 0.178$ no. = 72	$\mu = 0.845$ $\sigma = 0.136$ no. = 8	$\mu = 0.930$ $\sigma = 0.181$ no. = 64

- Notes:
1. The soil types are the soil types at the tip.
 2. BBC side – pile cases with Boston Blue Clay as the major soil type on the side of the pile.
 3. K_{SP} – ratio of static load test results to the Energy Approach predictions at the EOD.
 4. K_{SW} – ratio of static load test results to the CAPWAP/TEPWAP predictions at the BOR.
 5. K_{WP} – ratio of the CAPWAP/TEPWAP predictions at the BOR to the Energy Approach predictions at the EOD.
 6. EOD – End of Driving
 7. BOR – Beginning of Restrike and in this instance is the last restrike.
 8. 16 BP10cm is approximately 4 BPI.
 9. Two pile-cases had unknown soil types at the tip.

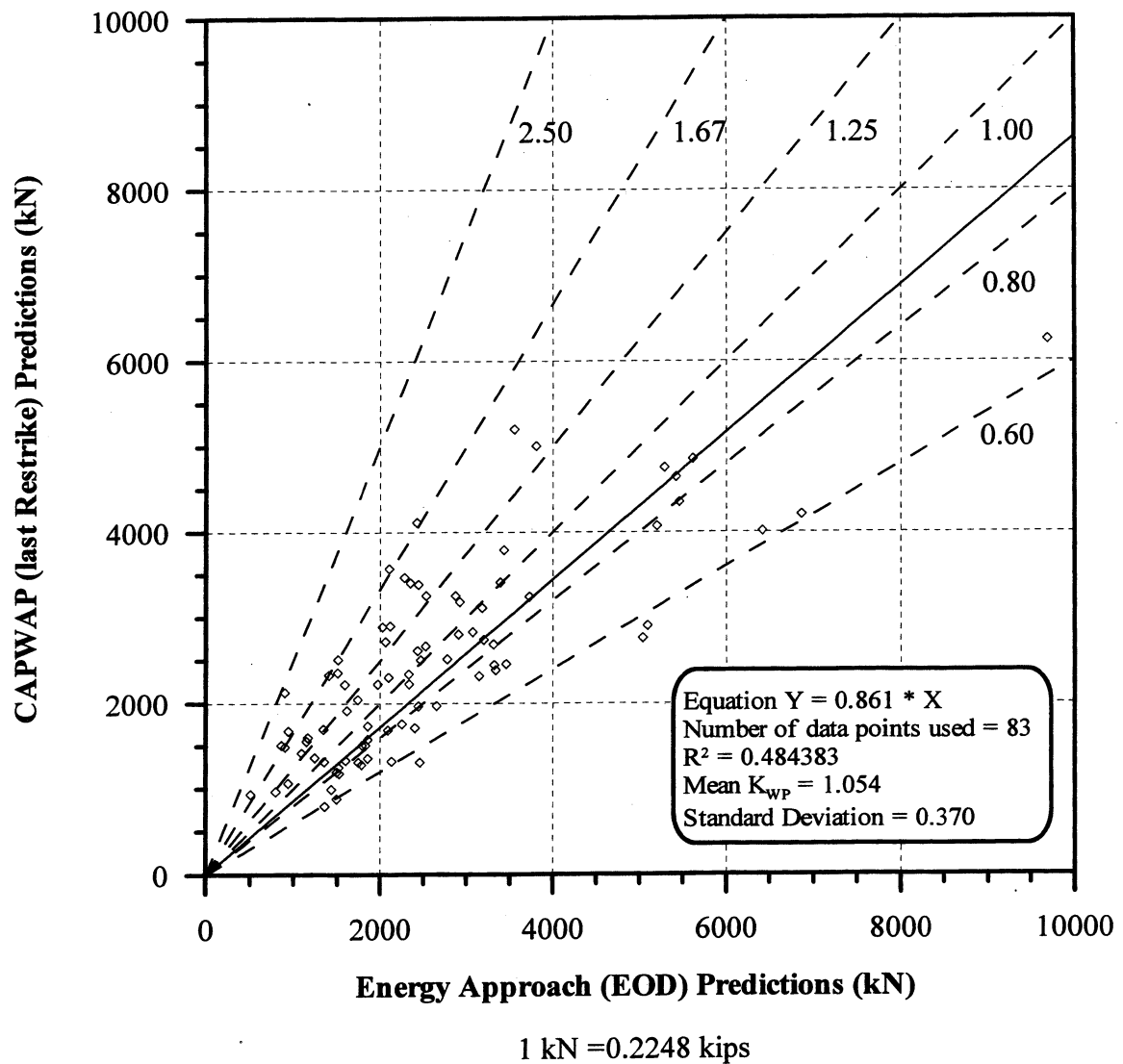


Figure 7.1. CAPWAP (last Restrike) Predictions vs. Energy Approach (EOD) Predictions for 83 PD/LT2000 pile-cases in all types of soils (AAA).

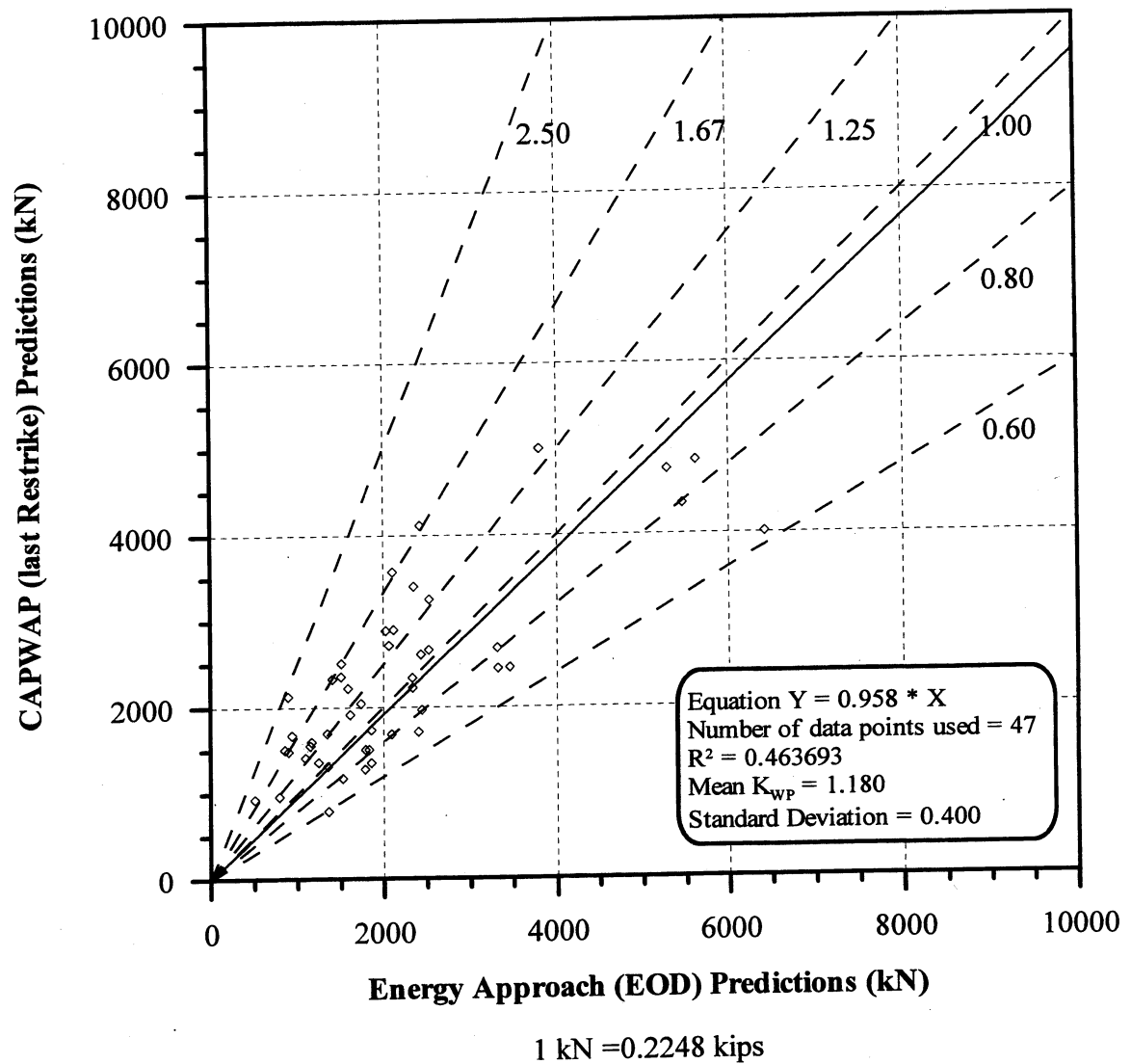


Figure 7.2. CAPWAP (last Restrike) Predictions vs. Energy Approach (EOD) Predictions for 47 PD/LT2000 pile-cases with Blow Count < 16 BP10cm in all types of soils (AAA).

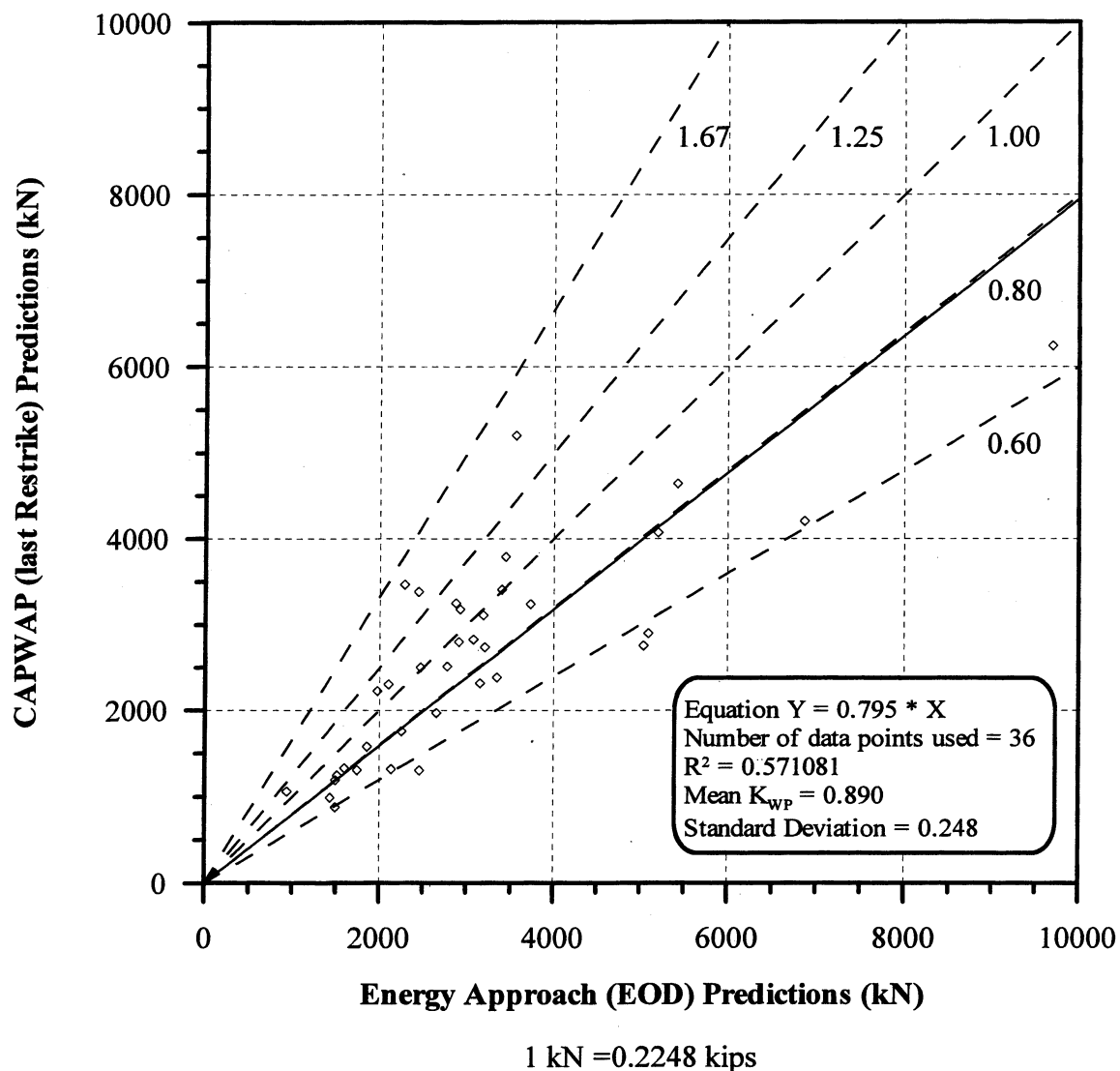


Figure 7.3. CAPWAP (last Restrike) Predictions vs. Energy Approach (EOD) Predictions for 36 PD/LT2000 pile-cases with Blow Count ≥ 16 BP10cm in all types of soils (AAA).

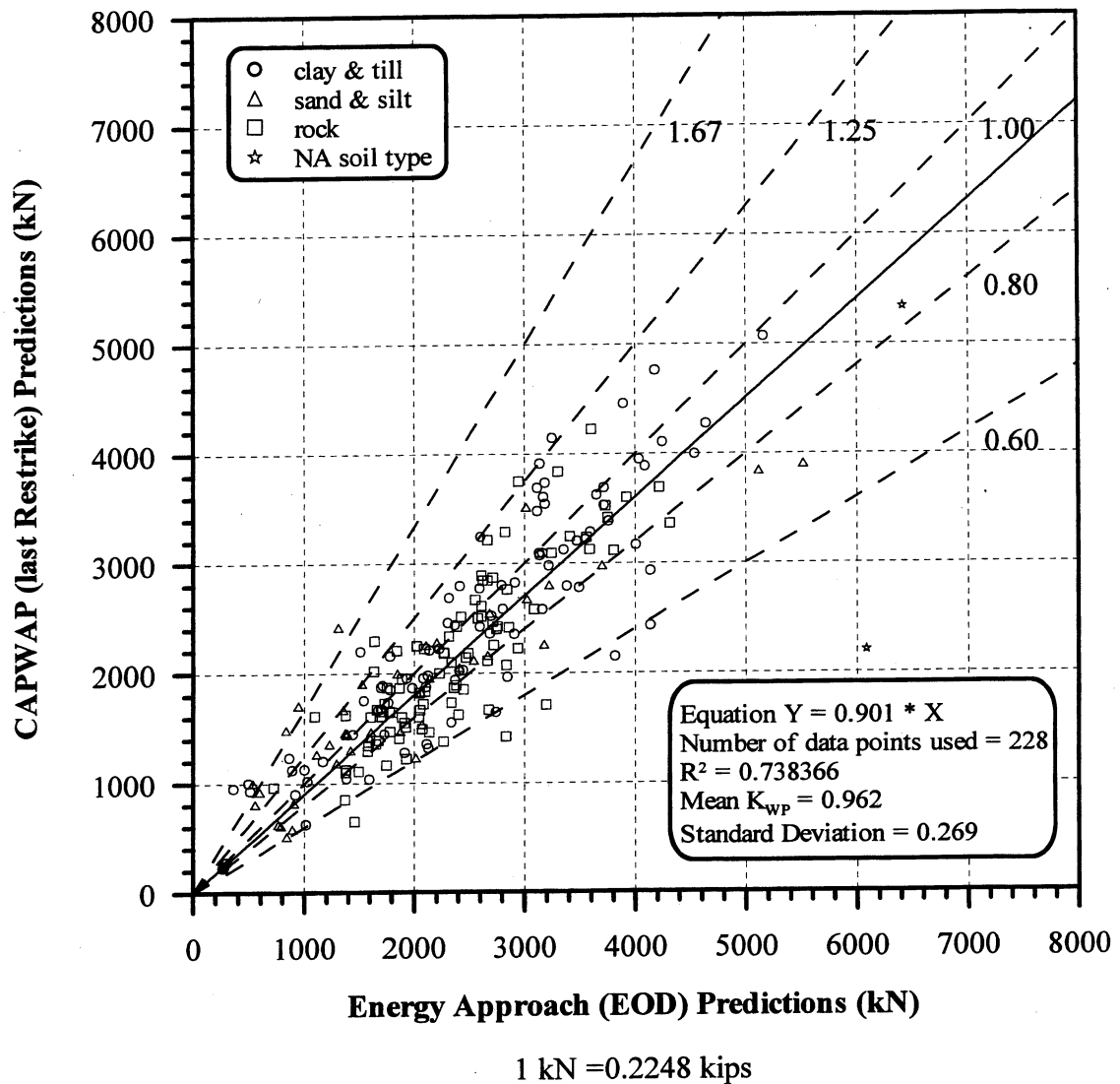


Figure 7.4. CAPWAP (last Restrike) Predictions vs. Energy Approach (EOD) Predictions for 228 PD2000 pile-cases in all soil types.

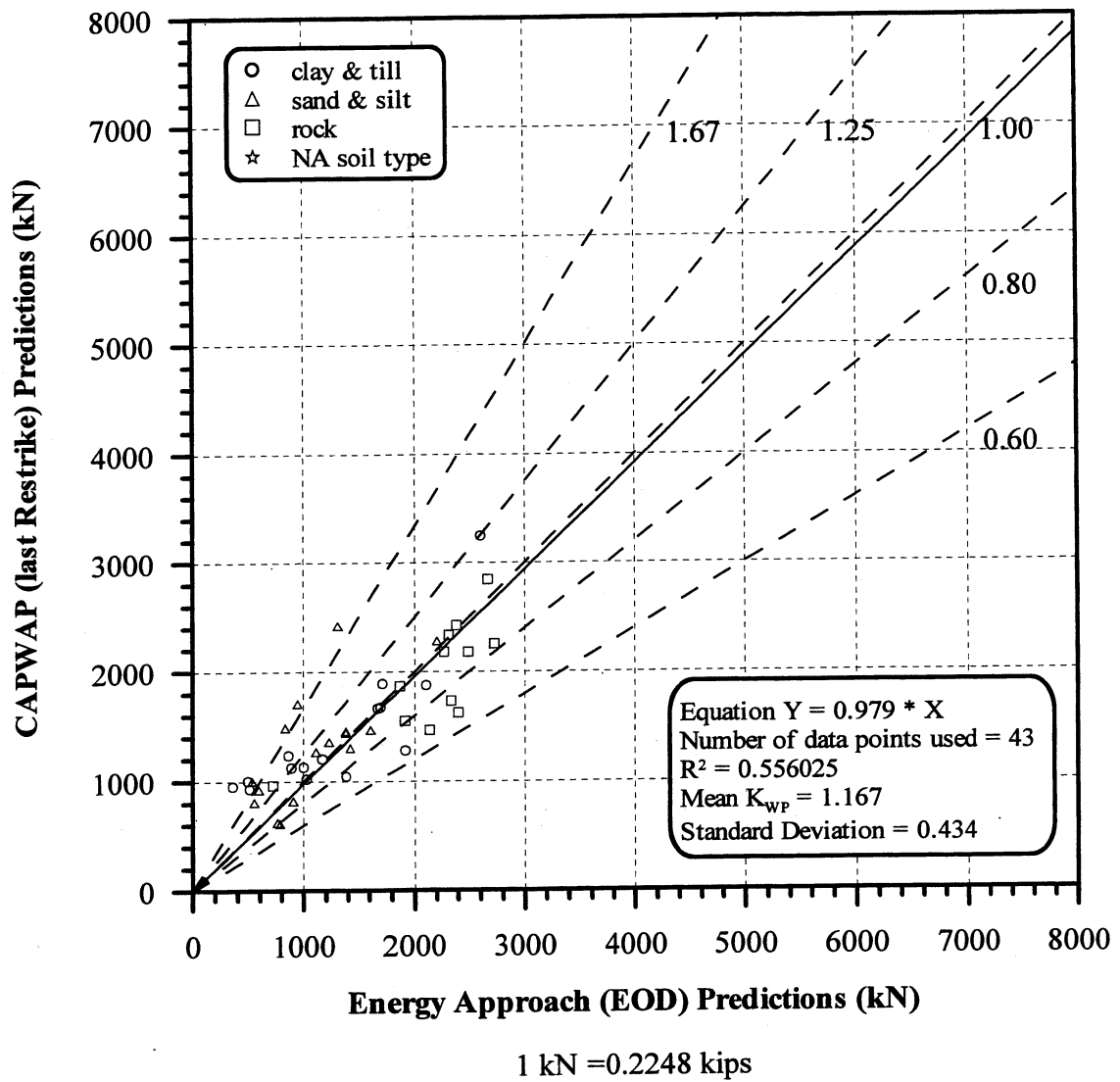


Figure 7.5. CAPWAP (last Restrike) Predictions vs. Energy Approach (EOD) Predictions for 43 PD2000 pile-cases with Blow Count < 16 BP10cm in all soil types.

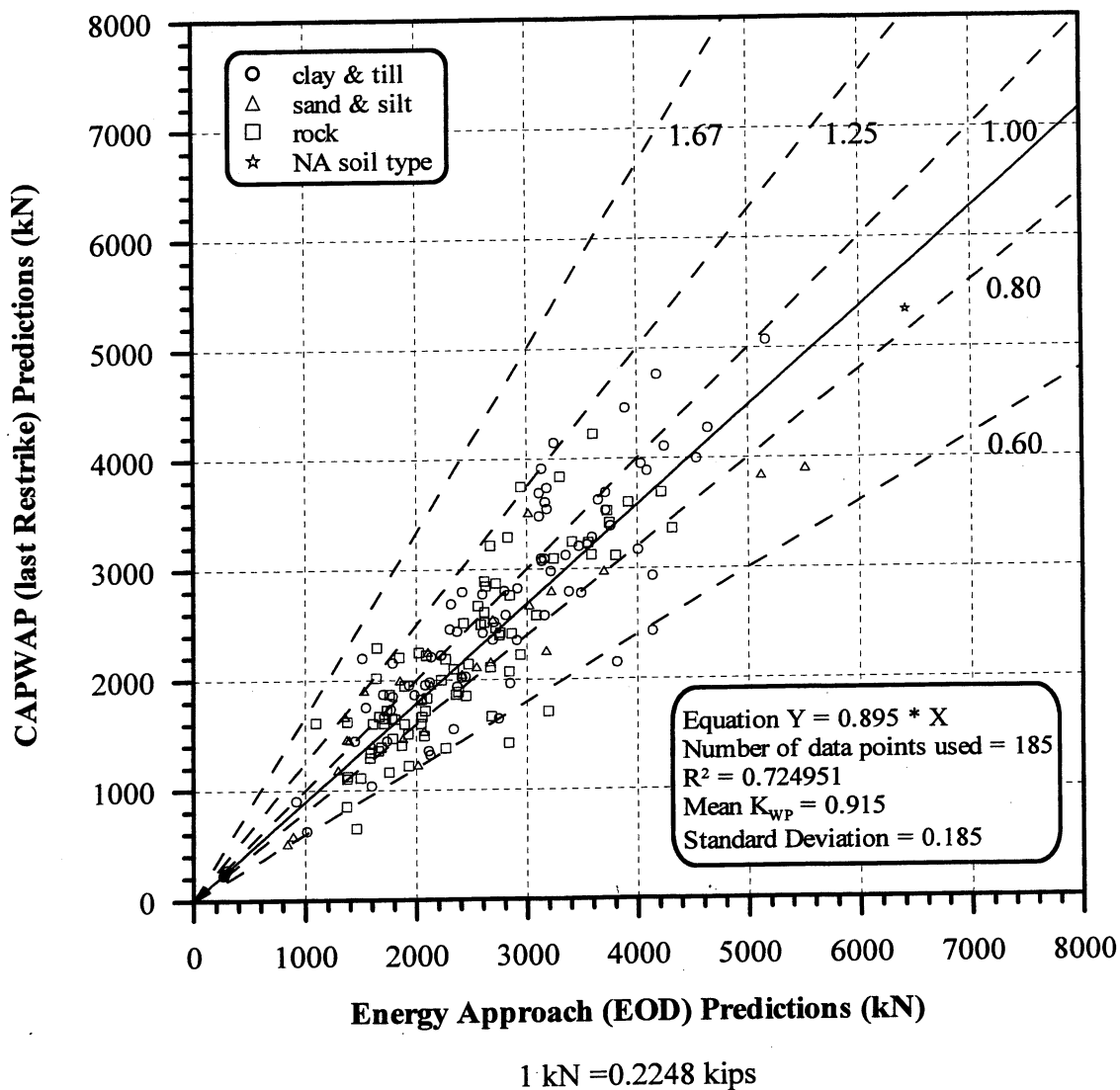


Figure 7.6. CAPWAP (last Restrike) Predictions vs. Energy Approach (EOD) Predictions for 185 PD2000 pile-cases with Blow Count ≥ 16 BP10cm in all soil types.

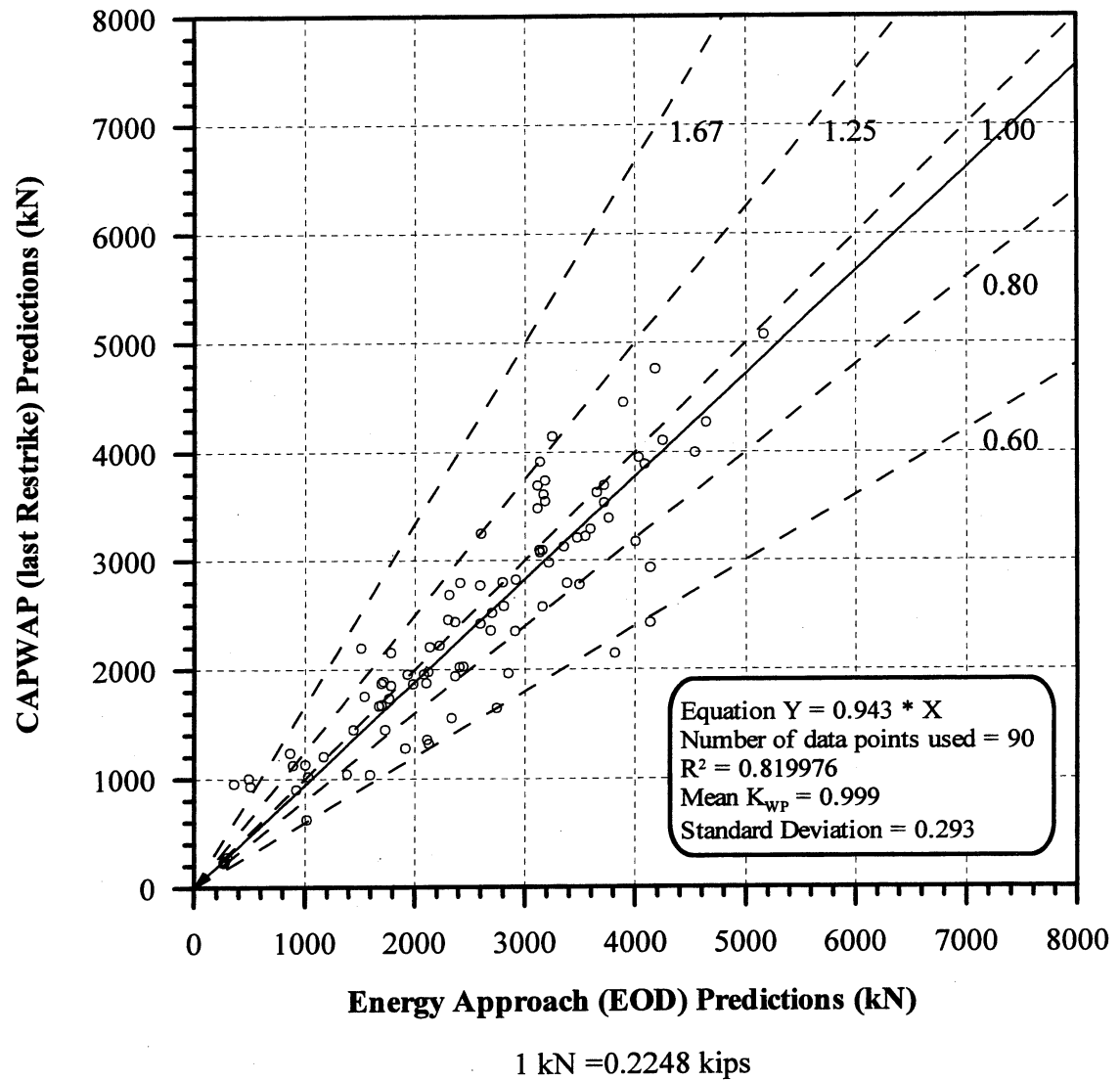


Figure 7.7. CAPWAP (last Restrike) Predictions vs. Energy Approach (EOD) Predictions for 90 PD2000 pile-cases in clay & till.

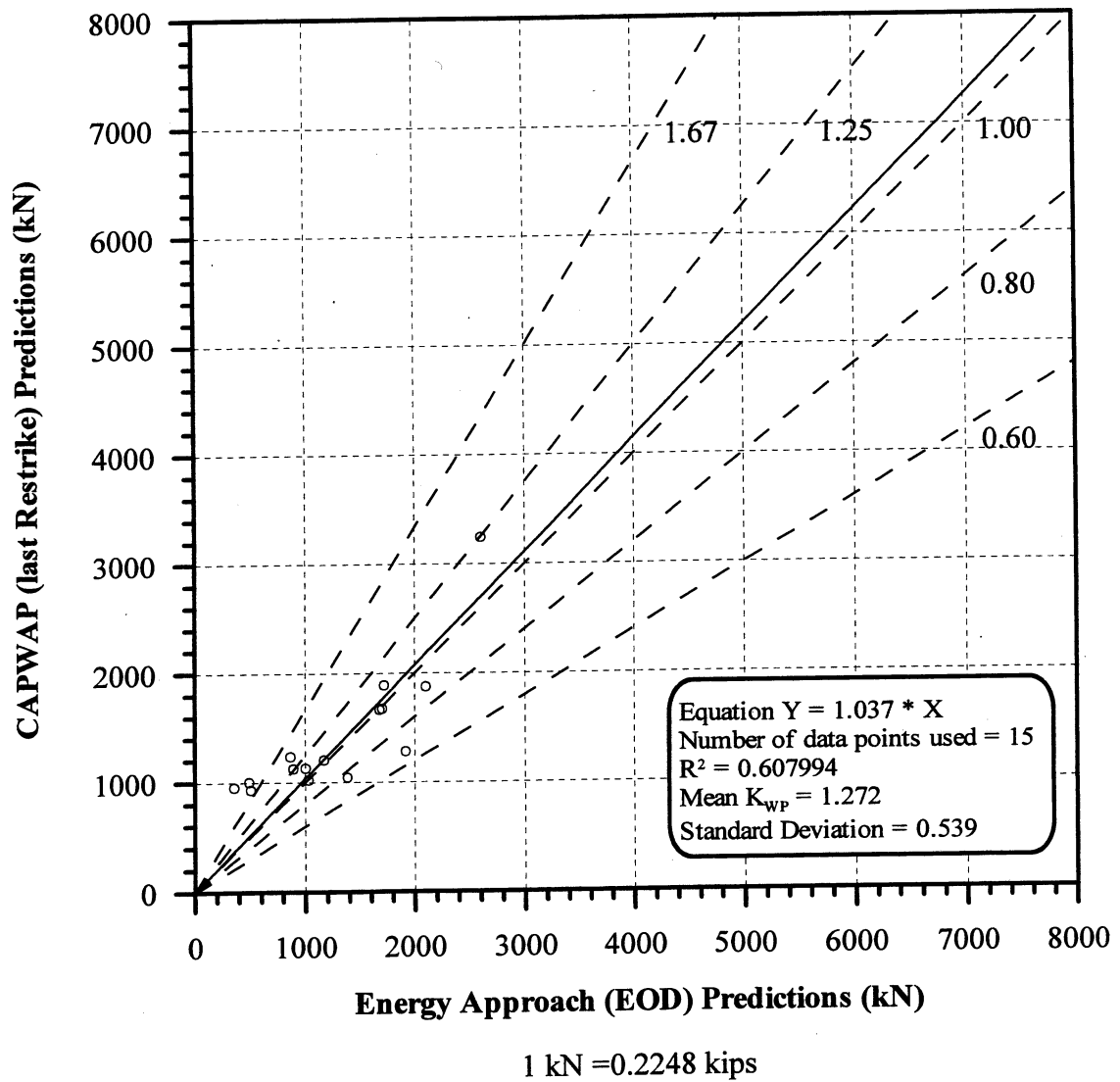


Figure 7.8. CAPWAP (last Restrike) Predictions vs. Energy Approach (EOD) Predictions for 15 PD2000 pile-cases with Blow Count < 16 BP10cm in clay & till.

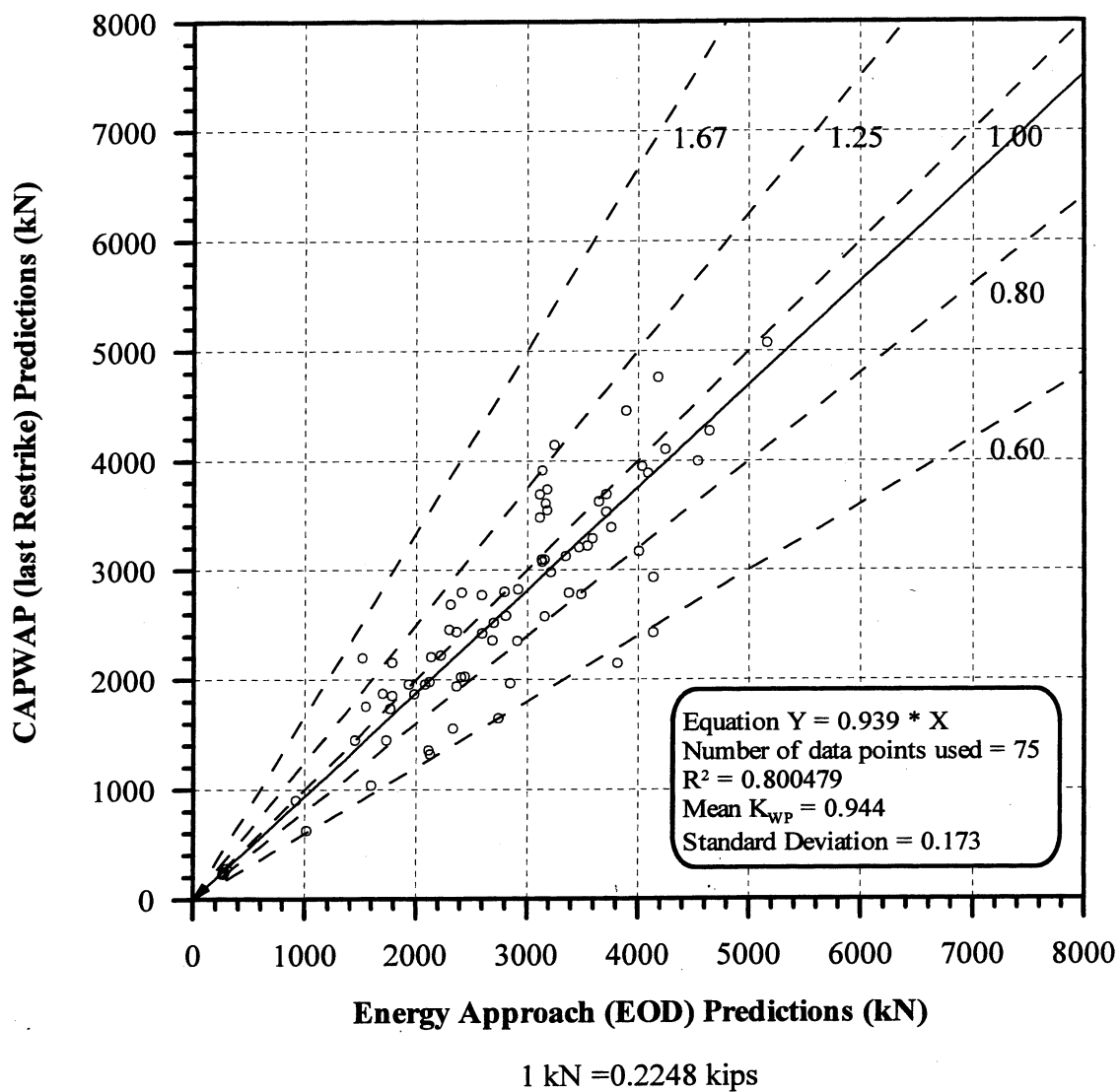


Figure 7.9. CAPWAP (last Restrike) Predictions vs. Energy Approach (EOD) Predictions for 75 PD2000 pile-cases with Blow Count ≥ 16 BP10cm in clay & till.

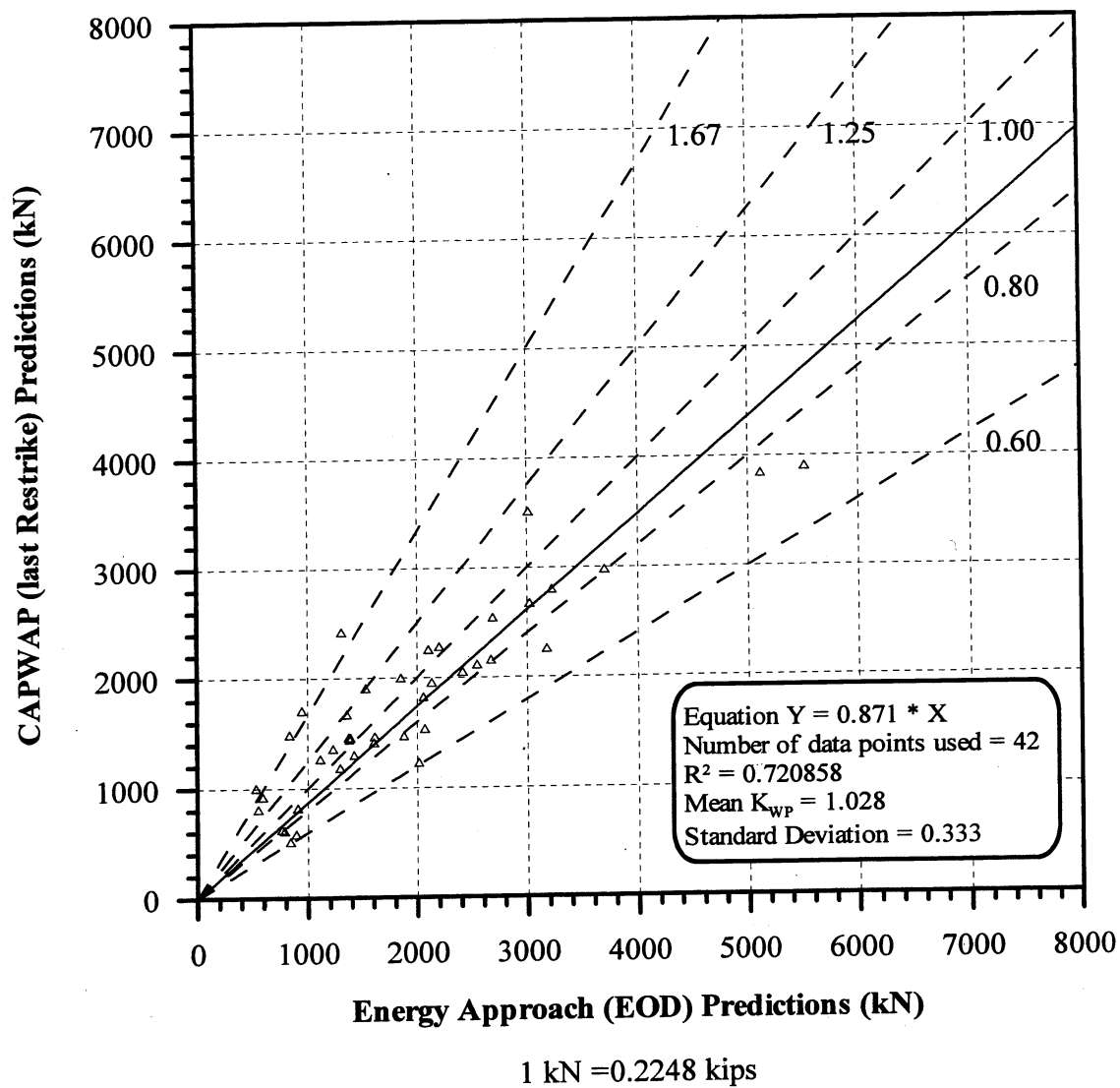


Figure 7.10. CAPWAP (last Restrike) Predictions vs. Energy Approach (EOD) Predictions for 42 PD2000 pile-cases in sand & silt.

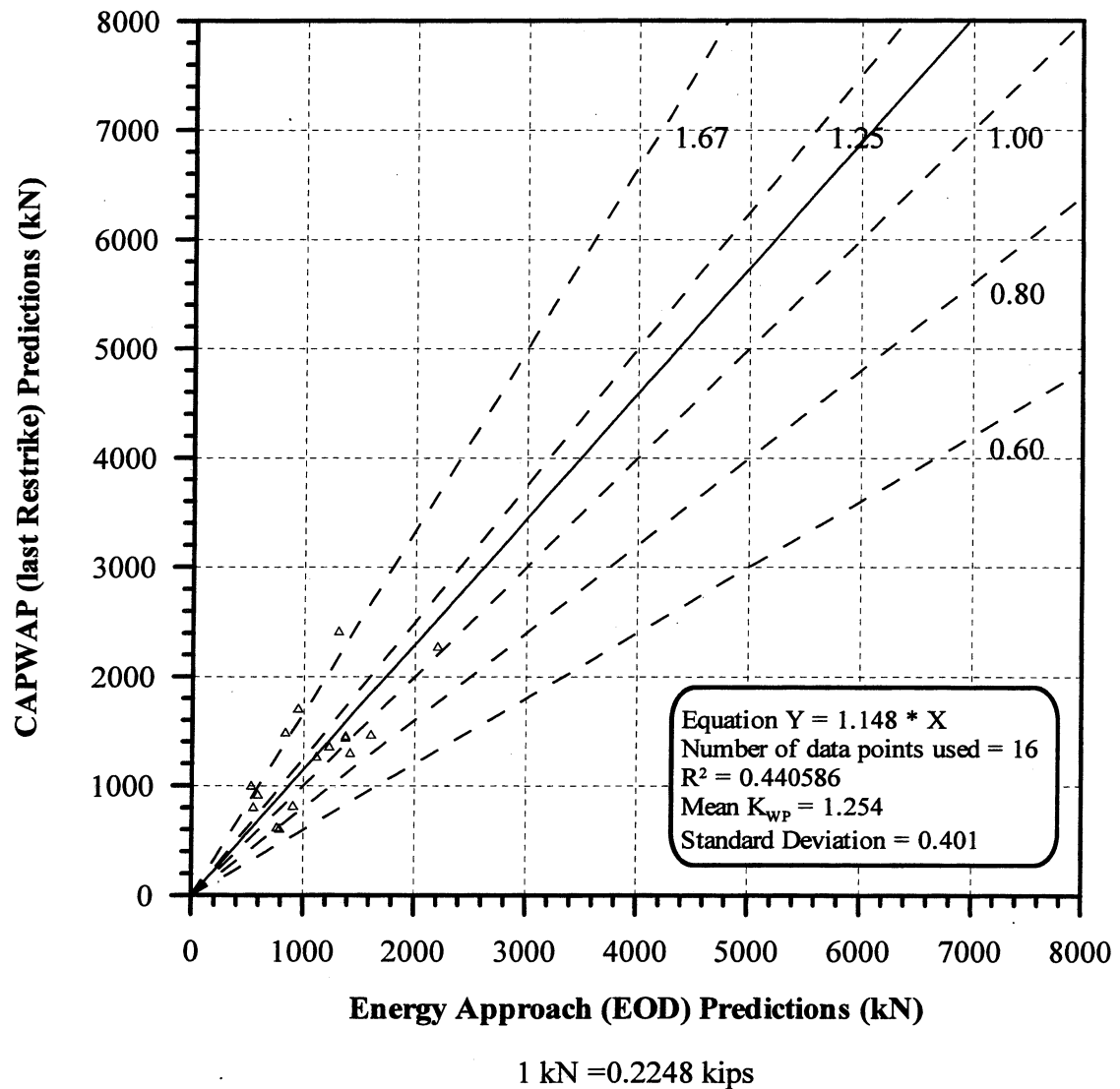


Figure 7.11. CAPWAP (last Restrike) Predictions vs. Energy Approach (EOD) Predictions for 16 PD2000 pile-cases with Blow Count < 16 BP10cm in sand & silt.

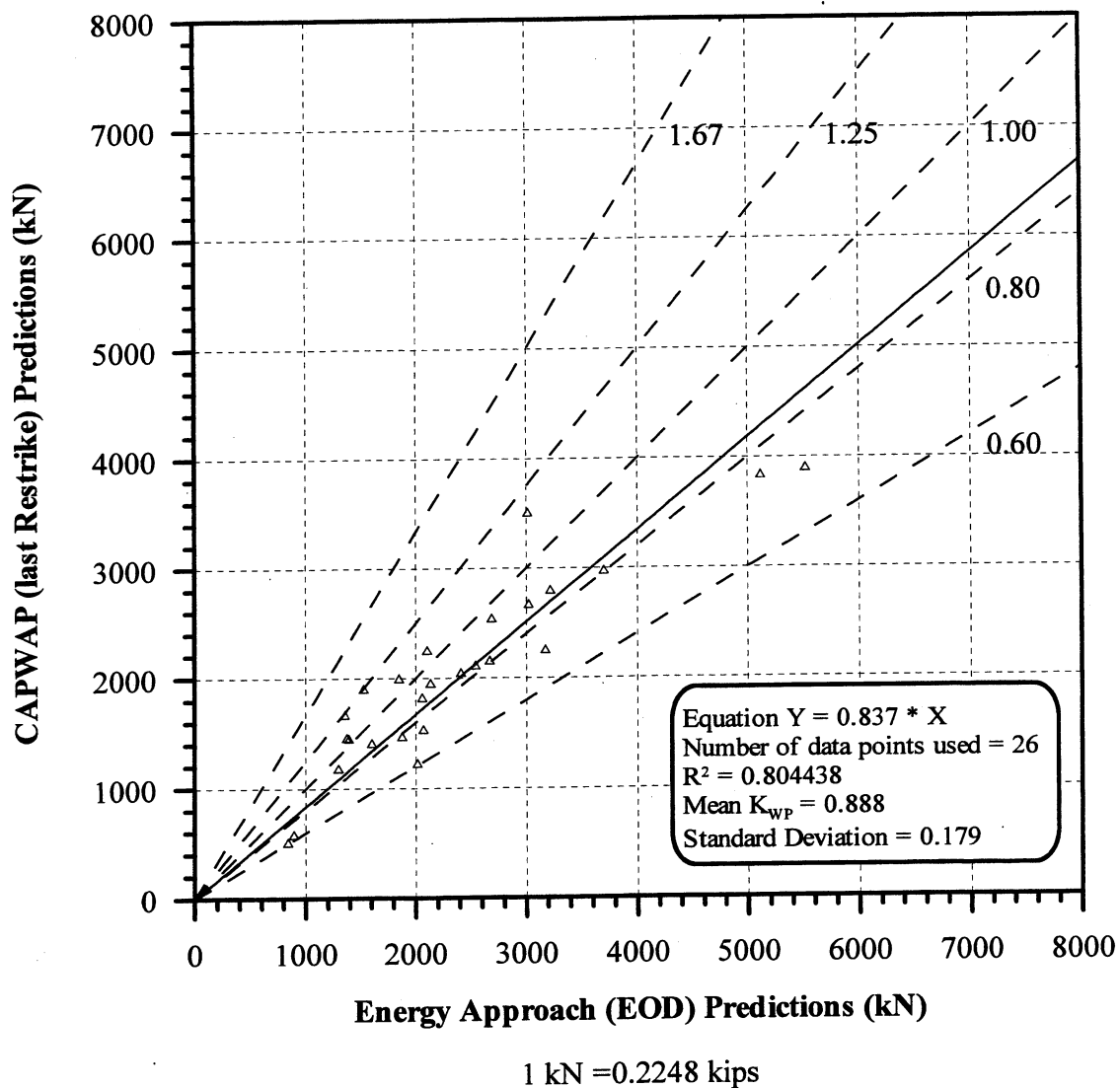


Figure 7.12. CAPWAP (last Restrike) Predictions vs. Energy Approach (EOD) Predictions for 26 PD2000 pile-cases with Blow Count ≥ 16 BP10cm in sand & silt.

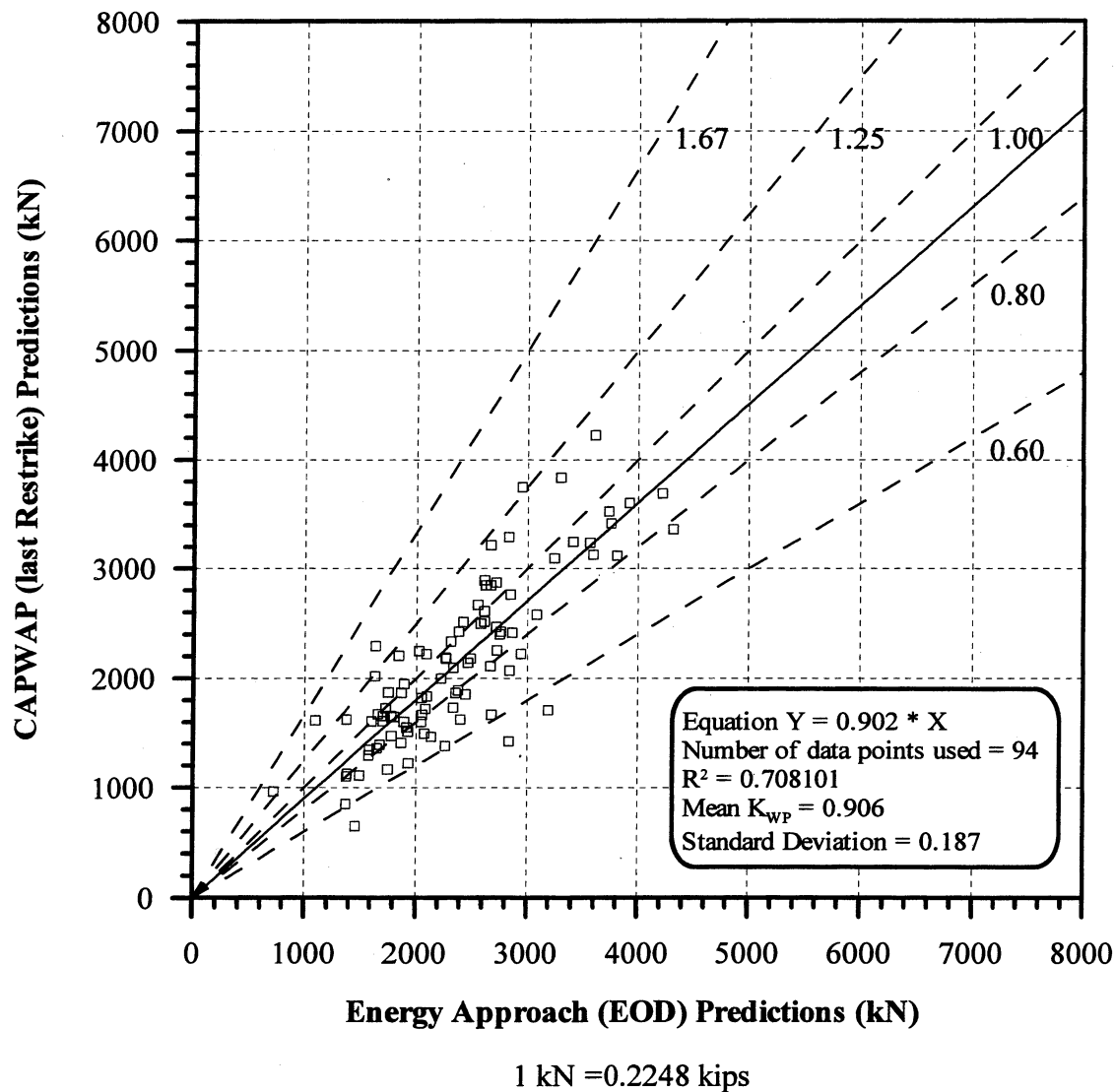


Figure 7.13. CAPWAP (last Restrike) Predictions vs. Energy Approach (EOD) Predictions for 94 PD2000 pile-cases in rock.

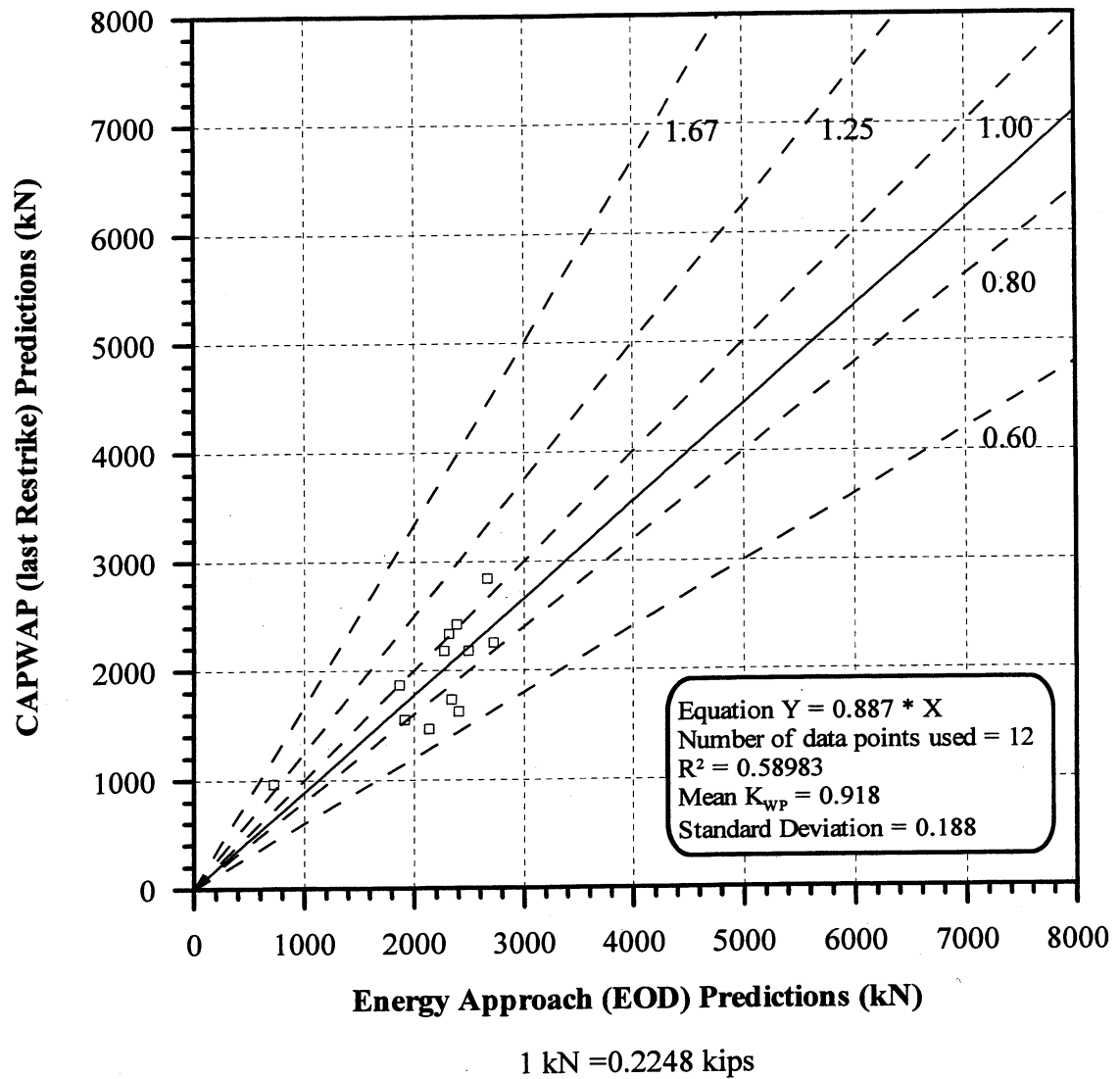


Figure 7.14. CAPWAP (last Restrike) Predictions vs. Energy Approach (EOD) Predictions for 12 PD2000 pile-cases with Blow Count < 16 BP10cm in rock.

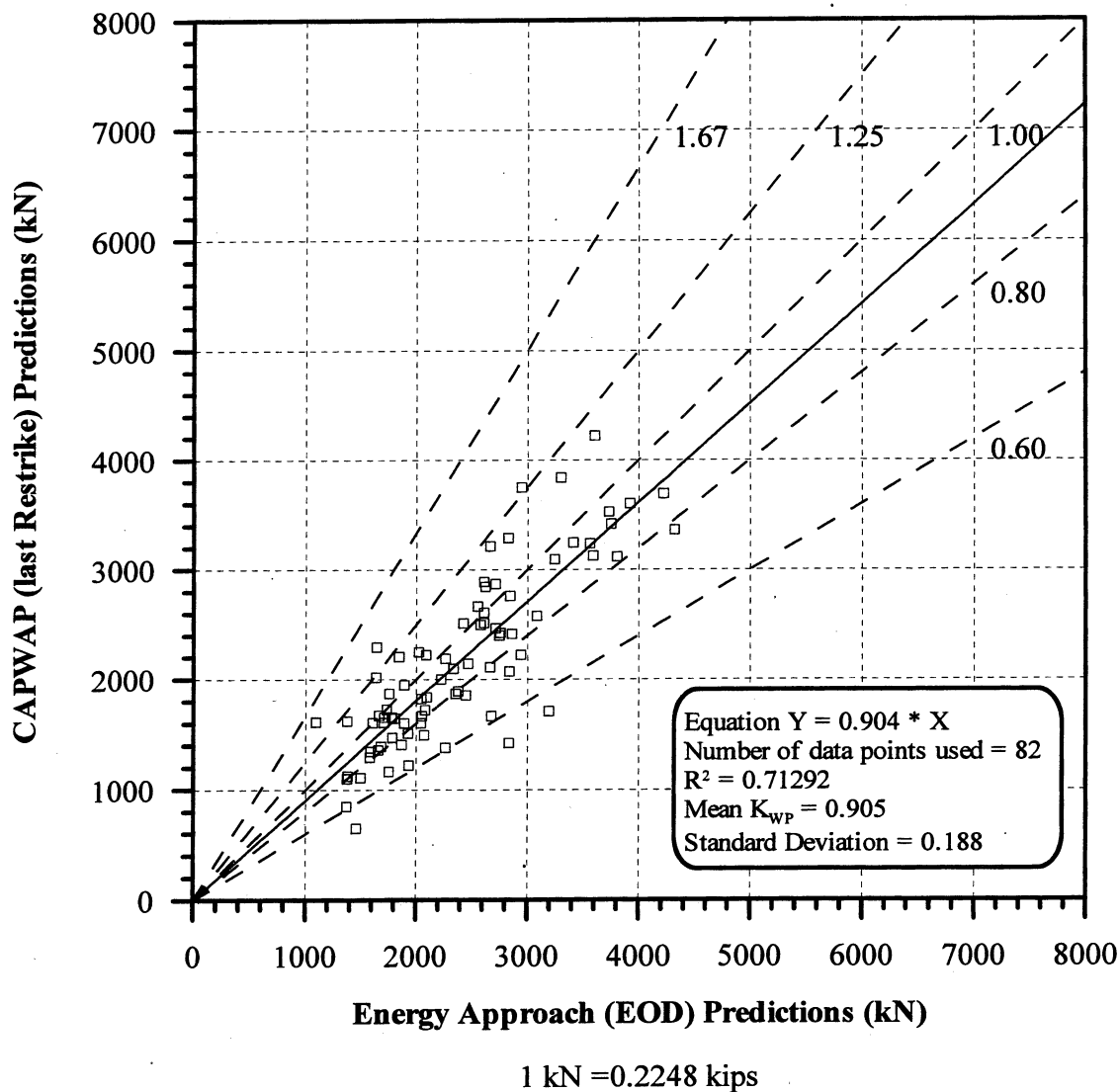


Figure 7.15. CAPWAP (last Restrike) Predictions vs. Energy Approach (EOD) Predictions for 82 PD2000 pile-cases with Blow Count ≥ 16 BP10cm in rock.

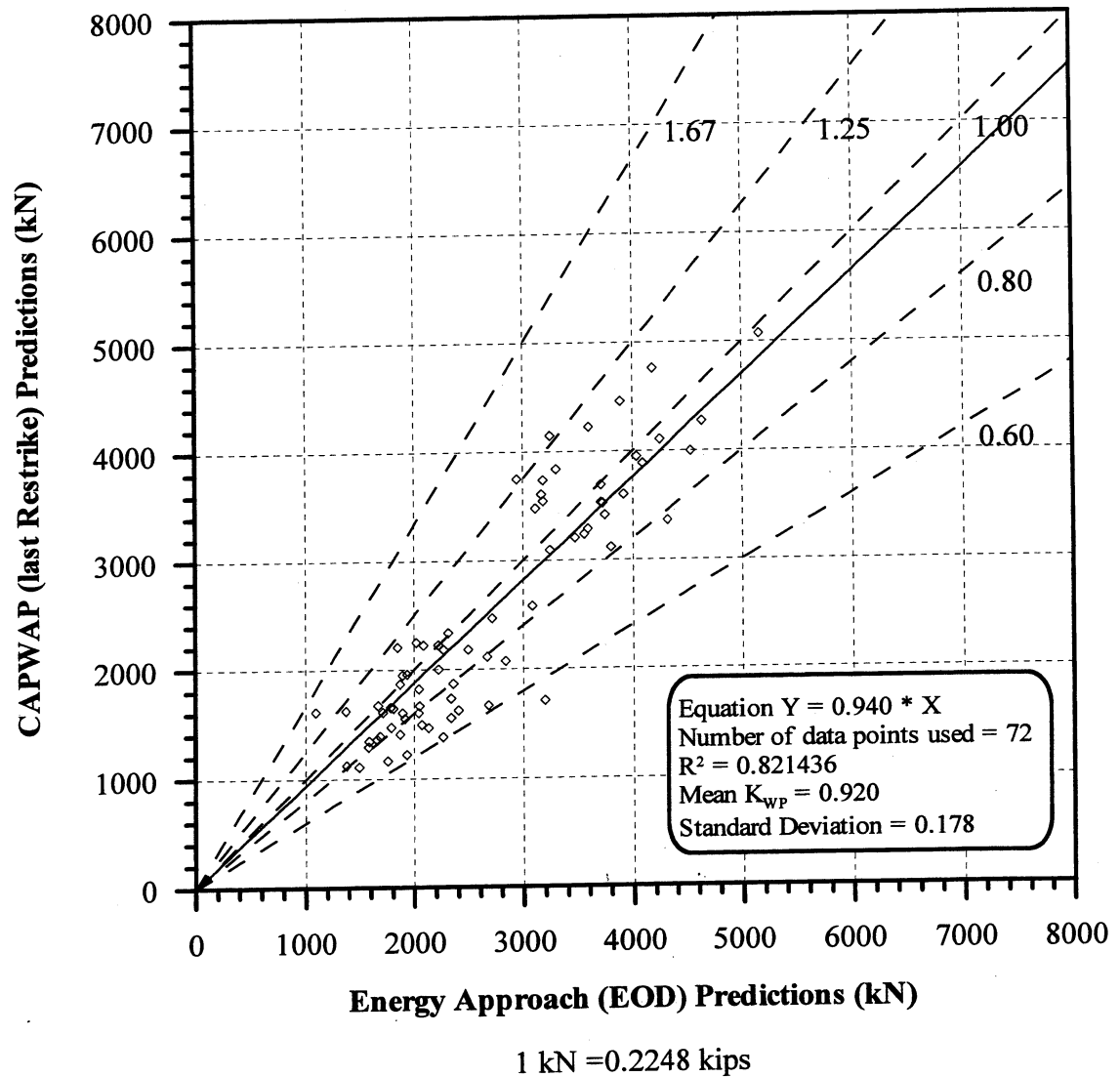


Figure 7.16. CAPWAP (last Restrike) Predictions vs. Energy Approach (EOD) Predictions for 72 PD2000 pile-cases with Boston Blue Clay.

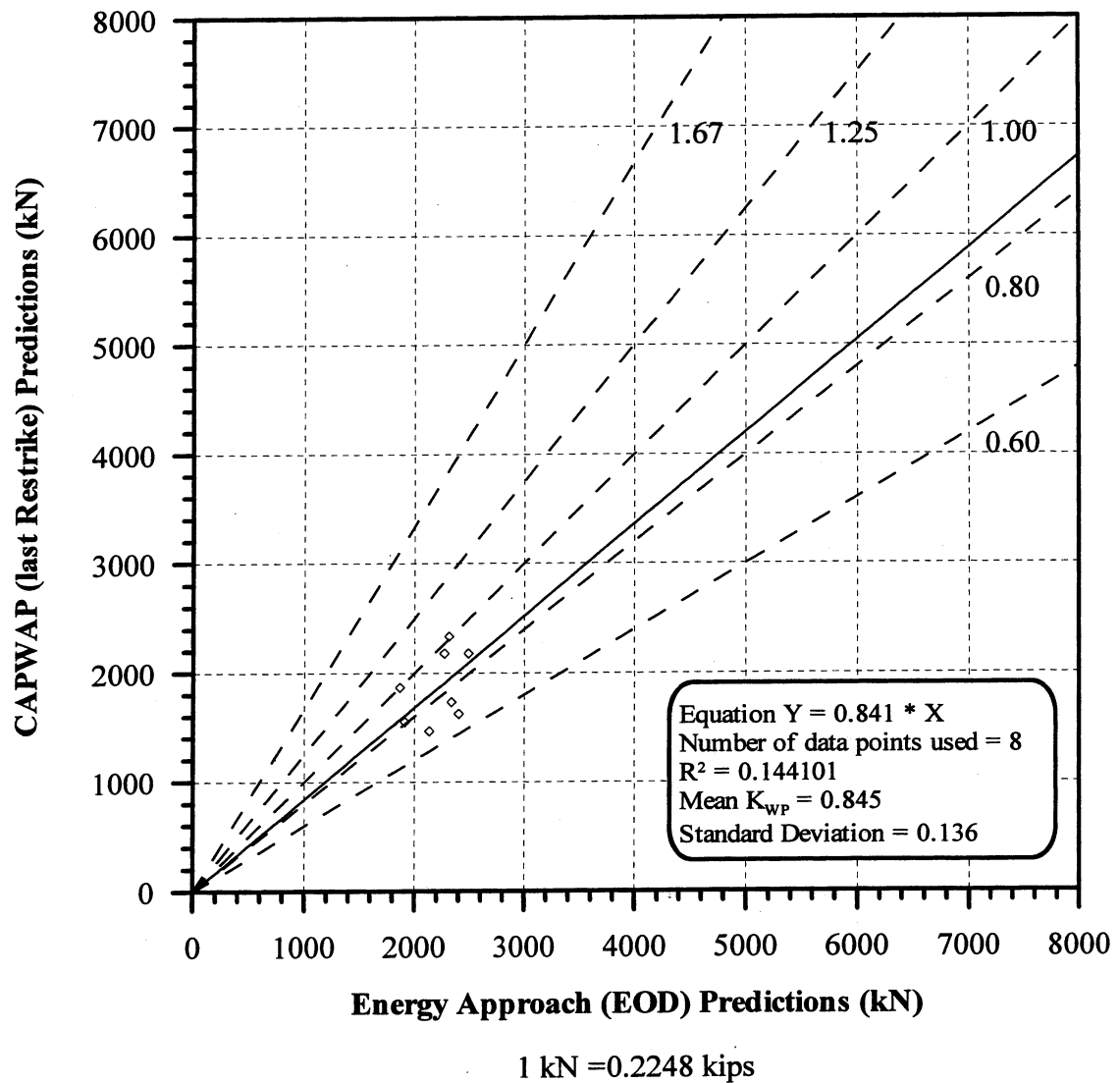


Figure 7.17. CAPWAP (last Restrike) Predictions vs. Energy Approach (EOD) Predictions for 8 PD2000 pile-cases with Blow Count < 16 BP10cm with Boston Blue Clay.

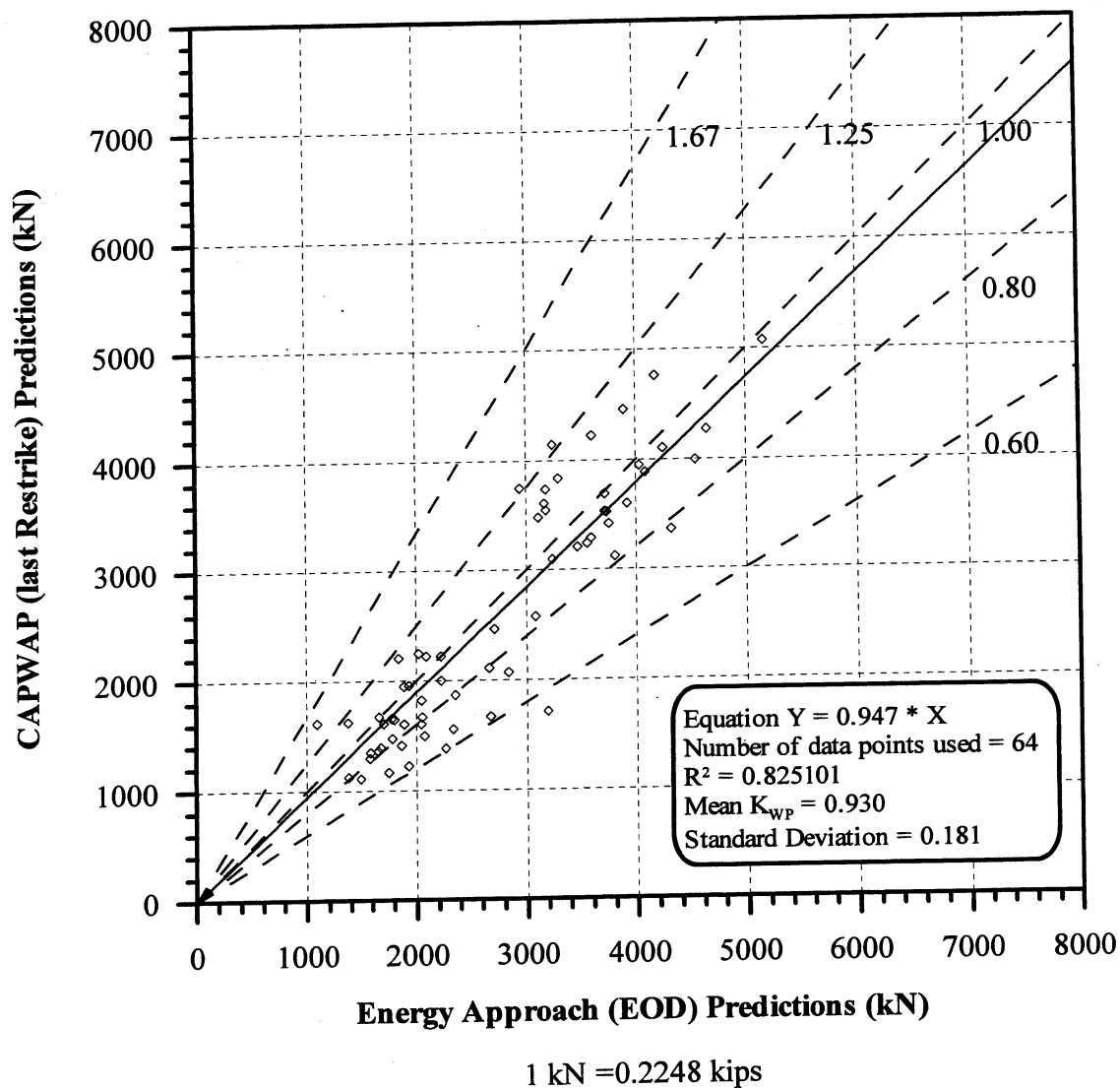


Figure 7.18. CAPWAP (last Restrike) Predictions vs. Energy Approach (EOD) Predictions for 64 PD2000 pile-cases with Blow Count ≥ 16 BP10cm with Boston Blue Clay.

CHAPTER 8

PILE CAPACITY GAIN WITH TIME

8.1 GENERAL

The concepts and information presented in this chapter makes use of data accumulated at the Geotechnical Engineering Research Laboratory under a long-term research project that investigates the gain of pile capacity with time. This work is not yet completed and thus far has been reported by Paikowsky et al. (1995), Paikowsky et al. (1996) and Paikowsky and Hart (1998). This chapter presents the relevant information concerning the pile capacity gain for design. For further details on the principles and procedures the reader is referred to one or all of the above references.

Data set PD/LTT2000 was initially reported by Paikowsky et al. (1995) as PD/LTT, has been modified in this work. The database contains fifteen piles that were dynamically monitored over time (EOD - End Of Driving and/or BOR - Beginning Of Restrike) and one load test to failure. Eight of the piles are pre-stressed concrete (PSC) ranging in widths from 250mm to 914mm, four of the piles are H-piles, two HP310×93 piles and two HP310×110 piles, and three of the piles are closed ended pipe piles (CEP) ranging in diameters from 245mm to 324mm. Table 8.1 and Table 8.2 summarize all the relevant data for the PD/LTT2000 pile cases, subdivided according to piles embedded predominately in clay (Table 8.1) and partially in clay

(Table 8.2). All dynamic capacities were determined through CAPWAP analysis (Case Pile Wave Analysis Program, Goble et al. 1970, GRL Inc., 1995). To allow comparison between the different cases, the data were presented in the form of capacity ratio versus the time on a logarithmic scale. The capacity ratio was determined by dividing the obtained CAPWAP capacity by the static load test capacity based on Davisson's failure criterion. The static load test capacity was not necessarily the maximum capacity, especially for the cases where the pile was dynamically monitored after the load test.

8.2 ANALYSIS OF PILE CAPACITY GAIN WITH TIME

Penetration of piles in fine-grained soils causes compression and disturbance, resulting in soil resistance during driving that differs from the long-term pile capacity. Although factors such as thixotropy and aging contribute to this phenomenon, the most significant cause for gain of capacity with time is associated with the migration of pore water. Measurements carried out on a model (Paikowsky & Hart 2000) and full-scale piles (Paikowsky & Hajduk 1999, 2000) show that pore pressure at magnitudes similar to the total soil pressures create in clays around the pile's shaft zones of about zero effective stresses, resulting in almost a complete loss of frictional resistance. Paikowsky et al. (1995, 1996) examined the static and dynamic gain of capacity with time based on radial consolidation; a normalization process was followed, allowing for a comparison between different pile sizes. Table 8.3 presents a summary of parameters describing the pile capacity gain with time based on static and dynamic testing. The presented data shows that while the rate of capacity gain

(normalized to the maximum capacity vs. time on log scale) is similar when based on static or dynamic measurements ($C_{gt} = 0.389$ and $C_{gtd} = 0.348$, respectively). The associated time for achieving 75% of the maximum capacity (normalized for all piles to 254mm (1ft) diameter) is about 20 times greater for the static data compared to the dynamic based data. In other words, dynamic testing (namely CAPWAP) while following the physical behavior of capacity gain, exhibit this gain much faster than the actual gain monitored by the static load test results.

Figure 8.1 presents the capacity gain curves based on dynamic measurements for the seven piles embedded in mostly clay, adjusted according to pile size. Also included on this graph are the equations of the best-fit lines, their corresponding coefficient of determination, and the number of points used for each curve. The slopes of the best-fit lines, termed C_{gtd} , represent the rate at which the pile gains capacity. The pile from Denmark (DN1) drastically shifted outside of the expected band. This pile was first load tested 29 days after its installation. This is a significant amount of time that elapsed between driving and testing for a 250mm square PSC pile. The data available, therefore, captures only the end of the capacity gain process and not the major event. As a result it is believed that the t_{75} value (the time needed for 75% of the capacity gain to be reached) does not reflect the actual time needed for this pile to gain 75% of its capacity. The t_{75} values ranged from 12.4 hours to 189.8 hours (8 days) with a mean value of 45.4 hours and a standard deviation of 64.1 hours. After eliminating the data from Denmark, the standard deviation substantially decreases to 7.9 hours with a mean of 21.3 hours.

The capacity gain curves for the eight piles partially embedded in clay are presented in Figure 8.2, adjusted according to pile size. Also included on this graph are the equations of the best-fit lines where the slope represents the rate at which the pile gains capacity, their corresponding coefficient of determination, and the number of points used for each curve. The t_{75} values ranged from 2.2 hours to 83.2 hours (3.5 days) with a mean value of 25.0 hours and a standard deviation of 28.4 hours. The two piles with t_{75} values of zero, also shown in Table 8.2, are not realistic. The unrealistic results are due to a combination of two factors. The first being that the dynamic tests over predicted the pile capacity compared to the actual static load test results, which causes a shift of the best-fit line upward. The other cause is that the rate at which the pile gains capacity is high, possibly due to the fast drainage through the sand and silt layers, which in turn creates a problem when attempting to linear interpolate back to the t_{75} value, at an adjusted time of one hour the K_{SW} value is greater than 0.75. This means that the time for the pile to gain 75 percent of the actual pile capacity is less than one hour. In a practical way, when the pile is embedded in mixed layers the sand and silt layers diminish the pile capacity gain with time phenomenon and need to be evaluated in a more detailed approach than the one presented.

8.3 INTERMEDIATE CONCLUSIONS

Since this data set is of limited size (especially if the two open-ended 36" \times 5" (0.914 m \times 0.127 m) PSC cylindrical piles (TP6 and TP7) are eliminated), it is difficult to make definitive conclusions regarding the applicability of the size/time

adjustment process based solely on the presented data. The practical conclusions offered for the presented data are:

- (i) actual gain of capacity is much slower than that exhibited by the dynamic methods,
- (ii) scheduling of construction or testing based on capacity gain should consider the reason for time evaluation (i.e. static loading in early construction or dynamic testing as part of quality control), and,
- (iii) at present, the dynamic methods evaluation should concentrate on the long term pile capacity.

Considering all of the above the following simplified relationships can be offered to determine the time elapsed from driving to the time for 75% of the maximum capacity:

For piles embedded completely in clay:

- For static testing purpose: $t_{75\%} = 1540 \times r^2$ (8.1)

- For dynamic testing purpose: $t_{75\%} = 85 \times r^2$ (8.2)

For piles embedded in alternating soil conditions (granular and cohesive):

- For dynamic testing purpose: $t_{75\%} = 39 \times r^2$ (8.3)

Where: $t_{75\%}$ = time to reach 75% of maximum capacity in hours
 r = pile radius in feet.

For example a 1 ft diameter pile in a clay deposit requires approximately a 1-day (21 hrs) delay for a restrike to present about 75% of the maximum capacity. A 2ft diameter pile will require a 3.5-day delay for a restrike under similar conditions.

The relationships for the piles embedded completely in clay were calculated using the t_{75} values presented in Table 8.3. The t_{75} value for the piles embedded in alternating soil conditions was determined by passing the best-fit line through all of the data points plotted in Figure 8.2 and using the resulting equation of that line. The obtained slope of the best-fit line (C_{gtd}) was 0.255 with a y-intercept of 0.499. The calculated t_{75} value was therefore 9.65 hours. The above relationships (equations 8.1-8.3) were determined by using the equation proposed by Paikowsky and Whitman (1990):

$$\frac{t_1}{t_2} = \left(\frac{r_1}{r_2} \right)^2 \quad (8.4)$$

Where:

t_1	=	elapsed time since driving for a pile of interest
r_1	=	radius of pile of interest
t_2	=	actual time since driving for a known pile
r_2	=	radius of known pile

For piles other than closed circular shapes, an equivalent radius (r_2) can be determined. In the presented analysis, the radius of open-ended pipe piles was taken as one-half of the outside diameter. For the square box shape, half of one side represents the radius. The depth from the outer edge of one flange to the outer edge of the other flange was considered the equivalent radius for H-piles.

Table 8.1. Soil properties, pile type, and relevant information for dynamic capacity gain - Data Set PD/LTT2000, predominately clay embedment (Paikowsky et al., 1995).

Location	Soil Type		Pile Type	Depth (m)	Davisson Capacity (kN)	t_{75}^* (hrs)	C_{gtd}
	Shaft	Tip					
Baton Rouge, LA	silty clay	silty sand	PSC 61 cm sq	25.7	1779	12.4	0.243
Denmark	sandy clay	clayey chalk	PSC 25cm sq	21.0	1250	189.8	0.332
Kenner, LA	clay	sand	PSC 61 cm sq	25.0	1842	29.3	0.332
Kenner, LA	clay	sand	PSC 76 cm sq	25.3	2273	32.7	0.341
Kenner, LA	clay	sand	PSC 76 cm sq	25.3	2469	19.5	0.315
Kenner, LA	clay	sand	91.4 cm ×; 12.7 cm PSC cyl	25.0	2411	16.4	0.431
Kenner, LA	clay	sand	91.4 cm ×; 12.7 cm PSC cyl	24.7	2402	17.6	0.439
Avg:						45.4	0.348
Stdev:						64.1	0.068
w/out Denmark, Avg:						21.3	
w/out Denmark, Stdev:						7.9	

Table 8.2. Soil properties, pile type, and relevant information for dynamic capacity gain - Data Set PD/LTT2000, partially in clay embedment.

Location	Soil Type		Pile Type	Depth (m)	Davisson Capacity (kN)	t ₇₅ (hrs)	C _{gtd}
	Shaft	Tip					
Jones Is., WI	sa-si-clay	silty sand	HP310×;93	47.5	1343	25.6	0.396
Jones Is., WI	sa-si-clay	silty sand	HP310×;93	43.5	890	0*	0.171
Newbury, MA	sa-si-clay	sand	CEP 324mm	21.1	667	41.2	0.455
Newbury, MA	sa-si-clay	sand	PSC 356mm sq	21.3	783	0*	0.134
Jones Is., WI	silty clay	silty clay	CEP 245mm	43.4	2936	83.2	0.139
Jones Is., WI	sa-si-clay	silty sand	CEP 324mm	37.5	2909	34.4	0.255
Newbury, MA	sa-si-clay	glacial till	HP310×;110	34.1	1806	2.2	0.103
Newbury, MA	sa-si-clay	silty sand	HP310×;110	33.1	2126	13.7	0.158
Avg:						25.0	0.226
Stdev:						28.4	0.131

*These two pile-cases are ones in which the dynamic predictions were considerably larger than the static load test results.

Table 8.3. Summary of static and dynamic based capacity gain data sets (Paikowsky et al. 1995).

	Static Data Sets LTT and PUT/LTT		Dynamic Data Set PD/LTT		All Data	
	C_{gtd}	t_{75}^*	C_{gtd}	t_{75}^{**}	C_{gtd}	t_{75}^{**}
No.	15	5	7	6	22	11
Average	0.389	385.0	0.348	21.3	0.376	186.6
Standard Deviation	0.119	226.3	0.068	7.9	0.106	237.9

* closed-ended piles only

** excluding the case from Denmark

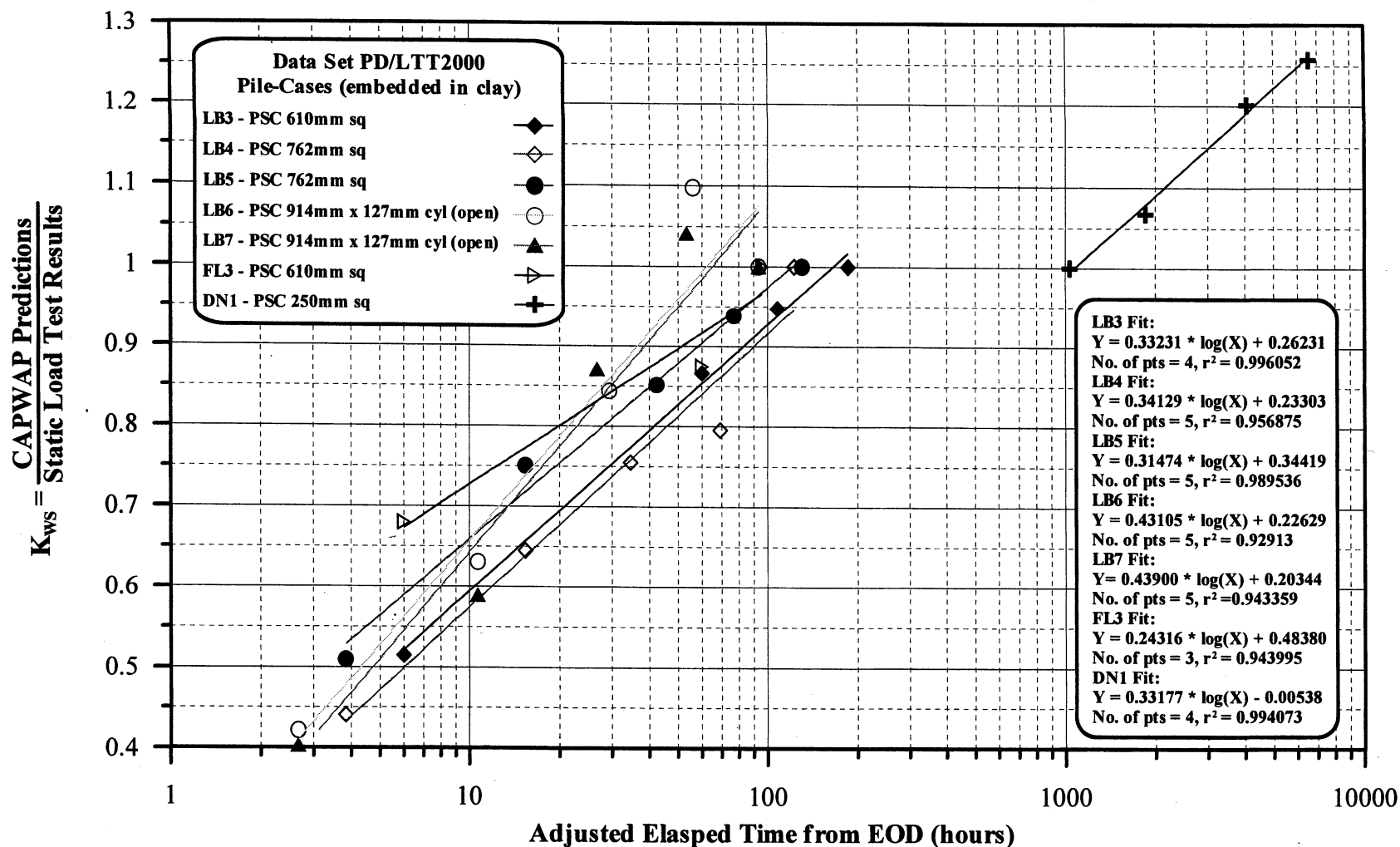


Figure 8.1. K_{ws} values vs. log - Time for PD/LTT2000 pile-cases with multiple Restrikes with the majority of the skin friction coming from the clay layers (Paikowsky et al., 1995).

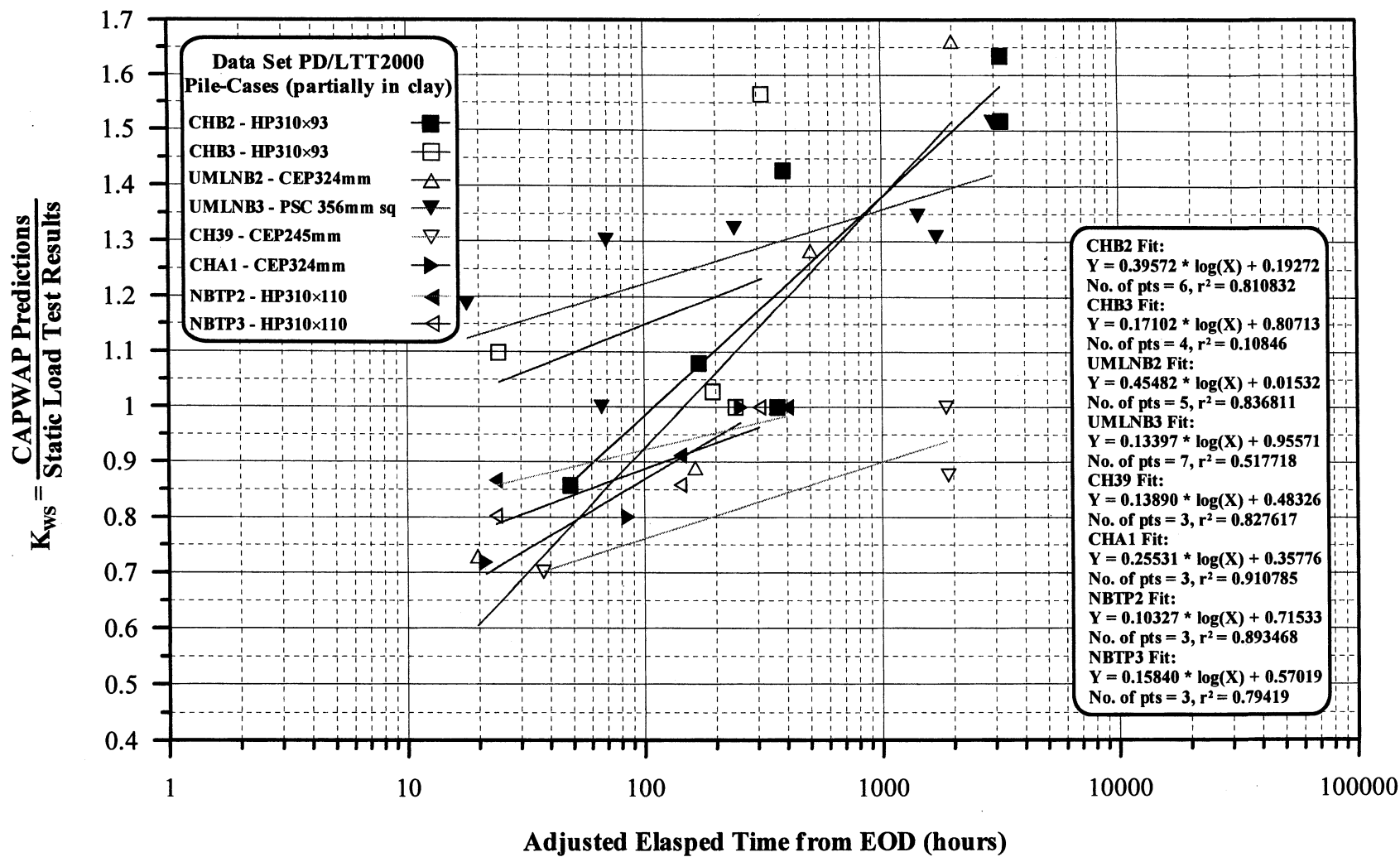


Figure 8.2. K_{ws} values vs. log - Time for PD/LTT2000 pile-cases with multiple Restrikes partially in clay.

CHAPTER 9

CALCULATION OF RESISTANCE FACTORS

9.1 METHODOLOGY

This section is based on contributions provided by Professor Bilal M. Ayyub and Gregory B. Baecher of the Department of Civil Engineering at the University of Maryland. The present project calibrates LRFD partial safety factors using the First-Order Reliability Method (FORM), (Hasofer and Lind, 1974). FORM can be used to assess the reliability of a pile with respect to specified limit states, and provides a means for calculating partial safety factors ϕ and γ_i for resistance and loads, respectively, against target reliability levels, β_0 . FORM requires only the first and second moment information on resistances and loads (i.e., means and standard deviations), and an assumption of distribution type (e.g., Normal, lognormal, etc.). The entire calibration process is presented in Figure 9.1.

In design practice, there are usually two types of limit states: ultimate limit states and serviceability limit state. Each can be represented by a performance function of the form,

$$g(X) = g(X_1, X_2, \dots, X_n) \quad (9.1)$$

in which X is a vector of basic random variables (X_1, X_2, \dots, X_n) for strengths and loads. The performance function $g(X)$ is sometimes called the limit state function. It relates

the random variables for the limit-state of interest. The limit state is defined when $g(\mathbf{X}) = 0$, and therefore, failure occurs when $g(\mathbf{X}) < 0$. The reliability index β is defined as the distance from the origin of the space of basic random variables (X_1, X_2, \dots, X_n) to the failure surface at the most probable failure point. The most probable failure point is that point on the limit state function at which the probability density of the basic random variables is greatest. This is also called, the design point. This relationship can also be used to back calculate representative values of the reliability index β from current design practice.

The computational scheme for determining β using FORM is the following:

1. Assume a design point x_i^* and obtain its corresponding point, $x_i'^*$ in a reduced coordinate system using the normalizing transformation:

$$x_i'^* = \frac{x_i^* - \mu_{X_i}}{\sigma_{X_i}} \quad (9.2)$$

where μ_{X_i} = mean value of the basic random variable X_i , and σ_{X_i} = standard deviation. The mean values of the basic random variables are often used as initial guesses for the design points,

2. For non-normal basic random variables, evaluate the equivalent normal distributions at the design point using:

$$\mu_X^N = x^* - \Phi^{-1}(F_X(x^*))\sigma_X^N \quad (9.3)$$

and

$$\sigma_X^N = \frac{\left(\Phi^{-1} \left(F_X(x^*) \right) \right)}{f_X(x^*)} \quad (9.4)$$

where μ_X^N = mean of the equivalent normal distribution, σ_X^N = standard deviation of the equivalent normal distribution, $F_X(x^*)$ = original cumulative distribution function (CDF) of X_i evaluated at the design point, $f_X(x^*)$ = original probability density function (PDF) of X_i evaluated at the design point, $\Phi(\cdot)$ = CDF of the standard normal distribution, and $\phi(\cdot)$ = PDF of the standard normal distribution.

3. Set $x_i^* = -\alpha_i^* \beta$, in which the α_i^* are direction cosines computed as,

$$\alpha_i^* = \frac{\left(\frac{\partial g}{\partial x_i} \right)_*}{\sqrt{\sum_{i=1}^n \left(\frac{\partial g}{\partial x_i} \right)_*^2}} \quad \text{for } i = 1, 2, \dots, n \quad (9.5)$$

where

$$\left(\frac{\partial g}{\partial x_i} \right)_* = \left(\frac{\partial g}{\partial x_i} \right)_* \sigma_{X_i}^N \quad (9.6)$$

4. With α_i^* , $\mu_{X_i}^N$, and $\sigma_{X_i}^N$ now known solve for β in the limit state function,

$$g \left[(\mu_{X_1}^N - \alpha_{X_1}^* \sigma_{X_1}^N \beta), \dots, (\mu_{X_n}^N - \alpha_{X_n}^* \sigma_{X_n}^N \beta) \right] = 0 \quad (9.7)$$

5. Using the β obtained from step 4, a new design point is obtained from:

$$x_i^* = \mu_{X_i}^N - \alpha_i^* \sigma_{X_i}^N \beta \quad (9.8)$$

6. Repeat steps 1 to 5 until it converges. This reliability index is the shortest distance to the failure surface from the origin in the reduced coordinates.

To estimate partial safety factors on resistance and loads, such as those found in the design format, consider that at the failure point $(R^*, L_1^*, \dots, L_n^*)$, the limit state is given by

$$g = R^* - L_1^* - \dots - L_n^* = 0 \quad (9.9)$$

or, in a general form

$$g(X) = g(x_1^*, x_2^*, \dots, x_n^*) = 0 \quad (9.10)$$

For given target reliability index β_0 ; probability distributions, means and standard deviations of load effects; and probability distribution, mean and coefficient of variation of resistance; partial safety factors can be determined by the iterative solution. The mean value of the resistance and the design point are then used to compute the mean required partial design safety factors as,

$$\phi = \frac{R^*}{\mu_R} \quad (9.11)$$

$$\gamma_i = \frac{L_i^*}{\mu_{L_i}} \quad (9.12)$$

In developing design code provisions for piles, it is necessary to follow the current design practice to ensure consistent levels of reliability over various pile types. Calibrations of existing design codes are needed to make the new design formats as simple as possible and to put them in a form that is familiar to users or designers. For

a given reliability index β and probability characteristics for the resistance and load effects, the partial safety factors determined by the FORM approach might be different for different failure modes for the same or differing component. For this reason, calibration of the calculated partial safety factors (PSF's) is important in order to maintain the same values for all loads at different failure modes. In the case of geotechnical codes, the calibration of resistance factors is performed for a set of load factors already specified in the structural code. Thus, the load factors are fixed. In this case, the following algorithm is used to determine resistance factors:

1. For a given value of the reliability index β , probability distributions and moments of the load variables, and the coefficient of variation for the resistance, compute mean resistance R using FORM
2. With the mean value for R computed in step 1, the partial safety factor ϕ is revised as:

$$\phi = \frac{\sum_{i=1}^n \gamma_i \mu_{L_i}}{\mu_R} \quad (9.13)$$

where μ_{L_i} and μ_R are the mean values of the loads and strength variables, respectively, and $\gamma_i, i = 1, 2, \dots, n$, are the given set of load factors.

9.2 LEVEL OF TARGET RELIABILITY

9.2.1 Overview

The utilization of the LRFD method requires the discussion of a target reliability which determines the probability of failure and hence the magnitude of the

resistance factors. The probability of failure represents the probability for the condition in which the resistance multiplied by the resistance factor will be less than the load multiplied by the load factors. An approximate relationship between the two for a lognormal distribution was presented by Rosenbleuth and Estava (1972): $p_f = 460 \exp(-4.3)$ and is presented in Table 9.1. Unfortunately, although Rosenbleuth and Estava say that the approximation pertains to log normal distributions (because they use the mean of the logs and the standard deviation of the logs to calculate β), the approximation is not so accurate below β of about 2.5. Table 9.2 prepared by Professor Gregory B. Baecher provides the comparison between the "exact" numbers to the approximation and suggests significant errors, especially in our zone of interest ($\beta = 2$ to 3). The "exact" numbers will be used in this research.

9.2.2 General Discussion

a) Target Reliability Levels

The discussion presented in this section was contributed by Professor Bilal M. Ayyub. Both codified and direct reliability-based design requires that a set of target reliability levels be defined. The selection of these levels is a difficult task (Payer *et al.* 1994). These values are not readily available and need to be generated or selected. Also, these levels might vary from one industry to another due to factors such as the implied reliability levels in currently used design practices by industries, failure consequences, public and media sensitivity, or response to failures that can depend on the industry type, types of users or owners, design life of a structure, and other political, economic, and societal factors. Two approaches for generating target

reliability levels were used by other industries. These approaches are: 1) calibrated reliability levels that are implied in currently used codes, and 2) cost benefit analysis.

The first approach was commonly used to develop reliability-based codified design such as the LRFD format. The target reliability levels according to this approach are based on calibrated values of implied levels in a currently used design practice. The argument behind this approach is that a code represents a documentation of an accepted practice. Therefore, since it is accepted, it can be used as a launching point for code revision and calibration. Any adjustments in the implied levels should be for the purpose of creating consistency in reliability among the resulting designs according to the reliability-based code. Using the same argument, it can be concluded that target reliability levels used in one industry might not be fully applicable to another industry.

The second approach is based on cost-benefit analysis. This approach was used effectively in dealing with designs for which failures result in only economic losses and consequences. Since structural failures might result in human injury or loss, this method might be very difficult to use because of its need for assigning a monetary value to human life. Although this method is logical on an economic basis, its main shortcoming is its need to measure the value of human life. Consequently, the first approach is favored for this study and is discussed further in the following sections.

b) *Calibrated Reliability Levels*

A number of efforts in which target reliability levels (i.e., safety indices or β values) were developed for the purpose of calibrating a new generation structural design code to an existing code have been completed.

According to *Structural Reliability: Analysis and Prediction*, Melchers (1987), the general methodology for code calibration based on specific reliability theories, using second-moment reliability concepts, is discussed by Allen (1975), Baker (1976), CIRIA (1977), Hawrenenk and Rackwitz (1976), Guiffre and Pinto (1976), Skov (1976), Ravindra and Galambos (1978), Ellingwood *et al.* (1980), Lind (1976), and Ravindra *et al.* (1969). The key steps in the process, following the discussion in Melchers (1987), are as follows. First, the scope of the design situation must be identified (e.g., material, loads, structural type) and narrowed to fit the specific situation. Next, a design space reflecting all key variables (nominal yield stresses, range of applied loads, continuity conditions, etc.) is chosen and divided into discrete zones. These zones are used to develop typical designs using existing codes. Next, performance functions for the failure modes, expressed in terms of the basic variables, are defined. The statistical properties (distributions, means, variances, and averagepoint-in-time values) of the basic variables are used for the determination of the β indices using a specified method for reliability analysis (e.g., moment methods).

Next, each of the designs obtained above, together with the performance functions and the statistical data derived above, are used to determine β for each zone. Repeated analyses will yield the variation of β . From these data, a weighted β is

obtained and used as a target reliability level β_t . Melchers notes that frequently the information is insufficient for this determination and one must make a "semi-intuitive" judgment in selecting β_t values. For example, recognizing a different β value is used for dead, live, and snow load combinations as compared to, dead, live, and wind load combinations or dead, live, and earthquake load combinations. Divergent β_t values should be corrected by means of the partial factor(s) on material strength or resistance (e.g., through the strength reduction factor).

While the specific reliabilities will be a function of the strength criteria needed for specific materials and load combinations within designated structures, it is useful to have an indication of the range of possible target reliability levels. Ellingwood *et al.* (1980) present ranges for reliability levels for metal structures, reinforced and prestressed concrete structures, heavy timber structures, and masonry structures, as well as discussions of issues that should be considered when making the calibrations. Table 9.3 provides typical values for target reliability levels. This table was developed based on values provided by Ellingwood *et al.* (1980). The target reliability levels shown in Table 9.4 were also used by Ellingwood and Galambos (1982) to demonstrate the development of partial safety factors.

Reed and Brown (1992) provide a summary of the target reliability levels used in the AISC LRFD specifications. In addition to the values provided in Tables 9.3 and 9.4, values for high strength bolts in tension and shear were given as 5.0 to 5.1, and 5.9 to 6.0, respectively. Also, a value for fillet welds of 4.4 is given. Detailed information about these values are provided by Galambos (1989).

Moses and Verma (1987) suggested target reliability levels in calibrating bridge codes (i.e. AASHTO Specifications). Assuming that bridge spans of less than 100 ft are most common, a β_t of 2.5 to 2.7 is suggested for redundant bridges, and a β_t of 3.5 for non-redundant bridges.

Wirsching (1984) estimated the safety index implied by the API specifications API RP2A (1989) for fixed offshore structures in fatigue of tubular welded joints to be 2.5. He reported that this value is on the low end, because of the reference wave values.

Madsen *et al.* (1986) discuss target reliability levels that were used by the National Building Code of Canada (1977) for hot-rolled steel structures. The target reliability values were selected as follows: $\beta_t = 4.00$ for yielding in tension and flexure, $\beta_t = 4.75$ for compression and buckling failure, and $\beta_t = 4.25$ for shear failures. These values are larger than the values in Tables 9.3 and 9.4 because they reflect different environmental loading conditions and possibly different design life. Also, the Canadian Standard Association presented the following target failure probabilities for developing design criteria for offshore installation in Canadian waters (Mansour *et al.* 1994): 10^{-5} per year for failures that result in great loss of life or a high potential for environmental damage; and 10^{-3} per year for failures that result in small risk to life or a low potential for environmental damage.

Madsen *et al.* (1986) also discuss target reliability levels that were used by the Nordic Building Code Committee (1978). The target reliability values were selected depending on the failure consequences of a building in the following ranges: $\beta_t = 3.1$

for less serious failure consequences, $\beta_t = 5.2$ for very serious failure consequences, and $\beta_t = 4.265$ for common cases.

For ship structures, A. S. Veritas (Lotsberg, 1991), a subsidiary of Det Norske Veritas, recommended target safety indices that depend on failure consequences and failure types. Table 9.5 provides a summary of these values. These values are annual probabilities. Therefore, they need to be multiplied by a design life to obtain the needed target values.

9.2.3 Geotechnical Perspective

The review provided in section 9.2.2 suggests that typical target reliability for members and structures relevant to bridge construction varies between 1.75 to 3.0 with a target reliability of 2.5 to 2.7 for relevant bridges.

Barker et al. (1991) have provided the following regarding target reliability index for driven piles (p.A-51): *"Meyerhof (1970) showed that the probability of failure of foundations should be between 10^{-3} and 10^{-4} , which corresponds to values of β between 3 and 3.6. The reliability index of offshore piles reported by Wu, et al. (1989) is between 2 and 3. They calculated that the reliability index for pile systems is somewhat higher and is approximately 4.0, corresponding to a lifetime probability of failure of 0.00005. Tang et al. (1990) reported that offshore piles have a reliability index ranging from 1.4 to 3.0.*

Reliability indices for driven piles are summarized in Table 5.4 (see Table 9.6). Values of β between 1.5 and 2.8 are generally obtained for the lognormal procedure. Thus a target value of β between 2.5 to 3 may be appropriate. However,

piles are usually used in groups. Failure of one pile does not necessarily imply that the pile group will fail. Because of this redundancy in pile groups, it is felt that the target reliability index for driven piles can be reduced from 2.5 to 3.0 to a value between 2.0 and 2.5."

Zhang et al. (2001) presented a method to evaluate the reliability of axially loaded pile groups designed using the traditional concept of group efficiency, along the line of load and resistance factor design (LRFD). Group effects and system effects were identified to be the major causes that led to a significantly greater observed reliability of pile foundations than calculated reliability of single piles. In group effect Zhang et al. referred to the combined action of any number of piles vs. a single pile. A system effect is the contribution of the superstructure to the load distribution and resistance as related to the stiffness of that structure. The calculated probability of failure of pile groups was found to be one to four orders of magnitude smaller than that of single piles, depending on significance of system effects. Based on their study Zhang et al. (2001) state that the target reliability index, β_T , for achieving a specified reliability level should be different for an isolated single pile, an isolated pile group, and a pile system. They give the following recommendations based on their research:

- (i) A β_T value as low as 1.7 may be adopted for design of pile groups if a system bias factor, λ_x , of 2.0 is justifiable.
- (ii) A β_T value in the range of 2.0 to 2.5 may be sufficient for pile groups with a λ_x factor not smaller than 1.5.

- (iii) A β_T value not smaller than 3.0 is required for pile groups without any system effect.

In presenting the resistance factors for driven piles, Barker et al. (1991) related to a target reliability between 2.0 to 2.5 and dead to live load ratio of 3.69. The following results were obtained based on the questionnaire distributed by the research team for this project: The estimated risk or failure probability of the group foundation design based on the safety factor used: 27% were less than 0.1%, 4% were between 0.1 to 1%, one percent (1%) of the responses were between 1% to 10%, and 67% were unknown. The assessment for the acceptable maximum failure probability ranged from about zero (0) to 1%. 14% of respondents had experienced pile failures.

Based on the presented review and data it seems reasonable to establish the target reliability for the dynamic analyses between 2.0 to 2.5 for pile groups, possibly in the middle, and as high as 3.0 for single piles. The evaluation of the resistance factors was carried out by using reliability indices of 2.0, 2.5, and 3.0. This provided a reasonable range before final target reliability values were set.

9.3 DEAD TO LIVE LOAD RATIO

Figure 9.2 presents examples of the resistance factors calculated based on the FORM procedure for the general CAPWAP and Energy Approach cases. Before exact target reliability was established, the resistance factors were evaluated for target reliability values of 2, 2.5, and 3.0 associated with probability of failure values of 2.3%, 0.62%, and 0.14%, respectively. The factors were evaluated using load factors of 1.25 and 1.75 for Dead Load (DL) and Live Load (LL), respectively, and for DL to

LL ratios ranging from 1 to 4. The obtained results presented in Figure 9.2 suggest very little sensitivity of the resistance factors to the DL to LL ratio. A parametric study was carried out for a generic coefficient of variation of 0.40 and dead to live load ratios ranging from 1 to 10. The large dead to live ratios represent a wide possibility of bridge construction, typically associated with very long bridge spans. No significant influence of the dead to live load ratio on the calculated resistance factors was found.

9.4 THE RESISTANCE FACTORS

9.4.1 Initial Evaluation

Figure 9.3 presents a flow chart that summarizes the parameters of the normal distribution (number of cases, mean and standard deviation) for all the dynamic analysis methods and their sub-categories established in Chapter 6. The statistical analysis presented in Figure 9.3 allows for the identification of the critical cases that require calibration and development into resistance factors. For example, the CAPWAP cases include (i) all data, (ii) EOD, (iii) BOR, and (iv) the worst combination of soil inertia (Blow count < 16 BP10cm and $A_R < 350$).

Table 9.7 presents a summary of the major categories of the dynamic methods that are identified from Figure 9.3 as the cases that require calibration for a resistance factor. The Case method was not included for the reasons discussed in section 6.3.4 and as it refers to a limited database (Florida), utilizing the RMX version of the method with variable Case damping coefficients, J_c .

Histogram and frequency distributions were prepared for the identified critical cases, presented in Table 9.7. This visual information enables to examine the match between the actual data and the probability distribution functions. Figure 9.4 through 9.19 present the data along with the calculated normal and lognormal distributions.

9.4.2 Intermediate Conclusions

This section presents the conclusions derived from the observed statistical performance. It is placed here for clarity and completeness. The data presented in Chapter 5 and summarized in Table 9.7 and Figures 9.3 through 9.19 lead to several preliminary conclusions:

- (i) The signal matching procedure generally under-predicts the pile's capacity. The method performs very well for the BOR (last restrike) cases.
- (ii) The simple Energy Approach provides excellent prediction for evaluating the pile's capacity during driving (EOD).
- (iii) The above suggests that construction delays due to restrike and costly signal matching analyses need to be examined in light of capacity time dependency and economical factors.
- (iv) The FHWA modified gates equation provides very reasonable predictions for evaluating the pile's capacity when dynamic methods are not carried out.
- (v) A reasonably good match exists for most cases between the calculated lognormal distribution and the observed data. For this reason lognormal functions were used in calibration procedures of the resistance factors.

9.4.3 Resistance Factors for a Range of Reliability Indices

Table 9.7 summarizes the resistance factors that were calculated for the critical investigated cases of the dynamic analyses. The resistance factors were calculated for reliability indices of 2.0, 2.5 and 3.0 and load factors of 1.25 and 1.75 for Dead Load (DL) and Live Load (LL), respectively, and for ratios of $DL/LL = 1$ and $DL/LL = 4$. The range of the reliability indices ($\beta = 2.0$ to 3.0) covers the expected range of probability of failure ($p_f = 2.28\%$ to $p_f = 0.14\%$) adequate for the dynamic methods. The obtained resistance factors presented in Table 9.7 allow (i) to assess the range of the obtained values and its sensitivity to the reliability index and (ii) reevaluate the 'critical' cases such that subcategories with similar resistance factors can be combined; e.g., Energy Approach EOD case and Energy Approach EOD for $A_R < 350$ and Blow Count < 16 BP10cm.

9.4.4 Recommended Resistance Factors

Based on the resistance factors presented in Table 9.7 the critical dynamic cases were reevaluated resulting in smaller number of categories, encompassing others, e.g., five versus eight for the methods of the dynamic measurements. The selected methods, their important categories and the recommended factors are presented in Table 9.8. Following review of existing common practice in probability of failure, review of the obtained parameters (to be presented in the following section) and discussion with the NCHRP 24-17 project panel, the following reliability indices and probability of failure are recommended:

- (i) For redundant piles, defined as five or more piles per pile cap, the recommended probability of failure is $p_f = 1\%$, corresponding to a reliability index of $\beta = 2.33$.
- (ii) For non-redundant piles, defined as four or less piles per pile cap, the recommended probability of failure is $p_f = 0.1\%$, corresponding to a reliability index of $\beta = 3.00$.

The obtained resistance factors for the methods that utilize dynamic measurements, range from 0.41 to 0.65 for the redundant pile cases and 0.23 to 0.51 for the non-redundant pile cases with typical decrease of about 25% in the resistance factor when moving from one category to the other. This practically means that the use of four piles with non-redundant resistance factors will be approximately equivalent to the use of five piles with redundant resistance factors.

The magnitude of the resistance factors by itself is not a measure that indicates the performance or economical value of the method. A comparison requires therefore an "efficiency" measure, discussed in the following section.

9.5 EVALUATION OF THE DYNAMIC METHODS EFFICIENCY

In the same way that a factor of safety alone is not a representative of the efficiency of a method, the resistance factors alone do not provide a measure for the evaluation of the efficiency of the dynamic methods. Such efficiency can be evaluated through the bias factor (mean of the ratio of the measured over predicted), its coefficient of variation (see Table 9.7) or the ratio of the resistance factor to the bias factor, i.e. $\phi/\text{mean } K_{sx}$, as proposed by McVay et al. (2000). This ratio is provided for

the final selected cases in Table 9.8. The efficiency values in Table 9.8 suggest that overall the higher efficiency is obtained by the signal matching analyses for the last restrike, followed by the Energy Approach at the end of driving (0.561 vs. 0.489 and 0.440 vs. 0.369 for redundant and non-redundant cases, respectively).

9.6 EVALUATION OF THE CHOSEN TARGET RELIABILITY AND RECOMMENDED RESISTANCE FACTORS

9.6.1 Resistance Factors Based on the Existing AASHTO Specifications

Utilizing the statistical parameters of the critical cases presented in Table 9.8, the same data and reliability indices were used to calculate the resistance factors based on the existing AASHTO methodology as presented by Barker et al. (1991) and reviewed in section 2.2.4b of this manuscript. Table 9.9 follows the format of Table 9.8 with the resistance factors from FORM compared with those of FOSM calculated using the existing AASHTO methodology as proposed by Barker et al. (1991).

The resistance factors obtained using FOSM (the existing AASHTO methodology) are approximately 10% lower than those obtained using FORM. In principle this shows that the methodology for calculating resistance factors using the existing AASHTO methodology is slightly more conservative than the method used to calculate the proposed resistance factors for the 2001 AASHTO code, assuming the same statistical data available for both.

9.6.2 Evaluation of the WSD Factors of Safety (AASHTO, 1997) in Light of the Obtained Results

The traditional WSD factors of safety presented in Table 2.1 can now be evaluated in light of the available data. For example, the coefficient of variation for

the WEAP analysis at the EOD is 0.724, which practically means that the method is unsuitable for the purpose of capacity prediction. The reduction in the factor of safety from 3.50 to 2.75 in Table 2.1 when adding WEAP analysis to static calculations is therefore unfounded. Moreover, considering the mean bias of the WEAP at EOD, ($K_{sx} = 1.656$), the F.S. = 2.75 actually means an average factor of safety of 4.55 (2.55×1.656), which is by no means of any "savings", compared to the static methods predictions assuming those to be accurate. The use of unspecified CAPWAP (general case) again does not justify the reduction of the factor of safety to 2.25 even though the average prediction is conservative (mean over prediction ratio of 1.368) and hence for the mean case with a F.S. = 2.25, the actual factor of safety is 3.1 (1.368×2.25). In comparison, the use of F.S. = 2.25 with a specified CAPWAP at the BOR is reasonable and is associated with an acceptable probability of failure for single pile application (approximately 1.85%, see Figure 9.7).

The conclusions of the above are:

- (i) The common wisdom accepting the recommended traditional factors of safety as accumulation of a long term knowledge must be evaluated in light of actual performance, hence the use of databases is as important for WSD as for LRFD, and
- (ii) The specific factors of safety recommended by AASHTO (1997) though seem to be logical and progressive (decrease of F.S. with increase of knowledge), are not so anymore when considering the bias of each method.

9.6.3 Evaluation of the Chosen Target Reliability

a) Overview

The chosen target reliability and probability of failure presented in section 9.4.4 need to be examined. The most desired method to determine the target reliability is by a calibration of accepted practice as described in Section 9.2.2. This is not possible in the case of the dynamic methods, due to the following reasons:

1. A large-scale analysis of the methods to produce calibration through design is beyond the scope of this work.
2. No direct relationship exist between the resistance factors calculated in this study and back calculated Factors of Safety.
3. The existing LRFD AASHTO specifications suggest in the case of the dynamic methods to multiply the resistance factor based on the static analysis by an additional factor (λ). There is not therefore a relationship between the current AASHTO resistance factor used for the dynamic methods and the one developed in the present study.
4. WSD Factors of Safety as used by AASHTO until 1997 (see Table 2.1 in Chapter 2) are questionable in light of the statistics presented in Table 9.7 (see section 9.6.2).

As a result of the above, two approaches have been adopted for evaluating the adequacy of the proposed target reliability in addition to the previously discussed material and comparisons. These approaches are described in the following sections.

(b) Approximate Factors of Safety

Barker et al. (1991) suggested calibration by fitting the resistance factors of the LRFD with WSD factors of safety, utilizing the following equation:

$$\phi \geq \frac{\gamma_D \frac{Q_D}{Q_L} + \gamma_L}{FS \left(\frac{Q_D}{Q_L} + 1 \right)} \quad (9.14)$$

This equation is not compatible with the FORM calibration procedure presented in section 9.1 but was used in order to obtain indicative factors of safety. The close agreement between FOSM and FORM presented in section 9.6.1 further supports this approach. Table 9.10 was developed using the load factors $\gamma_L=1.75$ $\gamma_D=1.25$, and the resistance factors corresponding to $\beta=2.33$ and $\beta=3.0$, presented in Table 9.8. In reviewing these factors of safety one should consider the bias factors as well. For example, the average F.S. for CAPWAP under the general case for non-redundant piles is 3.32, however the bias of the method under the general case is 1.368 (see Table 9.7) hence the “actual mean” factor of safety is 4.54 (3.32×1.37). Similarly the FS for the Energy Approach at EOD is 3.57, the bias is 1.084 hence the “actual mean” factor of safety is 3.87. The columns describing the actual mean F.S. in Table 9.10 describe therefore the “true” average F.S. considering the bias of the method.

(c) The Actual Probability of Failure

In this procedure the database was used directly (not through the calculated distribution function) to calculate the probability of failure when applying a certain

F.S. For example, if F.S.=2.0 would have been applied to the results of the Energy Approach analyses, in 9.16% of the cases, the obtained capacity would be still higher than the actual ultimate capacity. The results of this analysis are shown in Table 9.11, for factors of safety ranging from 2.00 to 4.00 in intervals of 0.25. Five factors are noticed when reviewing the data presented in Table 9.11:

1. The percent values are actual numbers from counting the cases for each category under certain F.S., with the total number of cases for each category provide in the table.
2. The prediction is compared to static analysis utilizing Davisson's failure criterion, which by itself, is not absolute. The meaning of "failure" in this regard is usually associated with larger settlement but not necessarily mean catastrophic failure or even structural damage.
3. When reviewing the obtained factors of safety one needs to consider the application of a factor of safety for the loads (or load factors) where as in the described analysis, the load is the actual failure load, i.e., the applied F.S. or γ is one. As a result the probability of failure presented in Table 9.11 is different than that discussed earlier, and in fact higher than the one actually expected in the field.
4. The factors of safety should again be judged in relation to the bias of the method as discussed earlier in relation to Table 9.10, e.g., a F.S. = 2.0 for the CAPWAP general case represents average actual F.S. = 2.736 or a F.S.

= 1.788 for the general case of the Energy Approach (bias of 1.368 and 0.894 for CAPWAP and Energy Approach, respectively).

9.7 THE CHOSEN TARGET RELIABILITY AND RESISTANCE FACTORS

Based on the presented material in this chapter the target reliability of 2.33 for pile groups and 3.0 for single piles seem to be adequate and compatible with existing and past work. These values are used therefore to calculate the resistance factors for the critical dynamic analysis methods and the obtained results are presented in Table 9.8. The resistance factors presented in Table 9.8 are therefore recommended to be used in the new AASHTO specifications and the ratio of evaluating the method's efficiency (comparison) is recommended to be used in conjunction with the resistance factors or as part of the commentary.

Table 9.1. Approximate Relationship Between Probability of Failure and Reliability Index for Lognormal Distribution, based on Rosenbleuth and Estava (1972), see Withiam et al. (1998).

Reliability Index, β	Probability of Failure, p_f	Probability of Failure, p_f	Reliability Index, β
2.0	8.47×10^{-2}	1×10^{-1}	1.96
2.5	9.86×10^{-2}	1×10^{-2}	2.50
3.0	1.15×10^{-3}	1×10^{-3}	3.03
3.5	1.34×10^{-4}	1×10^{-4}	3.57
4.0	1.56×10^{-5}	1×10^{-5}	4.10
4.5	1.82×10^{-6}	1×10^{-6}	4.64
5.0	2.12×10^{-7}	1×10^{-7}	5.17

Table 9.2. Comparison Between Rosenbleuth and Estava's Approximation and Series Expansion (Labeled "exact").

β	Rosenbleuth and Estavas' p_f	"exact" p_f	Percent Error
2.0	8.4689E-2	2.2750E-2	272.3%
2.5	9.8649E-3	6.2097E-3	58.9%
3.0	1.1491E-3	1.3500E-3	-14.9%
3.5	1.3385E-4	2.3267E-4	-42.5%
4.0	1.5592E-5	3.1686E-5	-50.8%
4.5	1.8162E-6	3.4008E-6	-46.6%
5.0	2.1156E-7	2.8711E-7	-26.3%
5.5	2.4643E-8	1.9036E-8	29.5%
6.0	2.8705E-9	9.9012E-10	189.9%

Table 9.3. Target Reliability Levels.

Structural Type	Target Reliability Level (β_t)
Metal structures for buildings (dead, live, and snow loads)	3
Metal structures for buildings (dead, live, and wind loads)	2.5
Metal structures for buildings (dead, live, snow, and earthquake loads)	1.75
Metal connections for buildings (dead, live, and snow loads)	4 to 4.5
Reinforced concrete for buildings (dead, live, and snow loads)	
- ductile failure	3
- brittle failure	3.5

The β_t values are for structural members designed for 50 years of service.

Table 9.4. Target Reliability Levels used by Ellingwood and Galambos (1982).

Member, Limit State	Target Reliability Level (β_t)
Structural Steel	
Tension member, yield	3.0
Beams in flexure	2.5
Beams in shear	3.0
Column, intermediate slenderness	3.5
Reinforced Concrete	
Beam in flexure	3.0
Beam in shear	3.0
Tied column, compressive failure	3.5
Masonry, unreinforced	
Wall in compression, uninspected	5.0
Wall in compression, inspected	7.5

The β_t values are for structural members designed for 50 years of service.

Table 9.5. Target Reliability Values Recommended
by A.S. Veritas (Lotsberg, 1991).

Failure Consequences	Failure Type		
	Ductile Failure with reserve capacity	Ductile failure without reserve capacity	Brittle fracture with instability
<u>Not serious:</u> Small possibility of human injury, pollution, or economic consequences	3.09	3.71	4.26
<u>Serious:</u> Possibility of human injury or fatality, pollution, or significant economic consequences	3.71	4.26	4.75
<u>Very serious:</u> Possibility of human injury or fatality, significant pollution, or very large economic consequences	4.26	4.75	5.20

Table 9.6. Reliability Indices for Driven Piles (Barker et al., 1991).

Dead to Live Load Ratio	Reliability Index, β	
	Lognormal	Advanced
1.00	1.6 – 2.8	1.6 – 3.0
3.69	1.7 – 3.1	1.8 – 3.3

Table 9.7. Summary of the Performance of the Dynamic Methods.

Method		Case	No. of Cases	Mean K_{SX}	Standard Deviation	COV	Preliminary Resistance Factors for given Reliability Index, β		
							2.0	2.5	3.0
Dynamic Measurements	CAPWAP	General	377	1.368	0.620	0.453	0.68	0.54	0.43
		EOD	125	1.626	0.797	0.490	0.75	0.59	0.46
		EOD - AR < 350 & Bl. Ct. < 16 BP10cm	37	2.589	2.385	0.921	0.52	0.35	0.23
		BOR	162	1.158	0.393	0.339	0.73	0.61	0.51
	Energy Approach	General	371	0.894	0.367	0.411	0.48	0.39	0.32
		EOD	128	1.084	0.431	0.398	0.60	0.49	0.40
		EOD - AR < 350 & Bl. Ct. < 16 BP10cm	39	1.431	0.727	0.508	0.63	0.49	0.39
		BOR	153	0.785	0.290	0.369	0.46	0.38	0.32
Dynamic Equations	ENR	General w/o FS = 6	384	0.267	0.243	0.910	0.04	0.03	0.02
	ENR	General w/ FS = 6	384	1.602	1.458	0.910	0.33	0.22	0.15
	Gates	General	384	1.787	0.848	0.475	0.85	0.67	0.53
	FHWA modified Gates	General	384	0.940	0.472	0.502	0.42	0.33	0.26
		EOD	135	1.073	0.573	0.534	0.45	0.35	0.27
		EOD Bl. Ct. < 16BP10cm	62	1.306	0.643	0.492	0.60	0.47	0.37
	WEAP	EOD	99	1.656	1.199	0.724	0.48	0.34	0.25
WEAP		BOR	99	0.939	0.399	0.425	0.49	0.40	0.32

See Notes on Table 9.8

Table 9.8. Recommended Resistance Factors for the Critical Dynamic Cases.

Method		Case	Resistance factor, ϕ		ϕ /Mean K_{SX}	
			Redundant $\beta = 2.33$ $p_f = 1.0\%$	Non-Redundant $\beta = 3.0$ $p_f = 0.1\%$	Redundant $\beta = 2.33$ $p_f = 1.0\%$	Non-Redundant $\beta = 3.0$ $p_f = 0.1\%$
Dynamic Measurements	Signal Matching	General	0.59	0.43	0.431	0.314
		EOD, AR<350, Bl. Ct.<16BP10cm	0.41	0.23	0.158	0.089
		BOR	0.65	0.51	0.561	0.440
	Energy Approach	General	0.42	0.32	0.470	0.358
		EOD	0.53	0.40	0.489	0.369
Dynamic Equations	ENR	General w/ FS = 6	0.26	0.15	0.162	0.094
	Gates	General	0.73	0.53	0.409	0.297
	FHWA modified	General	0.36	0.26	0.383	0.277
WEAP		EOD	0.39	0.25	0.236	0.151

Notes: β = Reliability Index p_f = Probability of Failure COV = Coefficient of Variation
EOD = End of Driving BOR = Beginning of Restrike ENR = Engineering News Record Equation
AR = Area Ratio Bl. Ct. = Blow Count
BP10cm = Blows per 10cm K_{SX} = Ratio of the Static Load Test Results to the predicted capacity
Redundant = Five piles or more under one pile cap.
Non-Redundant = Less than five piles under one pile cap.

Table 9.9. Resistance Factors for the Critical Dynamic Cases Based on FOSM using Barker et al., (1991) versus those developed through FORM (see Table 9.8).

Method		Case	Resistance factor, ϕ $\beta = 2.33, p_f = 1.0\%$		Resistance factor, ϕ $\beta = 3.00, p_f = 0.1\%$	
			FORM	FOSM	FORM	FOSM
Dynamic Measurements	Signal Matching	General	0.59	0.54	0.43	0.39
		EOD, AR<350, Bl. Ct.<16BP10cm	0.41	0.38	0.23	0.22
		BOR	0.65	0.56	0.51	0.45
	Energy Approach	General	0.42	0.39	0.32	0.29
		EOD	0.53	0.48	0.40	0.36
Dynamic Equations	ENR	General w/ FS = 6	0.26	0.24	0.15	0.14
	Gates	General	0.73	0.67	0.53	0.48
	FHWA modified	General	0.36	0.33	0.26	0.24
WEAP		EOD	0.39	0.37	0.25	0.23

Notes:

β	= Reliability Index	p_f	= Probability of Failure
EOD	= End of Driving	BOR	= Beginning of Restrike
AR	= Area Ratio	Bl. Ct.	= Blow Count
BP10cm	= Blows per 10cm	ENR	= Engineering News Record Equation
FORM	= First Order Reliability Method	FOSM	= First Order Second Moment

Table 9.10. Calculated Factors of Safety Based on the Resistance Factors in Table 9.8 and the Procedure Outlined by Barker et al. (1991).

Dynamic Method for Capacity Evaluation	Resistance Factor, ϕ		Factor of Safety (FS); $\gamma_L = 1.75, \gamma_D = 1.25$							
			Redundant - $\beta = 2.33$				Non-Redundant - $\beta = 3.0$			
	$\beta = 2.33$	$\beta = 3.00$	$\frac{DL}{LL} = 1$	$\frac{DL}{LL} = 4$	Mean FS	"Actual mean" FS	$\frac{DL}{LL} = 1$	$\frac{DL}{LL} = 4$	Mean FS	"Actual mean" FS
CAPWAP - General	0.59	0.43	2.54	2.29	2.42	3.31	3.49	3.14	3.32	4.54
CAPWAP - EOD, AR<350, Bl. Ct.<16 BP10cm	0.41	0.23	3.66	3.29	3.48	9.01	6.52	5.87	6.20	16.05
CAPWAP - BOR	0.65	0.51	2.31	2.08	2.20	2.55	2.94	2.65	2.80	3.24
Energy Approach - General	0.42	0.32	3.57	3.21	3.39	3.03	4.69	4.22	4.46	3.99
Energy Approach - EOD	0.53	0.40	2.88	2.60	2.74	2.97	3.75	3.38	3.57	3.87
ENR – General w/ FS = 6	0.26	0.15	5.77	5.19	5.48	8.78	10.00	9.00	9.50	15.21
Gates - General	0.73	0.53	2.05	1.85	1.95	3.48	2.83	2.55	2.69	4.81
FHWA - General	0.36	0.26	4.17	3.75	3.96	3.72	5.77	5.19	5.48	5.15
WEAP - EOD	0.39	0.25	3.85	3.46	3.66	6.06	6.00	5.40	5.70	9.44

Notes: β = Reliability Index DL/LL = Dead Load to Live Load Ratio AR = Area Ratio
 "Actual mean FS" = Mean FS \times Mean K_{SX} Bl. Ct. = Blow Count

Table 9.11. The Probability of Failures Associated with the Critical Dynamic Methods and Their Important Categories from the PD/LT2000 Database.

Factor of Safety	Probability of Failure - Risk							
	CAPWAP			Energy Approach		Gates	FHWA	WEAP
	General	BOR	EOD - AR<350 Bl. Ct. <16 BP10cm	General	EOD	General	General	EOD
2.00	0.27%	0%	2.70%	9.16%	1.56%	0.26%	10.42%	0%
2.25	0%	0%	0%	3.23%	0%	0.26%	5.47%	0%
2.50	0%	0%	0%	0.81%	0%	0.26%	3.13%	0%
2.75	0%	0%	0%	0.27%	0%	0%	1.56%	0%
3.00	0%	0%	0%	0.27%	0%	0%	0.78%	0%
3.25	0%	0%	0%	0%	0%	0%	0.52%	0%
3.50	0%	0%	0%	0%	0%	0%	0.52%	0%
3.75	0%	0%	0%	0%	0%	0%	0.26%	0%
4.00	0%	0%	0%	0%	0%	0%	0.26%	0%
No. of Cases	377	162	37	371	128	384	384	99

Notes: AR = Area Ratio
Bl. Ct. = Blow Count
EOD = End of Driving
BOR = Beginning of Restrike

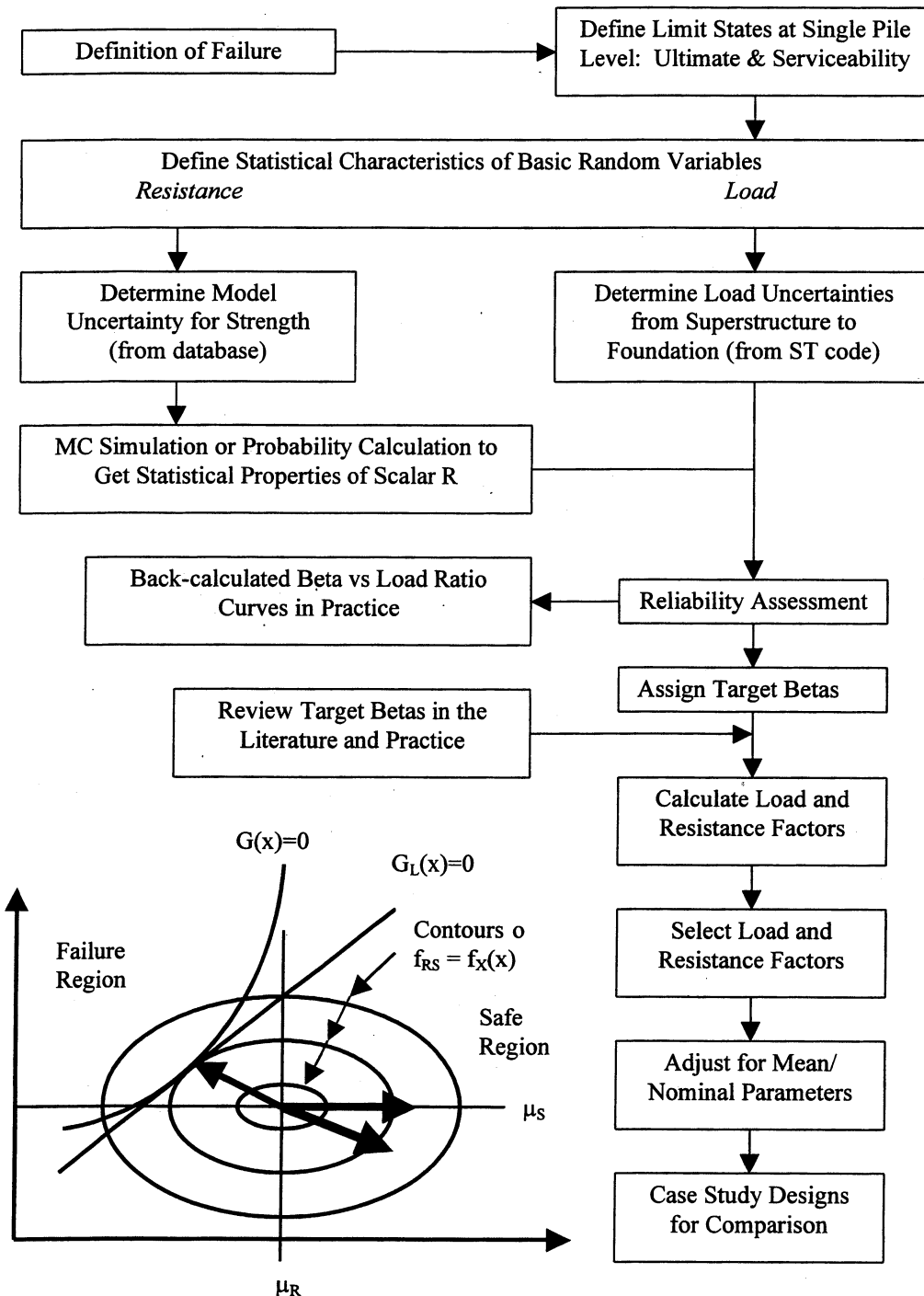


Figure 9.1. Resistance Factor Analysis Flow Chart (after Ayyub & Assakkaf, 1999, Ayyub et al., 2000).

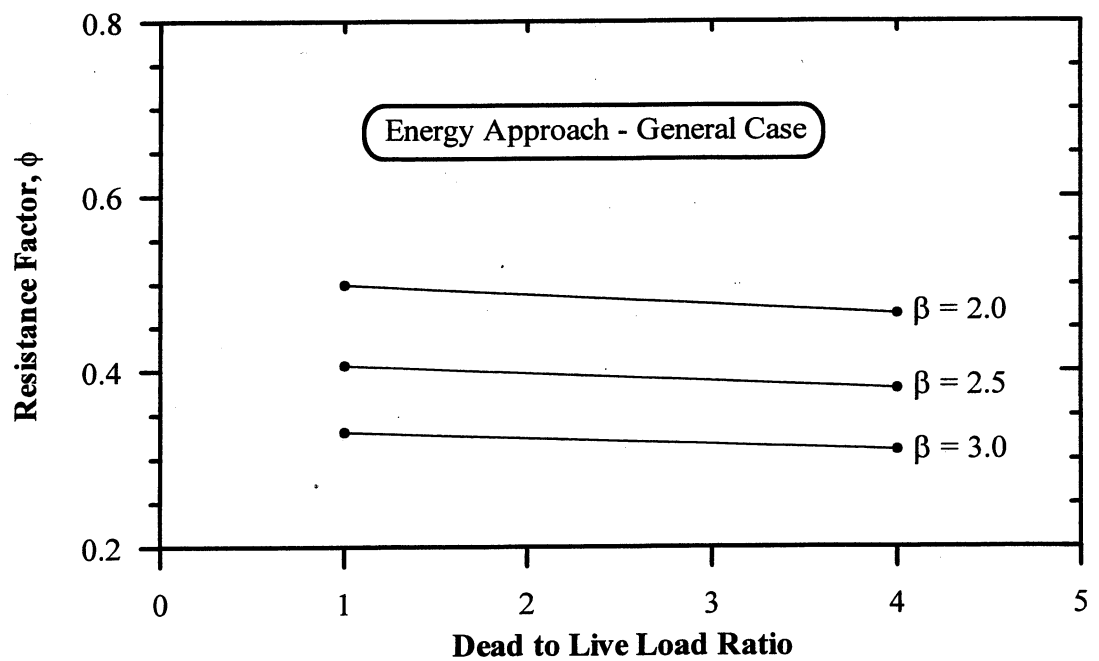
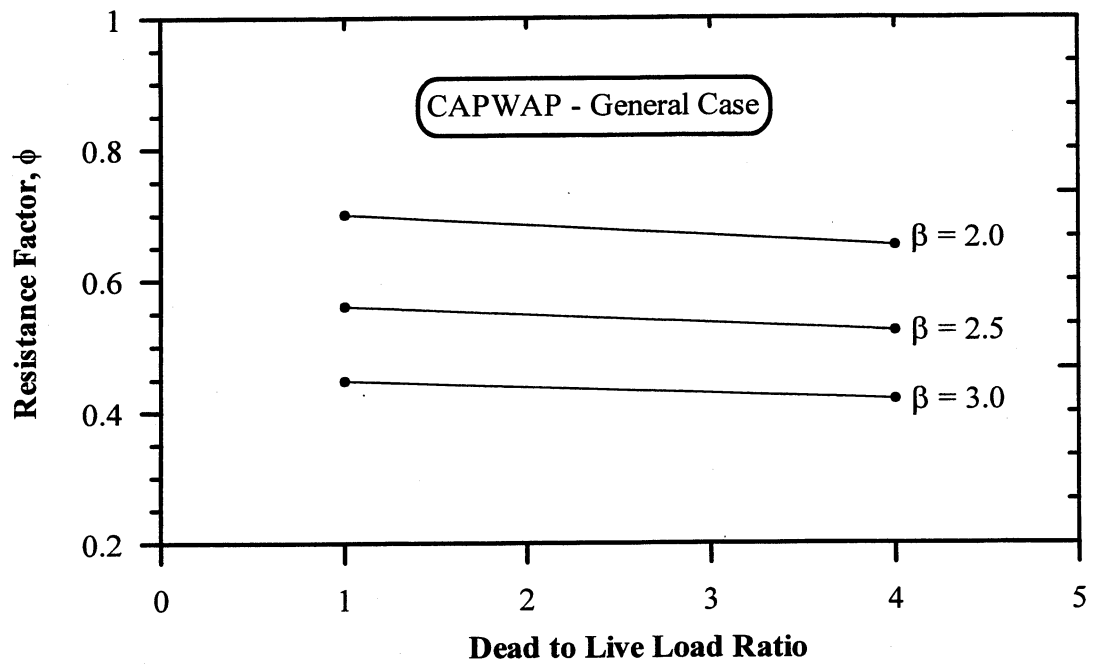


Figure 9.2. Calculated Resistance Factors for the CAPWAP and Energy Approach General Cases showing the Influence of the Dead to Live Load Ratio.

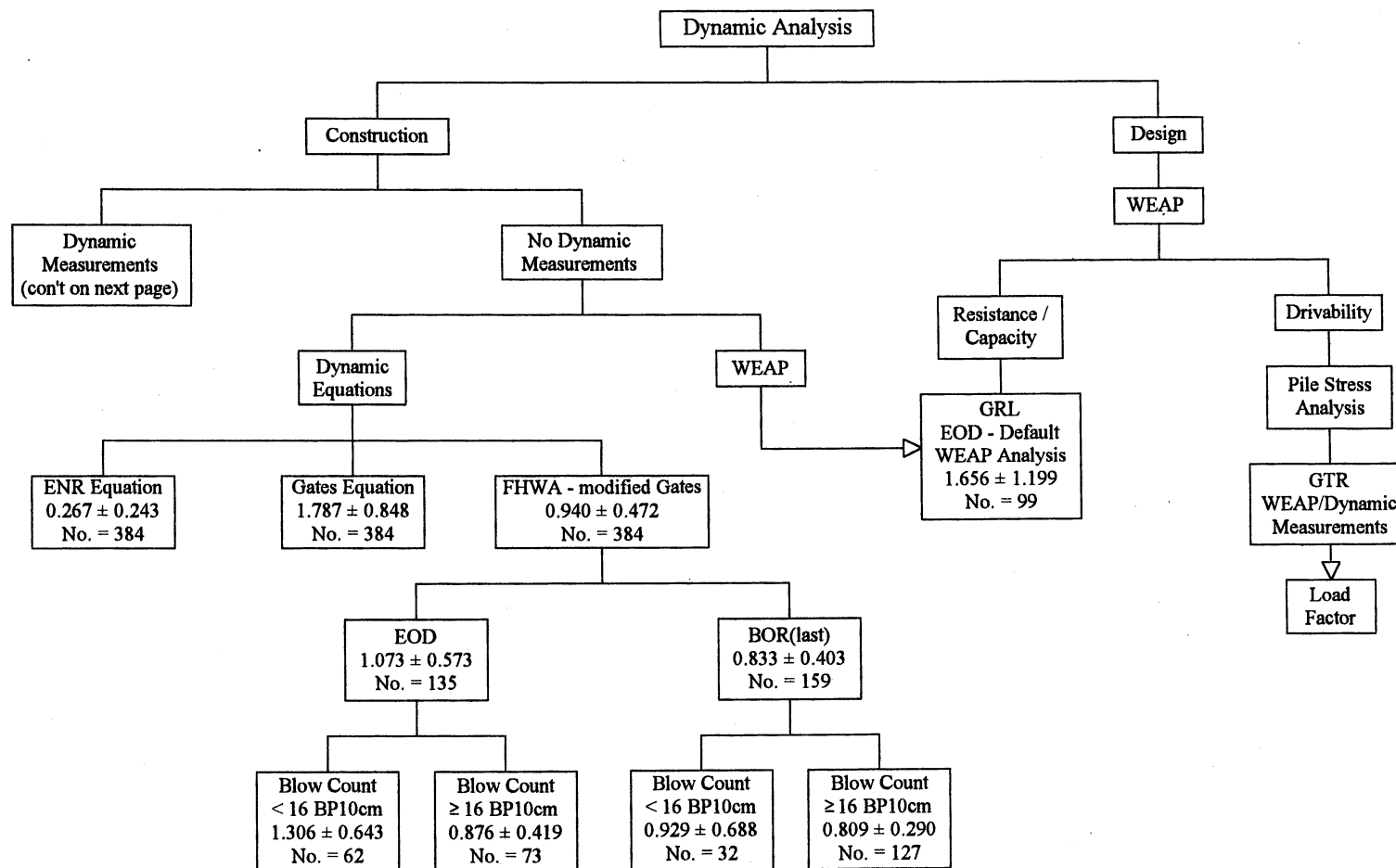


Figure 9.3. Flow Chart Presenting the Sub-Grouping of the Dynamic Analyses According to the Controlling Parameters and the Resulting Statistical Parameters for a Normal Distribution Function.

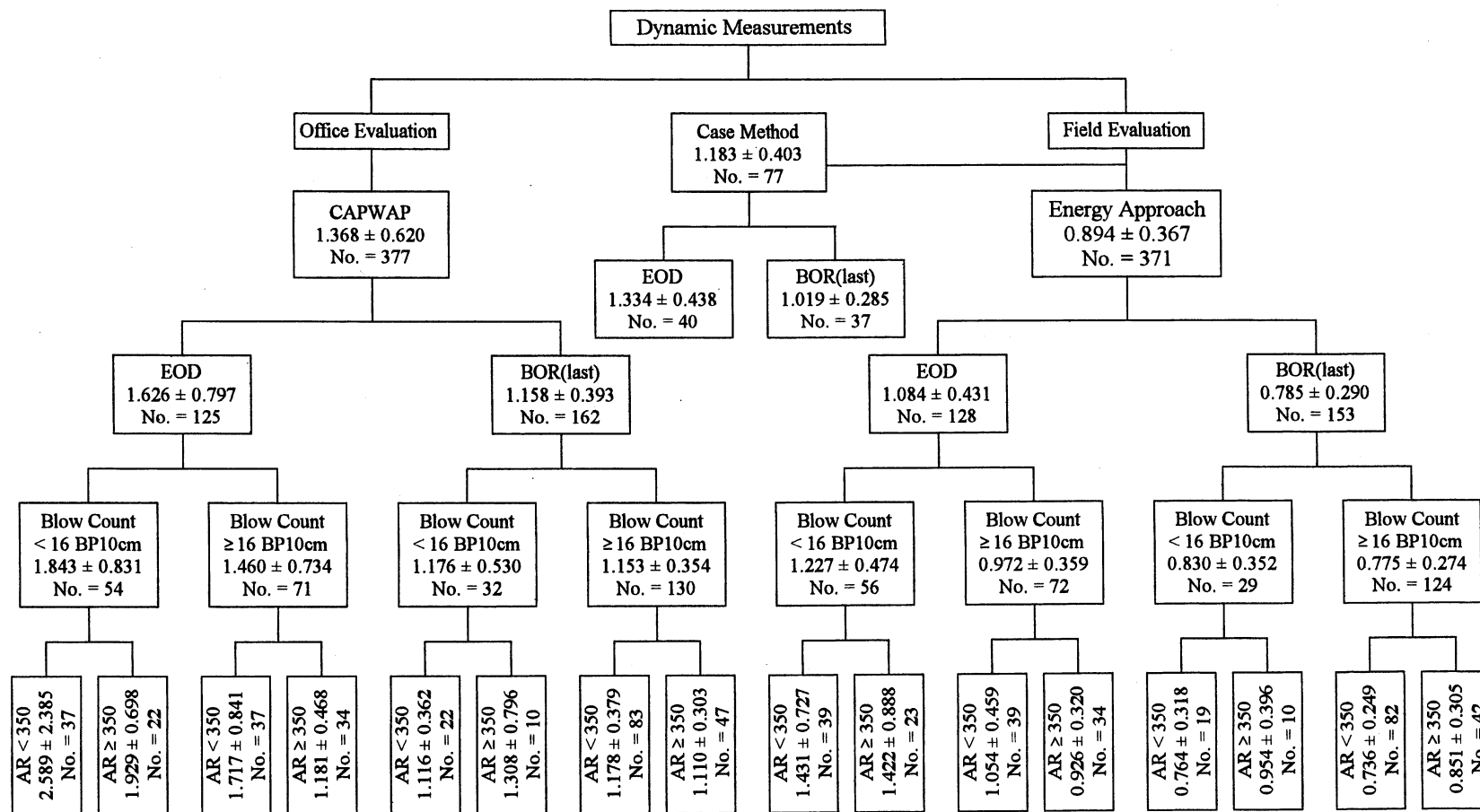


Figure 9.3 (con't). Flow Chart Presenting the Sub-Grouping of the Dynamic Analyses According to the Controlling Parameters and the Resulting Statistical Parameters for a Normal Distribution Function.

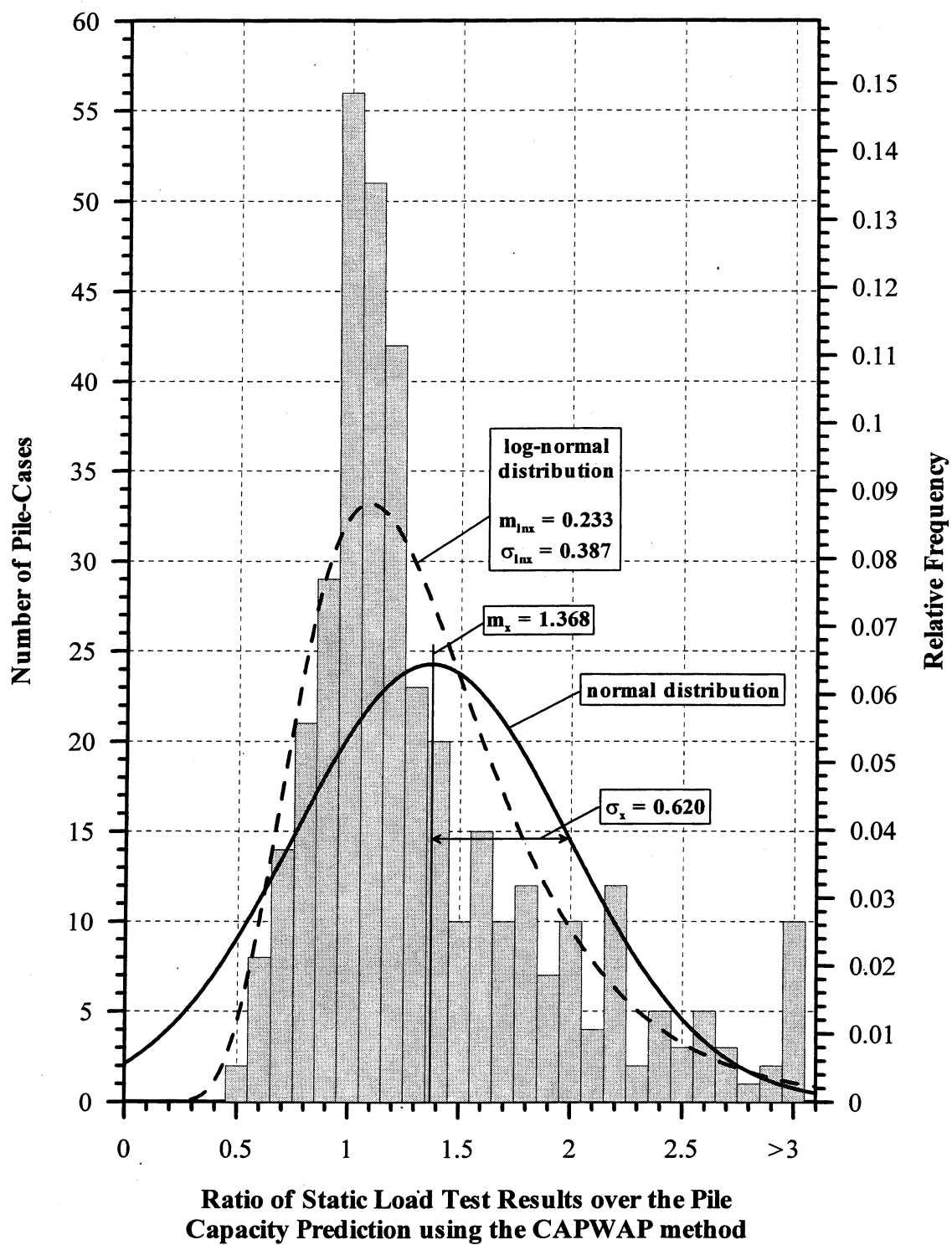


Figure 9.4. Histogram and frequency distributions of K_{sw} for 377 PD/LT2000 CAPWAP pile-cases in all types of soils (AAA).

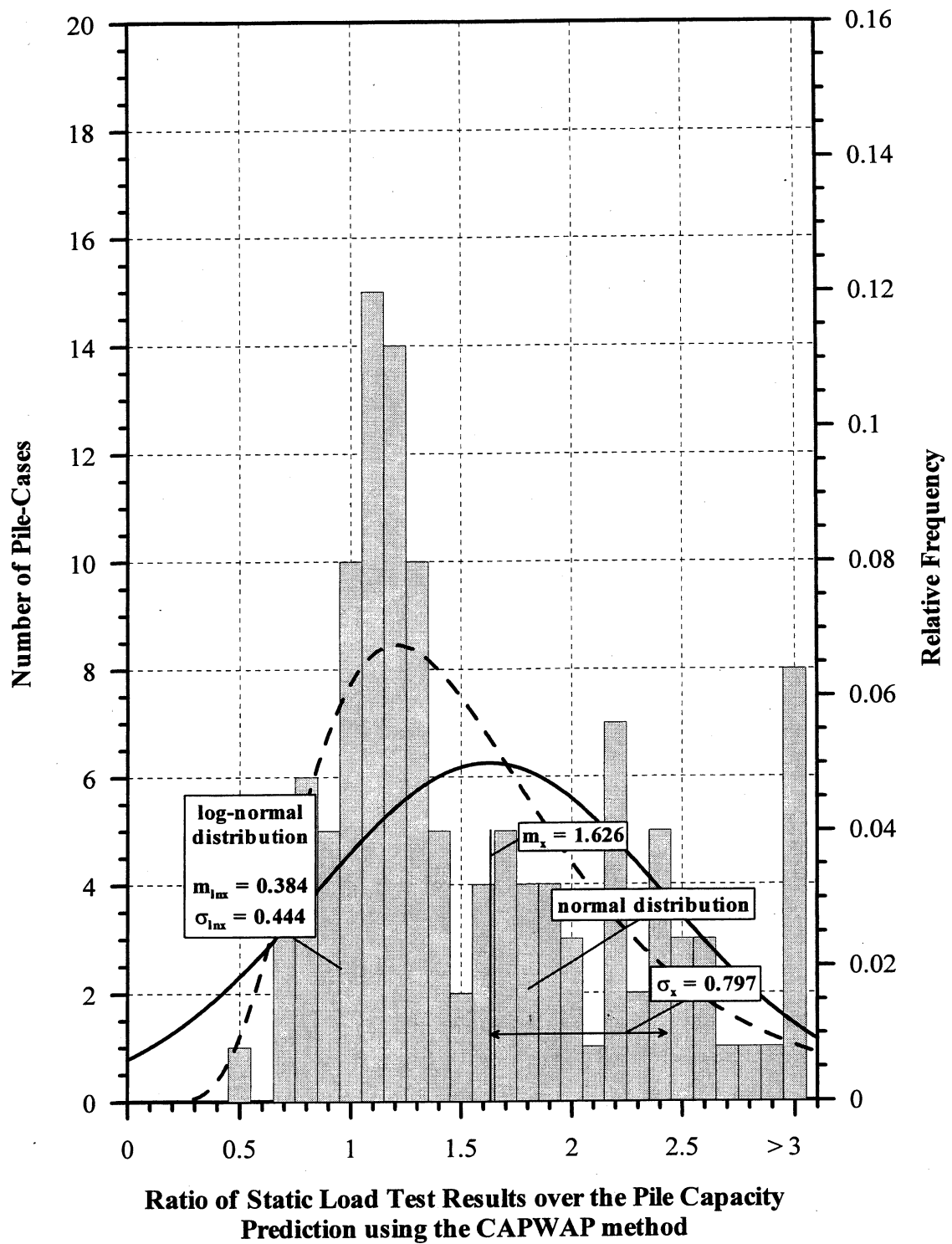


Figure 9.5. Histogram and frequency distributions of K_{sw} for 125 PD/LT2000 CAPWAP pile-cases at the EOD in all types of soils (AEA).

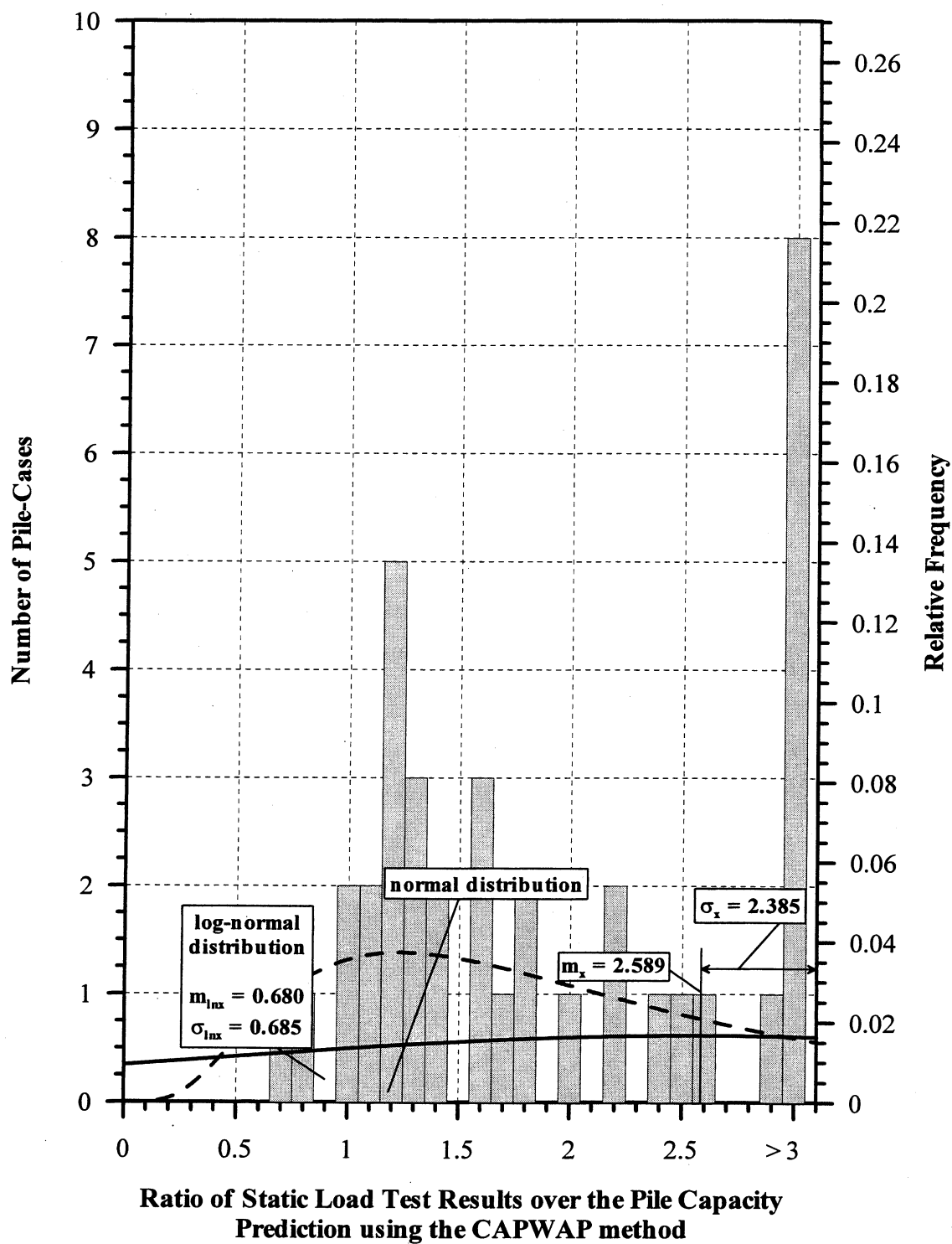


Figure 9.6. Histogram and frequency distributions of K_{sw} for 37 PD/LT2000 CAPWAP pile-cases at the EOD with Blow Counts < 16 BP10cm and Area Ratio < 350 in all types of soils (AEA).

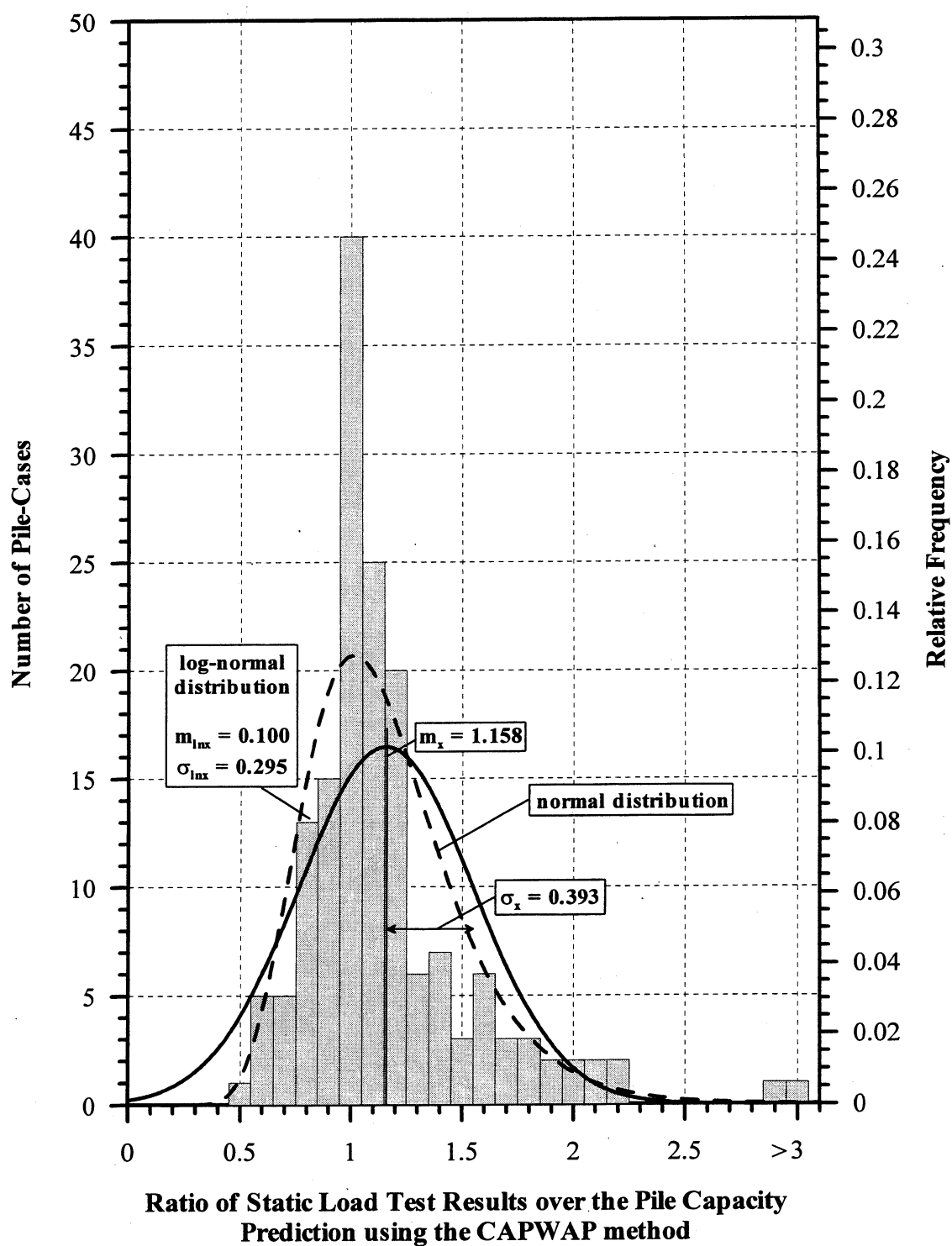


Figure 9.7. Histogram and frequency distributions of K_{sw} for 162 PD/LT2000 CAPWAP pile-cases at the BOR(last) in all types of soils (ABA).

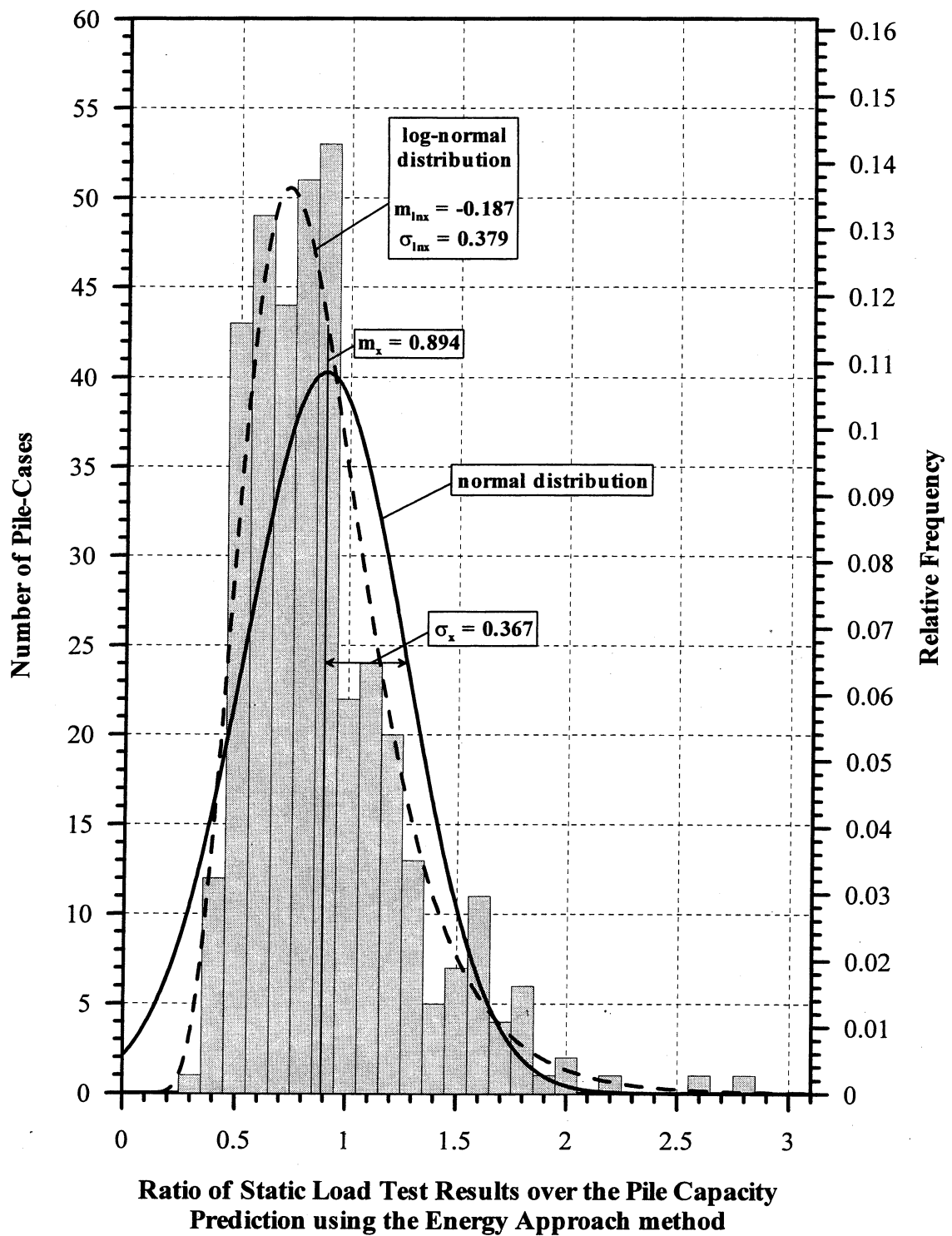


Figure 9.8. Histogram and frequency distributions of K_{SP} for 371 PD/LT2000 Energy Approach pile-cases in all types of soils (AAA).

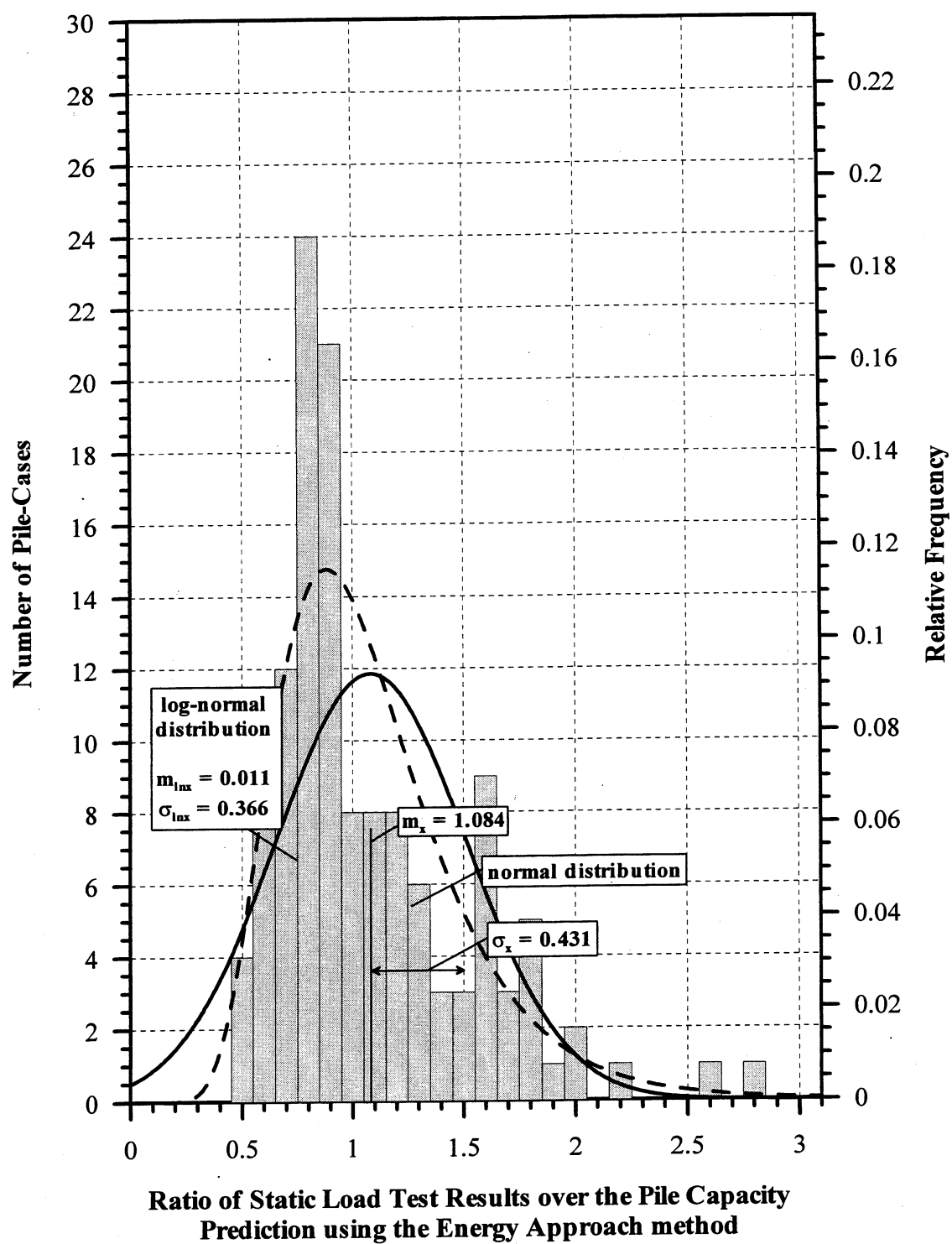


Figure 9.9. Histogram and frequency distributions of K_{SP} for 128 PD/LT2000 Energy Approach pile-cases at the EOD in all types of soils (AEA).

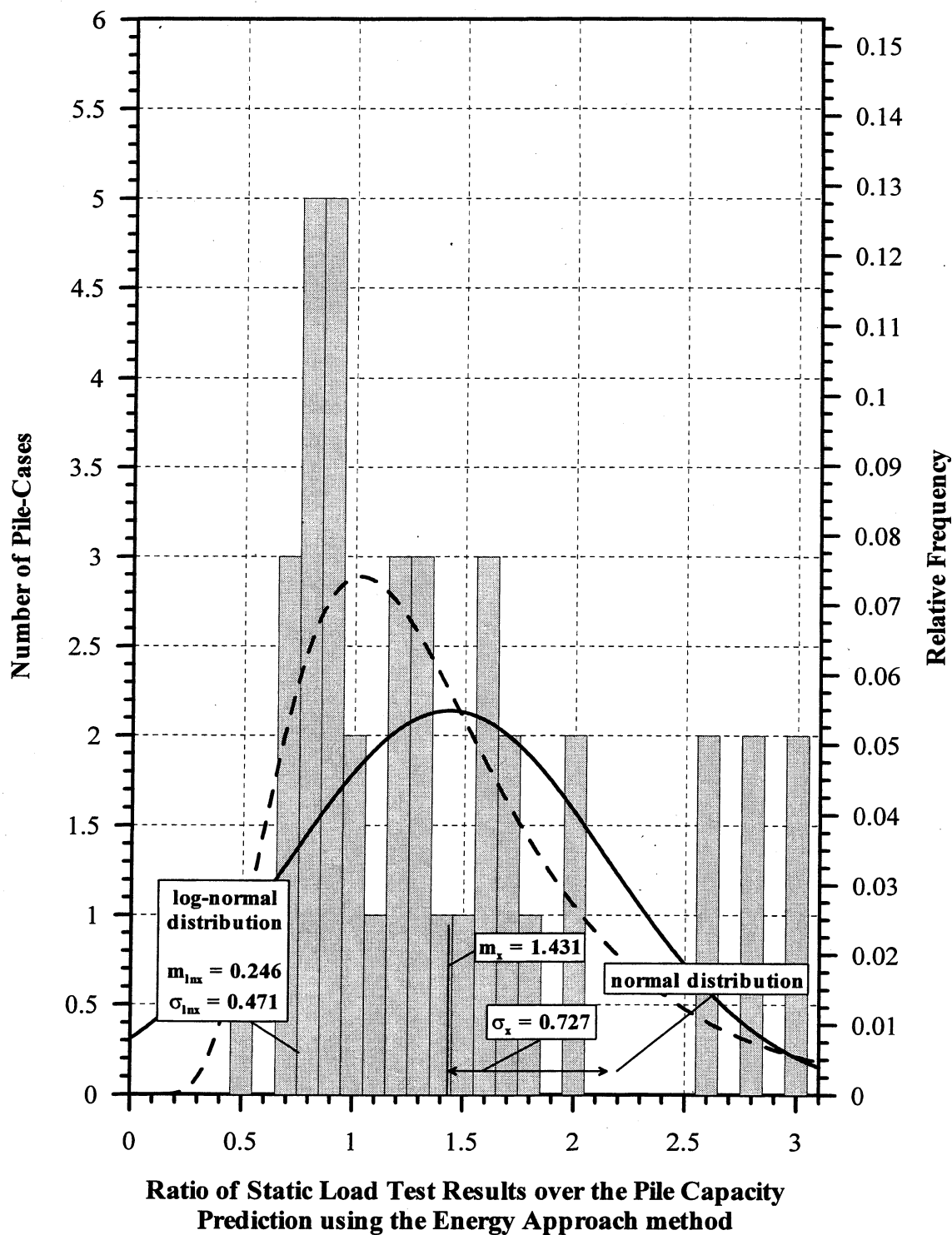


Figure 9.10. Histogram and frequency distributions of K_{sp} for 39 PD/LT2000 Energy Approach pile-cases at the EOD with Blow Counts < 16BP10cm and Area Ratio < 350 in all types of soils (AEA).

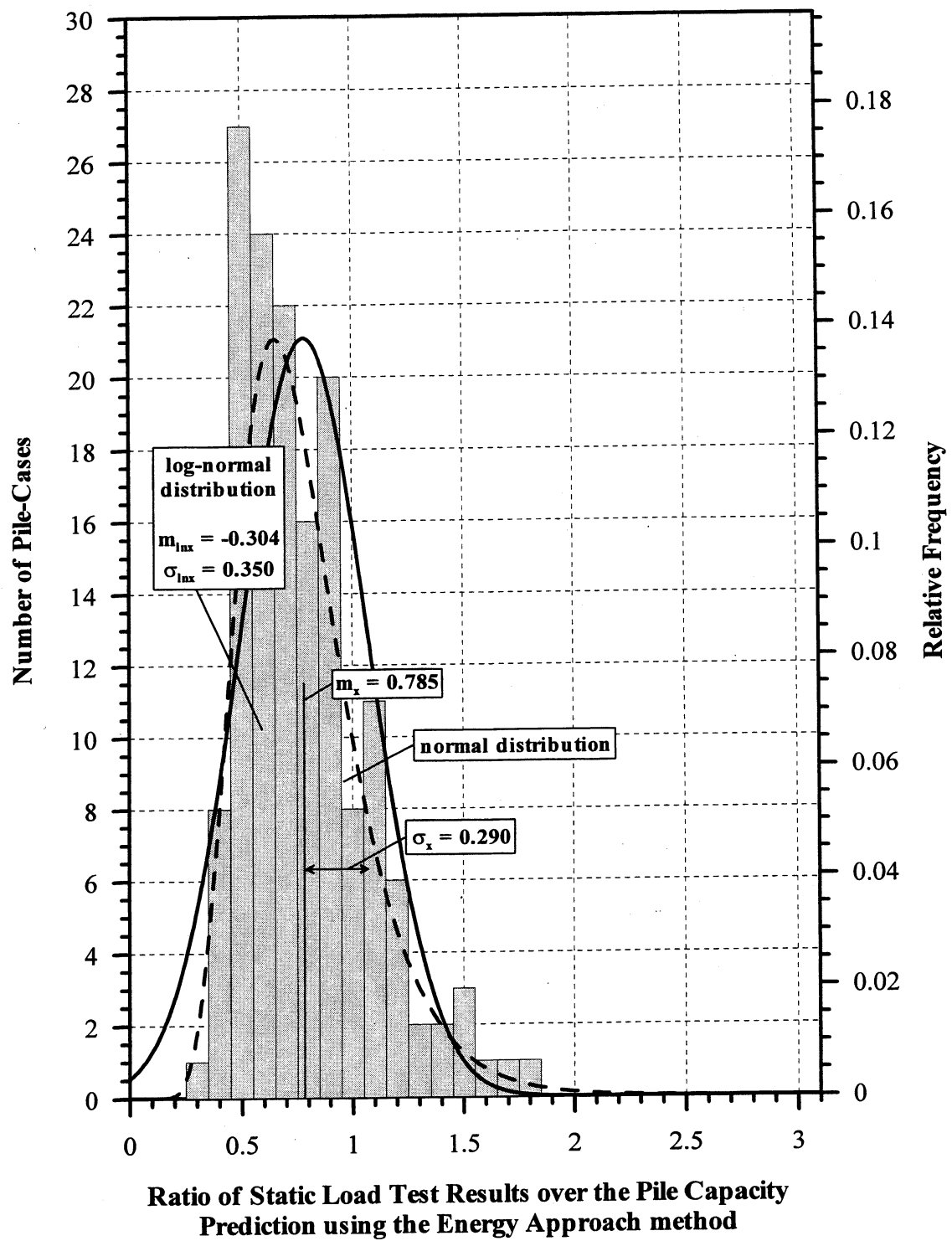


Figure 9.11. Histogram and frequency distributions of K_{sp} for 153 PD/LT2000 Energy Approach pile-cases at the BOR(last) in all types of soils (ABA).

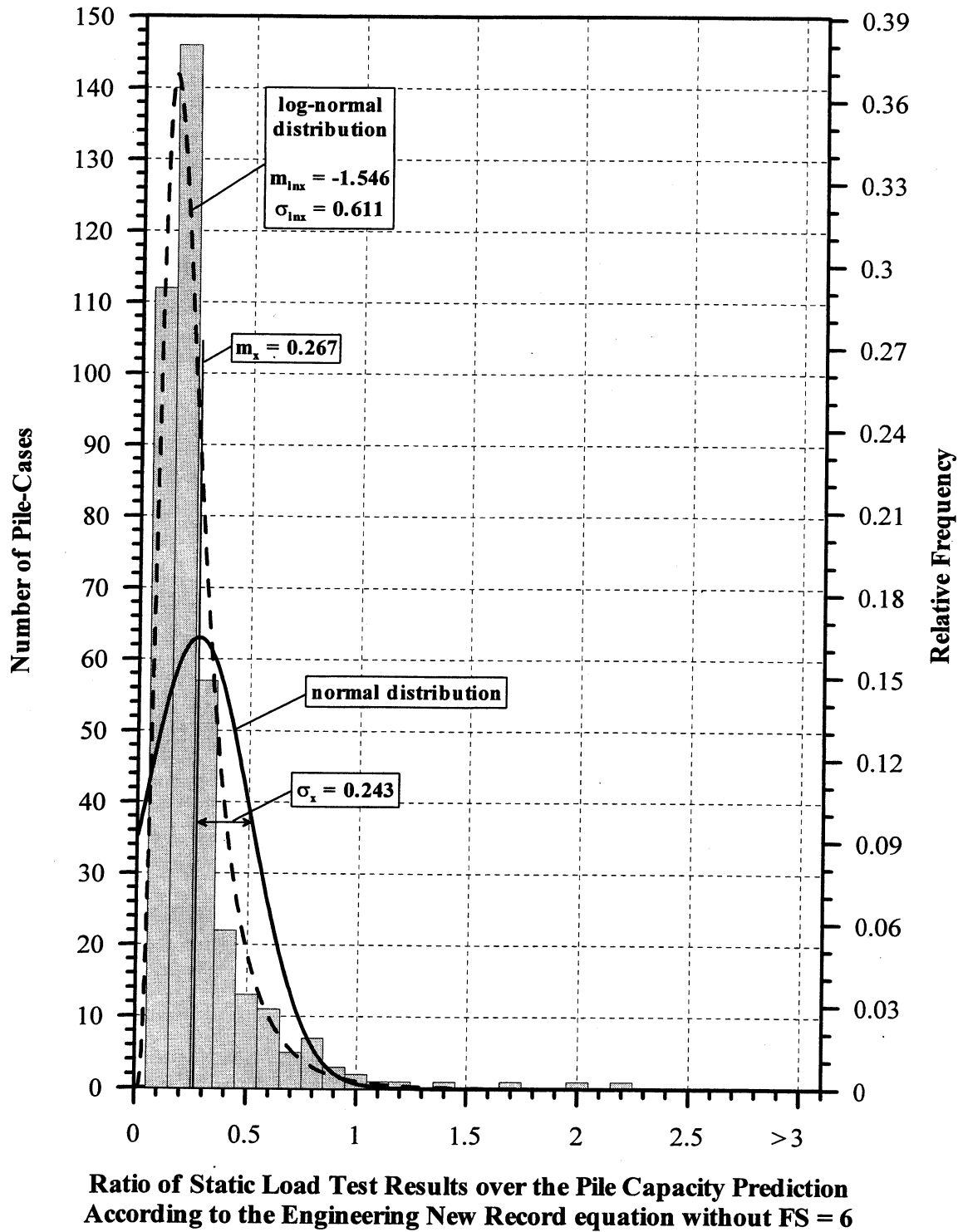


Figure 9.12. Histogram and frequency distributions of K_{SENR} (without FS = 6) for 384 PD/LT2000 pile-cases in all types of soils (AAA).

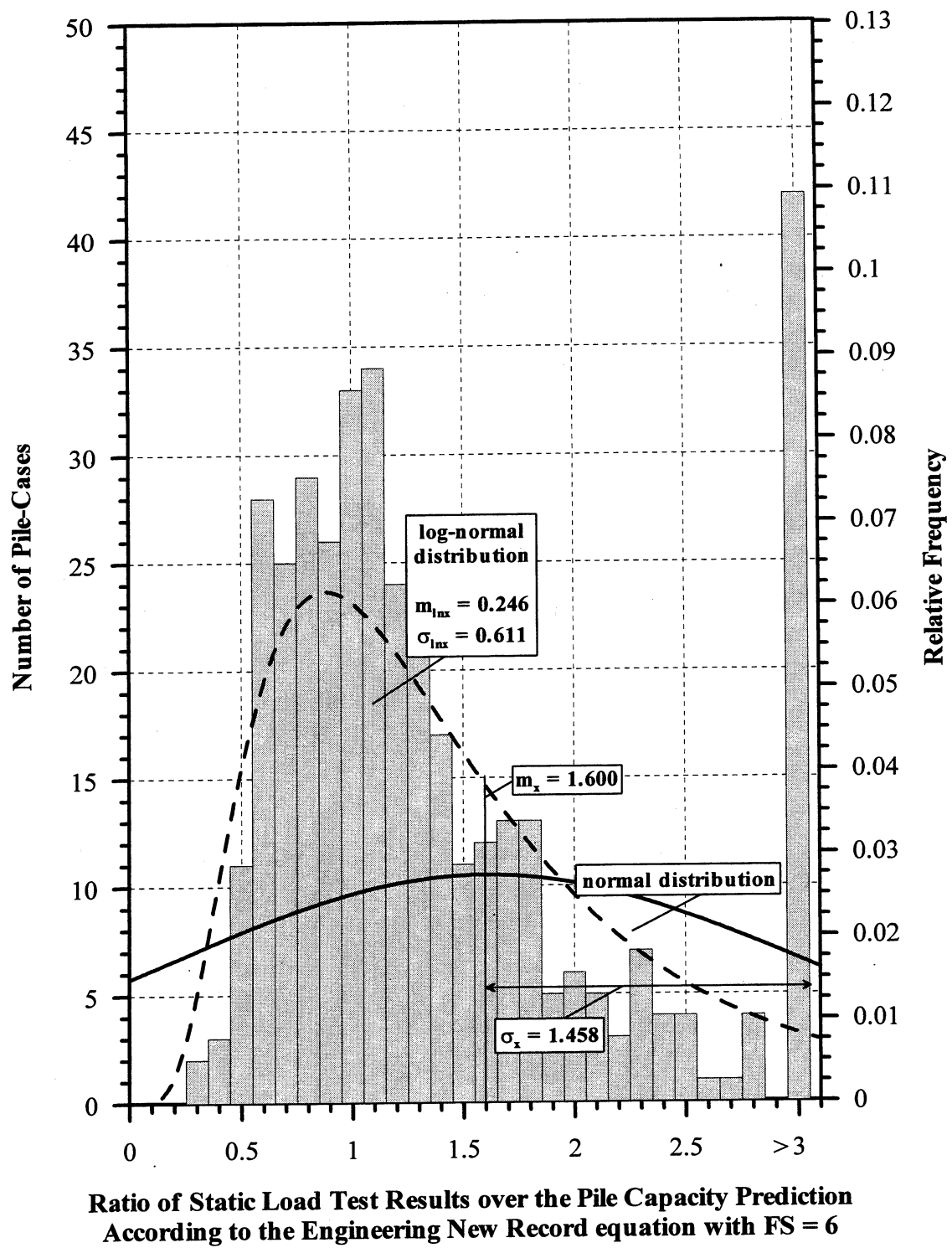


Figure 9.13. Histogram and frequency distributions of K_{SNER} (with FS = 6) for 384 PD/LT2000 pile-cases in all types of soils (AAA).

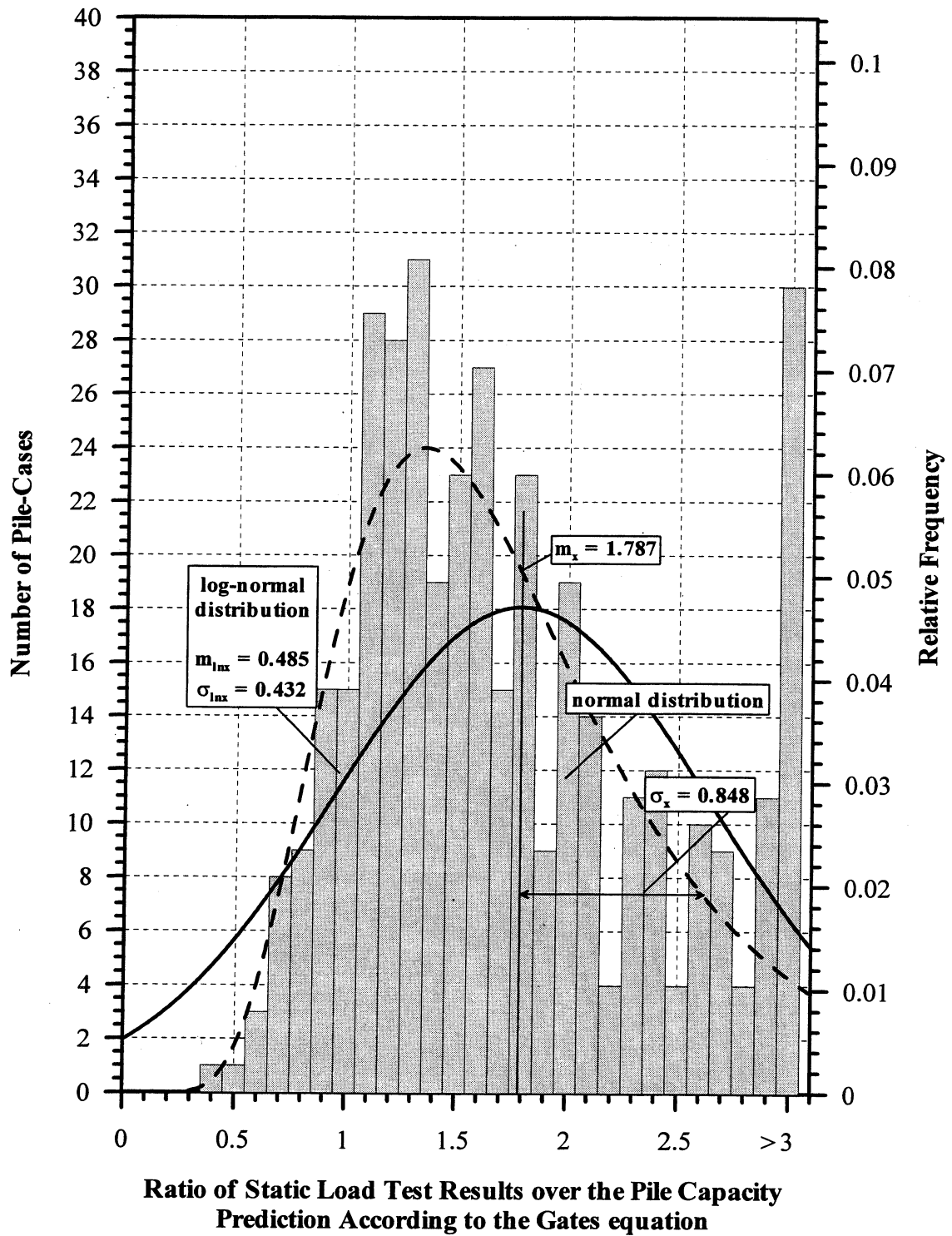


Figure 9.14. Histogram and frequency distributions of K_{SG} for 384 PD/LT2000 pile-cases in all types of soils (AAA).

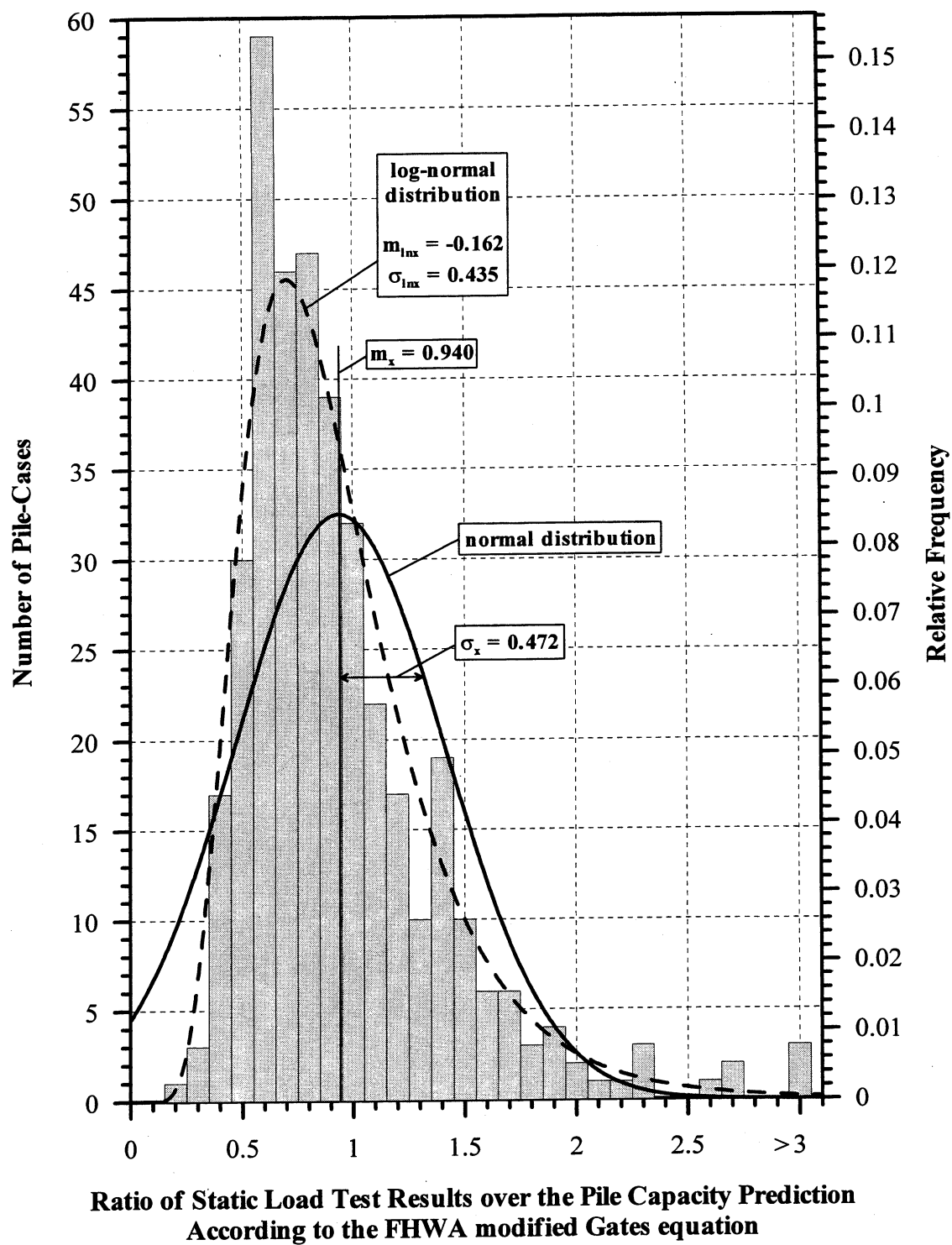


Figure 9.15. Histogram and frequency distributions of K_{SFG} for 384 PD/LT2000 pile-cases in all types of soils (AAA).

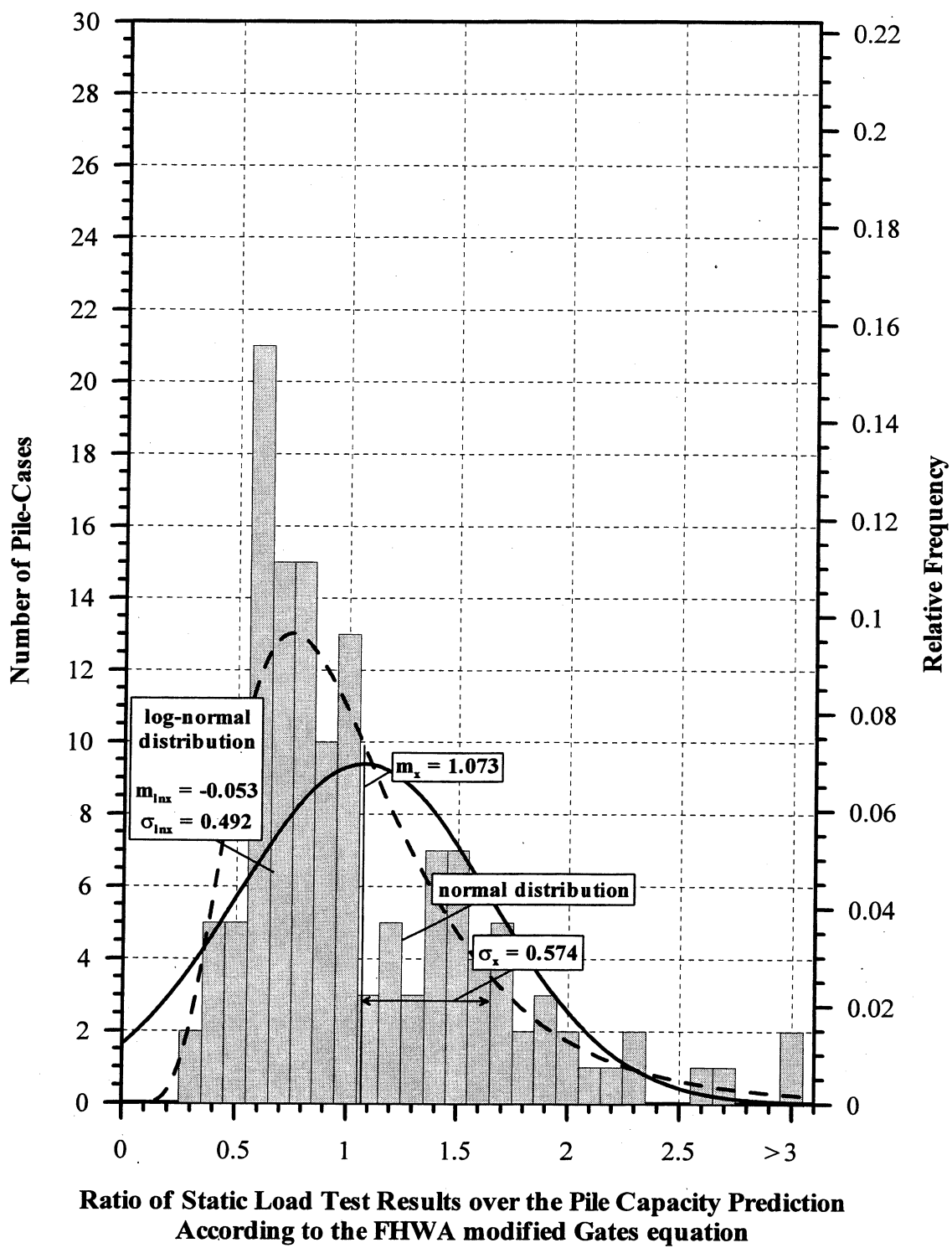


Figure 9.16. Histogram and frequency distributions of K_{SFG} for 135 PD/LT2000 pile-cases at the EOD in all types of soils (AAA).

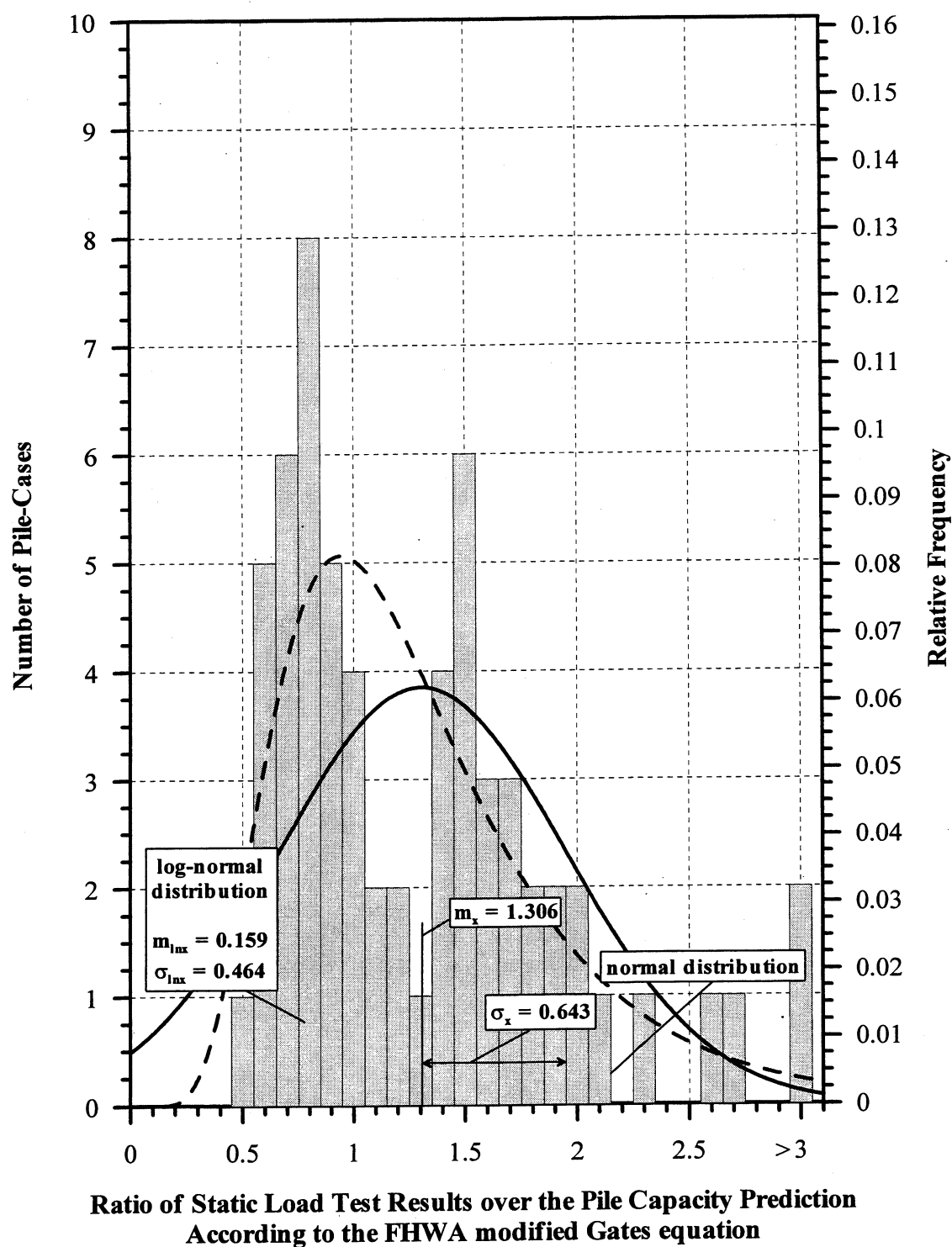


Figure 9.17. Histogram and frequency distributions of K_{SFG} for 62 PD/LT2000 pile-cases at the EOD with Blow Counts < 16 BP10cm in all types of soils (AAA).

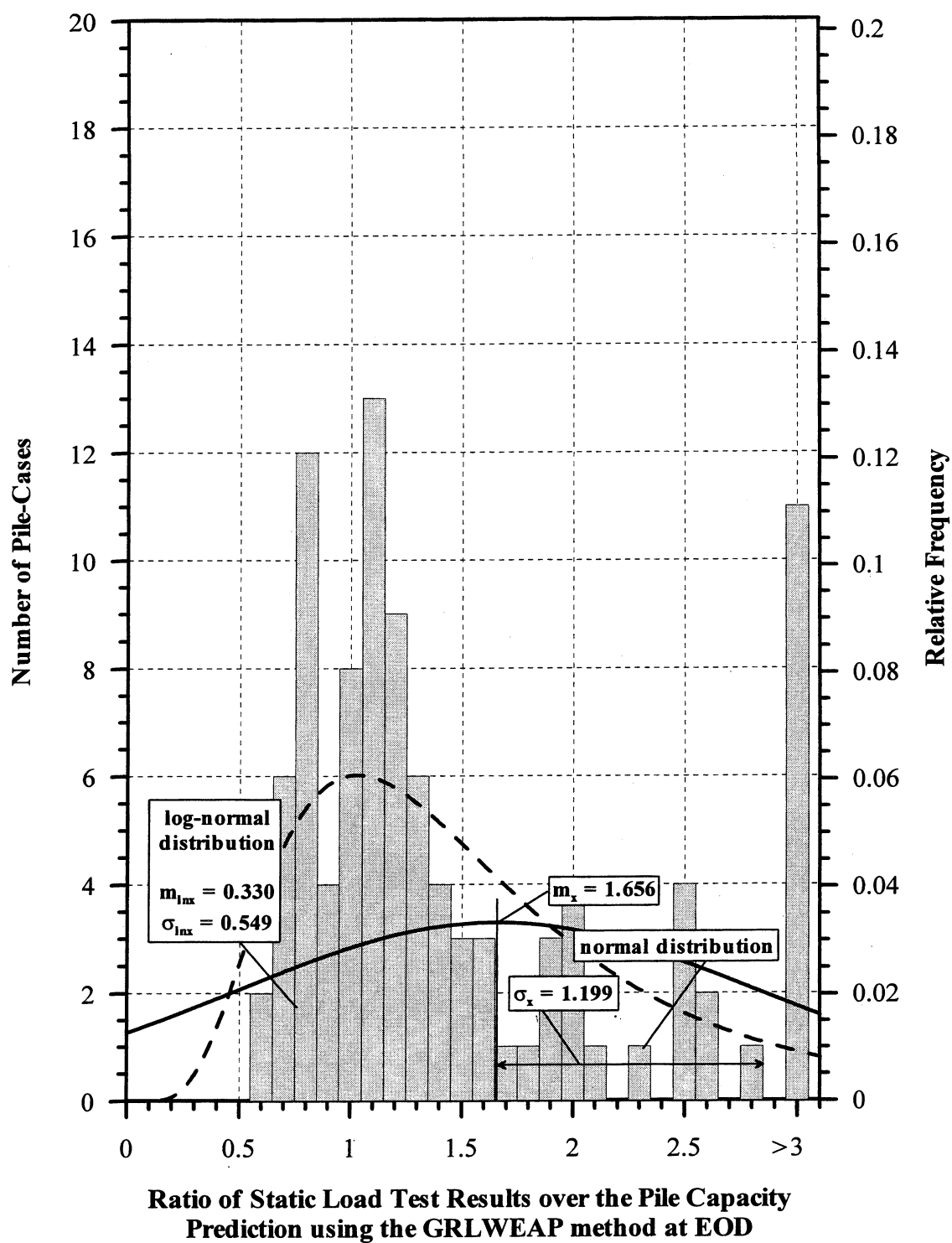


Figure 9.18. Histogram and frequency distributions of K_{swp} for 99 PD/LT2000 GRLWEAP pile-cases at the EOD in all types of soils.

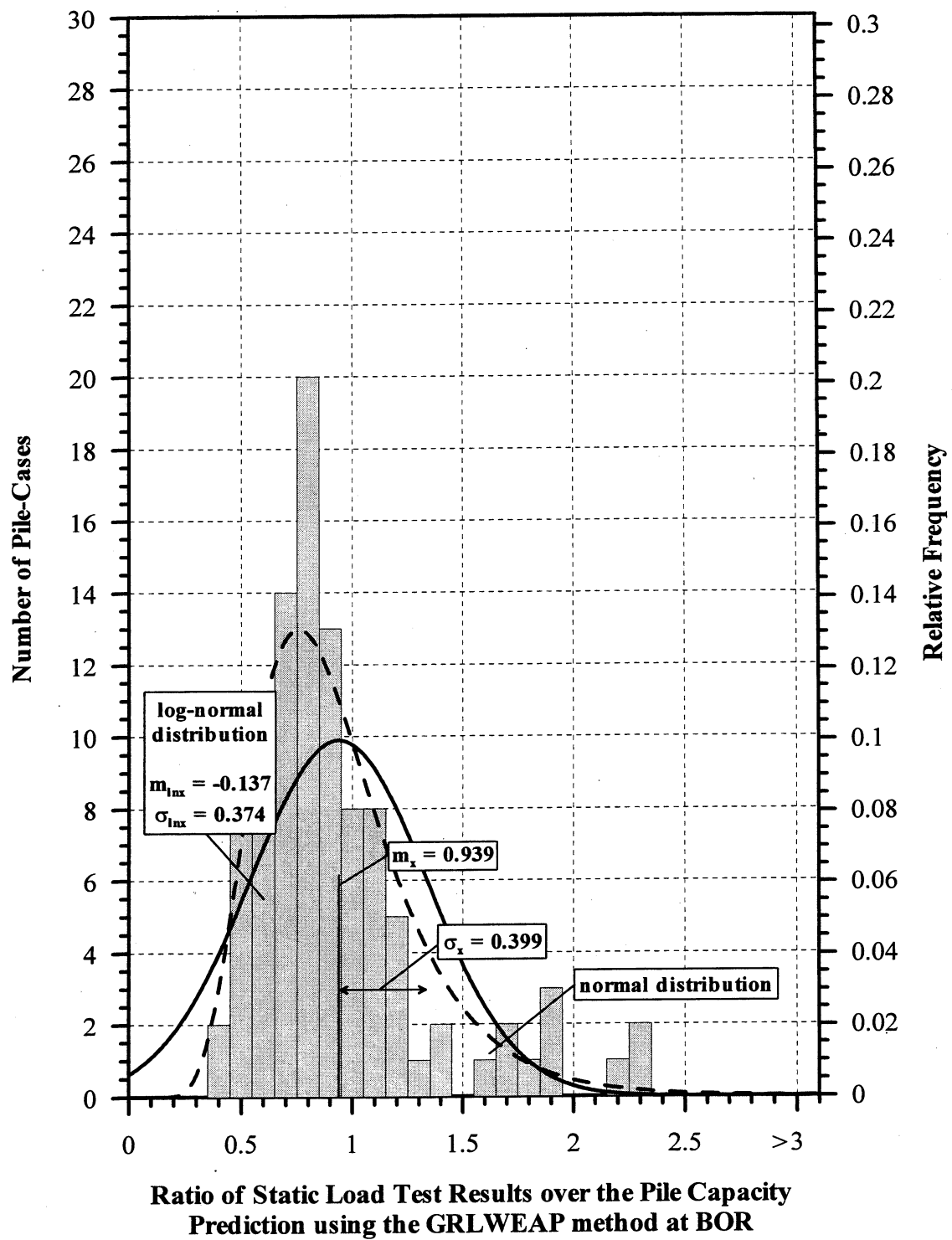


Figure 9.19. Histogram and frequency distributions of K_{SWP} for 99 PD/LT2000 GRLWEAP pile-cases at the BOR in all types of soils.

CHAPTER 10

EXAMPLE CASE HISTORIES

10.1 GENERAL

This chapter attempts to make a comparison between the LRFD method using the presented resistance factors, the 1998 AASHTO code and the Working Stress Design (WSD). This is a difficult task because there is no direct way to compare the 1998 AASHTO code with the proposed resistance factors as the code combines the static and dynamic methods for evaluating pile capacity. Appendix D presents the calculations for three test piles, two friction piles and one end bearing pile.

10.2 EVALUATION OF THE PROPOSED RESISTANCE FACTORS

The two test piles from Newbury, MA are considered friction piles, driven into a subsurface consisting of mostly clay as well as some sand and silt. The third test pile from the Choctawhatchee River project in Florida was driven into a sandy soil and is an end-bearing pile.

Table 10.1 summarizes the ultimate static pile capacities obtained for the three case history piles using a variety of the dynamic methods. Table 10.2 summarizes the allowed (design) pile capacities based on the different codes for the three case history piles. The pile capacities that are shown under the WSD headings were obtained by applying the appropriate factor of safety for each of the four methods used to

determine the piles' capacity (CAPWAP, Energy Approach, Gates formula, and the FHWA version of the Gates formula). The factors of safety that were used are 2.25 for the CAPWAP method, 3.50 for the two dynamic equations, and 2.75 for the Energy Approach. The determination of the pile capacities based on the 1998 AASHTO code is a challenge as the code uses static capacity methods to determine the pile's capacity and if specific dynamic methods are used to verify that pile capacity then the appropriate resistance factors can be used in conjunction with the static analysis results. The resistance factors based on the dynamic method used to verify pile capacities are 1.00 for CAPWAP verification, 0.90 for the Energy Approach verification, and 0.80 for the dynamic equation verification. For example the pile capacity for the Energy Approach method for test pile 2 was obtained by calculating the static pile capacity using the CPT method to be 883 kN, then applying a static resistance factor of 0.55 for the CPT method and finally applying the λ factor of 0.90 to the CPT prediction, resulting in 437 kN. The pile capacities listed under the heading Ch 9 ϕ 's are those capacities that were determined using the recommended resistance factors for non-redundant piles in Table 9.8. The pile capacities that were determined by each of the methods shown in Table 10.1 were simply multiplied by the appropriate resistance factor for that method, e.g., for the Energy Approach at the EOD for test pile 2, the predicted value was 792 kN, the resistance factor for non-redundant pile is $\phi = 0.40$ resulting in a design capacity of 320 kN, which represents an actual factor of safety of 2.06 in this case.

10.3 INTERMEDIATE CONCLUSIONS

Due to the different types of methods that were used to determine these pile capacities it is difficult to state whether the proposed resistance factors for the LRFD method are an improvement over the 1998 AASHTO code based strictly on pile capacities. Comparing between the existing code (AASHTO, 1998) and the recommended parameters obtained in this study is difficult. The comparison between the WSD factored capacities and the recommended parameters shows overall a very good agreement between the two, fully rationalizing the recommended resistance factors. The major improvement remains in the methodology, the ability to adopt the resistance factors to variable conditions (e.g. redundant versus non-redundant) and the method in which the load factors are determined and applied. The current concept is an immeasurable improvement compared to the existing AASHTO parameter application, separating the static and dynamic methods and their relevant resistance factors.

Table 10.1. Predictions of the Dynamic Methods for Three Case History Piles.

Type of Analysis	Method	Q _{ult} (kN)		
		Friction Piles		End Bearing Pile
		Newbury TP # 2	Newbury TP # 3	Choctawhatchee Pier 5
CAPWAP Analyses	CAPWAP EOD	418	738	-----
	CAPWAP BOR	-----	-----	2527
	CAPWAP BORL	1112	1228	2598
Simplified Methods	EA EOD	792	1228	-----
	EA BOR	-----	-----	4484
	EA BORL	1432	4075	5187
Dynamic Equations	ENR w/ FS = 6, EOD	347	409	-----
	ENR w/ FS = 6, BOR	-----	-----	4857
	ENR w/ FS = 6, BORL	1041	2527	5480
	Gates EOD	721	783	-----
	Gates BOR	-----	-----	2304
	Gates BORL	1219	1708	2447
	FHWA EOD	1157	1299	-----
	FHWA BOR	-----	-----	4680
	FHWA BORL	2251	3354	4982
Static Load Test Results		Q _{ult} = 658 kN	Q _{ult} = 872 kN	Q _{ult} = 5560 kN

Note: 1 ton = 8.896 kN

Table 10.2. Summary of Design Capacity Comparisons for Three Case History Piles.

Type of Analysis	Method	Q _{all} (kN)								
		Friction Piles						End Bearing Pile		
		Newbury TP # 2			Newbury TP # 3			Choctawhatchee Peir 5		
		WSD	AASHTO	Ch 9 ϕ's	WSD	AASHTO	Ch 9 ϕ's	WSD	AASHTO	Ch 9 ϕ's
Wave Matching	CAPWAP EOD	187	667	178	329	943	320	-----	1246	-----
	CAPWAP BOR	-----		-----	-----		1121	1290		
	CAPWAP BORL	489		569	543		623	1157		1326
Simplified Methods	EA EOD	285	605	320	445	854	489	-----	1121	-----
	EA BOR	-----		-----	-----		1628	1432		
	EA BORL	525		463	1486		1308	1886		1664
Dynamic Equations	ENR EOD	98	534	53	116	756	62	-----	996	-----
	ENR BOR	-----		-----	-----		-----	1388		730
	ENR BORL	294		160	721		383	1566		818
	Gates EOD	205		383	222		418	-----		-----
	Gates BOR	-----		-----	-----		-----	658		1219
	Gates BORL	347		649	489		907	703		1299
	FHWA EOD	329		302	374		338	-----		-----
	FHWA BOR	-----		-----	-----		-----	1334		1219
	FHWA BORL	641		587	961		872	1423		1299
Static Load Test Results		Q _{ult} = 658 kN			Q _{ult} = 872 kN			Q _{ult} = 5560 kN		

Note: The wave matching techniques are not recommended by GRL to be used at the EOD (Rausche, 2001) and the Energy Approach is not recommended to be used during restrike.

CHAPTER 11

SUMMARY, CONCLUSIONS, AND RECOMMENDATIONS

11.1 SUMMARY

1. A summary of the principles of the Load and Resistance Factor Design (LRFD) method was provided. The intent of the LRFD method is to separate the uncertainties in loading from uncertainties in resistance and to assure a prescribed margin of safety. The principle of the LRFD method for piles is that the ultimate resistance (R_u) multiplied by a resistance factor (ϕ), which is equal to the factored resistance (R_f), must be greater than or equal to the summation of the loads (Q_i) multiplied by a modifier (η_i) and load factor (γ_i), (Refer to Chapter 2).
2. Six datasets were compiled as part of the presented research: PD/LT2000, U-Mass Lowell / Ukraine, GRLWEAP, Case method, PD2000, and PD/LTT2000. The methods and standards that were used in compiling the data for each of the databases used in the LRFD research are presented (Chapter 3) and the relevant information pertaining to each of the databases is presented in Appendix A.
3. In order to evaluate the performance of each of the dynamic methods, the actual static pile capacity needs to be determined. A comparison study between

different bearing capacity interpretation methods had shown that the most reasonable method for determining pile capacity using static load test loadsettlement curves was Davisson's criterion, (Chapter 4). It was also determined that the type of static load test performed, i.e., a slow maintained, short duration, or static cyclic does not greatly affect the representative pile capacity determined from the load test curves.

4. The controlling parameters of the dynamic methods were evaluated based on soil type, time of driving, and soil inertia effects. The effect of soil type was examined by determining the accuracy of the predictive methods relative to the soil type. The time of driving effect was examined by comparing the static load test results to the dynamic predictions at the End Of Driving (EOD) and the Beginning Of Restrike (BOR). The soil inertia effects are represented by the driving resistance and the displaced soil volume, which is defined by the area ratio, (Chapter 5). The driving resistance can be categorized as hard or easy depending on the blow count. The dividing blow count between easy and hard driving was determined to be 16 blows per 10 centimeters (4 blows per inch). The pile types categorized as small displacement and large displacement with the quantitative boundary of $A_R = 350$. This criterion was proposed by Paikowsky et al. (1994) and was confirmed in this research. Using the controlling parameters for the dynamic methods as described above, resistance factors for each of the important sub-categories were calculated.

11.2 CONCLUSIONS

Based on the presented data the following conclusions are derived:

1. The compilation of a large database allows for the evaluation of the dynamic methods, the examination of the Working Stress Design (WSD) methodology (e.g. validity of the assigned factors of safety), and the development of new methodologies such as the Load and Resistance Factor Design (LRFD).
2. The dynamic methods performance is controlled by the time of driving and soil inertia, which in turn is controlled by the driving resistance and the ratio of the soil displaced by the pile's tip to the area of the soil along the shaft of the pile.
3. The most commonly known dynamic equation, the Engineering News Record (ENR) equation, is shown to be completely unreliable and unreasonable for use. In contrast, the Gates equation and its variation, modified by the Federal Highway Administration (FHWA), seem to provide a reasonable assessment of the pile's capacity considering the absence of dynamic measurements.
4. The wave equation analysis performs poorly when used for pile capacity evaluation. However, this conclusion should not be mistaken with the importance of the wave equation analysis during the design stage. The drivability study and pile stress analysis often determine the pile type, geometry and the adequacy of the proposed equipment.
5. Signal matching techniques (e.g. CAPWAP) prove to be most reliable for long-term restrike measurements. However, when evaluated by its efficiency ($\phi / \text{mean } K_{sx}$), the application of the signal matching on restrikes seem to be

marginal compared to the Energy Approach at the End of Driving (EOD). These conclusions though representative of most cases, cannot be based on statistical data alone. For example, sites that exhibit a significant but highly variable setup may economically justify consistent and long-term restrikes along with signal matching analysis.

6. The field application of the Energy Approach provides an exceptionally efficient evaluation of pile capacity during driving.
7. The recommended resistance factors for the dynamic methods that performed reasonably well range from 0.42 to 0.73 for redundant piles ($p_f = 1\%$) and from 0.32 to 0.53 for non-redundant piles ($p_f = 0.1\%$).
8. The development of resistance factors based on FOSM as used by Barker et al. (1991) and the statistical data of this research resulted in resistance factors of about 10% lower than those obtained through FORM, used in this study.
9. A back calculated factors of safety from the obtained resistance factors and an evaluation of the actual risk suggested that the proposed resistance factors and the probability of failure they are based on are reasonable and compatible with common practice.
10. Examination of three case histories suggests good agreement between the recommended resistance factors and the traditional factors of safety of the WSD methodology.
11. The framework for the development of resistance factors as part of the LRFD methodology seem to facilitate a design which is better suitable for

geotechnical applications. The presented work is only an initial stage in that direction.

11.3 RECOMMENDATIONS

1. The presented research refers to single pile analysis while in reality pile groups are most commonly used. Additional data and research are needed for evaluating the reliability of pile groups in comparison to single piles and hence determine resistance factors based on the probability of failure of pile groups.
2. Soil inertia greatly affects the performance of the dynamic analyses. This suggests the need for development of new methods of dynamic analyses that will correctly account for the soil inertia during pile penetration.
3. A complete code based on LRFD needs to consider factors associated with subsurface variability, site-specific technology and previous experience, as well as amount and type of testing during construction. The gathering of data and the development of parameters considering such factors would greatly enhance Geotechnical design.

REFERENCES

AASHTO, 1994. *LRFD Highway Bridge Design Specifications*. American Association of State Highway and Transportation Officials, Washington D.C.

AASHTO, 1997. *Standard Specifications for Highway Bridges*, American Association of State Highway and Transportation Officials, Washington D.C., 16th Edition (1996 with 1997 interims).

AASHTO, 1998. *Standard Specifications for Highway Bridges*, American Association of State Highway and Transportation Officials, Washington D.C.

AISC, 1994. Load and Resistance Factor Design, *Manual of Steel Construction*, American Institute of Steel Construction, Chicago, IL.

Allen, D.E., 1975. Limit States Design - A Probabilistic Study, *Canadian Journal of Civil Engineering*, Vol. 2, No. 1, pp. 36-49.

Allen, D.E., 1994, *The History and Future of Limit States Design*, Journal of Thermal Insulation and Building Envelopes, Vol. 18: pp. 3-20

American Society for Testing and Materials (ASTM), 1996. Annual Book of ASTM Standards, Volume 04.08, Soil and Rock (I): D 420 - D 4914, Philadelphia, PA, p. 1,000.

American Society for Testing and Materials (ASTM), 1998. Standard Test Method for Individual Piles Under Static Axial Compressive Load. *Annual Book of ASTM Standards*, 4.08, Philadelphia.

API, 1989. Draft Recommended Practice for Planning, Designing and Constructing Fixed Offshore Platforms - Load and Resistance Factor Design. *API RP2A-LRFD*, American Petroleum Institute, Dallas, TX.

ASCE, 1993. Minimum Design Loads for Buildings and Other Structures. *ASCE 7-93 (formerly ANSI A58.1)*.

AUSTROADS, 1992. *AUSTROADS Bridge Design Code*, National Office, AUSTROADS, Surry Hills, NSW, Australia.

Ayyub, B. and Assakkaf, I., 1999. LRFD Rules for naval Surface Ship Structures: Reliability-Based Load and Resistance Factor Design Rules. Naval Surface Warfare Center, Carderock Division, U.S. Navy.

Ayyub, B.M., Assakkaf, I., and Atua, K., 1998. Development of LRFD Rules for Naval Surface Ship Structures: Reliability-Based Load and Resistance Factor Design Rules, Part III - Stiffened and Gross Panels. Naval Surface Warfare Center, Carderock Division, U.S. Navy.

Ayyub, B., Assakkaf, I., and Atua, K., 2000. Reliability-Based Load and Resistance Factor Design (LRFD) of Hull Girders for Surface Ships. *Naval Engineers Journal*, ASNE, May 2000.

Ayyub, B.M., Assakkaf, I., Atua, K.I., Melton, W., and Hess, P., 1997, "LRFD Rules for Naval Surface Ship Structures: Reliability-Based Load and Resistance Factor Design Rules," U.S. Navy, Naval Sea System Command, Washington, DC.

Ayyub, B.M., and Atua, K., 1996, "Development of LRFD Rules for Naval Surface Ship Structures: Reliability-Based Load and Resistance Factor Design Rules, Part I - Hull Girder Bending," Naval Surface Warfare Center, Carderock Division, U.S. Navy.

Ayyub, B.M., Beach, J., and Packard, T., 1995, "Methodology for the Development of Reliability-Based Design Criteria for Surface Ship Structures," *Naval Engineers Journal*, ASNE, 107(1), Jan. 1995, 45-61.

Ayyub, B.M. and McCuen, R.H., 1997, Probability, Statistics and Reliability for Engineers, CRC Press, FL.

Baecher, G.B., 1998. Personal Communication.

Baecher, G. and Rackwitz, R., 1982. Factors of Safety of Pile Load Tests, *Journal of Numerical and Analytical Methods in Geomechanics*, Vol. 6, pp. 409-424.

Baker, M.J., 1976. Evaluation of Partial Safety Factors for Level I Codes.

Barker, R.M., Duncan, J.M., Rojiani, K.B., Ooi, P.S.K., Tan, C.K., and Kim, S.G., 1991. *Manuals for the Design of Bridge Foundations*, NCHRP Report 343. Transportation Research Board, National Research Council, Washington, DC.

Becker, D.E., 1996. Eighteenth Canadian Geotechnical Colloquium: *Limit States Design for Foundations. Part I. An Overview of the Foundation Design Process*. Canadian Geotechnical Journal, Vol. 32: pp. 956-983.

Berezantzev, V. G., Khristoforov, V. and Golubkov, V., 1961. Load Bearing Capacity and Deformation of Piled Foundations. *Proceedings 5th International Conference*. S.M. & F.E., Vol. 2, pp. 11-15.

Bowles, J.E., 1996. Foundation Analysis and Design, 5th Edition. McGraw-Hill, USA.

Burland, J. B., 1973. Shaft friction of piles in clay - A simple fundamental approach. *Ground Engineering*, Vol. 6, No. 3, pp. 30-42.

Butler, H.D. and Hoy, H.E., 1977. *Users Manual for the Texas Quick-Load Method for Foundation Load Testing*. Federal Highway Administration, Office of Development, Report No. FHWA-IP-77-8, Washington DC.

Canadian Geotechnical Society, 1992. *Canadian Foundation Engineering Manual*, 3rd Edition, Bi-Tech publishers, Ltd., Richmond, British Columbia, Canada.

Chernauskas, L.R., 1993. Dynamic Analysis of Plugged Piles in Clay. *Master of Science Thesis submitted to the Department of Civil Engineering*, University of Massachusetts-Lowell, 1993.

CIRIA 63, 1977. Rationalization of Safety and Serviceability Factors in Structural Codes. Construction Industry Research and Information Association, SWIP 3AU, Report 63, London.

Coyle, H. M. and Castello, R.R., 1981. New Design Correlations for Piles in Sand. *J. Geotech. Eng. Div.*, Proc. ASCE, Vol. 107, No. GT7, pp. 965-986.

Danish Geotechnical Institute, 1985. Code of Practice for Foundation Engineering. DGI Bulletin 36, 1 Maglebjergvej, DK-2800 Lyngby, Denmark.

Davisson, M.T., 1972. High Capacity Piles. *Proceedings, Soil Mechanics Lecture Series on Innovations in Foundation Construction*. American Society of Civil Engineers, Illinois Section, Chicago, pp. 81-112.

DeBeer, E.E., 1970. Proefondervindelijke bijdrage tot de studie van het grandsdraagvermogen van zand onder funderinger op staal. English version, *Geotechnique*, Vol. 20, No. 4, pp. 387-411.

DiMaggio, 2000. Personal Communication.

Drewry, J. M., Weidler, J. B. and Hwong, S. T., 1977. Predicting axial pile capacities for offshore platforms, *Petroleum Engineer*, Vol. 41.

- Duncan, J.M., Tan, C.K., Barker, R.M., and Rojiani, K.B., 1989, Load and Resistance Factor Design of Bridge Structures. *In the Proceedings of the Symposium on Limit States Design in Foundation Engineering. Canadian Geotechnical Society Southern Ontario Section*, Toronto, May 26 - 27, pp. 47 - 63.
- Ellingwood, B. and Galambos, T.V., 1982. Probability-Based Criteria for Structural Design, *Structural Safety*, 1, pp. 15-26.
- Ellingwood, B., Galambos, T., MacGregor, J. and Cornell, C. 1980. Development of a Probability-Based Load Criterion for American National Standard A58. *National Bureau of Standards Publication 577*, Washington, DC.
- Ellingwood, B., Galambos, T., MacGregor, J. and Cornell, C. 1982a. Probability Based Load Criteria - Assessment of Current Design Practices. *Journal of the Structural Division*, ASCE, Vol. 108, ST5, pp. 959-977.
- Ellingwood, B., Galambos, T., MacGregor, J. and Cornell, C. 1982b. Probability Based Load Criteria - Load Factors and Load Combinations. *Journal of the Structural Division*, ASCE, Vol. 108, ST5, pp. 978-997.
- Eurocode 7, 1993. *Geotechnical Design, General Rules*, European Committee for Standardization. Pre-standard. Danish Geotechnical Institute, Copenhagen.
- Fellenius, H.B., 1989. Guidelines for the Interpretation and Analysis of the Static Loading Test. Deep Foundations Institute.
- Fellenius, H.B., 1994. Limit States Design for Deep Foundations. *Proceedings, U.S. DOT International Conference on Deep Foundations*, Orlando, FL, December 1994, p. 12.
- FHWA, 1988. FHWA Guide Specifications for Driven Piles. Federal Highway Administration.
- Freudenthal, A.M. 1947. Safety of Structures. *Transactions of the ASCE*. Vol. 112, pp. 125-180.
- Fox, E., 1932. Stress Phenomena Occurring in Pile Driving. *Engineering Journal*, London, England, Vol. 134.
- Galambos, T.V., 1989. Present and Future Developments in Steel Design Codes, *Proceedings 5th International Conference on Structural Safety and Reliability*, Ang, A., et al. (eds.), ASCE, New York, pp. 2011-2018.

Galambos, T.V. and Ravindra, M.K. 1978. Properties of Steel for Use in LRFD. *Journal of Structural Engineering, ASCE*, Vol. 104, No. 9, pp. 1459-1468.

Gates, 1957. Empirical Formula for Predicting Pile Bearing Capacity. *Civil Engineering*, Vol. 27, No. 3, pp. 65-66.

Goble, G., 1999. Geotechnical Related Development and Implementation of Load and Resistance Factor Design (LRFD) Methods. *NCHRP Report 276*, Transportation Research Board, Washington, DC, pp. 10-36.

Goble, G. G., Likens, G., and Rausche, F., 1970. Dynamic Studies on the Bearing Capacity of Piles - Phase III, Report No. 48. *Division of Solid Mechanics, Structures, and Mechanical Design*. Case Western Reserve University.

Goble, G. G., Likens, G. and Rausche, F., 1975. Bearing Capacity of Piles from Dynamic Measurements, Final Report, Ohio Department of Transportation, Ohio DOT-05-75.

Goble, G.G., Rausche, F. and Likins, G., 1980. The Analysis of Pile-Driving: A State of the Art. *Proceedings from the 2nd Conference on the Application of Stress-Wave Theory on Piles*, Stockholm, Sweden, June 1980, pp. 1-34.

Goble, Rausche, Likens and Associates, Inc. (GRL), 1996. "Design and Construction of Driven Pile Foundations," Volume I, NHI Course Nos. 13221 and 13222, US Department of Transportation, Federal Highway Administration, Washington DC.

Goble, G.G., Scanlan, R.H. and Tomko, J.J., 1967. Dynamic Studies on the Bearing Capacity of Piles, Phase II. Vol. I and II, Case Institute of Technology.

Graff, K.F., 1975. Wave Motion in Elastic Solids. Ohio State University Press, Columbus, Ohio.

GRL, 1999. *Pile-Driving Analyzer, PAK Users Manual*. Goble, Rausche, Likins and Associates, Inc.

GTR, 1997. *Dynamic Pile Testing Report, Central Artery/Tunnel Project C07D2, I-90/Airport Interchange Arrivals Tunnel - Phase I, East Boston, MA*. Geosciences Testing and Research, Inc., North Chelmsford, MA.

GTR, 1998. *Dynamic Pile Testing Report, Central Artery/Tunnel Project C07D2, I-90/Airport Interchange Toll Plaza, East Boston, MA*. Geosciences Testing and Research, Inc., North Chelmsford, MA.

Guiffre, N. and Pinto, P.E., 1976. Discretization from a Level II Method, Information Bulletin No. 112, CIB Joint Committee on Structural Safety, Paris, France, pp. 158-189.

Hasofer, A.M. and Lind, N.C., 1974. An Exact and Invariant First-Order Reliability Format. *Journal of Engineering Mechanics*, ASCE, Vol. 100, No. EM1, pp. 111-121.

Hawrenek, R. and Rackwitz, R., 1976. Reliability Calculations for Steel Columns, Information Bulletin No. 112, CIB Joint Committee on Structural Safety, Paris, France, pp. 125-157.

Isaacs, D. 1931. Reinforced Concrete Pile Formula. *Transactions of the Institute of Engineers*, Australia, Vol. 12, pp. 312-323.

Kusakabe, Osamu, 1998. Foundation Design Standards in the World - Toward Performance-Based Design. *Japanese Geotechnical Society*, September 1998.

Kyfor, Z.G., Schnore, A.S., Carlo, T.A. and Baily, D.F., 1992. Static Testing of Deep Foundations. Report No. FHWA-SA-91-042, U.S. Department of Transportation, Federal Highway Administration, Office of Technology Applications, Washington DC., p. 174.

Lind, N.C., 1976. Application to Design of Level I Codes, Information Bulletin No. 112, CIB Joint Committee on Structural Safety, Paris, France, pp. 73-89.

Lotsberg, I., 1991. Target Reliability Index, A Literature Survey, Report No. 91-2023, A.S. Veritas Research, Norway.

Lowery, L.L., Hirsh, T.J., Edwards, T.C., Coyle, H.M. and Samson, C.H., 1969. Pile-Driving Analysis - State of the Art, Research Report 33-13 (Final). Texas Highway Department, Research Study No. 2-5-62-33.

Madsen, H.O., Krenk, S. and Lind, N.C., 1986. Methods of Structural Safety. Prentice Hall, Englewood Cliffs, New Jersey.

Mansour, A.E., Wirsching, P.H., Ayyub, B.M. and White, G.J., 1994. Probability Based Ship Design Implementation of Design Guidelines for Ships, Ship Structures Committee Draft Report, U.S. Coast Guard, Washington, D.C.

Mansur, C.I. and Hunter, A.H., 1970. Pile Tests - Arkansas River Project. *JSMFD*, ASCE, Vol. 96, SM 5, September, pp. 1545-1582.

Massachusetts Highway Department, (Section 940), 1995. Driven Piles. *1995 Standard Specifications for Highways and Bridges*, Metric Edition, pp. 257-271.

- McClelland, B., Focht, J. A., & Emrich, W. J., 1969. Problems in Design and Installation of Offshore Piles. *JSMFD*, ASCE, Vol.95, SM6, pp. 1419-1514.
- McVay, M., Birgisson, B., Zhang, L., Perez, A. and Putcha, S., 2000. Load and Resistance Factor Design (LRFD) for Driven Piles Using Dynamic Methods - A Florida Perspective. *Geotechnical Testing Journal*, ASTM, Vo. 23, No. 1, pp. 55-66.
- McVay, M.C., Ching, K.L., and Singletary, W.A., 1998. Calibrating Resistance Factors in the Load and Resistance Factor Design for Florida Foundations. Final Report, Department of Civil Engineering, University of Florida, Submitted to the Florida Department of Transportation, December 1998.
- Melchers, R.E., 1987. Structural Reliability Analysis and Prediction. Ellis Horwood Limited, UK
- Meyerhof, G.G., 1956. Penetration Tests and Bearing Capacity of Cohesionless Soils. *JSMFD*, ASCE, Vol. 85, SM6, pp. 1-29.
- Meyerhof, G.G., 1970. Safety Factors in Soil Mechanics. *Canadian Geotechnical Journal*, Vol. 7, No. 4, pp. 349-355.
- Meyerhof, G.G., 1976. Bearing Capacity and Settlement of Pile Foundations. *J. Geotech, Div.*, ASCE, Vol. 102, No. GT 3, pp. 197-228.
- Meyerhof, G.G., 1994, Evolution of Safety Factors and Geotechnical Limit State Design. *Spencer J. Buchanan Lecture, Texas A and M University*, Nov. 4, pp. 32
- Moses, F., 1985. Implementation of a Reliability-Based API RP2A Format, Final Report. *API PRAC 83-22*. American Petroleum Institute.
- Moses, F., 1986. Development of Preliminary Load and Resistance Factor Design Document for Fixed Offshore Platforms, Final Report. *API-PRAC 95-22*. American Petroleum Institute.
- Moses, F. and Verma, D., 1987. Load Capacity Evaluation of Existing Bridges, NCHRP Report 301, Transportation Research Board, Washington, D.C.
- National Research Council of Canada, 1977. *National Building Code of Canada*. Ottawa.
- Nordic Building Code Committee, 1978. Recommendations for Loading and Safety Regulations for Structural Design, Report No. 36, Copenhagen, Denmark, p. 148.

Nottingham, L. and Schmertmann, J., 1975. An Investigation of Pile Capacity Design Procedures, Final Report D629 to Florida Department of Transportation from the Department of Civil Engineering, University of Florida, p. 159.

Nowak, A.S., 1993. Calibration of LRFD Bridge Design Code. Department of Civil and Environmental Engineering Report UMCE 92-25, University of Michigan, NCHRP 12-33.

Nowak, A.S., 1999. Calibration of LRFD Bridge Design Code. Department of Civil and Environmental Engineering Report UMCE 92-25. University of Michigan, NCHRP 12-33.

Olsen, R. and Flaate, K., 1967. Pile Driving Formulas for Friction Piles in Sand. *ASCE JSMFC*, Vol. 93, SM6, November 1967, pp. 279-297.

Ontario Ministry of Transportation and Communication, 1992. Ontario Highway Bridge Design Code and Commentary, 3rd ed.

O'Neill, Michael W., 1999. Personal Communication.

O'Neill, Michael W., 1995. LRFD Factors for Deep Foundations through Direct Experimentation. In *Proceedings of US/Taiwan Geotechnical Engineering Collaboration Workshop*. Sponsored by the National Science Foundation (USA) and the National Science Council (Taiwan, ROC) Taipei, January 1995, pp. 100 - 114.

Paikowsky, S., 1982. Use of Dynamic Measurements to Predict Pile Capacity Under Local Conditions. M.Sc. Thesis, Dept. of Civil Engineering Technion-Israel Institute of Technology.

Paikowsky, S., 1984. Use of Dynamic Measurements for Pile Analysis. Including PDAP-Pile-Driving Analysis Program, GZA Inc., Newton, MA.

Paikowsky, S., 1995. Using Dynamic Measurements for the Capacity Evaluation of Driven Piles. *Civil Engineering Practice, Journal of the Boston Society of Civil Engineers Section / ASCE*. Vol. 10, No. 2, pp. 61-76.

Paikowsky, S.G. and Chen, Y.L., 1998. Field and Laboratory Study of the Physical Characteristics and Engineering Parameters of the Subsurface at the Newbury Bridge Site. *Research Report submitted to the Massachusetts Highway Department, January 1998*, Boston, Massachusetts.

Paikowsky, S. and Chernauskas, L., 1992. Energy Approach for Capacity Evaluation of Driven Piles. *4th International Conference on the Application of Stress-Wave Theory to Piles*. The Hague, Netherlands, pp. 595-601.

Paikowsky, S. and Chernauskas, L., 1996. Soil Inertia and the Use of Pseudo Viscous Damping Parameters. *5th International Conference on the Application of Stress-Wave Theory to Piles*. Orlando, FL, pp. 203-216.

Paikowsky, S.G. and Hajduk, E.L., 1999. Design and Construction of an Instrumented Test Pile Cluster. *Research Report submitted to the Massachusetts Highway Department, Geotechnical Section, September 1999*, Boston, Massachusetts.

Paikowsky, S.G. and Hajduk, E.L., 2000. Theoretical Evaluation and Full Scale Field Testing Examination of Pile Capacity Gain with Time. *Research Report to be submitted to the Massachusetts Highway Department, December 2000*. Boston, MA.

Paikowsky, S. and Hart, L., 2000. Development and Field Testing of Multiple Deployment Model Pile (MDMP). *Research Report to be submitted to the Federal Highway Administration, April 2000*. FHWA-RD-99-194, Washington DC.

Paikowsky, S. and LaBelle, V. 1994. Examination of the Energy Approach for Capacity Evaluation of Driven Piles. *US FHWA International Conference on Design and Construction of Deep Foundations. December 6-8, 1994*. Orlando, FL. Vol. II, pp. 1133-1149.

Paikowsky, S., LaBelle, V. and Hourani, N., 1996. Dynamic Analyses and Time Dependent Pile Capacity. *5th International Conference on the Application of Stress-Wave Theory to Piles*. Orlando, FL, pp. 325-339.

Paikowsky, S., LaBelle, V. and Mynampaty, R., 1995. Static and Dynamic Time Dependent Pile Behavior. *Research Report submitted to the Massachusetts Highway Department, November 1995*. Boston, MA.

Paikowsky, S., Operstein, V. and Bachand, M., 1999. Express Method of Pile Testing by Static Cyclic Loading. *Research Report submitted to the Massachusetts Highway Department, October 1999*. Boston, MA.

Paikowsky, S. G., Regan, J. E., and McDowell, J. J., 1994. A Simplified Field Method for Capacity Evaluation of Driven Piles. *FHWA Report No. FHWA-RD-94-042, September 1994*. Washington DC.

Paikowsky, S.G. and Stenersen, K.L., 2000. The performance of the dynamic methods, their controlling parameters and deep foundation specifications. *6th International Conference on the Application of Stress-Wave Theory to Piles*. São Paulo, Brazil, September 2000, Editors; S. Niyama and J. Beim.

Paikowsky, S. and Whitman, R., 1990. The Effect of Plugging on Pile Performance and Design. *Canadian Geotechnical Journal*, Vol. 27, No. 4, pp. 429-440.

Paikowsky, S., Whitman, R. and Baligh, M., 1989. A New Look at the Phenomenon of Offshore Pile Plugging. *Marine Geotechnology*, Vol. 8, No. 3, pp. 213-230.

Payer, H.G., Huppmann, H., Jochum, C., Madsen, H.o.< Nittinger, K., Shibata, H., Wild, W., and Wingender, H. J., 1994. Plenary Panel Discussion on How Safe is Safe Enough? *Structural Safety and Reliability*, Schueller, Shinozuka and Yao (eds.), Balkema, Rotterdam, Netherlands, pp. 57-74.

PDA Manual, 1999. Pile Dynamics, Inc., Model PAK, Cleveland, Ohio.

Peck, R.P., Hanson, W.E., and Thornburn, T.H., 1974. *Foundation Engineering*, 2nd ed. John Wiley & Sons, Inc., New York.

Rausche, F., 2000. Personal Communication. February 2000.

Rausche, F., 2001. Personal Communication. February 2001.

Rausche, F., Goble, G. and Likens, G., 1975. Bearing Capacity of Piles from Dynamic Measurements, Final Report, Ohio Department of Transportation, Ohio DOT-05-75.

Ravindra, M.K. and Galambos, T.V., 1978. Load and Resistance Factor Design for Steel. *Journal of the Structural Division*, Proceedings of the American Society of Civil Engineers, New York, N.Y., Vol. 104, No. 9, pp. 1337-1354.

Ravindra, M.K., Heany, A.C. and Lind, N.C., 1969. Probabilistic Evaluation of Safety Factors, Final Report, Symposium on Concepts of Safety of Structures and Methods of Designs, IABSE, London, pp. 36-46.

Reed, D.A. and Brown, C.B., 1992. Reliability in the Context of Design, *Structural Safety*, 11, pp. 109-119.

Rosenblueth, E. and L. Esteva, 1972. Reliability Basis for Some Mexican Codes. *ACI Publication SP-31*, American Concrete Institute, Detroit, MI.

Ryan, T.P., 1989. Linear Regression. Chapter 13 of *Handbook of Statistical Methods for Engineers and Scientists*, H.M. Wadsworth, editor. McGraw-Hill.

Simpson, B., Pappin, J.W., and Croft, D.D. 1981. An Approach to Limit State Calculations in Geotechnics, *Ground Engineering*, Vol. 14(6): pp. 21 - 28.

Siu, W.W.C., Parimi, S.R., and Lind, N.C., 1975. Practical Approach to Code Calibration. *Journal of the Structural Division*. ASCE, Vol. 101, No. ST7, pp. 1469-1480.

Smith, E., 1960. Pile Driving Analysis by the Wave Equation. *Journal of Soil Mechanics and Foundations, American Society of Civil Engineers*, August 1960, pp. 35-61.

Standards Association of Australia, 1995. Australian Standards, Piling-Design and Installation. Homebush, NSW.

Tang, W.H., Woodford, D.L. and Pelletier, J.J., 1990. Performance Reliability of Offshore Pile. *22nd Annual Offshore Technology Conference*, Paper No. OTC 6379, Houston, TX.

Taylor, D.W., 1948. *Fundamentals of Soil Mechanics*. John Wiley & Sons, New York, p. 700.

Terzaghi, K., 1942. Discussion of the Progress Report of the Committee on the Bearing Value of Pile Foundations. *Proceedings, ASCE*. Vol. 68, pp. 311-323.

The Massachusetts State Building Code, (Section 1213.0), 1996. Pile Foundations. *The Massachusetts Building Code 5th Edition*, 780 CMR, pp. 14-25.

Thoft-Christensen, P. and Baker, M.J., 1982. Structural Reliability Theory and Its Application. Springer-Verlag, New York.

Veneziano, D., 1993. Personal Communication.

Vesic, A. S., 1965. Ultimate Loads and Settlements of Deep Foundations in Sands. *Proceedings of the Symposium on Bearing Capacity and Settlement of Foundations*. Duke University, Durham, NC, pp. 53-68.

Vesic, A. S., 1977. Design of Pile Foundations. Transportation Research Board, National Research Council, Washington, DC.

Vijayvergiya, V. N. and Focht Jr., J. A., 1972. A new way to predict capacity of piles in clay. *Proceedings, 4th Offshore Technology Conference*, Houston, TX, Vol. 2, pp. 856-874.

Wellington, 1892. Discussion of "the Iron Wharf at Fort Monroe, VA." By J.B. Cuncklee. *Transactions, ASCE* Vol. 27, paper No. 543, August 1892, pp. 129-137.

Wirsching, P.H., 1984. Fatigue Reliability for Offshore Structures. *Journal of Structural Engineering*, American Society of Civil Engineers, New York, Vol. 110, No. 10, pp. 2340-2356.

Withiam, J. L., Voytko, E.P., Barker, R.M., Duncan, M.J., Kelly, B.C., Musser, S.C. and Elias, V., 1997. Load and Resistance Factor Design (LRFD) of Highway Bridge Substructures. Washington D.C.: U.S. DOT Federal Highway Administration.

Withiam, J. L., Voytko, E.P., Barker, R.M., Duncan, M.J., Kelly, B.C., Musser, S.C. and Elias, V., 1998. Load and Resistance Factor Design (LRFD) of Highway Bridge Substructures. *FHWA Publication No. HI-98-032*, July 1998. Washington D.C.

Wu, T.H., Tang, W.H., Sangrey, D.A. and Baecher, G.B., 1989. Reliability of Offshore Foundations - State of the Art. *Journal of Geotechnical Engineering*, ASCE, Vol. 115, No. 2, pp. 157-178.

Yoon, Gil and O'Neill, Michael, 1997. Resistance Factors for Single Driven Piles from Experiments. Transportation Research Board, 76th Annual Meeting, January 12-16. Washington DC.